

FRAMEWORK FOR DETERMINING THE PULLOUT  
RESISTANCE OF INEXTENSIBLE 2-WIRE  
SOIL-REINFORCING ELEMENTS EMBEDDED IN SAND

by

THOMAS PATRICK TAYLOR

Presented to the Faculty of the Graduate School of  
The University of Texas at Arlington in Partial Fulfilment  
of the Requirements  
for the Degree of

DOCTOR OF PHILOSOPHY

THE UNIVERSITY OF TEXAS AT ARLINGTON  
APRIL 2018

Copyright © by Thomas P. Taylor 2018  
All Rights Reserved



## Acknowledgements

I would like to extend my sincere appreciation and gratitude to my advisor, Dr. Anand J. Puppala for his guidance and constant encouragement throughout my studies. He provided unstinting encouragement to continue my educational pursuit. His support, patience, and friendship throughout my pursuit of my Doctor of Philosophy is sincerely appreciated. I would also like to thank Dr. James Collin, Dr. Xinbao Yu, and Dr. Shih-Ho Chao for serving on my examination committee. A special thanks to Dr. Richard Bathurst of the GeoEngineering Centre at Queen's-RMC, as well, for providing guidance in the development of the statistical analysis. Thanks to Richard Witasse of Plaxis Expert Services, for his help and advice with the numerical model. A special debt of gratitude is extended to Big-R Bridge for their unending support of this research.

I would also like to extend my sincere appreciation and gratitude to my friend, mentor, colleague, and committee member, Dr. James Collin, of The Collin Group, for his support during my research work and studies. His constant encouragement in the pursuit of my Doctor of Philosophy degree will never be forgotten.

There are few words that can express my gratitude and appreciation to family. To my parents, Herb and Armena, thank you for being excellent role models, leading by example, and for your support and encouragement all throughout my life. To my children, Jessica, Michael, Courtney, and Matthew, thank you for understanding how important this educational goal was to me, and for your sacrifice during my studies. And finally, a special debt of gratitude and sincere thanks is given to my wife, and best friend, Monica, who without her support, encouragement, understanding, and patience, none of this would have been possible.

**This Page Intentionally Left Blank**

Abstract

FRAMEWORK FOR DETERMINING THE PULLOUT  
RESISTANCE OF INEXTENSIBLE 2-WIRE  
SOIL-REINFORCING ELEMENTS EMBEDDED IN SAND

Thomas P Taylor, P.E., P.Eng., D.GE.

The University of Texas at Arlington, 2018

Supervising Professor: Dr. Anand J. Puppala, P.E., D.GE.

Mechanically Stabilized Earth (MSE) has been successfully used as a commercial retaining structure since its development in 1963 by Henry Vidal (Schlosser 1990). MSE is a ground improvement system that consists of soil-reinforcing, compacted backfill, and a facing. The initial soil-reinforcing developed for commercial use by Vidal consisted of a smooth steel strip. Since then, a diverse range of soil-reinforcing has been developed, including extensible and inextensible reinforcing. The various geometric configurations of soil-reinforcing have included wide width and narrow width elements comprising planar strips, planar grids, co-planar strips, co-planar grids, and wide sheets. General specifications categorize inextensible soil-reinforcing into metallic linear strips, metallic welded-wire mesh, and metallic bar mats, while extensible soil-reinforcing is categorized into geogrids and polymer strips. A soil-reinforcing element that consists of metallic welded wire, also known as a bar-mat, with only two longitudinal wires and a series of transverse wires is currently being utilized as soil-reinforcing in MSE systems. The 2-Wire soil-reinforcing element is a linear strip that resembles a ladder. The 2-Wire configuration of inextensible soil-reinforcing is not technically

categorized or defined within the general specification. In other words this raises the question, is the 2-Wire element a linear strip, a welded-wire system, a bar-mat system, or should it be uniquely identified?

The semi-empirical equations used to determine the pullout resistance of an inextensible grid system include a pullout coefficient, also known as a bearing resistance factor. The bearing resistance factor is soil-reinforcing dependent. For inextensible grid systems, it has been empirically established that the bearing resistance factor is a function of the transverse wire size and the transverse wire spacing. The spacing of the longitudinal wire is not considered in the equation. As an illustration, a grid system of a given width, for example 1220 mm, with 300 mm spaced longitudinal wires, is assumed to act in the same manner as a grid system with 50 mm spaced longitudinal wires. The objective of this research is to develop a bearing resistance factor for commonly used 2-Wire soil-reinforcing elements. This will be accomplished by performing pullout test on 2-Wire elements utilizing a state-of-practice pullout program.

## Table of Contents

|   |           |
|---|-----------|
| Acknowledgments .....                                     | i         |
| Abstract .....  | iii       |
| List of Figures .....                                     | xi        |
| List of Tables .....                                      | xvii      |
| List of Photographs .....                                 | xxi       |
| <b>CHAPTER 1 INTRODUCTION .....</b>                       | <b>1</b>  |
| 1.1 General.....  | 1         |
| 1.2 Statement of Problem.....                             | 9         |
| 1.3 Objectives and Scope of Research.....                 | 11        |
| 1.3.1 Goal of Research.....                               | 12        |
| 1.3.2 Hypothesis .....                                    | 12        |
| 1.3.3 Tasks.....  | 12        |
| 1.4 Organization of Dissertation.....                     | 13        |
| 1.5 Conventions and Units .....                           | 14        |
| <b>CHAPTER 2 LITERATURE REVIEW .....</b>                  | <b>15</b> |
| 2.1 Mechanically Stabilized Earth .....                   | 15        |
| 2.1.1 Soil-Reinforcing Classification .....               | 16        |
| 2.1.1.1 Linear Steel Strips.....                          | 17        |
| 2.1.1.1.1 RECo High Adherence (HA) Reinforcing Strip..... | 17        |
| 2.1.1.1.2 Sine Wall Corrugated Steel Strip.....           | 19        |
| 2.1.1.2 Grid Systems.....                                 | 20        |
| 2.1.1.2.1 Welded Wire Mesh.....                           | 21        |
| 2.1.1.2.2 Bar-Mats.....                                   | 23        |
| 2.1.1.2.3 RECo High Adherence (HA) Ladder .....           | 26        |
| 2.1.1.2.4 Keystone KeySystem KeyStrip .....               | 28        |
| 2.1.1.2.5 Grid-Strip™ .....                               | 29        |
| 2.1.1.3 Other Soil-Reinforcing Systems.....               | 31        |
| 2.1.2 Horizontal Earth Pressure.....                      | 31        |
| 2.1.2.1 Lateral Earth Pressure Coefficient.....           | 31        |
| 2.1.2.2 Coulomb Theory.....                               | 34        |
| 2.1.2.3 Rankine Theory.....                               | 35        |
| 2.1.2.4 Earth Pressure and MSE .....                      | 35        |
| 2.1.3 MSE Design Methodologies .....                      | 36        |
| 2.1.3.1 MSE External and Global Stability Design .....    | 37        |
| 2.1.3.2 MSE Internal Stability Design .....               | 39        |
| 2.1.3.3 Internal Failure Surface.....                     | 41        |

|           |  |            |
|-----------|--|------------|
| 2.1.3.4   | MSE Design Theories.....   | 44         |
| 2.1.3.4.1 | Coherent Gravity Design Method .....                                       | 45         |
| 2.1.3.4.2 | Tieback Wedge Method.....  | 48         |
| 2.1.3.4.3 | Stiffness Design Method.....   | 50         |
| 2.1.3.4.4 | Simplified Method .....  | 53         |
| 2.1.3.4.5 | K-Stiffness.....   | 55         |
| 2.1.3.5   | Description of Lateral Stress Ratio .....                                  | 56         |
| 2.1.3.6   | Effect of Soil Confinement on lateral Stress Ratio .....                   | 61         |
| 2.1.3.7   | Reinforcement Stiffness and Soil Stiffness .....                           | 63         |
| 2.1.3.8   | Coverage Ratio .....   | 63         |
| 2.1.3.9   | Tensile Resistance of Soil-Reinforcing.....                                | 65         |
| 2.1.3.10  | Pullout Resistance of Soil-Reinforcing .....                               | 68         |
| 2.2       | State of Practice for Pullout Resistance .....                             | 70         |
| 2.2.1     | Pullout of Grid Reinforcing.....   | 74         |
| 2.2.1.1   | Frictional Resistance.....   | 77         |
| 2.2.1.2   | Passive Resistance.....  | 81         |
| 2.2.1.3   | Bearing Resistance Factor, $N_q$ , for Grid Soil-Reinforcing Systems<br>94 |            |
| 2.2.2     | System Stiffness .....   | 96         |
| 2.2.3     | Effect of Boundary Conditions .....  | 99         |
| 2.2.3.1   | Soil Reinforcement Cover.....  | 99         |
| 2.2.3.2   | Sidewall Interference .....  | 100        |
| 2.2.3.3   | Vertical Load Application .....  | 101        |
| 2.2.4     | Pullout Resistance Models .....  | 101        |
| 2.2.4.1   | Peterson and Anderson (1980).....  | 103        |
| 2.2.4.2   | Jewell (1984).....   | 103        |
| 2.2.4.3   | Beragado, Chai, and Miura (1996) .....                                     | 105        |
| 2.2.4.4   | Federal Highway Administration (2009) .....                                | 107        |
| 2.2.4.5   | Jayawickrama et al., (2013).....   | 108        |
| 2.2.4.6   | Yu and Bathurst (2015).....  | 110        |
|           | <b>CHAPTER 3 EXPERIMENTAL TEST PROGRAM .....</b>                           | <b>113</b> |
| 3.1       | Introduction.....  | 113        |
| 3.2       | Pullout Apparatus.....   | 113        |
| 3.2.1     | Soil-Box.....  | 115        |
| 3.2.2     | Vertical Load Reaction Frame .....   | 119        |
| 3.2.3     | Horizontal Load Frame .....  | 121        |
| 3.2.4     | Hydraulic Load System.....   | 122        |
| 3.2.5     | Clamping System.....   | 124        |
| 3.2.6     | Hydraulic System .....   | 125        |
| 3.2.7     | Load Cells .....   | 127        |
| 3.2.8     | Position Sensors .....   | 127        |
| 3.2.9     | Inflatable Pneumatic Diaphragm .....                                       | 129        |
| 3.2.10    | Data Acquisition System.....   | 131        |
| 3.3       | 2-Wire Soil-Reinforcing Element.....                                       | 131        |



|     |   |            |
|-----|---|------------|
| 3.4 | Pullout Study Soil .....                                | 133        |
| 3.5 | Test Set-Up - Parametric Program .....                  | 136        |
|     | 3.5.1 Soil Density .....                                | 136        |
|     | 3.5.2 Vertical Load .....                               | 139        |
| 3.6 | Test Set-Up .....                                       | 141        |
|     | 3.6.1 Prepare Bottom-Half of Soil-Box .....             | 141        |
|     | 3.6.2 Place Soil-Reinforcing Element.....               | 142        |
|     | 3.6.3 Clamp Soil-Reinforcing.....                       | 143        |
|     | 3.6.4 Position Sensors.....                             | 144        |
|     | 3.6.5 Prepare Top-Half of the Soil-Box.....             | 145        |
|     | 3.6.6 Apply Overburden Pressure .....                   | 146        |
|     | 3.6.7 Pullout Test .....                                | 148        |
|     | 3.6.8 Post Pullout Test.....                            | 149        |
|     | 3.6.9 Repeat Test.....                                  | 150        |
|     | <b>CHAPTER 4 EXPERIMENTAL TEST PROGRAM RESULTS.....</b> | <b>151</b> |
| 4.1 | Introduction.....                                       | 151        |
| 4.2 | Test Matrix.....  | 151        |
| 4.3 | General Test Procedure for 2-Wire Element .....         | 153        |
| 4.4 | Pullout Test Results .....                              | 157        |
|     | 4.4.1 Group-1 Pullout Test Results .....                | 160        |
|     | 4.4.1.1 Set-1 Pullout Test Results .....                | 160        |
|     | 4.4.1.2 Set-2 Pullout Test Results .....                | 164        |
|     | 4.4.1.3 Set-3 Pullout Test Results .....                | 167        |
|     | 4.4.2 Group-2 Pullout Test Results .....                | 170        |
|     | 4.4.2.1 Set-1 Pullout Test Results .....                | 170        |
|     | 4.4.2.2 Set-3 Pullout Test Results .....                | 173        |
|     | 4.4.2.3 Set-3 Pullout Test Results .....                | 175        |
| 4.5 | Bearing Resistance Factor Equations .....               | 178        |
|     | 4.5.1 RE1 Equation.....                                 | 182        |
|     | 4.5.2 RE2 Equation.....                                 | 183        |
|     | 4.5.3 RE3 Equation.....                                 | 184        |
|     | 4.5.4 Yu and Bathurst Equation.....                     | 186        |
| 4.6 | Bearing Resistance Factor from Test Data.....           | 187        |
|     | 4.6.1 Group-1 Set-1 Bearing Resistance Factor .....     | 187        |
|     | 4.6.1.1 RE1 Group-1 / Set-1 .....                       | 189        |
|     | 4.6.1.2 RE2 Group-1 / Set-1 .....                       | 191        |
|     | 4.6.1.3 RE3 Group-1 / Set-1 .....                       | 194        |
|     | 4.6.1.4 Yu Group-1 / Set-1.....                         | 197        |
|     | 4.6.2 Group-1 Set-2 Bearing Resistance Factor .....     | 200        |
|     | 4.6.2.1 RE1 Group-1 / Set-2 .....                       | 201        |

|         |   |     |
|---------|---|-----|
| 4.6.2.2 | RE2 Group-1 / Set-2 .....                     | 203 |
| 4.6.2.3 | RE3 Group-1 / Set-2 .....                     | 205 |
| 4.6.2.4 | YU Group-1 / Set-2 .....                      | 208 |
| 4.6.3   | Group-1 Set-3 Bearing Resistance Factor ..... | 211 |
| 4.6.3.1 | RE1 Group-1 / Set-3 .....                     | 212 |
| 4.6.3.2 | RE2 Group-1 / Set-3 .....                     | 214 |
| 4.6.3.3 | RE3 Group-1 / Set-3 .....                     | 217 |
| 4.6.3.4 | YU Group-1 / Set-3 .....                      | 219 |
| 4.6.4   | Group-2 Set-1 Bearing Resistance Factor ..... | 222 |
| 4.6.4.1 | RE1 Group-2 / Set-1 .....                     | 223 |
| 4.6.4.2 | RE2 Group-2 / Set-1 .....                     | 225 |
| 4.6.4.3 | RE3 Group-2 / Set-1 .....                     | 228 |
| 4.6.4.4 | YU Group-2 / Set-1 .....                      | 230 |
| 4.6.5   | Group-2 Set-2 Bearing Resistance Factor ..... | 233 |
| 4.6.5.1 | RE1 Group-2 / Set-2 .....                     | 234 |
| 4.6.5.2 | RE2 Group-2 / Set-2 .....                     | 236 |
| 4.6.5.3 | RE3 Group-2 / Set-2 .....                     | 239 |
| 4.6.5.4 | Yu Group-2 / Set-2 .....                      | 242 |
| 4.6.6   | Group-2 Set-3 Bearing Resistance Factor ..... | 244 |
| 4.6.6.1 | RE1 Group-2 / Set-3 .....                     | 245 |
| 4.6.6.2 | RE2 Group-2 / Set-3 .....                     | 248 |
| 4.6.6.3 | RE3 Group-2 / Set-3 .....                     | 250 |
| 4.6.6.4 | Yu Group-2 / Set-3 .....                      | 253 |
| 4.7     | Bearing Resistance Equation Comparison .....  | 255 |
| 4.7.1   | Group-1 Set-1 - MW71 $S_T = 300$ mm .....     | 257 |
| 4.7.1.1 | MW71 x MW71 50 x 300 .....                    | 257 |
| 4.7.1.2 | MW71 x MW71 100 x 300 .....                   | 258 |
| 4.7.1.3 | MW71 x MW71 200 x 300 .....                   | 259 |
| 4.7.2   | Group-1 Set-2 – MW71 $S_T = 150$ mm .....     | 260 |
| 4.7.2.1 | MW71 x MW71 50 x 150 .....                    | 260 |
| 4.7.2.2 | MW71 x MW71 100 x 150 .....                   | 261 |
| 4.7.2.3 | MW71 x MW71 - 200 x 150 .....                 | 262 |
| 4.7.3   | Group-1 Set-3 – MW71 $S_T = 1W$ .....         | 263 |
| 4.7.3.1 | MW71 x MW71 - 50 x 1W .....                   | 263 |
| 4.7.3.2 | MW71 x MW71 - 100 x 1W .....                  | 264 |
| 4.7.3.3 | MW71 x MW71 - 200 x 1W .....                  | 265 |
| 4.7.4   | Group-2 Set-1- MW45 $S_T = 300$ mm .....      | 266 |
| 4.7.4.1 | MW45 x MW45 - 50 x 300 .....                  | 266 |
| 4.7.4.2 | MW45 x MW45 - 100 x 300 .....                 | 267 |
| 4.7.4.3 | MW45 x MW45 - 200 x 300 .....                 | 268 |
| 4.7.5   | Group-2 Set-2 – MW45 $S_T = 150$ mm .....     | 269 |
| 4.7.5.1 | MW45 x MW45 - 50 x 150 .....                  | 269 |
| 4.7.5.2 | MW45 x MW45 - 100 x 150 .....                 | 270 |
| 4.7.5.3 | MW45 x MW45 - 200 x 150 .....                 | 271 |
| 4.7.6   | Group-2 Set-3 – MW45 $S_T = 1W$ .....         | 272 |
| 4.7.6.1 | MW45 x MW45 - 50 x 1W .....                   | 272 |
| 4.7.6.2 | MW45 x MW45 - 100 x 1W .....                  | 273 |

|         |   |            |
|---------|---|------------|
| 4.7.6.3 | MW45 x MW45 - 200 x 1W.....   | 274        |
| 4.8     | Equation Analysis for Predicting the Bearing Resistance Factor..... | 275        |
| 4.9     | Spacing of Longitudinal and Transverse Elements.....                | 276        |
| 4.10    | Bending of Transverse Element and Bearing Resistance.....           | 282        |
| 4.11    | Using the Developed Equations for Design.....                       | 302        |
|         | <b>CHAPTER 5 SUMMARY, CONCLUSIONS, AND RECOMMENDATIONS .....</b>    | <b>311</b> |
| 5.1     | Summary .....   | 311        |
| 5.2     | Conclusions .....   | 317        |
| 5.3     | Recommendations for Future Studies .....                            | 318        |
|         | <b>REFERENCES .....</b>   | <b>319</b> |
|         | <b>BIOGRAPHICAL INFORMATION .....</b>                               | <b>329</b> |
|         | <b>APPENDIX A TEST DATA.....</b>                                    | <b>331</b> |
|         | <b>APPENDIX B TEST SET-UP .....</b>                                 | <b>55</b>  |
|         | <b>APPENDIX C PLAXIS-3D MODEL PARAMETERS.....</b>                   | <b>7</b>   |

|  |            |
|--|------------|
| <b>REFERENCES .....</b>                              | <b>317</b> |
| <b>BIOGRAPHICAL INFORMATION .....</b>                | <b>327</b> |
| <b>APPENDIX A – TEST DATA .....</b>                  | <b>A1</b>  |
| <b>APPENDIX B – TEST SET-UP .....</b>                | <b>B1</b>  |
| <b>APPENDIX C – PLAXIS-3D MODEL PARAMETERS .....</b> | <b>C1</b>  |

**This Page Intentionally Left Blank**

## List of Figures

|             |   |    |
|-------------|---|----|
| Figure 1-1  | Typical MSE Structure .....   | 1  |
| Figure 1-2  | AASHTO Figure 11.10.6.2.2-2 .....   | 11 |
| Figure 2-1  | Cross section of conventional MSE structure .....                             | 15 |
| Figure 2-2  | RECo HA Ribbed Strip (FDOT 2018).....   | 18 |
| Figure 2-3  | Corrugated Steel Soil-Reinforcing System (Sine Wall 2018).....                | 19 |
| Figure 2-4  | RECo HA Ladder (FDOT, 2018).....  | 27 |
| Figure 2-5  | External Stability Modes of Failure .....                                     | 38 |
| Figure 2-6  | Deep Seated Global Failure .....  | 38 |
| Figure 2-7  | Internal Stability Modes of Failure .....                                     | 39 |
| Figure 2-8  | Stress Envelope for a Soil-Reinforcing Element .....                          | 43 |
| Figure 2-10 | Meyerhof Vertical Stress.....   | 46 |
| Figure 2-11 | Tieback Wedge Method.....   | 49 |
| Figure 2-12 | AASHTO Figure 11.10.6.2.1-3 .....   | 54 |
| Figure 2-13 | Tributary Volume of Soil for a Discrete 2-Wire Element .....                  | 57 |
| Figure 2-14 | Lateral strain in soil element (Jones, 1985) .....                            | 62 |
| Figure 2-15 | Coverage Ratio of Soil-Reinforcing .....                                      | 64 |
| Figure 2-16 | Local Stability for Calculation of Tension .....                              | 66 |
| Figure 2-17 | Location of Maximum Tension.....  | 67 |
| Figure 2-18 | Shear Stress Transfer During Pullout.....                                     | 69 |
| Figure 2-20 | Soil-Reinforcing – Grid (Plan View) .....                                     | 76 |
| Figure 2-21 | Soil-Reinforcing – Grid (Side View) .....                                     | 76 |
| Figure 2-22 | Soil-Reinforcing – Grid (End View).....                                       | 76 |
| Figure 2-23 | Plastic Flow Along a Surface (Prandtl 1920).....                              | 81 |
| Figure 2-24 | Plastic Flow Along a Surface (Reissner 1924).....                             | 83 |
| Figure 2-25 | Shallow Foundation Shear Pattern (Terzaghi 1943).....                         | 85 |
| Figure 2-26 | Shallow Foundation Shear Pattern (Meyerhof 1953).....                         | 86 |
| Figure 2-27 | Shear Pattern for Deep Foundation (Adapted from Meyerhof 1951).....           | 89 |
| Figure 2-28 | Shear Pattern for Circular Profile Shallow Foundation (Gao et al., 2015)..... | 90 |
| Figure 2-29 | Transverse Wire Passive Failure Mechanism (Peterson, 1980) .....              | 91 |
| Figure 2-30 | Load on a Foundation.....   | 96 |
| Figure 2-31 | Free-Body Diagram for 3-Wire Grid Soil-Reinforcing System .....               | 96 |

|             |  |     |
|-------------|--|-----|
| Figure 2-32 | BoEF Load Diagram for 3-Wire Grid Soil-Reinforcing System .....              | 98  |
| Figure 2-33 | Jewell Punching Shear Model .....  | 104 |
| Figure 2-34 | Bergado et al., Punching Shear Model.....                                    | 106 |
| Figure 3-2  | Pullout Box with Diaphragm Insert .....                                      | 118 |
| Figure 3-3  | Cross Section at Horizontal Cylinder.....                                    | 123 |
| Figure 3-4  | Plan View 2-Wire Soil-Reinforcing Elements .....                             | 132 |
| Figure 3-5  | Backfill Gradation Curve .....   | 135 |
| Figure 4-1  | 2-Wire Soil-Reinforcing Element Experimental Test Matrix.....                | 152 |
| Figure 4-2  | Typical 2-Wire Pullout Test - Displacement Data.....                         | 156 |
| Figure 4-3  | Typical 2-Wire Pullout Test - Displacement<br>Data (Transverse Element)..... | 157 |
| Figure 4-4  | Pullout Resistance for Set-1 – Force vs Depth .....                          | 162 |
| Figure 4-5  | Pullout Resistance for Set-2 – Force vs Depth .....                          | 165 |
| Figure 4-6  | Pullout Resistance for Set-3 – Force vs Depth .....                          | 168 |
| Figure 4-7  | Pullout Resistance of Set-4 –Force vs Depth .....                            | 171 |
| Figure 4-8  | Pullout Resistance of Set-5 – Force vs Depth .....                           | 173 |
| Figure 4-9  | Pullout Resistance of Set-6 – Force vs Depth .....                           | 176 |
| Figure 4-10 | Measured Bearing Resistance Factor with<br>Best-Fit Trend MW71 50 x 300..... | 180 |
| Figure 4-11 | RE1 – Bearing Resistance Factor (MW71 $S_T = 300$ mm).....                   | 190 |
| Figure 4-12 | RE1 – Bias (MW71 $S_T = 300$ mm).....  | 191 |
| Figure 4-13 | RE2 – Bearing Resistance Factor (MW71 $S_T = 300$ mm).....                   | 193 |
| Figure 4-14 | RE2 – Bias (MW71 $S_T = 300$ mm).....  | 193 |
| Figure 4-16 | RE3 – Bias (MW71 $S_T = 300$ mm).....  | 196 |
| Figure 4-17 | $Y_u$ – Bearing Resistance Factor (MW71 $S_T = 300$ mm) .....                | 199 |
| Figure 4-18 | $Y_u$ – Bias (MW71 $S_T = 300$ mm) .....                                     | 199 |
| Figure 4-19 | RE1 – Bearing Resistance Factor (MW71 $S_T = 150$ mm).....                   | 202 |
| Figure 4-20 | RE1 – Bias (MW71 $S_T = 150$ mm).....  | 202 |
| Figure 4-21 | RE2 – Bearing Resistance Factor (MW71 $S_T = 150$ mm).....                   | 204 |
| Figure 4-22 | RE2 – Bias (MW71 $S_T = 150$ mm).....  | 205 |
| Figure 4-23 | RE3 – Bearing Resistance Factor (MW71 $S_T = 150$ mm).....                   | 207 |
| Figure 4-24 | RE3 – Bias (MW71 $S_T = 150$ mm).....  | 207 |
| Figure 4-25 | $Y_u$ – Bearing Resistance Factor (MW71 $S_T = 150$ mm) .....                | 209 |

|             |  |     |
|-------------|--|-----|
| Figure 4-26 | Yu – Bias (MW71 $S_T = 150$ mm) .....                      | 210 |
| Figure 4-27 | RE1 – Bearing Resistance Factor (MW71 $S_T = 1W$ ) .....   | 213 |
| Figure 4-28 | RE1 – Bias (MW71 $S_T = 1W$ ).....                         | 214 |
| Figure 4-29 | RE2 – Bearing Resistance Factor (MW71 $S_T = 1W$ ) .....   | 216 |
| Figure 4-30 | RE2 – Bias (MW71 $S_T = 1W$ ).....                         | 216 |
| Figure 4-31 | RE3 – Bearing Resistance Factor (MW71 $S_T = 1W$ ) .....   | 218 |
| Figure 4-32 | RE3 – Bias (MW71 $S_T = 1W$ ).....                         | 219 |
| Figure 4-33 | Yu – Bearing Resistance Factor (MW71 $S_T = 1W$ ) .....    | 221 |
| Figure 4-34 | Yu – Bias (MW71 $S_T = 1W$ ) .....                         | 221 |
| Figure 4-35 | RE1 – Bearing Resistance Factor (MW45 $S_T = 300$ ).....   | 224 |
| Figure 4-36 | RE1 – Bias (MW45 $S_T = 300$ ).....                        | 225 |
| Figure 4-37 | RE2 – Bearing Resistance Factor (MW45 $S_T = 300$ ).....   | 227 |
| Figure 4-38 | RE2 – Bias (MW45 $S_T = 300$ ).....                        | 227 |
| Figure 4-39 | RE3 – Bearing Resistance Factor (MW45 $S_T = 300$ ).....   | 229 |
| Figure 4-40 | RE3 – Bias (MW45 $S_T = 300$ ).....                        | 230 |
| Figure 4-41 | Yu – Bearing Resistance Factor (MW45 $S_T = 300$ ).....    | 232 |
| Figure 4-42 | Yu – Bias (MW45 $S_T = 300$ ).....                         | 232 |
| Figure 4-43 | RE1 – Bearing Resistance Factor (MW45 $S_T = 150$ ).....   | 235 |
| Figure 4-44 | RE1 – Bias (MW45 $S_T = 150$ ).....                        | 236 |
| Figure 4-45 | RE2 – Bearing Resistance Factor (MW45 $S_T = 150$ ).....   | 238 |
| Figure 4-46 | RE2 – Bias (MW45 $S_T = 150$ ).....                        | 238 |
| Figure 4-47 | RE3 – Bearing Resistance Factor (MW45 $S_T = 150$ ).....   | 241 |
| Figure 4-48 | RE3 – Bias (MW45 $S_T = 150$ ).....                        | 241 |
| Figure 4-49 | Yu – Bearing Resistance Factor (MW45 $S_T = 150$ ).....    | 243 |
| Figure 4-50 | Yu – Bias (MW45 $S_T = 150$ ).....                         | 244 |
| Figure 4-51 | RE1 – Bearing Resistance Factor (MW45 $S_T = 1W$ ) .....   | 247 |
| Figure 4-52 | RE1 – Bias (MW45 $S_T = 1W$ ).....                         | 247 |
| Figure 4-53 | RE2 – Bearing Resistance Factor<br>(MW45 $S_T = 1W$ )..... | 249 |
| Figure 4-54 | RE2 – Bias (MW45 $S_T = 1W$ ).....                         | 250 |
| Figure 4-55 | RE3 – Bearing Resistance Factor (MW45 $S_T = 1W$ ) .....   | 252 |
| Figure 4-56 | RE3 – Bias (MW45 $S_T = 1W$ ).....                         | 252 |
| Figure 4-57 | Yu – Bearing Resistance Factor (MW45 $S_T = 1W$ ) .....    | 254 |

|             |  |     |
|-------------|--|-----|
| Figure 4-58 | Yu – Bias (MW45 ST = 1W) .....   | 255 |
| Figure 4-59 | Bias (MW71 x MW71 - 50 x 300).....   | 257 |
| Figure 4-60 | Bias (MW71 x MW71 - 100 x 300).....  | 258 |
| Figure 4-61 | Bias ((MW71 x MW71 - 200 x 300)).....                                      | 259 |
| Figure 4-62 | Bias (MW71 x MW71 - 50 x 150).....   | 260 |
| Figure 4-63 | Bias (MW71 x MW71 - 100 x 150).....  | 261 |
| Figure 4-64 | Bias (MW71 x MW71 - 200 x 150).....  | 262 |
| Figure 4-65 | Bias (MW71 x MW71 - 50 x 1W) .....   | 263 |
| Figure 4-66 | Bias (MW71 x MW71 - 100 x 1W) .....  | 264 |
| Figure 4-67 | Bias (MW71 x MW71 - 200 x 1W) .....  | 265 |
| Figure 4-68 | Bias (MW45 x MW45 - 50 x 300).....   | 266 |
| Figure 4-69 | Bias (MW45 x MW45 - 100 x 300).....  | 267 |
| Figure 4-70 | Bias (MW45 x MW45 - 200 x 300).....  | 268 |
| Figure 4-71 | Bias (MW45 x MW45 - 50 x 150).....   | 269 |
| Figure 4-72 | Bias (MW45 x MW45 - 100 x 150).....  | 270 |
| Figure 4-73 | Bias (MW45 x MW45 - 200 x 150).....  | 271 |
| Figure 4-74 | Bias (MW45 x MW45 - 50 x 1W) .....   | 272 |
| Figure 4-75 | Bias (MW45 x MW45 - 100 x 1W) .....  | 273 |
| Figure 4-76 | Bias (MW45 x MW45 - 200 x 1W) .....  | 274 |
| Figure 4-77 | RE2 Equation MW71 .....  | 275 |
| Figure 4-78 | RE2 Equation MW45 .....  | 276 |
| Figure 4-79 | Pullout Resistance Based on Spacing<br>of Transverse Element (RE2).....    | 277 |
| Figure 4-80 | Pullout Resistance Based on Spacing<br>of Transverse Element (AASHTO)..... | 280 |
| Figure 4-81 | Pullout Resistance Based on Spacing<br>of Transverse Element (RE2).....    | 281 |
| Figure 4-82 | Transverse Bar Bending (MW71 x MW71 - 50 x 300) .....                      | 283 |
| Figure 4-83 | Transverse Bar Bending (MW71 x MW71 - 100 x 300) .....                     | 284 |
| Figure 4-84 | Transverse Bar Bending (MW71 x MW71 - 200 x 300) .....                     | 285 |
| Figure 4-85 | Plaxis 3D Model for MW71 x MW71 – 200 mm x 1-Wire.....                     | 289 |
| Figure 4-86 | Moment Diagram for Transverse Bar Bending.....                             | 289 |
| Figure 4-87 | Transverse Bar Bending (MW71 x MW71 - 50 x 150) .....                      | 291 |
| Figure 4-88 | Transverse Bar Bending (MW71 x MW71 - 100 x 150) .....                     | 292 |



|             |  |     |
|-------------|--|-----|
| Figure 4-89 | Transverse Bar Bending (MW71 x MW71 - 200 x 150).....        | 293 |
| Figure 4-93 | Total Displacement Contours for MW71 x MW71 – 50 x 1W .....  | 299 |
| Figure 4-94 | Total Displacement Contours for MW71 x MW71 – 100 x 1W ..... | 300 |
| Figure 4-95 | Total Displacement Contours for MW71 x MW71 – 200 x 1W ..... | 301 |

**This Page Intentionally Left Blank**

## List of Tables

|            |   |     |
|------------|---|-----|
| Table 1-1  | Common Welded Wire Sizes for MSE Soil-Reinforcing ..... | 9   |
| Table 2-1  | Coverage Ratio for 50 mm 2-Wire Soil-Reinforcing.....   | 65  |
| Table 2-2  | Wide Width Bar-Mats .....                               | 65  |
| Table 3-1  | 2-Wire Soil-Reinforcing Element Description .....       | 132 |
| Table 3-2  | Backfill Gradation (Florida Sand).....                  | 135 |
| Table 3-3  | Backfill Properties (Florida Sand).....                 | 136 |
| Table 3-4  | Vertical Reaction Frame Parametric Test Results .....   | 140 |
| Table 3-5  | Vertical Reaction Frame Parametric Test Statistics..... | 140 |
| Table 4-1  | Test Matrix for 2-Wire Element - Group MW71 (W11).....  | 152 |
| Table 4-2  | Test Matrix for 2-Wire Element - Group MW45 (W7).....   | 153 |
| Table 4-3  | Resistance vs Depth MW71 x MW71 – 50 mm x 300 mm .....  | 162 |
| Table 4-4  | Resistance vs Depth MW71 x MW71 – 100 mm x 300 mm ..... | 163 |
| Table 4-5  | Resistance vs Depth MW71 x MW71 – 200 mm x 300 mm ..... | 164 |
| Table 4-6  | Resistance vs Depth MW71 x MW71 – 50 mm x 150 mm .....  | 165 |
| Table 4-7  | Resistance vs Depth MW71 x MW71 – 100 mm x 150 mm ..... | 166 |
| Table 4-8  | Resistance vs Depth MW71 x MW71 – 200 mm x 150 mm ..... | 166 |
| Table 4-9  | Resistance vs Depth MW71 x MW71 – 50 mm x 1-Wire.....   | 168 |
| Table 4-10 | Resistance vs Depth MW71 x MW71 – 100 mm x 1-Wire.....  | 169 |
| Table 4-11 | Resistance vs Depth MW71 x MW71 – 200 mm x 1-Wire.....  | 169 |
| Table 4-12 | Resistance vs Depth MW45 x MW45 – 50 mm x 300 mm .....  | 171 |
| Table 4-13 | Resistance vs Depth MW45 x MW45 – 100 mm x 300 mm ..... | 172 |
| Table 4-14 | Resistance vs Depth MW45 x MW45 – 200 mm x 300 mm ..... | 172 |
| Table 4-15 | Resistance vs Depth MW45 x MW45 – 50 mm x 150 mm .....  | 174 |
| Table 4-16 | Resistance vs Depth MW45 x MW45 – 100 mm x 150 mm ..... | 174 |
| Table 4-17 | Resistance vs Depth MW45 x MW45 – 200 mm x 150 mm ..... | 175 |
| Table 4-18 | Resistance vs Depth MW45 x MW45 – 50 mm x 1-Wire.....   | 177 |
| Table 4-19 | Resistance vs Depth MW45 x MW45 – 100 mm x 1-Wire.....  | 177 |
| Table 4-20 | Resistance vs Depth MW45 x MW45 – 200 mm x 1-Wire.....  | 177 |
| Table 4-21 | RE1 - Regression Variables .....                        | 183 |
| Table 4-22 | RE2 - Regression Variables .....                        | 184 |
| Table 4-23 | RE3 - Regression Variables .....                        | 185 |

|            |  |     |
|------------|--|-----|
| Table 4-24 | Yu - Regression Variables .....                  | 187 |
| Table 4-25 | MW71 x MW71 – ST = 300 Pullout Test Results..... | 188 |
| Table 4-26 | RE1 - Regression Variables for $S_T = 300$ ..... | 189 |
| Table 4-27 | RE1 – $S_T = 300$ .....                          | 189 |
| Table 4-28 | RE2 - Regression Variables for $S_T = 300$ ..... | 191 |
| Table 4-29 | RE2 – $S_T = 300$ .....                          | 191 |
| Table 4-30 | RE3 - Regression Variables for $S_T = 300$ ..... | 194 |
| Table 4-31 | RE3 – $S_T = 300$ .....                          | 194 |
| Table 4-32 | Yu - Regression Variables for $S_T = 300$ .....  | 197 |
| Table 4-33 | Yu - Regression Variables .....                  | 197 |
| Table 4-34 | Yu – $S_T = 300$ .....                           | 198 |
| Table 4-35 | MW71 x MW71 – ST = 150 Pullout Test Results..... | 200 |
| Table 4-36 | RE1 - Regression Variables for $S_T = 150$ ..... | 201 |
| Table 4-37 | RE1 ST = 150 .....                               | 201 |
| Table 4-38 | RE2 - Regression Variables for $S_T = 150$ ..... | 203 |
| Table 4-39 | RE2 ST = 150 .....                               | 203 |
| Table 4-40 | RE3 - Regression Variables for $S_T = 150$ ..... | 205 |
| Table 4-41 | RE3 ST = 150 .....                               | 206 |
| Table 4-42 | Yu - Regression Variables for $S_T = 150$ .....  | 208 |
| Table 4-43 | Yu ST = 150 .....                                | 208 |
| Table 4-44 | MW71 x MW71 – ST = 1W Pullout Test Results ..... | 211 |
| Table 4-45 | RE1 - Regression Variables for $S_T = 1W$ .....  | 212 |
| Table 4-46 | RE1 – $S_T = 1W$ .....                           | 212 |
| Table 4-47 | RE2 - Regression Variables for $S_T = 1W$ .....  | 214 |
| Table 4-48 | RE2 – $S_T = 1W$ .....                           | 215 |
| Table 4-49 | RE3 - Regression Variables for $S_T = 1W$ .....  | 217 |
| Table 4-50 | RE3 – $S_T = 1W$ .....                           | 217 |
| Table 4-51 | Yu - Regression Variables for $S_T = 1W$ .....   | 219 |
| Table 4-52 | Yu – $S_T = 1W$ .....                            | 220 |
| Table 4-53 | MW45 x MW45 – ST = 300 Pullout Test Results..... | 222 |
| Table 4-54 | RE1 - Regression Variables for $S_T = 300$ ..... | 223 |
| Table 4-55 | RE1 – $S_T = 300$ .....                          | 223 |
| Table 4-56 | RE2 - Regression Variables for $S_T = 300$ ..... | 225 |

|             |  |     |
|-------------|--|-----|
| Table 4-57  | RE2 – $S_T = 300$ .....  | 226 |
| Table 4-58  | RE3 - Regression Variables for $S_T = 300$ .....                                     | 228 |
| Table 4-59  | RE3 – $S_T = 300$ .....  | 228 |
| Table 4-60  | Yu - Regression Variables for $S_T = 300$ .....                                      | 230 |
| Table 4-61  | Yu – $S_T = 300$ .....   | 231 |
| Table 4-62  | MW45 x MW45 – $S_T = 150$ Pullout Test Results .....                                 | 233 |
| Table 4-63  | RE1 - Regression Variables for $S_T = 150$ .....                                     | 234 |
| Table 4-64  | RE1 – $S_T = 150$ .....  | 234 |
| Table 4-65  | RE2 - Regression Variables for $S_T = 150$ .....                                     | 236 |
| Table 4-66  | RE2 – $S_T = 150$ .....  | 237 |
| Table 4-67  | RE3 - Regression Variables for $S_T = 150$ .....                                     | 239 |
| Table 4-68  | RE3 – $S_T = 150$ .....  | 239 |
| Table 4-69  | Yu - Regression Variables for $S_T = 150$ .....                                      | 242 |
| Table 4-70  | Yu – $S_T = 150$ .....   | 242 |
| Table 4-71  | MW45 x MW45 – $S_T = 1W$ Pullout Test Results .....                                  | 244 |
| Table 4-72  | RE1 - Regression Variables for $S_T = 1W$ .....                                      | 245 |
| Table 4-73  | RE1 – $S_T = 1W$ .....   | 246 |
| Table 4-74  | RE2 - Regression Variables for $S_T = 1W$ .....                                      | 248 |
| Table 4-75  | RE2 – $S_T = 1W$ .....   | 248 |
| Table 4-76  | RE3 - Regression Variables for $S_T = 1W$ .....                                      | 250 |
| Table 4-77  | RE3 – $S_T = 1W$ .....   | 251 |
| Table 4-78  | Yu - Regression Variables for $S_T = 1W$ .....                                       | 253 |
| Table 4-79  | Yu – $S_T = 1W$ .....  | 253 |
| Table 4-100 | Displacement of Plaxis 3D Transverse Element<br>Bending MW71 x MW71 – 50 x 1W .....  | 294 |
| Table 4-101 | Displacement of Plaxis 3D Transverse Element<br>Bending MW71 x MW71 – 100 x 1W ..... | 294 |
| Table 4-102 | Displacement of Plaxis 3D Transverse Element<br>Bending MW71 x MW71 – 200 x 1W ..... | 294 |
| Table 4-103 | Pullout Comparison (Table of Forces) .....   | 309 |

**This Page Intentionally Left Blank**

## List of Photographs

|                 |  |     |
|-----------------|--|-----|
| Photograph 1-1  | First Reinforced Earth Wall Constructed in United States (NCHRP 1987)..... | 2   |
| Photograph 1-2  | Facing Systems .....   | 4   |
| Photograph 1-3  | Inextensible Soil-Reinforcing .....  | 4   |
| Photograph 1-4  | Extensible Soil-Reinforcing.....   | 5   |
| Photograph 1-5  | Grid Type Soil-Reinforcing.....  | 7   |
| Photograph 2-1  | HA Ribbed Soil-Reinforcing Placement (ReCO, 2018).....                     | 19  |
| Photograph 2-2  | Sinusoidal Soil-Reinforcing Element (Sine Wall, 2018) .....                | 20  |
| Photograph 2-3  | Welded Wire Soil-Reinforcing (One-Piece).....                              | 22  |
| Photograph 2-4  | Welded Wire Continuous Coverage .....                                      | 22  |
| Photograph 2-5  | Bar-Mat Soil-Reinforcing.....  | 25  |
| Photograph 2-6  | Bar-Mat Soil-Reinforcing Placement .....                                   | 26  |
| Photograph 2-7  | RECo HA Ladder Soil-Reinforcing (ReCO, 2018) .....                         | 27  |
| Photograph 2-9  | Grid-Strip™ Soil-Reinforcing .....   | 30  |
| Photograph 2-10 | Grid-Strip™ Soil-Reinforcing Placement.....                                | 30  |
| Photograph 2-11 | Bending of Transverse Element in Pullout Test (Lawson et al., 2013).....   | 97  |
| Photograph 3-2  | Pullout Box with Closed-Mount.....   | 119 |
| Photograph 3-3  | Vertical Elevated Reaction Frame (Side View) .....                         | 121 |
| Photograph 3-4  | Vertical Elevated Reaction Frame (End View).....                           | 121 |
| Photograph 3-5  | Horizontal Load Frame .....  | 122 |
| Photograph 3-6  | Horizontal Cylinder.....   | 123 |
| Photograph 3-8  | Soil-Reinforcing Clamp (2).....  | 125 |
| Photograph 3-9  | Hydraulic Power Unit and Chiller.....                                      | 125 |
| Photograph 3-10 | Hydraulic Flow Control System .....  | 126 |
| Photograph 3-11 | Load Cells .....   | 127 |
| Photograph 3-12 | Position Sensors .....   | 129 |
| Photograph 3-13 | Inflatable Pneumatic Diaphragm Large Soil-Box .....                        | 130 |
| Photograph 3-14 | Inflatable Pneumatic Diaphragm .....                                       | 130 |
| Photograph 3-15 | Data Acquisition system .....  | 131 |
| Photograph 3-16 | Speedy Moisture Test Kit and Sand Cone Test.....                           | 138 |

|                 |  |     |
|-----------------|--|-----|
| Photograph 3-17 | Preparation of Bottom Half of Soil-box.....                            | 142 |
| Photograph 3-18 | Placement of Soil-Reinforcing in Soil-Box.....                         | 143 |
| Photograph 3-19 | Placement of Soil-Reinforcing in Soil-Box.....                         | 144 |
| Photograph 3-20 | Placement of Position Sensors.....                                     | 144 |
| Photograph 3-21 | Placing Exit Gate .....  | 145 |
| Photograph 3-22 | Placing and Compacting Soil.....                                       | 145 |
| Photograph 3-23 | Level Soil Surface .....   | 146 |
| Photograph 3-24 | Reaction Frame Set-Up .....  | 147 |
| Photograph 3-25 | Reaction Frame Set-Up .....  | 147 |
| Photograph 3-26 | Apply Overburden Pressure .....  | 148 |
| Photograph 3-27 | Apply Overburden Pressure .....  | 148 |
| Photograph 3-28 | Exhuming Soil-Reinforcing Element After Test.....                      | 149 |
| Photograph 3-29 | Exhumed Soil-Reinforcing Element After Test.....                       | 150 |
| Photograph 3-30 | Exhumed Soil-Reinforcing Showing Weld Failure .....                    | 150 |
| Photograph 4-1  | Wire Rope Potentiometers on<br>50 mm, 100 mm, and 200 mm Element ..... | 155 |
| Photograph 4-2  | Wire Rope Potentiometers on 100 mm Element.....                        | 167 |
| Photograph 4-3  | Transverse Bar Bending in MW71 x MW71 – 200 x 300.....                 | 286 |
| Photograph 4-4  | Weld Failure MW71 x MW71 – 100 x 300.....                              | 287 |
| Photograph 4-5  | Weld Shear for Welded Wire Mesh .....                                  | 288 |



# Chapter 1

## Introduction

### 1.1 General

Mechanically Stabilized Earth (MSE) is a ground improvement technology that is used to construct earth retaining walls and steep slopes (Anderson 2012, Collin 1986, NCHRP 1987, NHI 2009). MSE is characterized as a composite structure that consists of tensile resisting inclusions and compacted soil as shown in Figure 1-1. The structure may or may not contain a facing element. MSE is a retaining structure that is constructed using a bottom up construction method. In this method the compacted backfill, soil-reinforcing, and facing elements are placed in a repetitive manner that progresses from a prepared foundation to the top of surcharge.

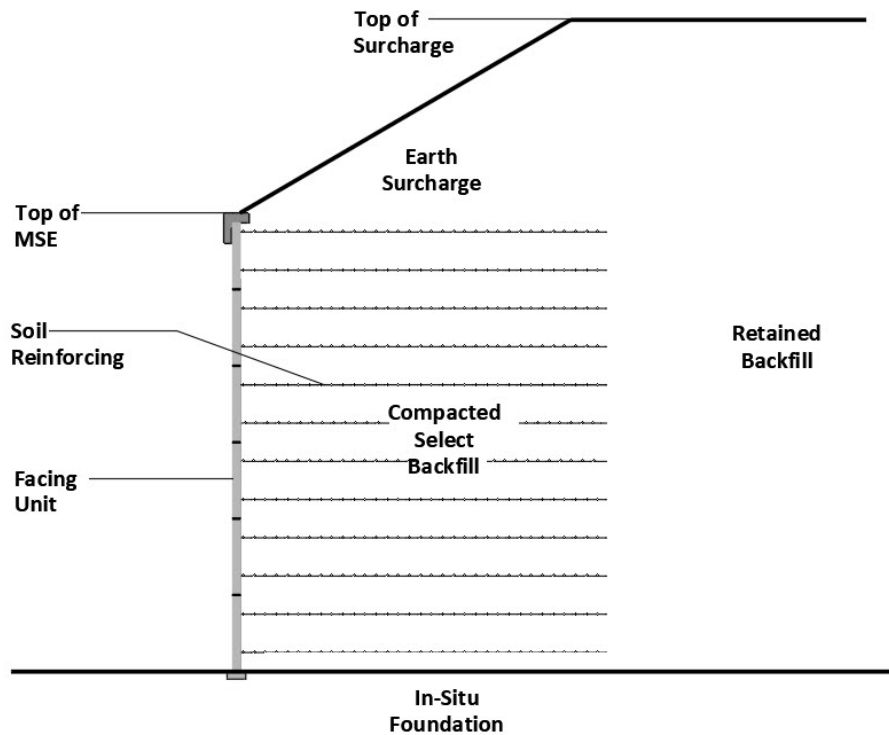


Figure 1-1 Typical MSE Structure

The commercial use of MSE was introduced in 1963 in France, by Henri Vidal. In 1971, the Reinforced Earth Company (RECO) constructed the first MSE structure in the United States on a transportation project for the California Department of Transportation (Caltrans) along Highway 39 in the San Gabriel Mountains shown in Photograph 1-1 (NCHRP 1987).

The San Gabriel structure soil-reinforcing consisted of smooth, steel strips that were mechanically attached to a steel elliptical shaped, segmental panel (ESP). The steel strips reinforced the soil while the ESP prevented the soil between the steel strips from eroding, sloughing, or raveling at the face of the structure. Since 1971, numerous commercial and proprietary MSE systems have been developed that utilize both steel and polymer soil-reinforcing elements and different forms of facing elements.



Photograph 1-1 First Reinforced Earth Wall Constructed in United States (NCHRP 1987)

MSE systems have been known to be faced with concrete panels, steel panels, mesh panels, and modular concrete blocks. The soil-reinforcing may be mechanically attached to the facing or may be attached using frictional resistance through the placement of the reinforcing at the interface between successive facing elements. It has

been estimated that every Department of Transportation (DOT) in the United States has constructed an MSE retaining wall (NHI, 2009).

A state-of-practice design manual for MSE has been developed by the United States Department of Transportation Federal Highway Administration (FHWA), Publication Number FHWA-NHI-10-024 (Berg, Christopher, and Samatani, 2009). This manual describes the design methodology and construction process for MSE and reinforced soil slopes (RSS). The design methodology for MSE is also covered in many geotechnical engineering text books.

The facings that are currently used in MSE structures include segmental concrete blocks, segmental concrete panels, full height concrete panels, and flexible face panel systems consisting of welded wire mesh. These facing systems are shown in the photo array in Photograph 1-2. Soil-reinforcing consists of linear discrete strips and wide width sheets. The soil-reinforcing can be fabricated from inextensible steel, or extensible plastic materials as shown in Photograph 1-3 and Photograph 1-4, respectively.



(a) Segmental Concrete Block



(b) Segmental Concrete Panel



(c) Full Height Panel



(d) Flexible Face Panel

Photograph 1-2 Facing Systems



(a) Linear Discrete Strips



(b) Wide Width Mesh

Photograph 1-3 Inextensible Soil-Reinforcing



(c) Linear Discrete Strips



(d) Wide Width Mesh

Photograph 1-4 Extensible Soil-Reinforcing

The design of MSE requires that global, external, and internal stability issues be considered. The state-of-practice assumes that the MSE structure performs as a rigid mass. The MSE structure height, in combination with the extent of the soil-reinforcing, i.e., distance from the facing element to the terminal end of the soil-reinforcing, defines the rigid mass. Global and external stability items follow similar methods that are used to design gravity retaining structures, e.g., cast-in-place reinforced concrete. Internal stability of the MSE investigates the inner stability of the composite soil mass. The internal stability is a function of the interaction of the components that make up the composite structure. Internal stability analysis has been simplified by defining a theoretical location of the failure surface. The internal stability analysis requires that the tensile strength and pullout resistance of the soil-reinforcement be known. The tensile strength and pullout resistance of the soil-reinforcing is material dependent.

The tensile strength of the soil-reinforcing is a measure of the force that is required to fail the soil-reinforcing element under tension. Failure of the soil-reinforcing element in tension can be defined either by strain, or by rupture, limits. The methods that are used to test tensile strength of the soil-reinforcing elements are performed in

isolation, outside the soil system. In other words, the soil-reinforcing is decoupled from the soil (i.e., they are not tested in soil) and therefore, the tests are performed in the absence of confinement. For inextensible soil-reinforcing tensile testing follows ASTM E8/E8M - *Standard Test Methods for Tension Testing of Metallic Materials* and for extensible soil-reinforcing tensile testing follows ASTM D6637/D6637M - *Standard Test Method for Determining Tensile Properties of Geogrids by the Single or Multi-Rib Tensile Method*.

The pullout resistance of a soil-reinforcing element is a function of the type of soil-reinforcing element, soil strength properties, soil density, soil confinement, and the overburden pressure. The pullout tests for a soil-reinforcing element are required to be performed insitu, or in the laboratory using a specially designed soil-box. For testing that is not performed insitu, ASTM D6706 - *Standard Test Method for Measuring Geosynthetic Pullout Resistance in Soil* is typically followed. This ASTM test method is designed for testing geosynthetic soil-reinforcing element i.e., extensible soil-reinforcing, but is routinely used as a guide specification to test metallic soil-reinforcing, i.e., inextensible soil-reinforcing. ASTM D6706 will be the test method used in this research program. It will be modified when required.

For structures using inextensible soil-reinforcing, the density of steel that is required in the MSE structure is a function of the tensile and pullout requirements. In typical metallic MSE structures, pullout controls in the upper 2 m of the structure while tension controls at 2 m and below. If the pullout resistance is underestimated, then the required density of steel will increase. If the density of steel increases then the total cost

of the structure increases; therefore, it is economically advantageous to have accurate pullout equations, including the bearing resistance factors.

Metallic soil-reinforcing consisting of inextensible welded-wire grid systems and bar-mat systems are comprised of a series of longitudinal and transverse wires that form a matrix, lattice, mesh, or grid. It should be noted that there is no physical difference between the welded-wire grid and bar-mat systems. The use of “welded-wire grid” and “bar-mat” was based on early trade names given to the soil-reinforcing system by MSE suppliers who developed them (NCHRP, 1987). Therefore, “welded-wire grid” and “bar-mat,” are interchangeable and the equations that are used to determine the tensile resistance and the pullout resistance, as defined in AASHTO, is equal for each reinforcing type. A grid type soil-reinforcing system is shown in Photograph 1-5.



(a) Welded Wire

(b) Bar Mat

Photograph 1-5 Grid Type Soil-Reinforcing

For grid type soil-reinforcing systems, the longitudinal wires are placed perpendicular to the MSE facing and the transverse wires are positioned parallel to the MSE facing. The transverse wires are joined, or fused, to the longitudinal wires by the method of resistance welding. Fabrication by resistance welding creates a condition where the longitudinal wires are positioned in a different plane than the transverse wires.

Because of this, the grid type soil-reinforcing is classified as a co-planar system. Within the MSE industry the grid type soil-reinforcing systems have longitudinal wire spacings that vary. The longitudinal wire spacing has been known to be 50 mm (2 in.), 150 mm (6 in.), 175 mm (7 in.), 200 mm (8 in.), 220 mm (9 in.), and 300 mm (12 in.) on center. The same spacing variations hold true for the transverse wire. The spacing of the transverse wire has been known to be 150 mm (6 in.), 300 mm (12 in.), 450 mm (18 in.), and 600 mm (24 in.). The transverse wire typically overhangs the outside longitudinal wires by 12 mm (1/2 in.) to 25 mm (1 in.). The state-of-practice classification system that is used to identify the longitudinal and transverse wire is based on the wire area, for instance, MW71. Where the M stands for “metric,” the W stands for smooth wire, and the 71 is the area of the wire in square millimeters. In the state-of-practice for MSE structures the grid type soil-reinforcing has wire sizes that vary. Sizes that are typically used are shown in Table 1-1. Table 1-1 lists the metric wire designation and the imperial equivalency for smooth welded wire reinforcement. This list is not complete. Reference should be made to the Wire Reinforcement Institute, Inc., Manual of Standard Practice – Structural Welded Wire Reinforcement (9<sup>th</sup> ed., 2016), for common sizes and designations.



Table 1-1 Common Welded Wire Sizes for MSE Soil-Reinforcing

| Metric Units     |                         |               | Imperial Units   |                         |               |
|------------------|-------------------------|---------------|------------------|-------------------------|---------------|
| Size Designation | Area (mm <sup>2</sup> ) | Diameter (mm) | Size Designation | Area (in <sup>2</sup> ) | Diameter (in) |
| MW22             | 23                      | 3.36          | W3.5             | 0.035                   | 0.211         |
| MW29             | 29                      | 6.08          | W4.5             | 0.045                   | 0.239         |
| MW45             | 45                      | 7.60          | W7.0             | 0.070                   | 0.299         |
| MW61             | 61                      | 8.81          | W9.5             | 0.095                   | 0.348         |
| MW71             | 71                      | 9.51          | W11.0            | 0.110                   | 0.374         |
| MW97             | 97                      | 11.11         | W15.0            | 0.150                   | 0.437         |
| MW129            | 129                     | 12.82         | W20.0            | 0.200                   | 0.505         |

## 1.2 Statement of Problem

Pullout of soil-reinforcing has been studied by numerous researchers. Tests have been performed insitu and in laboratories using soil-boxes of various sizes and configurations. Tests have been performed on linear elements and skewed elements. For welded-wire grid soil-reinforcing most of the pullout tests have been performed on elements that contain more than 2-longitudinal wires.

Based on the available research, the empirical equation that is used in the state-of-practice to determine the pullout resistance of welded-wire grid soil-reinforcing only considers the contribution of the bearing area of the transverse wires that are contained in the internal resisting zone of the reinforced soil volume in the MSE structure. The welded-wire grid bearing area is a function of the width, diameter, and number of transverse wires. The equation that is given in AASHTO is shown in Equation 1-1 and Equation 1-2. Equation 1-1 is used with soil-reinforcing that are placed at the top of the structure extending to a depth of 6 m. Equation 1-2 is used for soil-reinforcing that extend below 6 m. The bearing resistance factor is defined by the variable,  $N_p$ . The

bearing resistance factor varies with depth. AASHTO defines the bearing resistance factor as shown in Figure 1-2. The bearing resistance factor is defined in AASHTO as lower-bound default values. The default bearing resistance factors are to be used in the absence of specific soil-reinforcing pullout data.

$$P_p = N_p \cdot \frac{d_t}{S_t} \cdot \alpha \cdot \sigma_v \cdot L_e \cdot C \cdot R_c \text{ for } z < 20.00' \quad \text{Equation 1-1}$$

$$P_p = 20 \cdot \frac{d_t}{S_t} \cdot \alpha \cdot \sigma_v \cdot L_e \cdot C \cdot R_c \text{ for } z \geq 20.00' \quad \text{Equation 1-2}$$

- where:
- $P_p$  = Pullout resistance (kN/m)
  - $N_p$  = Bearing resistance factor (dim)
 
$$20 - \frac{20 - 10}{10} \cdot z \text{ -- for 0 m to 6 m}$$
  - $z$  = Depth to soil-reinforcing (m)
  - $d_t$  = Diameter of transverse wire (m)
  - $S_t$  = Spacing of transverse wire (m)
  - $\alpha$  = Scale effect correction factor and is equal to 1 for inextensible systems (dim)
  - $\sigma_v$  = Vertical pressure (kPa)
  - $L_e$  = Length of reinforcement in resistive zone (m)
  - $C$  = Unit perimeter factor default value equal to 2 (dim)
  - $R_c$  = Coverage ratio (dim)

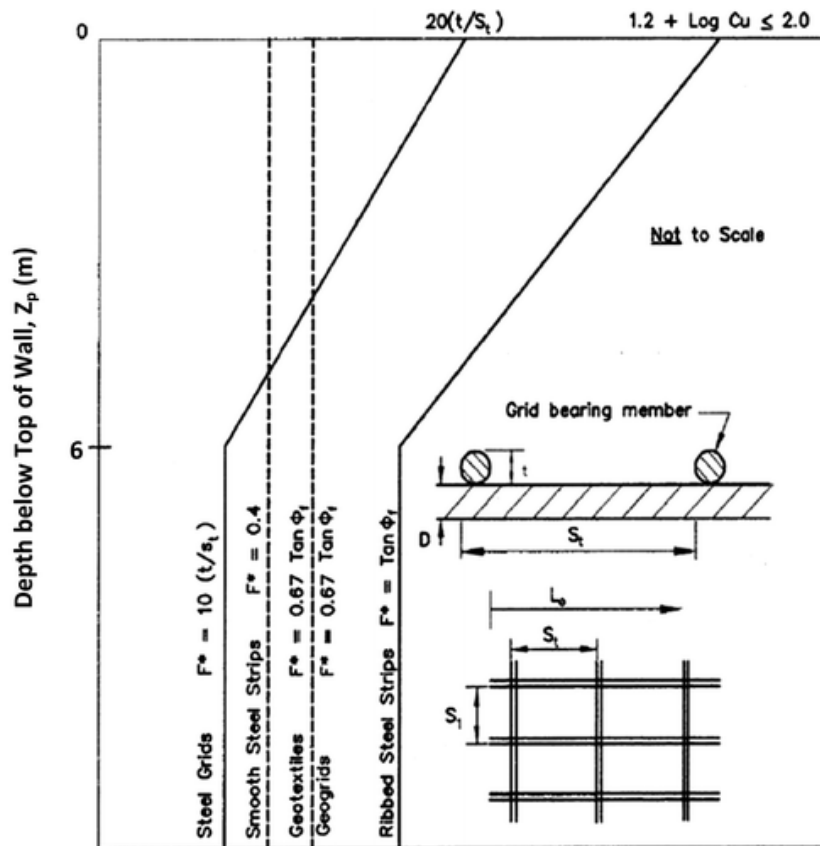


Figure 1-2 AASHTO Figure 11.10.6.2.2-2

As is demonstrated in the equation, the bearing resistance factor for any width of grid type soil-reinforcing system is the same. In other words, a system that is one meter wide and has six longitudinal wires will have the same bearing resistance factor as a system that is 0.5 meters wide and contains only two longitudinal wires. The geometrical configuration of the soil-reinforcing is not part of the pullout resistance equation.

### 1.3 Objectives and Scope of Research

The objective of the research program is to determine the bearing resistance factor for commonly used 2-Wire soil-reinforcing systems that are embedded in sand using the State of Practice pullout testing methodology.

### 1.3.1 *Goal of Research*

The goal of the research is to develop an equation for the bearing resistance factor that can be used to determine the pullout resistance of a 2-Wire soil-reinforcing element embedded in sand.

### 1.3.2 *Hypothesis*

The bearing resistance factor for a 2-Wire soil-reinforcing element is not a linear function that is correlated to the total bearing area, e.g., the number of transverse elements and the length and diameter of the transverse bearing elements. A proper understanding by comprehensive testing on the 2-Wire reinforcement elements will evaluate the current methods as well as provide a methodology to better predict bearing resistance factor and the pullout resistance.

### 1.3.3 *Tasks*

The tasks required to complete this research program include the following:

- (1) Perform literature review.
- (2) Develop Large-Scale Pullout Box.
- (3) Determine the soil properties of soil.
- (4) Fabricate and test 2-Wire soil-reinforcing elements.
- (5) Perform pullout testing.
- (6) Perform analysis of pullout testing results.
- (7) Develop equation to predict pullout bearing resistance factor.

## 1.4 Organization of Dissertation

Chapter 1 provides information on the objective, goal, and tasks of the research program. It also provides a brief summary of the organization of the research program.

Chapter 2 presents the results of the literature review. The literature review is presented in two sections. The first section reviews Mechanically Stabilized Earth and the second section reviews the state-of-practice for pullout testing and pullout theories. The MSE section includes a first subsection that presents a review of the classification soil-reinforcing systems that are presently being utilized in MSE construction. The second subsection discusses earth pressure theory and how it is applied to MSE. The third subsection describes the MSE design methodologies. The state-of-practice section includes a first subsection that introduces pullout testing of soil-reinforcing systems. The second subsection reviews the concept of soil-reinforcing stiffness and the effects on pullout resistance. The third subsection discusses test apparatus boundary conditions and their effect on pullout test results. The final subsection discusses bearing resistance factors and pullout resistance models.

Chapter 3 presents the Large-Scale experimental testing program in six subsections. Subsection one is an introduction of the experimental testing program. Subsection two describes the pullout test equipment. Subsection three describes the 2-Wire Soil-Reinforcing that were used in the test program. Subsection four provides information about the soil that was used in the test program. Subsection five describes a parametric study that was performed to assure consistent results in the test program. Subsection six describes steps for the experimental testing program setup.

Chapter 4 presents the experimental test program results in eleven subsections. Subsection one includes an introduction. Subsection two provides the test matrix used in

the experimental testing program. Subsection three provides a general overview of the test procedures. Subsection four presents the test results for each of the tests performed in the experimental testing program. Subsection five describes the proposed equations that will be used to determine the pullout bearing resistance factor. Subsection six presents the predicted pullout bearing resistance factor for each of the equations used in subsection five. Subsection seven compares the calculated pullout bearing resistance factor against each equation. Subsection eight determines the best equation for predicting the bearing resistance factor against the measured bearing resistance factor. Subsection nine discusses the impact that the longitudinal and transverse element has on the pullout resistance. Subsection ten discusses the impact of the bending of the transverse element on the pullout resistance. Subsection eleven describes how to use the equation in the design of an MSE structure.

Chapter 6 provides the dissertation summary, conclusions and recommendations.

The Appendix includes the detailed test results from the test program, the test set-up procedures, and the material properties used for the Plaxis-3D numerical model.

## 1.5 Conventions and Units

The dissertation is presented in international metric units with imperial (English) units given in parentheses. When a definition of a variable is provided, the units of the variable are located at the end of the definition and are enclosed in parentheses. In this case the units are defined using the international unit system (metric). When a variable is dimensionless it is defined in parentheses as (dim).

## Chapter 2

### Literature Review

#### 2.1 Mechanically Stabilized Earth

Mechanically Stabilized Earth (MSE) walls also known as reinforced soil structures, are a form of ground improvement (Han, 2015). The conventional MSE structure is a composite structure. Standard components that make up the composite MSE structure include compacted soil, a soil-reinforcing element, a facing unit, and a means to structurally connect the soil-reinforcing element to the facing element (Figure 2-1). The soil-reinforcing element may consist of discrete steel strips, discrete steel mesh, wide steel mesh, discrete polymer strips or wide polymer geogrids.

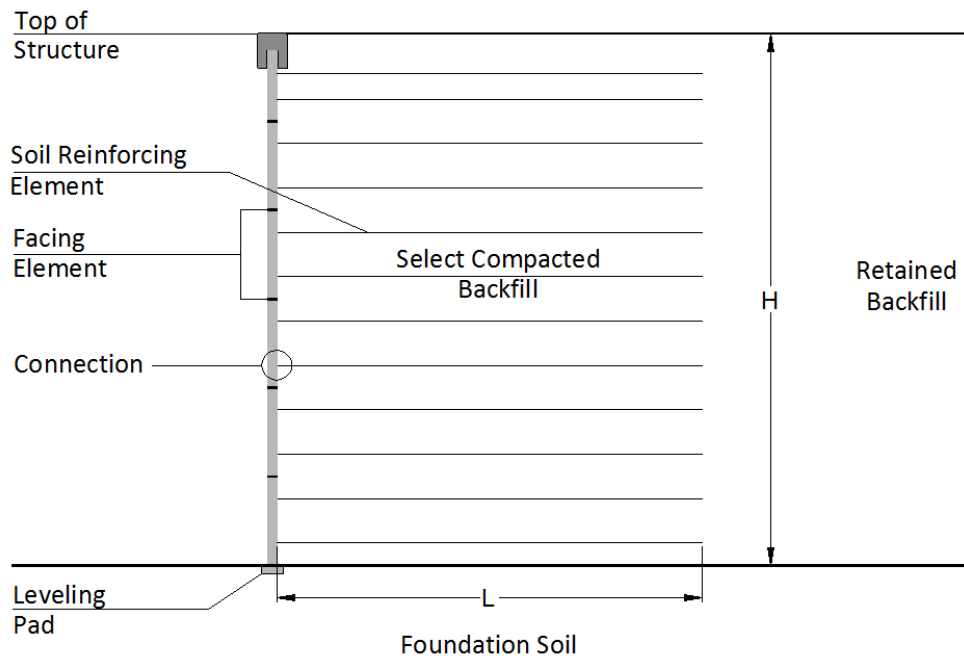


Figure 2-1 Cross section of conventional MSE structure

The current State of Practice for the Design of MSE structures in the United States follows the AASHTO LRFD Bridge Design Specification (AASHTO 2014), Article

11. AASHTO Article 11 has evolved significantly since 1990 to account for the increasing variations of soil-reinforcing systems. In 1994, a unified design specification was developed under the direction of the AASHTO T-15 Technical Committee on Substructures and Walls. The T-15 committee is part of the AASHTO Bridge Subcommittee (Allan, 2001). This unified design procedure was implemented by the State Departments of Transportation (DOT) to assure that MSE walls were designed using a standard that protected the public through the use of a simplistic design approach. The goal of the T-15 committee was to develop one design methodology that could be easily applied to all soil-reinforcing systems.

The properties of the soil-reinforcing system have an influence on how the composite earth structure performs under confinement and applied loading. This requires a unique design criterion. The original intent of the modification of Article-11 of the AASHTO design specification in early 1990 was to permit designers and reviewers a simplified method to validate the structural adequacy of an MSE structure using any type of soil-reinforcing system. The modification of the design methodology to the current form that is used today was not intended to be a radical change from design methodologies that had performed well historically but was intended to be an improvement to them (Christopher, 1993).

#### *2.1.1 Soil-Reinforcing Classification*

A method of classifying an MSE soil-reinforcing structure is based on the extensibility of the soil-reinforcing element. Soil-reinforcing systems that have mobilized strains that are less than the strain of the compacted soil are classified as inextensible. Soil-reinforcing systems with mobilized strains that are greater than the strain of the compacted soil are classified as extensible (McGowan, 1978; Collin, 1988; Christopher,



1990; NHI, 2009). Based on this classification system, steel soil-reinforcing elements are typically categorized as inextensible, whereas polymer soil-reinforcing elements are typically categorized as extensible. Inextensible soil reinforcing systems include, Linear Strips, Bar-Mats, and Welded-Wire grids. Extensible polymer soil-reinforcing elements are also known as geosynthetics. Extensible geosynthetics include sheets, grids, and strips. The geosynthetic element can be extruded, woven, or nonwoven. AASHTO is currently exploring the classification of new soil reinforcing systems such as, twisted wire mesh, corrugated steel strip, and polymer strip soil-reinforcements as extensible. In this dissertation, only inextensible soil-reinforcing systems will be discussed.

#### 2.1.1.1 Linear Steel Strips

Linear steel strips were one of the earliest forms of commercially used soil-reinforcing systems (Vidal, 1969, Schlosser, 1978, Anderson et al., 2012). The early soil-reinforcing consisted of flat steel bars, in widths of 100 mm (4 in.) and thickness of 5 mm (0.2 in.). The steel strips were used with segmental concrete panels and elliptical steel panels. As MSE technology progressed the steel-strip surface was modified to include raised ribs, punched tabs and corrugated profiles. Changing the surface configuration from a flat profile to one with a raised or corrugated profile increases the systems resistance to pullout. A brief description of the commonly used inextensible steel strip soil-reinforcing systems follows.

##### 2.1.1.1.1 RECo High Adherence (HA) Reinforcing Strip

The Reinforced Earth Company (RECo) uses a soil-reinforcing element called the High Adherence (HA) Reinforcing Strip. The HA strip is manufactured from hot-rolled steel plate. During the rolling process raised transverse ribs are formed on the top and

bottom surface of the strip. The steel strip width is 40 mm (1.5 in.) to 50 mm (2 in.) wide and has a nominal thickness of 4 mm (0.157 in.) to 6 mm (0.236 in.). The rib that is rolled on the element is elevated approximately 3 mm (0.118 in.) from the nominal surface of the steel strip. In most HA strip configurations there are two raised ribs for every 150 mm (6 in.) of strip surface. The elevated ribs are formed on both the top and bottom surface of the HA strip. The distance between the two ribs is equal to 25 mm (1 in.). The bottom set of ribs are positioned so the first rib is located between the top two ribs. Figure 2-2 shows a detail of the HA strip as shown in the Florida Department of Transportation (FDOT 2018) approved product list details. The units shown are imperial.

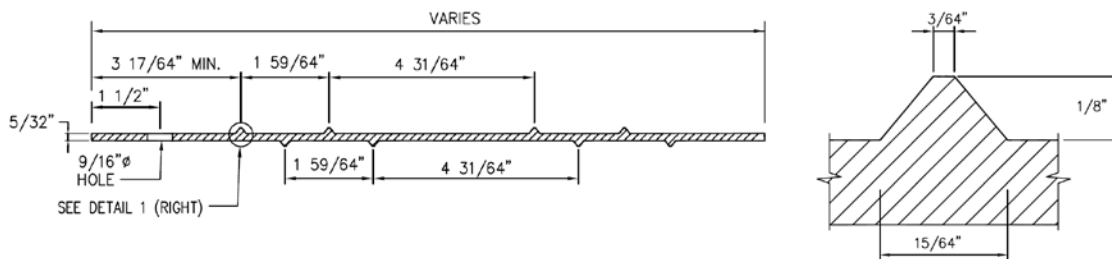


Figure 2-2 RECo HA Ribbed Strip (FDOT 2018)

The HA strip is classified as inextensible. The HA strip raised surface ribs in relationship to the flat surface of the strip create a bi-planar soil-reinforcing system. The height of the ribs on both the top and bottom surface adds 6 mm (0.236 in.) of thickness to the nominal plate thickness. There is normally only one type of HA strip used on a project. Adding additional HA strips in the horizontal plane increases the steel density. A standard spacing is shown in Photograph 2-1. The coverage ratio, (i.e., width of the element to the horizontal spacing of the element), of the HA strip ranges from 0.07 to 0.17. The connection to the SCP is made by passing the lead end of the HA strip into a panel anchor called a Tie-Strip, where it is then secured using a nut and bolt.



Photograph 2-1 HA Ribbed Soil-Reinforcing Placement (ReCO, 2018)

#### 2.1.1.1.2 Sine Wall Corrugated Steel Strip

The Sine Wall Company uses a soil-reinforcing element that is a flat bar formed into a sinusoidal shape as shown in Photograph 2-2. The Sine Wall strip is manufactured from hot-rolled steel plate. The sinusoidal shape is cold-formed on the top and bottom surface of the strip. The strip profile is defined as Corrugated. The Corrugated steel strip is 50 mm (2 in.) wide and has a nominal thickness of 4 mm (0.157 in.). The distance between peaks of the sine wave are 50 mm (2 in.) and the height to the peak is 6 mm (0.25 in.). Figure 2-2 shows a detail of the Sine Wall strip as shown in the FDOT approved product list details (FDOT, 2018).

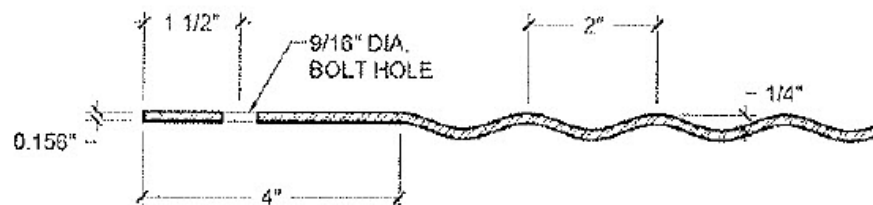


Figure 2-3 Corrugated Steel Soil-Reinforcing System (Sine Wall 2018)

There is normally only one Corrugated strip type used on a project. Adding additional Corrugated strips in the horizontal plane increases the steel density. The coverage ratio of the Corrugated strip ranges from 0.07 to 0.17. The connection to the SCP is made by passing the lead end of the Corrugated strip into a panel anchor called a Tie-Strip, where it is then secured using a nut and bolt.



Photograph 2-2 Sinusoidal Soil-Reinforcing Element (Sine Wall, 2018)

#### 2.1.1.2 Grid Systems

Inextensible grid soil-reinforcing systems are formed by longitudinal and transverse elements that are perpendicular to each other. The grid elements are typically round and are positioned one atop the other in different planes and are classified as a bi-planar. The grid configuration creates an apparent opening between the adjacent perpendicular and parallel elements. The longitudinal element is defined as the member that is perpendicular to the MSE structure facing and is parallel to the direction of shear stress transfer in the soil mass. The transverse element, sometimes referred to as a cross element, or passive element, is defined as the member that is parallel to the MSE structure facing and perpendicular to the direction of shear stress transfer in the soil mass. A brief description of the commonly used inextensible grid soil-reinforcing systems follows.

#### 2.1.1.2.1 Welded Wire Mesh

Welded-wire mesh is an inextensible, steel, bi-planar grid soil-reinforcing system. The welded-wire mesh element consists of round metal longitudinal wires and round metal transverse wires that are resistance welded at their intersection. Welded-wire mesh systems are fabricated in accordance with ASTM A1064, *Standard Specification for Steel Wire and Welded Wire Reinforcement, Plain and Deformed, for Concrete*. For MSE structures, the welded-wire mesh systems are typically used as both the soil-reinforcing element and the facing element. In this case, the welded-wire mesh facing is fabricated from continuous welded-wire sheets. The facing is formed into an “L” at the lead end of the welded-wire sheet by bending it 90-degrees from the horizontal (Photograph 2-3). This combination of soil-reinforcing and facing is sometimes called a One-Piece, wide-mesh, system. The metal welded-wire grid wire sizes range from MW23 to MW129. The physical parameters of the wire were given in Table 1-1. The longitudinal wires center-to-center spacing can vary but are commonly equal to 150 mm (6 in.). The spacings of the longitudinal wires have been known to be 100 mm (4 in.), 150 mm (6 in.), 225 (9 in.), 250 mm (10 in.) and 300 mm (12 in.). The transverse wires center-to-center spacing can vary and have been known to range from 100 mm (4 in.) to 1220 mm (48 in.). Typical transverse spacing increments are multiples of some number such as a multiple of, 50 mm (2 in.), 75 mm (3 in.) 150 mm (6 in.) or 300 mm (12 in.). As previously stated, the transverse wires are resistance welded to the longitudinal wires at their point of intersection, forming the rectangular, bi-planar, grid element. The overall width of the welded wire mesh is typically 1220 mm (4 ft. -0 in.) or 2440 mm (8 ft. - 0 in.).



Photograph 2-3 Welded Wire Soil-Reinforcing (One-Piece)

The welded wire mesh soil-reinforcing element is placed in the soil in a manner where the coverage ratio is considered continuous. Continuous coverage assumes that the adjacent soil-reinforcing elements have little to no horizontal spacing between them (Photograph 2-4).



Photograph 2-4 Welded Wire Continuous Coverage

On a particular project, there can be many assorted sizes and configurations of welded-wire mesh. The required steel density at each layer of soil-reinforcing is a function of the forces that are required to be resisted. As the required force increases so does the required steel density. From a commercial perspective, it is advantageous to have several different soil-reinforcing elements that have varying steel densities. The density of a system can be changed in several ways. One method that is used to increase the steel density is by increasing the wire size and at the same time maintain a uniform longitudinal spacing.

Another method that is used to increase the steel density is to maintain a consistent wire size and at the same time decrease the longitudinal spacing. Yet another method is to maintain a consistent transverse and longitudinal wire size and at the same time decrease the center-to-center horizontal spacing of the soil-reinforcing elements. Typically, and purely as a result of commercial considerations, the first method is commonly practiced.

The nomenclature to describe this type of system was commercially produced by The Hilfiker Company in the late 1970's (Hilfiker, 2018). Hilfiker called this MSE system a Welded Wire Wall (WWW) system and used welded-wire mesh or welded-wire grids to refer to the soil-reinforcing. The WWW system is a one-piece system.

#### 2.1.1.2.2 Bar-Mats

MSE soil-reinforcing grid elements that are attached to a facing element consisting of a segmental concrete panel (SCP) are called Bar-Mats. Bar-Mat is a generic name commercially produced by the VSL Retained Earth Company to describe their soil-reinforcing system (Neely, 1995). It has now become a universally accept

synonym for welded-wire soil-reinforcing. Welded-Wire Mesh was the name used to describe the soil-reinforcing for the Reinforced Soil Embankment system used by The Hilfiker Corporation (Hilfiker, 2018). There is no physical difference between “Welded-Wire Mesh,” “Welded-Wire Grids,” and “Bar-Mats” soil-reinforcing, except in the configuration of the reinforcing. In this dissertation, Bar-Mat systems are classified as “wide-width” systems that contain more than two longitudinal reinforcing elements. Bar-Mats are shown in Photograph 2-5. Typical MSE suppliers fabricate the Bar-Mat system with a configuration consisting of longitudinal and transverse metal bars designated as MW71, MW97 and MW129 (W11, W15, and W20 respectively). Larger bar sizes have been used. The Bar-Mat system longitudinal bars center-to-center spacing is characteristically equal to 150 mm (6 in.), 200 mm (8 in.), or 225 mm (9 in.). The transverse bars center-to-center spacing is uniform over the length of the longitudinal bar and ranges between spacings equal to 150 mm (6 in.) to 600 mm (24 in.). There are MSE suppliers that space the transverse bar greater than 600 mm (24 in.) and have been known to use a transverse bar spacing equal to 900 mm (36 in.) and 1200 mm (48 in.) on-center. In some State Department of Transportation (DOT) specifications, the wire diameter is required to be greater than MW64 (W10), the longitudinal and transverse wires are required to be of the same size, and the maximum transverse wire spacing is designated to be no greater than 600 mm (24 in.).





Photograph 2-5 Bar-Mat Soil-Reinforcing

In the Bar-Mat soil-reinforcing system, the round longitudinal and transverse bars form a rectangular, bi-planar grid pattern. The round longitudinal and transverse bars are fused together by electrical resistance welds at their intersecting points as is the case with welded wire mesh systems. The Bar-Mat is also fabricated in conformance with ASTM A1064 as before. The widths of the Bar-Mat range from 450 mm (18 in.) to 1100 mm (42 in.).

There can be many different types of Bar-Mats for a single project. Changing to a larger size longitudinal bar and maintaining the longitudinal spacing increases the steel density. Another way to increase the steel density is to increase the width of the Bar-Mat, and at the same time hold the longitudinal spacing equal, thereby increasing the number of longitudinal bars. Typically, the vertical spacing of the Bar-Mats is uniform throughout the structure and is almost always equal to 760 mm (30 in.). The vertical spacing of the Bar-Mats may vary at the top of the wall and is dependent on the top of wall treatment, i.e., coping element. The Bar-Mats have coverage ratios that range from continuous coverage equal to 1.00 decreasing to a coverage ratio equal to 0.30. As defined previously, the coverage ratio is the relation between the width of the soil-

reinforcing element, and the center-to-center horizontal spacing of the soil-reinforcing element.



Photograph 2-6 Bar-Mat Soil-Reinforcing Placement

#### 2.1.1.2.3 RECo High Adherence (HA) Ladder

The RECo HA ladder is a discreet grid-system containing two, round, metal longitudinal bars that are spaced at 50 mm (2 in.) centers. Spanning the longitudinal bars are 100 mm (4 in.) long round, metal, transverse bars that are spaced at 150 mm (6 in.) on-center. The transverse bars overhang the longitudinal bars by 25 mm (1 in.) on each side and are fused to the longitudinal bars at their intersection using a resistance weld. The standard HA ladder is shown in Photograph 2-1. The final configuration of the longitudinal and transverse bars forms a rectangular, bi-planar grid pattern. The transverse bar is positioned 9 mm (3/8 in.) above the surface of the longitudinal bar. The longitudinal and transverse bar sizes are equal and typically consist of a MW64 (W10) bar. The lead ends of the longitudinal bars are welded to the outside edge of a flat plate forming the connection component (Figure 2-4). As is the case with the HA strip there is

only one HA ladder type for any one project. Adding HA ladders in the horizontal plane increases the steel density. The coverage ratio of the HA strip ranges from 0.07 to 0.17. The connection to the SCP is the same for the HA Ladder as it was for the HA Strip.



Photograph 2-7 RECo HA Ladder Soil-Reinforcing (ReCO, 2018)

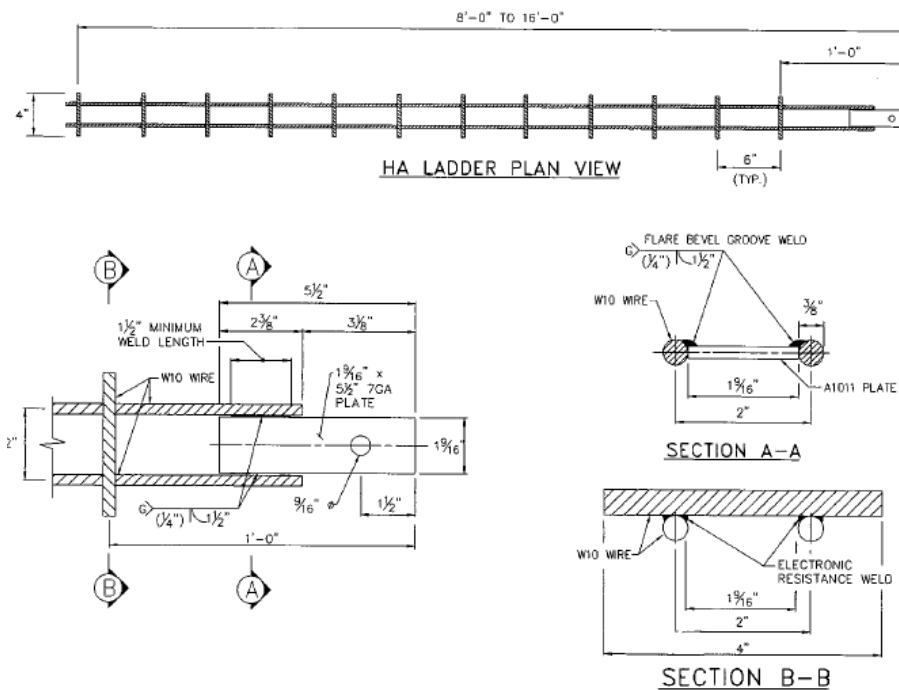


Figure 2-4 RECo HA Ladder (FDOT, 2018)

#### 2.1.1.2.4 Keystone KeySystem KeyStrip

The Keystone KeySystem KeyStrip is a discreet grid-system containing two metal longitudinal bars similar to the ReCO HA ladder. The KeyStrip is typically used with a modular block facing element (Keystone, 2018). The Highway Innovative Technology Evaluation Center (HITEC) Civil Engineering Research Foundation (CERF) evaluated the Keystone Retaining Wall KeySystem and issued report #40478. The KeyStrip is a discreet, bi-planar, grid element containing two metal longitudinal bars that are spaced on 325 mm (7 in.) centers (Photograph 2-8). Spanning the longitudinal bars are transverse bars that consist of 200 mm (8 in.) long metal bars that are spaced at 150 mm (6 in.) on-center. The transverse bars overhang the longitudinal bars by 12 mm (1/2 in.) on each side. The longitudinal and transverse bars are resistance welded at their intersection. The longitudinal bar and transverse bar sizes are equal and consist of MW50 (W7.5), MW70 (W11), MW90 (W14), and MW110 (W17) bars. There can be many different “grid-types” of KeyStrip soil-reinforcing for a single project. Changing to a larger size KeyStrip configuration or by decreasing the vertical spacing and, or, horizontal spacing, of the KeyStrip between the modular block facing units increases the steel density. The lead end of the KeyStrip longitudinal wire is welded to a flat plate to form the connection. The connection element is attached to the top of the block facing units (Photograph 2-8). Alternatively, the lead end may be formed into a loop. The KeyStrip has been attached to SCP; however, this system is typically used in conjunction with modular block facing elements. The KeyStrip is horizontally spaced in plan-view at every-other block or in every block. The coverage ratio is between 0.23 to 0.58.



Photograph 2-8 KeyStrip Soil-Reinforcing

#### 2.1.1.2.5 Grid-Strip™

The Grid-Strip™ soil-reinforcing system is marketed by Big-R Bridge (Vistawall, 2018). The Grid-Strip™, like the HA ladder, and KeyStrip, is a narrow, discrete grid-system containing two, round, metal, longitudinal bars that are spaced at 50 mm (2 in.) centers. The longitudinal bars are spanned by 75 mm (3 in.) long, round, metal, transverse bars spaced on 300 mm (12 in.) centers. The transverse bars overhang the longitudinal bars by 12 mm (1/2 in.). The transverse bars are fused to the longitudinal bars at the intersection by an electrical resistance weld. The Grid-Strip™ is shown in Photograph 2-9. The longitudinal bars and transverse bars form a rectangular, bi-planar, grid pattern. The transverse bar is positioned 9 mm (3/8 in.) above the surface of the longitudinal bar. The longitudinal bar and transverse bar size are equal and use MW70 (W11) wire. The lead end of the longitudinal bars is resistance welded to an end connector consisting of a flat steel plate or a special steel plate called a TAB.



Photograph 2-9 Grid-Strip™ Soil-Reinforcing

As is the case with the HA strip, and the HA ladder, there is only one type of Grid-Strip™ for a project. Adding additional Grid-Strip™ in the horizontal plane increases the steel density. Photograph 2-10 shows the standard placement of the Grid-Strip on the back of a 1.574 m (5 ft.) by 3.058 m (10 ft.) SCP. The coverage ratio of the Grid-Strip™ ranges from 0.07 to 0.17. The connection to the SCP is made by passing the lead end of the Grid-Strip™ into a panel anchor called a Tie-Strip, where it is then secured using a nut and bolt.



Photograph 2-10 Grid-Strip™ Soil-Reinforcing Placement

### 2.1.1.3 Other Soil-Reinforcing Systems

There are other inextensible soil-reinforcing systems that have not been described. For a list of other types of soil-reinforcing, the reader should refer to the Design and Construction of Mechanically Stabilized Earth Walls and Reinforced Soil Slopes manual prepared by FHWA (Berg et al., 2009).

### 2.1.2 Horizontal Earth Pressure

The internal stability of the MSE structure requires that the state of stress within the reinforced soil mass be determined. This requires knowledge of earth pressure theories. The basic principle of earth pressure on retaining walls was introduced by the French physicist, Charles-Augustin de Coulomb in 1776, and refined by William Rankine in 1857 (Terzaghi, 1943). All present retaining wall theory is an extension of these classical earth pressure concepts.

#### 2.1.2.1 Lateral Earth Pressure Coefficient

The fundamental principle of earth pressure theory states that the horizontal earth pressure,  $\sigma_h$ , is a function of the vertical earth pressure,  $\sigma_v$ . To determine the horizontal earth pressure the vertical earth pressure is multiplied by a coefficient, K (Equation 2-1).

$$\sigma_h = K \cdot \sigma_v \quad \text{Equation 2-1}$$

Based on this relationship, the factor K is known as the coefficient of lateral earth pressure and is the ratio of the horizontal pressure to the vertical pressure (Equation 2-2).

$$K = \frac{\sigma_h}{\sigma_v} \quad \text{Equation 2-2}$$

The magnitude of the coefficient  $K$  is a function of the state of stress of the soil. If the soil is under natural conditions, with no movement, the soil is said to be at-rest. Under these conditions,  $K$  is referenced as the at-rest earth pressure coefficient and is denoted by the variable  $K_o$ . If on the application of a vertical load to the surface of a retaining structure, the soil behind the structure moves, reaching a state of equilibrium, the state of stress in the soil changes. If the soil expands laterally, the coefficient  $K$  is known as the active earth pressure coefficient and is denoted by the variable  $K_a$ . If the soil contracts laterally, the coefficient  $K$  is known as the passive earth pressure coefficient and is denoted by the variable  $K_p$ . The at-rest, active, and passive, lateral earth pressure cases are the three fundamental states of stress that can occur within a soil mass.

For an earth retaining structure, when the face of the structure moves away from the retained soil it is in the active state of stress. In this case, the vertical stress remains unchanged, but, the horizontal stress decreases,  $\sigma_h < \sigma_v$ . The active case represents a state of minimum horizontal stress. When the face of the retaining structure moves toward the retained soil, the soil is in a state of passive stress. In this case, and as in the active case, the vertical stress remains unchanged, whereas the horizontal stress increases,  $\sigma_h > \sigma_v$ . The passive case represents a state of maximum horizontal stress.

The at-rest coefficient  $K_o$  for a cohesionless soil, is estimated according to the Jaky equation as shown in Equation 2-3 (Jaky, 1944).



$$K_o = 1.0 - \sin(\phi')$$

Equation 2-3

Where:  $K_o$  = At-rest earth pressure coefficient (dim)  
 $\phi'$  = The effective friction angle of the soil (deg)

As the friction angle of the soil decreases the at-rest coefficient increases. Typical values of the at-rest earth pressure coefficient for soil used as backfill in earth retaining structures ranges between the value of 0.35 and the value of 0.50. These values equate to soils with internal friction angles equal to 40 degrees to 30 degrees, respectively (Adib, 1988). For earth retaining structures it has been shown that the act of compacting soil near the face changes the at-rest state of stress to values greater than the Jaky at-rest state of stress and can approach values as large as 1.50 (Duncan, 1984).

The passive pressure coefficient (Equation 2-4) and active pressure coefficient (Equation 2-5) is a function of the effective internal friction angle of the soil,  $\phi'$ . For a level surcharge the coefficients are determined using the Rankine stress state.

$$K_p = \tan^2 \left( 45^\circ + \frac{\phi'}{2} \right) = \frac{1 + \sin(\phi')}{1 - \sin(\phi')}$$

Equation 2-4

$$K_a = \tan^2 \left( 45^\circ - \frac{\phi'}{2} \right) = \frac{1 - \sin(\phi')}{1 + \sin(\phi')}$$

Equation 2-5

The passive resistance increases with decreasing internal friction angles and the active resistance decreases with increasing internal friction angles.

### 2.1.2.2 Coulomb Theory

Coulomb in 1776 developed a method for the analysis of forces on retaining walls. In this method Coulomb assumed a soil wedge that is bound by the interface of the retaining wall and by a failure surface that originates at an angle from the base of the wall to the soil surface (Ketchum, 1919). This is known as the sliding wedge method of analysis. The lateral earth pressure coefficient was determined by Equation 2-6 and is a function of the internal friction angle of the soil, the slope at the top of the structure, the slope angle of the structures backs face, and the interface shear that develops between the soil and the structure (Coulomb 1776).

$$K_a = \frac{\cos^2(\phi - \alpha)}{\cos^2(\alpha) \cdot \cos(\alpha + \delta) \cdot \left( 1 + \sqrt{\frac{\sin(\phi + \delta) \cdot \sin(\phi - \beta)}{\cos(\alpha + \delta) \cdot \cos(\alpha - \beta)}} \right)^2} \quad \text{Equation 2-6}$$

- Where:
- $\phi$  = Internal friction angle of the soil (deg)
  - $\delta$  = Interface friction angle of the soil and structure (deg)
  - $\beta$  = Slope of surcharge at top of structure (deg)
  - $\alpha$  = Slope of back face of structure from vertical (deg)

Note that in Equation 2-6 that the earth pressure coefficient for a level back slope, with no interface friction, and a vertical back face structure, reduces to the Rankine earth pressure coefficient shown in Equation 2-5. Based on this, the horizontal earth pressure can be determined using Equation 2-7.

$$\sigma_H = \gamma \cdot h \cdot K_a \quad \text{Equation 2-7}$$

|        |            |   |  |
|--------|------------|---|--|
| Where: | $\sigma_H$ | = | Horizontal earth pressure (kPa)              |
|        | $h$        | = | Height of the retaining structure (m)        |
|        | $\gamma$   | = | Unit weight of backfill (kN/m <sup>3</sup> ) |
|        | $K_a$      | = | Active earth pressure coefficient (dim)      |

### 2.1.2.3 Rankine Theory

William Rankine in 1875 developed an equation to determine the horizontal pressure on a retaining wall for an incompressible, cohesionless, granular mass of soil with an assumed indefinite extent (Terzaghi, 1996). Rankine defined two equations to determine the horizontal earth pressure, one for the active case (Equation 2-8) and one for the passive case (Equation 2-9). These equations are based on the pressure coefficients as defined in Equation 2-4 and Equation 2-5, respectively.

$$\sigma_H = \gamma \cdot h \cdot \left[ \frac{1 - \sin \phi}{1 + \sin \phi} \right] = \sigma_v \cdot K_a \quad \text{Equation 2-8}$$

$$\sigma_H = \gamma \cdot h \cdot \left[ \frac{1 + \sin \phi}{1 - \sin \phi} \right] = \sigma_v \cdot K_p \quad \text{Equation 2-9}$$

### 2.1.2.4 Earth Pressure and MSE

For the internal stability analysis for an MSE structure, the earth pressure coefficient that is used to determine the horizontal force required for the analysis uses a variation of the Jaky at rest earth pressure (Equation 2-3) and the Rankine active earth pressure coefficient (Equation 2-5). For MSE structures that utilize inextensible soil-reinforcing, a hybrid approach applies the Rankine active earth pressure coefficient multiplied by an empirically derived earth pressure coefficient ratio,  $K_r$ . The ratio is

maximum at the top of the structure, decreasing linearly to a constant value equal to 1.2 below 6 meters. The ratio is a function of the stiffness of the soil-reinforcing system that is being used. This ratio implies that for an MSE structure that utilizes inextensible soil-reinforcing that the reinforced soil mass never achieves the active state of stress.

### 2.1.3 *MSE Design Methodologies*

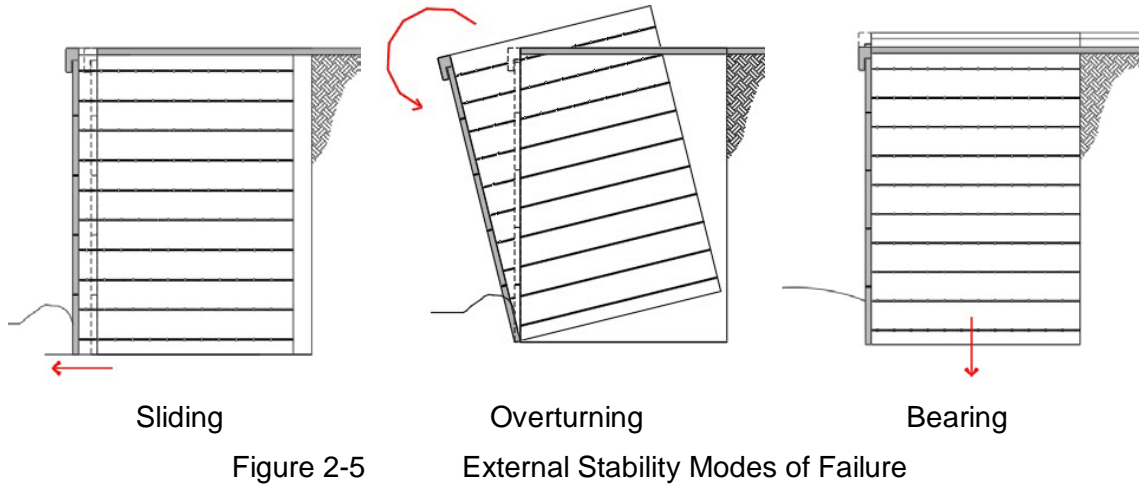
Several recognized design specifications dictate the analysis requirements for MSE structures. Two specifications that are recognized as being the most comprehensive and authoritative manuals on the subject include, the American Association of State Highway and Transportation Officials (AASHTO), Load and Resistance Factored Design (LRFD), Bridge Specification (AASHTO, 2014), and the Federal Highway Administration (FHWA) NHI-10-024 Mechanically Stabilized Earth and Reinforced Slope Design Manual (Berg et al., 2009). In addition, there are several computer programs that use Limit Equilibrium for the analysis of MSE structures. There are also computer software programs that use the AASHTO and FHWA methodology to design and analyze MSE structures. One such software program is called, MSEW, developed by Adama Engineering.

MSE structures are designed using an approach that was developed based on design methods that are used for gravity retaining structures and anchored retaining structures. The intent of MSE design is to determine geometric requirements of the structure that prevent global, local, external, and internal modes of failure. Geometrically the MSE structure is defined by a height (H) and a length (L). The height is defined by the extent of the facing system measured from the interface of the foundation to the top of the top panel. The length is defined by the length of the soil-reinforcing measured from the back face of the facing panel, to the terminal end of the soil-reinforcing. The

length of soil-reinforcing is increased until global and external stability requirements are satisfied. Based on design specifications the conventional MSE structure is typically required to have a soil-reinforcing length to structure height (L:H) ratio that is greater than, or equal to, 70% (AASHTO, 2014). The value of 70% is an arbitrary value that has been selected based on experience with, and success of structures that are in service today. The 70% rule typically yields structures that satisfy all external, internal, and global stability requirements. The length to height ratio is also known as the aspect ratio. It should be noted that structures have been successfully constructed with aspect ratios less than 70% (AASHTO, 2014; Anderson, 2010; NHI, 2009). In reality, the length of the soil-reinforcing must be long enough to produce a structure that is stable. In addition, external loads can be applied anywhere to the MSE structure. The external loads include both dead-loads and live-loads.

#### 2.1.3.1 MSE External and Global Stability Design

External and global stability requirements consider that the combined wall facing, and the reinforced soil mass, functions as a coherent gravity mass that is modelled as a rigid block. External modes of failure of the coherent gravity mass include sliding, overturning, and bearing as shown in Figure 2-5.



Global modes of failure of the rigid block include deep seated rotation and block shear as shown in Figure 2-6 (AASHTO, 2014; NHI, 2009; NHCRP, 1987).

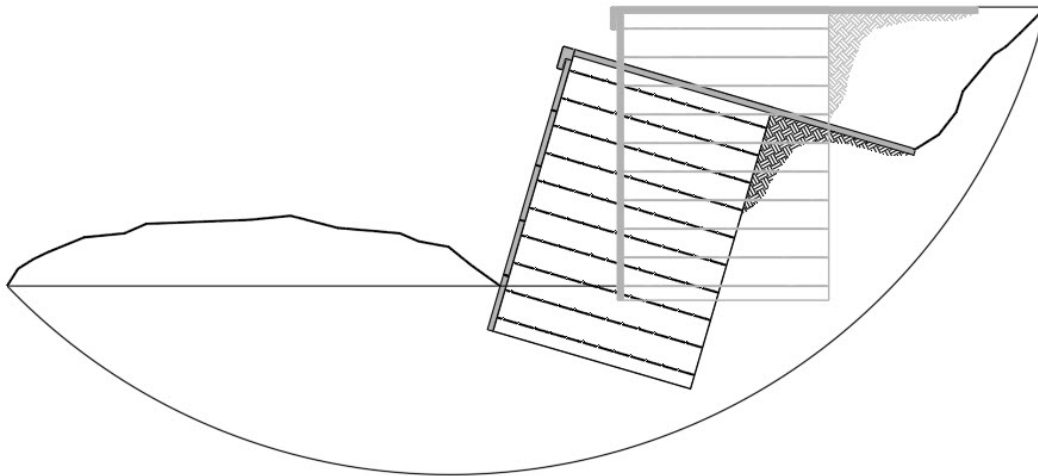


Figure 2-6 Deep Seated Global Failure

The external stability of the MSE structure follows classical design methods used for gravity retaining wall structures. The analysis is discussed in most principle of foundation engineering books and manuals (Clayton, 2013; Macnab, 2002; Bowels, 1996), therefore, it is not presented in this dissertation.

### 2.1.3.2 MSE Internal Stability Design

The difference in the design procedures between gravity retaining structures, anchored retaining structures, and MSE structures, is in the analysis of the internal modes of failure. In the internal stability design of gravity structures, such as the CIP concrete, the concrete elements, i.e., stem and footing, are reinforced with steel bars. The stem and footing of the structure are designed to assure that the combined strength of the concrete and steel reinforcing can prevent tensile and bond failures from occurring (Bowels, 1996). For an MSE structure the internal modes of failure are shown in Figure 2-7, and include tensile failure and bond failure of the soil-reinforcing from within the compacted soil mass. Bond failure is commonly called pullout failure, of the soil-reinforcing. In addition, as shown in Figure 2-7, the connection strength between the soil-reinforcing and the facing element must also be analyzed (AASHTO, 2014; NHI, 2009; Christopher, 1990; NCHRP, 1987; Collin, 1986).

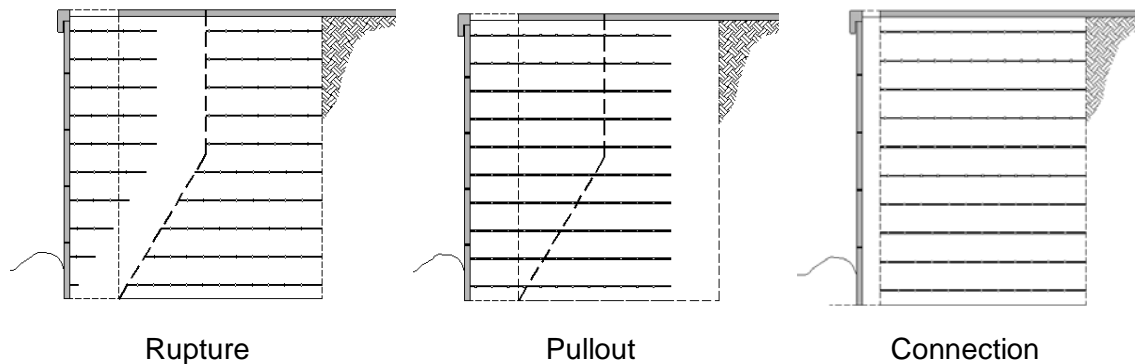


Figure 2-7 Internal Stability Modes of Failure

Internal stability analysis of the MSE structure requires that the soil-reinforcing geometric parameters and strength properties be identified. The geometric parameters that are required to be known include the soil-reinforcing length, soil-reinforcing width, soil-reinforcing vertical spacing, and soil-reinforcing horizontal spacing. The strength

properties that are required to be known include, the soil-reinforcing tensile resistance and the soil-reinforcing pullout resistance. The soil-reinforcement is required to be strong enough to prevent rupture from occurring at the location of a critical failure surface that passes through the reinforced mass of soil and to be long enough beyond that critical failure surface to prevent pullout of the element (Jewel, 1984). There are numerous design methodologies that can be used to design an MSE structure as discussed in Section 2.1.3.4. Many of these design methodologies were developed based on methodologies that were used in the design of earth slopes without soil-reinforcing. Furthermore, the design methodology is based on the classification of the soil-reinforcing i.e., inextensible or extensible. These design methodologies include empirical, semi-empirical, analytical, and numerical methods (Leshchinsky et al., 2014; NHI, 2009). Limit equilibrium (LE) methods that satisfy the Mohr-Coulomb failure criteria, where yielding coincides with failure, are used to determine the internal stability of an MSE structure. The LE method uses classical slope stability procedures and theories to determine the forces in the soil-reinforcing. The methods include, but are not limited to, the Bishop Simplified, Janbu Simplified, Morgenstern-Price, GLE, etc. These methods search the soil mass for the location of a critical failure surface.

Other MSE design methods are also used to determine the forces in the soil-reinforcing. In these methods, instead of searching for the critical surface, they incorporate a predefined failure surface and use a local equilibrium analysis technique that is based on Coulomb and Rankine earth pressure theories. The MSE design methodologies are based on a simplification of actual soil-interaction. These design methods are acceptable design tools because they allow for quick and easy modelling or



MSE structures that can be used with, or without, a computer (Christopher, 1990; Collin, 1986).

### 2.1.3.3 Internal Failure Surface

The first requirement in the internal design of an MSE structure is to define the location of the critical failure surface. Classical theories used for slope stability problems including sliding wedge, circular, logarithmic spiral, 2-part wedge and 3-part wedge analysis can be used to define the location of the critical failure surface (Collin, 1986). The critical failure surface for MSE structures is unique and is a function of the extensibility of the soil-reinforcing. The failure surface was identified based on results of instrumented structures. The results from the instrumented structures identified a unique and consistent failure surface location for structures reinforced with inextensible soil-reinforcing and one for structures with extensible soil-reinforcing. The application of a fixed failure surface location in the design process greatly simplified the internal stability analysis of the MSE structure.

In the late 1970's field measurements of constructed MSE structures were commissioned by Terra Armee of France and the Reinforced Earth Company of the United States (Schlosser, 1978). These early studies were used to determine and verify the location of the failure surface for the inextensible, steel strip soil-reinforcing system. Similar studies have been performed by other researchers on other forms of soil-reinforcing systems (Christopher, 1990). In the instrumentation program strain gauges were placed at intervals along the length of the soil-reinforcing before they were placed in the soil. The strain gauges were used to record the stress pattern in the soil. The strain gauges measured the strain in the reinforcing at working stress conditions and were not taken to failure (Christopher et al., 1989). The maximum tensile force in the

soil-reinforcing can be back-calculated based on the strain gauge information as shown in Equation 2-10.

$$T_{\max} = A_r \cdot E_r \cdot \varepsilon_r \quad \text{Equation 2-10}$$

Where:

|                 |   |  |
|-----------------|---|--|
| $T_{\max}$      | = | Maximum tension force (kN)                   |
| $A_r$           | = | Area of soil-reinforcement (m <sup>2</sup> ) |
| $E_r$           | = | Soil reinforcement elastic modulus (kPa)     |
| $\varepsilon_r$ | = | Soil reinforcement strain (dim)              |

Based on instrumentation programs, it was determined that the internal failure surface of the MSE structure coincided with the location of the maximum tension in the soil-reinforcing. The instrumentation programs demonstrated that the maximum tensile forces in the reinforcements are not located at the facing, but at a distance behind it. The internal failure surface is the location of maximum stress, dividing the reinforced soil mass into two distinct zones. The zones are defined as the active zone and a passive zone. The passive zone is also sometimes referred to as the resistive zone or resistance zone. The active zone is closest to the facing, while the passive zone is closest to the retained soil. In the active zone the tangential stresses, also known as the tensile forces, are directed toward the wall face and the proximal end of the soil-reinforcing. In the passive zone the tangential stresses (tensile forces), are directed toward the terminal end of the soil-reinforcing. The axial force increases parabolically from the terminal end of the soil-reinforcement to the point of maximum tension (Wood, 2018). The axial force decreases from the maximum at the failure surface toward the wall face. It is not equal to zero at the wall face for structures using a stiff facing element. This stress envelope was

confirmed in instrumented structures and through numerical modeling (Adib, 1988; Collin, 1988; Christopher, 1993). The stress envelope for a soil-reinforcing element is shown in Figure 2-8.

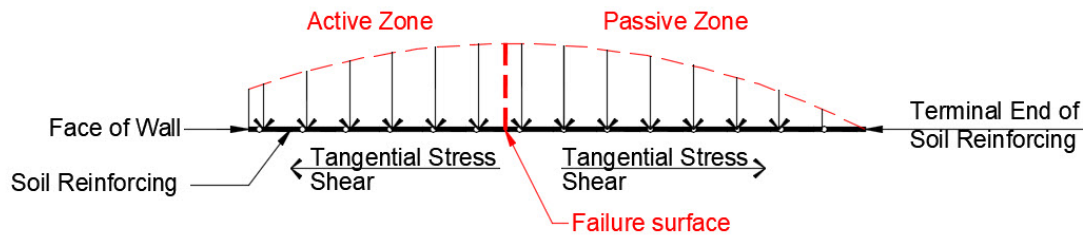
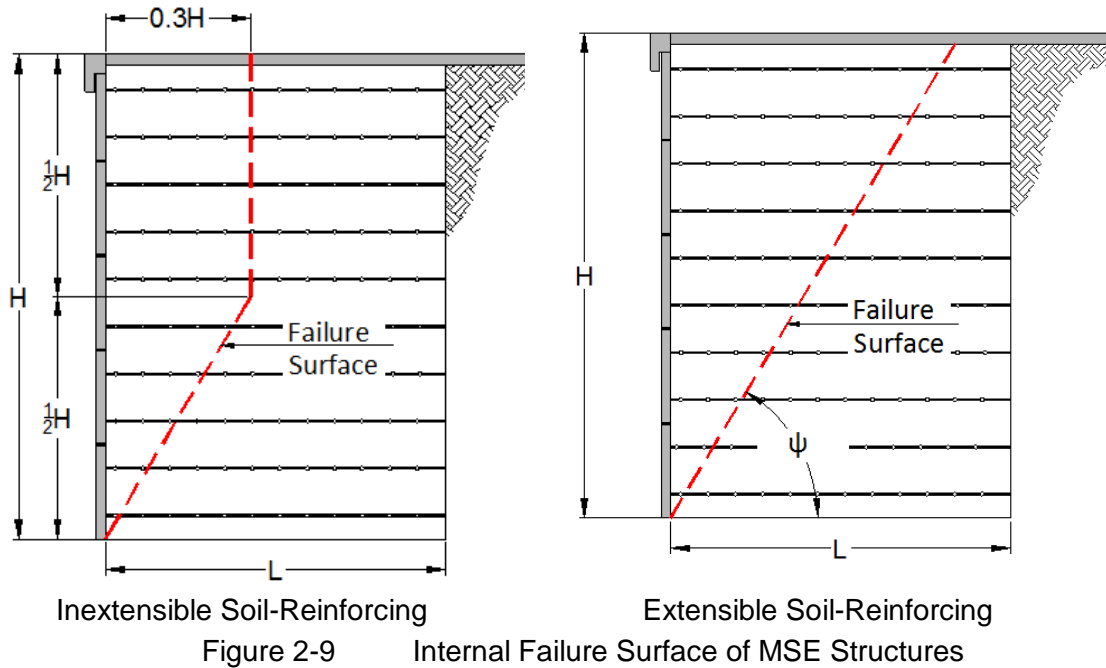


Figure 2-8 Stress Envelope for a Soil-Reinforcing Element

The location and shape of the failure surface that develops in the reinforced soil mass was shown to be a function of the stiffness of the soil-reinforcing system (McGowan, 1978). Because of this there are two failure surfaces used in the design of MSE structures, one for extensible soil-reinforcing and one for inextensible soil-reinforcing as shown in Figure 2-9. Based on instrumented structures, it was demonstrated that the failure surface for inextensible soil-reinforcing systems formed a logarithmic spiral. In order to simplify the calculation process, the logarithmic spiral was geometrically idealized into a bi-linear surface as shown in Figure 2-9 (Juran, 1978). The bilinear failure surface is assumed to occur because the soil-reinforcing system's stiffness is greater than the soil it reinforces, in other words, the presence of soil-reinforcing in the soil mass alters the strain and stress when compared to an unreinforced soil mass. For instrumented structures using extensible soil-reinforcing the failure surface was demonstrated to be linear and nearly follow the Rankine failure surface. The linear nature of failure surface for the extensible soil-reinforcing is also a function of the stiffness of the reinforcing system. The stiffness of the extensible soil-

reinforcing is less than the stiffness of the soil. Because of this, the soil mass can move to the active state. In other words, the extensible soil-reinforcing allows full mobilization of the shear strength of the soil (Leshchinsky, 2014).



$$\psi = 45^\circ + \frac{\phi}{2} \qquad \text{Equation 2-11}$$

Where:       $\psi$       =      Angle of failure surface (deg)

$\phi$       =      Internal friction angle of soil (deg)

After locating the failure surface, the internal stability of the MSE may be analyzed.

#### 2.1.3.4    MSE Design Theories

The internal design methodology for MSE structures has evolved since the introduction of the technology in the United States in the early 1970's. In the beginning, the proprietors of the MSE systems developed unique design methodologies for their

soil-reinforcing system. The design models were semi-empirical in nature and used limit equilibrium concepts. These methods were incorporated into working stress models that fit what had been observed in full-scale structures. In the development of these methods it was assumed that that soil-reinforcement loads could be associated directly to the state of stress in the soil and that limit equilibrium concepts were applicable. In each of these design methods the predicted loads were modified to match the empirical data (Allen et al., 2003).

#### 2.1.3.4.1 Coherent Gravity Design Method

Early design methods for inextensible soil-reinforcing systems used the Meyerhof design method for an eccentrically loaded concrete footing (Meyerhof, 1953; Juran, 1978; Schlosser, 1978; and Schlosser, 1979). This method is called the Coherent Gravity Design Method (CG). In the CG method, the volume of soil that is above the soil-reinforcing interface is assumed to act as a rigid block that can support bending moments. Based on this assumption, the horizontal pressures acting on the back of the reinforced soil mass is used to increase the vertical stress of the soil-reinforcing by decreasing the contact area at the soil-reinforcing interface. Therefore, the calculated vertical stress is greater than the overburden stress. The use of eccentricity at the interface of the soil-reinforcing decreases the contact area of the applied vertical forces. The decreased contact area at the soil-reinforcing interface utilizes the approach that is used in the external stability of the MSE structure to calculate the applied bearing pressure. The horizontal stress is then calculated by multiplying the vertical stress by the internal earth pressure coefficient. This concept is shown in Figure 2-10, and is presented in Equation 2-12, Equation 2-13, and Equation 2-14. As was previously discussed, this calculation method is used at each soil-reinforcement level.

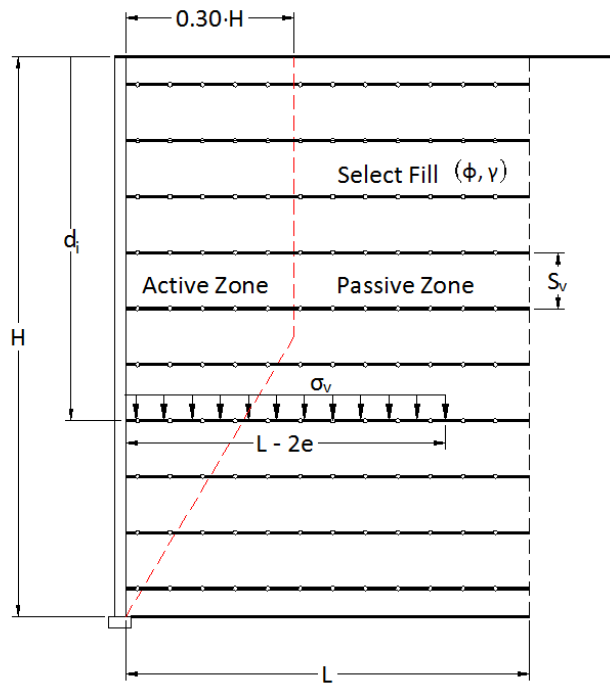


Figure 2-10 Meyerhof Vertical Stress

$$\sigma_v = \frac{\sum V}{L - 2 \cdot e} \quad \text{Equation 2-12}$$

$$e = \frac{L}{2} - \frac{\sum M_r - \sum M_o}{\sum V} \quad \text{Equation 2-13}$$

- Where:
- $\sigma_v$  = Meyerhof vertical pressure (kPa)
  - $e$  = Eccentricity (m)
  - $\sum V$  = Sum of vertical forces (kN)
  - $L$  = Length of soil-reinforcing (m)
  - $\sum M_r$  = Sum of resisting moments (kN-m)
  - $\sum M_o$  = Sum of overturning moments (kN-m)

$$\sigma_H = K_i \cdot \sigma_v \quad \text{Equation 2-14}$$

Where:  $\sigma_H$  = Horizontal pressure (kPa)  
 $K_i$  = Internal earth pressure coefficient (varies with depth) (dim)

The lateral stress that is to be resisted by the soil-reinforcement is assumed to be a function of the horizontal pressure applied over a tributary area. The tributary area is a function of the vertical and horizontal spacing of the soil-reinforcing, which is a function of the facing system. Based on the CG method if the length of reinforcement is increased, the stress in the reinforcement decreases, and in contrast, if the length of reinforcement is decreased, the stress in the reinforcement is increased. The method of superposition is used to include any externally applied load to the structure, both dead-loads and live-loads.

The magnitude of the internal earth pressure coefficient is a function of the soil-reinforcing system. In the CG method, and for inextensible soil-reinforcing, the lateral earth pressure coefficient is empirically determined. It is shown to be nearly equal to the at-rest pressure coefficient,  $K_o$ , at the top of the structure, decreasing to the active earth pressure coefficient,  $K_a$ , at a depth of 6 m (20 ft.) and below the top of the structure. The  $K_o$  conditions were assumed to occur at the top of the structure due to locked-in-compaction stresses. The compaction stress that is locked-in is a function of the lateral restraint of the soil-reinforcing. For relatively stiff, inextensible, soil-reinforcement the locked-in stress can be greater than the vertical overburden pressure (Collin, 1988). It is assumed that the stiffer the soil-reinforcing is, the less the soil can strain (Leshchinsky et al., 2016). The prevention of strain in the soil also prevents the active state of stress from developing. As the depth below the top of structure increases, the locked-in-

compaction stresses are overcome by the increasing overburden stress. At some distance below the top of the structure the deformations became large enough to mobilize the active state stress (Schlosser, 1978; Duncan, 1984; Allan, 2001; Leshchinsky et al., 2016). The CG method is a well-established methodology that is still used today (Anderson, et al, 2010).

#### 2.1.3.4.2 Tieback Wedge Method

Early design methods for extensible soil-reinforcing systems used the Tieback Wedge Method (TW). The TW method assumes that the MSE structure is flexible. For extensible soil-reinforcement, it is assumed that sufficient lateral deformation can occur in the soil mass allowing the active state of stress to develop (McGowan, 1978; Collin, 1988; Christopher, 1990). The failure surface for the TW method is shown in Figure 2-11. As previously discussed, the CG method assumes that the horizontal soil stresses at the soil interface located at the terminal end of the soil-reinforcement influences the state of internal stress. In the TW method it is assumed that the vertical stress within the soil mass is equal to the overburden stress. In other words, the forces at the interface of the retained soil do not influence the state of stress. Because the active wedge develops, the lateral earth pressure coefficient for the Rankine active case is used to calculate the horizontal stress (Bell 1983). At the time of development of this method, the facing elements that were being used for most of the extensible soil-reinforcing systems, were considered to be flexible. The flexible facing elements would not prevent large lateral deformations to take place. The calculation methodology is shown in Equation 2-15 and Equation 2-16.



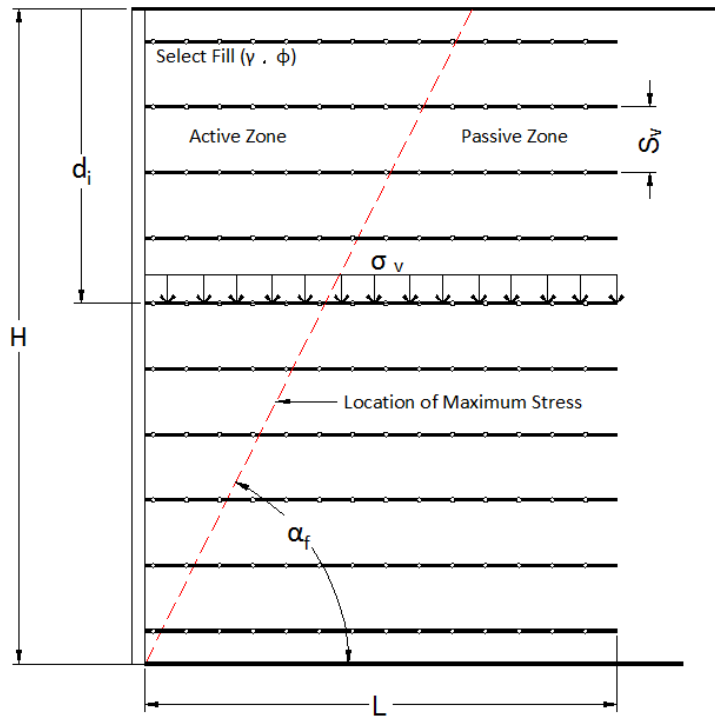


Figure 2-11 Tieback Wedge Method

$$\sigma_v = \gamma \cdot d_i \quad \text{Equation 2-15}$$

Where:  $\sigma_v$  = Meyerhof vertical pressure (kPa)  
 $\gamma$  = Unit weight of soil ( $\text{kN/m}^3$ )  
 $d_i$  = Depth to soil-reinforcing (m)

$$\sigma_H = K_a \cdot \sigma_v \quad \text{Equation 2-16}$$

Where:  $\sigma_H$  = Horizontal pressure (kPa)  
 $K_a$  = Active earth pressure coefficient (dim)

#### 2.1.3.4.3 Stiffness Design Method

A research project sponsored by the FHWA from 1983 through 1989 was used to unify the design methodology for the inextensible and extensible soil-reinforcing systems and is known as the Stiffness Design Method (SD). The development of the SD method is well documented in the FHWA-RD-89-043 Reinforced Soil Structures Design and Construction Guidelines (Christopher et al. 1989). The SD methodology was developed from the results of full scale instrumented MSE structures. The research project combined case studies, numerical models (Adib, 1988; Schmertman et al., 1989), analytical models, pullout tests (Bonczkiewicz, 1990), small scale models (Juran, 1985; Juran, 1986), centrifuge models (Jabar, 1989) and instrumented full-scale walls (Christopher et al., 1989) built specifically for the research project. Many other researchers contributed to this effort including an earlier NCHRP literature review performed by Mitchell and Villet (1987), along with supporting work by Collin (1998). The research program is summarized in Volume II of Christopher (1989).

The SD method incorporated the global stiffness of soil-reinforcing system into the calculation of the lateral earth pressure coefficient. A detailed description of the research and the results concerning the development of a global stiffness factor is provided by Christopher (1993). The SD method also classified the failure surface based on the stiffness of the soil-reinforcing. The stiffness of the soil-reinforcing was based on the geometrical parameters of the soil-reinforcing element. The SD method developed equations that can be used to determine the global stiffness of the soil-reinforcing for both extensible and inextensible systems. For inextensible soil-reinforcing systems a factor was applied to the global stiffness factor. This additional factor was represented by the variable, omega ( $\Omega$ ). The omega factor ( $\Omega$ ) increased the lateral earth pressure

coefficient (Christopher, 1993). There is no known published documentation on how the Omega factors were determined. The use of the SD method requires a full knowledge of the soil-reinforcing system that is being used. The methodology is an iterative calculation procedure. It is well suited for use with a computer. To perform calculations by hand can be long and tedious making the method difficult to check (Allen, 2001).

In the SD method, the global stiffness of the soil-reinforcing system is calculated using the relationship shown in Equation 2-17 (Christopher, 1993).

$$S_r = \frac{E_r \cdot A_r}{\left(\frac{H}{n}\right)} \quad \text{Equation 2-17}$$

Where:

- $S_r$  = Global Stiffness (kPa)
- $E_r$  = Modulus of reinforcement (kPa)
- $A_r$  = Area of reinforcement (m<sup>2</sup>)
- $H$  = Height of the MSE structure (m)
- $n$  = Number of rows of soil-reinforcing (dim)

Based on this method the lateral earth pressure coefficient can be calculated using the relationships shown in Equation 2-18 and Equation 2-19.

$$K_r = K_a \left( \Omega_1 \left( 1 + 0.4 \frac{S_r}{47880(kPa)} \right) \right) \left( 1 - \frac{Z}{6(m)} \right) + \Omega_2 \frac{Z}{6(m)} \quad \text{if } Z \leq 6 \text{ m} \quad \text{Equation 2-18}$$

$$K_r = K_a \Omega_2 \quad \text{if } Z > 6 \text{ m} \quad \text{Equation 2-19}$$

Where:

- $K_r$  = Coefficient of active earth pressure (dim)
- $\Omega_1$  = 1.0 for strips and polymer sheet reinforcement (dim)

$$\begin{aligned} & 1.5 \text{ for Bar-Mats and welded wire mesh (dim)} \\ \Omega_2 &= 1.0 \text{ if } S_r \leq 47880 \text{ kPa} \\ & 1.2 \text{ if } S_r > 47880 \text{ kPa} \\ Z &= \text{Depth from top of structure to soil-reinforcing (m)} \end{aligned}$$

The vertical overburden pressure is used to determine the horizontal pressure. The SM method does not assume that the soil pressure at the terminal end of the soil-reinforcing, located at the interface of the reinforced soil and retained soil, affects the stress in the soil-reinforcing like the CG method did.

$$\sigma_v = \gamma \cdot d_i \quad \text{Equation 2-20}$$

Where:  $\sigma_v$  = Meyerhof vertical pressure (kPa)  
 $\gamma$  = Unit weight of soil (kN/m<sup>3</sup>)  
 $d_i$  = Depth to soil-reinforcing (m)

$$\sigma_H = K_a \cdot \sigma_v \quad \text{Equation 2-21}$$

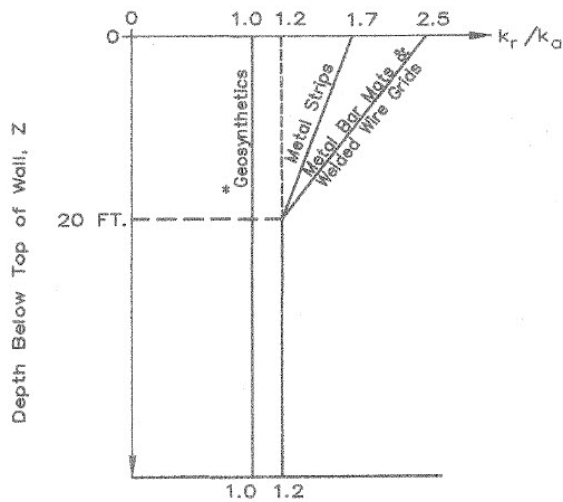
Where:  $\sigma_H$  = Horizontal pressure (kPa)  
 $K_a$  = Active earth pressure coefficient (dim)

As previously indicated, the development of this method was based on several full-scale instrumented structures and then was verified through numerical modeling. In 1994, the Stiffness Design Method was introduced in the AASHTO Bridge Design Specification for the first time.

#### 2.1.3.4.4 Simplified Method

The method that is recognized by AASHTO and FHWA today is called the Simplified Method. The method was developed jointly by FHWA and AASHTO and was an attempt to combine the best, and simplest features of various design methods that had been allowed by the AASHTO specifications into a single unifiable method (Allan, 2001). The objective was to account for the differences among the various reinforcement types, including the soil-reinforcing global stiffness, through the simplification and removal of the need to have full knowledge of the soil-reinforcing systems by introducing default values. It was a further objective to limit the iteration that was required when using Equation 2-18 and Equation 2-19.

Another objective was to develop a method that could easily be adapted to new MSE reinforcing systems as they became available. To do this, they developed a lateral earth pressure ratio,  $K_r/K_a$  for the common soil-reinforcing systems. In the AASHTO Article 11.10, the lateral stress ratio for several common soil-reinforcing systems is shown in figure 11.10.6.2.1-3 that is reproduced in Figure 2-12 and the method to determine the lateral stress ratio is shown in Equation 2-22, Equation 2-23, and Equation 2-24.



\* Does not apply to polymer strip reinforcement

Figure 2-12 AASHTO Figure 11.10.6.2.1-3

$$K_r = 1.7 - \frac{1.7 - 1.2}{6(m)} \cdot Z \rightarrow Z \leq 6 \text{ m [Metal Strips]} \quad \text{Equation 2-22}$$

$$K_r = 2.5 - \frac{2.5 - 1.2}{6(m)} \cdot Z \rightarrow Z \leq 6 \text{ m [Bar Mats]} \quad \text{Equation 2-23}$$

$$K_r = 1.2 \rightarrow Z > 20 \text{ m} \quad \text{Equation 2-24}$$

Where:  $K_r$  = Lateral earth pressure ratio (dim)

$Z$  = Depth below top of wall (m)

As before, the vertical overburden pressure is used to determine the horizontal pressure. The Simplified method does not assume that the soil pressure at the terminal end of the soil-reinforcing, located at the interface of the reinforced soil and retained soil, affects the stress in the soil-reinforcing like the CG method did. The horizontal pressure is a function of the vertical pressure, lateral earth pressure ratio, and is indexed to the Rankine earth pressure coefficient.

$$\sigma_v = \gamma \cdot d_i \quad \text{Equation 2-25}$$

Where:  $\sigma_v$  = Meyerhof vertical pressure (kPa)  
 $\gamma$  = Unit weight of soil (kN/m<sup>3</sup>)  
 $d_i$  = Depth to soil-reinforcing (m)

$$\sigma_H = K_r K_a \cdot \sigma_v \quad \text{Equation 2-26}$$

Where:  $\sigma_H$  = Horizontal pressure (kPa)  
 $K_a$  = Active earth pressure coefficient (dim)

#### 2.1.3.4.5 K-Stiffness

The K-Stiffness design method was developed by Allan et al. (2003). The focus was to provide a more accurate estimate of reinforcement loads and strains at working stress. The K-Stiffness design method was developed to encompass the full range of the soil-reinforcement system properties to remove the arbitrary distinctions that are made between the soil-reinforcement systems used to match the empirical data. It was the objective of the K-Stiffness method to develop a seamless design approach that was consistent with the limit states and that was consistent with the levels of safety for all soil-reinforcement systems (Allen et al., 2003).

The K-Stiffness approach used a similar approach as the Stiffness Method. To improve the calculation of the maximum tension in the soil-reinforcing the K-Stiffness method incorporated additional variables with the general equations. The K-Stiffness method considers both the local stiffness of the soil-reinforcement and the facing stiffness when compared to the Stiffness and Simplified Methods. This was done by

incorporating influence factors. The application of influence factors to the soil-reinforcing and to the facing improved the evaluation mechanisms that were used to determine the distribution of loads in the soil-reinforcement layers (Allen et al., 2003).

#### 2.1.3.5 Description of Lateral Stress Ratio

In the current state-of-practice, in the design of an MSE structure, to determine the horizontal earth pressure at a given depth, the coefficient of active earth pressure is multiplied by the lateral stress ratio. This is shown in Equation 2-27.

$$K_r = K \cdot K_a \rightarrow K = \frac{K_r}{K_a} \quad \text{Equation 2-27}$$

Where:

|       |   |  |
|-------|---|--|
| $K_r$ | = | Internal earth pressure coefficient at any depth (dim) |
| $K$   | = | Internal earth pressure ratio (dim)                    |
| $K_a$ | = | Coefficient of active earth pressure (dim)             |

The lateral stress ratio is a simplification of the Stiffness Design Method where it was established that that the lateral stress was a function of the stiffness of the soil-reinforcing system. This is also similar to the method used in the Coherent Gravity method where the horizontal earth pressure was a combination of a variable earth pressure coefficient and an increased vertical pressure. Based on the Simplified Method, in conjunction with the Stiffness Design Method, it can be offered that lateral stress ratio is a combination of the stiffness of the soil-reinforcing, the soil material properties, and the tributary volume of soil that the soil and soil-reinforcement occupy. The tributary volume of soil is a function of the soil-reinforcing horizontal spacing ( $S_H$ ), vertical spacing ( $S_V$ ), and length ( $L$ ) as shown in the isometric drawing in Figure 2-13. Note that as the width of the soil-reinforcing increases, the stiffness of the soil volume increases.



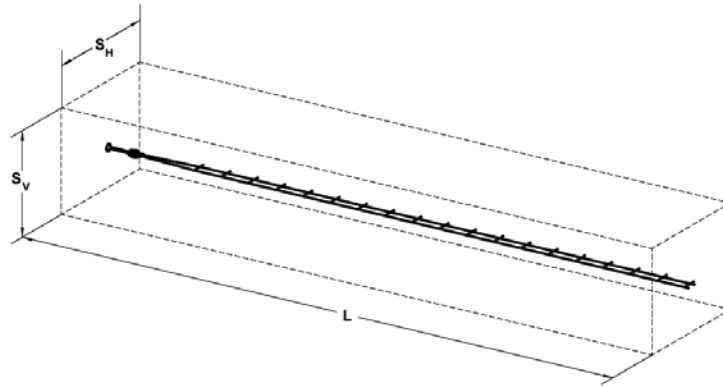


Figure 2-13 Tributary Volume of Soil for a Discrete 2-Wire Element

As specified in the AASHTO LRFD Bridge Design Specification (2014) and as described in the derivation of the stiffness design method (Christopher, 1993; Allen, 2001), the lateral stress ratio varies with the soil-reinforcing type, including the soil-reinforcing extensibility. For systems using an inextensible soil-reinforcing element, the lateral stress ratio varies linearly with depth. For systems using an extensible soil-reinforcing element, the lateral stress ratio is linear. The coefficient of active earth pressure is a function of the effective internal friction angle of the soil. The coefficient of active earth pressure,  $K_a$ , was only used as a convenient index for calibration purposes (Allen, 1991).

As shown in Figure 2-12, for inextensible metal strips, the lateral stress ratio,  $K_r$ , is equal to 1.7 times  $K_a$  at the top of the structure decreasing linearly to 1.2 times  $K_a$ , at a depth of 20 feet and below. The  $K$  ratios of 1.7 to 1.2 are equal to, or slightly more conservative than, the  $K_o$  to  $K_a$  values that are used in the Coherent Gravity design method as defined in Section 2.1.3.4.1. Also, as shown in Figure 2-12, for inextensible Welded Wire Grids and Bar-Mats, the lateral stress ratio is equal to 2.5 times  $K_a$  at the top of the structure decreasing linearly to 1.2 times  $K_a$  at depths equal to, or greater

than, 6.1 m (20'). The 2.5 value is approximately 1.6 times greater than the value used in the coherent gravity method when using a soil with an internal friction angle equal to 34 degrees.

Most MSE structures are designed for durations (life) equal to 75 or 100 years depending on the critical nature of the structure. In all AASHTO design methodologies the density of required steel is based on the steel area after considering corrosion for the specified design life. Due to degradation of steel, the stiffness of the soil-reinforcing system varies over the design life of the structure. In practical terms, the soil-reinforcing system decreases in stiffness as the system ages. The monitoring for the test structures that were used to develop the above correlations were conducted at the time of construction, and continued in many cases, for approximately one year after completion of construction. Because of this, the steel soil-reinforcing had not degraded due to being buried in soil, and therefore, they were at their greatest stiffness. In order to fully develop the stress ratio, the area of steel would need to be considered. It is evident that this was considered in the development of the stress ratio theory from Christopher (1989) as the area of the longitudinal steel is in the equation that is used to determine the coefficient of active earth pressure. This equation is shown in Equation 2-18 and Equation 2-19.

The FHWA-89-043 Reinforced Soil Structures (1989) design manual contained the derivation of the equation that was used to develop the stress ratio. In the FHWA manual it was recognized that the earth pressure coefficient should be determined based on the decreased area of the steel. This is described in Figure 26 of the FHWA-89-043 manual (Christopher et al., 1989) where the soil-reinforcing steel area, after corrosion,  $A_c$ , is used to determine the stiffness. This is an extremely important concept that appears to have been lost in the continued update of the methodologies.

As stated earlier, the labels “Bar-Mats” and “Welded Wire Grids” were proprietary trade-names used by the VSL Company and the Hilfiker Retaining Wall Company, respectively, to identify their soil-reinforcing systems. When the stiffness design method was created the retaining wall companies using metal soil-reinforcing elements were RECo, VSL, and Hilfiker (NHI, 2009). The soil-reinforcing trade-names used by these companies are labels that are used in the AASHTO and FHWA charts, figures, and text (Figure 2-12). The “Welded Wire Grids” label has been incorrectly interpreted to categorize anything that has a grid arrangement and that is fabricated to form a steel wire mesh. The derivation of the ratios in the Stiffness method are based on the stiffness of the soil-reinforcing correlated to the confinement of the soil they were tested in. Therefore, the identifier names that are referenced in these charts, figures, and graphs, have no literal meaning. The narrow, discrete configuration of the 2-Wire soil-reinforcing element for the RECo HA Ladder, and the Grid-Strip™, coupled with the stiffness theory, separates them in both form, and function, when compared to the “Bar-Mats” and “Welded Wire Grid” soil-reinforcing systems. Therefore, they should be identified in a unique fashion. The KeyStrip soil-reinforcing systems width, and wire sizes are different than the two previously identified 2-Wire systems and therefore would also most likely have a unique K-Ratio as well.

The label used by AASHTO to classify a “metal strip” does not provide a definition concerning at what width the strip transitions to a sheet. In other words, there are no geometrical dimensions given for any of the soil-reinforcing identified on Figure 2-12. One could speculate that a strip would encompass elements that have widths between 50 mm (2 in.) and 100 mm (4 in.) since these are the widths that have been used in the industry and that were used during the development of the methodology. In

addition, the classification “strip” has nothing to do with its appearance, i.e., it is not limited to only a smooth metal plate. The K-ratio values for the strip have been used in the internal design analysis for linear strips with transverse raised ribs, corrugated strips, as well as discrete 2-wire elements. Each of these elements have a bi-planar structure. The discrete 2-Wire soil-reinforcing elements have similarities that are more in common with the RECo HA strip than a wide, multiple longitudinal wire system such as the Welded Wire Grid and Bar-Mat. The discrete 2-Wire soil-reinforcing element and the RECo HA strip all transfer the soil stress into the soil-reinforcing through passive and frictional means. They both are fabricated from metal, and, therefore, have the same modulus of elasticity. They each have a similar thickness and metal areas. The difference between the 2-Wire element and the RECo HA strip, is that the 2-Wire elements are configured to have a narrow, apparent opening along their length. Because of these similarities the 2-Wire element classification is closer to a “metal strip” than a “Bar-Mat” or “Welded-Wire”.

In a study conducted by Stuedlein, A. W., Allen, T. M., Holtz, R. D., and Christopher, B. R. (2012), it was demonstrated in a structure that was reinforced with steel, linear strips, that the stress ratio can be greater than maximum value equal to 1.7 specified in the AASHTO specifications. The structure defined in this study was highly reinforced in the lower section of the wall. In the lower sections of the structure there where 25 linear strips that were attached to a single, 1.524 m x 1.524 m (5 ft. x 5 ft.) segmental concrete panel (SCP). The density of steel and, therefore, the stiffness of the system was very large. Because of the large density of steel, the soil was highly confined, preventing lateral deformation. The study conducted by Stuedlein (2012), clearly demonstrated that a structure that is reinforced with a very high density of soil-

reinforcing increases the system stiffness. It further demonstrated that as the stiffness increased, the lateral confinement increased and, therefore, the lateral stress ratio increased. For the structure described in Stuedlein (2012), the lateral stress ratio that is defined in AASHTO would have underestimated the stress in the bottom of the structure. From this study it can clearly be surmised that the stiffness of the soil-reinforcing system is highly dependent on the coverage ratio defined in Figure 2-13, and that the lateral stress ratio defined in AASHTO as shown in Figure 2-12 are ambiguous, and incomplete.

#### 2.1.3.6 Effect of Soil Confinement on lateral Stress Ratio

When a vertical load is applied to a non-reinforced soil mass, it strains both axially and laterally. In the axial direction the soil is contracting and in the lateral direction the soil is expanding. When a vertical load is applied to the surface of a non-reinforced soil mass of finite width, and the lateral expansion is not restricted, there is no lateral stress and the mass will fail by shear. When a soil-reinforcing element is placed horizontally in the same soil mass, and the same vertical load is applied, the soil-reinforcing restricts the lateral deformation as if acted on by an outside lateral force as shown in Figure 2-14 (Jones, 1985). If full restriction of movement is provided, the lateral force that is assumed to restrain the lateral deformation is equivalent to the at-rest soil condition. For wide Bar-Mat and Welded-Wire soil-reinforcement, the stresses from mechanically compacting the soil can cause the soil mass to contract. This restraining lateral force is equivalent to the passive soil condition (Duncan, 1984). Likewise, if the soil-reinforcing allows for some lateral expansion of the soil, the lateral force is considered equivalent to the active soil condition (Adib, 1988). The amount of restraint that is provided by the soil-reinforcing has been directly correlated to the stiffness of the

soil-reinforcing system (Collin, 1986; Mitchel, 1987; Buonaparte, et. al., 1987; Adib, 1988; Christopher, 1993; Allen, et. al., 2001). Consequently, the internal earth pressure coefficient in an MSE structure is a function of the stiffness of the soil-reinforcing system as well as the lateral restraint provided by the soil-reinforcing. The soil interaction in a mass of soil that is reinforced is a three-dimensional problem where the vertical spacing as well as the horizontal spacing of the soil-reinforcing becomes a critical aspect to the overall soil system stiffness.

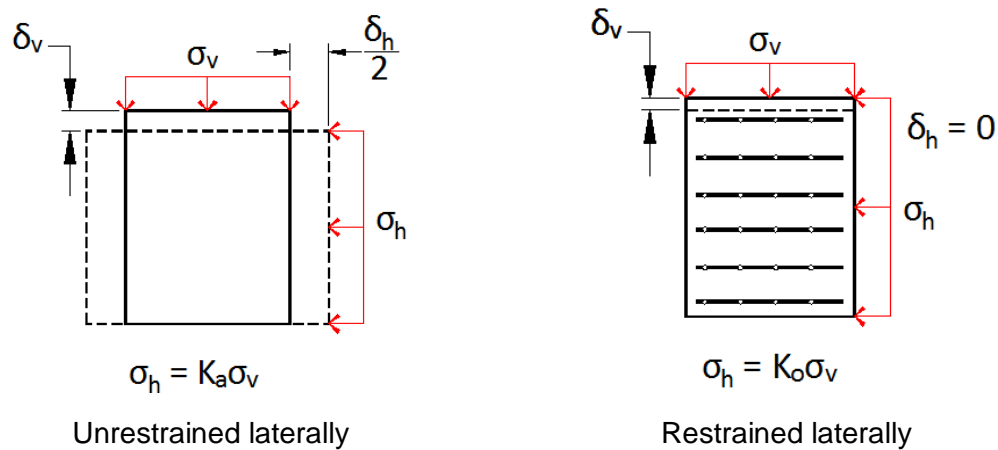


Figure 2-14 Lateral strain in soil element (Jones, 1985)

The stiffness of the soil-reinforcing system is, therefore, an extremely important parameter in the design of MSE structures. The stiffer the soil-reinforcing system, the lower the strain, and the higher the stress in the soil-reinforcing element will be. The stiffness of the soil-reinforcing system dictates the internal forces that occur in the reinforced soil mass. The global stiffness of the reinforced soil mass is a function of the stiffness of the soil, the number of soil-reinforcing elements, and the vertical and horizontal spacing of the soil-reinforcing elements as demonstrated in Equation 2-28.

### 2.1.3.7 Reinforcement Stiffness and Soil Stiffness

Research of instrumented MSE structures demonstrates that the width of the soil-reinforcing will affect the load-deformation behavior of the soil and, therefore, it will affect the lateral stress ratio (Adib, 1989). As the width of the soil-reinforcing decreases the lateral restraint of the tributary volume of soil decreases. As demonstrated previously in this dissertation, the lateral earth coefficient is directly related to the amount of lateral restraint of the soil mass. The ratio of the reinforcement stiffness to the soil stiffness can be calculated based on the specific material stiffness and on Poisson's ratio for the soil that is reinforced.

$$\theta = \frac{A_r \cdot E_r}{A_s \cdot E_s} \cdot (1 - \mu_s^2) \quad \text{Equation 2-28}$$

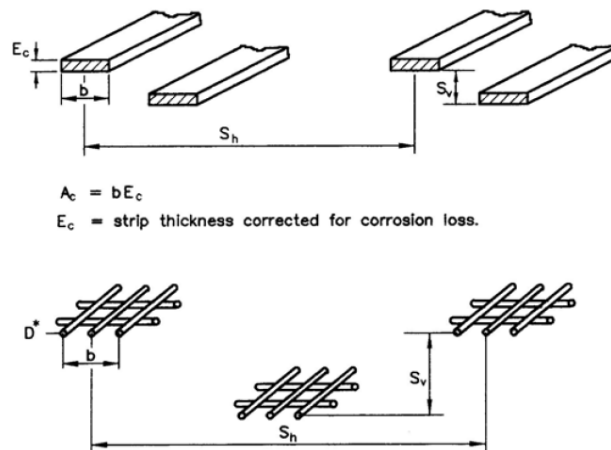
|        |          |   |   |
|--------|----------|---|---|
| Where: | $\theta$ | = | Reinforcement stiffness to the soil stiffness (dim) |
|        | $A_r$    | = | Area of reinforcement (m <sup>2</sup> )             |
|        | $E_r$    | = | Modulus of reinforcement (MPa)                      |
|        | $A_s$    | = | Area of soil (m <sup>2</sup> )                      |
|        | $E_s$    | = | Modulus of soil (MPa)                               |
|        | $\mu_s$  | = | Poisson's ratio for soil (dim)                      |

The lower the value of  $\theta$  is, the lower the stiffness of the composite mass (Adib, 1989).

### 2.1.3.8 Coverage Ratio

The soil-reinforcing occupies a tributary volume of soil as shown in Figure 2-13. In reference to Figure 2-15, the coverage ratio is a function of the width of the soil-reinforcing element ( $b$ ), the horizontal center-to-center spacing of the soil-reinforcing

element ( $S_h$ ) and the vertical spacing of the soil-reinforcing element ( $S_v$ ). The larger the width of the soil-reinforcing is for a given volume of soil, the larger the coverage ratio will be. The coverage ratio can be calculated using Equation 2-29 and is in conformance with the method shown in the AASHTO LRFD Bridge Design Specification (2014), Article 11.10.6.4.1.



[AASHTO (2014) Figure 11.10.6.4.1-1]

Figure 2-15 Coverage Ratio of Soil-Reinforcing

$$R_c = \frac{b}{S_h} \quad \text{Equation 2-29}$$

Where:  $R_c$  = Reinforcement coverage ratio (dim)

$b$  = Width of reinforcement (m)

$S_h$  = Horizontal spacing of reinforcement (m)

Table 2-1 and Table 2-2 provide the calculated coverage ratios for a 2-Wire soil-reinforcing element and for a Bar-Mat system assuming the use of a 1.524 m x 3.048 m (5 ft. x 10 ft.) and 1.524 m x 1.524 m (5 ft. x 5 ft.) facing element, respectively. Based on



Equation 2-29, a system utilizing a 2-Wire soil-reinforcing element with a 50 mm (2 in.) spaced longitudinal wire has a coverage ratio that ranges from 0.067 to 0.100. Based on the definition provided in Section 2.1.1.2.1 the Welded Wire Mesh system will typically have a coverage ratio equal to 1.00. Further, and based on the definition provided in Section 2.1.1.2.2, Bar-Mats will have coverage ratios that range from 0.30 to 0.75. The lower the coverage ratio, the lower the amount of soil-reinforcing that is occupying the soil and, therefore, the lower the stiffness of the composite soil mass.

Table 2-1 Coverage Ratio for 50 mm 2-Wire Soil-Reinforcing

| Panel Size        | Number of Elements per Row | Total Soil-Reinforcing Width | Coverage Ratio |
|-------------------|----------------------------|------------------------------|----------------|
| 1.524 m x 3.048 m | 3                          | 150 mm                       | 0.050          |
| 1.524 m x 3.048 m | 4                          | 200 mm                       | 0.067          |
| 1.524 m x 1.524 m | 2                          | 150 mm                       | 0.067          |
| 1.524 m x 1.524 m | 3                          | 200 mm                       | 0.100          |

Table 2-2 Wide Width Bar-Mats

| Panel Size        | Number of Bar-Mats per Row | Total Soil-Reinforcing Width | Coverage Ratio |
|-------------------|----------------------------|------------------------------|----------------|
| 1.524 m x 3.048 m | 2                          | 450                          | 0.300          |
| 1.524 m x 3.048 m | 2                          | 760                          | 0.500          |
| 1.524 m x 1.524 m | 1                          | 450                          | 0.300          |
| 1.524 m x 1.524 m | 1                          | 760                          | 0.500          |

#### 2.1.3.9 Tensile Resistance of Soil-Reinforcing

In an MSE structure the tensile forces that develop in the soil-reinforcements occur by the transfer of shear stress along the reinforcement. The magnitude of the stress is a function of the overburden pressure. As discussed previously, the equations and methods used to determine the tension in the soil-reinforcing are empirically derived. These equations are idealized, conservative conditions that are not completely

representative of the actual conditions that occur in a reinforced soil structure. In the state-of-practice local stability is used to determine the tension in each soil-reinforcing element. In other words, no other soil-reinforcing element that is located above, or below, the location of the soil-reinforcement that is being analyzed, is considered to contribute to the resistance. The structural model used for the calculation of local stability for a single soil-reinforcing element located at depth,  $d_i$ , is shown in Figure 2-16.

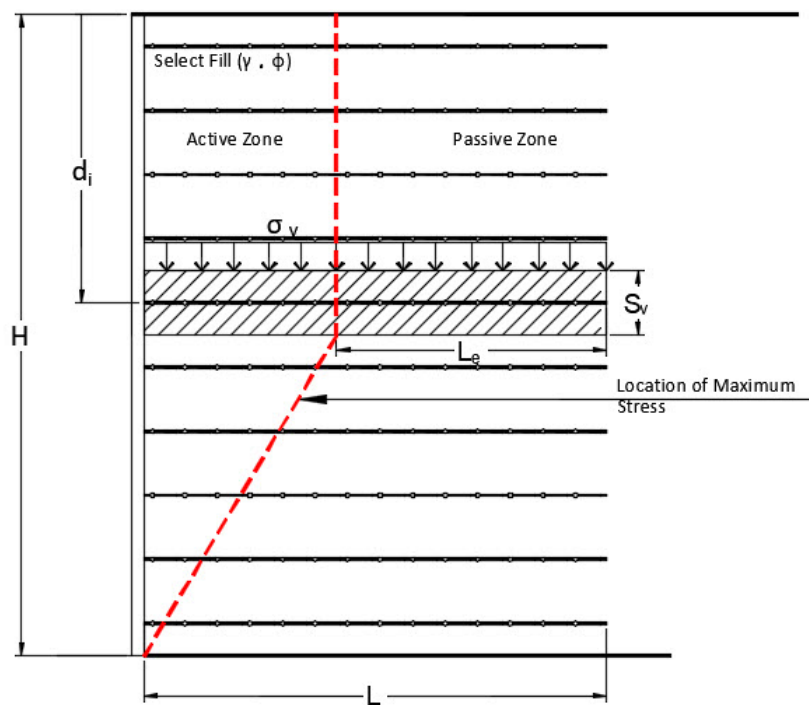


Figure 2-16 Local Stability for Calculation of Tension

The overburden pressure from the soil mass above the soil-reinforcing, in addition to all externally applied loads, cause the soil to expand laterally transferring shear stress to the soil-reinforcing element. The shear stress creates tangential forces in the soil-reinforcing. The tangential forces are acting in opposite directions at the location of the intersection of the failure surface. The free body diagram for a soil-reinforcing

element acted on by tangential stresses at the interface of the failure surface is shown in Figure 2-17.

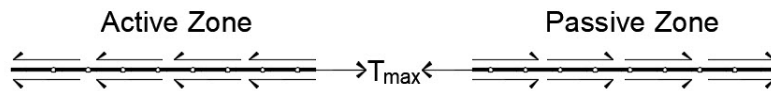


Figure 2-17 Location of Maximum Tension

The maximum tension in the soil-reinforcing is a function of the vertical pressure, lateral earth pressure coefficient, and the tributary area that the soil-reinforcing is resisting. Using the method prescribed by the current AASHTO (2014) specification the maximum tensile force in the soil-reinforcing element is calculated as shown in Equation 2-30.

$$T_{\max} = K_r \cdot \sigma_v \cdot A_T \quad \text{Equation 2-30}$$

- Where:
- $T_{\max}$  = Maximum soil-reinforcement tension (kN)
  - $K_r$  = Lateral earth pressure ratio (dim)
  - $\sigma_v$  = Vertical pressure (kPa)
  - $A_T$  = Tributary area (m<sup>2</sup>)

The soil-reinforcing system is required to be strong enough to prevent rupture and excessive lateral deformation. The allowable tensile resistance of the soil-reinforcing element must be greater than the maximum tension the soil-reinforcing element is required to resist at each local elevation. When determining the allowable tensile resistance of the soil-reinforcing element all degradation factors that may reduce the tensile capacity must be considered. For steel soil-reinforcing elements reduction in the

tensile capacity by degradation is caused by corrosion of the element. Therefore, the design cross sectional area of the soil-reinforcing element is reduced accordingly. The allowable tensile capacity is required to be greater than or equal to the maximum tensile force that is required to be resisted as shown in Equation 2-31.

$$T_a \geq T_{\max} \quad \text{Equation 2-31}$$

Where:  $T_a$  = Allowable soil-reinforcement tension (kN)

#### 2.1.3.10 Pullout Resistance of Soil-Reinforcing

The pullout resistance of soil-reinforcing systems is based on laboratory and insitu testing. Because of the high cost of insitu testing, laboratory testing is typically preferred. It is not possible to completely recreate the actual field conditions of the reinforced soil structure in the laboratory. The field conditions that are difficult to reproduce include: the difference in the density of the soil between lift placements, the development of the position of maximum tensile force occurring during construction, the interaction of the reinforcements that are positioned above, below, and adjacent; the soil-reinforcement, the difference in the moisture content of the soil, and the difference in backfill gradation, among others (Palmeira, 1989). Laboratory and insitu testing are instrumented, to reduce the factors that affect the accuracy of the pullout testing. The ability to instrument the soil-reinforcing system provides information on the soil-structure interaction that occurs during the pullout of the soil-reinforcement from the soil.

Several methods of determining the magnitude of the tension force in the soil-reinforcing have been described. To satisfy the pullout requirements for the internal stability of the structure, as defined in the state-of-practice, the soil-reinforcing pullout

resistance must be greater than the tension force that develops at the local elevation of the soil-reinforcing as shown in Equation 2-32.

$$P_r \geq T_{\max} \quad \text{Equation 2-32}$$

Pullout of a soil-reinforcing system is a function of frictional and passive resistance. For grid type soil-reinforcing systems, pullout resistance is a function of the frictional resistance that develops along the longitudinal member and the passive resistance that develops in front of the transverse member. The frictional resistance is a result of the transfer of shear stress along the longitudinal surface. Passive resistance, also called bearing resistance, is a result of the soil that bears on the transverse element. The longitudinal member is positioned parallel to the direction of the pullout force and the passive member is positioned perpendicular to the pullout force. It has been shown that passive resistance contributes far more than the frictional resistance (Chang, 1977). The frictional and passive resistance components, for a grid type soil-reinforcing system, that occur during pullout are shown in Figure 2-18.

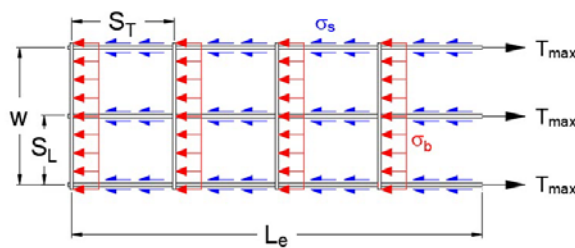


Figure 2-18 Shear Stress Transfer During Pullout

- Where:
- $w$  = Width of soil-reinforcement (m)
  - $S_L$  = Spacing of longitudinal element (m)
  - $S_T$  = Spacing of transverse element (m)

|            |   |  |
|------------|---|--|
| $L_e$      | = | Length of embedment behind failure surface (m) |
| $\sigma_b$ | = | Passive resistance (kPa)                       |
| $\sigma_s$ | = | Frictional resistance (kPa)                    |

## 2.2 State of Practice for Pullout Resistance

Pullout of soil-reinforcing has been studied by numerous researchers. To determine the resistance to pullout, and the parameters that occur during mobilization of the soil-reinforcing, laboratory pullout tests are routinely used (Khedkar and Mandal, 2009; Palmeira, 2009). Pullout testing has been used to develop empirical relationships that are referenced to known geotechnical theories. The advantage of the pullout test is that it can simulate the load-displacement relationship that occurs during the application of a tensile force to the reinforcing element at varying levels of confinement. Pullout testing of soil-reinforcing systems has been performed insitu and in specially designed soil-boxes. Pullout tests have been performed on both inextensible, and extensible, soil-reinforcing consisting of sheets, strips, and grids.

The simplest and most cost-effective pullout test is performed in a laboratory using a soil-box. The equipment that has been used to perform pullout tests varies significantly. In the majority of laboratory pullout tests, the soil-reinforcement is buried in a soil-box. The proximal end of the soil-reinforcement passes through a slot at the front of the soil-box and is clamped to a load application device. The terminal end of the soil-reinforcement is placed a distance from the sidewalls and backwall of the soil-box. This combination creates a condition where the soil-reinforcement is free to displace in the soil during application of a horizontal tensile force. Displacement of the soil-reinforcing is measured at varying locations using sensors that are attached to the soil-reinforcement.

Displacement measurements are recorded inside the soil-box and outside the soil-box. A vertical loading device located at the top of the soil-box, is used to simulate soil overburden applied to the soil-reinforcement. A pullout test is performed by applying a gradually increasing horizontal force to the proximal end of the soil-reinforcement until a predetermined displacement magnitude occurs. Several tests are performed by applying different overburden surcharges to simulate the soil-reinforcing being located at varying depths in a soil structure. The variation of the overburden pressures provides a relationship of the resistance to pullout as a function of depth in the soil. A simple cross section of a pullout soil-box is shown Figure 2-19.

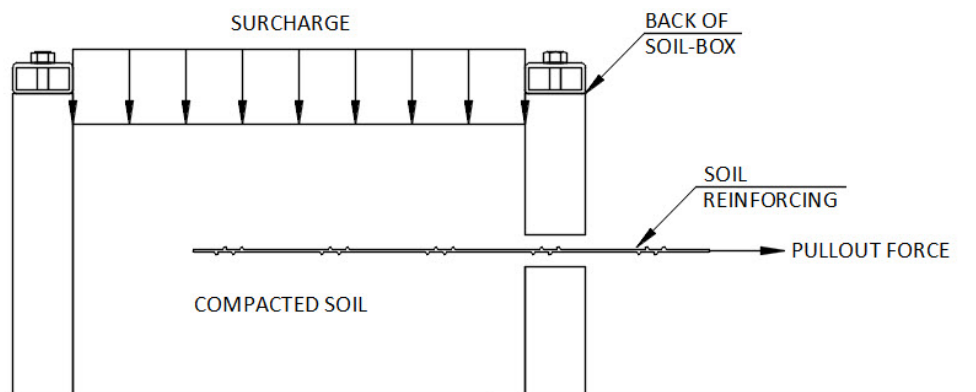


Figure 2-19 Cross Section of a Simple Pullout Box

As was previously discussed, tensile stress in the soil-reinforcement is a result of the shear stress that is transferred to the soil-reinforcement by the soil in response to a vertical overburden pressure. Therefore, it is intuitive that the pullout resistance of the soil-reinforcing would be a function of the shear stress distribution along the length of the reinforcement. It was demonstrated by Schlosser and Guilloux (1981) that the pullout resistance that develops is not a local phenomenon and that the combined deformation of the soil and the reinforcement both contribute to the pullout resistance.

Schlosser and Elias (1978) investigated the pullout-resistance of steel strip soil-reinforcing. The test was developed to understand how the mobilization of friction, coupled with the magnitude of the coefficient of friction, on a steel strip soil-reinforcing element influenced the design of a reinforced earth structure. In their test program the pullout tests were performed on two distinct types of steel strip soil-reinforcing and consisted of a smooth strip, and a strip that had ribs formed on the top and bottom surface. It was generally understood at the time of their study that two factors influenced the soil-reinforcements resistance to pullout, the internal friction angle of the soil and how the soil interacted with the surface of the reinforcement. The general equation used to determine the pullout resistance of a smooth steel strip at the time of the Schlosser and Elias (1978) test was of the form shown in Equation 2-33.

$$P_r = \sigma_v \cdot w \cdot 2 \cdot L_e \cdot \tan(\phi) \quad \text{Equation 2-33}$$

- Where:
- $P_r$  = Resistance to pullout (kN)
  - $\sigma_v$  = Average overburden pressure (kPa)
  - $w$  = Width of the steel strip (m)
  - $L_e$  = Portion of soil-reinforcing resisting pullout (m)
  - $\phi$  = Internal friction angle of the soil (deg)
  - 2 = Constant to account for two sides of the strip (dim)

From their testing they determined that the mobilization of the friction along the surface of the soil-reinforcement was not consistent at different soil densities. At low density they determined that the friction was almost uniformly mobilized along the length of the strip soil-reinforcement. While at high density they determined that the friction was



mobilized only on a portion of the strip soil-reinforcement. The difference appeared to be due to deformation of the strip soil-reinforcement at higher overburden. At the higher overburden, as the tensile force applied to the strip soil-reinforcement increased, the portion of mobilized friction along the strip soil-reinforcement increased.

To differentiate between how the surface of the soil-reinforcing affected the resistance to pullout, Equation 2-33 was rewritten to introduce a friction factor,  $f^*$ , as shown in Equation 2-34.

$$P_r = \sigma_v \cdot w \cdot 2 \cdot L_e \cdot f^* \quad \text{Equation 2-34}$$

In Equation 2-33, and Equation 2-34, all the parameters are known except the friction factor,  $f^*$ . The only parameter that is variable is the overburden pressure. Based on this, pullout tests using the smooth steel strip, and the ribbed steel strip, could be performed at varying overburden pressures and the magnitude of  $f^*$  could be back calculated and then compared. This would demonstrate how the surface of the strip soil-reinforcement affects the pullout resistance.

$$f^* = \frac{P_r}{\sigma_v \cdot w \cdot 2 \cdot L_e} \quad \text{Equation 2-35}$$

The tests demonstrated that the surface of the steel strip influenced the pullout resistance. The tests showed that the ribbed steel strip provided more resistance to pullout than the smooth steel strip. It was hypothesized that the ribs provided an additional resistance to pullout through passive resistance at the rib interface. The friction factor was calculated to be higher than the frictional resistance factor of the soil. For a ribbed strip this was attributed to soil-to-soil shear at the surface area positioned between the ribs and along the total surface area of the smooth strips. At low

overburdened pressure the increase in the friction factor from just the frictional resistance of the soil was attributed to soil dilatancy. Because of this the friction factor was renamed to the *apparent friction factor*. It was further demonstrated that the friction factor for both the smooth strip and the ribbed strip decreased with an increasing overburden. These tests demonstrated that the resistance to pullout for a smooth strip was a function of frictional resistance, and when the soil-reinforcing strip includes a rib, thus making the soil-reinforcement bi-planar, passive resistance contributes to the resistance to pullout.

### 2.2.1 *Pullout of Grid Reinforcing*

Pullout testing of grid type soil-reinforcing confirmed the hypothesis that the resistance to pullout is a function of the overburden pressure, soil density, and the configuration of the soil-reinforcing. This was previously established from pullout testing of steel strip soil-reinforcing. It had been demonstrated that pullout resistance of steel soil-reinforcing strips that had ribs on the strip surface, was a combination of frictional resistance and passive resistance (Schlosser, 1978). Frictional resistance occurred in the direction of displacement along the surface of the strip and passive resistance occurred perpendicularly to the direction of displacement at the location of the raised rib.

In a steel grid soil-reinforcing system, the resistance to pullout is governed by the friction that develops at the interface between the soil and the longitudinal elements of the grid and the bearing resistance from the soil on the transverse element of the grid (Chang et al., 1977; Peterson et al., 1980; Ingold, 1983; Anderson, 1984; Bergado et al.; 1992, 2010; Jayawickrama et al., 2013). The passive resistance to pullout that is provided by the transverse element of the grid is far greater than the frictional resistance

that is provided by the longitudinal element (Chang et al., 1977; Bishop et. al., 1979).

Based on this relationship, the general equation for the pullout resistance of a steel grid soil-reinforcing system is given by Equation 2-36.

$$P_r = P_f + P_p \quad \text{Equation 2-36}$$

Where:

|       |   |                                    |
|-------|---|------------------------------------|
| $P_r$ | = | Pullout resistance (kN)            |
| $P_f$ | = | Frictional pullout resistance (kN) |
| $P_p$ | = | Passive pullout resistance (kN)    |

Grid soil-reinforcement can be configured in numerous ways. The grid soil-reinforcement is defined by a combination of longitudinal elements and transverse elements. The number, length, and size of the elements have been known to vary as discussed in Section 2.1.1.2 and Section 2.1.1.2.2. The size of the element is based on standard wire nomenclature used by the Wire Reinforcement Institute, Inc. (2016) as referenced in Section 2.1.1.2 and Section 2.1.1.2.2. The size of the grid element is defined by the element diameter and the element length. A detailed drawing showing a plan view, side view, and end view for a multiple wire grid element is shown in Figure 2-20, Figure 2-21, and Figure 2-22, respectively.

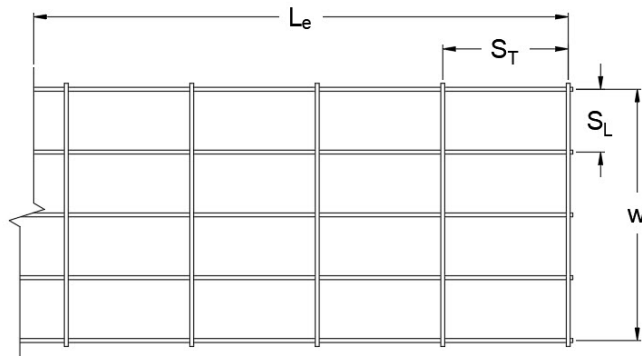


Figure 2-20 Soil-Reinforcing – Grid (Plan View)

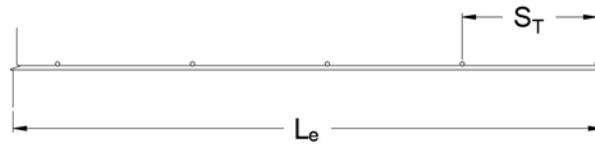


Figure 2-21 Soil-Reinforcing – Grid (Side View)

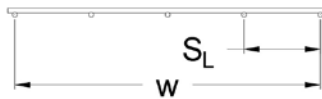


Figure 2-22 Soil-Reinforcing – Grid (End View)

- Where:
- $w$  = Width of grid element (m)
  - $L_e$  = Length of grid element available for pullout (m)
  - $S_L$  = Spacing of longitudinal grid element (m)
  - $S_T$  = Spacing of transverse grid element (m)

The number of longitudinal grid elements and transverse grid elements are calculated as shown in Equation 2-37 and Equation 2-38, respectively.

$$n_L = \frac{w}{S_L} + 1 \quad \text{Equation 2-37}$$

$$n_T = \frac{W}{S_T} + 1 \quad \text{Equation 2-38}$$

Where:       $n_L$       =      Number of longitudinal grid elements (dim)  
                   $n_T$       =      Number of transverse grid elements (dim)

As shown in Figure 2-20, Figure 2-21, and Figure 2-22, the grid soil-reinforcement element is composed of a series of apertures. The aperture is defined as the opening created by the space between the adjacent longitudinal elements ( $S_L$ ) and the adjacent transverse elements ( $S_T$ ). The aperture size has been shown to influence the pullout resistance of the grid element (Lawson et al., 2012; Jayawickrama, 2013). It was demonstrated by Wilson-Fahmy and Koerner (1993), that flexibility of the transverse element delays the mobilization of the passive resistance. Based on this it was determined that the greater the flexural rigidity of the transverse element, the greater the resistance to pullout is. The flexural rigidity is a function of the length of the transverse element, i.e., spacing between the longitudinal elements, and the diameter of the transverse element. Therefore, as the length of the transverse element decreases the flexural rigidity increase.

#### 2.2.1.1 Frictional Resistance

Resistance to pullout in grid soil-reinforcing systems develop along the longitudinal elements through adhesion at the interface of the element and the soil. The manner of pullout is analogous to the frictional skin resistance that develops in a deeply embedded pile. The skin friction component, for a circular pile, is calculated using the relationship shown in Equation 2-39. Based on this relationship, the resistance to pullout is a combined function of the surface area of the element that is in contact with the soil,

the frictional properties at the interface between the soil and element, and the effective overburden pressure. The magnitude of the effective overburden pressure for a pile varies depending on the method of analysis (Bowels, 1996).

$$P_f = \pi \cdot b \cdot z \cdot \sigma_v \cdot \tan(\delta) \quad \text{Equation 2-39}$$

where:

|            |   |   |
|------------|---|---|
| $\pi$      | = | Perimeter factor for a circular pile (dim)                  |
| $b$        | = | Diameter of the pile (m)                                    |
| $z$        | = | Embedment length of pile (m)                                |
| $\sigma_v$ | = | Effective stress (kPa)                                      |
| $\delta$   | = | Coefficient of friction for pile and soil interaction (dim) |

Equation 2-39 is the same equation that was used to determine the pullout resistance of a horizontally positioned smooth strip that was shown in Equation 2-33. As is demonstrated in the equations, the frictional pullout resistance is a function of the shear stress distribution along the length of the reinforcement. The frictional resistance is a function of the surface area, the frictional properties at the interface of the surface, and the overburden pressure.

Empirical evidence has established that pile theory can be correlated to an element that is horizontally positioned in the soil (Peterson et. al., 1980; Nielsen et. al. 1984; Jewell et. al., 1984; Abdel-Motaleb, 1989; Palmeira et. al., 1989; Jewell, 1990). The correlation requires the addition of factors that account for the structural geometry of the soil-reinforcing system and the extensibility of the reinforcing system. In addition, the

overburden pressure, or effective stress, is calculated as the average vertical stress acting on the circumference of the element.

Based on the results of pullout tests, an empirical equation to calculate the frictional resistance of the grid soil-reinforcing systems comprised of a series of longitudinal elements embedded in soil was developed (Peterson et al., 1980; Nielsen et al., 1984). This relationship is shown in Equation 2-40.

$$P_f = \pi \cdot d_L \cdot L_e \cdot m \cdot K \cdot \sigma_v \cdot \tan(\delta) \quad \text{Equation 2-40}$$

- where:
- $\pi$  = Effective unit perimeter (dim)
  - $d_L$  = Diameter of longitudinal element (m)
  - $L_e$  = Length of embedment behind failure surface (m)
  - $m$  = Number of longitudinal elements (dim)
  - $K$  = Average overburden pressure factor (dim)
  - $\sigma_v$  = Vertical stress (kPa)
  - $\delta$  = Friction factor (dim)

The FHWA NHI-10-024 (2009) MSE publication defines the frictional resistance component for the pullout resistance of grid type soil-reinforcing systems, with the addition of a scale correction factor, a structural geometric factor, and overburden factor as shown in Equation 2-41.

$$P_f = \alpha \cdot \alpha_f \cdot K \cdot \tan(\delta) \cdot \sigma_v \cdot L_e \cdot C \quad \text{Equation 2-41}$$

|        |            |   |  |
|--------|------------|---|--|
| where: | $\alpha$   | = | Scale Correction Factor (dim)  |
|        | $\alpha_f$ | = | Structural Geometric Factor $\left(\frac{\pi \cdot d_L}{2 \cdot S_L}\right)$ (dim) |
|        | $d_L$      | = | Diameter of longitudinal bar (m)   |
|        | $S_L$      | = | Spacing of longitudinal bar (m)  |
|        | $K$        | = | Average overburden pressure factor (dim)   |
|        | $\sigma_v$ | = | Vertical stress (kPa)  |
|        | $L_e$      | = | Length of embedment behind failure surface (m)                                     |
|        | $C$        | = | Effective unit perimeter (dim)   |

Based on the numerical solution to Equation 2-40 and Equation 2-41, and the typical geometrical parameters of a steel grid soil-reinforcement, contribution of the frictional resistance to pullout is very small. This is due to the small diameter of the longitudinal elements that are used in steel grid soil-reinforcing systems. Because of this, several empirical pullout equations for steel grid systems have completely omitted the frictional component calculation from the equation.

Recent pullout tests performed by Texas Tech University (TTU) have demonstrated that the spacing of the longitudinal element influences the pullout resistance of grid type soil-reinforcing systems (Lawson et. al., 2013; Jayawickrama, 2013). In the TTU pullout testing research program, the results demonstrated that as the longitudinal element spacing decreased, the resistance to pullout increased. In the TTU study it was determined that narrower grids were more efficient and generate higher pullout friction factors than wider grids. The TTU pullout testing research also



demonstrated that the spacing of longitudinal element influences the overall stiffness of the grid soil-reinforcing system. It was established that the tested 3-wire soil-reinforcing system that had 50 mm spaced longitudinal elements had 1.5 times greater pullout resistance than the tested 3-wire soil-reinforcing system that has 150 mm spaced longitudinal elements.

#### 2.2.1.2 Passive Resistance

The failure mechanism of the transverse element of the steel grid soil-reinforcing system, as it is displacing in the soil, has been correlated to closely follow a modification of the general bearing resistance theory proposed by German Engineer Ludwig Prandtl (1920). Prandtl demonstrated that for a uniformly loaded, continuous, and smooth footing, bearing on the surface of a weightless soil possessing both cohesion and friction, that the soil will fail by plastic flow along the surface of the footing as shown in Figure 2-23.

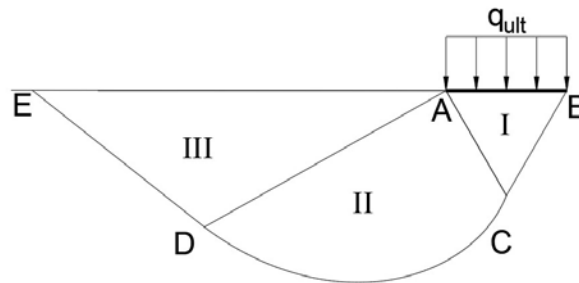


Figure 2-23 Plastic Flow Along a Surface (Prandtl 1920)

Prandtl demonstrated that at the boundary of the footing and soil, as the footing descends vertically downward into the soil at failure, the soil slides past it. His work was based on the observations of the penetration of a rigid stamp into a rigid-plastic solid (Prandtl, 1920; Vesic, 1963).

As the load applied to the footing is increased beyond a certain critical value, the soil gradually passes into a state of plastic equilibrium. During the transition from the elastic to plastic state, the distribution of the soil reactions over the base of the footing and the orientation of the principal stresses in the soil beneath the footings change (Terzaghi, 1943; Jumikis, 1962; Bowels, 1996). As the soil transitions from the state of elastic equilibrium to plastic equilibrium a shear plane develops. Referring to Figure 2-23, Prandtl considered that the shear plane was comprised of three distinct zones, identified by the roman numerals I, II, and III. The active zone of plastic failure was assumed to be triangular and is referenced by Zone-1. This zone is encompassed by line segments ABC. The inclination of the surface AC and BC was assumed to be at an angle equal to  $45^\circ + \phi/2$  from the base of the foundation as defined by surface AB. Line segments AB, BC, and AC, were assumed to consist of straight lines. A simplifying assumption was made that there was no friction at the interface of Zone-1 with Zone-2. This simplifying assumption reduces the directions of the principal stresses to being horizontal and vertical. Zone-2 is defined by an arc of a logarithmic spiral and is encompassed by line segments BCD. In this zone it was assumed that the principle stresses rotated  $90^\circ$  from Zone-1 toward Zone-3. As before, at the interface of Zone-1 and Zone-3 a simplifying assumption was made that there was no interface friction. Zone-3 is encompassed by line segments BDE, where line segment DE is a straight line. As before, no friction develops at the interface of Zone-2 and Zone-3. Therefore, the directions of the principal stresses are horizontal and vertical, with the horizontal stress having the largest magnitude. The boundaries between the ground surface and Zone-3 was assumed to be at an angle equal to  $45^\circ + \phi/2$ . In 1924, Reissner, expanded the Prandtl equation to include the surrounding surcharge,  $q$ , as shown in Figure 2-24.

Based on this, during plastic failure, Zone-1 will push on Zone-2, moving Zone-2 to the side which in turn pushes on Zone-3, moving Zone-3 upward.

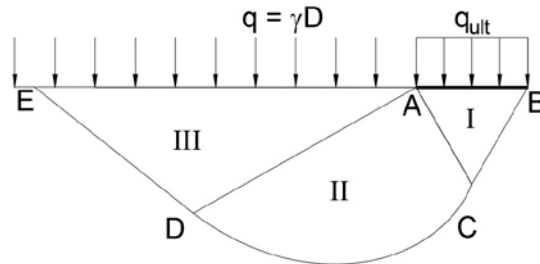


Figure 2-24 Plastic Flow Along a Surface (Reissner 1924)

Prandtl's and Reissner's analytical solution defined the bearing resistance equation as shown in Equation 2-42. The solution for the bearing resistance factors are shown in Equation 2-43 and Equation 2-44 and were solved using the method of superposition (Jumikis, 1962; Bowels, 1996).

$$q_{ult} = c \cdot N_c + q \cdot N_q \quad \text{Equation 2-42}$$

$$N_c = \cot(\phi) \cdot \left[ e^{\pi \cdot \tan(\phi)} \cdot \tan^2 \left( \left( \frac{\pi}{4} + \frac{\phi}{2} \right) - 1 \right) \right] \quad \text{Equation 2-43}$$

$$N_q = e^{\pi \cdot \tan(\phi)} \cdot \tan^2 \left( \frac{\pi}{4} + \frac{\phi}{2} \right) \quad \text{Equation 2-44}$$

- Where:
- $q_{ult}$  = Ultimate bearing resistance of foundation (kPa)
  - $N_c$  = Bearing resistance factor for cohesion (dim)
  - $c$  = Soil cohesion (kPa)
  - $\phi$  = Friction angle of the soil (deg)
  - $N_q$  = Bearing resistance factor for bearing (dim)

q = Applied normal pressure (kPa)

The equation shown in Equation 2-42 is commonly used as a model to determine the resistance to pullout for grid type soil-reinforcing systems that have transverse grid elements (Peterson et al., 1980; Neilson et al., 1983).

The original bearing resistance equations were developed considering a shallow footing. The classification of a shallow footing is a function of the footing width and the footing depth. It is classified as a shallow footing if the width of the footing, B, is equal to, or greater than, the depth from the ground surface to the base of the footing. The original bearing resistance derivations were based on plane-strain solutions. The classification for plane-strain is based on the length of footing being considerably larger than the width of the footing.

The solution for the bearing resistance of a shallow foundation system that included the weight of the soil wedge ABC in Figure 2-24 and Figure 2-25 was presented by Buisman (1940) and Terzaghi (1943). The equation derived by Buisman and Terzaghi is shown in Equation 2-45. This is the same equation developed by Prandtl and Reissner with the addition of the soil wedge component.

$$p_o = c \cdot N_c + q \cdot N_q + \frac{1}{2} \gamma \cdot B \cdot N_\gamma \quad \text{Equation 2-45}$$

where:

|          |   |  |
|----------|---|--|
| $p_o$    | = | Bearing resistance (kPa)                 |
| $c$      | = | Cohesion (kPa)                           |
| $q$      | = | Overburden pressure (kPa)                |
| $\gamma$ | = | Unit weight of soil (kN/m <sup>3</sup> ) |

B = Footing width (m)

$N_{c,q,\gamma}$  = Bearing resistance factors (dim)

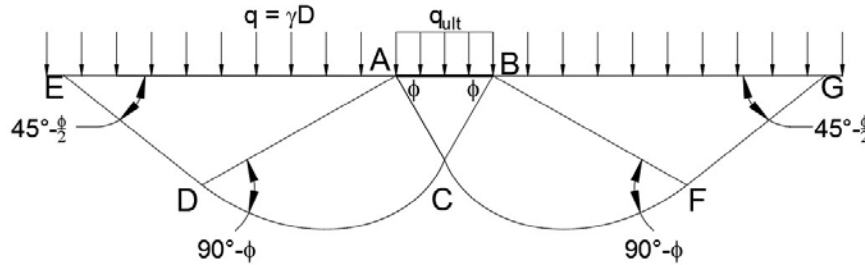


Figure 2-25 Shallow Foundation Shear Pattern (Terzaghi 1943)

As stated previously, the radial lines CD and CF as shown in Figure 2-25 are log spirals defined by Equation 2-46.

$$r = r_o \cdot e^{\theta \cdot \tan(\phi)} \quad \text{Equation 2-46}$$

Where:  $r$  = radius at point defined by angle  $\theta$  (m)

$r_o$  = radius of line segment AC or BC (m)

$\theta$  = angle between ACD and CBG (rad)

$\phi$  = internal friction angle of soil (deg)

Line segments AD, DE, BG, and GF shown in Figure 2-25 are assumed to be straight lines.

Early derivations neglected the shearing resistance of the soil that was above the base of the footing. With this assumption, an equivalent surcharge was used to replace the soil that was above the base of the footing. It has been shown that the error of

neglecting the shearing resistance and the replacement of the soil with an equivalent surcharge was conservative. By neglecting these two components the calculations used to derive the theory were greatly simplified.

When the shallow foundation criteria are exceeded, in other words, when the footing width,  $B$ , is less than the depth from the ground surface to the base of the footing, the shearing resistance of the soil above the footing should to be considered. Meyerhof (1953) extended the bearing resistance equation to take into consideration the shear strength of the soil above the base of the footing as shown in Figure 2-26.

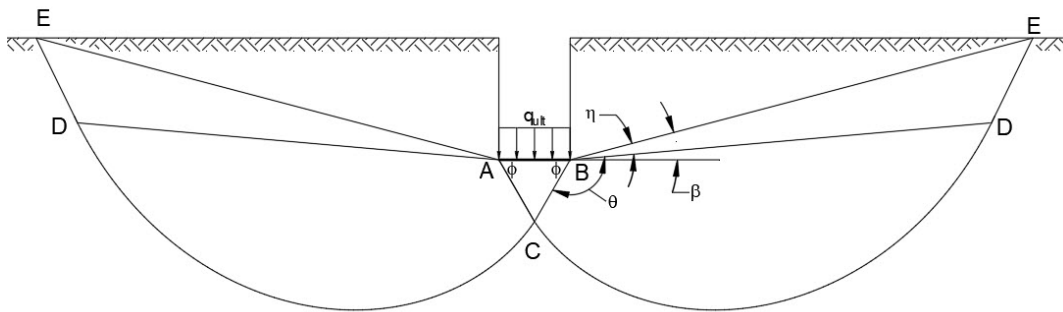


Figure 2-26 Shallow Foundation Shear Pattern (Meyerhof 1953)

The Meyerhof solution was of the same general form as Terzaghi's bearing resistance solution and equation. Meyerhof adjusted the bearing resistance equation to account for the difference in shape of the failure surface by including factors that accounted for the depth and shape of the footing. In addition, Meyerhof included a method to take into consideration the roughness of the base. The same three zones of plastic equilibrium were still considered, i.e., Zone-1 formed by ABC, Zone-2 formed by ACD, and Zone-3 formed by ADE. In the Meyerhof solution for determining the bearing resistance factors, the free surface AE and BD had a normal and tangential force applied to it that was a function of the angle of inclination given by  $\beta$ . Meyerhof's solution for the

bearing resistance factors  $N_c$  and  $N_q$  were the same as found by Prandtl and Reissner. The bearing resistance factor for the weight of the soil is shown in Equation 2-47.

$$N_\gamma = (N_q - 1) \cdot \tan(1.4 \cdot \phi) \quad \text{Equation 2-47}$$

The above theories are based on general shear failure. That is, the full mobilization along the shear planes. Failures of this type are often sudden. Because of full mobilization of the shear plane, coupled with the path of the three zones, the soil near the foundation typically heaves. This type of failure characteristically occurs in dense sand and stiff clay. A second failure type is known as local shear failure. When this occurs, there are large vertical displacements that occur before development of shear planes. Because of the large vertical displacements there is not a full extension of the shear planes to the soil surface because there is not full mobilization along the shear plane boundary. During local shear failure, instead of soil heave at the surface, there is bulging of the soil near the edge of the foundation. Local shear failures have been known to occur in loose soils and soft clays. A third common failure mode is called punching shear. In this failure mode the foundation punches into the soil with little to no development of the shear planes. With this type of failure, the soil is commonly dragged down at the surface, creating a depression. The original bearing resistance factors were derived based on the shape of the shear plane, as such, local shear failure and punching shear failure will have different bearing resistance factors.

The plane-strain bearing resistance problem for a shallow footing was advanced by De Beer (1943) and Jaky (1948) to include deep foundations. The enhancement of the method included an extension of the radial shear zone and the shear surface to intersect the pile interface. Vesic (1963) tested piles in sand and demonstrated that the

shear patterns are dependent on the relative density of the sand and that all three failure modes that occur in a shallow foundation can occur in deep foundations, i.e., general shear failure, local shear failure, and punching shear failure. At great depths Vesic (1963) showed that punching shear controlled and that the failure mode was not dependent on the relative density of the sand.

At shallow depths the end bearing, and skin resistances of a foundation increases linearly with depth. Typically, the end bearing, and skin resistance show a hyperbolic increase with depth that reaches a constant, final value at a certain depth. The final values were shown to be independent of overburden pressure and were attributed to arching. The values were found to be a function of the relative density of the sand, as was the case described in the pullout resistance of the strip type soil-reinforcing system investigated by Schlosser and Elias (1978).

For a deep foundation, the shear pattern was first modelled using the Prandtl method (Prandtl, 1920; Reissner 1924; Caquot 1934; Bulsman 1935; Terzaghi 1943) and then using the De Beer method (De Beer, 1945; Jaky, 1945; Meyerhof, 1951). These two shear patterns are shown in Figure 2-27. The Prandtl (1920) method is shown on the left side of the figure and the De Beer (1945) method is shown on the right side of the figure. The same three zones of failure are considered.



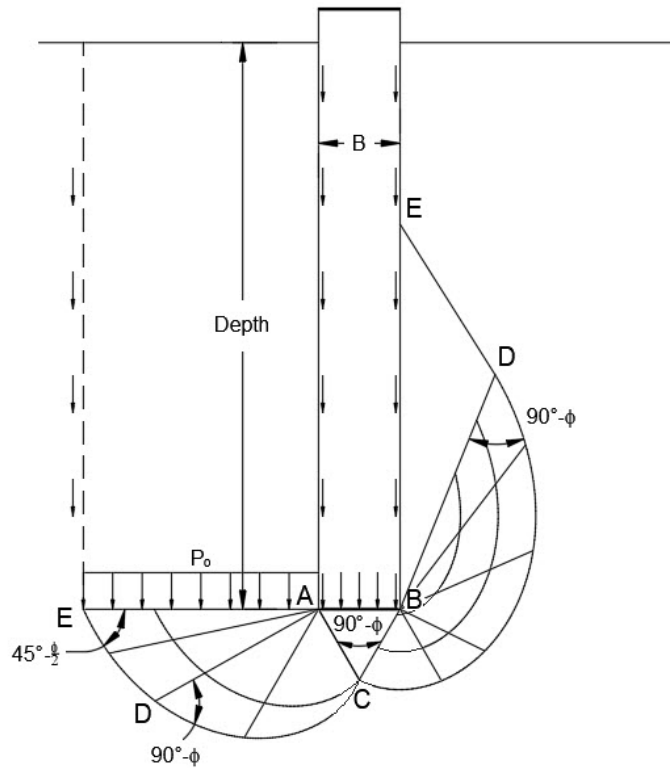


Figure 2-27 Shear Pattern for Deep Foundation (Adapted from Meyerhof 1951)

All bearing resistance equations for shallow foundations are based on a slip-line (stress field) theory. In the development of the bearing resistance theories the upper-bound theorem of classical plasticity theory was used. The upper bound theorem of plasticity is based on the principle that the soil mass will collapse if there is any compatible pattern of plastic deformation for which the rate of work of the external loads exceeds the part of internal dissipation (Chen and Liu, 1990).

The bearing resistance equations derived for foundations with a flat surface were extended to bearing resistance solutions for pipeline foundations with circular surfaces bearing on drained soils (Gao et al., 2015). This solution used the same bearing resistance equations and the application of the Mohr-Coulomb failure criteria as before. The shear pattern as shown in Figure 2-28, is like the flat-base solutions that are shown

in Figure 2-25. The failure zones are defined as the uniform zone, CFG, the extrusion region CBD, and the transition region CDF. Similar solutions of superposition were used to determine the bearing resistance factor.

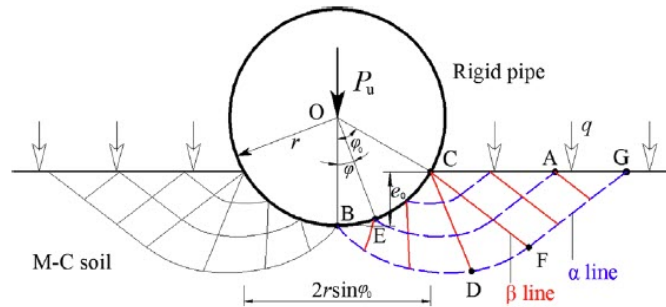


Figure 2-28 Shear Pattern for Circular Profile Shallow Foundation (Gao et al., 2015)

For the transverse grid element, the shear pattern of a deep foundation was used to model the failure of the transverse element as it was being pulled through the soil (Peterson, 1980). The displacement has been rotated from the vertical direction to a horizontal direction. As before, three zones were used to describe the areas inside the boundary of the shear surface of the model as shown in Figure 2-29. The zone of soil that is enclosed in the area defined by boundary ACD is Zone-1. The failure of Zone-1 is directed toward the displacement, and as before is analogous to the active Rankine state of stress. Zone-1 pushes on Zone-2. Zone-2 is defined by the areas to each side of Zone-1 and includes the boundaries defined by DAF and DCE. Zone-2 is considered a radial shear zone that is formed by a logarithmic spiral with point A defining the center. Zone-3 is defined by the areas to each side of Zone-2 and includes the boundary defined by AFEC. Likewise, as before, Zone-3 is analogous to the Rankine passive state of stress that is positioned tangential to the radial shear Zone-2

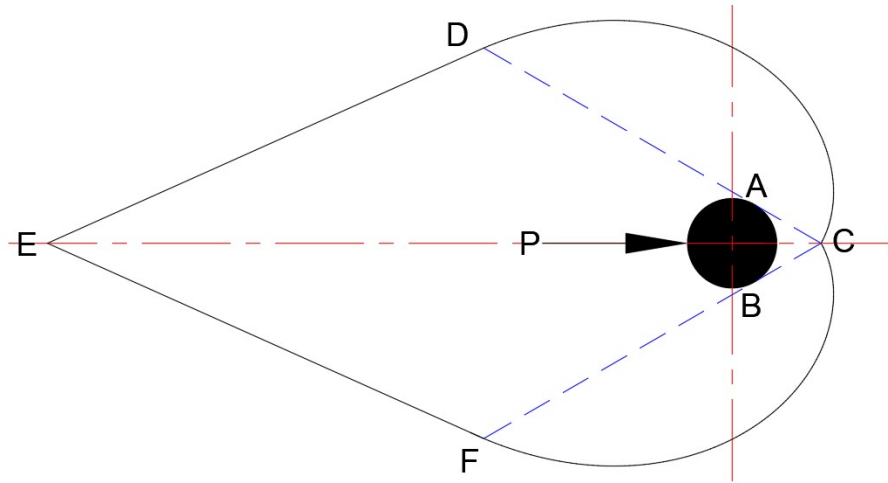


Figure 2-29 Transverse Wire Passive Failure Mechanism (Peterson, 1980)

As previously defined the backfill material that is routinely used in MSE structures is frictional with no cohesion. Therefore, Equation 2-42 is typically modified as shown in Equation 2-48.

$$q_{ult} = q \cdot N_q \quad \text{Equation 2-48}$$

The purpose of all pullout test programs that have been performed on grid soil-reinforcing systems was to determine an equation that then could be used to predict the pullout resistance of all grid soil-reinforcing systems regardless of the system configuration. All of the derived pullout equations have been developed using empirical correlations to known theory (Schlosser et al., 1978; Peterson, 1980; Nielsen, 1984; Palmier, 1989; FHWA, 1989; Christopher, 1990; Bergado et al., 1993) as well as statistically derived equations based on the results of pullout testing (Lawson, 2013; and Yu and Bathurst 2015; Miyata, Yu, and Bathurst, 2017).

The pullout resistance of the grid soil-reinforcing system is a function of the bearing resistance factor, scale correction factors, and geometric correction factors. The

equation defined in the FHWA NHI-10-024 (2010) to calculate the pullout resistance of steel grid soil-reinforcing systems that are imbedded in soil is given by Equation 2-49. This equation is like Equation 2-48 with the addition of the scale correction factors and geometric correction factors.

$$P_p = N_q \cdot \sigma_v \cdot \alpha \cdot \alpha_\beta \cdot L_e \cdot C \quad \text{Equation 2-49}$$

where:

|                |   |  |
|----------------|---|--|
| $P_p$          | = | Pullout resistance of steel grid system (kN/m)     |
| $N_q$          | = | Bearing resistance factor (dim)                    |
| $\sigma_v$     | = | Vertical stress (kPa)                              |
| $\alpha$       | = | Scale correction factor (dim)                      |
| $\alpha_\beta$ | = | Geometric correction factor (dim)                  |
| $L_e$          | = | Length of embedment behind the failure surface (m) |
| $C$            | = | Effective unit perimeter (dim)                     |

The scale correction factor,  $\alpha$ , as defined by FHWA NHI-10-024, accounts for a non-linear stress reduction over the embedded soil-reinforcing length of extensible soil-reinforcing elements. This factor is determined during the pullout test in combination with laboratory data and is based on non-uniform displacement. FHWA NHI-10-024 defines the scale correction factor to generally be equal to 1.0 for metallic reinforcements, and ranges from 0.6 to 1.0 for geosynthetic reinforcements. The geometric correction factor is a bearing factor for passive resistance which is a function of the thickness per unit width of the bearing member, i.e., transverse element of the grid. The geometric correction factor is defined in Equation 2-50.

$$\alpha_{\beta} = \frac{t}{S_T} \quad \text{Equation 2-50}$$

Where:       $t$       =      thickness of transverse element (m)  
                   $S_T$       =      Spacing of transverse element (m)

Equation 2-49 is calculated based on a unit width of the system, such as, one-meter of soil-reinforcing. To adjust the equation to calculate the pullout resistance for a discrete grid soil-reinforcing system, the width of the system,  $w$ , can be added to the equation. In addition, the thickness of the grid element,  $t$ , is typically referenced as the diameter of the element,  $d_b$ . Making these substitutions, and adjustments, Equation 2-49 becomes Equation 2-51. Note that the factor of 2 is required in the denominator to correct the presence of the effective unit perimeter variable,  $C$ , as there are not 2 sides to the grid element. This prevents a doubling of the pullout resistance.

$$P_p = N_q \cdot \sigma_v \cdot \alpha \cdot \left( \frac{d_b}{2 \cdot S_T} \right) \cdot L_e \cdot C \cdot w \quad \text{Equation 2-51}$$

Where:       $P_p$       =      Pullout resistance of steel grid system (kN)  
                   $d_b$       =      Diameter of transverse grid element (m)  
                   $w$       =      Width of transverse member (dim)

Not explicitly defined in Equation 2-51 is the number of transverse elements,  $n$ . The number of transverse elements is a function of the soil-reinforcing systems length of embedment and the center-to-center spacing of the transverse element as given in Equation 2-52. Further, because the scale correction factor,  $\alpha$ , is equal to 1 for metallic

systems, Equation 2-51 can be rearranged into Equation 2-53. The right side of the equation is identical to Equation 2-48.

$$n_T = \frac{L_e}{S_T} \quad \text{Equation 2-52}$$

$$\frac{P_p}{[n \cdot d_b \cdot w]} = N_q \cdot \sigma_v \quad \text{Equation 2-53}$$

Based on Equation 2-53, and holding all other variables constant, explicitly the equation demonstrates that the larger the bearing area, the greater the resistance to pullout becomes. This is true for the bearing resistance theories developed for the shallow and deep foundation systems. In other words, if the bearing area increases the bearing resistance will increase proportionally.

### 2.2.1.3 Bearing Resistance Factor, $N_q$ , for Grid Soil-Reinforcing Systems

As with bearing resistance failure of foundation systems, there is a difference of opinion in the literature as to what the bearing resistance factor,  $N_q$ , should be equal to. As has been shown, there are numerous correlations for determining the bearing resistance factor  $N_q$ . The majority of the  $N_q$  factors for foundation systems are indexed as a function of the internal friction angle of the soil. The upper bound and lower bound  $N_q$  factors for shallow foundation systems proposed by Terzaghi (1943) are shown in Equation 2-54 and Equation 2-55 respectively. The  $N_q$  factor proposed by Meyerhof (1963) is shown in and Equation 2-56. The  $N_q$  factor that is based on punching shear as proposed by Jewel is shown in Equation 2-57. Each of these  $N_q$  factors are purely a function of the internal friction angle of the soil.

$$N_{q_{upper}} = e^{\pi \cdot \tan(\phi)} \cdot \tan^2 \left( \frac{\pi}{4} + \frac{\phi}{2} \right) \quad \text{Equation 2-54}$$

$$N_{q_{Lower}} = e^{\frac{\pi}{2} \cdot \tan(\phi)} \cdot \tan^2 \left( \frac{\pi}{4} + \frac{\phi}{2} \right) \quad \text{Equation 2-55}$$

$$N_q = \frac{\left( e^{\left[ \frac{3}{4} \pi - \frac{\phi}{2} \right] \cdot \tan(\phi)} \right)^2}{2 \cdot \cos^2 \left( 45 + \frac{\phi}{2} \right)} \quad \text{Equation 2-56}$$

$$N_q = e^{\left( \frac{\pi}{2} + \phi \right) \tan(\phi)} \cdot \tan \left( \frac{\pi}{4} + \frac{\phi}{2} \right) \quad \text{Equation 2-57}$$

The deep foundation  $N_q$  factors proposed by Vesic (1963), Janbu (1976), and Meyerhof (1976) are shown in Equation 2-58, Equation 2-61, and Equation 2-62, respectively. The equations shown in Equation 2-59 and Equation 2-60 are the calculations for the rigidity factor in the Vesic equation an account for the soil compressibility.

$$N'_q = \frac{3}{3 - \sin(\phi)} \left\{ \exp \left[ \left( \frac{\pi}{2} - \phi \right) \right] \tan^2 \left( 45^\circ + \frac{\phi}{2} \right) \cdot I_{rr}^{\frac{1.333 \cdot \sin(\phi)}{1 + \sin(\phi)}} \right\} \quad \text{Equation 2-58}$$

$$I_r = \frac{I_r}{1 + \varepsilon_v \cdot I_r} \quad \text{Equation 2-59}$$

$$I_r = \frac{G'}{q \cdot \tan(\phi)} \quad \text{Equation 2-60}$$

$$N'_q = \left( \tan(\phi) + \sqrt{1 + \tan^2(\phi)} \right)^2 \cdot e^{(2 \cdot \psi \cdot \tan(\phi))} \quad \text{Equation 2-61}$$

$$N_q = \frac{(1 + \sin(\phi)) e^{2 \cdot \tan(\phi)}}{1 - \sin(\phi) \cdot \sin(2 \cdot \eta + \phi)} \quad \text{Equation 2-62}$$

### 2.2.2 System Stiffness

The equations that have been presented to determine the bearing resistance of a foundation thus far, are a function of the area of a single bearing element. Further, each method assumes that the element is rigid and that the loading is equally distributed over the element area as shown in Equation 2-44.

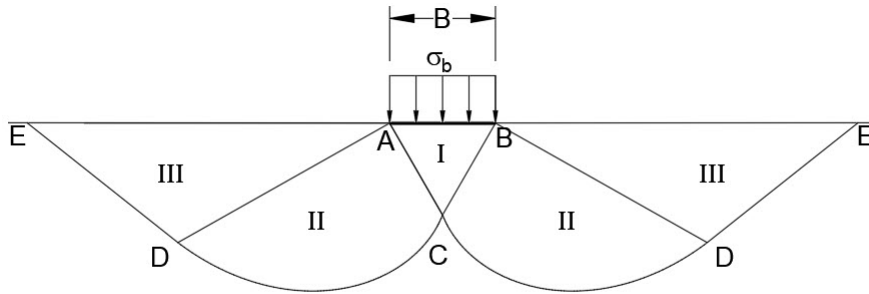


Figure 2-30 Load on a Foundation

The grid soil-reinforcing systems consist of a series of friction members and bearing members that resemble a structural frame. In the grid soil-reinforcing system the load is applied to the longitudinal element. Pullout has been shown to be primarily resisted by the transverse element. The free-body diagram for a 3-wire grid soil-reinforcing system displaying only passive resistance is shown in Equation 2-45.

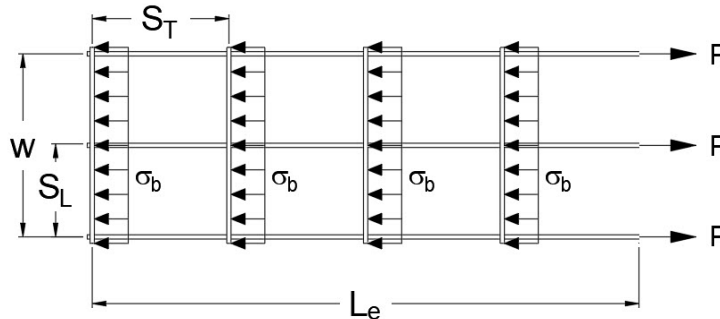
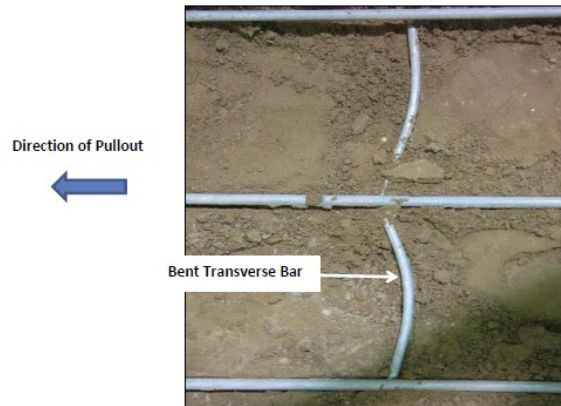


Figure 2-31 Free-Body Diagram for 3-Wire Grid Soil-Reinforcing System



The area located at the junction of the transverse and longitudinal member creates a condition where there is interference of the bearing area. In other words, the bearing failure surface cannot develop fully. Because of this it is instinctive to conclude that the bearing resistance will not be uniform along the length of the bearing member.

Pullout tests performed at Texas Tech University in 2013 (Lawson et al., 2013) demonstrated that the grid transverse element will not deflect uniformly under loading and may bend as shown in Photograph 2-11. The flexibility of the transverse element delays the mobilization of the passive resistance (Wilson-Fahmy et al., 1993).



Photograph 2-11 Bending of Transverse Element in Pullout Test (Lawson et al., 2013)

As the load in the reinforced soil mass is transferred to the longitudinal element through shear, displacement of the soil-reinforcing system is resisted primarily by the interaction of the transverse elements with the surrounding soil. As has been demonstrated through testing, the longitudinal wires provide very little resistance to pullout, and therefore displace easily in the soil. Based on this, the resistance to displacement of the soil-reinforcing system is a function of the applied force, modulus of subgrade reaction of the soil, and the rigidity of the transverse element. The theory used for a beam on an elastic foundation (BoEF) could be used to explain this phenomenon (Figure 2-32).

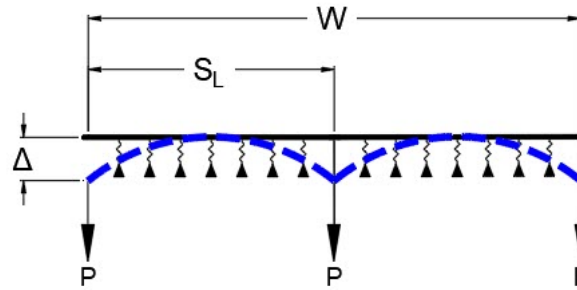


Figure 2-32 BoEF Load Diagram for 3-Wire Grid Soil-Reinforcing System

Bergado et al. (1996), introduced a dimensionless rigidity factor of the soil-reinforcing system by assuming that the transverse element was analogous to a fixed end beam. This index was used to develop a hyperbolic pullout resistance model that was then used to develop a bearing resistance factor  $N_q$ . The rigidity index was determined as shown in Equation 2-63.

$$I_d = \frac{E \cdot I \cdot d}{L^4 \cdot D \cdot P_a} \quad \text{Equation 2-63}$$

- Where:
- $I_d$  = Rigidity Index (dim)
  - $E$  = Elastic modulus of reinforcement (KPa)
  - $d$  = Unit length equal to 1.0 m (m)
  - $L$  = Length of the transverse element between the longitudinal elements (m)
  - $D$  = Diameter of transverse grid element (m)
  - $P_a$  = Atmospheric pressure (KPa)

### 2.2.3 *Effect of Boundary Conditions*

The soil-box creates boundary conditions that can influence the pullout resistance of the soil-reinforcing element. Boundary conditions created by the soil-box include, the depth of cover over the soil-reinforcing element, the soil-box wall interface (side, back, and front), the size of the exit slot, the configuration of the leading edge of the exit slot, the apparatus and configuration of the vertical load component, and the rate of application of the pullout load. Pullout test results were shown to be a function of the following boundary conditions (Christopher, 1986):

1. Pullout Box Equipment
  - a. Box Size
  - b. Depth of soil above and below soil-reinforcing
  - c. Method of horizontal load application
  - d. Pullout slot opening size
  - e. Method of vertical load application
2. Test Procedure
  - a. Rate of load application
  - b. Drainage
3. Material Evaluated
  - a. Reinforcement
  - b. Soil
4. Method of Interpretation

The ASTM D6707 specification was developed as a guide specification to limit boundary affects by providing requirements for the soil-box configuration, the placement of the soil reinforcing element, and the application of the pullout force.

#### 2.2.3.1 Soil Reinforcement Cover

To prevent soil-box interface boundary conditions from occurring the soil-reinforcement must be positioned away from the sides of the soil-box. The depth of

cover is defined as the distance between the soil-reinforcing element and the vertical load device and to the floor of the soil-box. ASTM D6707 requires that the soil-box allow for a minimum depth of 150 mm (6 in.) above and below the soil-reinforcement. In addition, the depth of cover is defined as the distance that separates the edge of the soil-reinforcing from the edge of the soil-box. ASTM D6707 requires the distance from the edge of the soil-box to the edge of the soil-reinforcement be a minimum distance that is the greater of 20 times the D<sub>85</sub> of the soil, or 6 times the maximum soil particle size. A further requirement in ASTM D6706 is the soil-box must allow for at least 610 mm (24 in.) embedment length beyond the load transfer sleeve, and that the minimum specimen length to width ratio be no less than 2.0. ASTM D6707 also states that when testing large aperture geosynthetics, the actual pullout soil-box may have to be larger than the stated minimum dimensions.

#### 2.2.3.2 Sidewall Interference

Palmeira et al. (1989), demonstrated that the front of the soil-box had an influence on the results. These influences were verified by Christopher (1993). Results from the Palmeira et al. (1989), tests demonstrated that higher peak and residual pullout resistances will be generated due to interface friction angles,  $\delta$ , at the front face of the soil-box. To limit the effects of the interface friction at the front face of the soil-box with the soil-reinforcing, the soil-reinforcing should be isolated using an embedded inclusion consisting of a sleeve, or tunnel, that is positioned at the front face of the soil-box as specified in ASTM D6706. The sleeve, or tunnel, should be configured to allow for the soil-reinforcing to pass through the front face of the soil-box without interference. Further, it was determined that the pullout test results were influenced by the location of the first bearing member. It was determined that the bearing member should be

positioned a minimum of 15 diameters away from the front face, or the leading edge of the sleeve. Christopher (1989) determined that you could limit the effect of sidewall friction on the soil-reinforcement interface by keeping the soil-reinforcing a minimum distance equal to 50 mm (2 in.) away from the sidewall.

#### 2.2.3.3 Vertical Load Application

The vertical load applied to the surface of the soil is typically applied using a pneumatic diaphragm or hydraulic system. The vertical load is transferred to the soil surface using rigid plates and beams. Pullout tests have used methods where the vertical load application system bears directly on the soil surface, or where it was separated from the soil surface using a flexible rubber membrane or rigid plates. It was demonstrated that the use of the rubber membrane system on the soil surface contact area allows for the application of a consistent normal stress. Test on different contact surface systems demonstrated that when using a flexible type load application device, the maximum pullout force is lower than the values obtained using a rigid load application device (Palmeira et al., 1989). It has been inferred by researchers that the flexible membrane provides a more uniform load distribution over the contact area (Farrag et al., 1993). The pneumatic load application also was shown to provide a more uniform pressure to the system when compared to a system that uses a hydraulic actuator or a series of hydraulic actuators (Weldu et al., 2015).

#### 2.2.4 *Pullout Resistance Models*

There are several different pullout resistance models detailed in the literature. Methods that are presented in the literature are for extensible and inextensible systems consisting of strip, grid, and sheet configurations. This section will discuss pullout

resistance models developed for grid systems. In each of the methods that follow a bearing resistance factor was developed that related the pullout resistance of the grid soil-reinforcing system with a frictional soil. As such, no cohesion is considered in the equations. The general bearing resistance equation is of the general form shown in Equation 2-64.

$$P_r = N_q \cdot \frac{d_b}{S_T} \cdot \sigma_v \cdot w \cdot L_e \quad \text{Equation 2-64}$$

- Where:
- $P_r$  = Pullout resistance (kN)
  - $N_q$  = Bearing resistance factor (dim)
  - $d_b$  = Diameter of bearing member (m)
  - $S_T$  = Spacing of transverse wire (m)
  - $n$  = Number of bearing members (dim)
  - $\sigma_v$  = Overburden pressure (kPa)
  - $w$  = Width of bearing member (m)
  - $L_e$  = Length of embedment (m)

The pullout bearing resistance factor  $N_q$ , is what is typically being investigated and determined in pullout testing. Based on the definition of Equation 2-64 the bearing resistance factor will have the influence of soil dilatancy, initial stress state of soil, soil friction angle, soil density, the geometry of the system, etc., intrinsically and explicitly, built in to it.

#### 2.2.4.1 Peterson and Anderson (1980)

Peterson and Anderson developed a pullout relationship for welded wire grid soil-reinforcing systems. The formulation of the bearing resistance factor was based on testing performed in a silty-sand soil. The soil-reinforcing that was tested consisted of systems with longitudinal and transverse element spacings equal to 50 mm x 150 mm (2 in. x 6 in.) respectively. The size of the element wires consisted of MW11 (W1.5), MW15 (W2.5), MW21 (W3.5) and MW32 (W5.0). For this experimental testing program 75 tests were performed. The resistance to pullout was based on a peak displacement equal to 5 mm (0.20 in.). The displacement criteria used in this program is below the pullout displacement criteria equal to 19 mm (3/4 in.) that is referenced in ASTM D6706. As such, it is possible that the peak pullout resistance was not achieved. Peterson and Anderson determined that the bearing resistance factor was nearly equal to the upper bound Terzaghi bearing resistance factor for general shear failure.

$$N_q = e^{(\pi \cdot \tan(\phi))} \cdot \tan^2\left(\frac{\pi}{4} + \frac{\phi}{2}\right) \quad \text{Equation 2-65}$$

#### 2.2.4.2 Jewell (1984)

Jewel tested the pullout resistance of an extensible grid type soil-reinforcing system. The soil-reinforcing was defined by a polymer sheet with small apertures. In addition, the soil-reinforcement had a small bearing member spacing to bearing member thickness ratio. His test results demonstrated that pullout resistance was a function of combination of the mobilization of direct sliding and bond strength and that three mechanisms of failure occur between the soil and the grid soil-reinforcing system. These mechanisms included the soil shearing over the plane of reinforcement surface areas, soil that is bearing on the grid reinforcement transverse surfaces, and soil shearing over

soil at the interface of the grid apertures. Because of the small aperture size, and the flexibility of the transverse element, results demonstrated that that the main contribution to pullout resistance was from the combined affect of the first and last mechanism. Jewel concluded that for aperture ratios between 10 and 20 the soil-reinforcing acts like a rough sheet and the contribution for bearing is limited.

It was theorized that when the grid performs as a perfectly rough sheet, the orientation of the principal axis of the compressive stress in the soil that is adjacent to the soil-reinforcement would be significantly inclined to the vertical. In a compacted granular soil the overall horizontal effective stress in the soil, adjacent to the soil-reinforcement, would approximately equal the overall vertical effective stress.

Jewel considered that the bearing stress of soil on a grid member is like the base pressure of deep foundations and that the punching shear failure mechanism in a deep footing would control.

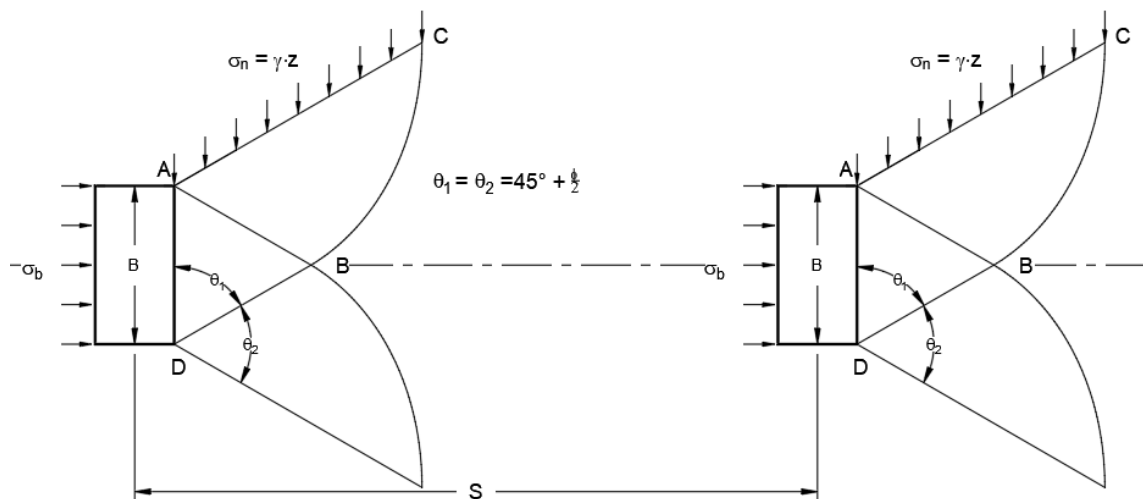


Figure 2-33 Jewell Punching Shear Model



It was determined that the bearing stress that was on the bearing member was primarily a function of the soil shear strength and that the  $N_q$  values had a lower bound and an upper bound relationship that was related to the Terzaghi bearing capacity lower and upper bound correlations.

$$N_q = e^{\left(\left(\frac{\pi}{2} + \phi\right) \cdot \tan(\phi)\right)} \cdot \tan\left(\frac{\pi}{4} + \frac{\phi}{2}\right) \quad \text{Equation 2-66}$$

$$N_q = e^{(\pi \cdot \tan(\phi))} \cdot \tan\left(\frac{\pi}{4} + \frac{\phi}{2}\right) \quad \text{Equation 2-67}$$

In addition, the test results demonstrated that the bearing stress on grid members varied and was a function of several factors besides the soil friction angle. Jewell recognized that the testing performed by Kerisel (1961) demonstrated that the soil density, the depth to the foundation, and the size of the foundation bearing area had an influence on the bearing pressures. In work performed by Vesic (1963) it was demonstrated that the ultimate bearing pressure for deeply embedded footings was a function of the relative density of the sand. Because of this Jewell recognized that the range of results for pullout resistance for soil-reinforcement that rely primarily on bearing resistance should be anticipated.

#### 2.2.4.3 Beragado, Chai, and Miura (1996)

Beragado et al., proposed a hyperbolic model that was used to simulate the pullout bearing resistance mobilization process for grid soil-reinforcing. The model simulated the effects of the grid geometry and the grid bearing rigidity on the bearing resistance by introducing the softening behaviour of the soil matrix. An analytical model was developed that was a modification of the theory developed for axial loaded piles introduced by Reese (1964). The bearing resistance factor was an extension of Jewell's

(1984) punching shear bearing resistance factor. The punching shear model for Bergado, et. al, is shown in Figure 2-34 and the proposed equation for the determining the bearing resistance factor is shown in Equation 2-68.

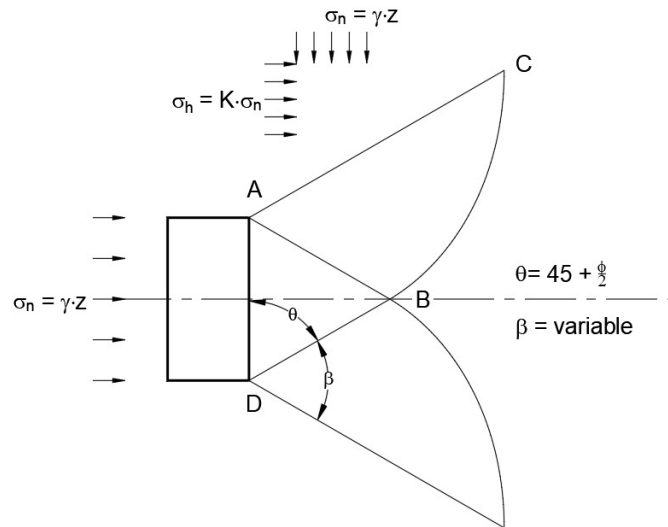


Figure 2-34 Bergado et al., Punching Shear Model

$$N_q = \left[ \frac{1+K}{2} + \frac{1-K}{2} \cdot \sin(2 \cdot \beta - \phi) \right] \frac{1}{\cos(\phi)} e^{(2 \cdot \beta \cdot \tan(\phi))} \cdot \tan^2 \left( \frac{\pi}{4} + \frac{\phi}{2} \right) \quad \text{Equation 2-68}$$

The Equation 2-68, was developed from the stress characteristic field shown in Figure 2-34. In this model the active failure zone and the rotational failure zone are only the two zones that are assumed to occur. The passive zone that is common in the general shear stress field, is replaced by the normal pressure that occurs on line AC.

In the new equation, consideration of the earth pressure coefficient, K, was introduced. Unlike, Jewell (1984), Bergado et al. theorized that the horizontal stress followed classical earth pressure models. For this analytical model the earth pressure coefficient was assumed to be related to compaction induced stresses and the applied normal pressure. From the analytical model and based on the best-fit to the test data, K

was assumed to be equal to 1.00 and beta was equal to  $\pi/2$ . When these two constraints are added to Equation 2-68 it reduces to Equation 2-69. As is apparent with this model, the internal friction angle governs the magnitude of the bearing resistance factor.

$$N_q = \frac{1}{\cos(\phi)} e^{(\pi \cdot \tan(\phi))} \cdot \tan^2\left(\frac{\pi}{4} + \frac{\phi}{2}\right) \quad \text{Equation 2-69}$$

#### 2.2.4.4 Federal Highway Administration (2009)

The Federal Highway Administration (FHWA) bearing resistance factor has an upper bound that decreases with increasing overburden. The bearing resistance factor was developed based on the collection and statistical analysis of pullout resistance information taken from different research projects that used grid type soil-reinforcing. The collected data was not separated by the variables used to determine the bearing resistance factor, such as the facing rigidity, the grid geometry, the structure design duration, the time at which the data was gathered, how the external load was applied, if the test was in-situ or in the laboratory, the soil-reinforcing geometry, the grid spacing, density of soil, among others. All known data for grid soil-reinforcing systems was used to determine the bearing resistance factor at a 95% confidence level. As such, a large scatter of pullout resistance values would be expected. Further, and because all data was used to calculate the bearing resistance factor, it was assumed that the FHWA bearing resistance equation could be conservatively used for any grid soil-reinforcing system and with any frictional soil. FHWA recognized that the bearing resistance factor was a lower-bound value and stipulated that systems that have bearing resistance factors developed from testing, that they could be used in the design process.

A two-piece linear regression analysis was used to determine the FHWA bearing resistance factor. Based on the linear regression the bearing resistance factor was determined to be equal to 20 at the surface, decreasing linearly to 10 at a depth of 6 m (20 ft.) and below. For depths that are between the structure surface, and 6 m (20 ft.), the bearing resistance value is linearly interpolated.

$$N_q = 20 \rightarrow d_i = 0 \quad \text{Equation 2-70}$$

$$N_q = 10 \rightarrow d_i \geq 6 \text{ m} \quad \text{Equation 2-71}$$

Where:  $d_i$  = Depth to soil-reinforcing (m)

When using this method, the surface factor  $C$ , equal to 2, must be included in Equation 2-64. The equation that is used with this method is shown in Equation 2-72.

$$P_r = N_q \left( \frac{d_b}{S_r} \right) \cdot \sigma_v \cdot w \cdot L_e \cdot C \quad \text{Equation 2-72}$$

#### 2.2.4.5 Jayawickrama et al., (2013)

Jayawickrama et al., performed a study that examined the pullout resistance of inextensible MSE reinforcements in backfills used in heavy-highway transportation structures in the state of Texas. The testing was funded by the Texas Department of Transportation (TxDOT). The study involved an extensive laboratory test program in which a total of 650 pullout tests were completed. The soil-box used for this study consisted of a large soil-box with dimensions of 3.658 m x 3.658 m x 1.220 m (12 ft. x 12 ft. x 4 ft.). The soil-box was capable of simulating overburden pressures equivalent to 12.120 m (40 ft.) of soil. Tests were conducted on soil-reinforcing systems consisting of

ribbed strips and welded steel grids. Two distinct types of select backfill that is used by the TxDOT was used in the program and are designated as Type A (gravelly) and Type B (sandy). A subset of the ribbed strip soil-reinforcing and the welded grid soil-reinforcing, in both soil types, were instrumented with strain gages to provide information on the mechanisms that may control pullout resistance.

The test program evaluated the pullout resistance factors for an assortment of independent variables including overburden pressure, reinforcement length, skew or splay angle, grid wire size, and grid geometry. The soil was compacted to a relative compaction density equal to 95%. The grid geometry investigated both the transverse and longitudinal wire spacing. A statistical analysis was performed on the test results to interpret and compare the data with the state-of-practice AASHTO design values. These tests were not used to develop an equation to determine the bearing resistance factor.

Test results demonstrated that the measured pullout resistance factor values were significantly higher than those predicted by the AASHTO equations. ANOVA analysis was performed on the test results and demonstrated that the transverse bar spacing has considerable influence on the pullout resistance factor. It showed that larger transverse spacing had higher pullout resistance. From the test results it was demonstrated that there were two mechanisms that may influence the observed increase pullout resistance factor. The first is the possible increase in frictional resistance provided by the longer length of longitudinal element in grids with larger transverse element spacing and that there is likely an interaction that may be taking place between adjacent transverse elements for small spacings. As a result, they concluded that grids with larger transverse bar spacings will yield higher pullout resistance.

ANOVA analysis was also performed on the test results to understand how the spacing of the longitudinal element affected the pullout resistance factor. The ANOVA demonstrated that the longitudinal element spacing is a highly significant variable that influences the pullout resistance factor. It demonstrated that the longitudinal element spacing is negatively correlated with the pullout resistance factor. The lowest correlation was for the 305 mm (12 in.) spacing and highest for the 50 mm (2 in.) spacing. It was theorized that a grid soil-reinforcing system that has closely spaced longitudinal bars would offer stiffer resistance during pullout because the transverse bars in these grids will not undergo as much deformation. As a result, they concluded that grids with smaller longitudinal bar spacings will yield higher pullout resistance.

#### 2.2.4.6 Yu and Bathurst (2015)

Yu and Bathurst, developed a method to calculate the pullout resistance factor based on the statistical evaluation of pullout test results. Statistical analysis was carried out on a large set of pullout test data. As a comparison, the state-of-practice FHWA model was performed first using the data base. For each method the pullout resistance factors were back-calculated using the measured test data. Two sets of analysis were performed. One analysis was performed to develop a general expression for  $N_q$ . Once the expression was established, the coefficient values were back-calculated. Once the coefficients were determined they were used as default values for projects that did not have test data. A second procedure was used to validate the accuracy of the model by comparing it to pullout test results from tests performed in soil-boxes.

The accuracy of the model was checked against the statistical analysis of the bias. The bias was set equal to the ratio of the measured pullout capacity to calculated pullout capacity ( $P_m/P_c$ ). For the test data the bias mean and the bias coefficient of

variation (COV) were calculated. Allen et al. (2005) and Bathurst et al. (2008) have demonstrated that a mean close to one that is correlated with a COV that is relatively small can be used to determine if the model is highly predictive. A third criterion that was used to test the accuracy of the model was based on the correlation of the bias value to the predicted pullout capacity. If the bias correlates with the predicted pullout capacity ( $p < 0.05$ ) then the accuracy of the model will depend on the magnitude of the predicted pullout capacity, which is undesirable for Allowable Stress Design (ASD) and renders the calibration of the Load and Resistance Factored Design challenging (Bathurst et al. 2011, 2013).

As discussed, the model equation was fit to a large data base of available pullout resistance tests. The coefficients  $\alpha$  and  $\beta$  were determined using the Solver optimization utility in Excel by using a power function that was fit to a dimensionless factor that was a function of the number of bearing members and the overburden pressure as shown in Equation 2-73.

$$N_q = \alpha \cdot \left( \frac{n \cdot \sigma_v}{p_a} \right)^\beta \quad \text{Equation 2-73}$$

Where:

|            |   |                                 |
|------------|---|---------------------------------|
| $N_q$      | = | Bearing resistance factor (dim) |
| $\alpha$   | = | Coefficient (dim)               |
| $\beta$    | = | Coefficient (dim)               |
| $n$        | = | Number of bearing members (dim) |
| $\sigma_v$ | = | Overburden pressure (kPa)       |
| $p_a$      | = | Atmospheric pressure (kPa)      |

To determine trial values of  $\alpha$  and  $\beta$ , the objective function was taken as the mean of bias values equal to one. The analysis was performed using the Excel Solver application. Based on the pullout data, the best fit coefficients were when  $\alpha$  equaled 46 and  $\beta$  equaled -0.5.

In this statistical model, it was demonstrated that the coefficients did not have the disadvantage of a hidden dependency with predicted pullout resistance. The lack of this dependency was an improvement over the other methods used to determine the bearing resistance factor. Because of the statistical nature of this model it was determined that it could be used for both ASD and LRFD design methods, as well as in LRFD calibration. Furthermore, the model could be used to develop soil-reinforcing specific values by using a regression analysis to determine  $\alpha$  and  $\beta$  for other systems.



## Chapter 3

### Experimental Test Program

#### 3.1 Introduction

The pullout tests for this experimental test program were performed using a state-of-practice pullout apparatus that was specifically developed for the program. The pullout apparatus was fabricated in conformance with the recommendations of the ASTM D 6706, *Standard Test Method for Measuring Geosynthetic Pullout Resistance in Soil* and modified to remove boundary affects that have been recognized and reported in the literature. Tests on various configurations of 2-Wire soil-reinforcing elements were performed in the experimental test program.

#### 3.2 Pullout Apparatus

The pullout apparatus used for this experimental test program is shown schematically in Figure 3-1. The main components of the pullout apparatus include the soil-box, reaction frame, load frame, hydraulic system, instrumentation components, and the data acquisition system. The soil-box, reaction frame, and load frame were fabricated using structural steel components.

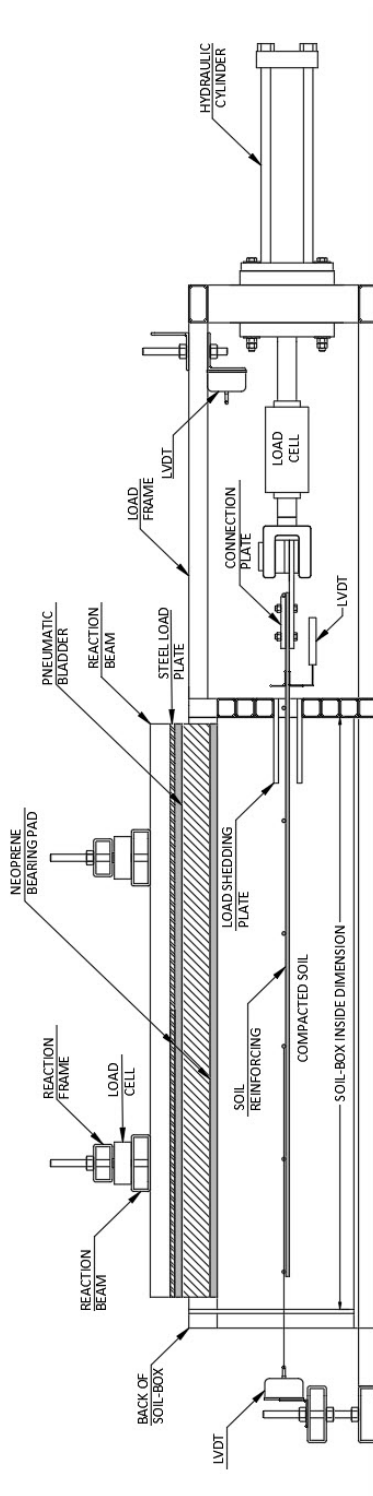


Figure 3-1 Cross Section Pullout Box

### 3.2.1 *Soil-Box*

The soil-box used in the experimental test program has an inside plan dimension equal to 450 mm (18 in.) wide by 1500 mm (60 in.) long by 375 mm (18 in.) deep. The soil-reinforcing element that is being tested exits the front of the soil-box through an opening called the exit gate. The exit gate consists of a series of 50 mm x 50 mm (2 in. x 2 in.) structural steel tubes that are stacked one atop the other inside a narrow slot. The opening slot is created by leaving a 50 mm (2 in.) gap that is positioned between two 50 mm x 50 mm structural steel tubes of the exit gate. The height of the slot opening is adjustable, but typically the height is set to 50 mm (2 in.). At the slot opening, position on opposing sides, and extending into the soil-box, are two sleeve plates. The sleeve plates consist of 12 mm x 300 mm (0.5 in. x 6 in.) steel plates that are welded to the top and bottom of the opposing 50 mm x 50 mm (2 in. x 2 in.) structural steel tubes in the exit gate. The sleeve plates are used to reduce the boundary effects from arching of the soil that can occur at the front of the soil-box during the application of the vertical and horizontal load. The soil-box, when looking toward the front, is shown in Photograph 3-1. In this photograph, only two of the 50 mm x 50 mm (2 in. x 2 in.) steel tubes for the exit gate are positioned in the slot at the front of the soil-box.



Photograph 3-1 Pullout Box Look Toward Exit Gate

The soil-box was designed to allow for a variable length of the inside chamber through the attachment of a special cross diaphragm. The cross diaphragm can be inserted inside the soil-box to create chambers of varying lengths. The cross diaphragm consists of two 100 mm x 100 mm x 6 mm (4 in. x 4 in. x ¼ in.) structural steel posts that are welded to a 50 mm x 100 mm x 6 mm (2 in. x 4 in. x ¼ in.) cross member. Each of the structural steel posts have a 62 mm x 62 mm x 6 mm (2 ½ in. x 2 ½ in. x ¼ in.) structural steel angle welded to their inside face. This angle-post combination creates a slot on the inside of the chamber. The slot is used to accommodate a series of 50 mm x 50 mm x 6 mm (2 in. x 2 in. x ¼ in.) structural steel tubes that serve to close the

chamber off. This is similar in concept to the exit gate at the front of the soil-box. The steel cross member and posts are inserted into the inside chamber of the soil-box with the structural steel angles, i.e., the slot, facing the front of the soil-box. The cross member is bolted to the top of each of the side rails of the soil-box. Each post is then braced at the bottom and the backside, at the interface of the soil-box floor, using an adjustable support strut. The support struts consist of a 100 mm x 100 mm x 6 mm (4 in. x 4 in. x ¼ in.) structural steel tubes. Positioned inside the support strut and extending from the end that is facing the back of the box is a 25 mm (1 in.) threaded rod. The threaded rod is held into position by a nut, that is welded to a plate, that is welded to the base of the post. This combination allows the threaded rod to extend and retract when the threaded rod is twisted. The threaded rod is twisted into a final position, so it is in contact with the inside back-wall of the soil-box. The support strut prevents the rotation of the base of the insert post inside the chamber. A series of 50 mm x 50 mm x 6 mm (2 in. x 2 in. x ¼ in.) structural steel tubes are placed in the slot that is formed inside the chamber by the combined posts and angles. The diaphragm configuration is shown schematically in Figure 3-2.

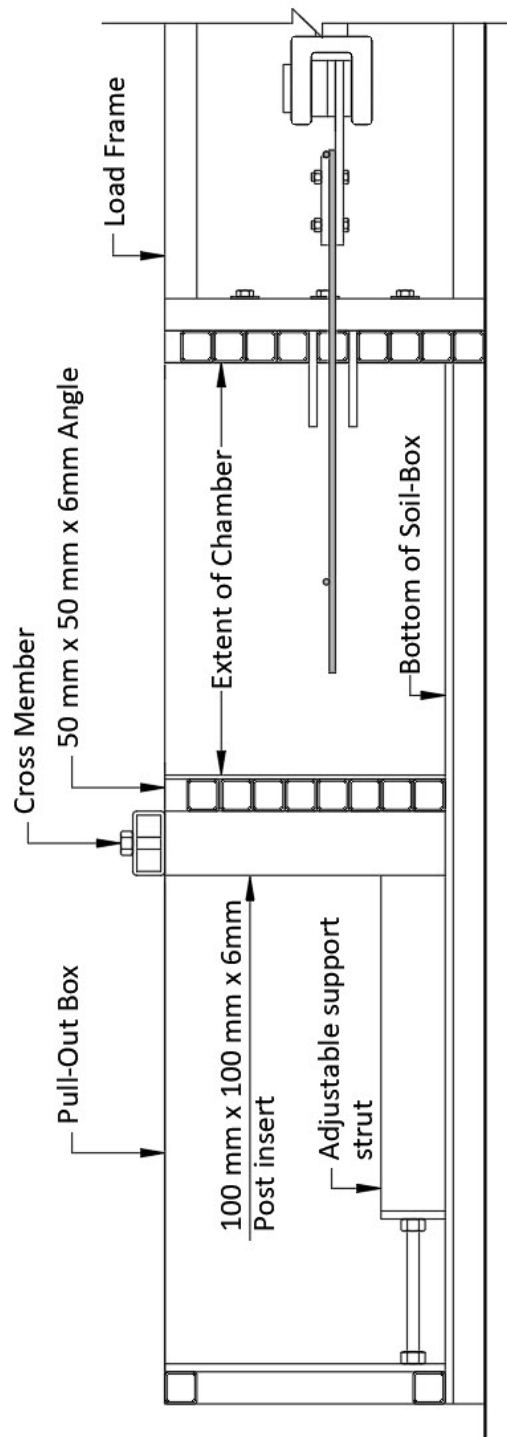


Figure 3-2 Pullout Box with Diaphragm Insert

### 3.2.2 Vertical Load Reaction Frame

The pullout soil-box was designed with two different vertical load reaction frame concepts. The first reaction frame concept consists of a Closed-Mount. The Closed-Mount reaction frame consists of a 12 mm ( $\frac{1}{2}$  in.) thick structural steel plate that has an area equal to the opening of the soil-box plus 100 mm in all directions. For the ease of handling, the steel plate is fabricated in two equal sized pieces. Each steel plate is attached to the top rails of the soil-box using a combination of four 50 mm x 100 mm x 6 mm (2 in. x 4 in. x  $\frac{1}{4}$  in.) structural steel rectangular tubes in combination with 16 mm ( $\frac{5}{8}$  in.) high-strength bolts, washers, and nuts. The rectangular tubes act to stiffen the plate. Each plate is fabricated with a borehole near one end to allow for passage and access to the pneumatic diaphragm inflation components. When the pneumatic diaphragm is placed in the box and inflated it pushes back on the 12 mm ( $\frac{1}{2}$  in.) thick structural steel plates and the surface of the compacted soil. The pressure inside the pneumatic diaphragm dictates the load that is applied to the surface of the soil inside the soil-box. The Closed-Mount concept is shown in Photograph 3-2.



Photograph 3-2 Pullout Box with Closed-Mount

The second vertical reaction frame concept consists of an Elevated-Mount. The Elevated-Mount consists of structural steel tubing and 19 mm ( $\frac{3}{4}$  in.) high strength all-thread rods, washers, and nuts. Two-high strength all-thread rods are attached to the opposing side rails of the soil-box. The structural tubing is placed over the high strength threaded rod, so they bridge over and span between the soil-box side rails and act as a reaction beam. The distance that the reaction beam is above the soil surface, or the top of the soil-box, is adjustable using nuts and washers. Included in the Elevated-Mount system are two, 12 mm ( $\frac{1}{2}$  in.) structural steel plates that are slightly smaller than the plan surface of the soil-box. The plates are fabricated so there is 25 mm (1 in.) gap between the edge of the soil-box and the edge of the plate.

Each plate is fabricated with a bore hole near the front-middle edge to allow for passage and access to the pneumatic diaphragm inflation components. The steel plates are placed on top of the pneumatic diaphragm that is bearing on the soil surface. Placed on top of the 12 mm ( $\frac{1}{2}$  in.) steel plates are two stiffener beams consisting of 75 mm x 150 mm x 6 mm (3 in. x 6 in. x  $\frac{1}{4}$  in.) structural steel rectangular tubes. Spanning between the rectangular tubes, and at the same location as the reaction beam, are 75 mm x 150 mm x 6 mm (3 in. x 6 in. x  $\frac{1}{4}$  in.) structural steel rectangular beams. The structural steel stiffener beams are used to distribute the load equally to the surface of the steel plates that are on top of the pneumatic diaphragm. Depending on the anticipated loading there may be one to four elevated reaction beams spanning the top of the soil-box. When the pneumatic diaphragm is inflated it pushes up on the 12 mm ( $\frac{1}{2}$  in.) thick structural steel plates and beams. The pressure inside the pneumatic diaphragm dictates the load that is applied to the surface of the soil inside the soil-box. Load cells are used between the reaction beams and the structural steel beams to



adjust, record, and monitor the applied surface load. The Elevated-Mount system is shown in Photograph 3-3 and in Photograph 3-4.



Photograph 3-3 Vertical Elevated Reaction Frame (Side View)



Photograph 3-4 Vertical Elevated Reaction Frame (End View)

### 3.2.3 *Horizontal Load Frame*

The horizontal load frame consists of welded 50 mm x 100 mm x 6 mm (2 in. x 4 in. x 1/4 in.) structural steel tubing. The horizontal load frame is used to mount the hydraulic actuator that is used to apply the horizontal load to the soil-reinforcing. The lead end of the load frame is attached to the soil-box using 19 mm (3/4 in.) structural steel

bolts, washers, and nuts. The lead end of the hydraulic actuator is mounted to the load frame by passing the rod end of the hydraulic actuator through a slot between two structural steel columns. The hydraulic actuator is then attached to the load frame using a special mounting plate and flange plate in combination with 12 mm high-strength steel bolts. The hydraulic actuator body rests on a special platform that is welded to an adjustable scissors-jack. The scissors-jack, in combination with the slot, defined by the steel columns, allows the elevation of the hydraulic actuator to be adjusted. Once the hydraulic rod end is positioned at the required elevation, the flange plate is tightened. The load frame and hydraulic actuator is shown in Photograph 3-5.



Photograph 3-5 Horizontal Load Frame

#### 3.2.4 *Hydraulic Load System*

The horizontal load system consists of a two-way hydraulic cylinder. The hydraulic cylinder used in the test program consisted of a body with a 125 mm (5 in.) bore and a 50 mm (2 in.) threaded rod. The maximum extension force of the hydraulic cylinder using 21 MPa (3000 psi) line pressure is equal to 260 kPa (58,000 lbf). The maximum retraction force of the hydraulic cylinder, using the same line pressure, is

equal to 220 kN (50,000 lbf). The maximum stroke of the hydraulic cylinder is 455 mm (18 in.). Attached to the threaded rod-end is a load cell, clevis and connection clamping system. The cylinder is mounted to the horizontal reaction frame using flange mounting plates as described in Section 3.2.3, as detailed in Figure 3-3, and as shown in Photograph 3-6.

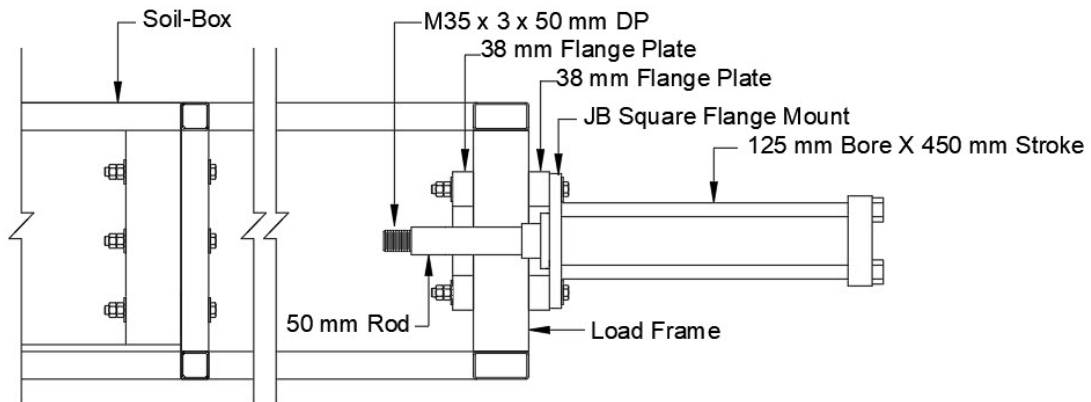


Figure 3-3 Cross Section at Horizontal Cylinder



Photograph 3-6 Horizontal Cylinder

### 3.2.5 *Clamping System*

The soil-reinforcing is clamped to the hydraulic actuator using a special compression clamp. The clamping system consists of two opposing harden steel plates. The harden steel plates are attached to the rod end using the clevis that is attached to the hydraulic cylinder rod-end. The connection is fabricated so the harden steel plates are free to rotate in all directions. Rotation of the connection components prevents uneven force application and allows the soil-reinforcing to displace freely. The inside surface of the connection plate is fabricated with a series of pointed serrations, like the hardened points that are on a steel file. Each of the steel connection plates are fabricated with a series of through-bores that allow for the attachments of all-thread bolts. The lower plate through-bores are threaded so all-thread bolts can be attached protruding through the top surface, then through the through-bores of the top plate. The soil-reinforcing element is compressed between the top and bottom serrated connection plate. A bearing element of the soil-reinforcing is typically positioned at the trailing edge of the top plate. Once the soil-reinforcing is placed in the connection plates, the plates are secured and tightened using a series of nuts.



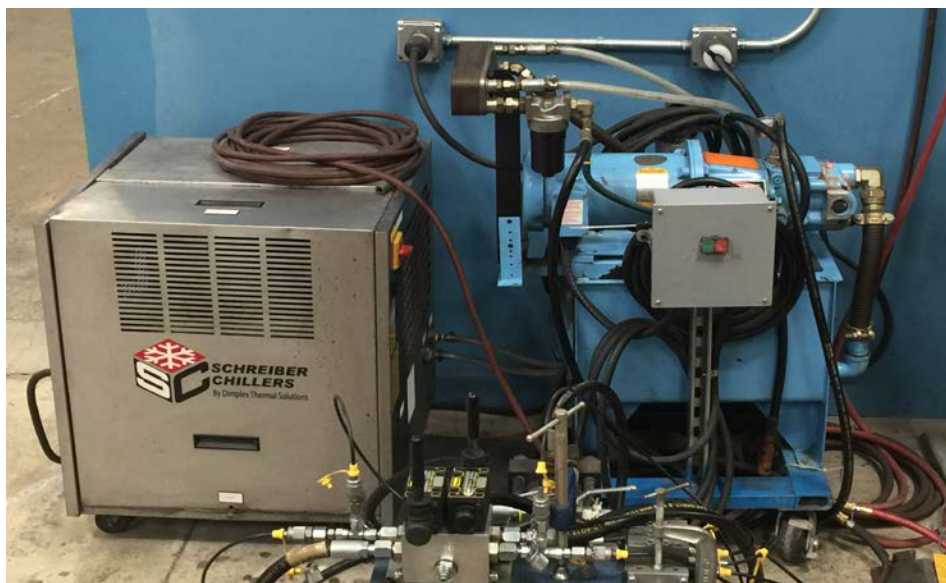
Photograph 3-7 Soil-Reinforcing Clamp (1)



Photograph 3-8 Soil-Reinforcing Clamp (2)

### 3.2.6 *Hydraulic System*

The hydraulic system consists of a power unit, flow controls and the hydraulic actuator. The power unit consists of a motor, hydraulic pump, and reservoir. The hydraulic system is placed in-line with a chiller. The chiller is used to cool the hydraulic fluid that is returned to the system before it is pumped back into the reservoir. The hydraulic unit and chiller is shown in Photograph 3-9.



Photograph 3-9 Hydraulic Power Unit and Chiller

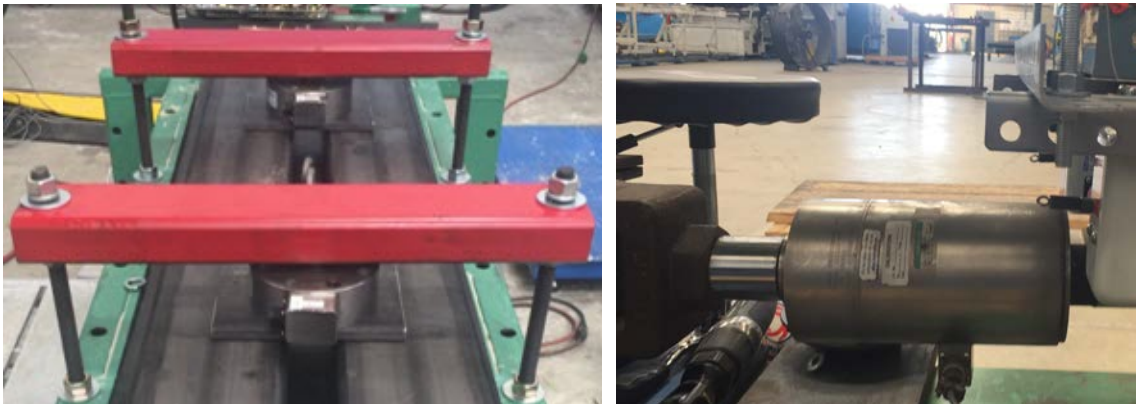
The hydraulic flow control consists of a series of directional control valves and flow reducers. The hydraulic system has been designed to allow for manual adjustment of the rate of retraction of the rod-end. The rate of retraction of the rod-end for this experimental test program varied from 1 mm/min to 3 mm/min. The rate of retraction varied due to system environmental fluctuations. Because of the large diameter bore of the cylinder, the amount of fluid required to retract the cylinder at a rate of 1 mm/min was very small. Any fluid that was not used was pushed back into the power unit. This movement of fluid through a reduced diameter hose, in combination with the pushing of excess fluid, generated a substantial amount of heat. The in-line chiller was added to the system to manage the heat variation of the fluid. The chiller is shown in Photograph 3-9. The flow control system is shown in Photograph 3-10.



Photograph 3-10 Hydraulic Flow Control System

### 3.2.7 Load Cells

The horizontal load cell that is used to measure the force applied to the soil-reinforcing consists of an Omega Cannister Load-Cell, type LC1102-25k. One end of the load cell is attached to the horizontal actuator rod end and the other end is attached to a rod extender that is then attached to a clevis. The vertical load cells consist of Omega Low-Profile Pancake load cells, type LCHD-15K. The vertical load cells are placed between the reaction frame and the structural steel beams above the pneumatic diaphragm. The vertical and horizontal load cells are shown in Photograph 3-11.



Vertical

Horizontal

Photograph 3-11 Load Cells

### 3.2.8 Position Sensors

There are two different position transducers used with the pullout soil-box. These include a Linear Variable Differential Transformer (LVDT) and a wire-rope potentiometer. Both transducers are mounted outside the soil-box at strategic locations. The position sensors monitor the displacement of the soil-reinforcing during application of the load.

LVDT's are electromechanical sensors that convert rectilinear motion of an object into a corresponding electrical signal. The LVDT consists of a housing and an armature. The armature passes in and out of the housing through a central core in a rectilinear

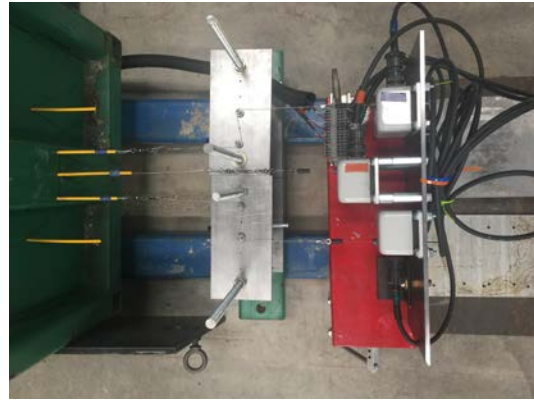
motion. As the armature moves in and out of the housing core it passes between a series of primary and secondary copper coil windings. The coil's primary winding is excited by alternating current at a predetermined amplitude and frequency. As the position of the armature changes in the central core, between the windings, an electrical output signal consisting of differential AC voltage is created. The electrical signal is read by the data acquisition module and converted into a unit of length. The LVDT's are type TR-100 manufactured by Novotechnik. The LVDT's are mounted at the front of the soil-box and are used to measure the displacement of the soil-reinforcing at the location of the connection clamp.

The potentiometer consists of an extensible wire rope that is contained in a housing. The end of the extensible wire rope is attached to the soil-reinforcing by passing it through bicycle cable housings. The bicycle cable housing prevents the soil pressure from being transferred to the wire attached to the soil-reinforcing element. As the soil-reinforcing displaces in the soil, the wire rope is pulled from the housing through the cable housing. As the wire rope extends it rotates an internal cylinder, called a capstan, about a sensing device. The rotation of the capstan about the sensing device produces an electrical output signal that is proportional to the wire rope extension. The electrical signal is read by the data acquisition module and converted into a unit of length. In the capstan an internal torsion spring is used to apply and maintain tension on the wire rope as it extends from the housing. The addition of tension to the wire rope allows it to retract back into the housing after the load is removed or during fluctuation of the load. The potentiometers used in this research project were manufactured by Unimeasure and are a type PA-4-S10-N1S-10C. The position sensors are shown in Photograph 3-12.





LVDT – Front of Soil-Box



Wire Rope – Back of Soil-Box

Photograph 3-12 Position Sensors

### 3.2.9 *Inflatable Pneumatic Diaphragm*

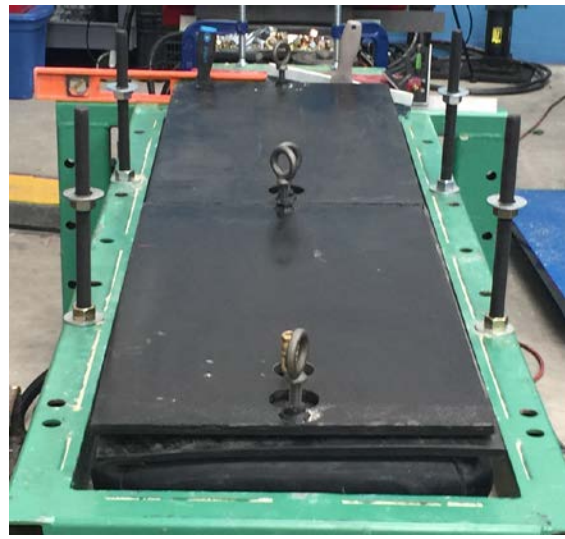
The inflatable pneumatic diaphragm was specifically manufactured for this application. The inflatable pneumatic diaphragm was manufactured by Matjack of Indianapolis, Indiana. The inflatable pneumatic diaphragm was manufactured to have flat sides to prevent binding in the soil-box. The profile of the inflatable pneumatic diaphragm was manufactured so it was less than the plan area of the soil-box chamber, i.e. 430 mm x 1500 mm (17 in. x 59 in.), by 25 mm (1 in.), in both length and in width and was equal to 405 mm x 1475 mm (16 in. x 58 in.). The smaller profile area prevents binding of the pneumatic diaphragm on the sides of the soil-box in the chamber during inflation. The pneumatic diaphragm was manufactured to be able to provide a simulated overburden pressure equal to 180 kPa (26 psi) for a depth equal to 9 m (30 ft.).

The pressure in the inflatable pneumatic diaphragm was controlled using a fine thread pressure regulator attached to an Omega general purpose pressure gauge, type DPG8000. The air-pressure could be controlled to within 68 Pa (0.01 psi). Attached in line, and near the inflatable pneumatic diaphragm, was a secondary pressure gauge that was used to verify the pneumatic diaphragm pressure. In addition to using line pressure,

and the pneumatic diaphragm pressure, load cells were used in the Elevated-Mount reaction frame method. The inflatable pneumatic diaphragm for the large soil-box is shown in Photograph 3-13. The inflatable pneumatic diaphragm for the small soil-box and the inflation control system are shown in Photograph 3-14.



Pnumeatic Diaphragm



Pnumeatic Diaphragm with Lid

Photograph 3-13 Inflatable Pneumatic Diaphragm Large Soil-Box



Pnumeatic Diaphragm – Small Soil-Box



Pnumeatic Control

Photograph 3-14 Inflatable Pneumatic Diaphragm

### 3.2.10 Data Acquisition System

The data acquisition system consists of Campbell Scientific components and software program. The datalogger consisted of a CR10X Wiring Panel. The wiring panel provided sensor measurements, timekeeping, data reduction, data/program storage and control functions. In addition to the CR10X, the AVW4 amplification and signal conditioning system was used to connect to vibrating-wire transducers. To collect the data the Campbell Scientific, PC400 datalogger software was used. The data acquisition system is shown in Photograph 3-15.



Photograph 3-15 Data Acquisition system

### 3.3 2-Wire Soil-Reinforcing Element

The soil-reinforcing used in the experimental test program consisted of 2-Wire soil-reinforcing elements. The 2-Wire soil-reinforcing elements were manufactured using cold drawn steel wire in conformance with ASTM A1064 and then hot-dip galvanized in conformance with ASTM A123. Three longitudinal element spacings were used for the 2-Wire elements and include, 50 mm, 100 mm, and 200 mm. Two different transverse element spacings for each of the longitudinal element spacings was used and consisted of 150 mm and 300 mm. The tests were set up so 8, 4, and 1 transverse wires were

contained in the soil-box. The transverse element of the 2-Wire system was always placed in the up position. The placement of the transverse element in the up position insured that the transverse element could not interact with the bottom sleeve of the exit gate in the soil-box. The 2-Wire soil-reinforcing elements for this research program are shown in Figure 3-4 and described in Table 3-1.

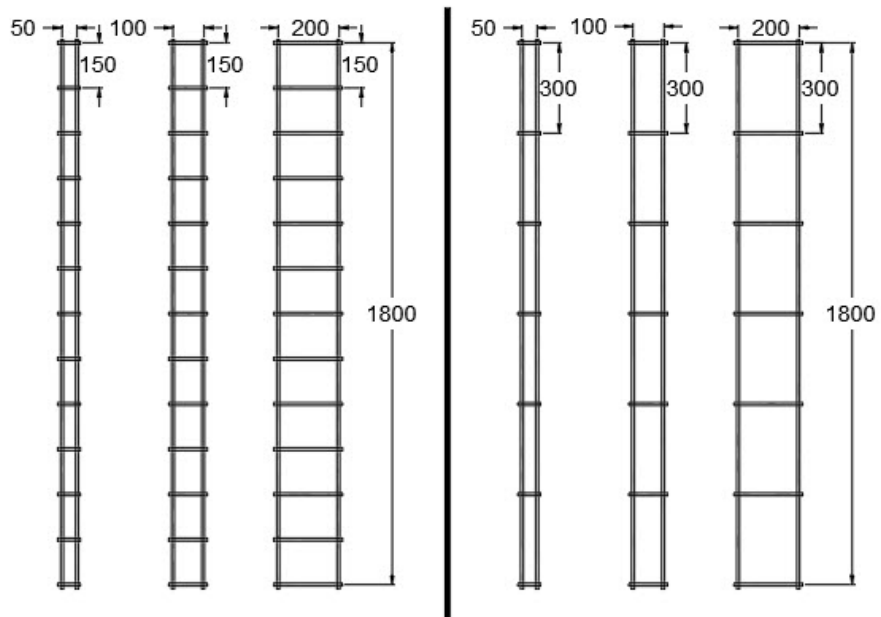


Figure 3-4 Plan View 2-Wire Soil-Reinforcing Elements

Table 3-1 2-Wire Soil-Reinforcing Element Description

| Test | Longitudinal Size | Transverse Size | Longitudinal Space (mm) | Transverse Space (mm) | Embedment Length (mm) |
|------|-------------------|-----------------|-------------------------|-----------------------|-----------------------|
| 1    | MW71              | MW71            | 50                      | 300                   | 1220                  |
| 2    | MW71              | MW71            | 100                     | 300                   | 1220                  |
| 3    | MW71              | MW71            | 200                     | 300                   | 1220                  |
| 4    | MW71              | MW71            | 50                      | 150                   | 1220                  |
| 5    | MW71              | MW71            | 100                     | 150                   | 1220                  |
| 6    | MW71              | MW71            | 200                     | 150                   | 1220                  |

Table 3-1 2-Wire Soil-Reinforcing Element Description

| Test | Longitudinal Size | Transverse Size | Longitudinal Space (mm) | Transverse Space (mm) | Embedment Length (mm) |
|------|-------------------|-----------------|-------------------------|-----------------------|-----------------------|
| 7    | MW45              | MW45            | 50                      | 300                   | 1220                  |
| 8    | MW45              | MW45            | 100                     | 300                   | 1220                  |
| 9    | MW45              | MW45            | 200                     | 300                   | 1220                  |
| 10   | MW45              | MW45            | 50                      | 150                   | 1220                  |
| 11   | MW45              | MW45            | 100                     | 150                   | 1220                  |
| 12   | MW45              | MW45            | 200                     | 150                   | 1220                  |
| 13   | MW71              | MW71            | 50                      | 1-Wire                | 300                   |
| 14   | MW71              | MW71            | 100                     | 1-Wire                | 300                   |
| 15   | MW71              | MW71            | 200                     | 1-Wire                | 300                   |
| 16   | MW45              | MW45            | 50                      | 1-Wire                | 300                   |
| 17   | MW45              | MW45            | 100                     | 1-Wire                | 300                   |
| 18   | MW45              | MW45            | 200                     | 1-Wire                | 300                   |

### 3.4 Pullout Study Soil

The soil used for the experimental test program consisted of a sand obtained in Jacksonville, Florida. The sand was classified as SP, in conformance with the Unified Soil Classification. The sand gradation and strength parameters are shown in Figure 3-5 and in Table 3-2 and Table 3-3. This material was selected to be used in the pullout study because it is a lower-bound material that is used as backfill in MSE structures. Based on this, the results that are developed from this experimental testing program can conservatively be used with other higher-bound material.

The target compaction for each of the tests was set equal to 95% of standard proctor in conformance with ASTM D698. The density of the sand for each pullout test was determined based on the use of a volume relationship. The plan area of the soil-box

is fixed and only the height of soil volume was required to be determined. The required height of the volume of soil was calculated based on the unit weight of the sand required to achieve a 95% density, divided by the plan area as shown in Equation 3-1. The unit weight of the soil was calculated based on a target weight at the optimum moisture content.

$$H_s = 0.95 \cdot \frac{A_{sb}}{\gamma_d \cdot \left(1 + \frac{w_{opt}}{100}\right)} \quad \text{Equation 3-1}$$

Where:

- $H_s$  = Height of soil column (m)
- $A_{sb}$  = Plan area of soil-box (m<sup>2</sup>)
- $\gamma_d$  = Dry unit weight of soil (kN/m<sup>3</sup>)
- $w$  = optimum moisture content (%)

Based on this methodology the sand was placed in 9-20 litre buckets (5-gallon bucket) with equal soil weight. Typically, each 20-litre bucket contained 0.33 kN (75 lbf) of soil for a total soil weight of 3 kN (675 lbf). The soil was weighed using a low-profile floor scale and digital readout.

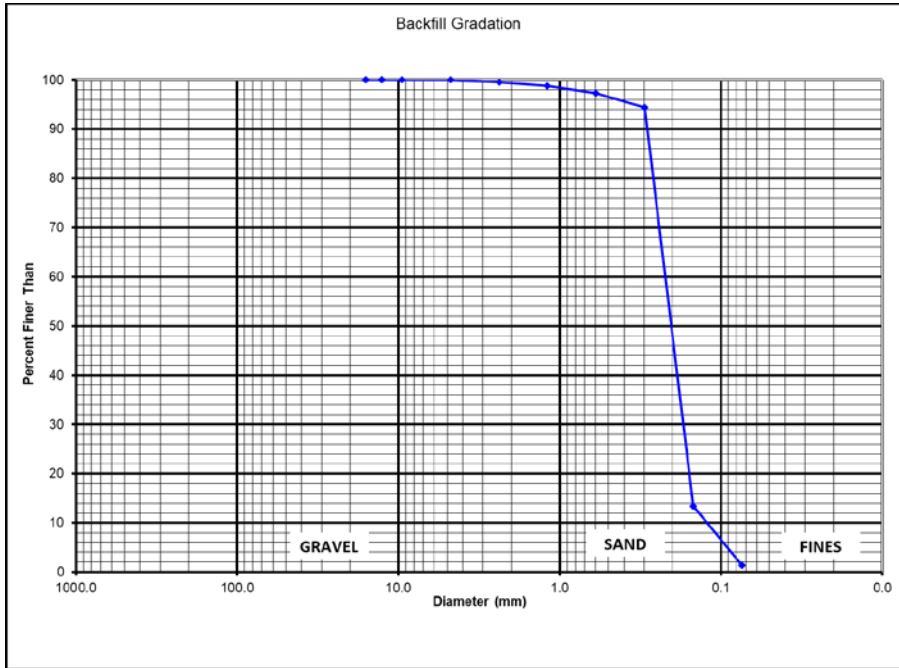


Figure 3-5 Backfill Gradation Curve

Table 3-2 Backfill Gradation (Florida Sand)

| Nominal Opening       |                       | Percent Passing<br>by Weight<br>(%) |
|-----------------------|-----------------------|-------------------------------------|
| Sieve<br>Size<br>(US) | Sieve<br>Size<br>(mm) |                                     |
| 1.000                 | 25.4                  | 100                                 |
| 0.750                 | 16.0                  | 100                                 |
| 0.500                 | 12.7                  | 100                                 |
| 0.375                 | 9.51                  | 100                                 |
| 0.187                 | 4.76                  | 100                                 |
| 0.0937                | 2.38                  | 99.6                                |
| 0.0496                | 1.19                  | 98.8                                |
| 0.0234                | 0.595                 | 97.3                                |
| 0.0117                | 0.297                 | 94.4                                |
| 0.0059                | 0.149                 | 13.38                               |
| 0.0029                | 0.074                 | 1.4                                 |

Table 3-3 Backfill Properties (Florida Sand)

| D <sub>10</sub><br>(mm) | D <sub>30</sub><br>(mm) | D <sub>60</sub><br>(mm) | C <sub>u</sub> | C <sub>c</sub> | Class | Dry Unit Weight<br>(kN/m <sup>3</sup> ) | Optimum Moisture Content<br>(%) | Bulk Unit Weight<br>(kN/m <sup>3</sup> ) | Peak Friction Angle<br>(deg) | Dilatancy<br>(deg) |
|-------------------------|-------------------------|-------------------------|----------------|----------------|-------|---|---------------------------------|--|------------------------------|--------------------|
| 1.4                     | 1.8                     | 2.3                     | 1.64           | 1.00           | SP    | 15.35                                   | 16.8                            | 17.93                                    | 44                           |                    |

The internal friction angle of the soil was determined by the Direct Shear (DST) test in conformance with ASTM D3080. The tests were performed at Texas A&M University (TAMU). The direct shear tests were performed using a Geocomp, Large ShearTrac III system. The DST was performed at 14% optimum moisture and compacted to 95% density. The DST were performed at a normal stress equal to 10, 30, and 50 KPa. The 10 kPa DST was performed three times as a measure of the repeatability of the test. Based on the TAMU DST program the peak friction angle was determined to be equal to 44 degrees with 0.44 kPa cohesion and the residual friction angle was determined to be equal to 41 degrees with 0.90 kPa cohesion.

### 3.5 Test Set-Up - Parametric Program

The pullout test requires accuracy, predictability and repeatability. A parametric study was performed to limit and understand the effects of boundary conditions associated with the experimental testing program. A parametric study was performed to determine a method of soil placement to achieve a consistent density. In addition, a parametric study was completed to determine the application of the vertical overburden pressure.

#### 3.5.1 Soil Density

The density of the soil in the soil-box is a function of the soil moisture content and the method that is used to place and compact it. The target moisture content for this



experimental test program was based on the standard proctor test. The results of the proctor test determined that the optimum moisture content was equal to 16%. At the beginning of each day's testing, the moisture content of the soil was tested. Then, at a minimum, the moisture content was tested two additional times during the day. The moisture content was determined using a Speedy Moisture Tester by Humboldt Mfg. Co. as shown in Photograph 3-16. The moisture test was performed in conformance with the Florida Department of Transportation test method, FM5-507 - *Method of Test for Determination of Moisture Content by Means of a Calcium Carbide Gas Pressure Moisture Tester*. Corrections to the measured moisture from the Speedy Tester were adjusted based on the requirements of FM5-507. When necessary, water was added to the soil to keep the soil within a range of -2% of optimum. To prevent the soil from drying out it was always stored in containers with sealed lids.

A parametric study was used to develop a method of soil placement to assure that the density of the soil was uniform in each lift and in each test. The density of the soil in the soil-box was verified using the Sand-Cone method in conformance with ASTM D1556 Standard Test Method for Density and Unit Weight of Soil in Place by Sand-Cone Method. The final method that was selected for placing the soil for the experimental test program was verified by placing and measuring the density in three separate lift placements. In addition, for the first 10 tests, a sand-cone test (Photograph 3-16) was performed to verify that the method was working. Thereafter, a minimum of one sand-cone test per day was performed to verify the method specification was still performing as required.



Photograph 3-16 Speedy Moisture Test Kit and Sand Cone Test

The method used to place the soil was based on a volume to weight ratio. To achieve the required density in the soil-box, it was determined that the soil was required to be placed and compacted in three lifts of equal weight. The soil weight was verified using an industrial floor scale. The scale was calibrated each day using a 50-kg calibrated weight. The soil was compacted using a Bosh-Hammer Drill outfitted with a 250 mm compaction plate. The soil was dumped, spread, and levelled manually. Once the surface was levelled it was compacted using the Bosh-Hammer Drill to a known thickness. This typically required that the hammer be passed over the soil surface twice.

The tested soil had a dry density equal to  $15.35 \text{ kN/m}^3$  (97.7 pcf) and an optimum moisture content equal to 16.8%. The unit weight of the soil at 100% density was equal to  $17.93 \text{ kN/m}^3$  (114.1 pcf). As previously stated, the soil was placed and compacted in

three identical lift thicknesses. Each compacted soil lift thickness was calculated based on the relationship shown in Equation 3-2.

$$t_{lift} = \frac{P_{soil}}{\sigma_{soil} \cdot A_{box}} \quad \text{Equation 3-2}$$

Where:

|                 |   |  |
|-----------------|---|--|
| $t_{lift}$      | = | Thickness of lift (mm)                       |
| $P_{soil}$      | = | Weight of soil to be placed (kN)             |
| $\sigma_{soil}$ | = | Unit weight of the soil (kN/m <sup>3</sup> ) |
| $A_{box}$       | = | Area of the soil-box (m <sup>2</sup> )       |

Before placement of each lift of soil the sides of the soil-box were marked with an indicator-line. The indicator-line was placed at a distance above the in-place soil equal to the required lift thickness,  $t_{lift}$ . This soil was compacted to the elevation of this line to assure that the soil density was 95% of optimum.

### 3.5.2 Vertical Load

The Elevated-Mount reaction frame was selected for use in the experimental testing program. This was based on parametric tests performed using both the Closed-Mount and Elevated-Mount. A total of eight tests were performed to determine the reaction frame system to use. For the parametric study a 2-Wire element with longitudinal spacing equal to 50 mm and transverse spacing equal to 300 mm was used in each of the tests. All eight of the tests were performed using a simulated soil depth equal to 1.524 (5 ft.). Four tests were performed for the Closed-Mount system and four tests were performed for the Elevated-Mount system. The method-specification was developed to assure that a consistent test set-up and soil density was used for each parametric test. For the parametric tests, the soil-reinforcing was pulled at an average

rate of 2 mm/min. For two of tests in each of the vertical load methods, i.e., closed-mount and elevated-mount, the sides of the soil-box were covered with a sheet of 4-mil plastic. For the closed-mount tests, the gauge pressure from the pneumatic diaphragm was used to set and monitor the required overburden pressure. For the Elevated-Mount tests two load cells were used to set and monitor the required overburden pressure. The results of the test are shown in Table 3-4.

Table 3-4 Vertical Reaction Frame Parametric Test Results

| Test | Mount    | Side    | Pullout Force (kN) |
|------|----------|---------|--------------------|
| 1    | Closed   | Plastic | 3.3                |
| 2    | Closed   | Plastic | 4.0                |
| 3    | Closed   | None    | 2.2                |
| 4    | Closed   | None    | 3.6                |
| 5    | Elevated | Plastic | 4.4                |
| 6    | Elevated | Plastic | 3.8                |
| 7    | Elevated | None    | 3.9                |
| 8    | Elevated | None    | 4.7                |

Table 3-5 Vertical Reaction Frame Parametric Test Statistics

| Test     | Min | Max | Mean | Std  | COV  |
|----------|-----|-----|------|------|------|
| Closed   | 2.2 | 4.0 | 3.3  | 0.77 | 0.24 |
| Elevated | 3.8 | 4.7 | 4.3  | 0.42 | 0.10 |

Based on the parametric tests it was determined that the Elevated-Mount provided the best repeatability. Furthermore, it was determined that the soil-box interface had no effect on the application of the load to the soil-reinforcing. Therefore, the Elevated-Mount was selected, and the soil was placed in the soil-box without the 4-mil sheet plastic liner.

### 3.6 Test Set-Up

The test set-up for the pullout test was sequential and repetitive. A series of controlled parametric test set-up procedures were determined prior to beginning the test program. To limit test-set up bias, the required steps for each test were followed. Furthermore, to limit set-up bias, all tests in the experimental test program were completely set-up and performed by the author of this dissertation. The set-up sequence is shown in the Appendix B. For each of test set-up steps provided in the Appendix B, a picture is provided when appropriate. A general set-up procedure that has been modified from the test set-up defined in ASTM D 6706, *Standard Test Method for Measuring Geosynthetic Pullout Resistance in Soil*, is given in the following subsections.

#### 3.6.1 *Prepare Bottom-Half of Soil-Box*

Assemble the soil-box with only the bottom half of the exit gate in place. Calculate the weight and volume of soil that is necessary to attain the required moist unit weight of the soil when placed in the lower half of the soil-box. When the soil is placed in the bottom of the soil-box it should be placed so that it is slightly above the exit gate sleeve (approximately 10 mm (0.4 in.)). This will prevent the soil-reinforcing from dragging on the exit gate sleeve. Place and compact the soil in the bottom of the soil-box using the method specification. After compaction, the soil surface should be leveled.



Photograph 3-17 Preparation of Bottom Half of Soil-box

### 3.6.2 *Place Soil-Reinforcing Element*

Place the soil-reinforcing in the soil-box so it is in the center of the soil-box and so the terminal end is at the required distance from the back-face of the soil-box.

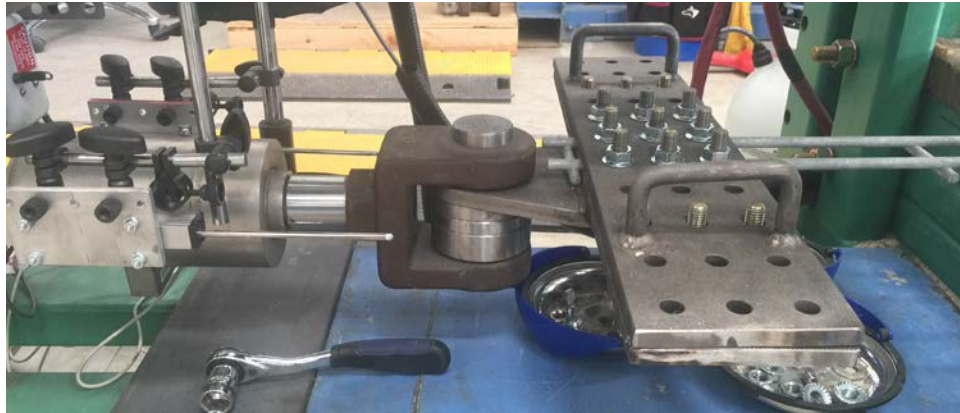
Measure the location of the soil-reinforcement and record.



Photograph 3-18 Placement of Soil-Reinforcing in Soil-Box

### 3.6.3 *Clamp Soil-Reinforcing*

Place the soil-reinforcement in the connection-clamp. The lead-end of the transverse wire should be positioned so it is behind, and in contact with, the trailing edge of the connection-clamp. Place the top plate of the connection-clamp over the threaded bolts. Verify that the soil-reinforcing is centred in the connection-clamp. Secure the top plate using the nuts and the air impact wrench. The nuts should be finger tight, then tightened using the air impact wrench. Remeasure the location of the soil-reinforcing in the soil-box and re-center as required.



Photograph 3-19 Placement of Soil-Reinforcing in Soil-Box

#### 3.6.4 *Position Sensors*

Place and attach the LVDT's at the front of the soil-box, at the location of each side of the connection clamp. Connect the wire-rope potentiometers to the soil-reinforcing element in the soil-box. Verify that the bicycle brake housing cables each wire-rope is contained in are as close to the soil-reinforcing as possible. Remove all slack from the wire rope potentiometers.



Photograph 3-20 Placement of Position Sensors



### 3.6.5 *Prepare Top-Half of the Soil-Box*

Place the spacer on the bottom exit gate sleeve at the interface of the side of the soil-box and then place the top exit gate sleeve on the spacer. Assure that the gap formed between the top and bottom sleeves is unobstructed. In the slots place the remaining top half of the exit gate, i.e., the 50 mm structural steel tubes. Calculate the weight and volume of soil that is necessary to attain the required moist unit weight of the soil when placed in the upper half of the soil-box. Place and compact the soil in the top of the soil-box using the method specification. After compaction the soil surface should be leveled.



Photograph 3-21 Placing Exit Gate



Photograph 3-22 Placing and Compacting Soil



Photograph 3-23 Level Soil Surface

### 3.6.6 *Apply Overburden Pressure*

Place the rubber bearing pad on the soil surface at the top of the soil-box and center (Photograph 3-24). The neoprene bearing pad should be placed so it is approximately 12 mm from all edges of the soil-box. Place the pneumatic diaphragm and center on the neoprene bearing pad (Photograph 3-24). Place the second neoprene bearing pad on top of the pneumatic diaphragm. Place the steel plates on the top neoprene bearing pad and center (Photograph 3-25). Place the reaction frame components on the steel plates and center so they are symmetric about the center-lines of the soil-box. Place the load cells on the small reaction frame cross beams and center (Photograph 3-25). Apply the required normal pressure by using the pneumatic diaphragm inflation system (Photograph 3-26).



Photograph 3-24 Reaction Frame Set-Up



Photograph 3-25 Reaction Frame Set-Up



Photograph 3-26 Apply Overburden Pressure

### 3.6.7 *Pullout Test*

The pullout test is initiated by applying a small seating load with the pullout force device. This is followed by zeroing the gauge readings. The system is set so it will pull at a constant rate of displacement. The soil-reinforcing is then loaded by initiating the system. The soil reinforcing is loaded until failure, or until pullout occurs, or until the predetermined displacement has been reached. The test is halted and the maximum pullout load and mode of failure are recorded.



Photograph 3-27 Apply Overburden Pressure

### 3.6.8 Post Pullout Test

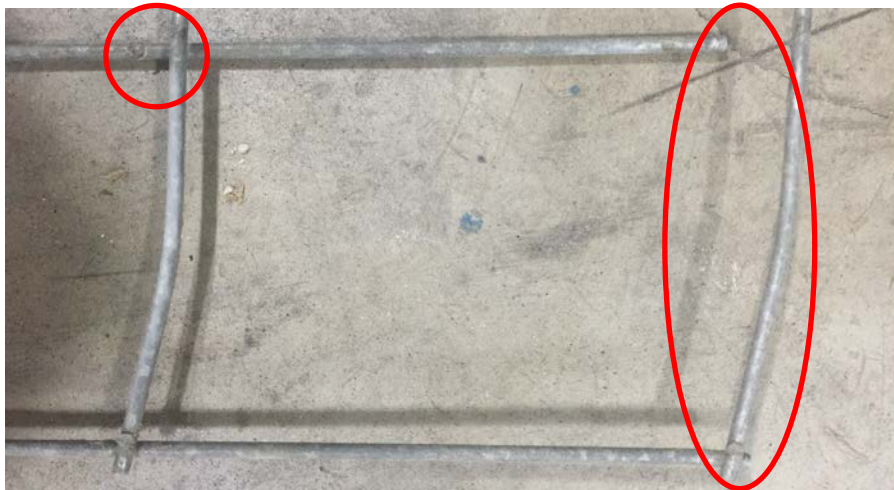
After the test is completed the normal stress is removed and the reaction frame and vertical load device are disassembled. The soil is removed from the soil-box using a large aluminium scoop to the elevation of the soil-reinforcing element. The removed soil is placed back in the 20-litre buckets to the required weight. The 20-litre buckets of soil are placed the floor scale, covered, and sealed with the bucket lid. The soil-reinforcing is inspected, photograph, and any system failures noted, i.e., weld failure, bar deformation, etc.



Photograph 3-28 Exhuming Soil-Reinforcing Element After Test



Photograph 3-29 Exhumed Soil-Reinforcing Element After Test



Photograph 3-30 Exhumed Soil-Reinforcing Showing Weld Failure

### 3.6.9 *Repeat Test*

The procedure is repeated as required under additional overburden pressures until the required number of tests have been performed.

## Chapter 4

### Experimental Test Program Results

#### 4.1 Introduction

In Chapter 4 the test results for the experimental test program are presented. The soil-reinforcing used in the experimental test program consisted of discrete, 2-Wire soil-reinforcing elements. Details and descriptions of the 2-Wire soil-reinforcing elements used in the experimental test program were provided in Section 3.3. The data presented in Chapter 4 should be supplemented with the information provided in Appendix-A. Appendix-A includes a detailed presentation of the data that was collected for each test in the experimental test program. Each pullout test was performed in sand using the state-of-practice ASTM D6706 pullout apparatus described in Section 3.2.

#### 4.2 Test Matrix

The experimental testing program was organized into test groups, sets, and subsets. The groups, sets, and subsets were classified according to the 2-Wire element size and configuration. Two different groups of 2-Wire element sizes were tested. These included an MW71 (W11) and MW45 (W7.0). The test groups were separated based on the element size, i.e., Group-1 (MW71) and Group-2 (MW45). Each group was divided into three sets based on the spacing of the transverse element. The 2-Wire transverse element spacings that were tested included 300 mm (12 in.), 150 mm (6 in.), and elements with only one cross wire (1W). The sets were Set-1 (300 mm), Set-2 (150 mm) and Set-3 (1W). Each set was subdivided into three subsets. The subsets were classified according to the 2-Wire longitudinal element spacing. The 2-Wire longitudinal element spacings that were tested consisted of 50 mm (2 in.), 100 mm (4 in.), and 200

mm (8 in.). The subsets were Subset-1 (50 mm), Subset-2 (100 mm) and Subset-3 (200 mm). The Group-1 test matrix is shown in Table 4-1 and the Group-2 test matrix is shown in Table 4-2. A total of 142 pullout tests were performed.

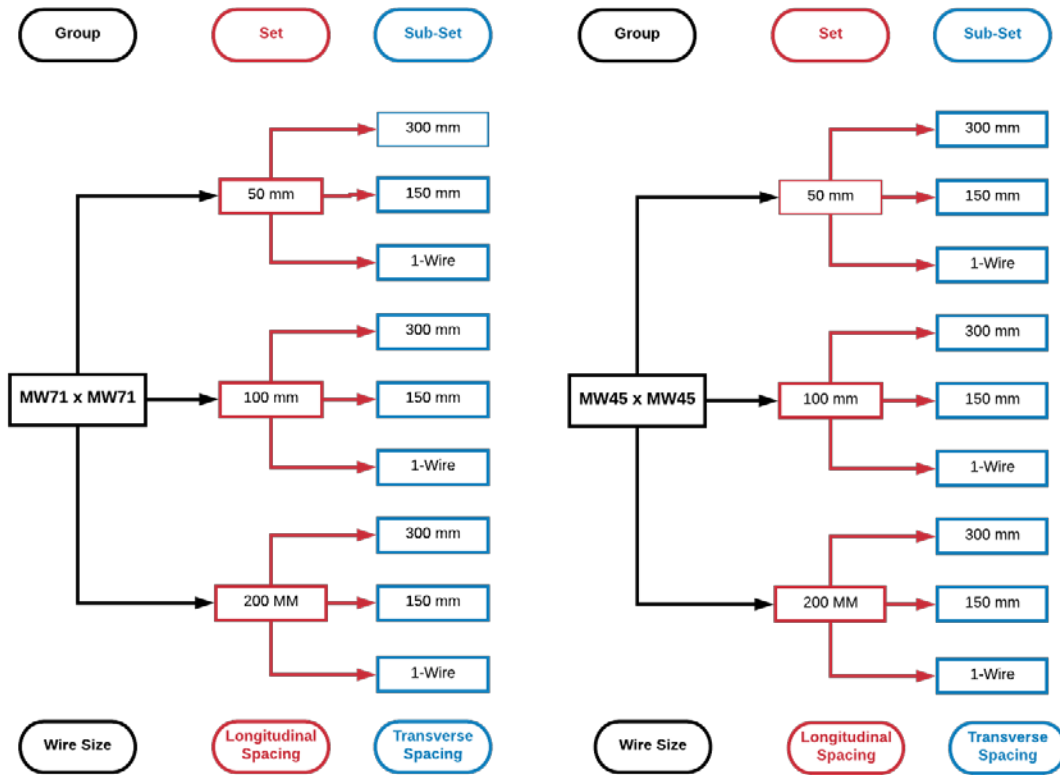


Figure 4-1 2-Wire Soil-Reinforcing Element Experimental Test Matrix

Table 4-1 Test Matrix for 2-Wire Element - Group MW71 (W11)

| Set | Subset | Test | Longitudinal Size | Transverse Size | Longitudinal Space (mm) | Transverse Space (mm) | Embedment Length (mm) | Number of tests |
|-----|--------|------|-------------------|-----------------|-------------------------|-----------------------|-----------------------|-----------------|
| 1   | 1      | 1    | MW71              | MW71            | 50                      | 300                   | 1220                  | 17              |
|     | 2      | 2    | MW71              | MW71            | 100                     | 300                   | 1220                  | 7               |
|     | 3      | 3    | MW71              | MW71            | 200                     | 300                   | 1220                  | 11              |
| 2   | 1      | 4    | MW71              | MW71            | 50                      | 150                   | 1220                  | 6               |
|     | 2      | 5    | MW71              | MW71            | 100                     | 150                   | 1220                  | 7               |
|     | 3      | 6    | MW71              | MW71            | 200                     | 150                   | 1220                  | 6               |



Table 4-1 Test Matrix for 2-Wire Element - Group MW71 (W11)

| Set | Subset | Test | Longitudinal Size | Transverse Size | Longitudinal Space (mm) | Transverse Space (mm) | Embedment Length (mm) | Number of tests |
|-----|--------|------|-------------------|-----------------|-------------------------|-----------------------|-----------------------|-----------------|
| 3   | 1      | 13   | MW71              | MW71            | 50                      | 1-Wire                | 300                   | 8               |
|     | 2      | 14   | MW71              | MW71            | 100                     | 1-Wire                | 300                   | 7               |
|     | 3      | 15   | MW71              | MW71            | 200                     | 1-Wire                | 300                   | 7               |

Table 4-2 Test Matrix for 2-Wire Element - Group MW45 (W7)

| Set | Subset | Test | Longitudinal Size | Transverse Size | Longitudinal Space (mm) | Transverse Space (mm) | Embedment Length (mm) | Number of tests |
|-----|--------|------|-------------------|-----------------|-------------------------|-----------------------|-----------------------|-----------------|
| 1   | 1      | 7    | MW45              | MW45            | 50                      | 300                   | 1220                  | 8               |
|     | 2      | 8    | MW45              | MW45            | 100                     | 300                   | 1220                  | 7               |
|     | 3      | 9    | MW45              | MW45            | 200                     | 300                   | 1220                  | 8               |
| 2   | 1      | 10   | MW45              | MW45            | 50                      | 150                   | 1220                  | 7               |
|     | 2      | 11   | MW45              | MW45            | 100                     | 150                   | 1220                  | 9               |
|     | 3      | 12   | MW45              | MW45            | 200                     | 150                   | 1220                  | 6               |
| 3   | 1      | 16   | MW45              | MW45            | 50                      | 1-Wire                | 300                   | 8               |
|     | 2      | 17   | MW45              | MW45            | 100                     | 1-Wire                | 300                   | 7               |
|     | 3      | 18   | MW45              | MW45            | 200                     | 1-Wire                | 300                   | 6               |

#### 4.3 General Test Procedure for 2-Wire Element

Each sub-set was tested at overburden depths equal to 300 mm (1 ft.), 1525 mm (5 ft.), 3050 mm (10 ft.), 4575 mm (15 ft.) and 6100 mm (20 ft.). The overburden pressures for each of the corresponding depths was equal to 6 kPa (125 psf), 30 kPa (625 psf), 60 kPa (1250 psf), 90 kPa (1875 psf), and 120 kPa (2500 psf). The overburden pressure was applied using the pneumatic diaphragm and the Elevated-Mount reaction frame described in Section 3.2.2. The overburdened pressure was controlled using a pressure regulator system that was described in Section 3.2.9. The overburden pressure was measured by the vertical load cells described in Section 3.2.7.

The Campbell Scientific PC400 software module described in Section 3.2.10 recorded the overburden pressure.

The horizontal pullout force was applied using the hydraulic load system described in Section 3.2.4. The horizontal pullout force was applied at a prescribed retraction rate of 1 mm/min. Because of environmental factors, such as the temperature of the hydraulic fluid, the rate of application of the horizontal pullout force varied from ½ mm/min to 3 mm/min. Based on the frictional, gradation, moisture, and drainage characteristics of the sand soil used in the test program, it was determined that the variation in the rate of application of the horizontal pullout force did not affect the results of the test.

The displacement of the 2-Wire element was recorded using the LVDT's described in Section 3.2.8 that were positioned on each side of the connection clamp at the front of the soil-box. As described in Section 3.2.8, three wire-rope potentiometers were used to monitor the displacement of the 2-Wire element inside the soil-box. Two of the wire-rope potentiometers were placed at the location of the welds that join the longitudinal element to the transverse element. The third wire-rope potentiometer was placed at the midpoint of the transverse element as shown in Photograph 4-1.



Photograph 4-1 Wire Rope Potentiometers on 50 mm, 100 mm, and 200 mm Element

In conformance with ASTM D-6706, the front LVDT displacement points were used as the limiting criteria for the determination of the maximum pullout force. The maximum pullout force was recorded at 19 mm (3/4 in.) of displacement. If the maximum pullout force occurred before the 19 mm (3/4 in.) displacement, it was recorded as the maximum pullout force. Each test was performed to a maximum displacement of 38 mm (1 1/2 in.). The maximum pullout force at 19 mm (3/4 in.) and 38 mm (1 1/2 in.) was recorded for each of the pullout tests.

Data from a typical pullout test showing the displacement of the soil-reinforcing as measured from the front of the soil-box is shown in Figure 4-2. Data from a typical pullout test showing the displacement of the soil-reinforcing inside the soil-box is shown in Figure 4-3. Data showing the maximum pullout force for a complete set of pullout tests for a subset is shown in Figure 4-4.

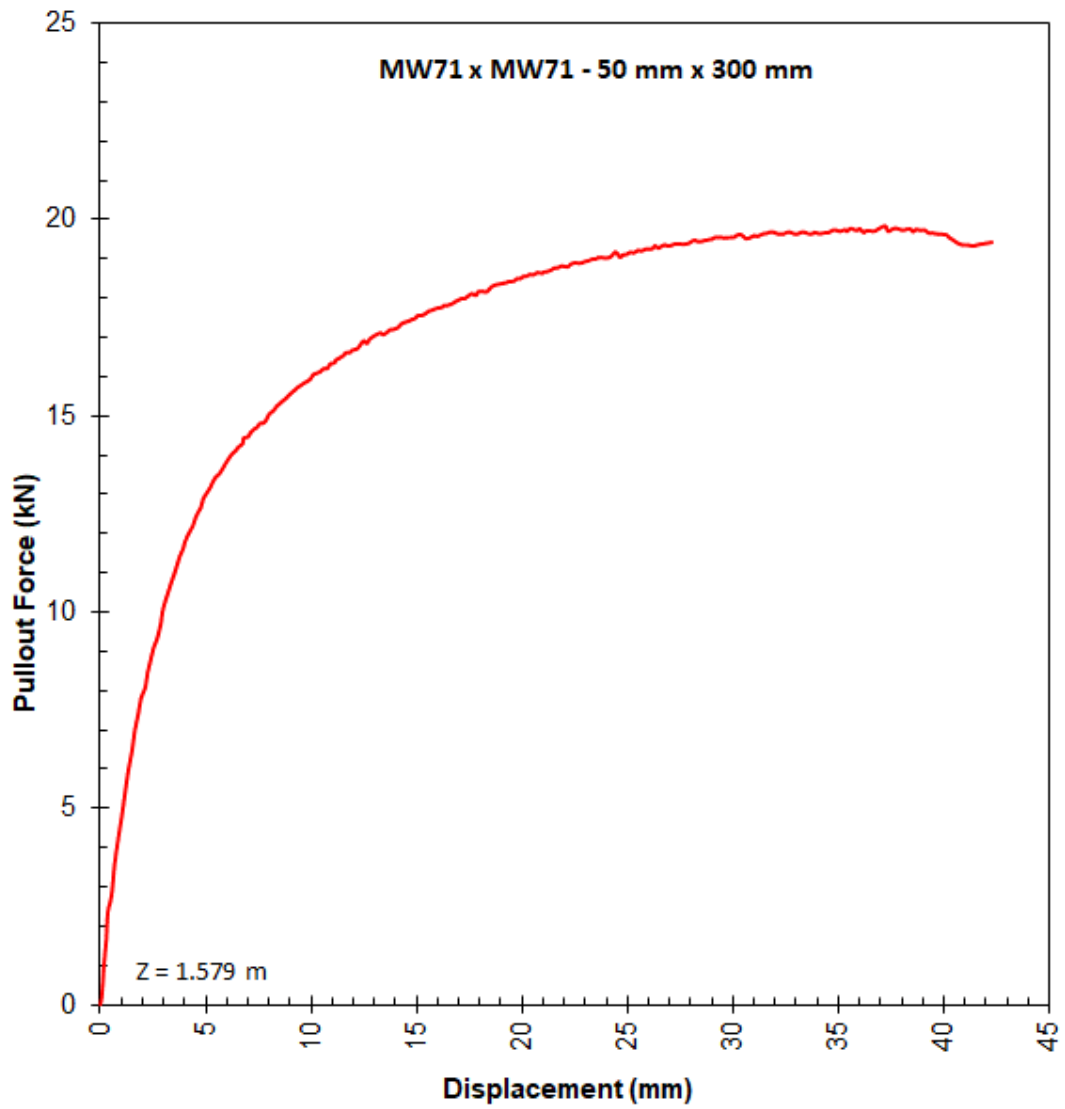


Figure 4-2 Typical 2-Wire Pullout Test - Displacement Data

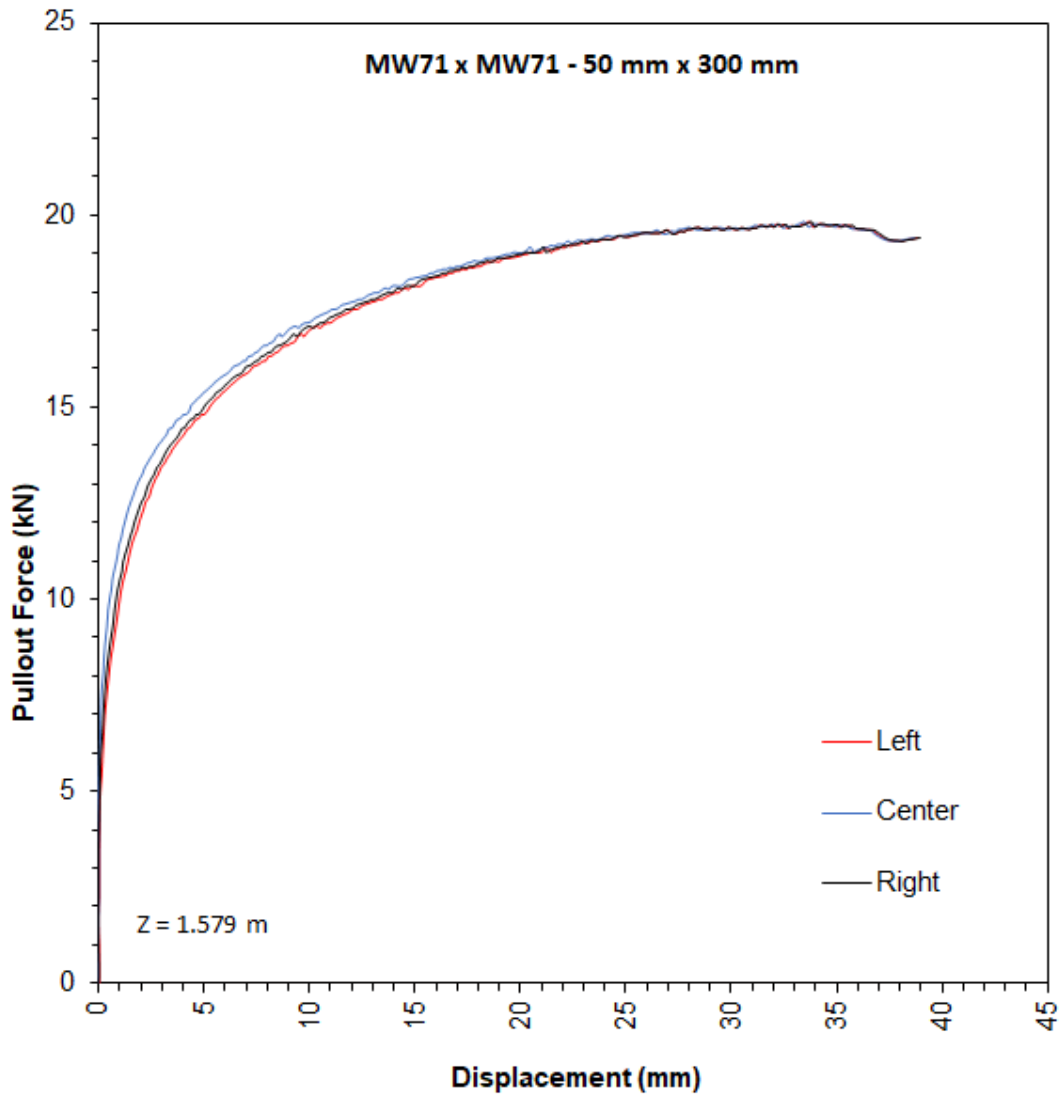


Figure 4-3 Typical 2-Wire Pullout Test - Displacement Data (Transverse Element)

#### 4.4 Pullout Test Results

The data for the experimental testing program in this section is presented in graphical form. The graph in this section presents the results as a function of the measured pullout resistance versus the depth the element is from the top of the structure. The pullout resistance of a soil-reinforcing system is a function of the depth the

soil-reinforcing is below the soil surface. Based on the results of the experimental testing program a power function can be used to represent the pullout resistance of the soil-reinforcing elements as a function of the depth the element is from the top of the structure. The power function shown in Equation 4-1 was used to generate the best-fit line to the measured pullout resistance.

$$P_{Le} = \alpha \cdot x^\beta \quad \text{Equation 4-1}$$

Where:

|          |   |   |
|----------|---|---|
| $P_{Le}$ | = | Pullout resistance per meter of soil-reinforcing (kN/m) |
| $\alpha$ | = | Coefficient (dim)                                       |
| $x$      | = | Depth to soil-reinforcing (m)                           |
| $\beta$  | = | Coefficient (dim)                                       |

It should be noted that Equation 4-1 is based on a normalized length of one meter of embedment. In order to use this function in design, it is required that the Equation 4-1 be multiplied by the length of embedment of the soil-reinforcing element in the passive zone as shown in Equation 4-2.

$$P_r = P_{Le} \cdot L_e \quad \text{Equation 4-2}$$

Where:

|       |   |   |
|-------|---|---|
| $P_r$ | = | Pullout resistance (kN)                       |
| $L_e$ | = | Length of embedment of soil-reinforcing (dim) |

Using the power function shown in Equation 4-1, a regression analysis can be performed on each of the test groups to create a unique equation for each of the 18 sub-set tests. For each of the sub-set tests, the measured pullout resistance and the corresponding depth the test is performed at are used to generate the alpha and beta

coefficient that best fits the data. Once the alpha and beta coefficient are determined they then can be used to calculate the pullout resistance at the specified depth.

A statistical analysis was performed on Equation 4-1 using the appropriate alpha and beta coefficients for each of the configurations tested in this experimental program. The mean, coefficient of variance (COV), standard deviation (STD), and the R value were calculated and are shown on the data tables for each of the systems in the experimental test program. The P-Value for the measured and calculated pullout resistance using the PPMC method was determined for each subset. The P-Value was required to be less than or equal to 0.05. If this is true, there is a statistical significance of the equation.

The bias ratio of the calculated pullout resistance to the measured pullout resistance for each test was also calculated.

$$Bias = \frac{P_m}{P_c} \quad \text{Equation 4-3}$$

Where:  $P_m$  = Measured pullout resistance (kN)

$P_c$  = Calculated pullout resistance (kN)

The P-Value of the bias, compared to the calculated pullout resistance was determined. The P-Value in this case, was required to be greater than 0.05. This was preformed to show the bias is not statistically significant when compared to the calculated pullout resistance.

The relationship shown in Equation 4-1 and in Equation 4-2 can be used to predict the pullout resistance for a 2-Wire of soil-reinforcing element embedded in sand when applying the alpha and beta values shown in the graphs for each of the 2-Wire configurations tested in this experimental program. Other configurations that were not tested in this experimental program, and that have pullout test data, can use this function and procedure to determine specific alpha and beta coefficients that fit the configuration. It should also be noted that because pullout resistance is a function of the soil unit weight, the function can be adjusted for soil unit weights that differ from the tested unit weight using a simple ratio of the actual unit weight to that of the tested soil unit weight equal to  $19.6 \text{ kN/m}^3$ .

Based on this method, and the test results, there is a significant statistical significance of each of the equations in predicting the pullout resistance for each of the soil-reinforcing configuration used in this experimental test program.

#### *4.4.1 Group-1 Pullout Test Results*

The Group-1 test program consisted of a 2-Wire system with longitudinal and transverse member size equal to MW71 (W11). The MW71 (W11) has a diameter equal to 9.5 mm (0.374 in) and a cross-sectional area equal to  $71 \text{ mm}^2$  ( $0.11 \text{ in}^2$ ). Pullout test results for Sets 1 through 3 follows.

##### *4.4.1.1 Set-1 Pullout Test Results*

The Set-1 2-Wire element had transverse element spacings equal to 300 mm. The pullout test results for the 50 mm, 100 mm, and 200 mm longitudinal element spacing are presented in the graph in Figure 4-4. A trend-line consisting of a power



function for each sub-set is shown on the graph in Figure 4-4. The trendline is based on the power function defined in Equation 4-1.

Based on the statistical data shown in Table 4-3 through Table 4-5, when comparing the bias of the calculated pullout resistance to the tested pullout resistance, each equation has a P-Value that is less than 0.05. In addition, the P-Values for the calculated pullout resistance to the bias were all significantly greater than 0.05.

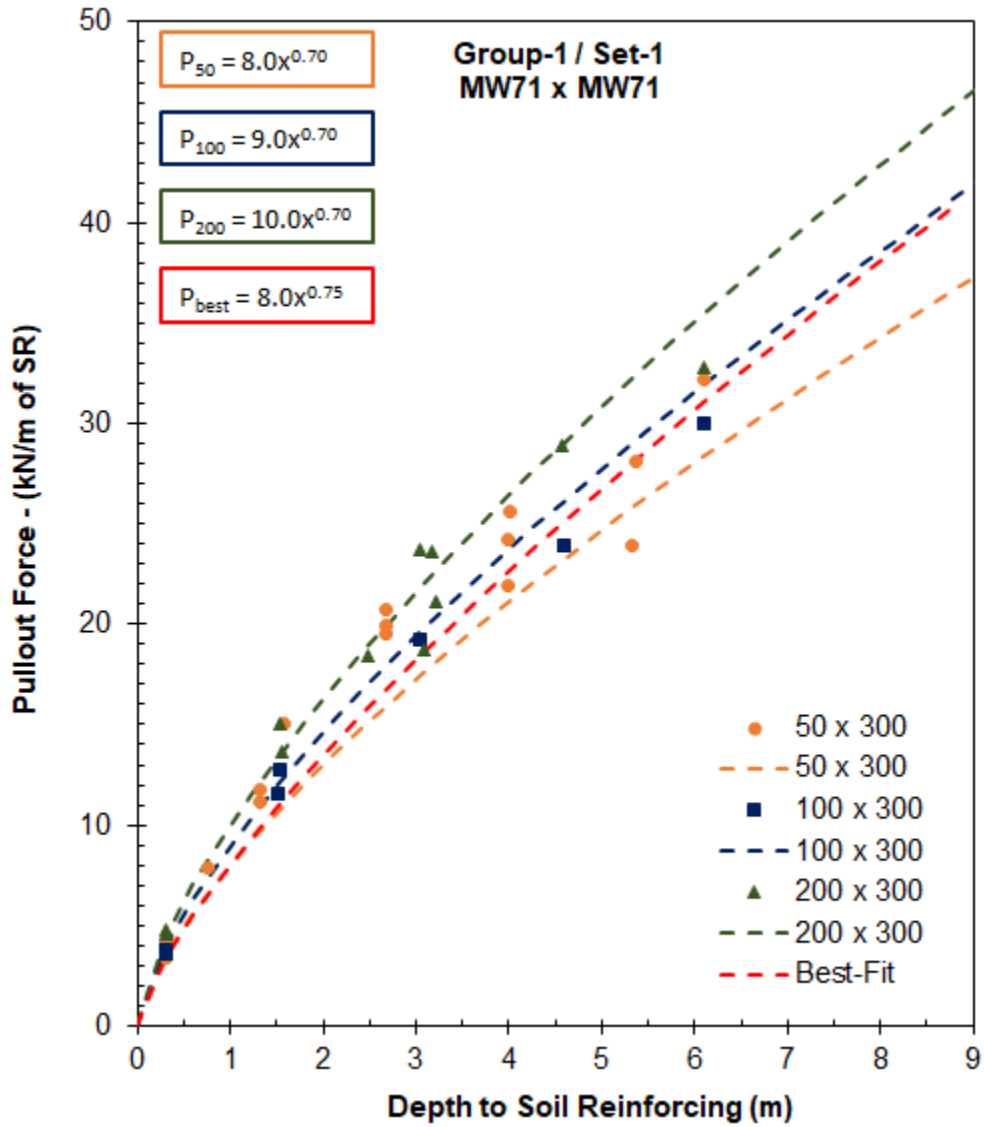


Figure 4-4 Pullout Resistance for Set-1 – Force vs Depth

Table 4-3 Resistance vs Depth MW71 x MW71 – 50 mm x 300 mm

| Depth (m) | Measured Force (kN) | Measured Force (kN/m) | Calculated Force (kN/m) | Bias | Statistics Value | Statistic |
|-----------|---------------------|-----------------------|-------------------------|------|------------------|-----------|
| 0.305     | 5.10                | 4.19                  | 3.48                    | 0.83 |                  |           |
| 0.305     | 4.09                | 3.35                  | 3.48                    | 1.04 |                  |           |

Table 4-3 Resistance vs Depth MW71 x MW71 – 50 mm x 300 mm

| Depth (m) | Measured Force (kN) | Measured Force (kN/m) | Calculated Force (kN/m) | Bias | Statistics Value | Statistic |
|-----------|---------------------|-----------------------|-------------------------|------|------------------|-----------|
| 0.305     | 4.35                | 3.57                  | 3.48                    | 0.98 |                  |           |
| 0.305     | 4.48                | 3.67                  | 3.48                    | 0.95 |                  |           |
| 1.329     | 14.31               | 11.73                 | 9.76                    | 0.83 |                  |           |
| 1.317     | 13.65               | 11.19                 | 9.70                    | 0.87 |                  |           |
| 1.580     | 18.37               | 15.06                 | 11.02                   | 0.73 |                  |           |
| 2.680     | 23.87               | 19.58                 | 15.95                   | 0.81 |                  |           |
| 2.680     | 25.26               | 20.72                 | 15.95                   | 0.77 |                  |           |
| 2.672     | 24.30               | 19.93                 | 15.92                   | 0.80 |                  |           |
| 3.999     | 29.55               | 24.24                 | 21.11                   | 0.87 |                  |           |
| 3.999     | 26.72               | 21.91                 | 21.11                   | 0.96 | 0.98             | CC        |
| 4.021     | 31.20               | 25.59                 | 21.19                   | 0.83 | 0.01             | P-Value   |
| 5.364     | 34.33               | 28.15                 | 25.93                   | 0.92 | 0.88             | Mean      |
| 5.325     | 29.22               | 23.97                 | 25.80                   | 1.08 | 0.11             | COV       |
| 6.111     | 39.20               | 32.15                 | 28.40                   | 0.88 | 0.09             | STD       |
| 0.763     | 9.63                | 7.90                  | 6.62                    | 0.84 | 0.98             | R         |

CC = Correlation Coefficient, COV = Coefficient of Variance, STD = Standard Deviation, R = Measure of Fit

Table 4-4 Resistance vs Depth MW71 x MW71 – 100 mm x 300 mm

| Depth (m) | Measured Force (kN) | Measured Force (kN/m) | Calculated Force (kN/m) | Bias | Statistics Value | Statistic |
|-----------|---------------------|-----------------------|-------------------------|------|------------------|-----------|
| 0.305     | 4.57                | 3.74                  | 3.92                    | 1.05 |                  |           |
| 0.305     | 4.40                | 3.61                  | 3.92                    | 1.08 | 0.99             | CC        |
| 1.526     | 15.58               | 12.78                 | 12.10                   | 0.95 | 0.01             | P-Value   |
| 1.517     | 14.03               | 11.51                 | 12.05                   | 1.05 | 1.04             | Mean      |
| 3.053     | 23.48               | 19.26                 | 19.66                   | 1.02 | 0.05             | COV       |
| 4.589     | 29.17               | 23.93                 | 26.15                   | 1.09 | 0.05             | STD       |
| 6.103     | 36.58               | 30.01                 | 31.93                   | 1.06 | 1.00             | R         |

CC = Correlation Coefficient, COV = Coefficient of Variance, STD = Standard Deviation, R = Measure of Fit

Table 4-5 Resistance vs Depth MW71 x MW71 – 200 mm x 300 mm

| Depth (m) | Measured Force (kN) | Measured Force (kN/m) | Calculated Force (kN/m) | Bias | Statistics Value | Statistic |
|-----------|---------------------|-----------------------|-------------------------|------|------------------|-----------|
| 0.305     | 5.60                | 4.59                  | 4.35                    | 0.95 |                  |           |
| 0.305     | 5.86                | 4.81                  | 4.35                    | 0.91 |                  |           |
| 1.553     | 16.63               | 13.64                 | 13.61                   | 1.00 |                  |           |
| 1.534     | 18.33               | 15.03                 | 13.49                   | 0.90 |                  |           |
| 2.494     | 22.50               | 18.45                 | 18.96                   | 1.03 |                  |           |
| 3.082     | 22.88               | 18.77                 | 21.99                   | 1.17 | 0.98             | CC        |
| 3.209     | 25.79               | 21.15                 | 22.62                   | 1.07 | 0.01             | P-Value   |
| 3.180     | 28.81               | 23.63                 | 22.47                   | 0.95 | 1.00             | Mean      |
| 3.038     | 28.96               | 23.75                 | 21.77                   | 0.92 | 0.09             | COV       |
| 4.570     | 35.18               | 28.86                 | 28.97                   | 1.00 | 0.09             | STD       |
| 6.096     | 39.96               | 32.77                 | 35.44                   | 1.08 | 0.99             | R         |

CC = Correlation Coefficient, COV = Coefficient of Variance, STD = Standard Deviation, R = Measure of Fit

#### 4.4.1.2 Set-2 Pullout Test Results

The Set-2, 2-Wire element had transverse element spacings equal to 150 mm. The pullout test results for the 50 mm, 100 mm, and 200 mm longitudinal element spacing are presented in the graph in Figure 4-5. A trend-line consisting of a power function for each sub-set is shown on the graph in Figure 4-5. The trendline is based on the power function defined in Equation 4-1.

Based on the statistical data shown in Table 4-6 through Table 4-8, when comparing the bias of the calculated pullout resistance to the tested pullout resistance, each equation has a P-Value that is less than 0.05. In addition, the P-Values for the calculated pullout resistance to the bias were all significantly greater than 0.05.

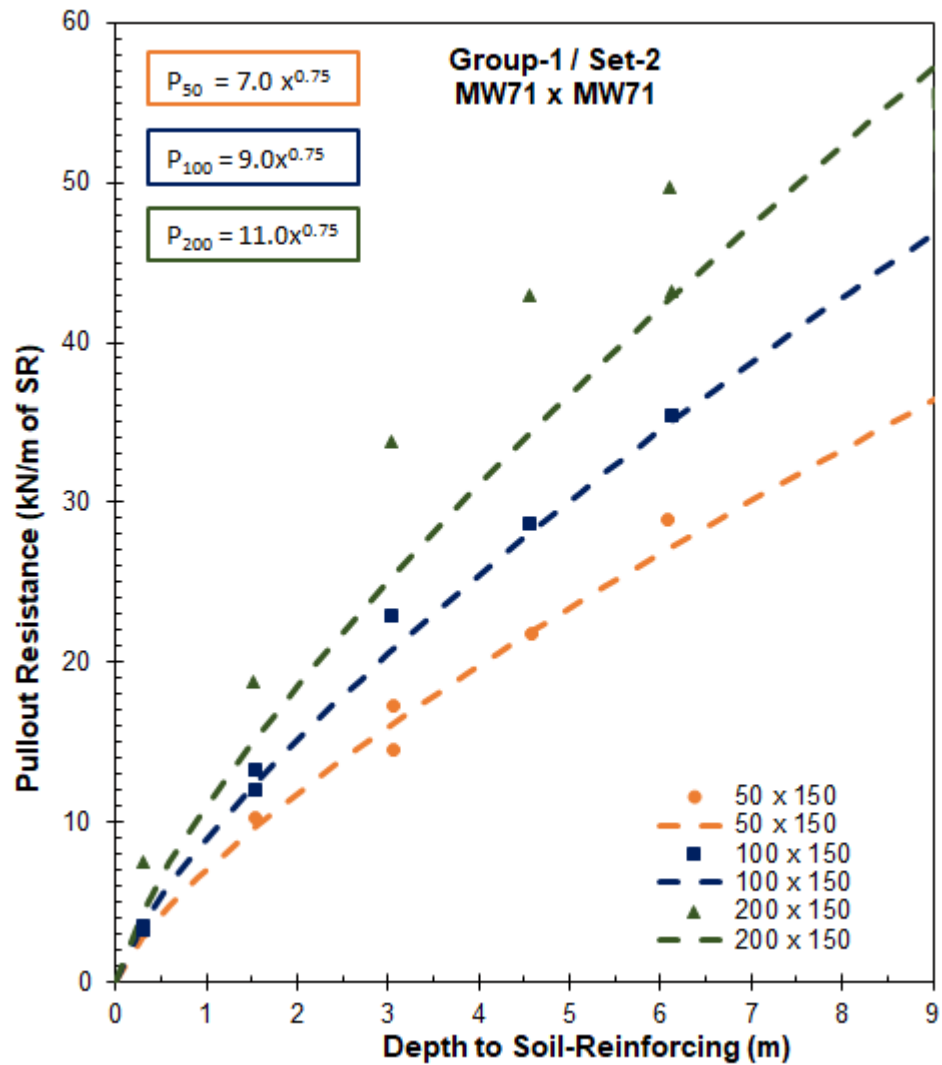


Figure 4-5 Pullout Resistance for Set-2 – Force vs Depth

Table 4-6 Resistance vs Depth MW71 x MW71 – 50 mm x 150 mm

| Depth (m) | Measured Force (kN) | Measured Force (kN/m) | Calculated Force (kN/m) | Bias | Statistics Value | Statistic |
|-----------|---------------------|-----------------------|-------------------------|------|------------------|-----------|
| 0.305     | 3.77                | 3.10                  | 2.87                    | 0.93 | 0.99             | CC        |
| 1.529     | 12.56               | 10.30                 | 9.62                    | 0.93 | 0.01             | P-Value   |
| 3.068     | 21.10               | 17.31                 | 16.23                   | 0.94 | 0.97             | Mean      |

Table 4-6 Resistance vs Depth MW71 x MW71 – 50 mm x 150 mm

| Depth (m) | Measured Force (kN) | Measured Force (kN/m) | Calculated Force (kN/m) | Bias | Statistics Value | Statistic |
|-----------|---------------------|-----------------------|-------------------------|------|------------------|-----------|
| 3.058     | 17.80               | 14.60                 | 16.19                   | 1.11 | 0.07             | COV       |
| 4.570     | 26.64               | 21.85                 | 21.88                   | 1.00 | 0.07             | STD       |
| 6.089     | 35.31               | 28.97                 | 27.13                   | 0.94 | 0.99             | R         |

CC = Correlation Coefficient, COV = Coefficient of Variance, STD = Standard Deviation, R = Measure of Fit

Table 4-7 Resistance vs Depth MW71 x MW71 – 100 mm x 150 mm

| Depth (m) | Measured Force (kN) | Measured Force (kN/m) | Calculated Force (kN/m) | Bias | Statistics Value | Statistic |
|-----------|---------------------|-----------------------|-------------------------|------|------------------|-----------|
| 0.305     | 4.00                | 3.28                  | 3.69                    | 1.13 |                  |           |
| 0.305     | 4.24                | 3.48                  | 3.69                    | 1.06 | 0.99             | CC        |
| 1.541     | 16.23               | 13.31                 | 12.45                   | 0.93 | 0.01             | P-Value   |
| 1.529     | 14.62               | 11.99                 | 12.37                   | 1.03 | 1.00             | Mean      |
| 3.046     | 28.00               | 22.97                 | 20.75                   | 0.90 | 0.08             | COV       |
| 4.552     | 34.91               | 28.63                 | 28.05                   | 0.98 | 0.08             | STD       |
| 6.120     | 43.19               | 35.42                 | 35.02                   | 0.99 | 1.00             | R         |

CC = Correlation Coefficient, COV = Coefficient of Variance, STD = Standard Deviation, R = Measure of Fit

Table 4-8 Resistance vs Depth MW71 x MW71 – 200 mm x 150 mm

| Depth (m) | Measured Force (kN) | Measured Force (kN/m) | Calculated Force (kN/m) | Bias | Statistics Value | Statistic |
|-----------|---------------------|-----------------------|-------------------------|------|------------------|-----------|
| 0.305     | 7.54                | 6.18                  | 4.51                    | 0.73 | 0.97             | CC        |
| 1.522     | 18.75               | 15.38                 | 15.07                   | 0.98 | 0.01             | P-Value   |
| 3.041     | 33.79               | 27.72                 | 25.33                   | 0.91 | 0.98             | Mean      |
| 4.560     | 42.93               | 35.21                 | 34.32                   | 0.97 | 0.16             | COV       |
| 6.120     | 43.19               | 35.42                 | 42.80                   | 1.21 | 0.16             | STD       |
| 6.108     | 49.74               | 40.80                 | 42.74                   | 1.05 | 0.98             | R         |

CC = Correlation Coefficient, COV = Coefficient of Variance, STD = Standard Deviation, R = Measure of Fit

#### 4.4.1.3 Set-3 Pullout Test Results

The Set-3, 2-Wire element had only one transverse wire embed in the soil as shown in Photograph 4-2. The pullout test results for the 2-Wire element with a 50 mm, 100 mm, and 200 mm longitudinal element spacings are presented on the graph shown in Figure 4-6. The trend-line consisting of a power function for each sub-set are shown also shown on the graph in Figure 4-6.



Photograph 4-2 Wire Rope Potentiometers on 100 mm Element

Based on the statistical data shown in Table 4-9 through Table 4-11, when comparing the bias of the calculated pullout resistance to the tested pullout resistance, each equation has a P-Value that is less than 0.05. In addition, the P-Values for the calculated pullout resistance to the bias were all significantly greater than 0.05.

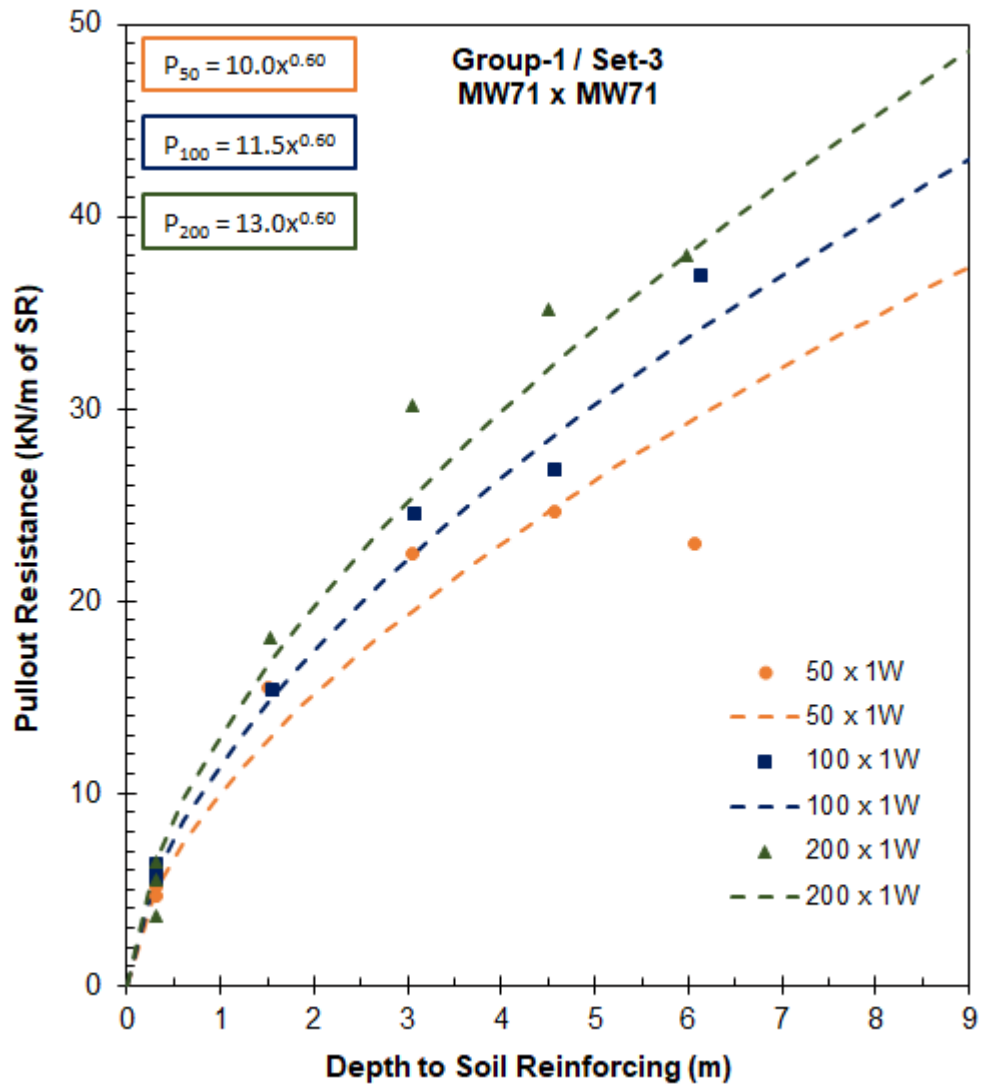


Figure 4-6 Pullout Resistance for Set-3 – Force vs Depth

Table 4-9 Resistance vs Depth MW71 x MW71 – 50 mm x 1-Wire

| Depth (m) | Measured Force (kN) | Measured Force (kN/m) | Calculated Force (kN/m) | Bias | Statistics Value | Statistic |
|-----------|---------------------|-----------------------|-------------------------|------|------------------|-----------|
| 0.305     | 1.58                | 5.19                  | 4.90                    | 0.94 |                  |           |
| 0.305     | 1.43                | 4.68                  | 4.90                    | 1.05 |                  |           |
| 0.305     | 1.57                | 5.14                  | 4.90                    | 0.95 |                  |           |



Table 4-9 Resistance vs Depth MW71 x MW71 – 50 mm x 1-Wire

| Depth (m) | Measured Force (kN) | Measured Force (kN/m) | Calculated Force (kN/m) | Bias | Statistics Value | Statistic |
|-----------|---------------------|-----------------------|-------------------------|------|------------------|-----------|
| 1.509     | 4.72                | 15.48                 | 12.80                   | 0.83 |                  |           |
| 3.048     | 6.84                | 22.44                 | 19.52                   | 0.87 | 0.98             | Mean      |
| 4.572     | 7.50                | 24.60                 | 24.89                   | 1.01 | 0.14             | COV       |
| 4.574     | 8.19                | 26.86                 | 24.90                   | 0.93 | 0.14             | STD       |
| 6.057     | 7.00                | 22.98                 | 29.47                   | 1.28 | 0.96             | R         |

CC = Correlation Coefficient, COV = Coefficient of Variance, STD = Standard Deviation, R = Measure of Fit

Table 4-10 Resistance vs Depth MW71 x MW71 – 100 mm x 1-Wire

| Depth (m) | Measured Force (kN) | Measured Force (kN/m) | Calculated Force (kN/m) | Bias | Statistics Value | Statistic |
|-----------|---------------------|-----------------------|-------------------------|------|------------------|-----------|
| 0.305     | 1.79                | 5.86                  | 5.64                    | 0.96 |                  |           |
| 0.305     | 1.70                | 5.59                  | 5.64                    | 1.01 |                  |           |
| 0.305     | 1.92                | 6.31                  | 5.64                    | 0.89 |                  |           |
| 1.551     | 4.68                | 15.37                 | 14.96                   | 0.97 | 0.96             | Mean      |
| 3.075     | 7.47                | 24.51                 | 22.56                   | 0.92 | 0.06             | COV       |
| 6.133     | 11.27               | 36.96                 | 34.14                   | 0.92 | 0.06             | STD       |
| 4.577     | 8.19                | 26.86                 | 28.64                   | 1.07 | 0.99             | R         |

CC = Correlation Coefficient, COV = Coefficient of Variance, STD = Standard Deviation, R = Measure of Fit

t

Table 4-11 Resistance vs Depth MW71 x MW71 – 200 mm x 1-Wire

| Depth (m) | Measured Force (kN) | Measured Force (kN/m) | Calculated Force (kN/m) | Bias | Statistics Value | Statistic |
|-----------|---------------------|-----------------------|-------------------------|------|------------------|-----------|
| 0.305     | 1.11                | 3.64                  | 6.37                    | 1.75 |                  |           |
| 0.305     | 1.97                | 6.48                  | 6.37                    | 0.98 |                  |           |
| 0.305     | 1.66                | 5.46                  | 6.37                    | 1.17 |                  |           |
| 1.524     | 5.50                | 18.06                 | 16.74                   | 0.93 | 1.08             | Mean      |
| 3.043     | 9.18                | 30.12                 | 25.35                   | 0.84 | 0.29             | COV       |
| 4.509     | 10.72               | 35.18                 | 32.09                   | 0.91 | 0.31             | STD       |
| 5.981     | 11.57               | 37.96                 | 38.02                   | 1.00 | 0.99             | R         |

CC = Correlation Coefficient, COV = Coefficient of Variance, STD = Standard Deviation, R = Measure of Fit

#### 4.4.2 *Group-2 Pullout Test Results*

The Group-2 test program consisted of a 2-Wire system with longitudinal and transverse members size equal to MW45 (W7). The MW45 (W7) has a diameter equal to 7.5 mm (0.299 in) and a cross-sectional area equal to 45 mm<sup>2</sup> (0.07 in<sup>2</sup>). Pullout test results for Sets 1, 2, and 3 follows.

##### 4.4.2.1 Set-1 Pullout Test Results

The Set-1, 2-Wire element had transverse element spacings equal to 300 mm. The pullout test results for the 50 mm, 100 mm, and 200 mm longitudinal element spacing are presented on the graph in Figure 4-7. A trend-line consisting of a power function for each sub-set is also shown on the graph in Figure 4-7.

Based on the statistical data shown in Table 4-12 through Table 4-14, when comparing the bias of the calculated pullout resistance to the tested pullout resistance, each equation has a P-Value that is less than 0.05. In addition, the P-Values for the calculated pullout resistance to the bias were all significantly greater than 0.05.

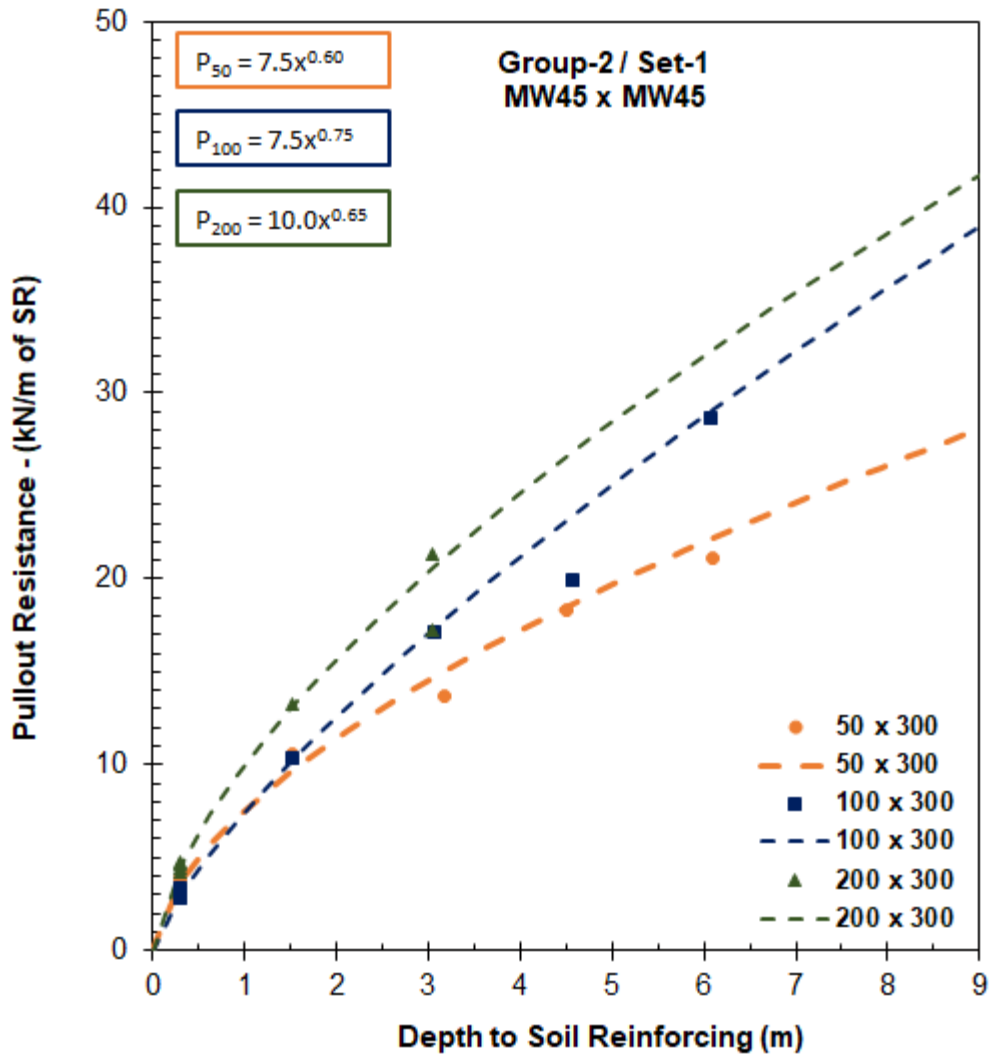


Figure 4-7 Pullout Resistance of Set-4 –Force vs Depth

Table 4-12 Resistance vs Depth MW45 x MW45 – 50 mm x 300 mm

| Depth (m) | Measured Force (kN) | Measured Force (kN/m) | Calculated Force (kN/m) | Bias | Statistics Value | Statistic |
|-----------|---------------------|-----------------------|-------------------------|------|------------------|-----------|
| 0.305     | 4.47                | 3.66                  | 3.68                    | 1.75 |                  |           |
| 0.305     | 4.73                | 3.88                  | 3.68                    | 0.98 |                  |           |
| 0.305     | 4.09                | 3.36                  | 3.68                    | 1.17 | 0.99             | CC        |

Table 4-12 Resistance vs Depth MW45 x MW45 – 50 mm x 300 mm

| Depth (m) | Measured Force (kN) | Measured Force (kN/m) | Calculated Force (kN/m) | Bias | Statistics Value | Statistic |
|-----------|---------------------|-----------------------|-------------------------|------|------------------|-----------|
| 1.524     | 12.91               | 10.59                 | 9.66                    |      | 0.00             | P-Value   |
| 3.172     | 16.70               | 13.70                 | 14.99                   | 0.93 | 1.08             | Mean      |
| 4.513     | 22.39               | 18.36                 | 18.53                   | 0.84 | 0.29             | COV       |
| 6.096     | 25.71               | 21.09                 | 22.19                   | 0.91 | 0.31             | STD       |
| 9.103     | 30.18               | 24.76                 | 28.22                   | 1.00 | 0.99             | R         |

CC = Correlation Coefficient, COV = Coefficient of Variance, STD = Standard Deviation, R = Measure of Fit

Table 4-13 Resistance vs Depth MW45 x MW45 – 100 mm x 300 mm

| Depth (m) | Measured Force (kN) | Measured Force (kN/m) | Calculated Force (kN/m) | Bias | Statistics Value | Statistic |
|-----------|---------------------|-----------------------|-------------------------|------|------------------|-----------|
| 0.305     | 3.44                | 2.82                  | 3.08                    | 1.09 |                  |           |
| 0.305     | 3.80                | 3.11                  | 3.08                    | 0.99 | 0.99             | CC        |
| 0.305     | 4.06                | 3.33                  | 3.08                    | 0.92 | 0.01             | P-Value   |
| 1.524     | 12.57               | 10.31                 | 10.29                   | 1.00 | 1.03             | Mean      |
| 3.055     | 20.94               | 17.18                 | 17.33                   | 1.01 | 0.08             | COV       |
| 4.572     | 24.29               | 19.92                 | 23.45                   | 1.18 | 0.08             | STD       |
| 6.084     | 34.90               | 28.63                 | 29.05                   | 1.01 | 0.99             | R         |

CC = Correlation Coefficient, COV = Coefficient of Variance, STD = Standard Deviation, R = Measure of Fit

Table 4-14 Resistance vs Depth MW45 x MW45 – 200 mm x 300 mm

| Depth (m) | Measured Force (kN) | Measured Force (kN/m) | Calculated Force (kN/m) | Bias | Statistics Value | Statistic |
|-----------|---------------------|-----------------------|-------------------------|------|------------------|-----------|
| 0.305     | 5.81                | 4.76                  | 3.08                    | 0.65 |                  |           |
| 0.305     | 5.42                | 4.45                  | 4.62                    | 1.04 | 0.97             | CC        |
| 0.305     | 5.09                | 4.18                  | 4.62                    | 1.11 | 0.01             | P-Value   |
| 3.048     | 26.04               | 21.36                 | 20.64                   | 0.97 | 0.99             | Mean      |
| 1.524     | 16.21               | 13.29                 | 13.15                   | 0.99 | 0.17             | COV       |
| 3.048     | 21.00               | 17.22                 | 20.64                   | 1.20 | 0.17             | STD       |
| 0.305     | 5.68                | 4.66                  | 4.62                    | 0.99 | 0.98             | R         |

CC = Correlation Coefficient, COV = Coefficient of Variance, STD = Standard Deviation, R = Measure of Fit

#### 4.4.2.2 Set-3 Pullout Test Results

The Set-3, 2-Wire element had transverse element spacings equal to 150 mm. The pullout test results for the 50 mm, 100 mm, and 200 mm longitudinal spacing are presented in the graph that is shown in Figure 4-8. A trend-line consisting of a power function for each sub-set is also shown on the graph in Figure 4-8.

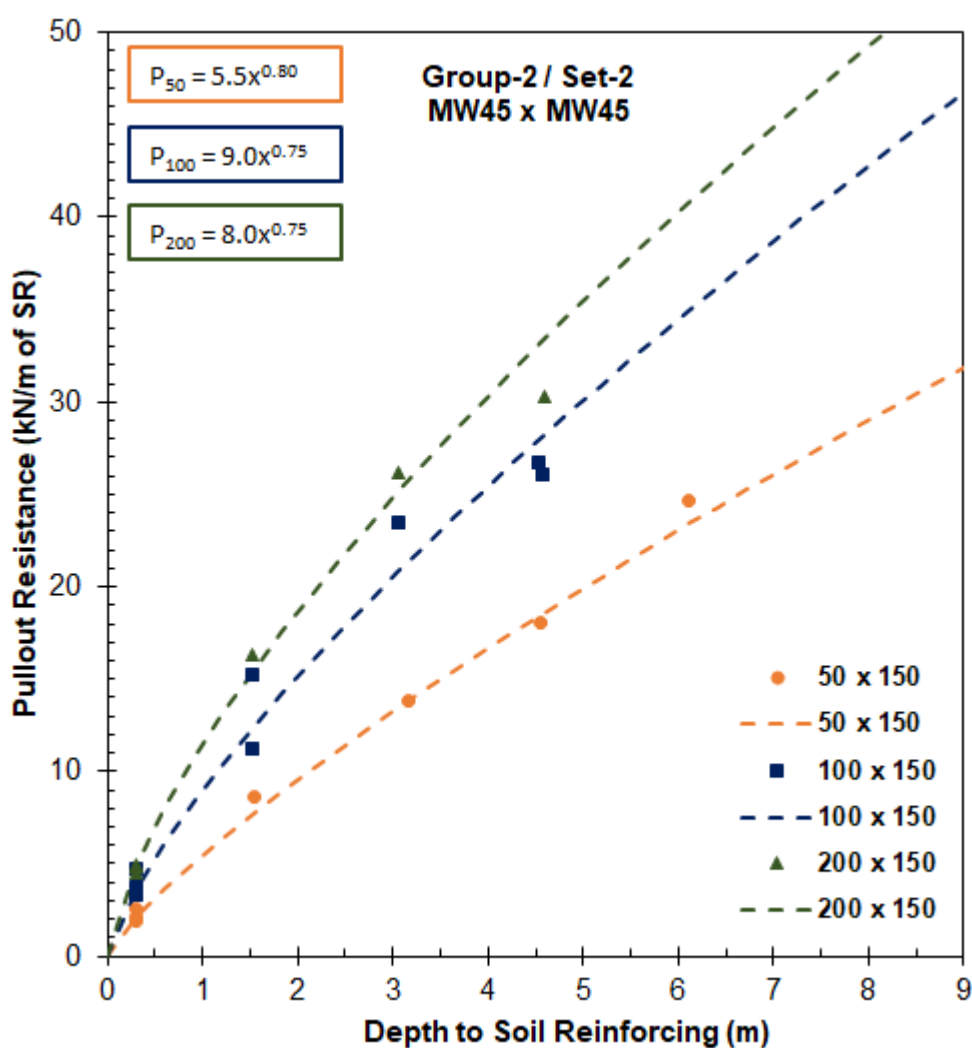


Figure 4-8 Pullout Resistance of Set-5 – Force vs Depth

Based on the statistical data shown in Table 4-15 through Table 4-17, when comparing the bias of the calculated pullout resistance to the tested pullout resistance, each equation has a P-value that is less than 0.05. In addition, the P-Values for the calculated pullout resistance to the bias were all significantly greater than 0.05.

Table 4-15 Resistance vs Depth MW45 x MW45 – 50 mm x 150 mm

| Depth (m) | Measured Force (kN) | Measured Force (kN/m) | Calculated Force (kN/m) | Bias | Statistics Value | Statistic |
|-----------|---------------------|-----------------------|-------------------------|------|------------------|-----------|
| 0.305     | 5.81                | 4.76                  | 3.08                    | 0.65 |                  |           |
| 0.305     | 5.42                | 4.45                  | 4.62                    | 1.04 | 0.97             | CC        |
| 0.305     | 5.09                | 4.18                  | 4.62                    | 1.11 | 0.01             | P-Value   |
| 3.048     | 26.04               | 21.36                 | 20.64                   | 0.97 | 0.99             | Mean      |
| 1.524     | 16.21               | 13.29                 | 13.15                   | 0.99 | 0.17             | COV       |
| 3.048     | 21.00               | 17.22                 | 20.64                   | 1.20 | 0.17             | STD       |
| 0.305     | 5.68                | 4.66                  | 4.62                    | 0.99 | 0.98             | R         |

CC = Correlation Coefficient, COV = Coefficient of Variance, STD = Standard Deviation, R = Measure of Fit

Table 4-16 Resistance vs Depth MW45 x MW45 – 100 mm x 150 mm

| Depth (m) | Measured Force (kN) | Measured Force (kN/m) | Calculated Force (kN/m) | Bias | Statistics Value | Statistic |
|-----------|---------------------|-----------------------|-------------------------|------|------------------|-----------|
| 0.305     | 4.03                | 3.31                  | 3.69                    | 1.12 |                  |           |
| 0.305     | 4.32                | 3.54                  | 3.69                    | 1.04 |                  |           |
| 0.305     | 4.56                | 3.74                  | 3.69                    | 0.99 |                  |           |
| 1.531     | 13.70               | 11.24                 | 12.39                   | 1.10 | 0.98             | CC        |
| 4.570     | 31.76               | 26.05                 | 28.13                   | 1.08 | 0.01             | P-Value   |
| 3.060     | 28.61               | 23.47                 | 20.82                   | 0.89 | 0.98             | Mean      |
| 1.526     | 18.61               | 15.26                 | 12.36                   | 0.81 | 0.13             | COV       |
| 0.305     | 5.71                | 4.68                  | 3.69                    | 0.79 | 0.13             | STD       |
| 4.540     | 32.60               | 26.74                 | 27.99                   | 1.05 | 0.99             | R         |

CC = Correlation Coefficient, COV = Coefficient of Variance, STD = Standard Deviation, R = Measure of Fit

Table 4-17 Resistance vs Depth MW45 x MW45 – 200 mm x 150 mm

| Depth (m) | Measured Force (kN) | Measured Force (kN/m) | Calculated Force (kN/m) | Bias | Statistics Value | Statistic |
|-----------|---------------------|-----------------------|-------------------------|------|------------------|-----------|
| 0.305     | 5.56                | 4.56                  | 5.01                    | 1.10 | 0.99             | CC        |
| 0.305     | 5.92                | 4.86                  | 5.01                    | 1.03 | 0.01             | P-Value   |
| 0.305     | 6.08                | 4.99                  | 5.01                    | 1.00 | 1.02             | Mean      |
| 1.519     | 19.85               | 16.28                 | 15.41                   | 0.95 | 0.07             | COV       |
| 3.050     | 31.86               | 26.13                 | 25.10                   | 0.96 | 0.07             | STD       |
| 4.596     | 36.93               | 30.29                 | 33.45                   | 1.10 | 0.99             | R         |

CC = Correlation Coefficient, COV = Coefficient of Variance, STD = Standard Deviation, R = Measure of Fit

#### 4.4.2.3 Set-3 Pullout Test Results

The Set-3, 2-Wire element had only one transverse wire embed in the soil as shown in Photograph 4-2. The pullout test results for the 2-Wire element with a 50 mm, 100 mm, and 200 mm longitudinal element spacings are presented in on the graph shown in Figure 4-9. The trend-line consisting of a power function for each sub-set are shown on the graph in Figure 4-9.

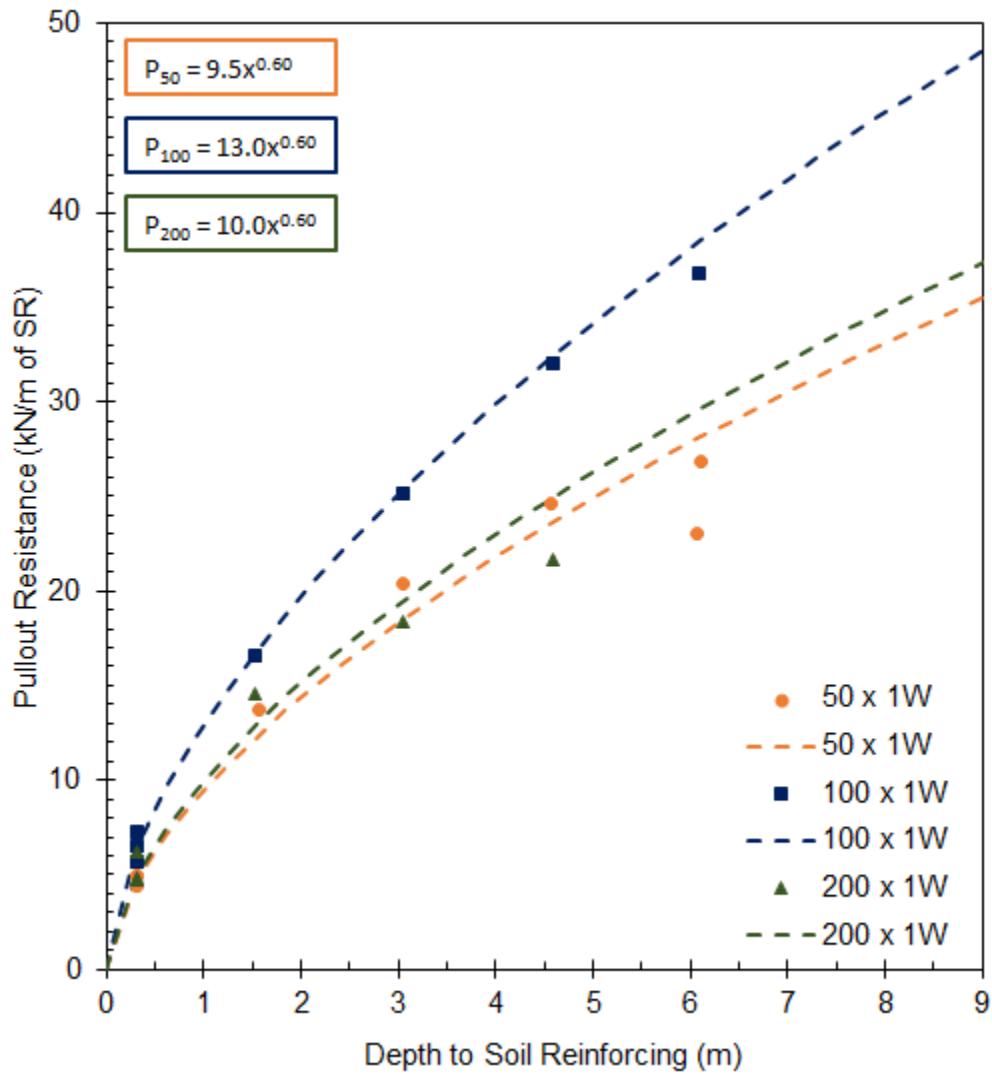


Figure 4-9 Pullout Resistance of Set-6 – Force vs Depth

Based on the statistical data shown in Table 4-18 through Table 4-20, when comparing the bias of the calculated pullout resistance to the tested pullout resistance, each equation has a P-value that is less than 0.05. In addition, the P-Values for the calculated pullout resistance to the bias were all significantly greater than 0.05.



Table 4-18 Resistance vs Depth MW45 x MW45 – 50 mm x 1-Wire

| Depth (m) | Measured Force (kN) | Measured Force (kN/m) | Calculated Force (kN/m) | Bias | Statistics Value | Statistic |
|-----------|---------------------|-----------------------|-------------------------|------|------------------|-----------|
| 0.305     | 1.36                | 4.46                  | 4.66                    | 1.04 |                  |           |
| 0.305     | 1.49                | 4.90                  | 4.66                    | 0.95 |                  |           |
| 0.305     | 1.49                | 4.90                  | 4.66                    | 0.95 | 0.98             | CC        |
| 1.565     | 4.18                | 13.72                 | 12.43                   | 0.91 | 0.01             | P-Value   |
| 3.050     | 6.22                | 20.40                 | 18.55                   | 0.91 | 1.00             | Mean      |
| 4.572     | 7.51                | 24.63                 | 23.65                   | 0.96 | 0.10             | COV       |
| 6.103     | 8.19                | 26.86                 | 28.12                   | 1.05 | 0.10             | STD       |
| 6.057     | 7.00                | 22.98                 | 27.99                   | 1.22 | 0.98             | R         |

CC = Correlation Coefficient, COV = Coefficient of Variance, STD = Standard Deviation, R = Measure of Fit

Table 4-19 Resistance vs Depth MW45 x MW45 – 100 mm x 1-Wire

| Depth (m) | Measured Force (kN) | Measured Force (kN/m) | Calculated Force (kN/m) | Bias | Statistics Value | Statistic |
|-----------|---------------------|-----------------------|-------------------------|------|------------------|-----------|
| 0.305     | 2.21                | 7.24                  | 6.37                    | 0.88 |                  |           |
| 0.305     | 1.73                | 5.67                  | 6.37                    | 1.12 | 1.00             | CC        |
| 0.305     | 1.97                | 6.48                  | 6.37                    | 0.98 | 0.00             | P-Value   |
| 1.522     | 5.04                | 16.53                 | 16.72                   | 1.01 | 1.01             | Mean      |
| 3.041     | 7.66                | 25.13                 | 25.34                   | 1.01 | 0.07             | COV       |
| 4.582     | 9.75                | 31.98                 | 32.40                   | 1.01 | 0.07             | STD       |
| 6.094     | 11.21               | 36.77                 | 38.45                   | 1.05 | 1.00             | R         |

CC = Correlation Coefficient, COV = Coefficient of Variance, STD = Standard Deviation, R = Measure of Fit

Table 4-20 Resistance vs Depth MW45 x MW45 – 200 mm x 1-Wire

| Depth (m) | Measured Force (kN) | Measured Force (kN/m) | Calculated Force (kN/m) | Bias | Statistics Value | Statistic |
|-----------|---------------------|-----------------------|-------------------------|------|------------------|-----------|
| 0.305     | 1.89                | 6.21                  | 4.90                    | 0.79 | 0.98             | CC        |
| 0.305     | 1.44                | 4.74                  | 4.90                    | 1.03 | 0.01             | P-Value   |
| 0.305     | 1.47                | 4.81                  | 4.90                    | 1.02 | 0.99             | Mean      |
| 1.531     | 4.44                | 14.57                 | 12.91                   | 0.89 | 0.13             | COV       |

Table 4-20 Resistance vs Depth MW45 x MW45 – 200 mm x 1-Wire

| Depth (m) | Measured Force (kN) | Measured Force (kN/m) | Calculated Force (kN/m) | Bias | Statistics Value | Statistic |
|-----------|---------------------|-----------------------|-------------------------|------|------------------|-----------|
| 3.043     | 5.61                | 18.40                 | 19.50                   | 1.06 | 0.13             | STD       |
| 4.582     | 6.61                | 21.67                 | 24.92                   | 1.15 | 0.99             | R         |

CC = Correlation Coefficient, COV = Coefficient of Variance, STD = Standard Deviation, R = Measure of Fit

#### 4.5 Bearing Resistance Factor Equations

The relationship that is shown in Equation 4-4 can also be used to determine the pullout resistance of grid type soil-reinforcing elements. It is based on the general equation provided in AASHTO (2017) and FHWA (2010). This equation is commonly used in the state-of-practice. It is therefore familiar to practitioners. The only unknown in the equation for an inextensible soil-reinforcing system is the bearing resistance factor  $F_q$ . The bearing resistance factor can be directly determined from pullout testing.

$$P_r = \phi \cdot F_q \cdot \alpha \cdot \sigma_v \cdot C \cdot R_c \cdot L_e \quad \text{Equation 4-4}$$

- Where:
- $P_r$  = Pullout resistance at  $\frac{3}{4}$  in. displacement (kN/m)
  - $\phi$  = Pullout resistance factor for LRFD (dim)
  - $F_q$  = Bearing resistance factor (dim)
  - $\alpha$  = Scale correction factor (dim)
  - $\sigma_v$  = Vertical overburden pressure (kPa)
  - $C$  = Surface area geometry factor (dim)
  - $R_c$  = Reinforcement coverage ratio (dim)
  - $L_e$  = Length of embedment (m)

The value of  $\alpha$  is equal to 1.0 and the value of C is equal to 2 for inextensible soil-reinforcing. To reduce the equation to calculate the pullout resistance for one soil-reinforcing element the reinforcement coverage ratio is replaced by the width of the soil-reinforcing element,  $w$ .

In this research program, pullout tests were performed on 2-Wire, grid, soil-reinforcing systems. From the results of the test program the bearing resistance factor  $F_q$  was back-calculated using Equation 4-5. In Equation 4-5 the reinforcing coverage ratio has been replaced with the width of the soil-reinforcing,  $w$ , and the default numerical values for the scale correction factor,  $\alpha$ , the surface area geometry factor, C, and have been added.

$$F_q = \frac{P_r}{2 \cdot w \cdot L_e \cdot \sigma_v} \quad \text{Equation 4-5}$$

Pullout tests of the 2-Wire soil-reinforcement in this experimental test program showed a tendency for the bearing resistance factor versus the depth of soil cover to have a shape of a decaying exponential function or in some cases a power function. At low overburden pressure the bearing resistance factor was higher than predicted by all equations described in Section 2.2.4. As the overburden pressure increased the bearing resistance factor decreased.

An example of the shape of the bearing resistance factor curve, based on actual pullout test results for the MW71 - 50 mm x 300 mm 2-Wire element is shown in Figure 4-10. In this figure it clearly shows a tendency for the bearing resistance factor be substantially higher than the two-piece linear trend that is given in the state-of-practice

by FHWA (2009) and AASHTO (2017). The results shown in Figure 4-10 are very similar to the results given by Jayawickrama et al. (2013).

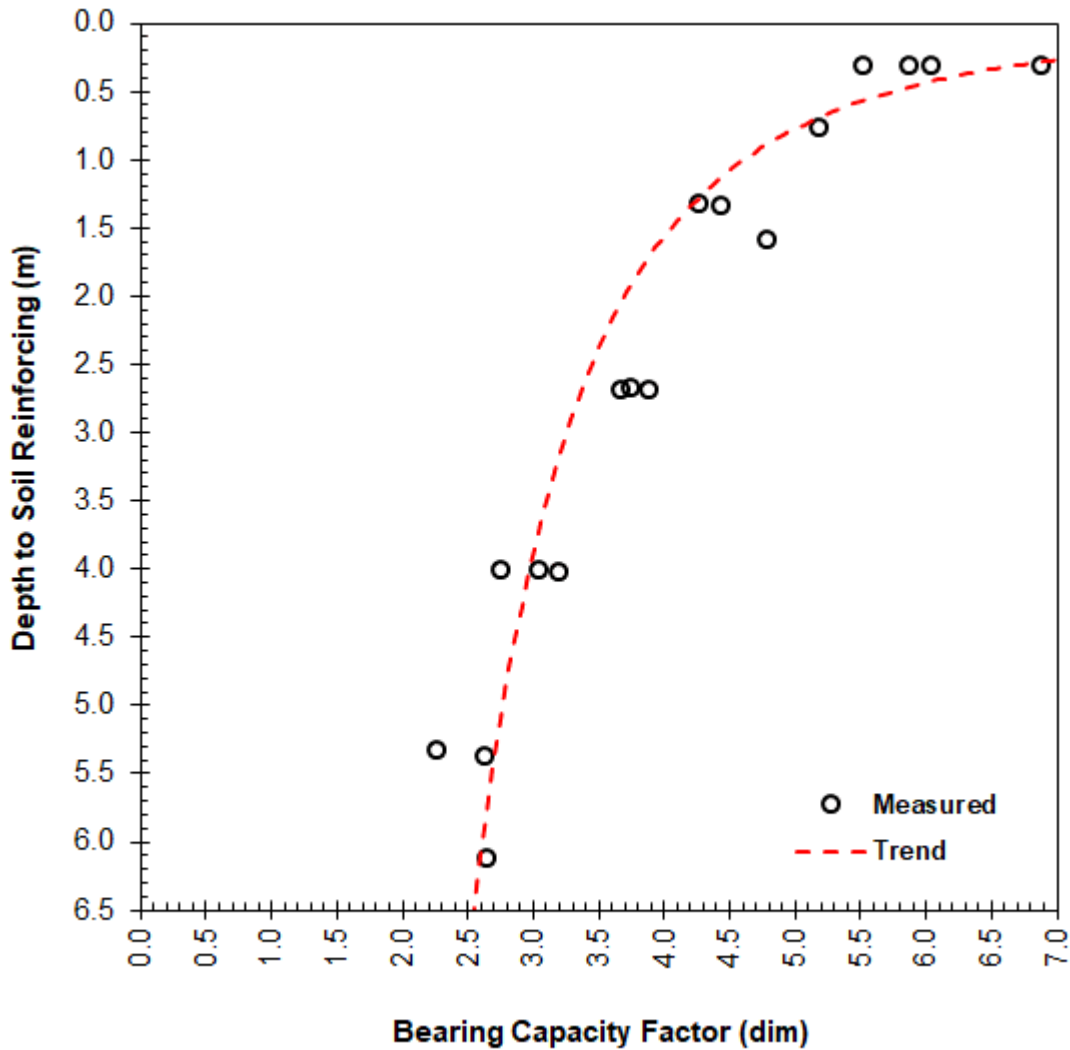


Figure 4-10 Measured Bearing Resistance Factor with Best-Fit Trend MW71 50 x 300

In this experimental test program, a parametric study was performed to determine the best-fit function for calculating the bearing resistance factor. The parametric study investigated various functions to determine the bearing resistance

factor. The power functions, two parameter decaying exponential functions, three parameter decaying exponential functions, and linear piece-wise functions were investigated. As a means of comparison, the Yu and Bathurst (2015) power function was also used. Regression analysis was used to estimate the coefficients in each of the functions. After the coefficients were determined for each of the bearing resistance functions, the function was used to predict the pullout resistance of the soil-reinforcing system. The predicted value was then compared to the measured value and the bias determined. This was performed for each of the tests in the experimental test program.

To test the significance of the function a Pearson Product Moment Correlation (PPMC) was used. The PPMC was used to calculate a correlation coefficient and the corresponding P-Value. In the PPMC, the pair of variables with positive correlation coefficients and with P-Values below 0.05 tend to increase together. For the pair of variables with negative correlation coefficients and with P-Values below 0.05, one variable tends to decrease, while the other increases. For the pair of variables with P-Values less than 0.05, there is a significant relationship between the two variables. For the pair of variables with P-Values greater than 0.05, there is *not* a significant relationship between the two variables (Yu et al., 2015).

The PPMC method was used as a means to check the significance of the relationship between the measured pullout resistance versus the predicted pullout resistance and for the bias value versus the predicted pullout resistance. The bias in this case was equal to the ratio of the predicted pullout resistance to the measured pullout resistance. If the bias is less than one, then the predicted pullout resistance is less than the measured pullout resistance. If the bias is greater than one, then the predicted

pullout resistance is greater than the measured pullout resistance. The function that was used to calculate the bearing resistance factor was determined to be satisfactory if the P-Value was less than 0.05 for the comparison of the measured pullout resistance to the predicted pullout resistance.

In addition, the P-Value was required to be greater than 0.05 for the comparison of the bias to the calculated pullout resistance. If these two conditions held true, the function can be used to calculate the pullout resistance of the 2-Wire element. The software program SigmaPlot 14 was used to perform the regression analysis and the PPMC comparisons. Based on the parametric study, three different functions tend to satisfy the PPMC requirements. The equations that will be presented are titled Research Equation 1 (RE1), Research Equation 2 (RE2), and Research Equation 3 (RE3). Also, as a comparison, each of the research equations (RE1, RE2, and RE3) were compared to the equation as provide in the literature by Yu and Bathurst (2015), labeled as “Yu”.

#### 4.5.1 RE1 Equation

Research Equation 1 (RE1) is a 2-parameter exponential decay equation. The unknown coefficients are the alpha factor and the beta factor. RE1 is shown in Equation 4-6 and the results from a regression analysis defining the alpha and beta coefficients are shown in Table 4-21.

RE1 
$$F_q = \alpha \cdot e^{-\beta \cdot z}$$
 Equation 4-6

Where:

- $\alpha$  = Geometric factor (dim)
- $\beta$  = Depth factor (dim)
- $z$  = Depth to soil-reinforcing (m)

Table 4-21 RE1 - Regression Variables

| Type                       | Longitudinal Spacing (mm) |         |          |         |          |         |
|----------------------------|---------------------------|---------|----------|---------|----------|---------|
|                            | 50                        |         | 100      |         | 200      |         |
|                            | $\alpha$                  | $\beta$ | $\alpha$ | $\beta$ | $\alpha$ | $\beta$ |
| MW71 x MW71<br>$S_T = 300$ | 6.17                      | 0.178   | 3.00     | 0.192   | 2.00     | 0.250   |
| MW71 x MW71<br>$S_T = 150$ | 4.86                      | 0.164   | 2.73     | 0.122   | 2.39     | 0.215   |
| MW71 x MW71<br>$S_T = 1W$  | 8.78                      | 0.268   | 5.15     | 0.288   | 2.23     | 0.199   |
| MW45 x MW45<br>$S_T = 300$ | 6.25                      | 0.261   | 2.60     | 0.176   | 2.04     | 0.332   |
| MW45 x MW45<br>$S_T = 150$ | 3.67                      | 0.127   | 3.25     | 0.190   | 2.08     | 0.221   |
| MW45 x MW45<br>$S_T = 1W$  | 7.24                      | 0.265   | 5.64     | 0.298   | 2.33     | 0.373   |

#### 4.5.2 RE2 Equation

Research Equation 2 (RE2) is a 3-parameter exponential decay equation. The unknown coefficients are the minimum bearing resistance factor, maximum bearing resistance factor, and the beta factor. RE2 is shown in Equation 4-7 and the results from a regression analysis defining the alpha and beta coefficients are shown in Table 4-22.

$$\text{RE2} \quad F_q = F_0 + F_{\max} \cdot e^{-\beta \cdot z} \quad \text{Equation 4-7}$$

Where:  $F_0$  = Minimum bearing resistance factor (dim)

$\alpha$  = Maximum bearing resistance factor (dim)

$z$  = depth to soil-reinforcing (m)

Table 4-22 RE2 - Regression Variables

| Type                                   | Longitudinal Spacing (mm) |      |      |                |      |      |                |      |      |
|--|---------------------------|------|------|----------------|------|------|----------------|------|------|
|  | 50                        |      |      | 100            |      |      | 200            |      |      |
|  | F <sub>0</sub>            | α    | β    | F <sub>0</sub> | α    | β    | F <sub>0</sub> | α    | β    |
| MW71 x<br>MW71<br>S <sub>T</sub> = 300 | 2.00                      | 4.50 | 0.38 | 1.25           | 2.25 | 0.75 | 0.70           | 1.50 | 0.75 |
| MW71 x<br>MW71<br>S <sub>T</sub> = 150 | 2.33                      | 3.54 | 0.81 | 1.45           | 1.55 | 0.55 | 0.86           | 2.25 | 0.99 |
| MW71 x<br>MW71<br>S <sub>T</sub> = 1W  | 1.78                      | 7.40 | 0.48 | 1.52           | 4.38 | 0.89 | 0.90           | 1.46 | 0.55 |
| MW45 x<br>MW45<br>S <sub>T</sub> = 300 | 1.54                      | 5.39 | 0.65 | 1.11           | 1.75 | 0.68 | 0.70           | 1.53 | 0.92 |
| MW45 x<br>MW45<br>S <sub>T</sub> = 150 | 1.88                      | 2.06 | 0.52 | 1.50           | 1.55 | 0.55 | 0.74           | 1.45 | 0.54 |
| MW45 x<br>MW45<br>S <sub>T</sub> = 1W  | 2.06                      | 6.95 | 0.63 | 1.63           | 4.89 | 0.94 | 0.52           | 2.04 | 0.72 |

#### 4.5.3 RE3 Equation

Research Equation 3 (RE3) is a 3-segment linear piecewise equation. The unknown coefficients are the maximum bearing resistance factor, intermediate bearing resistance factor, minimum bearing resistance factor, depth factor to intermediate bearing resistance factor, and the depth factor to minimum bearing resistance factor. RE3 is shown in Equation 4-8 and the results from a regression analysis defining the coefficients are shown in Table 4-23.



$$RE3 \quad F_q = \begin{cases} F_{\max} - \frac{F_{\max} - F_1}{z_1} \cdot z \rightarrow 0 \leq z \leq z_1 \\ F_1 - \frac{F_1 - F_{\min}}{z_2 - z_1} \cdot (z_2 - z) \rightarrow z_1 \leq z \leq z_2 \\ F_{\min} \rightarrow z \geq z_2 \end{cases} \quad \text{Equation 4-8}$$

- Where:
- $F_{\max}$  = Maximum bearing resistance factor (dim)
  - $F_1$  = Intermediate bearing resistance factor (dim)
  - $F_{\min}$  = Maximum bearing resistance factor (dim)
  - $z_1$  = Depth factor to intermediate bearing resistance factor (m)
  - $z_2$  = Depth factor to minimum bearing resistance factor (m)

Table 4-23 RE3 - Regression Variables

| Type                       |   | Longitudinal Spacing (mm) |       |       |       |       |       |       |       |       |
|----------------------------|---|---------------------------|-------|-------|-------|-------|-------|-------|-------|-------|
|                            |   | 50                        |       |       | 100   |       |       | 200   |       |       |
|                            |   | Max                       | 1     | Min   | Max   | 1     | Min   | Max   | 1     | Min   |
| MW71 x MW71<br>$S_T = 300$ | F | 6.00                      | 4.00  | 2.50  | 3.50  | 2.00  | 1.25  | 2.00  | 1.00  | 0.75  |
|                            | z | 0.000                     | 1.524 | 4.572 | 0.000 | 1.524 | 4.572 | 0.000 | 1.524 | 4.572 |
| MW71 x MW71<br>$S_T = 150$ | F | 5.00                      | 3.50  | 2.25  | 5.00  | 3.50  | 2.25  | 5.00  | 3.50  | 2.25  |
|                            | z | 0.000                     | 1.524 | 4.572 | 0.000 | 1.524 | 4.572 | 0.000 | 1.524 | 4.572 |
| MW71 x MW71<br>$S_T = 1W$  | F | 8.50                      | 5.00  | 2.50  | 5.00  | 2.50  | 1.50  | 2.50  | 1.50  | 1.00  |
|                            | z | 0.000                     | 1.524 | 4.572 | 0.000 | 1.524 | 4.572 | 0.000 | 1.524 | 4.572 |
| MW45 x MW45<br>$S_T = 300$ | F | 6.00                      | 3.00  | 1.50  | 2.75  | 1.50  | 1.00  | 2.00  | 1.00  | 0.50  |
|                            | z | 0.000                     | 1.524 | 4.572 | 0.000 | 1.524 | 4.572 | 0.000 | 1.524 | 4.572 |
| MW45 x MW45<br>$S_T = 150$ | F | 4.00                      | 2.50  | 2.00  | 3.00  | 1.75  | 1.50  | 2.00  | 1.00  | 0.75  |
|                            | z | 0.000                     | 1.524 | 4.572 | 0.000 | 1.524 | 4.572 | 0.000 | 1.524 | 4.572 |
| MW45 x MW45<br>$S_T = 1W$  | F | 8.00                      | 4.00  | 2.25  | 5.00  | 2.50  | 1.50  | 2.50  | 1.00  | 0.50  |
|                            | z | 0.000                     | 1.524 | 4.572 | 0.000 | 1.524 | 4.572 | 0.000 | 1.524 | 4.572 |

#### 4.5.4 Yu and Bathurst Equation

Yu and Bathurst (2015), calculated the pullout resistance factor,  $N_q$ , as shown in Equation 4-9, for grid type soil-reinforcing elements so it could be used to calculate the pullout resistance using Equation 4-10. In order to perform a direct comparison of the RE equations with the Yu and Bathurst. equations, the bearing resistance factor  $F_q$  is required to be calculated as shown in Equation 4-11. Once the  $F_q$  value is calculated it can be directly compared to the results of the RE equations. As stipulated in the literature for the and Bathurst method, the alpha and beta factors are required to be determined using a regression analysis. Based on this, the bearing resistance factor,  $N_q$ , using the results from the experimental test program, and a regression analysis, was performed to determine the required alpha and beta coefficients. The alpha and beta coefficients for the soil-reinforcing used in the experimental test program are shown in Table 4-24.

$$N_q = \alpha \left( \frac{n \cdot \sigma_v}{p_a} \right)^{-\beta} \quad \text{Equation 4-9}$$

Yu  $P_r = w \cdot n \cdot d_b \cdot N_q \cdot \sigma_v$  Equation 4-10

$$N_q = \frac{F_q \cdot S_T}{d_b} \rightarrow F_q = \frac{N_q \cdot d_b}{S_T} \quad \text{Equation 4-11}$$

|        |            |   |                                      |
|--------|------------|---|--------------------------------------|
| Where: | $\alpha$   | = | Bearing resistance coefficient (dim) |
|        | $n$        | = | Number of transverse bars (dim)      |
|        | $\sigma_v$ | = | Vertical pressure (kPa)              |
|        | $p_a$      | = | Atmospheric pressure(dim)            |
|        | $N_q$      | = | Bearing resistance factor (dim)      |

- $\beta$  = Bearing resistance coefficient (dim)
- $d_b$  = Diameter of transverse element (dim)
- $S_T$  = Spacing of transverse element (m)
- $F_q$  = Bearing resistance factor (dim)

Table 4-24 Yu - Regression Variables

| Type                       | Longitudinal Spacing (mm) |         |          |         |          |         |
|----------------------------|---------------------------|---------|----------|---------|----------|---------|
|                            | 50                        |         | 100      |         | 200      |         |
|                            | $\alpha$                  | $\beta$ | $\alpha$ | $\beta$ | $\alpha$ | $\beta$ |
| MW71 x MW71<br>$S_T = 300$ | 145                       | 0.263   | 69       | 0.288   | 42       | 0.338   |
| MW71 x MW71<br>$S_T = 150$ | 59                        | 0.274   | 35       | 0.198   | 26       | 0.380   |
| MW71 x MW71<br>$S_T = 1W$  | 83                        | 0.386   | 48       | 0.403   | 27       | 0.318   |
| MW45 x MW45<br>$S_T = 300$ | 149                       | 0.405   | 74       | 0.271   | 49       | 0.360   |
| MW45 x MW45<br>$S_T = 150$ | 57                        | 0.202   | 49       | 0.253   | 29       | 0.278   |
| MW45 x MW45<br>$S_T = 1W$  | 98                        | 0.402   | 65       | 0.414   | 26       | 0.435   |

#### 4.6 Bearing Resistance Factor from Test Data

##### 4.6.1 Group-1 Set-1 Bearing Resistance Factor

Group-1, Set-1 consists of an MW71 x MW71, 2-Wire soil-reinforcing element with transverse element spacings equal to 300 mm. Group-1, Set-1, had three sub-sets with longitudinal element spacings equal to 50 mm, 100 mm, and 200 mm. The pullout test results from the experimental test program for the Group-1 Set-1 are shown in Table 4-25. The  $F_q$  value shown in Table 4-25 is based on back-calculation using Equation 4-5.

Table 4-25 MW71 x MW71 – ST = 300 Pullout Test Results

| Type                     | Test | Depth<br>m | Surcharge<br>kPa | $P_{r,3/4}$<br>kN | $F_q$ | $\sigma_v$<br>kPa | $N_q$ |
|--------------------------|------|------------|------------------|-------------------|-------|-------------------|-------|
| MW71 X MW71<br>50 x 300  | 1    | 0.305      | 6.0              | 5.10              | 6.88  | 5.99              | 440   |
|                          | 2    | 0.305      | 6.0              | 4.09              | 5.51  | 6.0               | 353   |
|                          | 3    | 0.305      | 6.0              | 4.35              | 5.87  | 6.0               | 376   |
|                          | 4    | 0.305      | 6.0              | 4.48              | 6.04  | 6.0               | 386   |
|                          | 5    | 1.329      | 26.1             | 14.30             | 4.42  | 26.1              | 283   |
|                          | 6    | 1.317      | 25.9             | 13.64             | 4.26  | 25.9              | 273   |
|                          | 7    | 1.580      | 31.0             | 18.36             | 4.78  | 31.0              | 306   |
|                          | 8    | 2.680      | 52.6             | 23.86             | 3.66  | 52.6              | 234   |
|                          | 9    | 2.680      | 52.6             | 25.25             | 3.87  | 52.6              | 248   |
|                          | 10   | 2.672      | 52.5             | 24.29             | 3.74  | 52.5              | 239   |
|                          | 11   | 3.999      | 78.5             | 29.54             | 3.04  | 78.5              | 194   |
|                          | 12   | 3.999      | 78.5             | 26.70             | 2.75  | 78.5              | 176   |
|                          | 13   | 4.021      | 79.0             | 31.18             | 3.19  | 79.0              | 204   |
|                          | 14   | 5.364      | 105.3            | 34.31             | 2.63  | 105.3             | 168   |
|                          | 15   | 5.325      | 104.6            | 29.21             | 2.26  | 104.6             | 144   |
|                          | 16   | 6.111      | 120.0            | 39.19             | 2.64  | 120.0             | 169   |
|                          | 17   | 0.763      | 15.0             | 9.62              | 5.18  | 15.0              | 332   |
| MW71 X MW71<br>100 x 300 | 18   | 0.305      | 6.0              | 4.56              | 3.08  | 6.0               | 197   |
|                          | 19   | 0.305      | 6.0              | 4.40              | 2.97  | 6.0               | 190   |
|                          | 20   | 1.526      | 30.0             | 15.58             | 2.10  | 30.0              | 134   |
|                          | 21   | 1.517      | 29.8             | 14.02             | 1.90  | 29.8              | 122   |
|                          | 22   | 3.053      | 59.9             | 23.47             | 1.58  | 59.9              | 101   |
|                          | 23   | 4.589      | 90.1             | 29.16             | 1.31  | 90.1              | 84    |
|                          | 24   | 6.103      | 119.8            | 36.57             | 1.23  | 119.8             | 79    |
| MW71 X MW71<br>200 x 300 | 25   | 0.305      | 6.0              | 5.60              | 1.89  | 6.0               | 121   |
|                          | 26   | 0.305      | 6.0              | 5.86              | 1.98  | 6.0               | 126   |
|                          | 27   | 1.553      | 30.5             | 16.62             | 1.10  | 30.5              | 70    |
|                          | 28   | 1.534      | 30.1             | 18.32             | 1.23  | 30.1              | 79    |
|                          | 29   | 2.494      | 49.0             | 22.49             | 0.93  | 49.0              | 59    |
|                          | 30   | 3.082      | 60.5             | 22.87             | 0.76  | 60.5              | 49    |
|                          | 31   | 3.209      | 63.0             | 25.78             | 0.83  | 63.0              | 53    |
|                          | 32   | 3.180      | 62.4             | 28.80             | 0.93  | 62.4              | 60    |
|                          | 33   | 3.038      | 59.7             | 28.94             | 0.98  | 59.7              | 63    |
|                          | 34   | 4.570      | 89.7             | 35.17             | 0.79  | 89.7              | 51    |
|                          | 35   | 6.096      | 119.7            | 39.94             | 0.67  | 119.7             | 43    |

4.6.1.1 RE1 Group-1 / Set-1

RE1

$$F_q = \alpha \cdot e^{-\beta \cdot z}$$

Equation 4-6

Table 4-26 RE1 - Regression Variables for  $S_T = 300$

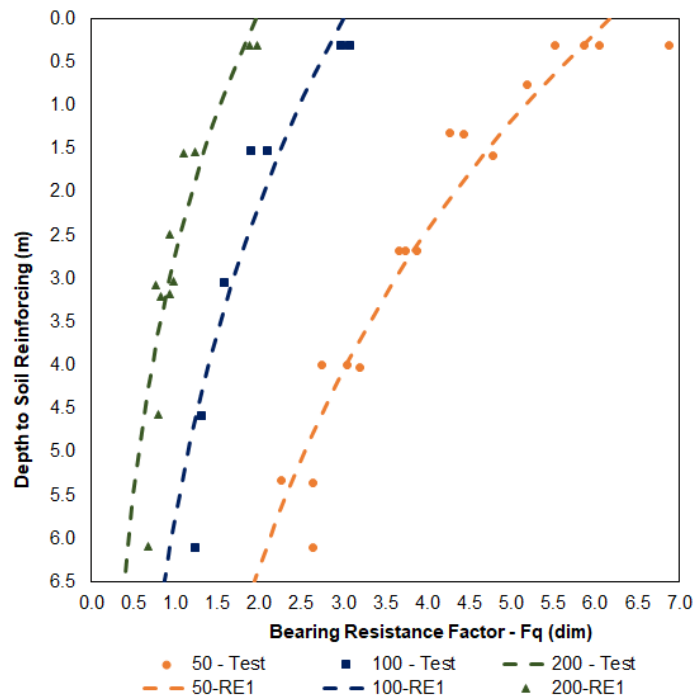
| Type        | Longitudinal Spacing (mm) |         |          |         |          |         |
|-------------|---------------------------|---------|----------|---------|----------|---------|
|             | 50                        |         | 100      |         | 200      |         |
|             | $\alpha$                  | $\beta$ | $\alpha$ | $\beta$ | $\alpha$ | $\beta$ |
| MW71 x MW71 | 6.17                      | 0.178   | 3.00     | 0.192   | 2.00     | 0.250   |

Table 4-27 RE1 –  $S_T = 300$

| Type                     | Test | Z (m) | $P_{test}$ (kN/m <sup>3</sup> ) | $P_{calc}$ (kN/m <sup>3</sup> ) | Bias | Statistics |         |
|--------------------------|------|-------|---------------------------------|---------------------------------|------|------------|---------|
| MW71 X MW71<br>50 x 300  | 1    | 0.305 | 5.10                            | 4.33                            | 0.85 |            |         |
|                          | 2    | 0.305 | 4.09                            | 4.33                            | 1.06 |            |         |
|                          | 3    | 0.305 | 4.35                            | 4.33                            | 1.00 |            |         |
|                          | 4    | 0.305 | 4.48                            | 4.33                            | 0.97 |            |         |
|                          | 5    | 1.329 | 14.30                           | 15.74                           | 1.10 |            |         |
|                          | 6    | 1.317 | 13.64                           | 15.63                           | 1.15 |            |         |
|                          | 7    | 1.580 | 18.36                           | 17.90                           | 0.97 |            |         |
|                          | 8    | 2.680 | 23.86                           | 24.96                           | 1.05 |            |         |
|                          | 9    | 2.680 | 25.25                           | 24.96                           | 0.99 |            |         |
|                          | 10   | 2.672 | 24.29                           | 24.92                           | 1.03 |            |         |
|                          | 11   | 3.999 | 29.54                           | 29.46                           | 1.00 |            |         |
|                          | 12   | 3.999 | 26.70                           | 29.46                           | 1.10 | 0.09       | COV     |
|                          | 13   | 4.021 | 31.18                           | 29.51                           | 0.95 | -0.09      | Cor-C   |
|                          | 14   | 5.364 | 34.31                           | 31.00                           | 0.90 | 0.74       | P-Bias  |
|                          | 15   | 5.325 | 29.21                           | 30.99                           | 1.06 | 0.98       | Pearson |
|                          | 16   | 6.111 | 39.19                           | 30.93                           | 0.79 | 0.09       | STD     |
|                          | 17   | 0.763 | 9.62                            | 10.00                           | 1.04 | 1.00       | Mean    |
| MW71 X MW71<br>100 x 300 | 18   | 0.305 | 4.56                            | 4.20                            | 0.92 |            |         |
|                          | 19   | 0.305 | 4.40                            | 4.20                            | 0.95 | 0.14       | COV     |
|                          | 20   | 1.526 | 15.58                           | 16.63                           | 1.07 | -0.13      | Cor-C   |
|                          | 21   | 1.517 | 14.02                           | 16.56                           | 1.18 | 0.78       | P-Bias  |
|                          | 22   | 3.053 | 23.47                           | 24.82                           | 1.06 | 0.95       | Pearson |
|                          | 23   | 4.589 | 29.16                           | 27.79                           | 0.95 | 0.13       | STD     |
|                          | 24   | 6.103 | 36.57                           | 27.65                           | 0.76 | 0.98       | Mean    |

Table 4-27 RE1 –  $S_T = 300$

| Type                     | Test | Z (m) | $P_{test}$ (kN/m <sup>3</sup> ) | $P_{calc}$ (kN/m <sup>3</sup> ) | Bias | Statistics |         |
|--------------------------|------|-------|---------------------------------|---------------------------------|------|------------|---------|
| MW71 X MW71<br>200 x 300 | 25   | 0.305 | 5.60                            | 5.38                            | 0.96 |            |         |
|                          | 26   | 0.305 | 5.86                            | 5.38                            | 0.92 |            |         |
|                          | 27   | 1.553 | 16.62                           | 20.07                           | 1.21 |            |         |
|                          | 28   | 1.534 | 18.32                           | 19.92                           | 1.09 |            |         |
|                          | 29   | 2.494 | 22.49                           | 25.48                           | 1.13 |            |         |
|                          | 30   | 3.082 | 22.87                           | 27.18                           | 1.19 | 0.18       | COV     |
|                          | 31   | 3.209 | 25.78                           | 27.41                           | 1.06 | 0.01       | Cor-C   |
|                          | 32   | 3.180 | 28.80                           | 27.36                           | 0.95 | 0.98       | P-Bias  |
|                          | 33   | 3.038 | 28.94                           | 27.09                           | 0.94 | 0.86       | Pearson |
|                          | 34   | 4.570 | 35.17                           | 27.79                           | 0.79 | 0.17       | STD     |
|                          | 35   | 6.096 | 39.94                           | 25.31                           | 0.63 | 0.99       | Mean    |



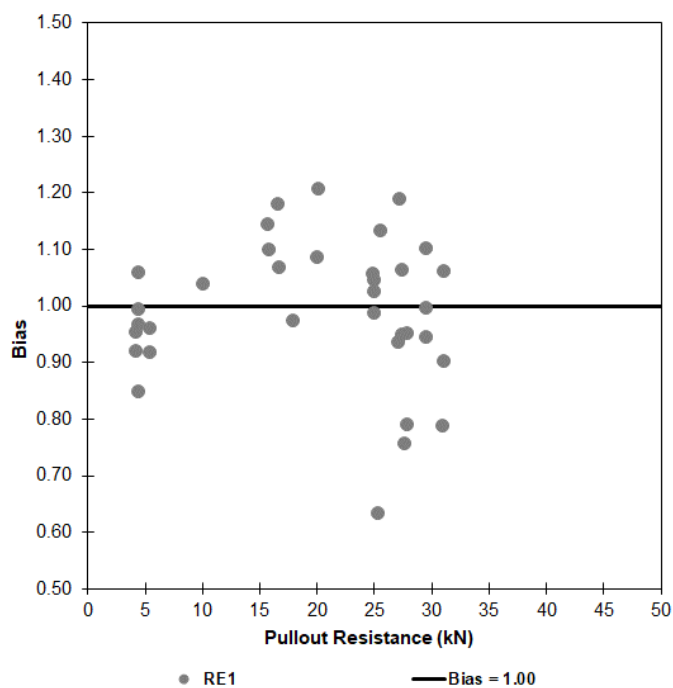


Figure 4-12 RE1 – Bias (MW71 S<sub>T</sub> = 300 mm)

4.6.1.2 RE2 Group-1 / Set-1

RE2

$$F_q = F_0 + F_{max} \cdot e^{-\beta \cdot z}$$

Equation 4-7

Table 4-28 RE2 - Regression Variables for S<sub>T</sub> = 300

| Type        | Longitudinal Spacing (mm) |      |      |                |      |      |                |      |      |
|-------------|---------------------------|------|------|----------------|------|------|----------------|------|------|
|             | 50                        |      |      | 100            |      |      | 200            |      |      |
|             | F <sub>0</sub>            | α    | β    | F <sub>0</sub> | α    | β    | F <sub>0</sub> | α    | β    |
| MW71 x MW71 | 2.00                      | 4.50 | 0.38 | 1.25           | 2.25 | 0.75 | 0.70           | 1.50 | 0.75 |

Table 4-29 RE2 – S<sub>T</sub> = 300

| Type                 | Test | Z (m) | P <sub>test</sub> (kN/m <sup>3</sup> ) | P <sub>calc</sub> (kN/m <sup>3</sup> ) | Bias | Statistics |
|----------------------|------|-------|--|--|------|------------|
| MW71 X MW71 50 x 300 | 1    | 0.305 | 5.10                                   | 4.46                                   | 0.87 |            |
|                      | 2    | 0.305 | 4.09                                   | 4.46                                   | 1.09 |            |
|                      | 3    | 0.305 | 4.35                                   | 4.46                                   | 1.02 |            |
|                      | 4    | 0.305 | 4.48                                   | 4.46                                   | 1.00 |            |

Table 4-29 RE2 – S<sub>T</sub> = 300

| Type                     | Test | Z<br>(m) | P <sub>test</sub><br>(kN/m <sup>3</sup> ) | P <sub>calc</sub><br>(kN/m <sup>3</sup> ) | Bias | Statistics |         |
|--------------------------|------|----------|---|---|------|------------|---------|
|                          | 5    | 1.329    | 14.30                                     | 15.30                                     | 1.07 |            |         |
|                          | 6    | 1.317    | 13.64                                     | 15.20                                     | 1.11 |            |         |
|                          | 7    | 1.580    | 18.36                                     | 17.25                                     | 0.94 |            |         |
|                          | 8    | 2.680    | 23.86                                     | 23.77                                     | 1.00 |            |         |
|                          | 9    | 2.680    | 25.25                                     | 23.77                                     | 0.94 |            |         |
|                          | 10   | 2.672    | 24.29                                     | 23.74                                     | 0.98 |            |         |
|                          | 11   | 3.999    | 29.54                                     | 29.22                                     | 0.99 |            |         |
|                          | 12   | 3.999    | 26.70                                     | 29.22                                     | 1.09 | 0.08       | COV     |
|                          | 13   | 4.021    | 31.18                                     | 29.30                                     | 0.94 | -0.01      | Cor-C   |
|                          | 14   | 5.364    | 34.31                                     | 33.95                                     | 0.99 | 0.98       | P-Bias  |
|                          | 15   | 5.325    | 29.21                                     | 33.82                                     | 1.16 | 0.99       | Pearson |
|                          | 16   | 6.111    | 39.19                                     | 36.49                                     | 0.93 | 0.08       | STD     |
|                          | 17   | 0.763    | 9.62                                      | 9.99                                      | 1.04 | 1.01       | Mean    |
| MW71 X MW71<br>100 x 300 | 18   | 0.305    | 4.56                                      | 4.51                                      | 0.99 |            |         |
|                          | 19   | 0.305    | 4.40                                      | 4.51                                      | 1.02 | 0.04       | COV     |
|                          | 20   | 1.526    | 15.58                                     | 14.60                                     | 0.94 | 0.15       | Cor-C   |
|                          | 21   | 1.517    | 14.02                                     | 14.54                                     | 1.04 | 0.75       | P-Bias  |
|                          | 22   | 3.053    | 23.47                                     | 21.95                                     | 0.94 | 1.00       | Pearson |
|                          | 23   | 4.589    | 29.16                                     | 29.51                                     | 1.01 | 0.04       | STD     |
|                          | 24   | 6.103    | 36.57                                     | 37.80                                     | 1.03 | 1.00       | Mean    |
| MW71 X MW71<br>200 x 300 | 25   | 0.305    | 5.60                                      | 5.61                                      | 1.00 |            |         |
|                          | 26   | 0.305    | 5.86                                      | 5.61                                      | 0.96 |            |         |
|                          | 27   | 1.553    | 16.62                                     | 17.65                                     | 1.06 |            |         |
|                          | 28   | 1.534    | 18.32                                     | 17.53                                     | 0.96 |            |         |
|                          | 29   | 2.494    | 22.49                                     | 22.59                                     | 1.00 |            |         |
|                          | 30   | 3.082    | 22.87                                     | 25.45                                     | 1.11 | 0.11       | COV     |
|                          | 31   | 3.209    | 25.78                                     | 26.07                                     | 1.01 | 0.12       | Cor-C   |
|                          | 32   | 3.180    | 28.80                                     | 25.93                                     | 0.90 | 0.74       | P-Bias  |
|                          | 33   | 3.038    | 28.94                                     | 25.23                                     | 0.87 | 0.96       | Pearson |
|                          | 34   | 4.570    | 35.17                                     | 33.29                                     | 0.95 | 0.11       | STD     |
|                          | 35   | 6.096    | 39.94                                     | 50.70                                     | 1.27 | 1.01       | Mean    |



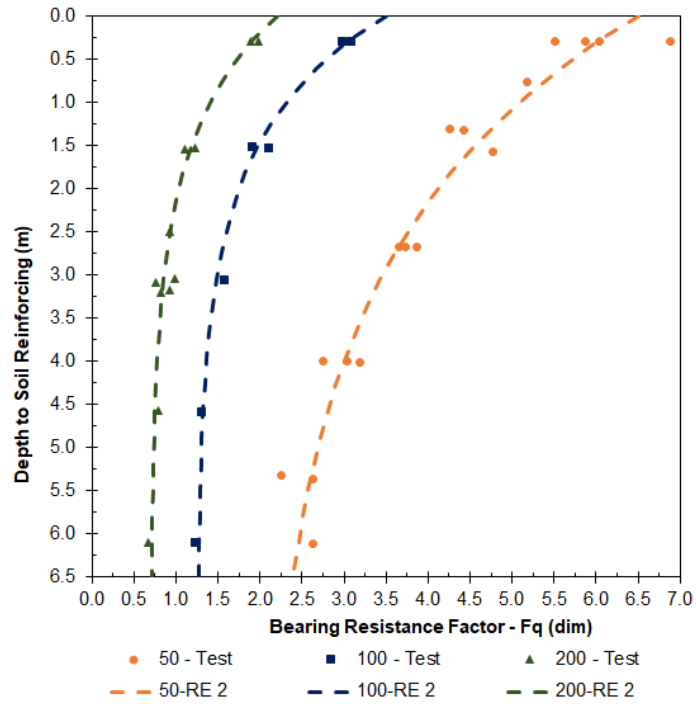


Figure 4-13 RE2 – Bearing Resistance Factor (MW71  $S_T = 300$  mm)

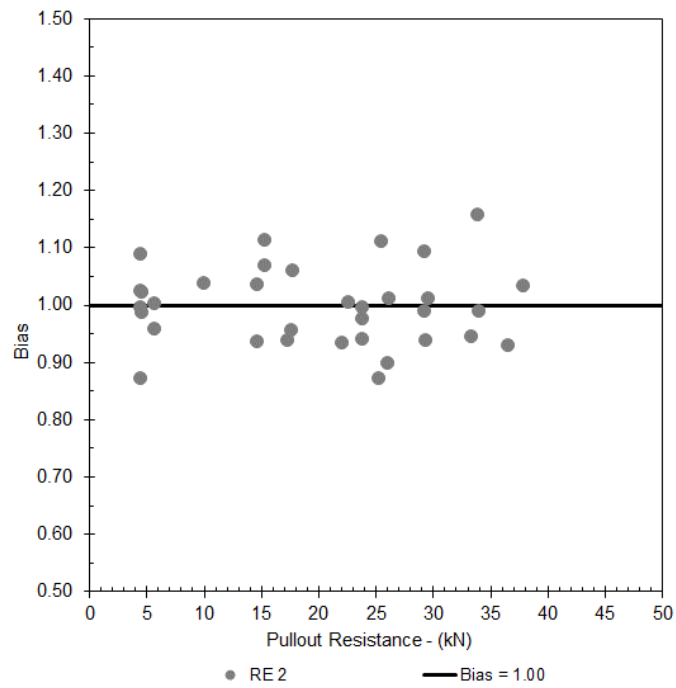


Figure 4-14 RE2 – Bias (MW71  $S_T = 300$  mm)

4.6.1.3 RE3 Group-1 / Set-1

$$RE3 \quad F_q = \begin{cases} F_{\max} - \frac{F_{\max} - F_1}{z_1} \cdot z \rightarrow 0 \leq z \leq z_1 \\ F_1 - \frac{F_1 - F_{\min}}{z_2 - z_1} \cdot (z - z_1) \rightarrow z_1 \leq z \leq z_2 \\ F_{\min} \rightarrow z \geq z_2 \end{cases} \quad \text{Equation 4-8}$$

Table 4-30 RE3 - Regression Variables for  $S_T = 300$

| Type        |   | Longitudinal Spacing (mm) |       |       |       |       |       |       |       |       |
|-------------|---|---------------------------|-------|-------|-------|-------|-------|-------|-------|-------|
|             |   | 50                        |       |       | 100   |       |       | 200   |       |       |
|             |   | Max                       | 1     | Min   | Max   | 1     | Min   | Max   | 1     | Min   |
| MW71 x MW71 | F | 6.00                      | 4.00  | 2.50  | 3.50  | 2.00  | 1.25  | 2.00  | 1.00  | 0.75  |
|             | z | 0.000                     | 1.524 | 4.572 | 0.000 | 1.524 | 4.572 | 0.000 | 1.524 | 4.572 |

Table 4-31 RE3 –  $S_T = 300$

| Type                    | Test | Z (m) | $P_{\text{test}}$ (kN/m <sup>3</sup> ) | $P_{\text{calc}}$ (kN/m <sup>3</sup> ) | Bias | Statistics |         |
|-------------------------|------|-------|--|--|------|------------|---------|
| MW71 X MW71<br>50 x 300 | 1    | 0.305 | 5.10                                   | 4.15                                   | 0.81 |            |         |
|                         | 2    | 0.305 | 4.09                                   | 4.15                                   | 1.02 |            |         |
|                         | 3    | 0.305 | 4.35                                   | 4.15                                   | 0.95 |            |         |
|                         | 4    | 0.305 | 4.48                                   | 4.15                                   | 0.93 |            |         |
|                         | 5    | 1.329 | 14.30                                  | 13.76                                  | 0.96 |            |         |
|                         | 6    | 1.317 | 13.64                                  | 13.68                                  | 1.00 |            |         |
|                         | 7    | 1.580 | 18.36                                  | 15.27                                  | 0.83 |            |         |
|                         | 8    | 2.680 | 23.86                                  | 22.36                                  | 0.94 |            |         |
|                         | 9    | 2.680 | 25.25                                  | 22.36                                  | 0.89 |            |         |
|                         | 10   | 2.672 | 24.29                                  | 22.33                                  | 0.92 |            |         |
|                         | 11   | 3.999 | 29.54                                  | 27.06                                  | 0.92 |            |         |
|                         | 12   | 3.999 | 26.70                                  | 27.06                                  | 1.01 | 0.08       | COV     |
|                         | 13   | 4.021 | 31.18                                  | 27.10                                  | 0.87 | 0.20       | Cor-C   |
|                         | 14   | 5.364 | 34.31                                  | 32.62                                  | 0.95 | 0.44       | P-Bias  |
|                         | 15   | 5.325 | 29.21                                  | 32.38                                  | 1.11 | 0.99       | Pearson |
|                         | 16   | 6.111 | 39.19                                  | 37.16                                  | 0.95 | 0.07       | STD     |
|                         | 17   | 0.763 | 9.62                                   | 9.28                                   | 0.96 | 0.94       | Mean    |

Table 4-31 RE3 –  $S_T = 300$

| Type                     | Test | Z (m) | $P_{test}$ (kN/m <sup>3</sup> ) | $P_{calc}$ (kN/m <sup>3</sup> ) | Bias | Statistics |         |
|--------------------------|------|-------|---------------------------------|---------------------------------|------|------------|---------|
| MW71 X MW71<br>100 x 300 | 18   | 0.305 | 4.56                            | 4.74                            | 1.04 |            |         |
|                          | 19   | 0.305 | 4.40                            | 4.74                            | 1.08 | 0.05       | COV     |
|                          | 20   | 1.526 | 15.58                           | 14.85                           | 0.95 | -0.47      | Cor-C   |
|                          | 21   | 1.517 | 14.02                           | 14.81                           | 1.06 | 0.24       | P-Bias  |
|                          | 22   | 3.053 | 23.47                           | 24.11                           | 1.03 | 0.99       | Pearson |
|                          | 23   | 4.589 | 29.16                           | 27.90                           | 0.96 | 0.05       | STD     |
|                          | 24   | 6.103 | 36.57                           | 37.11                           | 1.01 | 1.02       | Mean    |
| MW71 X MW71<br>200 x 300 | 25   | 0.305 | 5.60                            | 5.34                            | 0.95 |            |         |
|                          | 26   | 0.305 | 5.86                            | 5.34                            | 0.91 |            |         |
|                          | 27   | 1.553 | 16.62                           | 15.08                           | 0.91 |            |         |
|                          | 28   | 1.534 | 18.32                           | 14.91                           | 0.81 |            |         |
|                          | 29   | 2.494 | 22.49                           | 22.34                           | 0.99 |            |         |
|                          | 30   | 3.082 | 22.87                           | 26.15                           | 1.14 | 0.10       | COV     |
|                          | 31   | 3.209 | 25.78                           | 26.90                           | 1.04 | 0.12       | Cor-C   |
|                          | 32   | 3.180 | 28.80                           | 26.73                           | 0.93 | 0.74       | P-Bias  |
|                          | 33   | 3.038 | 28.94                           | 25.89                           | 0.89 | 0.98       | Pearson |
|                          | 34   | 4.570 | 35.17                           | 33.35                           | 0.95 | 0.10       | STD     |
|                          | 35   | 6.096 | 39.94                           | 44.48                           | 1.11 | 0.97       | Mean    |

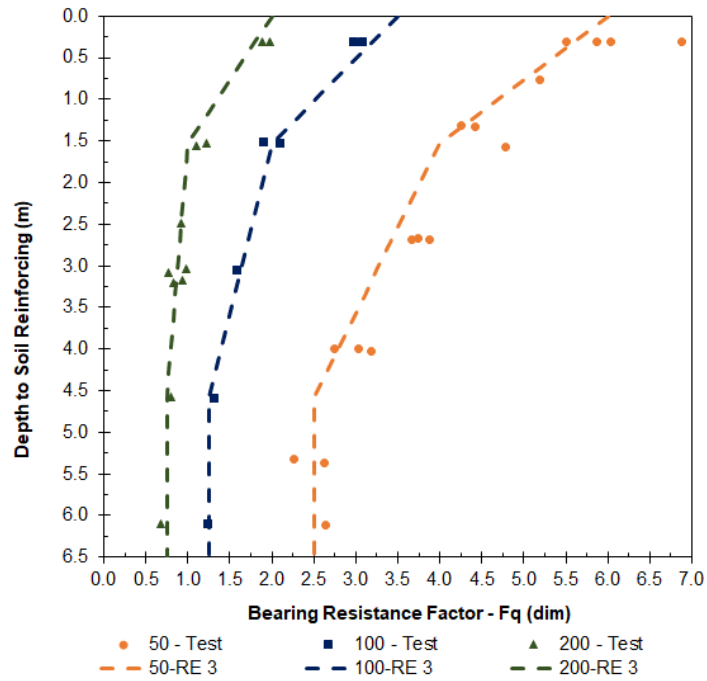


Figure 4-15 RE3 – Bearing Resistance Factor (MW71  $S_T = 300$  mm)

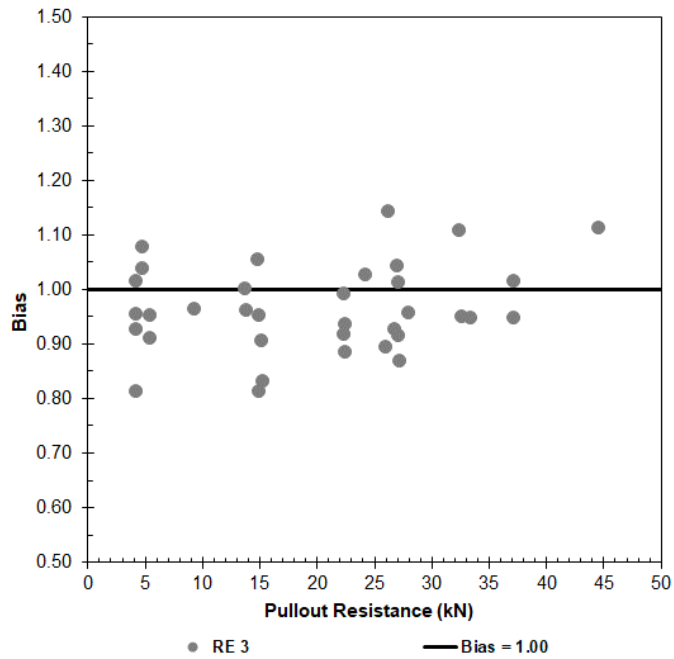


Figure 4-16 RE3 – Bias (MW71  $S_T = 300$  mm)

4.6.1.4 Yu Group-1 / Set-1

Table 4-32 Yu - Regression Variables for  $S_T = 300$

| Type        | Longitudinal Spacing (mm) |         |          |         |          |         |
|-------------|---------------------------|---------|----------|---------|----------|---------|
|             | 50                        |         | 100      |         | 200      |         |
|             | $\alpha$                  | $\beta$ | $\alpha$ | $\beta$ | $\alpha$ | $\beta$ |
| MW71 x MW71 | 145                       | 0.263   | 69       | 0.288   | 42       | 0.338   |

$$N_q = \alpha \left( \frac{n \cdot \sigma_v}{p_a} \right)^{-\beta} \quad \text{Equation 4-9}$$

Yu

$$N_q = \frac{F_q \cdot S_T}{d_b} \rightarrow F_q = \frac{N_q \cdot d_b}{S_T} \quad \text{Equation 4-11}$$

Table 4-33 Yu - Regression Variables

| Type                       | Longitudinal Spacing (mm) |         |          |         |          |         |
|----------------------------|---------------------------|---------|----------|---------|----------|---------|
|                            | 50                        |         | 100      |         | 200      |         |
|                            | $\alpha$                  | $\beta$ | $\alpha$ | $\beta$ | $\alpha$ | $\beta$ |
| MW71 x MW71<br>$S_T = 300$ | 145                       | 0.263   | 69       | 0.288   | 42       | 0.338   |

Table 4-34  $Y_u - S_T = 300$

| Type                     | Test | Z (m) | $P_{test}$ (kN/m <sup>3</sup> ) | $P_{calc}$ (kN/m <sup>3</sup> ) | Bias | Statistics |         |
|--------------------------|------|-------|---------------------------------|---------------------------------|------|------------|---------|
| MW71 X MW71<br>50 x 300  | 1    | 0.305 | 5.10                            | 4.90                            | 0.96 |            |         |
|                          | 2    | 0.305 | 4.09                            | 4.90                            | 1.20 |            |         |
|                          | 3    | 0.305 | 4.35                            | 4.90                            | 1.13 |            |         |
|                          | 4    | 0.305 | 4.48                            | 4.90                            | 1.10 |            |         |
|                          | 5    | 1.329 | 14.30                           | 14.52                           | 1.02 |            |         |
|                          | 6    | 1.317 | 13.64                           | 14.42                           | 1.06 |            |         |
|                          | 7    | 1.580 | 18.36                           | 16.49                           | 0.90 |            |         |
|                          | 8    | 2.680 | 23.86                           | 24.35                           | 1.02 |            |         |
|                          | 9    | 2.680 | 25.25                           | 24.35                           | 0.96 |            |         |
|                          | 10   | 2.672 | 24.29                           | 24.30                           | 1.00 |            |         |
|                          | 11   | 3.999 | 29.54                           | 32.70                           | 1.11 |            |         |
|                          | 12   | 3.999 | 26.70                           | 32.70                           | 1.22 | 0.11       | COV     |
|                          | 13   | 4.021 | 31.18                           | 32.83                           | 1.05 | 0.43       | Cor-C   |
|                          | 14   | 5.364 | 34.31                           | 40.60                           | 1.18 | 0.01       | P-Bias  |
|                          | 15   | 5.325 | 29.21                           | 40.39                           | 1.38 | 0.98       | Pearson |
|                          | 16   | 6.111 | 39.19                           | 44.70                           | 1.14 | 0.12       | STD     |
|                          | 17   | 0.763 | 9.62                            | 9.65                            | 1.00 | 1.08       | Mean    |
| MW71 X MW71<br>100 x 300 | 18   | 0.305 | 4.56                            | 4.74                            | 1.06 |            |         |
|                          | 19   | 0.305 | 4.40                            | 4.74                            | 1.10 | 0.05       | COV     |
|                          | 20   | 1.526 | 15.58                           | 14.85                           | 0.98 | 0.47       | Cor-C   |
|                          | 21   | 1.517 | 14.02                           | 14.81                           | 1.09 | 0.29       | P-Bias  |
|                          | 22   | 3.053 | 23.47                           | 24.11                           | 1.07 | 1.00       | Pearson |
|                          | 23   | 4.589 | 29.16                           | 27.90                           | 1.15 | 0.05       | STD     |
|                          | 24   | 6.103 | 36.57                           | 37.11                           | 1.12 | 1.08       | Mean    |
| MW71 X MW71<br>200 x 300 | 25   | 0.305 | 5.60                            | 5.34                            | 1.12 |            |         |
|                          | 26   | 0.305 | 5.86                            | 5.34                            | 1.07 |            |         |
|                          | 27   | 1.553 | 16.62                           | 15.08                           | 1.11 |            |         |
|                          | 28   | 1.534 | 18.32                           | 14.91                           | 1.00 |            |         |
|                          | 29   | 2.494 | 22.49                           | 22.34                           | 1.12 |            |         |
|                          | 30   | 3.082 | 22.87                           | 26.15                           | 1.27 | 0.07       | COV     |
|                          | 31   | 3.209 | 25.78                           | 26.90                           | 1.15 | 0.16       | Cor-C   |
|                          | 32   | 3.180 | 28.80                           | 26.73                           | 1.03 | 0.65       | P-Bias  |
|                          | 33   | 3.038 | 28.94                           | 25.89                           | 0.99 | 0.99       | Pearson |
|                          | 34   | 4.570 | 35.17                           | 33.35                           | 1.07 | 0.08       | STD     |
|                          | 35   | 6.096 | 39.94                           | 44.48                           | 1.14 | 1.10       | Mean    |

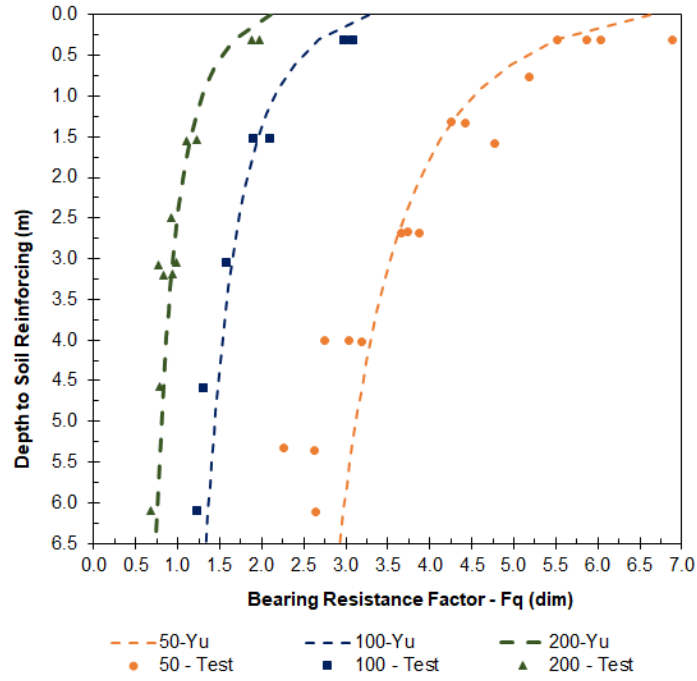


Figure 4-17 Yu – Bearing Resistance Factor (MW71  $S_T = 300$  mm)

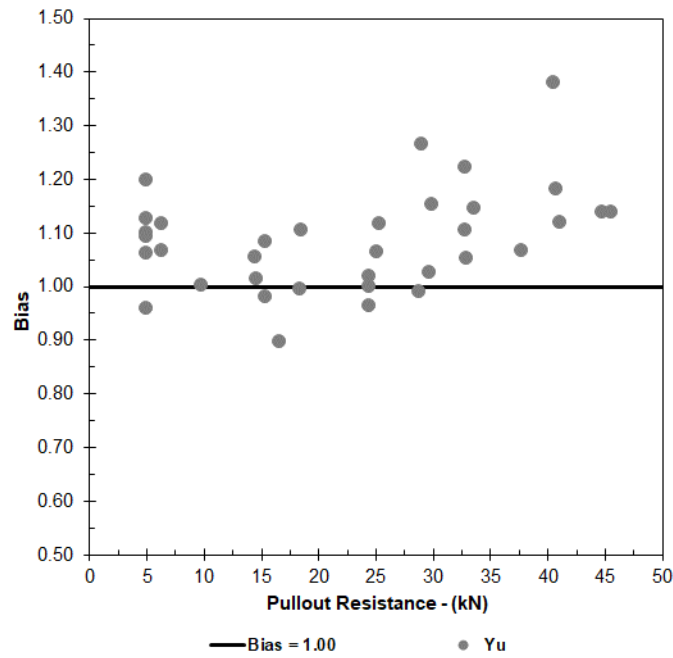


Figure 4-18 Yu – Bias (MW71  $S_T = 300$  mm)

#### 4.6.2 Group-1 Set-2 Bearing Resistance Factor

Group-1, Set-2 consists of an MW71 x MW71, 2-Wire soil-reinforcing element with transverse element spacings equal to 150 mm. Group-1, Set-2, had three sub-sets with longitudinal element spacings equal to 50 mm, 100 mm, and 200 mm.

Table 4-35 MW71 x MW71 – ST = 150 Pullout Test Results

| Type                     | Test | Depth<br>m | Surcharge<br>kPa | $P_{r,3/4}$<br>kN | $F^*_{19\text{ mm}}$ | $\sigma_v$<br>kPa | $N_q$ |
|--------------------------|------|------------|------------------|-------------------|----------------------|-------------------|-------|
| MW71 x MW71<br>50 x 150  | 1    | 0.305      | 5.99             | 3.77              | 5.09                 | 5.99              | 326   |
|                          | 2    | 1.529      | 30.02            | 12.55             | 3.37                 | 30.02             | 216   |
|                          | 3    | 3.068      | 60.23            | 21.10             | 2.83                 | 60.23             | 181   |
|                          | 4    | 3.058      | 60.04            | 17.79             | 2.39                 | 60.04             | 153   |
|                          | 5    | 4.570      | 89.73            | 26.63             | 2.40                 | 89.73             | 153   |
|                          | 6    | 6.089      | 119.56           | 35.30             | 2.38                 | 119.56            | 153   |
| MW71 x MW71<br>100 x 150 | 7    | 0.305      | 5.99             | 4.00              | 2.70                 | 5.99              | 173   |
|                          | 8    | 0.305      | 5.99             | 4.24              | 2.86                 | 5.99              | 183   |
|                          | 9    | 1.541      | 30.26            | 16.23             | 2.16                 | 30.26             | 139   |
|                          | 10   | 1.529      | 30.02            | 14.61             | 1.96                 | 30.02             | 126   |
|                          | 11   | 3.046      | 59.80            | 27.99             | 1.89                 | 59.80             | 121   |
|                          | 12   | 4.552      | 89.39            | 34.89             | 1.58                 | 89.39             | 101   |
|                          | 13   | 6.120      | 120.18           | 43.17             | 1.45                 | 120.18            | 93    |
| MW71 x MW71<br>200 x 150 | 14   | 0.305      | 5.99             | 7.53              | 2.54                 | 5.99              | 163   |
|                          | 15   | 1.522      | 29.88            | 18.74             | 1.27                 | 29.88             | 81    |
|                          | 16   | 3.041      | 59.71            | 33.77             | 1.14                 | 59.71             | 73    |
|                          | 17   | 4.560      | 89.54            | 42.91             | 0.97                 | 89.54             | 62    |
|                          | 18   | 6.120      | 120.18           | 43.17             | 0.72                 | 120.18            | 46    |
|                          | 19   | 6.108      | 119.94           | 49.72             | 0.84                 | 119.94            | 54    |



4.6.2.1 RE1 Group-1 / Set-2

RE1

$$F_q = \alpha \cdot e^{-\beta \cdot z}$$

Equation 4-6

Table 4-36 RE1 - Regression Variables for  $S_T = 150$

| Type        | Longitudinal Spacing (mm) |         |          |         |          |         |
|-------------|---------------------------|---------|----------|---------|----------|---------|
|             | 50                        |         | 100      |         | 200      |         |
|             | $\alpha$                  | $\beta$ | $\alpha$ | $\beta$ | $\alpha$ | $\beta$ |
| MW71 x MW71 | 4.86                      | 0.164   | 2.73     | 0.122   | 2.39     | 0.215   |

Table 4-37 RE1  $S_T = 150$

| Type                     | Test | Depth M | $P_{test}$ (kN/m <sup>3</sup> ) | $P_{calc}$ (kN/m <sup>3</sup> ) | Bias | Statistics |         |
|--------------------------|------|---------|---------------------------------|---------------------------------|------|------------|---------|
| MW71 x MW71<br>50 x 150  | 1    | 0.305   | 3.77                            | 3.43                            | 0.91 | 0.17       | COV     |
|                          | 2    | 1.529   | 12.55                           | 14.06                           | 1.12 | -0.09      | Cor-C   |
|                          | 3    | 3.068   | 21.10                           | 21.90                           | 1.04 | 0.74       | P-Bias  |
|                          | 4    | 3.058   | 17.79                           | 21.86                           | 1.23 | 0.93       | Pearson |
|                          | 5    | 4.570   | 26.63                           | 25.48                           | 0.96 | 0.17       | STD     |
|                          | 6    | 6.089   | 35.30                           | 26.45                           | 0.75 | 1.00       | Mean    |
| MW71 x MW71<br>100 x 150 | 7    | 0.305   | 4.00                            | 3.90                            | 0.98 |            |         |
|                          | 8    | 0.305   | 4.24                            | 3.90                            | 0.92 | 0.09       | COV     |
|                          | 9    | 1.541   | 16.23                           | 16.97                           | 1.05 | -0.13      | Cor-C   |
|                          | 10   | 1.529   | 14.61                           | 16.86                           | 1.15 | 0.78       | P-Bias  |
|                          | 11   | 3.046   | 27.99                           | 27.93                           | 1.00 | 0.95       | Pearson |
|                          | 12   | 4.552   | 34.89                           | 34.76                           | 1.00 | 0.09       | STD     |
|                          | 13   | 6.120   | 43.17                           | 38.61                           | 0.89 | 1.00       | Mean    |
| MW71 x MW71<br>200 x 150 | 14   | 0.305   | 7.53                            | 6.64                            | 0.88 | 0.21       | COV     |
|                          | 15   | 1.522   | 18.74                           | 25.53                           | 1.36 | 0.01       | Cor-C   |
|                          | 16   | 3.041   | 33.77                           | 36.79                           | 1.09 | 0.98       | P-Bias  |
|                          | 17   | 4.560   | 42.91                           | 39.79                           | 0.93 | 0.93       | Pearson |
|                          | 18   | 6.120   | 43.17                           | 38.17                           | 0.88 | 0.21       | STD     |
|                          | 19   | 6.108   | 49.72                           | 38.19                           | 0.77 | 0.99       | Mean    |

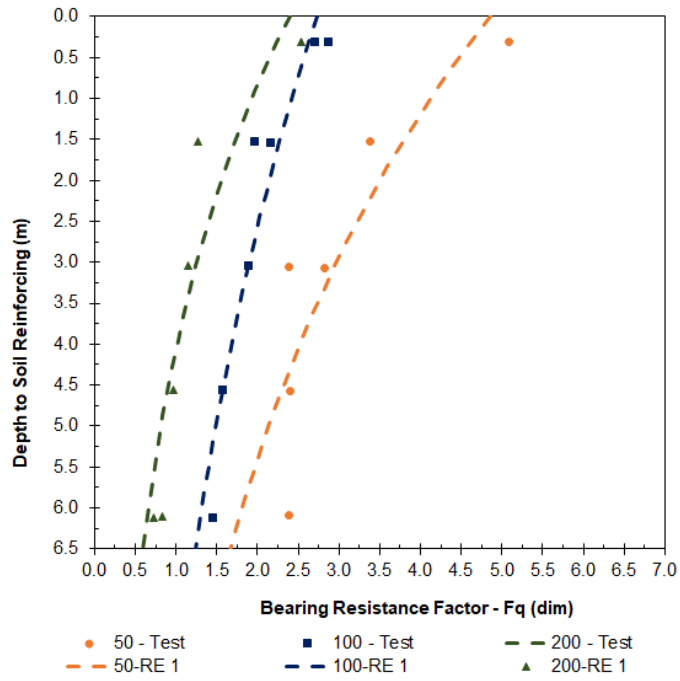


Figure 4-19 RE1 – Bearing Resistance Factor (MW71  $S_T = 150$  mm)

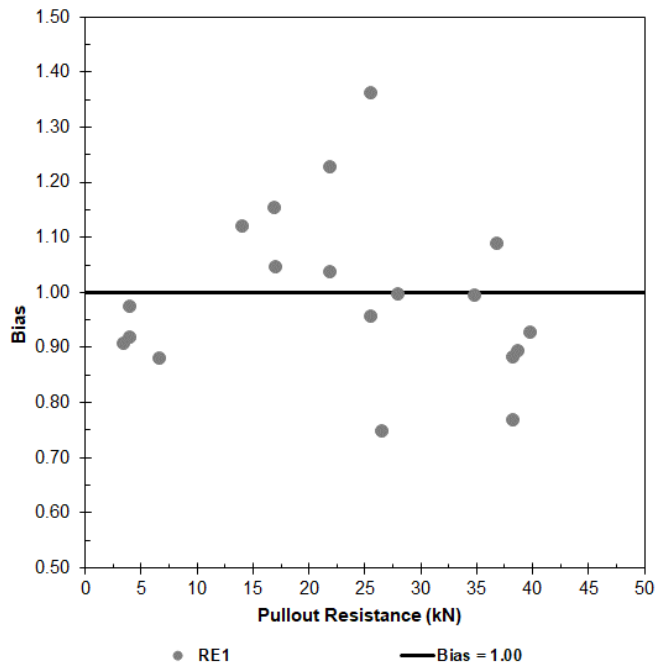


Figure 4-20 RE1 – Bias (MW71  $S_T = 150$  mm)

4.6.2.2 RE2 Group-1 / Set-2

RE2

$$F_q = F_0 + F_{\max} \cdot e^{-\beta \cdot z}$$

Equation 4-7

Table 4-38 RE2 - Regression Variables for  $S_T = 150$

| Type        | Longitudinal Spacing (mm) |          |         |       |          |         |       |          |         |
|-------------|---------------------------|----------|---------|-------|----------|---------|-------|----------|---------|
|             | 50                        |          |         | 100   |          |         | 200   |          |         |
|             | $F_0$                     | $\alpha$ | $\beta$ | $F_0$ | $\alpha$ | $\beta$ | $F_0$ | $\alpha$ | $\beta$ |
| MW71 x MW71 | 2.33                      | 3.54     | 0.81    | 1.45  | 1.55     | 0.55    | 0.86  | 2.25     | 0.99    |

Table 4-39 RE2 ST = 150

| Type                     | Test | Depth M | $P_{\text{test}}$ (kN/m <sup>3</sup> ) | $P_{\text{calc}}$ (kN/m <sup>3</sup> ) | Bias | Statistics |         |
|--------------------------|------|---------|--|--|------|------------|---------|
| MW71 x MW71<br>50 x 150  | 1    | 0.305   | 3.77                                   | 3.78                                   | 1.00 | 0.05       | COV     |
|                          | 2    | 1.529   | 12.55                                  | 12.46                                  | 0.99 | -0.01      | Cor-C   |
|                          | 3    | 3.068   | 21.10                                  | 19.56                                  | 0.93 | 0.98       | P-Bias  |
|                          | 4    | 3.058   | 17.79                                  | 19.52                                  | 1.10 | 1.00       | Pearson |
|                          | 5    | 4.570   | 26.63                                  | 26.84                                  | 1.01 | 0.05       | STD     |
|                          | 6    | 6.089   | 35.30                                  | 34.86                                  | 0.99 | 1.00       | Mean    |
| MW71 x MW71<br>100 x 150 | 7    | 0.305   | 4.00                                   | 4.10                                   | 1.02 |            |         |
|                          | 8    | 0.305   | 4.24                                   | 4.10                                   | 0.97 | 0.05       | COV     |
|                          | 9    | 1.541   | 16.23                                  | 15.88                                  | 0.98 | 0.15       | Cor-C   |
|                          | 10   | 1.529   | 14.61                                  | 15.78                                  | 1.08 | 0.75       | P-Bias  |
|                          | 11   | 3.046   | 27.99                                  | 25.84                                  | 0.92 | 1.00       | Pearson |
|                          | 12   | 4.552   | 34.89                                  | 34.99                                  | 1.00 | 0.05       | STD     |
|                          | 13   | 6.120   | 43.17                                  | 44.86                                  | 1.04 | 1.00       | Mean    |

Table 4-39 RE2 ST = 150

| Type                     | Test | Depth M | P <sub>test</sub> (kN/m <sup>3</sup> ) | P <sub>calc</sub> (kN/m <sup>3</sup> ) | Bias | Statistics |         |
|--------------------------|------|---------|--|--|------|------------|---------|
| MW71 x MW71<br>200 x 150 | 14   | 0.305   | 7.53                                   | 7.49                                   | 0.99 | 0.12       | COV     |
|                          | 15   | 1.522   | 18.74                                  | 20.11                                  | 1.07 | 0.12       | Cor-C   |
|                          | 16   | 3.041   | 33.77                                  | 28.77                                  | 0.85 | 0.74       | P-Bias  |
|                          | 17   | 4.560   | 42.91                                  | 39.36                                  | 0.92 | 0.96       | Pearson |
|                          | 18   | 6.120   | 43.17                                  | 51.70                                  | 1.20 | 0.12       | STD     |
|                          | 19   | 6.108   | 49.72                                  | 51.60                                  | 1.04 | 1.01       | Mean    |

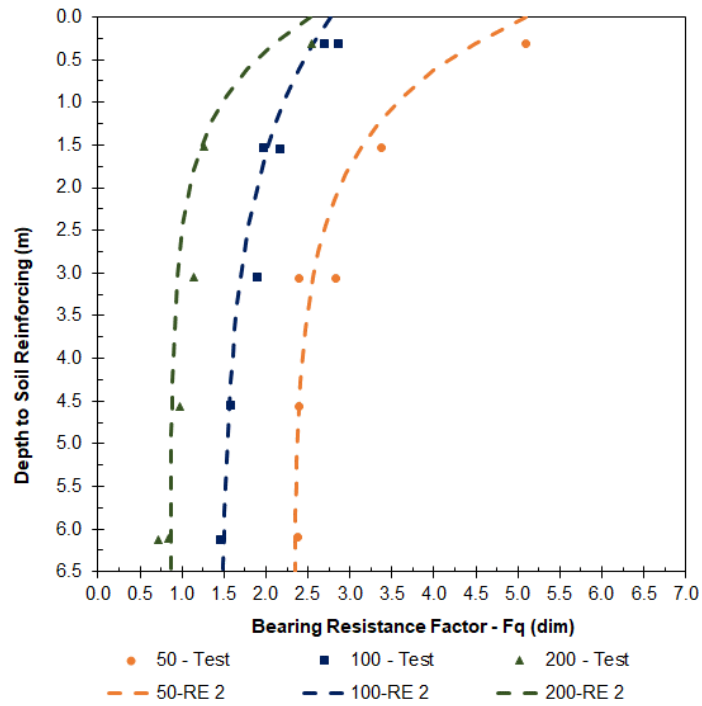


Figure 4-21 RE2 – Bearing Resistance Factor (MW71 S<sub>T</sub> = 150 mm)

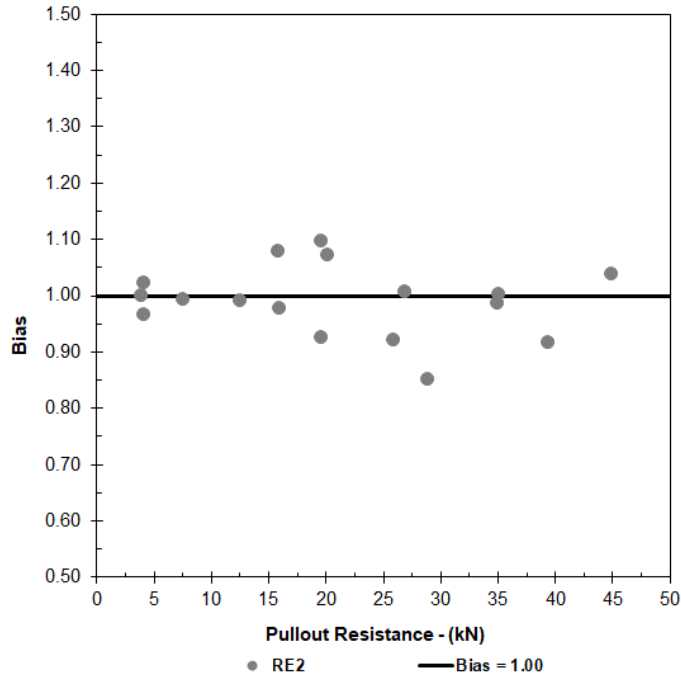


Figure 4-22 RE2 – Bias (MW71 S<sub>T</sub> = 150 mm)

#### 4.6.2.3 RE3 Group-1 / Set-2

$$RE3 \quad F_q = \begin{cases} F_{\max} - \frac{F_{\max} - F_1}{z_1} \cdot z \rightarrow 0 \leq z \leq z_1 \\ F_1 - \frac{F_1 - F_{\min}}{z_2 - z_1} \cdot (z_2 - z) \rightarrow z_1 \leq z \leq z_2 \\ F_{\min} \rightarrow z \geq z_2 \end{cases} \quad \text{Equation 4-8}$$

Table 4-40 RE3 - Regression Variables for S<sub>T</sub> = 150

| Type        |   | Longitudinal Spacing (mm) |       |       |       |       |       |       |       |       |
|-------------|---|---------------------------|-------|-------|-------|-------|-------|-------|-------|-------|
|             |   | 50                        |       |       | 100   |       |       | 200   |       |       |
|             |   | Max                       | 1     | Min   | Max   | 1     | Min   | Max   | 1     | Min   |
| MW71 x MW71 | F | 5.00                      | 3.50  | 2.25  | 5.00  | 3.50  | 2.25  | 5.00  | 3.50  | 2.25  |
|             | z | 0.000                     | 1.524 | 4.572 | 0.000 | 1.524 | 4.572 | 0.000 | 1.524 | 4.572 |

Table 4-41 RE3 ST = 150

| Type                     | Test | Depth<br>M | P <sub>test</sub><br>(kN/m <sup>3</sup> ) | P <sub>calc</sub><br>(kN/m <sup>3</sup> ) | Bias | Statistics |         |
|--------------------------|------|------------|---|---|------|------------|---------|
| MW71 x MW71<br>50 x 150  | 1    | 0.305      | 3.77                                      | 3.48                                      | 0.92 | 0.10       | COV     |
|                          | 2    | 1.529      | 12.55                                     | 13.01                                     | 1.04 | 0.20       | Cor-C   |
|                          | 3    | 3.068      | 21.10                                     | 21.39                                     | 1.01 | 0.44       | P-Bias  |
|                          | 4    | 3.058      | 17.79                                     | 21.35                                     | 1.20 | 0.98       | Pearson |
|                          | 5    | 4.570      | 26.63                                     | 25.02                                     | 0.94 | 0.10       | STD     |
|                          | 6    | 6.089      | 35.30                                     | 33.32                                     | 0.94 | 1.01       | Mean    |
| MW71 x MW71<br>100 x 150 | 7    | 0.305      | 4.00                                      | 4.15                                      | 1.04 |            |         |
|                          | 8    | 0.305      | 4.24                                      | 4.15                                      | 0.98 | 0.05       | COV     |
|                          | 9    | 1.541      | 16.23                                     | 14.97                                     | 0.92 | -0.47      | Cor-C   |
|                          | 10   | 1.529      | 14.61                                     | 14.87                                     | 1.02 | 0.24       | P-Bias  |
|                          | 11   | 3.046      | 27.99                                     | 25.93                                     | 0.93 | 1.00       | Pearson |
|                          | 12   | 4.552      | 34.89                                     | 33.29                                     | 0.95 | 0.05       | STD     |
|                          | 13   | 6.120      | 43.17                                     | 44.66                                     | 1.03 | 0.98       | Mean    |
| MW71 x MW71<br>200 x 150 | 14   | 0.305      | 7.53                                      | 5.34                                      | 0.71 | 0.14       | COV     |
|                          | 15   | 1.522      | 18.74                                     | 14.83                                     | 0.79 | 0.12       | Cor-C   |
|                          | 16   | 3.041      | 33.77                                     | 25.90                                     | 0.77 | 0.74       | P-Bias  |
|                          | 17   | 4.560      | 42.91                                     | 33.32                                     | 0.78 | 0.97       | Pearson |
|                          | 18   | 6.120      | 43.17                                     | 44.66                                     | 1.03 | 0.12       | STD     |
|                          | 19   | 6.108      | 49.72                                     | 44.57                                     | 0.90 | 0.83       | Mean    |

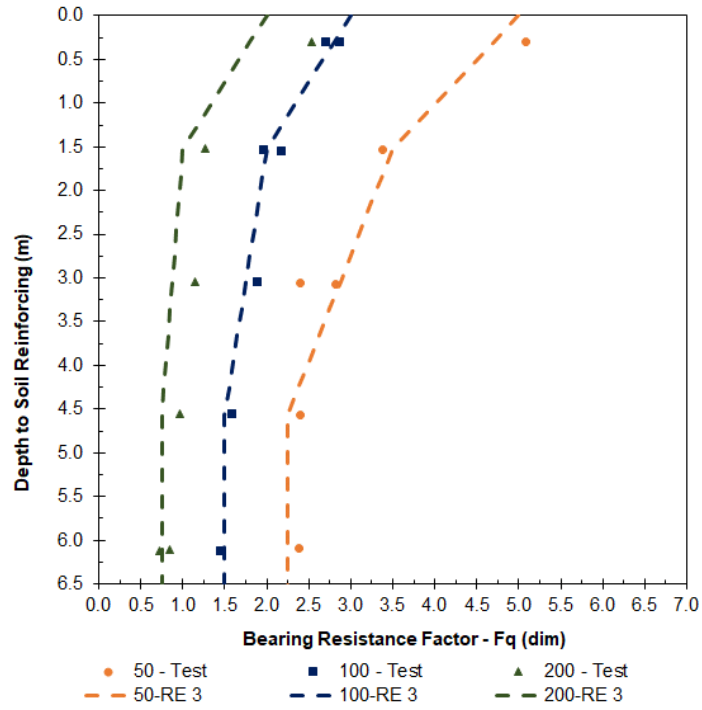


Figure 4-23 RE3 – Bearing Resistance Factor (MW71  $S_T = 150$  mm)

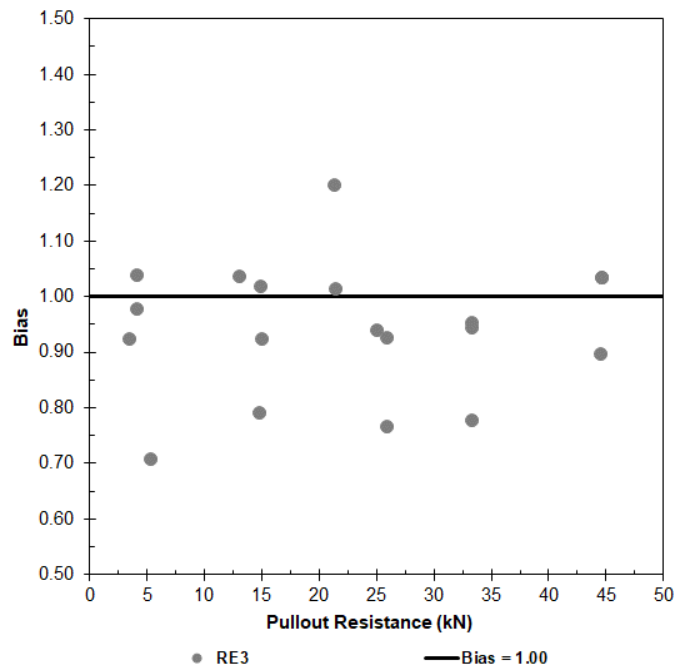


Figure 4-24 RE3 – Bias (MW71  $S_T = 150$  mm)

4.6.2.4 YU Group-1 / Set-2

$$N_q = \alpha \left( \frac{n \cdot \sigma_v}{p_a} \right)^{-\beta} \quad \text{Equation 4-9}$$

Yu

$$N_q = \frac{F_q \cdot S_T}{d_b} \rightarrow F_q = \frac{N_q \cdot d_b}{S_T} \quad \text{Equation 4-11}$$

Table 4-42 Yu - Regression Variables for  $S_T = 150$

| Type        | Longitudinal Spacing (mm) |         |          |         |          |         |
|-------------|---------------------------|---------|----------|---------|----------|---------|
|             | 50                        |         | 100      |         | 200      |         |
|             | $\alpha$                  | $\beta$ | $\alpha$ | $\beta$ | $\alpha$ | $\beta$ |
| MW71 x MW71 | 59                        | 0.274   | 35       | 0.198   | 26       | 0.380   |

Table 4-43 Yu ST = 150

| Type                     | Test | Depth M | $P_{\text{test}}$ (kN/m <sup>3</sup> ) | $P_{\text{calc}}$ (kN/m <sup>3</sup> ) | Bias | Statistics |         |
|--------------------------|------|---------|--|--|------|------------|---------|
| MW71 x MW71<br>50 x 150  | 1    | 0.305   | 3.77                                   | 3.35                                   | 0.89 | 0.07       | COV     |
|                          | 2    | 1.529   | 12.55                                  | 10.79                                  | 0.86 | -0.12      | Cor-C   |
|                          | 3    | 3.068   | 21.10                                  | 17.90                                  | 0.85 | 0.82       | P-Bias  |
|                          | 4    | 3.058   | 17.79                                  | 17.86                                  | 1.00 | 0.99       | Pearson |
|                          | 5    | 4.570   | 26.63                                  | 23.91                                  | 0.90 | 0.06       | STD     |
|                          | 6    | 6.089   | 35.30                                  | 29.45                                  | 0.83 | 0.89       | Mean    |
| MW71 x MW71<br>100 x 150 | 7    | 0.305   | 4.00                                   | 3.80                                   | 0.95 |            |         |
|                          | 8    | 0.305   | 4.24                                   | 3.80                                   | 0.90 | 0.05       | COV     |
|                          | 9    | 1.541   | 16.23                                  | 13.93                                  | 0.86 | 0.36       | Cor-C   |
|                          | 10   | 1.529   | 14.61                                  | 13.85                                  | 0.95 | 0.43       | P-Bias  |
|                          | 11   | 3.046   | 27.99                                  | 24.06                                  | 0.86 | 1.00       | Pearson |
|                          | 12   | 4.552   | 34.89                                  | 33.21                                  | 0.95 | 0.05       | STD     |
|                          | 13   | 6.120   | 43.17                                  | 42.11                                  | 0.98 | 0.92       | Mean    |



Table 4-43 Yu ST = 150

| Type                     | Test | Depth M | P <sub>test</sub> (kN/m <sup>3</sup> ) | P <sub>calc</sub> (kN/m <sup>3</sup> ) | Bias | Statistics |         |
|--------------------------|------|---------|--|--|------|------------|---------|
| MW71 x MW71<br>200 x 150 | 14   | 0.305   | 7.53                                   | 6.33                                   | 0.84 | 0.08       | COV     |
|                          | 15   | 1.522   | 18.74                                  | 17.16                                  | 0.92 | 0.00       | Cor-C   |
|                          | 16   | 3.041   | 33.77                                  | 26.37                                  | 0.78 | 1.00       | P-Bias  |
|                          | 17   | 4.560   | 42.91                                  | 33.90                                  | 0.79 | 0.98       | Pearson |
|                          | 18   | 6.120   | 43.17                                  | 40.69                                  | 0.94 | 0.07       | STD     |
|                          | 19   | 6.108   | 49.72                                  | 40.64                                  | 0.82 | 0.85       | Mean    |

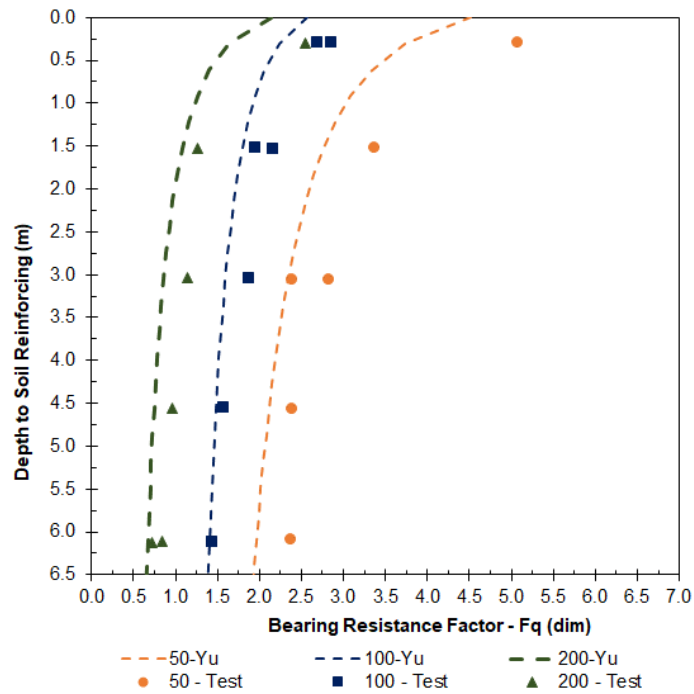


Figure 4-25 Yu – Bearing Resistance Factor (MW71 S<sub>T</sub> = 150 mm)

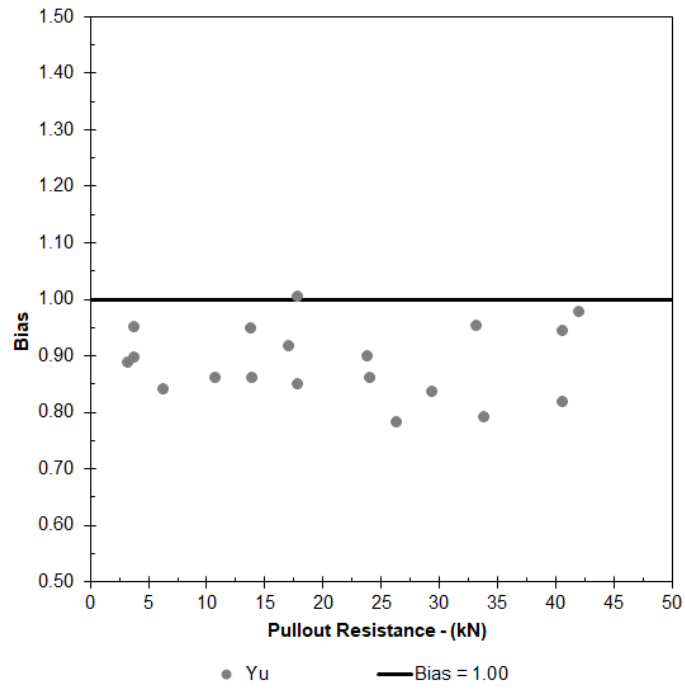


Figure 4-26 Yu – Bias (MW71  $S_T = 150$  mm)

#### 4.6.3 Group-1 Set-3 Bearing Resistance Factor

Group-1, Set-3 consists of an MW71 x MW71, 2-Wire soil-reinforcing element with transverse element spacings equal to 150 mm. Group-1, Set-3, had three sub-sets with longitudinal element spacings equal to 50 mm, 100 mm, and 200 mm.

Table 4-44 MW71 x MW71 – ST = 1W Pullout Test Results

| Type                    | Test | Depth<br>m | Surcharge<br>kPa | $P_{r_{3/4}}$<br>kN | $F^*_{19\text{ mm}}$ | $\sigma_v$<br>kPa | $N_q$ |
|-------------------------|------|------------|------------------|---------------------|----------------------|-------------------|-------|
| MW71 x MW71<br>50 x 1W  | 1    | 0.305      | 5.99             | 1.58                | 8.54                 | 5.99              | 546   |
|                         | 2    | 0.305      | 5.99             | 1.42                | 7.69                 | 5.99              | 492   |
|                         | 3    | 0.305      | 5.99             | 1.57                | 8.45                 | 5.99              | 541   |
|                         | 4    | 1.509      | 29.64            | 4.71                | 5.14                 | 29.64             | 329   |
|                         | 5    | 3.048      | 59.85            | 6.84                | 3.69                 | 59.85             | 236   |
|                         | 6    | 4.572      | 89.78            | 7.50                | 2.70                 | 89.78             | 173   |
|                         | 7    | 4.574      | 89.82            | 8.18                | 2.94                 | 89.82             | 188   |
|                         | 8    | 6.057      | 118.93           | 7.00                | 1.90                 | 118.93            | 122   |
| MW71 x MW71<br>100 x 1W | 9    | 0.305      | 5.99             | 1.79                | 4.82                 | 5.99              | 308   |
|                         | 10   | 0.305      | 5.99             | 1.70                | 4.60                 | 5.99              | 294   |
|                         | 11   | 0.305      | 5.99             | 1.92                | 5.18                 | 5.99              | 332   |
|                         | 12   | 1.551      | 30.45            | 4.68                | 2.53                 | 30.45             | 162   |
|                         | 13   | 3.075      | 60.38            | 7.47                | 2.02                 | 60.38             | 129   |
|                         | 14   | 6.133      | 120.42           | 11.26               | 1.52                 | 120.42            | 97    |
|                         | 15   | 4.577      | 89.87            | 8.18                | 1.47                 | 89.87             | 94    |
| MW71 x MW71<br>200 x 1W | 16   | 0.305      | 5.99             | 1.11                | 1.49                 | 5.99              | 96    |
|                         | 17   | 0.305      | 5.99             | 1.97                | 2.66                 | 5.99              | 170   |
|                         | 18   | 0.305      | 5.99             | 1.66                | 2.24                 | 5.99              | 143   |
|                         | 19   | 1.524      | 29.93            | 5.50                | 1.48                 | 29.93             | 95    |
|                         | 20   | 3.043      | 59.75            | 9.18                | 1.24                 | 59.75             | 79    |
|                         | 21   | 4.509      | 88.53            | 10.72               | 0.98                 | 88.53             | 63    |
|                         | 22   | 5.981      | 117.45           | 11.56               | 0.80                 | 117.45            | 51    |

4.6.3.1 RE1 Group-1 / Set-3

RE1

$$F_q = \alpha \cdot e^{-\beta \cdot z}$$

Equation 4-6

Table 4-45 RE1 - Regression Variables for  $S_T = 1W$

| Type        | Longitudinal Spacing (mm) |         |          |         |          |         |
|-------------|---------------------------|---------|----------|---------|----------|---------|
|             | 50                        |         | 100      |         | 200      |         |
|             | $\alpha$                  | $\beta$ | $\alpha$ | $\beta$ | $\alpha$ | $\beta$ |
| MW71 x MW71 | 8.78                      | 0.268   | 5.15     | 0.288   | 2.23     | 0.199   |

Table 4-46 RE1 –  $S_T = 1W$

| Type                    | Z (m) | $P_{test}$ (kN/m <sup>3</sup> ) | $P_{calc}$ (kN/m <sup>3</sup> ) | Bias | Statistics |          |
|-------------------------|-------|---------------------------------|---------------------------------|------|------------|----------|
| MW71 X MW71<br>50 x 1W  | 0.305 | 1.58                            | 1.50                            | 0.98 |            |          |
|                         | 0.305 | 1.42                            | 1.50                            | 1.08 |            |          |
|                         | 0.305 | 1.57                            | 1.50                            | 0.99 | 0.08       | COV      |
|                         | 1.509 | 4.71                            | 5.38                            | 1.20 | -0.12      | Cor-Bias |
|                         | 3.048 | 6.84                            | 7.19                            | 1.14 | 0.77       | P-Bias   |
|                         | 4.572 | 7.50                            | 7.17                            | 1.06 | 0.99       | Pearson  |
|                         | 4.574 | 8.18                            | 7.16                            | 0.97 | 0.08       | STD      |
|                         | 6.057 | 7.00                            | 6.38                            | 1.04 | 1.06       | Mean     |
| MW71 X MW71<br>100 x 1W | 0.305 | 1.79                            | 1.75                            | 0.86 |            |          |
|                         | 0.305 | 1.70                            | 1.75                            | 0.90 | 0.22       | COV      |
|                         | 0.305 | 1.92                            | 1.75                            | 0.80 | 0.00       | Cor-Bias |
|                         | 1.551 | 4.68                            | 6.22                            | 1.17 | 0.99       | P-Bias   |
|                         | 3.075 | 7.47                            | 7.96                            | 0.95 | 0.87       | Pearson  |
|                         | 6.133 | 11.26                           | 6.59                            | 0.54 | 0.19       | STD      |
|                         | 4.577 | 8.18                            | 7.69                            | 0.85 | 0.87       | Mean     |

Table 4-46 RE1 –  $S_T = 1W$

| Type                    | Z (m) | $P_{test}$ (kN/m <sup>3</sup> ) | $P_{calc}$ (kN/m <sup>3</sup> ) | Bias | Statistics |          |
|-------------------------|-------|---------------------------------|---------------------------------|------|------------|----------|
| MW71 X MW71<br>200 x 1W | 0.305 | 1.11                            | 1.56                            | 1.39 | 0.25       | COV      |
|                         | 0.305 | 1.97                            | 1.56                            | 0.78 | -0.18      | Cor-Bias |
|                         | 0.305 | 1.66                            | 1.56                            | 0.93 | 0.74       | P-Bias   |
|                         | 1.524 | 5.50                            | 6.11                            | 1.04 | 0.98       | Pearson  |
|                         | 3.043 | 9.18                            | 9.02                            | 0.85 | 0.24       | STD      |
|                         | 4.509 | 10.72                           | 9.99                            | 0.75 | 0.96       | Mean     |

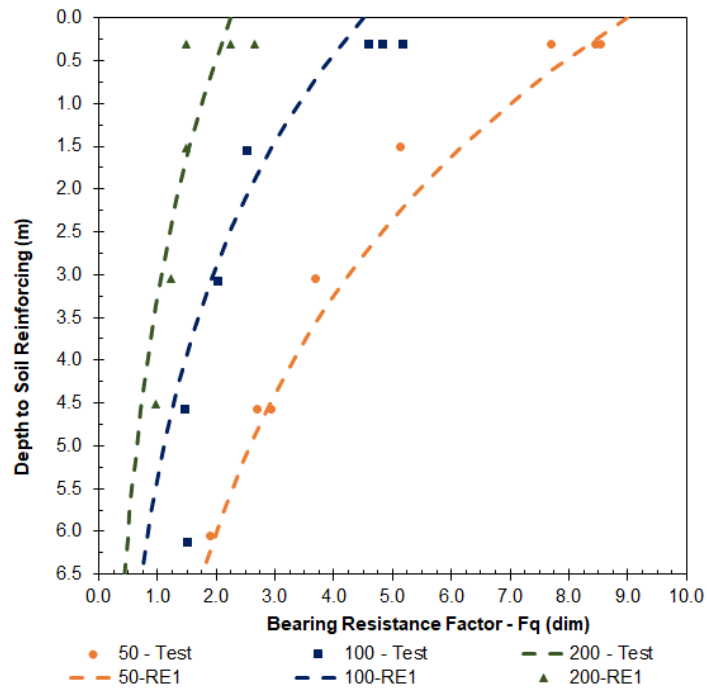


Figure 4-27 RE1 – Bearing Resistance Factor (MW71  $S_T = 1W$ )

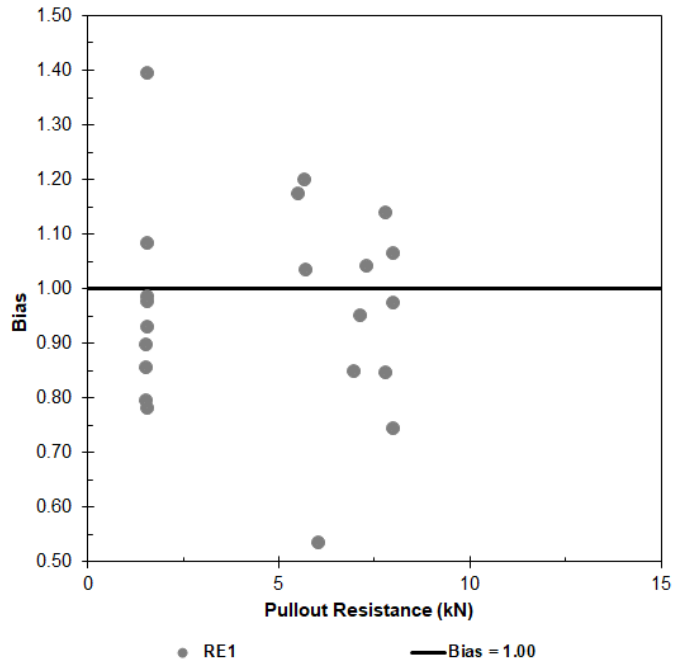


Figure 4-28 RE1 – Bias (MW71 S<sub>T</sub> = 1W)

4.6.3.2 RE2 Group-1 / Set-3

RE2

$$F_q = F_0 + F_{max} \cdot e^{-\beta \cdot z}$$

Equation 4-7

Table 4-47 RE2 - Regression Variables for S<sub>T</sub> = 1W

| Type        | Longitudinal Spacing (mm) |      |      |                |      |      |                |      |      |
|-------------|---------------------------|------|------|----------------|------|------|----------------|------|------|
|             | 50                        |      |      | 100            |      |      | 200            |      |      |
|             | F <sub>0</sub>            | α    | β    | F <sub>0</sub> | α    | β    | F <sub>0</sub> | α    | β    |
| MW71 x MW71 | 1.78                      | 7.40 | 0.48 | 1.52           | 4.38 | 0.89 | 0.90           | 1.46 | 0.55 |

Table 4-48 RE2 –  $S_T = 1W$

| Type                    | Z (m) | $P_{test}$ (kN/m <sup>3</sup> ) | $P_{calc}$ (kN/m <sup>3</sup> ) | Bias | Statistics |          |
|-------------------------|-------|---------------------------------|---------------------------------|------|------------|----------|
| MW71 X MW71<br>50 x 1W  | 0.305 | 1.58                            | 1.52                            | 0.96 |            |          |
|                         | 0.305 | 1.42                            | 1.52                            | 1.06 |            |          |
|                         | 0.305 | 1.57                            | 1.52                            | 0.97 | 0.08       | COV      |
|                         | 1.509 | 4.71                            | 4.95                            | 1.05 | 0.08       | Cor-Bias |
|                         | 3.048 | 6.84                            | 6.53                            | 0.95 | 0.85       | P-Bias   |
|                         | 4.572 | 7.50                            | 7.30                            | 0.97 | 0.98       | Pearson  |
|                         | 4.574 | 8.18                            | 7.30                            | 0.89 | 0.08       | STD      |
|                         | 6.057 | 7.00                            | 8.10                            | 1.16 | 1.00       | Mean     |
| MW71 X MW71<br>100 x 1W | 0.305 | 1.79                            | 1.80                            | 1.01 |            |          |
|                         | 0.305 | 1.70                            | 1.80                            | 1.06 | 0.07       | COV      |
|                         | 0.305 | 1.92                            | 1.80                            | 0.94 | 0.14       | Cor-Bias |
|                         | 1.551 | 4.68                            | 4.95                            | 1.06 | 0.76       | P-Bias   |
|                         | 3.075 | 7.47                            | 6.74                            | 0.90 | 0.99       | Pearson  |
|                         | 6.133 | 11.26                           | 11.45                           | 1.02 | 0.07       | STD      |
|                         | 4.577 | 8.18                            | 8.86                            | 1.08 | 1.01       | Mean     |
| MW71 X MW71<br>200 x 1W | 0.305 | 1.11                            | 1.58                            | 1.42 | 0.20       | COV      |
|                         | 0.305 | 1.97                            | 1.58                            | 0.80 | -0.12      | Cor-Bias |
|                         | 0.305 | 1.66                            | 1.58                            | 0.95 | 0.82       | P-Bias   |
|                         | 1.524 | 5.50                            | 5.65                            | 1.03 | 0.99       | Pearson  |
|                         | 3.043 | 9.18                            | 8.65                            | 0.94 | 0.21       | STD      |
|                         | 4.509 | 10.72                           | 11.16                           | 1.04 | 1.03       | Mean     |

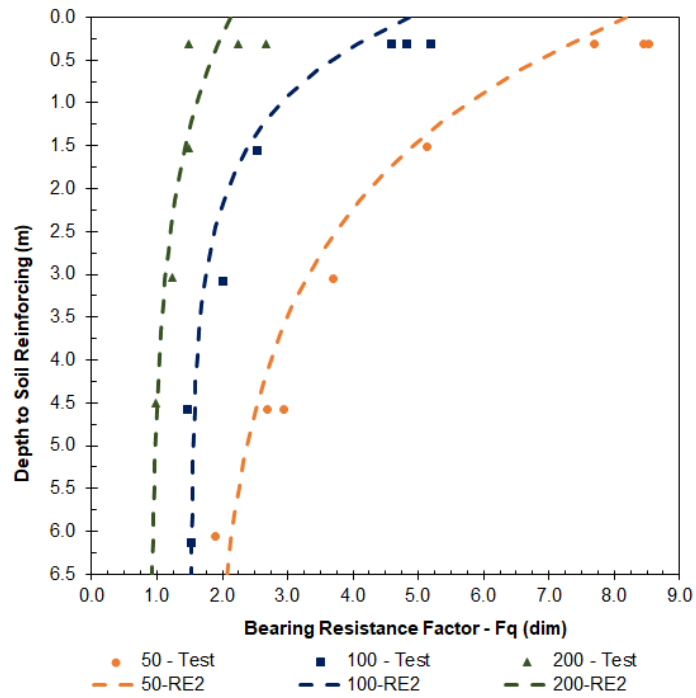


Figure 4-29 RE2 – Bearing Resistance Factor (MW71  $S_T = 1W$ )

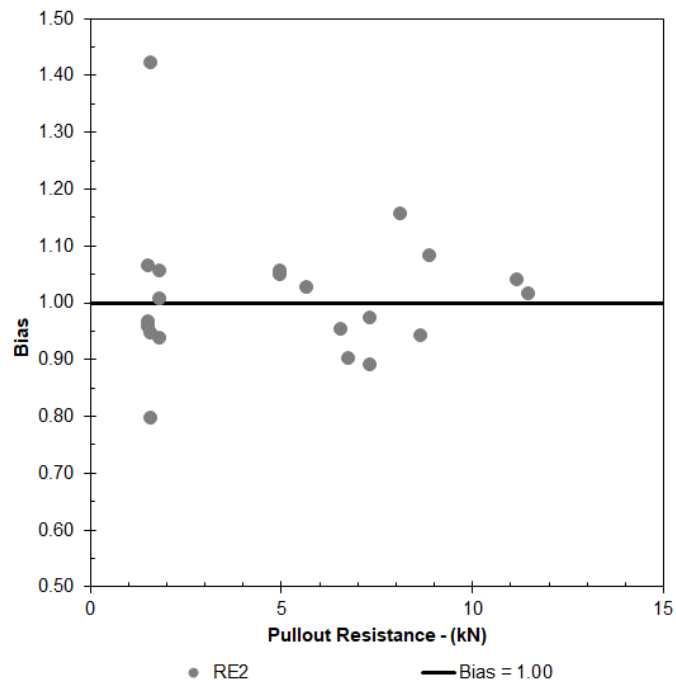


Figure 4-30 RE2 – Bias (MW71  $S_T = 1W$ )



4.6.3.3 RE3 Group-1 / Set-3

RE3

$$F_q = \begin{cases} F_{\max} - \frac{F_{\max} - F_1}{z_1} \cdot z \rightarrow 0 \leq z \leq z_1 \\ F_1 - \frac{F_1 - F_{\min}}{z_2 - z_1} \cdot (z - z_1) \rightarrow z_1 \leq z \leq z_2 \\ F_{\min} \rightarrow z \geq z_2 \end{cases} \quad \text{Equation 4-8}$$

Table 4-49 RE3 - Regression Variables for  $S_T = 1W$

| Type        |   | Longitudinal Spacing (mm) |       |       |       |       |       |       |       |       |
|-------------|---|---------------------------|-------|-------|-------|-------|-------|-------|-------|-------|
|             |   | 50                        |       |       | 100   |       |       | 200   |       |       |
|             |   | Max                       | 1     | Min   | Max   | 1     | Min   | Max   | 1     | Min   |
| MW71 x MW71 | F | 8.50                      | 5.00  | 2.50  | 5.00  | 2.50  | 1.50  | 2.50  | 1.50  | 1.00  |
|             | z | 0.000                     | 1.524 | 4.572 | 0.000 | 1.524 | 4.572 | 0.000 | 1.524 | 4.572 |

Table 4-50 RE3 –  $S_T = 1W$

| Type                    | Z (m) | P <sub>test</sub> (kN/m <sup>3</sup> ) | P <sub>calc</sub> (kN/m <sup>3</sup> ) | Bias | Statistics |          |
|-------------------------|-------|--|--|------|------------|----------|
| MW71 X MW71<br>50 x 1W  | 0.305 | 1.58                                   | 1.45                                   | 0.91 |            |          |
|                         | 0.305 | 1.42                                   | 1.45                                   | 1.01 |            |          |
|                         | 0.305 | 1.57                                   | 1.45                                   | 0.92 | 0.14       | COV      |
|                         | 1.509 | 4.71                                   | 4.62                                   | 0.98 | 0.47       | Cor-Bias |
|                         | 3.048 | 6.84                                   | 6.95                                   | 1.02 | 0.24       | P-Bias   |
|                         | 4.572 | 7.50                                   | 6.95                                   | 0.93 | 0.95       | Pearson  |
|                         | 4.574 | 8.18                                   | 6.95                                   | 0.85 | 0.14       | STD      |
|                         | 6.057 | 7.00                                   | 9.21                                   | 1.32 | 0.99       | Mean     |
| MW71 X MW71<br>100 x 1W | 0.305 | 1.79                                   | 1.67                                   | 0.93 |            |          |
|                         | 0.305 | 1.70                                   | 1.67                                   | 0.98 | 0.05       | COV      |
|                         | 0.305 | 1.92                                   | 1.67                                   | 0.87 | 0.66       | Cor-Bias |
|                         | 1.551 | 4.68                                   | 4.70                                   | 1.00 | 0.11       | P-Bias   |
|                         | 3.075 | 7.47                                   | 7.45                                   | 1.00 | 1.00       | Pearson  |
|                         | 6.133 | 11.26                                  | 11.19                                  | 0.99 | 0.05       | STD      |
|                         | 4.577 | 8.18                                   | 8.35                                   | 1.02 | 0.97       | Mean     |

Table 4-50 RE3 –  $S_T = 1W$

| Type                    | Z (m) | $P_{test}$ (kN/m <sup>3</sup> ) | $P_{calc}$ (kN/m <sup>3</sup> ) | Bias | Statistics |          |
|-------------------------|-------|---------------------------------|---------------------------------|------|------------|----------|
| MW71 X MW71<br>200 x 1W | 0.305 | 1.11                            | 1.71                            | 1.54 | 0.22       | COV      |
|                         | 0.305 | 1.97                            | 1.71                            | 0.86 | -0.25      | Cor-Bias |
|                         | 0.305 | 1.66                            | 1.71                            | 1.03 | 0.63       | P-Bias   |
|                         | 1.524 | 5.50                            | 5.56                            | 1.01 | 1.00       | Pearson  |
|                         | 3.043 | 9.18                            | 9.26                            | 1.01 | 0.23       | STD      |
|                         | 4.509 | 10.72                           | 11.08                           | 1.03 | 1.08       | Mean     |

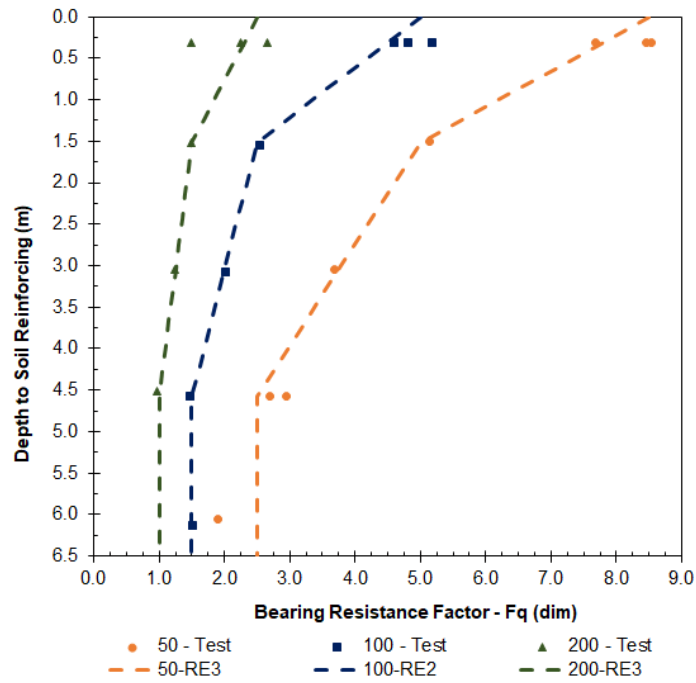


Figure 4-31 RE3 – Bearing Resistance Factor (MW71  $S_T = 1W$ )

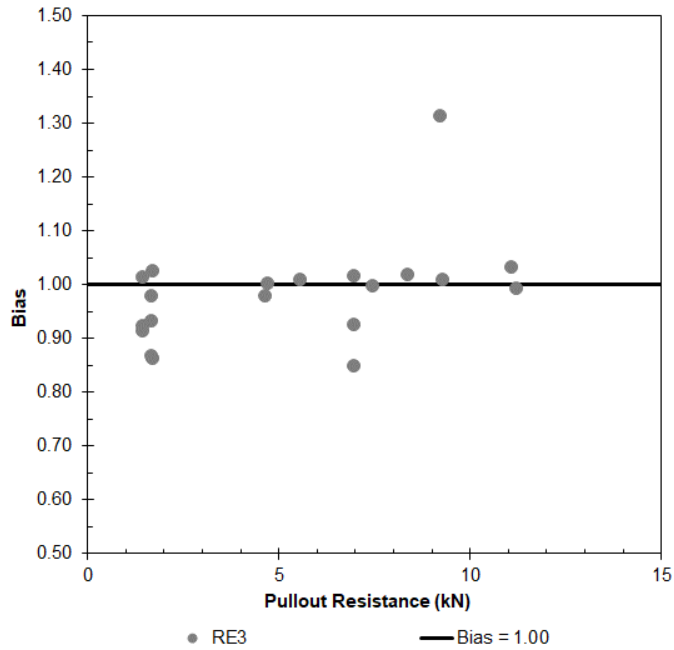


Figure 4-32 RE3 – Bias (MW71 S<sub>T</sub> = 1W)

4.6.3.4 YU Group-1 / Set-3

$$N_q = \alpha \left( \frac{n \cdot \sigma_v}{p_a} \right)^{-\beta} \quad \text{Equation 4-9}$$

Yu

$$N_q = \frac{F_q \cdot S_T}{d_b} \rightarrow F_q = \frac{N_q \cdot d_b}{S_T} \quad \text{Equation 4-11}$$

Table 4-51 Yu - Regression Variables for S<sub>T</sub> = 1W

| Type        | Longitudinal Spacing (mm) |       |     |       |     |       |
|-------------|---------------------------|-------|-----|-------|-----|-------|
|             | 50                        |       | 100 |       | 200 |       |
|             | α                         | β     | α   | β     | α   | β     |
| MW71 x MW71 | 83                        | 0.386 | 48  | 0.403 | 27  | 0.318 |

Table 4-52  $Y_u - S_T = 1W$

| Type                    | Z (m) | $P_{test}$ (kN/m <sup>3</sup> ) | $P_{calc}$ (kN/m <sup>3</sup> ) | Bias | Statistics |          |
|-------------------------|-------|---------------------------------|---------------------------------|------|------------|----------|
| MW71 X MW71<br>50 x 1W  | 0.305 | 1.58                            | 1.44                            | 0.91 |            |          |
|                         | 0.305 | 1.42                            | 1.44                            | 1.01 |            |          |
|                         | 0.305 | 1.57                            | 1.44                            | 0.92 | 0.15       | COV      |
|                         | 1.509 | 4.71                            | 3.85                            | 0.82 | 0.50       | Cor-Bias |
|                         | 3.048 | 6.84                            | 5.92                            | 0.87 | 0.21       | P-Bias   |
|                         | 4.572 | 7.50                            | 7.59                            | 1.01 | 0.96       | Pearson  |
|                         | 4.574 | 8.18                            | 7.59                            | 0.93 | 0.15       | STD      |
|                         | 6.057 | 7.00                            | 9.02                            | 1.29 | 0.97       | Mean     |
| MW71 X MW71<br>100 x 1W | 0.305 | 1.79                            | 1.75                            | 0.98 |            |          |
|                         | 0.305 | 1.70                            | 1.75                            | 1.02 | 0.06       | COV      |
|                         | 0.305 | 1.92                            | 1.75                            | 0.91 | 0.07       | Cor-Bias |
|                         | 1.551 | 4.68                            | 4.61                            | 0.98 | 0.87       | P-Bias   |
|                         | 3.075 | 7.47                            | 6.94                            | 0.93 | 0.99       | Pearson  |
|                         | 6.133 | 11.26                           | 10.48                           | 0.93 | 0.06       | STD      |
|                         | 4.577 | 8.18                            | 8.80                            | 1.08 | 0.98       | Mean     |
| MW71 X MW71<br>200 x 1W | 0.305 | 1.11                            | 1.53                            | 1.38 | 0.24       | COV      |
|                         | 0.305 | 1.97                            | 1.53                            | 0.78 | 0.14       | Cor-Bias |
|                         | 0.305 | 1.66                            | 1.53                            | 0.92 | 0.83       | P-Bias   |
|                         | 1.524 | 5.50                            | 4.59                            | 0.83 | 0.99       | Pearson  |
|                         | 3.043 | 9.18                            | 7.36                            | 0.80 | 0.23       | STD      |
|                         | 4.509 | 10.72                           | 9.63                            | 0.90 | 0.94       | Mean     |

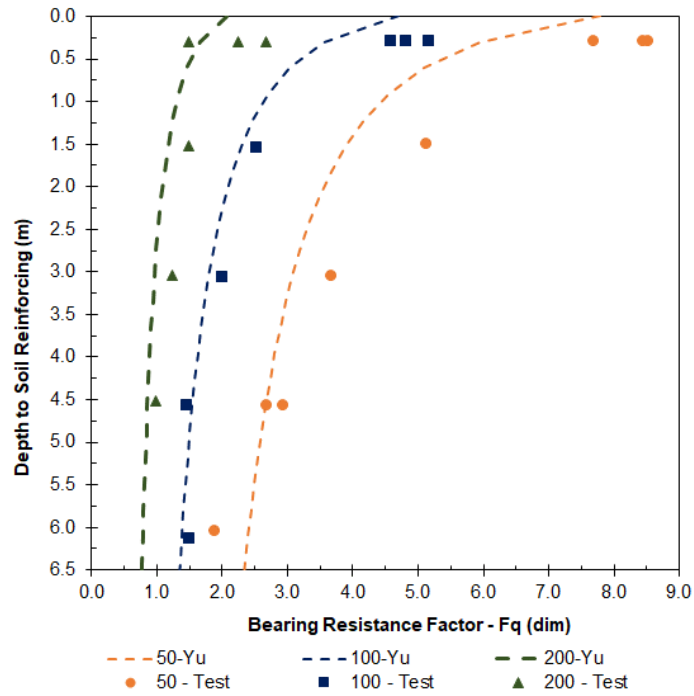


Figure 4-33 Yu – Bearing Resistance Factor (MW71  $S_T = 1W$ )

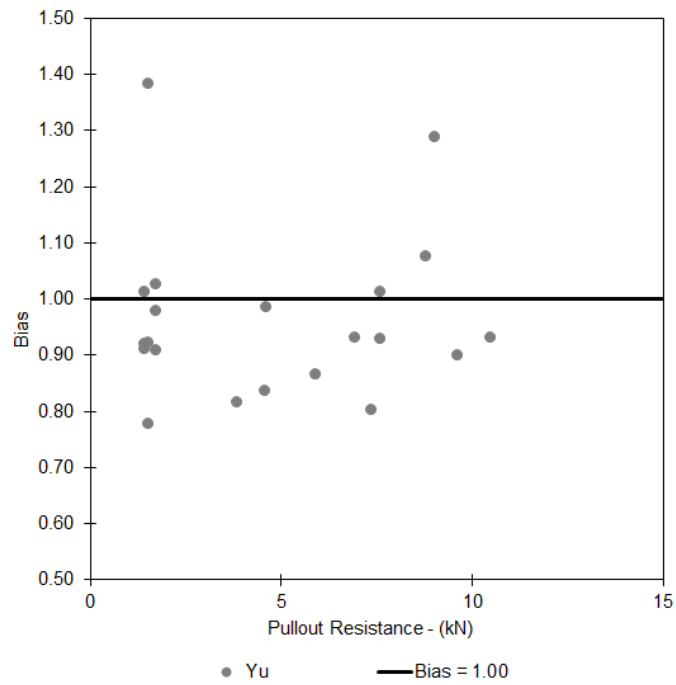


Figure 4-34 Yu – Bias (MW71  $S_T = 1W$ )

#### 4.6.4 Group-2 Set-1 Bearing Resistance Factor

Group-2, Set-1 consists of an MW45 x MW45, 2-Wire soil-reinforcing element with transverse element spacings equal to 300 mm. Group-2, Set-1, had three sub-sets with longitudinal element spacings equal to 50 mm, 100 mm, and 200 mm.

Table 4-53 MW45 x MW45 – ST = 300 Pullout Test Results

| Type                     | Test | Depth<br>m | Surcharge<br>kPa | $P_{r_{3/4}}$<br>kN | $F^*_{19\text{ mm}}$ | $\sigma_v$<br>kPa | $N_q$ |
|--------------------------|------|------------|------------------|---------------------|----------------------|-------------------|-------|
| MW45 x MW45<br>50 x 300  | 1    | 0.305      | 5.99             | 4.46                | 6.02                 | 5.99              | 483   |
|                          | 2    | 0.305      | 5.99             | 4.72                | 6.37                 | 5.99              | 511   |
|                          | 3    | 0.305      | 5.99             | 4.09                | 5.52                 | 5.99              | 443   |
|                          | 4    | 1.524      | 29.93            | 12.90               | 3.48                 | 29.93             | 279   |
|                          | 5    | 3.172      | 62.29            | 16.69               | 2.16                 | 62.29             | 174   |
|                          | 6    | 4.513      | 88.63            | 22.38               | 2.04                 | 88.63             | 164   |
|                          | 7    | 6.096      | 119.70           | 25.70               | 1.73                 | 119.70            | 139   |
|                          | 8    | 9.103      | 178.74           | 30.17               | 1.36                 | 178.74            | 109   |
| MW45 x MW45<br>100 x 300 | 9    | 0.305      | 5.99             | 3.44                | 2.32                 | 5.99              | 186   |
|                          | 10   | 0.305      | 5.99             | 3.79                | 2.56                 | 5.99              | 205   |
|                          | 11   | 0.305      | 5.99             | 4.05                | 2.73                 | 5.99              | 220   |
|                          | 12   | 1.524      | 29.93            | 12.57               | 1.70                 | 29.93             | 136   |
|                          | 13   | 3.055      | 59.99            | 20.93               | 1.41                 | 59.99             | 113   |
|                          | 14   | 4.572      | 89.78            | 24.28               | 1.09                 | 89.78             | 88    |
|                          | 15   | 6.084      | 119.46           | 34.88               | 1.18                 | 119.46            | 95    |
| MW45 x MW45<br>200 x 300 | 16   | 0.305      | 5.99             | 5.42                | 1.96                 | 5.99              | 157   |
|                          | 17   | 0.305      | 5.99             | 5.09                | 1.83                 | 5.99              | 147   |
|                          | 18   | 0.305      | 5.99             | 15.99               | 1.72                 | 5.99              | 138   |
|                          | 19   | 3.048      | 59.85            | 26.03               | 0.88                 | 59.85             | 71    |
|                          | 20   | 1.524      | 29.93            | 16.20               | 1.08                 | 29.93             | 87    |
|                          | 21   | 3.048      | 59.85            | 20.99               | 0.71                 | 59.85             | 57    |
|                          | 22   | 0.305      | 5.99             | 5.68                | 1.92                 | 5.99              | 154   |

4.6.4.1 RE1 Group-2 / Set-1

RE1

$$F_q = \alpha \cdot e^{-\beta \cdot z}$$

Equation 4-6

Table 4-54 RE1 - Regression Variables for  $S_T = 300$

| Type        | Longitudinal Spacing (mm) |         |          |         |          |         |
|-------------|---------------------------|---------|----------|---------|----------|---------|
|             | 50                        |         | 100      |         | 200      |         |
|             | $\alpha$                  | $\beta$ | $\alpha$ | $\beta$ | $\alpha$ | $\beta$ |
| MW45 x MW45 | 6.25                      | 0.261   | 2.60     | 0.176   | 2.04     | 0.332   |

Table 4-55 RE1 –  $S_T = 300$

| Type                     | Test | Z (m) | $P_{test}$ (kN/m <sup>3</sup> ) | $P_{calc}$ (kN/m <sup>3</sup> ) | Bias | Statistics |         |
|--------------------------|------|-------|---------------------------------|---------------------------------|------|------------|---------|
| MW45 X MW45<br>50 x 300  | 1    | 0.305 | 4.46                            | 4.28                            | 0.96 |            |         |
|                          | 2    | 0.305 | 4.72                            | 4.28                            | 0.91 |            |         |
|                          | 3    | 0.305 | 4.09                            | 4.28                            | 1.05 | 0.28       | COV     |
|                          | 4    | 1.524 | 12.90                           | 15.58                           | 1.21 | 0.10       | Cor-C   |
|                          | 5    | 3.172 | 16.69                           | 21.11                           | 1.26 | 0.82       | P-Bias  |
|                          | 6    | 4.513 | 22.38                           | 21.18                           | 0.95 | 0.75       | Pearson |
|                          | 7    | 6.096 | 25.70                           | 18.94                           | 0.74 | 0.27       | STD     |
|                          | 8    | 9.103 | 30.17                           | 12.93                           | 0.43 | 0.94       | Mean    |
| MW45 X MW45<br>100 x 300 | 9    | 0.305 | 3.44                            | 3.65                            | 1.06 |            |         |
|                          | 10   | 0.305 | 3.79                            | 3.65                            | 0.96 | 0.14       | COV     |
|                          | 11   | 0.305 | 4.05                            | 3.65                            | 0.90 | -0.08      | Cor-C   |
|                          | 12   | 1.524 | 12.57                           | 14.72                           | 1.17 | 0.87       | P-Bias  |
|                          | 13   | 3.055 | 20.93                           | 22.54                           | 1.08 | 0.96       | Pearson |
|                          | 14   | 4.572 | 24.28                           | 25.82                           | 1.06 | 0.14       | STD     |
|                          | 15   | 6.084 | 34.88                           | 26.33                           | 0.75 | 1.00       | Mean    |

Table 4-55 RE1 –  $S_T = 300$

| Type                     | Test | Z (m) | $P_{test}$ (kN/m <sup>3</sup> ) | $P_{calc}$ (kN/m <sup>3</sup> ) | Bias | Statistics |         |
|--------------------------|------|-------|---------------------------------|---------------------------------|------|------------|---------|
| MW45 X MW45<br>200 x 300 | 16   | 0.305 | 5.42                            | 5.47                            | 1.01 |            |         |
|                          | 17   | 0.305 | 5.09                            | 5.47                            | 1.07 | 0.29       | COV     |
|                          | 18   | 0.305 | 15.99                           | 5.47                            | 0.34 | 0.28       | Cor-C   |
|                          | 19   | 3.048 | 26.03                           | 21.94                           | 0.84 | 0.55       | P-Bias  |
|                          | 20   | 1.524 | 16.20                           | 18.22                           | 1.12 | 0.86       | Pearson |
|                          | 21   | 3.048 | 20.99                           | 21.94                           | 1.05 | 0.27       | STD     |
|                          | 22   | 0.305 | 5.68                            | 5.47                            | 0.96 | 0.91       | Mean    |

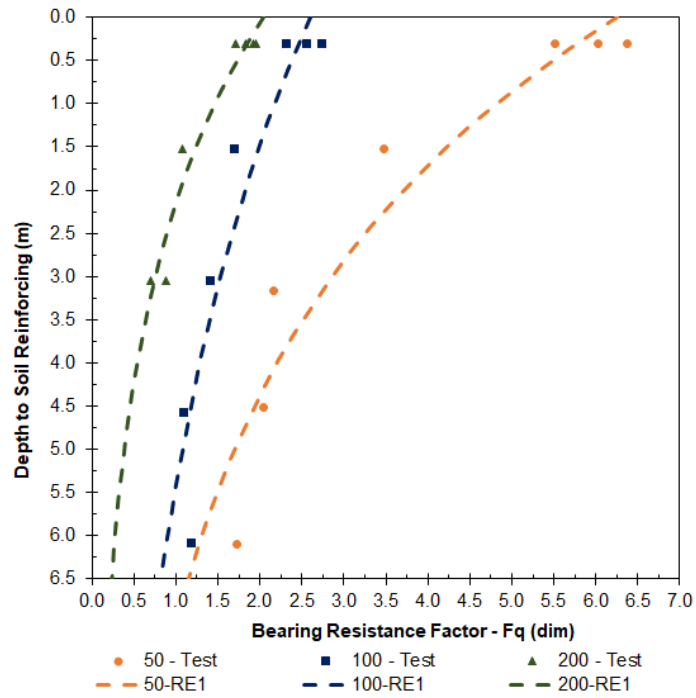


Figure 4-35 RE1 – Bearing Resistance Factor (MW45  $S_T = 300$ )



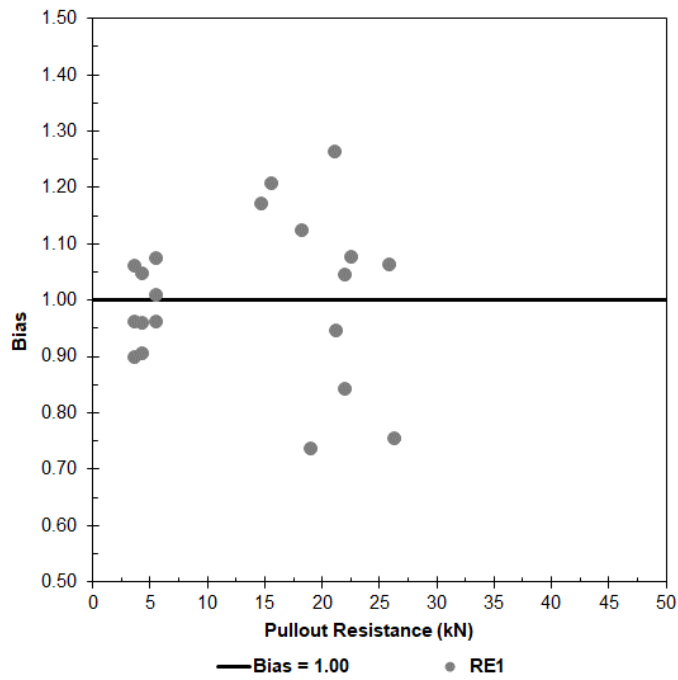


Figure 4-36 RE1 – Bias (MW45 S<sub>T</sub> = 300)

4.6.4.2 RE2 Group-2 / Set-1

RE2

$$F_q = F_0 + F_{max} \cdot e^{-\beta \cdot z}$$

Equation 4-7

Table 4-56 RE2 - Regression Variables for S<sub>T</sub> = 300

| Type        | Longitudinal Spacing (mm) |      |      |                |      |      |                |      |      |
|-------------|---------------------------|------|------|----------------|------|------|----------------|------|------|
|             | 50                        |      |      | 100            |      |      | 200            |      |      |
|             | F <sub>0</sub>            | α    | β    | F <sub>0</sub> | α    | β    | F <sub>0</sub> | α    | β    |
| MW45 x MW45 | 1.54                      | 5.39 | 0.65 | 1.11           | 1.75 | 0.68 | 0.70           | 1.53 | 0.92 |

Table 4-57 RE2 –  $S_T = 300$

| Type                     | Z (m) | $P_{test}$ (kN/m <sup>3</sup> ) | $P_{calc}$ (kN/m <sup>3</sup> ) | Bias | Statistics |         |
|--------------------------|-------|---------------------------------|---------------------------------|------|------------|---------|
| MW45 X MW45<br>50 x 300  | 0.305 | 4.46                            | 4.42                            | 0.99 |            |         |
|                          | 0.305 | 4.72                            | 4.42                            | 0.94 |            |         |
|                          | 0.305 | 4.09                            | 4.42                            | 1.08 | 0.08       | COV     |
|                          | 1.524 | 12.90                           | 13.13                           | 1.02 | 0.27       | Cor-C   |
|                          | 3.172 | 16.69                           | 17.18                           | 1.03 | 0.52       | P-Bias  |
|                          | 4.513 | 22.38                           | 20.06                           | 0.90 | 0.99       | Pearson |
|                          | 6.096 | 25.70                           | 24.35                           | 0.95 | 0.08       | STD     |
|                          | 9.103 | 30.17                           | 34.41                           | 1.14 | 1.00       | Mean    |
| MW45 X MW45<br>100 x 300 | 0.305 | 3.44                            | 3.76                            | 1.09 |            |         |
|                          | 0.305 | 3.79                            | 3.76                            | 0.99 | 0.07       | COV     |
|                          | 0.305 | 4.05                            | 3.76                            | 0.93 | -0.01      | Cor-C   |
|                          | 1.524 | 12.57                           | 12.83                           | 1.02 | 0.98       | P-Bias  |
|                          | 3.055 | 20.93                           | 19.75                           | 0.94 | 1.00       | Pearson |
|                          | 4.572 | 24.28                           | 26.42                           | 1.09 | 0.07       | STD     |
|                          | 6.084 | 34.88                           | 33.68                           | 0.97 | 1.00       | Mean    |
| MW45 X MW45<br>200 x 300 | 0.305 | 5.42                            | 5.51                            | 1.02 |            |         |
|                          | 0.305 | 5.09                            | 5.51                            | 1.08 | 0.29       | COV     |
|                          | 0.305 | 15.99                           | 5.51                            | 0.34 | 0.31       | Cor-C   |
|                          | 3.048 | 26.03                           | 23.57                           | 0.91 | 0.50       | P-Bias  |
|                          | 1.524 | 16.20                           | 16.01                           | 0.99 | 0.88       | Pearson |
|                          | 3.048 | 20.99                           | 23.57                           | 1.12 | 0.26       | STD     |

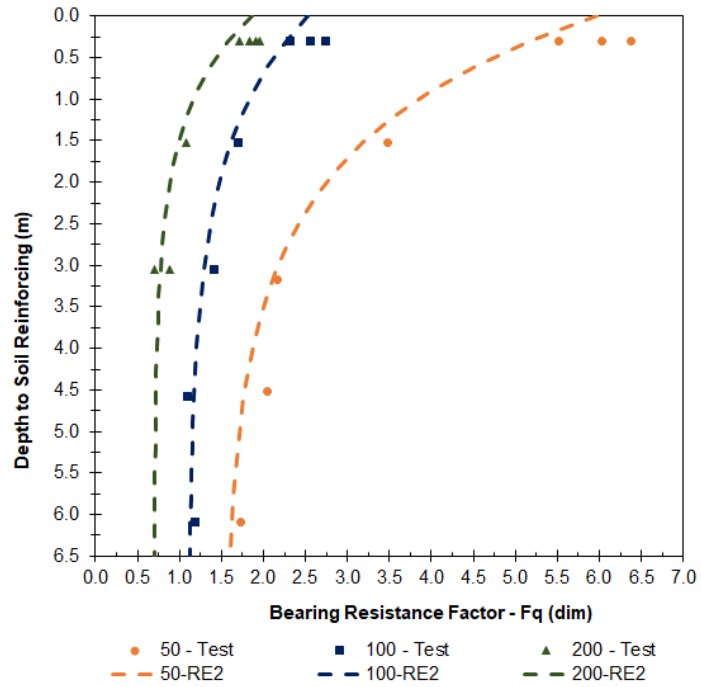


Figure 4-37 RE2 – Bearing Resistance Factor (MW45  $S_T = 300$ )

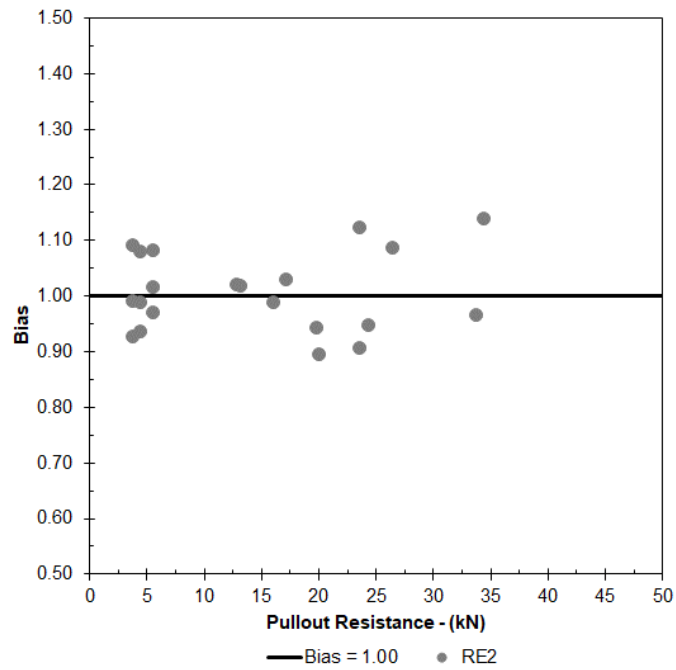


Figure 4-38 RE2 – Bias (MW45  $S_T = 300$ )

4.6.4.3 RE3 Group-2 / Set-1

RE3

$$F_q = \begin{cases} F_{\max} - \frac{F_{\max} - F_1}{z_1} \cdot z \rightarrow 0 \leq z \leq z_1 \\ F_1 - \frac{F_1 - F_{\min}}{z_2 - z_1} \cdot (z_2 - z_1) \rightarrow z_1 \leq z \leq z_2 \\ F_{\min} \rightarrow z \geq z_2 \end{cases} \quad \text{Equation 4-8}$$

Table 4-58 RE3 - Regression Variables for  $S_T = 300$

| Type        |   | Longitudinal Spacing (mm) |       |       |       |       |       |       |       |       |
|-------------|---|---------------------------|-------|-------|-------|-------|-------|-------|-------|-------|
|             |   | 50                        |       |       | 100   |       |       | 200   |       |       |
|             |   | Max                       | 1     | Min   | Max   | 1     | Min   | Max   | 1     | Min   |
| MW45 x MW45 | F | 6.00                      | 3.00  | 1.50  | 2.75  | 1.50  | 1.00  | 2.00  | 1.00  | 0.50  |
|             | z | 0.000                     | 1.524 | 4.572 | 0.000 | 1.524 | 4.572 | 0.000 | 1.524 | 4.572 |

Table 4-59 RE3 –  $S_T = 300$

| Type                     | Z (m) | P <sub>test</sub> (kN/m <sup>3</sup> ) | P <sub>calc</sub> (kN/m <sup>3</sup> ) | Bias | Statistics |         |
|--------------------------|-------|--|--|------|------------|---------|
| MW45 X MW45<br>50 x 300  | 0.305 | 4.46                                   | 4.00                                   | 0.90 |            |         |
|                          | 0.305 | 4.72                                   | 4.00                                   | 0.85 |            |         |
|                          | 0.305 | 4.09                                   | 4.00                                   | 0.98 | 0.12       | COV     |
|                          | 1.524 | 12.90                                  | 11.12                                  | 0.86 | 0.42       | Cor-C   |
|                          | 3.172 | 16.69                                  | 16.89                                  | 1.01 | 0.31       | P-Bias  |
|                          | 4.513 | 22.38                                  | 16.78                                  | 0.75 | 0.97       | Pearson |
|                          | 6.096 | 25.70                                  | 22.24                                  | 0.87 | 0.11       | STD     |
|                          | 9.103 | 30.17                                  | 33.21                                  | 1.10 | 0.91       | Mean    |
| MW45 X MW45<br>100 x 300 | 0.305 | 3.44                                   | 3.71                                   | 1.08 |            |         |
|                          | 0.305 | 3.79                                   | 3.71                                   | 0.98 | 0.08       | COV     |
|                          | 0.305 | 4.05                                   | 3.71                                   | 0.91 | -0.62      | Cor-C   |
|                          | 1.524 | 12.57                                  | 11.12                                  | 0.88 | 0.09       | P-Bias  |
|                          | 3.055 | 20.93                                  | 18.56                                  | 0.89 | 1.00       | Pearson |
|                          | 4.572 | 24.28                                  | 22.24                                  | 0.92 | 0.08       | STD     |

Table 4-59 RE3 –  $S_T = 300$

| Type                     | Z (m) | $P_{test}$ (kN/m <sup>3</sup> ) | $P_{calc}$ (kN/m <sup>3</sup> ) | Bias | Statistics |         |
|--------------------------|-------|---------------------------------|---------------------------------|------|------------|---------|
|                          | 6.084 | 34.88                           | 29.59                           | 0.85 | 0.93       | Mean    |
| MW45 X MW45<br>200 x 300 | 0.305 | 5.42                            | 5.34                            | 0.98 |            |         |
|                          | 0.305 | 5.09                            | 5.34                            | 1.05 | 0.29       | COV     |
|                          | 0.305 | 15.99                           | 5.34                            | 0.33 | 0.26       | Cor-C   |
|                          | 3.048 | 26.03                           | 22.24                           | 0.85 | 0.58       | P-Bias  |
|                          | 1.524 | 16.20                           | 14.83                           | 0.92 | 0.88       | Pearson |
|                          | 3.048 | 20.99                           | 22.24                           | 1.06 | 0.25       | STD     |

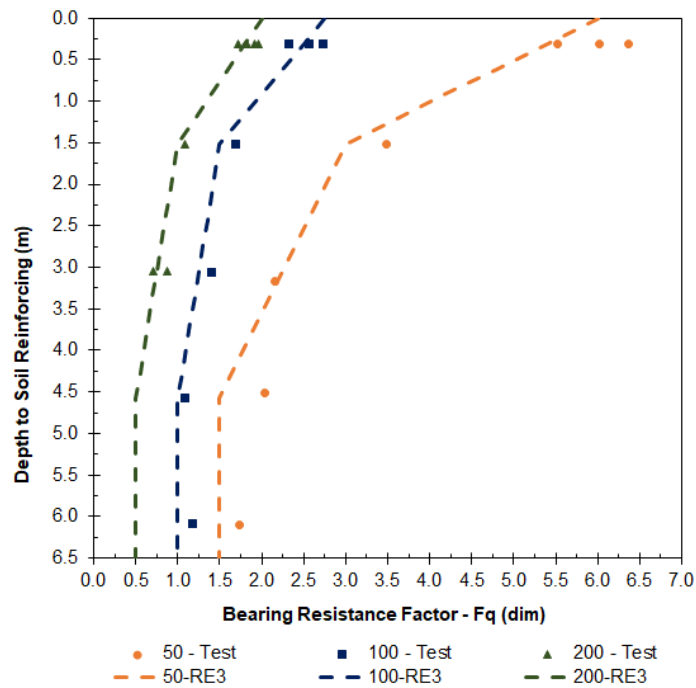


Figure 4-39 RE3 – Bearing Resistance Factor (MW45  $S_T = 300$ )

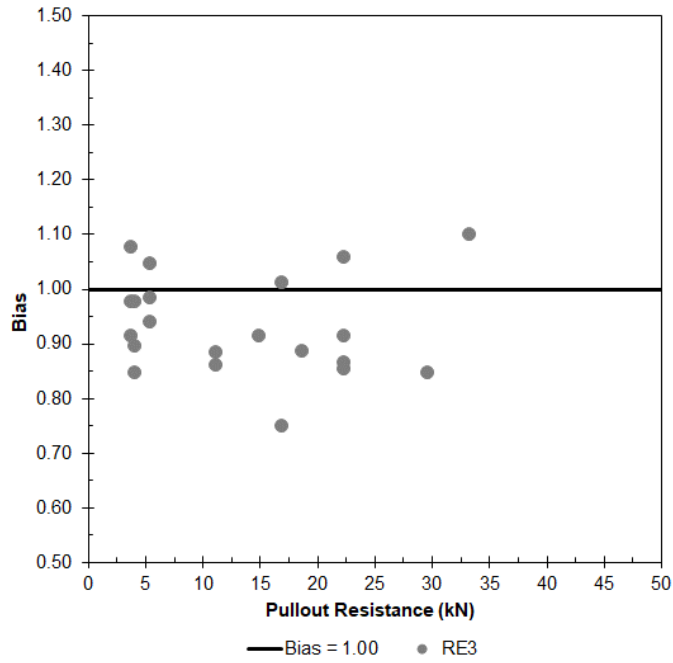


Figure 4-40 RE3 – Bias (MW45  $S_T = 300$ )

4.6.4.4 YU Group-2 / Set-1

$$N_q = \alpha \left( \frac{n \cdot \sigma_v}{p_a} \right)^{-\beta} \tag{Equation 4-9}$$

Yu

$$N_q = \frac{F_q \cdot S_T}{d_b} \rightarrow F_q = \frac{N_q \cdot d_b}{S_T} \tag{Equation 4-11}$$

Table 4-60 Yu - Regression Variables for  $S_T = 300$

| Type        | Longitudinal Spacing (mm) |         |          |         |          |         |
|-------------|---------------------------|---------|----------|---------|----------|---------|
|             | 50                        |         | 100      |         | 200      |         |
|             | $\alpha$                  | $\beta$ | $\alpha$ | $\beta$ | $\alpha$ | $\beta$ |
| MW45 x MW45 | 149                       | 0.405   | 74       | 0.271   | 49       | 0.360   |

Table 4-61  $Y_u - S_T = 300$

| Type                     | Z (m) | $P_{test}$ (kN/m <sup>3</sup> ) | $P_{calc}$ (kN/m <sup>3</sup> ) | Bias | Statistics |         |
|--------------------------|-------|---------------------------------|---------------------------------|------|------------|---------|
| MW45 X MW45<br>50 x 300  | 0.305 | 4.46                            | 4.92                            | 1.10 |            |         |
|                          | 0.305 | 4.72                            | 4.92                            | 1.04 |            |         |
|                          | 0.305 | 4.09                            | 4.92                            | 1.20 | 0.07       | COV     |
|                          | 1.524 | 12.90                           | 12.83                           | 0.99 | 0.44       | Cor-C   |
|                          | 3.172 | 16.69                           | 19.84                           | 1.19 | 0.28       | P-Bias  |
|                          | 4.513 | 22.38                           | 24.47                           | 1.09 | 1.00       | Pearson |
|                          | 6.096 | 25.70                           | 29.26                           | 1.14 | 0.08       | STD     |
|                          | 9.103 | 30.17                           | 37.15                           | 1.23 | 1.12       | Mean    |
| MW45 X MW45<br>100 x 300 | 0.305 | 3.44                            | 4.04                            | 1.17 |            |         |
|                          | 0.305 | 3.79                            | 4.04                            | 1.06 | 0.07       | COV     |
|                          | 0.305 | 4.05                            | 4.04                            | 1.00 | 0.08       | Cor-C   |
|                          | 1.524 | 12.57                           | 13.06                           | 1.04 | 0.87       | P-Bias  |
|                          | 3.055 | 20.93                           | 21.69                           | 1.04 | 0.99       | Pearson |
|                          | 4.572 | 24.28                           | 29.10                           | 1.20 | 0.08       | STD     |
|                          | 6.084 | 34.88                           | 35.85                           | 1.03 | 1.08       | Mean    |
| MW45 X MW45<br>200 x 300 | 0.305 | 5.42                            | 6.03                            | 1.11 |            |         |
|                          | 0.305 | 5.42                            | 6.03                            | 1.18 | 0.29       | COV     |
|                          | 0.305 | 5.09                            | 6.03                            | 0.38 | 0.33       | Cor-C   |
|                          | 0.305 | 15.99                           | 6.03                            | 1.01 | 0.47       | P-Bias  |
|                          | 3.048 | 26.03                           | 26.29                           | 1.04 | 0.88       | Pearson |
|                          | 1.524 | 16.20                           | 16.88                           | 1.25 | 0.29       | STD     |
|                          | 3.048 | 20.99                           | 26.29                           | 1.06 | 1.01       | Mean    |

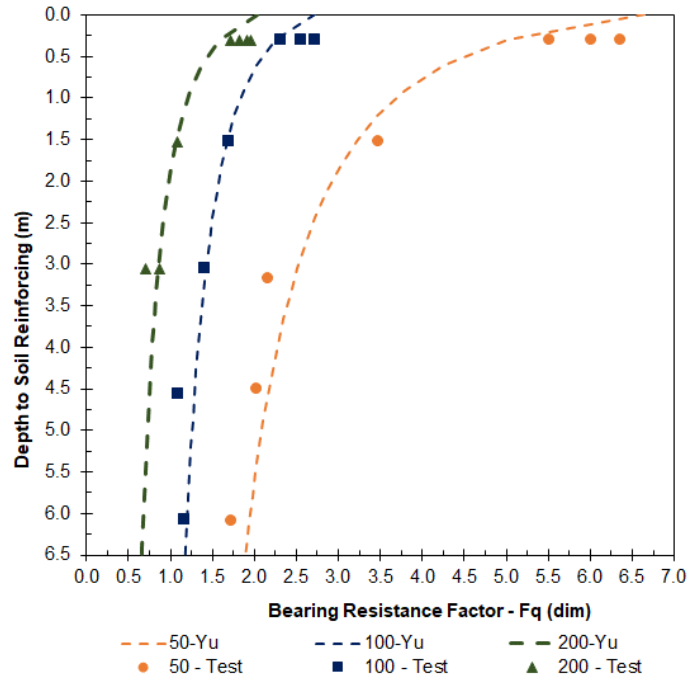


Figure 4-41 Yu – Bearing Resistance Factor (MW45  $S_T = 300$ )

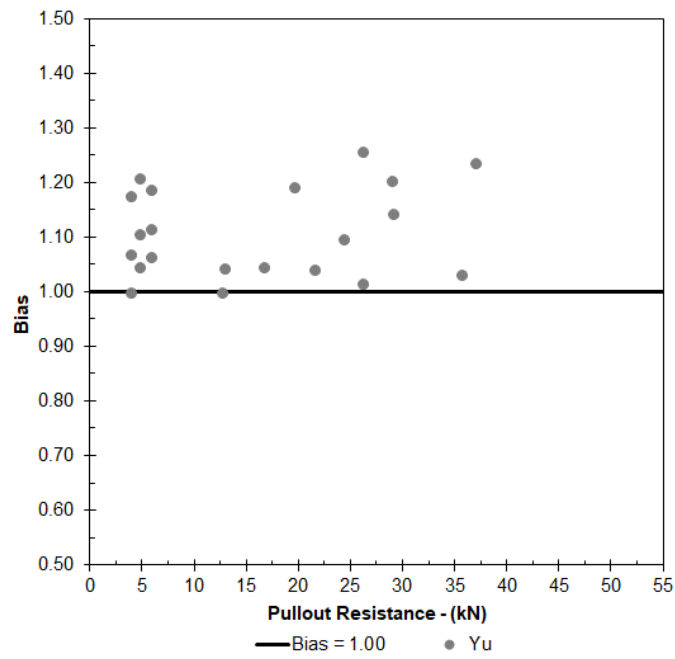


Figure 4-42 Yu – Bias (MW45  $S_T = 300$ )



#### 4.6.5 Group-2 Set-2 Bearing Resistance Factor

Group-2, Set-2 consists of an MW45 x MW45, 2-Wire soil-reinforcing element with transverse element spacings equal to 150 mm. Group-2, Set-2, had three sub-sets with longitudinal element spacings equal to 50 mm, 100 mm, and 200 mm.

Table 4-62 MW45 x MW45 – ST = 150 Pullout Test Results

| Type                     | Test | Depth<br>m | Surcharge<br>kPa | $P_{r_{3/4}}$<br>kN | $F^*_{19\text{ mm}}$ | $\sigma_v$<br>kPa | $N_q$ |
|--------------------------|------|------------|------------------|---------------------|----------------------|-------------------|-------|
| MW45 x MW45<br>50 x 150  | 1    | 0.305      | 5.99             | 3.08                | 4.15                 | 125.0             | 333   |
|                          | 2    | 0.305      | 5.99             | 2.37                | 3.19                 | 125.0             | 256   |
|                          | 3    | 0.305      | 5.99             | 2.59                | 3.49                 | 125.0             | 280   |
|                          | 4    | 1.544      | 30.31            | 10.58               | 2.82                 | 633.0             | 226   |
|                          | 5    | 3.170      | 62.24            | 16.89               | 2.19                 | 1300.0            | 176   |
|                          | 6    | 4.555      | 89.44            | 21.99               | 1.98                 | 1868.0            | 159   |
|                          | 7    | 6.103      | 119.84           | 30.05               | 2.02                 | 2503.0            | 163   |
| MW45 x MW45<br>100 x 150 | 8    | 0.305      | 5.99             | 4.03                | 2.72                 | 125.0             | 218   |
|                          | 9    | 0.305      | 5.99             | 4.32                | 2.91                 | 125.0             | 234   |
|                          | 10   | 0.305      | 5.99             | 4.56                | 3.07                 | 125.0             | 247   |
|                          | 11   | 1.531      | 30.07            | 13.70               | 1.84                 | 628.0             | 148   |
|                          | 12   | 4.570      | 89.73            | 31.75               | 1.43                 | 1874.0            | 115   |
|                          | 13   | 3.060      | 60.09            | 28.60               | 1.92                 | 1255.0            | 154   |
|                          | 14   | 1.526      | 29.97            | 18.60               | 2.51                 | 626.0             | 201   |
|                          | 15   | 0.305      | 5.99             | 5.71                | 3.85                 | 125.0             | 309   |
|                          | 16   | 4.540      | 89.15            | 32.58               | 1.48                 | 1862.0            | 118   |
| MW45 x MW45<br>200 x 150 | 17   | 0.305      | 5.99             | 5.56                | 1.87                 | 125.0             | 150   |
|                          | 18   | 0.305      | 5.99             | 5.92                | 2.00                 | 125.0             | 160   |
|                          | 19   | 0.305      | 5.99             | 6.08                | 2.05                 | 125.0             | 165   |
|                          | 20   | 1.519      | 29.83            | 19.84               | 1.34                 | 623.0             | 108   |
|                          | 21   | 3.050      | 59.90            | 31.85               | 1.07                 | 1251.0            | 86    |
|                          | 22   | 4.596      | 90.25            | 36.91               | 0.83                 | 1885.0            | 66    |

4.6.5.1 RE1 Group-2 / Set-2

RE1

$$F_q = \alpha \cdot e^{-\beta \cdot z}$$

Equation 4-6

Table 4-63 RE1 - Regression Variables for  $S_T = 150$

| Type        | Longitudinal Spacing (mm) |         |          |         |          |         |
|-------------|---------------------------|---------|----------|---------|----------|---------|
|             | 50                        |         | 100      |         | 200      |         |
|             | $\alpha$                  | $\beta$ | $\alpha$ | $\beta$ | $\alpha$ | $\beta$ |
| MW45 x MW45 | 3.67                      | 0.127   | 3.25     | 0.190   | 2.08     | 0.221   |

Table 4-64 RE1 –  $S_T = 150$

| Type                     | Test | Z (m) | $P_{test}$ (kN/m <sup>3</sup> ) | $P_{calc}$ (kN/m <sup>3</sup> ) | Bias | Statistics |         |
|--------------------------|------|-------|---------------------------------|---------------------------------|------|------------|---------|
| MW45 x MW45<br>50 x 150  | 1    | 0.305 | 3.08                            | 2.62                            | 0.85 |            |         |
|                          | 2    | 0.305 | 2.37                            | 2.62                            | 1.11 | 0.12       | COV     |
|                          | 3    | 0.305 | 2.59                            | 2.62                            | 1.01 | -0.01      | Cor-C   |
|                          | 4    | 1.544 | 10.58                           | 11.32                           | 1.07 | 0.83       | P-Bias  |
|                          | 5    | 3.170 | 16.89                           | 18.91                           | 1.12 | 0.98       | Pearson |
|                          | 6    | 4.555 | 21.99                           | 22.79                           | 1.04 | 0.12       | STD     |
|                          | 7    | 6.103 | 30.05                           | 25.07                           | 0.83 | 1.00       | Mean    |
| MW45 x MW45<br>100 x 150 | 8    | 0.305 | 4.03                            | 4.55                            | 1.13 |            |         |
|                          | 9    | 0.305 | 4.32                            | 4.55                            | 1.05 |            |         |
|                          | 10   | 0.305 | 4.56                            | 4.55                            | 1.00 |            |         |
|                          | 11   | 1.531 | 13.70                           | 18.11                           | 1.32 | 0.15       | COV     |
|                          | 12   | 4.570 | 31.75                           | 30.30                           | 0.95 | -0.10      | Cor-C   |
|                          | 13   | 3.060 | 28.60                           | 27.05                           | 0.95 | 0.79       | P-Bias  |
|                          | 14   | 1.526 | 18.60                           | 18.07                           | 0.97 | 0.99       | Pearson |
|                          | 15   | 0.305 | 5.71                            | 4.55                            | 0.80 | 0.15       | STD     |
|                          | 16   | 4.540 | 32.58                           | 30.27                           | 0.93 | 0.99       | Mean    |

Table 4-64 RE1 –  $S_T = 150$

| Type                     | Test | Z (m) | $P_{test}$ (kN/m <sup>3</sup> ) | $P_{calc}$ (kN/m <sup>3</sup> ) | Bias | Statistics |         |
|--------------------------|------|-------|---------------------------------|---------------------------------|------|------------|---------|
| MW45 x MW45<br>200 x 150 | 17   | 0.305 | 5.56                            | 5.77                            | 1.04 | 0.80       | COV     |
|                          | 18   | 0.305 | 5.92                            | 5.77                            | 0.98 | -0.13      | Cor-C   |
|                          | 19   | 0.305 | 6.08                            | 5.77                            | 0.95 | 0.98       | P-Bias  |
|                          | 20   | 1.519 | 19.84                           | 22.00                           | 1.11 | 0.99       | Pearson |
|                          | 21   | 3.050 | 31.85                           | 31.50                           | 0.99 | 0.80       | STD     |
|                          | 22   | 4.596 | 36.91                           | 33.74                           | 0.91 | 1.00       | Mean    |

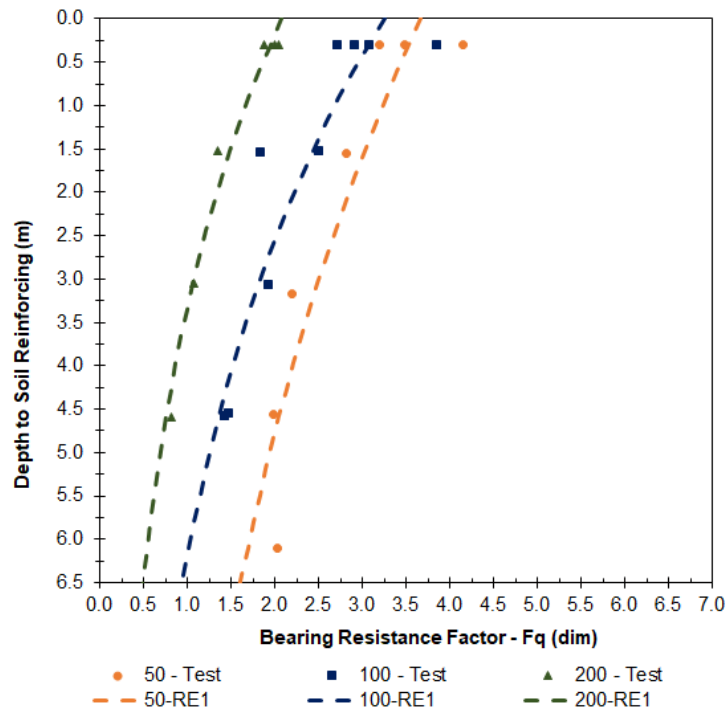


Figure 4-43 RE1 – Bearing Resistance Factor (MW45  $S_T = 150$ )

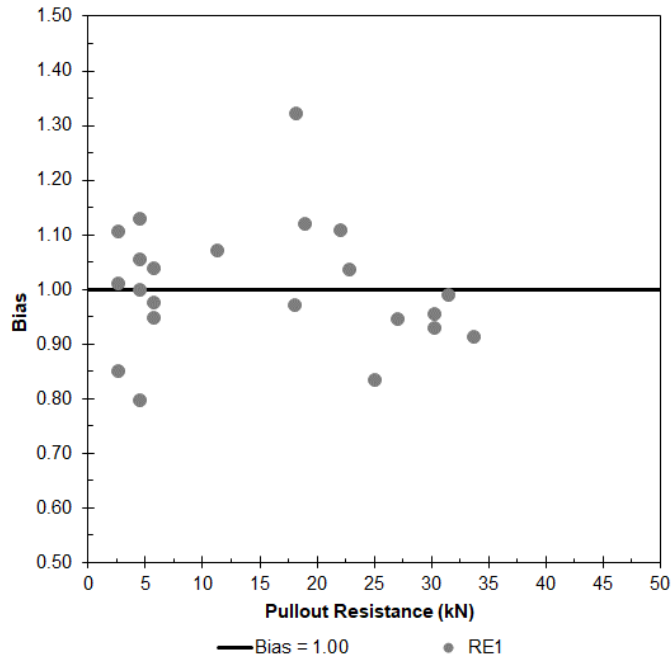


Figure 4-44 RE1 – Bias (MW45 S<sub>T</sub> = 150)

4.6.5.2 RE2 Group-2 / Set-2

RE2

$$F_q = F_0 + F_{max} \cdot e^{-\beta \cdot z}$$

Equation 4-7

Table 4-65 RE2 - Regression Variables for S<sub>T</sub> = 150

| Type        | Longitudinal Spacing (mm) |      |      |                |      |      |                |      |      |
|-------------|---------------------------|------|------|----------------|------|------|----------------|------|------|
|             | 50                        |      |      | 100            |      |      | 200            |      |      |
|             | F <sub>0</sub>            | α    | β    | F <sub>0</sub> | α    | β    | F <sub>0</sub> | α    | β    |
| MW45 x MW45 | 1.88                      | 2.06 | 0.52 | 1.50           | 1.55 | 0.55 | 0.74           | 1.45 | 0.54 |

Table 4-66 RE2 – S<sub>T</sub> = 150

| Type                     | Test | Z (m) | P <sub>test</sub> (kN/m <sup>3</sup> ) | P <sub>calc</sub> (kN/m <sup>3</sup> ) | Bias | Statistics |         |
|--------------------------|------|-------|--|--|------|------------|---------|
| MW45 x MW45<br>50 x 150  | 1    | 0.305 | 3.08                                   | 2.69                                   | 0.87 |            |         |
|                          | 2    | 0.305 | 2.37                                   | 2.69                                   | 1.14 | 0.08       | COV     |
|                          | 3    | 0.305 | 2.59                                   | 2.69                                   | 1.04 | -0.07      | Cor-C   |
|                          | 4    | 1.544 | 10.58                                  | 10.49                                  | 0.99 | 0.87       | P-Bias  |
|                          | 5    | 3.170 | 16.89                                  | 17.49                                  | 1.04 | 1.00       | Pearson |
|                          | 6    | 4.555 | 21.99                                  | 22.90                                  | 1.04 | 0.08       | STD     |
|                          | 7    | 6.103 | 30.05                                  | 29.12                                  | 0.97 | 1.01       | Mean    |
| MW45 x MW45<br>100 x 150 | 8    | 0.305 | 4.03                                   | 4.17                                   | 1.03 |            |         |
|                          | 9    | 0.305 | 4.32                                   | 4.17                                   | 0.97 |            |         |
|                          | 10   | 0.305 | 4.56                                   | 4.17                                   | 0.91 |            |         |
|                          | 11   | 1.531 | 13.70                                  | 16.15                                  | 1.18 | 0.14       | COV     |
|                          | 12   | 4.570 | 31.75                                  | 36.14                                  | 1.14 | 0.54       | Cor-C   |
|                          | 13   | 3.060 | 28.60                                  | 26.62                                  | 0.93 | 0.14       | P-Bias  |
|                          | 14   | 1.526 | 18.60                                  | 16.11                                  | 0.87 | 0.99       | Pearson |
|                          | 15   | 0.305 | 5.71                                   | 4.17                                   | 0.73 | 0.14       | STD     |
|                          | 16   | 4.540 | 32.58                                  | 35.95                                  | 1.10 | 0.99       | Mean    |
| MW45 x MW45<br>200 x 150 | 17   | 0.305 | 5.56                                   | 5.85                                   | 1.05 | 0.04       | COV     |
|                          | 18   | 0.305 | 5.92                                   | 5.85                                   | 0.99 | 0.08       | Cor-C   |
|                          | 19   | 0.305 | 6.08                                   | 5.85                                   | 0.96 | 0.88       | P-Bias  |
|                          | 20   | 1.519 | 19.84                                  | 20.35                                  | 1.03 | 1.00       | Pearson |
|                          | 21   | 3.050 | 31.85                                  | 30.18                                  | 0.95 | 0.04       | STD     |
|                          | 22   | 4.596 | 36.91                                  | 38.42                                  | 1.04 | 1.00       | Mean    |

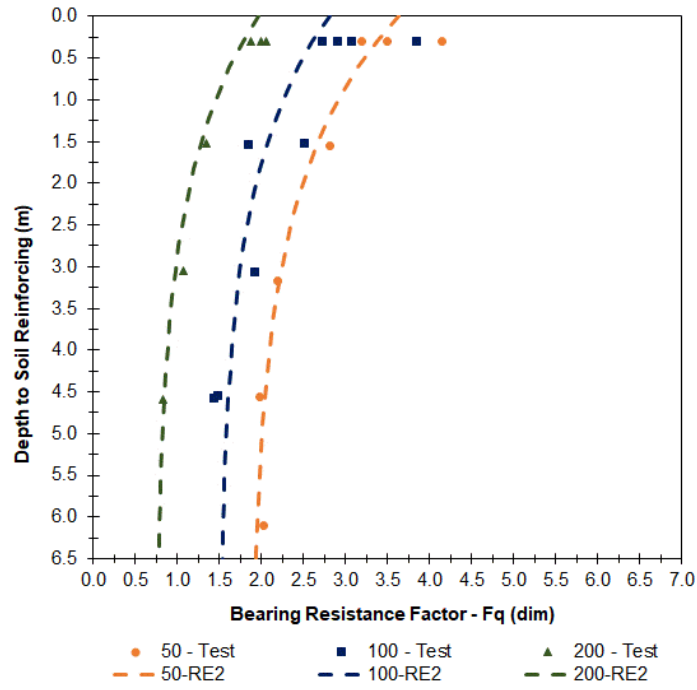


Figure 4-45 RE2 – Bearing Resistance Factor (MW45  $S_T = 150$ )

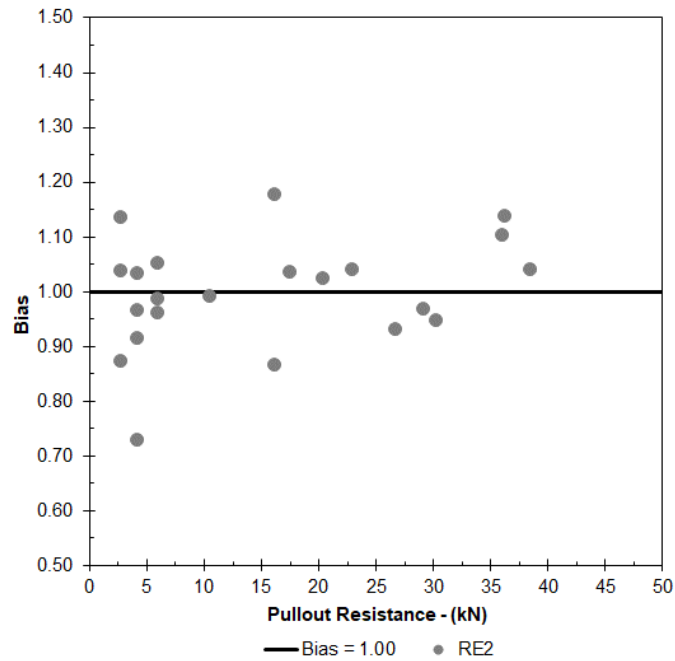


Figure 4-46 RE2 – Bias (MW45  $S_T = 150$ )

4.6.5.3 RE3 Group-2 / Set-2

$$RE3 \quad F_q = \begin{cases} F_{\max} - \frac{F_{\max} - F_1}{z_1} \cdot z \rightarrow 0 \leq z \leq z_1 \\ F_1 - \frac{F_1 - F_{\min}}{z_2 - z_1} \cdot (z_2 - z_1) \rightarrow z_1 \leq z \leq z_2 \\ F_{\min} \rightarrow z \geq z_2 \end{cases} \quad \text{Equation 4-8}$$

Table 4-67 RE3 - Regression Variables for  $S_T = 150$

| Type        |   | Longitudinal Spacing (mm) |       |       |       |       |       |       |       |       |
|-------------|---|---------------------------|-------|-------|-------|-------|-------|-------|-------|-------|
|             |   | 50                        |       |       | 100   |       |       | 200   |       |       |
|             |   | Max                       | 1     | Min   | Max   | 1     | Min   | Max   | 1     | Min   |
| MW45 x MW45 | F | 4.00                      | 2.50  | 2.00  | 3.00  | 1.75  | 1.50  | 2.00  | 1.00  | 0.75  |
|             | z | 0.000                     | 1.524 | 4.572 | 0.000 | 1.524 | 4.572 | 0.000 | 1.524 | 4.572 |
|             | z | 0.000                     | 1.524 | 4.572 | 0.000 | 1.524 | 4.572 | 0.000 | 1.524 | 4.572 |

Table 4-68 RE3 –  $S_T = 150$

| Type                    | Test | Z (m) | $P_{\text{test}}$ (kN/m <sup>3</sup> ) | $P_{\text{calc}}$ (kN/m <sup>3</sup> ) | Bias | Statistics |         |
|-------------------------|------|-------|--|--|------|------------|---------|
| MW45 x MW45<br>50 x 150 | 1    | 0.305 | 3.08                                   | 2.74                                   | 0.89 |            |         |
|                         | 2    | 0.305 | 2.37                                   | 2.74                                   | 1.16 | 0.09       | COV     |
|                         | 3    | 0.305 | 2.59                                   | 2.74                                   | 1.06 | -0.12      | Cor-C   |
|                         | 4    | 1.544 | 10.58                                  | 9.37                                   | 0.89 | 0.80       | P-Bias  |
|                         | 5    | 3.170 | 16.89                                  | 17.19                                  | 1.02 | 1.00       | Pearson |
|                         | 6    | 4.555 | 21.99                                  | 22.19                                  | 1.01 | 0.09       | STD     |
|                         | 7    | 6.103 | 30.05                                  | 29.69                                  | 0.99 | 1.00       | Mean    |

Table 4-68 RE3 –  $S_T = 150$

| Type                     | Test | Z<br>(m) | $P_{test}$<br>(kN/m <sup>3</sup> ) | $P_{calc}$<br>(kN/m <sup>3</sup> ) | Bias | Statistics |         |
|--------------------------|------|----------|------------------------------------|------------------------------------|------|------------|---------|
| MW45 x MW45<br>100 x 150 | 8    | 0.305    | 4.03                               | 4.08                               | 1.01 |            |         |
|                          | 9    | 0.305    | 4.32                               | 4.08                               | 0.94 |            |         |
|                          | 10   | 0.305    | 4.56                               | 4.08                               | 0.90 |            |         |
|                          | 11   | 1.531    | 13.70                              | 13.03                              | 0.95 | 0.15       | COV     |
|                          | 12   | 4.570    | 31.75                              | 33.35                              | 1.05 | 0.40       | Cor-C   |
|                          | 13   | 3.060    | 28.60                              | 24.17                              | 0.85 | 0.29       | P-Bias  |
|                          | 14   | 1.526    | 18.60                              | 12.99                              | 0.70 | 0.98       | Pearson |
|                          | 15   | 0.305    | 5.71                               | 4.08                               | 0.71 | 0.13       | STD     |
|                          | 16   | 4.540    | 32.58                              | 33.19                              | 1.02 | 0.88       | Mean    |
| MW45 x MW45<br>200 x 150 | 17   | 0.305    | 5.56                               | 5.34                               | 0.96 | 0.09       | COV     |
|                          | 18   | 0.305    | 5.92                               | 5.34                               | 0.90 | -0.24      | Cor-C   |
|                          | 19   | 0.305    | 6.08                               | 5.34                               | 0.88 | 0.65       | P-Bias  |
|                          | 20   | 1.519    | 19.84                              | 14.83                              | 0.75 | 0.99       | Pearson |
|                          | 21   | 3.050    | 31.85                              | 25.96                              | 0.82 | 0.08       | STD     |
|                          | 22   | 4.596    | 36.91                              | 33.54                              | 0.91 | 0.87       | Mean    |



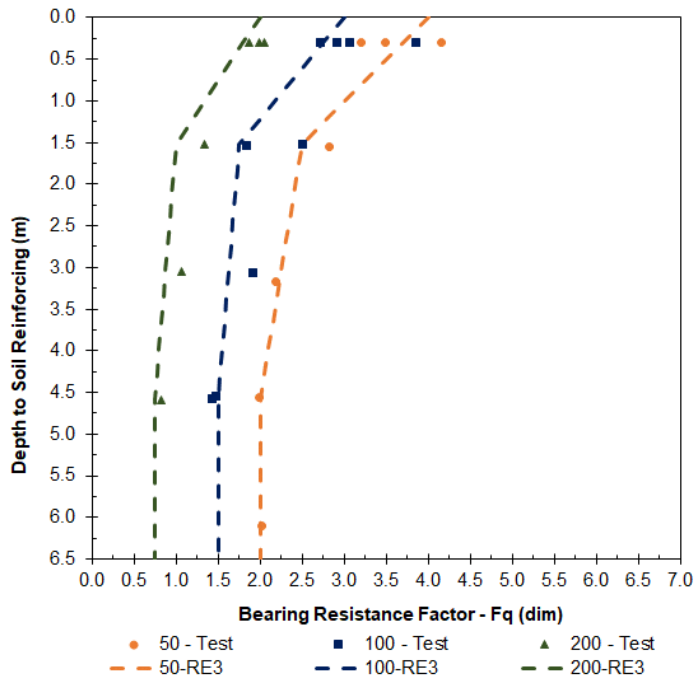


Figure 4-47 RE3 – Bearing Resistance Factor (MW45  $S_T = 150$ )

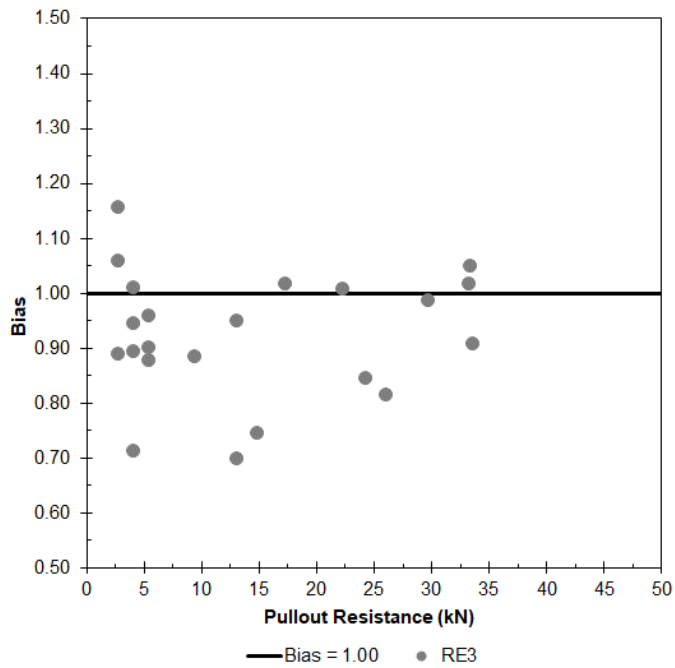


Figure 4-48 RE3 – Bias (MW45  $S_T = 150$ )

4.6.5.4 Yu Group-2 / Set-2

$$N_q = \alpha \left( \frac{n \cdot \sigma_v}{p_a} \right)^{-\beta} \quad \text{Equation 4-9}$$

Yu

$$N_q = \frac{F_q \cdot S_T}{d_b} \rightarrow F_q = \frac{N_q \cdot d_b}{S_T} \quad \text{Equation 4-11}$$

Table 4-69 Yu - Regression Variables for  $S_T = 150$

| Type        | Longitudinal Spacing (mm) |         |          |         |          |         |
|-------------|---------------------------|---------|----------|---------|----------|---------|
|             | 50                        |         | 100      |         | 200      |         |
|             | $\alpha$                  | $\beta$ | $\alpha$ | $\beta$ | $\alpha$ | $\beta$ |
| MW45 x MW45 | 57                        | 0.202   | 49       | 0.253   | 29       | 0.278   |

Table 4-70 Yu –  $S_T = 150$

| Type                     | Test | Z (m) | $P_{test}$ (kN/m <sup>3</sup> ) | $P_{calc}$ (kN/m <sup>3</sup> ) | Bias | Statistics |         |
|--------------------------|------|-------|---------------------------------|---------------------------------|------|------------|---------|
| MW45 x MW45<br>50 x 150  | 1    | 0.305 | 3.08                            | 2.46                            | 0.80 |            |         |
|                          | 2    | 0.305 | 2.37                            | 2.46                            | 1.04 | 0.09       | COV     |
|                          | 3    | 0.305 | 2.59                            | 2.46                            | 0.95 | 0.03       | Cor-C   |
|                          | 4    | 1.544 | 10.58                           | 8.99                            | 0.85 | 0.95       | P-Bias  |
|                          | 5    | 3.170 | 16.89                           | 15.98                           | 0.95 | 1.00       | Pearson |
|                          | 6    | 4.555 | 21.99                           | 21.34                           | 0.97 | 0.08       | STD     |
|                          | 7    | 6.103 | 30.05                           | 26.96                           | 0.90 | 0.92       | Mean    |
| MW45 x MW45<br>100 x 150 | 8    | 0.305 | 4.03                            | 4.36                            | 1.08 |            |         |
|                          | 9    | 0.305 | 4.32                            | 4.36                            | 1.01 |            |         |
|                          | 10   | 0.305 | 4.56                            | 4.36                            | 0.96 |            |         |
|                          | 11   | 1.531 | 13.70                           | 14.54                           | 1.06 | 0.13       | COV     |
|                          | 12   | 4.570 | 31.75                           | 32.90                           | 1.04 | 0.13       | Cor-C   |
|                          | 13   | 3.060 | 28.60                           | 24.39                           | 0.85 | 0.74       | P-Bias  |
|                          | 14   | 1.526 | 18.60                           | 14.51                           | 0.78 | 0.99       | Pearson |
|                          | 15   | 0.305 | 5.71                            | 4.36                            | 0.76 | 0.12       | STD     |
|                          | 16   | 4.540 | 32.58                           | 32.75                           | 1.00 | 0.92       | Mean    |

Table 4-70 Yu –  $S_T = 150$

| Type                     | Test | Z (m) | $P_{test}$ (kN/m <sup>3</sup> ) | $P_{calc}$ (kN/m <sup>3</sup> ) | Bias  | Statistics |         |
|--------------------------|------|-------|---------------------------------|---------------------------------|-------|------------|---------|
| MW45 x MW45<br>200 x 150 | 17   | 0.305 | 5.56                            | 5.20                            | 0.93  | 0.07       | COV     |
|                          | 18   | 0.305 | 5.92                            | 5.20                            | 0.88  | 0.47       | Cor-C   |
|                          | 19   | 0.305 | 6.08                            | 5.20                            | 0.85  | 0.65       | P-Bias  |
|                          | 20   | 1.519 | 19.84                           | 16.59                           | 0.84  | 0.99       | Pearson |
|                          | 21   | 3.050 | 31.85                           | 27.44                           | 0.86  | 0.06       | STD     |
|                          | 22   | 4.596 | 36.91                           | 36.90                           | 1.000 | 0.894      | Mean    |

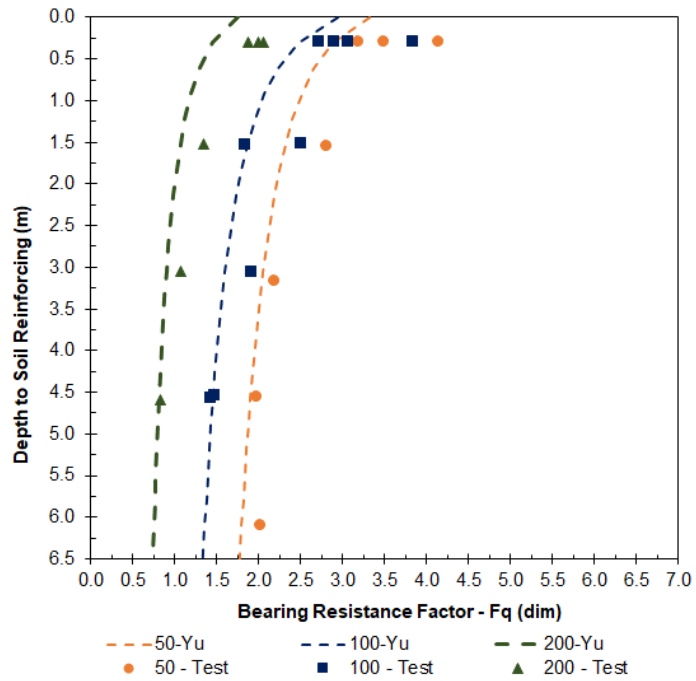


Figure 4-49 Yu – Bearing Resistance Factor (MW45  $S_T = 150$ )

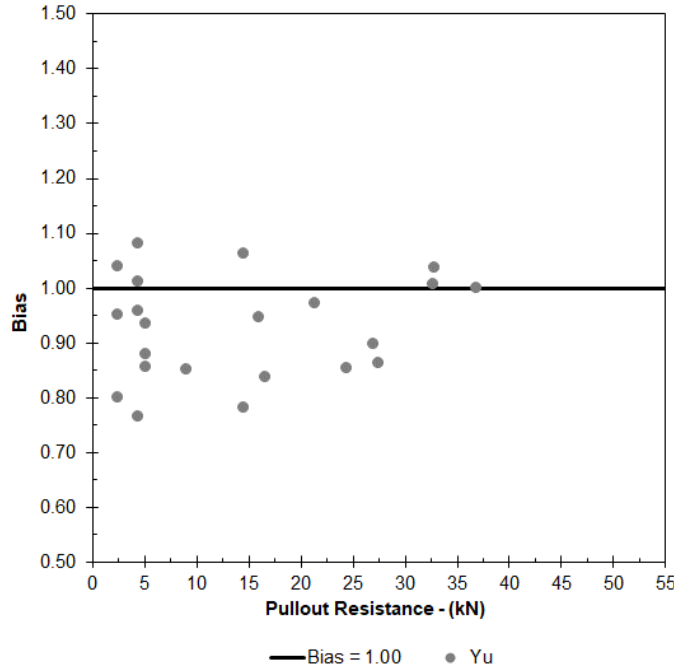


Figure 4-50 Yu – Bias (MW45 ST = 150)

#### 4.6.6 Group-2 Set-3 Bearing Resistance Factor

Group-2, Set-3 consists of an MW45 x MW45, 2-Wire soil-reinforcing element with one transverse element (1W). Group-2, Set-3, had three sub-sets with longitudinal element spacings equal to 50 mm, 100 mm, and 200 mm.

Table 4-71 MW45 x MW45 – ST = 1W Pullout Test Results

| Type                   | Test | Depth<br>m | Surcharge<br>kPa | $P_{r,3/4}$<br>kN | $F^*_{19\text{ mm}}$ | $\sigma_v$<br>kPa | $N_q$ |
|------------------------|------|------------|------------------|-------------------|----------------------|-------------------|-------|
| MW45 x MW45<br>50 x 1W | 1    | 0.305      | 5.99             | 1.36              | 7.33                 | 5.99              | 588   |
|                        | 2    | 0.305      | 5.99             | 1.49              | 8.06                 | 5.99              | 647   |
|                        | 3    | 0.305      | 5.99             | 1.49              | 8.06                 | 5.99              | 647   |
|                        | 4    | 1.565      | 30.74            | 4.18              | 4.39                 | 30.74             | 352   |
|                        | 5    | 3.050      | 59.90            | 6.22              | 3.35                 | 59.90             | 269   |
|                        | 6    | 4.572      | 89.78            | 7.50              | 2.70                 | 89.78             | 217   |
|                        | 7    | 6.103      | 119.84           | 8.18              | 2.21                 | 119.84            | 177   |

Table 4-71 MW45 x MW45 – ST = 1W Pullout Test Results

| Type                    | Test | Depth<br>m | Surcharge<br>kPa | P <sub>r,3/4</sub><br>kN | F* <sub>19 mm</sub> | σ <sub>v</sub><br>kPa | N <sub>q</sub> |
|-------------------------|------|------------|------------------|--------------------------|---------------------|-----------------------|----------------|
|                         | 8    | 6.057      | 118.93           | 7.00                     | 1.90                | 118.93                | 153            |
| MW45 x MW45<br>100 x 1W | 9    | 0.305      | 5.99             | 2.21                     | 5.95                | 5.99                  | 478            |
|                         | 10   | 0.305      | 5.99             | 1.73                     | 4.66                | 5.99                  | 374            |
|                         | 11   | 0.305      | 5.99             | 1.97                     | 5.33                | 5.99                  | 427            |
|                         | 12   | 1.522      | 29.88            | 5.04                     | 2.72                | 29.88                 | 218            |
|                         | 13   | 3.041      | 59.71            | 7.66                     | 2.07                | 59.71                 | 166            |
|                         | 14   | 4.582      | 89.97            | 9.74                     | 1.75                | 89.97                 | 140            |
|                         | 15   | 6.094      | 119.65           | 11.20                    | 1.51                | 119.65                | 121            |
| MW45 x MW45<br>200 x 1W | 16   | 0.305      | 5.99             | 1.89                     | 2.55                | 5.99                  | 205            |
|                         | 17   | 0.305      | 5.99             | 1.44                     | 1.95                | 5.99                  | 156            |
|                         | 18   | 0.305      | 5.99             | 1.47                     | 1.98                | 5.99                  | 159            |
|                         | 19   | 1.531      | 30.07            | 4.44                     | 1.19                | 30.07                 | 96             |
|                         | 20   | 3.043      | 59.75            | 5.61                     | 0.76                | 59.75                 | 61             |
|                         | 21   | 4.582      | 89.97            | 6.60                     | 0.59                | 89.97                 | 48             |

4.6.6.1 RE1 Group-2 / Set-3

RE1 
$$F_q = \alpha \cdot e^{-\beta \cdot z}$$
 Equation 4-6

Table 4-72 RE1 - Regression Variables for S<sub>T</sub> = 1W

| Type        | Longitudinal Spacing (mm) |       |      |       |      |       |
|-------------|---------------------------|-------|------|-------|------|-------|
|             | 50                        |       | 100  |       | 200  |       |
|             | α                         | β     | α    | β     | α    | β     |
| MW45 x MW45 | 7.24                      | 0.265 | 5.64 | 0.298 | 2.33 | 0.373 |

Table 4-73 RE1 –  $S_T = 1W$

| Type                    | Test | Z (m) | $P_{test}$ (kN/m <sup>3</sup> ) | $P_{calc}$ (kN/m <sup>3</sup> ) | Bias | Statistics |          |
|-------------------------|------|-------|---------------------------------|---------------------------------|------|------------|----------|
| MW45 X MW45<br>50 x 1W  | 1    | 0.305 | 1.36                            | 1.24                            | 0.91 |            |          |
|                         | 2    | 0.305 | 1.49                            | 1.24                            | 0.83 |            |          |
|                         | 3    | 0.305 | 1.49                            | 1.24                            | 0.83 | 0.16       | COV      |
|                         | 4    | 1.565 | 4.18                            | 4.55                            | 1.09 | -0.09      | Cor-Bias |
|                         | 5    | 3.050 | 6.22                            | 5.98                            | 0.96 | 0.84       | P-Bias   |
|                         | 6    | 4.572 | 7.50                            | 5.98                            | 0.80 | 0.95       | Pearson  |
|                         | 7    | 6.103 | 8.18                            | 5.32                            | 0.65 | 0.13       | STD      |
|                         | 8    | 6.057 | 7.00                            | 5.35                            | 0.76 | 0.85       | Mean     |
| MW45 X MW45<br>100 x 1W | 9    | 0.305 | 2.21                            | 1.91                            | 0.86 |            |          |
|                         | 10   | 0.305 | 1.73                            | 1.91                            | 1.10 | 0.24       | COV      |
|                         | 11   | 0.305 | 1.97                            | 1.91                            | 0.97 | -0.04      | Cor-Bias |
|                         | 12   | 1.522 | 5.04                            | 6.63                            | 1.32 | 0.93       | P-Bias   |
|                         | 13   | 3.041 | 7.66                            | 8.43                            | 1.10 | 0.87       | Pearson  |
|                         | 14   | 4.582 | 9.74                            | 8.02                            | 0.82 | 0.23       | STD      |
|                         | 15   | 6.094 | 11.20                           | 6.80                            | 0.61 | 0.97       | Mean     |
| MW45 X MW45<br>200 x 1W | 16   | 0.305 | 1.89                            | 1.54                            | 0.81 | 0.16       | COV      |
|                         | 17   | 0.305 | 1.44                            | 1.54                            | 1.07 | -0.09      | Cor-Bias |
|                         | 18   | 0.305 | 1.47                            | 1.54                            | 1.05 | 0.86       | P-Bias   |
|                         | 19   | 1.531 | 4.44                            | 4.90                            | 1.10 | 0.93       | Pearson  |
|                         | 20   | 3.043 | 5.61                            | 5.55                            | 0.99 | 0.16       | STD      |
|                         | 21   | 4.582 | 6.60                            | 4.71                            | 0.71 | 0.96       | Mean     |

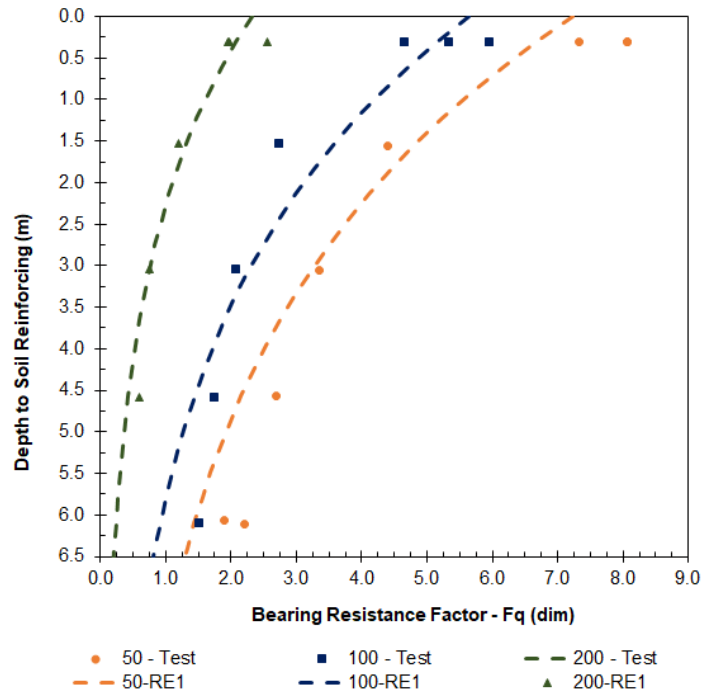


Figure 4-51 RE1 – Bearing Resistance Factor (MW45  $S_T = 1W$ )

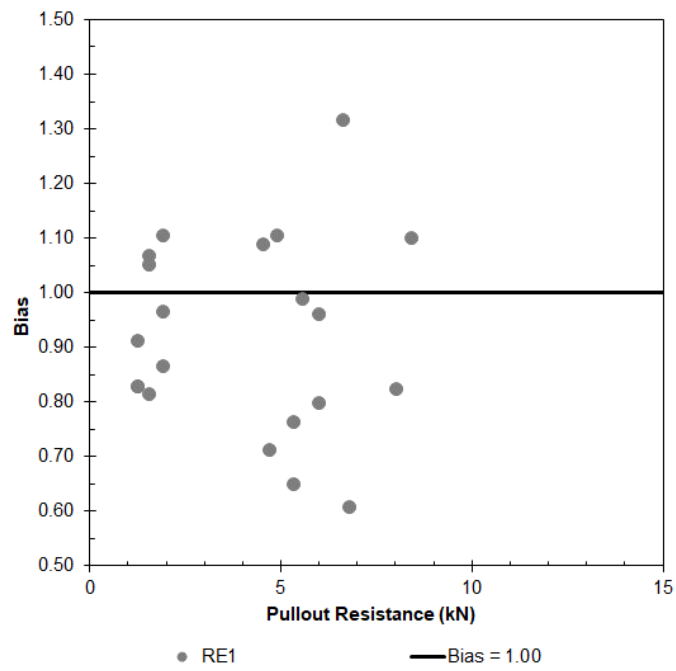


Figure 4-52 RE1 – Bias (MW45  $S_T = 1W$ )

4.6.6.2 RE2 Group-2 / Set-3

RE2

$$F_q = F_0 + F_{\max} \cdot e^{-\beta \cdot z}$$

Equation 4-7

Table 4-74 RE2 - Regression Variables for  $S_T = 1W$

| Type        | Longitudinal Spacing (mm) |          |         |       |          |         |       |          |         |
|-------------|---------------------------|----------|---------|-------|----------|---------|-------|----------|---------|
|             | 50                        |          |         | 100   |          |         | 200   |          |         |
|             | $F_0$                     | $\alpha$ | $\beta$ | $F_0$ | $\alpha$ | $\beta$ | $F_0$ | $\alpha$ | $\beta$ |
| MW45 x MW45 | 2.06                      | 6.95     | 0.63    | 1.63  | 4.89     | 0.94    | 0.52  | 2.04     | 0.72    |

Table 4-75 RE2 –  $S_T = 1W$

| Type                    | Z (m) | $P_{\text{test}}$ (kN/m <sup>3</sup> ) | $P_{\text{calc}}$ (kN/m <sup>3</sup> ) | Bias | Statistics |          |
|-------------------------|-------|--|--|------|------------|----------|
| MW45 X MW45<br>50 x 1W  | 0.305 | 1.36                                   | 1.44                                   | 1.06 |            |          |
|                         | 0.305 | 1.49                                   | 1.44                                   | 0.97 |            |          |
|                         | 0.305 | 1.49                                   | 1.44                                   | 0.97 | 0.08       | COV      |
|                         | 1.565 | 4.18                                   | 4.44                                   | 1.06 | 0.16       | Cor-Bias |
|                         | 3.050 | 6.22                                   | 5.72                                   | 0.92 | 0.71       | P-Bias   |
|                         | 4.572 | 7.50                                   | 6.82                                   | 0.91 | 0.98       | Pearson  |
|                         | 6.103 | 8.18                                   | 8.19                                   | 1.00 | 0.09       | STD      |
|                         | 6.057 | 7.00                                   | 8.15                                   | 1.16 | 1.01       | Mean     |
| MW45 X MW45<br>100 x 1W | 0.305 | 2.21                                   | 1.97                                   | 0.89 |            |          |
|                         | 0.305 | 1.73                                   | 1.97                                   | 1.14 | 0.09       | COV      |
|                         | 0.305 | 1.97                                   | 1.97                                   | 1.00 | 0.12       | Cor-Bias |
|                         | 1.522 | 5.04                                   | 5.19                                   | 1.03 | 0.81       | P-Bias   |
|                         | 3.041 | 7.66                                   | 7.08                                   | 0.92 | 0.99       | Pearson  |
|                         | 4.582 | 9.74                                   | 9.46                                   | 0.97 | 0.09       | STD      |
|                         | 6.094 | 11.20                                  | 12.21                                  | 1.09 | 1.01       | Mean     |



Table 4-75 RE2 –  $S_T = 1W$

| Type                    | Z (m) | $P_{test}$ (kN/m <sup>3</sup> ) | $P_{calc}$ (kN/m <sup>3</sup> ) | Bias | Statistics |          |
|-------------------------|-------|---------------------------------|---------------------------------|------|------------|----------|
| MW45 X MW45<br>200 x 1W | 0.305 | 1.89                            | 1.60                            | 0.85 | 0.09       | COV      |
|                         | 0.305 | 1.44                            | 1.60                            | 1.11 | -0.08      | Cor-Bias |
|                         | 0.305 | 1.47                            | 1.60                            | 1.09 | 0.88       | P-Bias   |
|                         | 1.531 | 4.44                            | 4.45                            | 1.00 | 1.00       | Pearson  |
|                         | 3.043 | 5.61                            | 5.54                            | 0.99 | 0.09       | STD      |
|                         | 4.582 | 6.60                            | 6.65                            | 1.01 | 1.01       | Mean     |

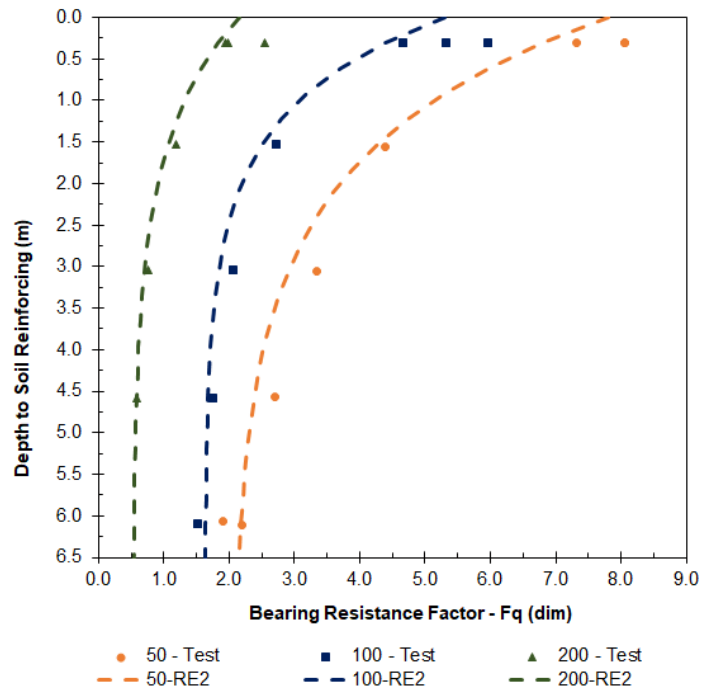


Figure 4-53 RE2 – Bearing Resistance Factor (MW45  $S_T = 1W$ )

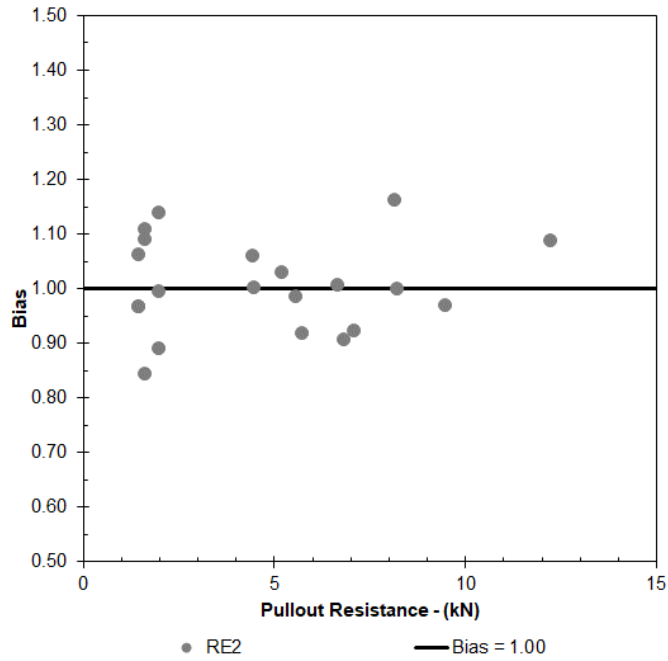


Figure 4-54 RE2 – Bias (MW45 S<sub>T</sub> = 1W)

4.6.6.3 RE3 Group-2 / Set-3

RE3

$$F_q = \begin{cases} F_{\max} - \frac{F_{\max} - F_1}{z_1} \cdot z \rightarrow 0 \leq z \leq z_1 \\ F_1 - \frac{F_1 - F_{\min}}{z_2 - z_1} \cdot (z - z_1) \rightarrow z_1 \leq z \leq z_2 \\ F_{\min} \rightarrow z \geq z_2 \end{cases} \quad \text{Equation 4-8}$$

Table 4-76 RE3 - Regression Variables for S<sub>T</sub> = 1W

| Type        |   | Longitudinal Spacing (mm) |       |       |       |       |       |       |       |       |
|-------------|---|---------------------------|-------|-------|-------|-------|-------|-------|-------|-------|
|             |   | 50                        |       |       | 100   |       |       | 200   |       |       |
|             |   | Max                       | 1     | Min   | Max   | 1     | Min   | Max   | 1     | Min   |
| MW45 x MW45 | F | 8.00                      | 4.00  | 2.25  | 5.00  | 2.50  | 1.50  | 2.50  | 1.00  | 0.50  |
|             | z | 0.000                     | 1.524 | 4.572 | 0.000 | 1.524 | 4.572 | 0.000 | 1.524 | 4.572 |

Table 4-77 RE3 –  $S_T = 1W$

| Type                    | Z (m) | $P_{test}$ (kN/m <sup>3</sup> ) | $P_{calc}$ (kN/m <sup>3</sup> ) | Bias | Statistics |          |
|-------------------------|-------|---------------------------------|---------------------------------|------|------------|----------|
| MW45 X MW45<br>50 x 1W  | 0.305 | 1.36                            | 1.33                            | 1.03 |            |          |
|                         | 0.305 | 1.49                            | 1.33                            | 0.94 |            |          |
|                         | 0.305 | 1.49                            | 1.33                            | 0.94 | 0.10       | COV      |
|                         | 1.565 | 4.18                            | 3.78                            | 0.89 | 0.46       | Cor-Bias |
|                         | 3.050 | 6.22                            | 5.79                            | 0.90 | 0.26       | P-Bias   |
|                         | 4.572 | 7.50                            | 6.26                            | 0.95 | 0.98       | Pearson  |
|                         | 6.103 | 8.18                            | 8.35                            | 1.03 | 0.10       | STD      |
|                         | 6.057 | 7.00                            | 8.29                            | 1.20 | 0.99       | Mean     |
| MW45 X MW45<br>100 x 1W | 0.305 | 2.21                            | 1.67                            | 0.88 |            |          |
|                         | 0.305 | 1.73                            | 1.67                            | 1.12 | 0.07       | COV      |
|                         | 0.305 | 1.97                            | 1.67                            | 0.98 | -0.04      | Cor-Bias |
|                         | 1.522 | 5.04                            | 4.63                            | 0.99 | 0.93       | P-Bias   |
|                         | 3.041 | 7.66                            | 7.40                            | 0.98 | 1.00       | Pearson  |
|                         | 4.582 | 9.74                            | 8.36                            | 0.97 | 0.07       | STD      |
|                         | 6.094 | 11.20                           | 11.12                           | 1.00 | 0.99       | Mean     |
| MW45 X MW45<br>200 x 1W | 0.305 | 1.89                            | 1.63                            | 0.87 | 0.12       | COV      |
|                         | 0.305 | 1.44                            | 1.63                            | 1.14 | 0.03       | Cor-Bias |
|                         | 0.305 | 1.47                            | 1.63                            | 1.12 | 0.58       | P-Bias   |
|                         | 1.531 | 4.44                            | 3.72                            | 0.92 | 0.99       | Pearson  |
|                         | 3.043 | 5.61                            | 5.56                            | 1.07 | 0.12       | STD      |
|                         | 4.582 | 6.60                            | 5.57                            | 1.15 | 1.04       | Mean     |

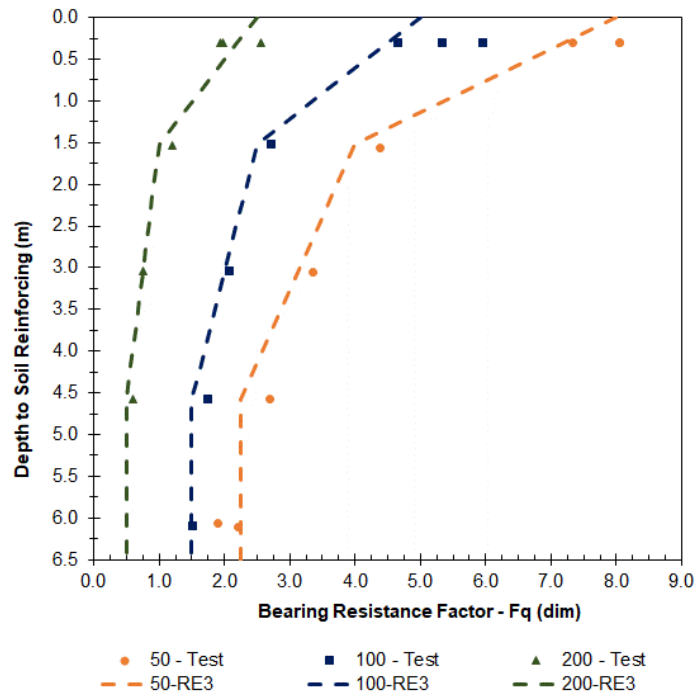


Figure 4-55 RE3 – Bearing Resistance Factor (MW45  $S_T = 1W$ )

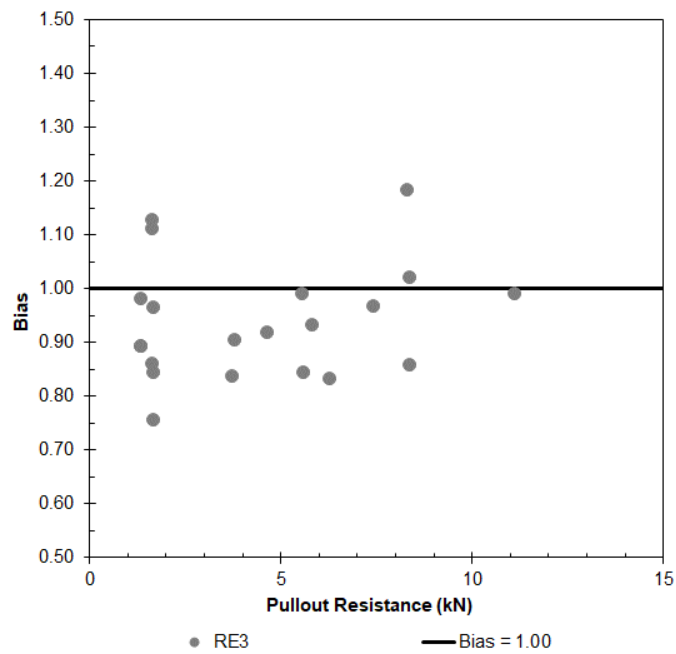


Figure 4-56 RE3 – Bias (MW45  $S_T = 1W$ )

4.6.6.4 Yu Group-2 / Set-3

$$N_q = \alpha \left( \frac{n \cdot \sigma_v}{p_a} \right)^{-\beta} \quad \text{Equation 4-9}$$

Yu

$$N_q = \frac{F_q \cdot S_T}{d_b} \rightarrow F_q = \frac{N_q \cdot d_b}{S_T} \quad \text{Equation 4-11}$$

Table 4-78 Yu - Regression Variables for  $S_T = 1W$

| Type        | Longitudinal Spacing (mm) |         |          |         |          |         |
|-------------|---------------------------|---------|----------|---------|----------|---------|
|             | 50                        |         | 100      |         | 200      |         |
|             | $\alpha$                  | $\beta$ | $\alpha$ | $\beta$ | $\alpha$ | $\beta$ |
| MW45 x MW45 | 98                        | 0.402   | 65       | 0.414   | 26       | 0.435   |

Table 4-79 Yu –  $S_T = 1W$

| Type                    | Z (m) | $P_{test}$ (kN/m <sup>3</sup> ) | $P_{calc}$ (kN/m <sup>3</sup> ) | Bias | Statistics |          |
|-------------------------|-------|---------------------------------|---------------------------------|------|------------|----------|
| MW45 X MW45<br>50 x 1W  | 0.305 | 1.36                            | 1.40                            | 1.03 |            |          |
|                         | 0.305 | 1.49                            | 1.40                            | 0.94 |            |          |
|                         | 0.305 | 1.49                            | 1.40                            | 0.94 | 0.10       | COV      |
|                         | 1.565 | 4.18                            | 3.74                            | 0.89 | 0.46       | Cor-Bias |
|                         | 3.050 | 6.22                            | 5.57                            | 0.90 | 0.26       | P-Bias   |
|                         | 4.572 | 7.50                            | 7.10                            | 0.95 | 0.98       | Pearson  |
|                         | 6.103 | 8.18                            | 8.43                            | 1.03 | 0.10       | STD      |
|                         | 6.057 | 7.00                            | 8.40                            | 1.20 | 0.99       | Mean     |
| MW45 X MW45<br>100 x 1W | 0.305 | 2.21                            | 1.94                            | 0.88 |            |          |
|                         | 0.305 | 1.73                            | 1.94                            | 1.12 | 0.07       | COV      |
|                         | 0.305 | 1.97                            | 1.94                            | 0.98 | -0.04      | Cor-Bias |
|                         | 1.522 | 5.04                            | 4.98                            | 0.99 | 0.93       | P-Bias   |
|                         | 3.041 | 7.66                            | 7.47                            | 0.98 | 1.00       | Pearson  |
|                         | 4.582 | 9.74                            | 9.50                            | 0.97 | 0.07       | STD      |
|                         | 6.094 | 11.20                           | 11.23                           | 1.00 | 0.99       | Mean     |

Table 4-79  $Y_u - S_T = 1W$

| Type                    | Z (m) | $P_{test}$ (kN/m <sup>3</sup> ) | $P_{calc}$ (kN/m <sup>3</sup> ) | Bias | Statistics |          |
|-------------------------|-------|---------------------------------|---------------------------------|------|------------|----------|
| MW45 X MW45<br>200 x 1W | 0.305 | 1.89                            | 1.64                            | 0.87 | 0.12       | COV      |
|                         | 0.305 | 1.44                            | 1.64                            | 1.14 | 0.03       | Cor-Bias |
|                         | 0.305 | 1.47                            | 1.64                            | 1.12 | 0.58       | P-Bias   |
|                         | 1.531 | 4.44                            | 4.08                            | 0.92 | 0.99       | Pearson  |
|                         | 3.043 | 5.61                            | 6.01                            | 1.07 | 0.12       | STD      |
|                         | 4.582 | 6.60                            | 7.57                            | 1.15 | 1.04       | Mean     |

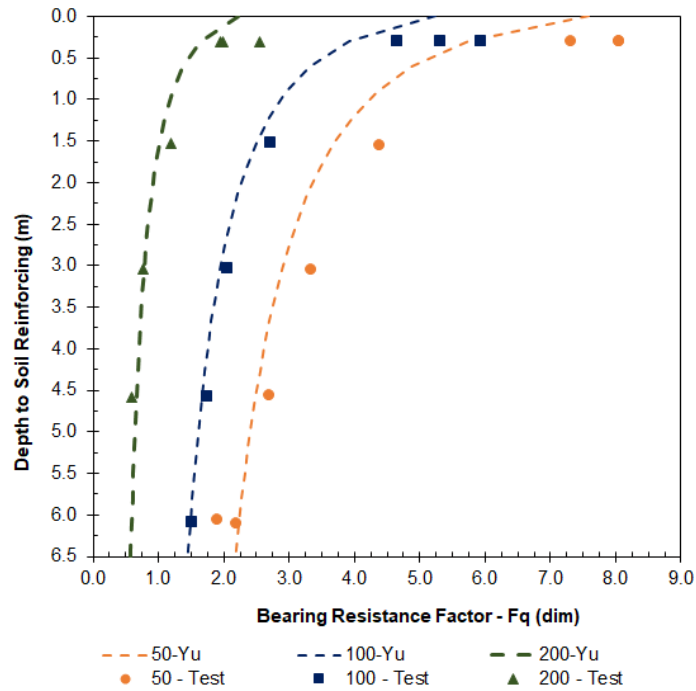


Figure 4-57  $Y_u - \text{Bearing Resistance Factor (MW45 } S_T = 1W)$

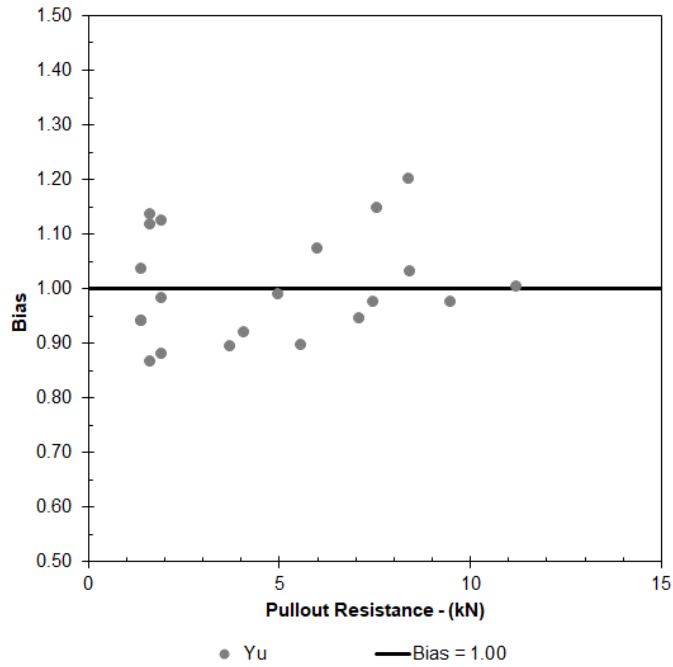


Figure 4-58 Yu – Bias (MW45 ST = 1W)

#### 4.7 Bearing Resistance Equation Comparison

In this section a comparison between the calculated bearing resistance using the equations developed for the research equations, i.e., RE1, RE2, and RE3, in addition to the Yu equation will be presented. The results will be presented numerically in a table and graphically. The values in the table will be presented as the mean, coefficient of variance (COV), standard deviation (STD) and the R coefficient. These values are calculated based on the bias that was presented in Section 4.6. As previously described, the bias is the predicted (calculated) pullout resistance ( $P_c$ ) divided by the measured pullout resistance ( $P_m$ ) from the pullout test data. The predicted pullout resistance and measure pullout resistance can be found on the data tables in Section 4.6.

A graphic representation will be presented that plots the Bias versus the predicted (calculated) pullout capacity. In the plot of the Bias versus Predicted Pullout Resistance a value less than one indicates that the equation that was used to predict (calculate) the pullout resistance is under estimated. In contrast, a value that is greater than one indicates that the equation that was used to predict (calculate) the pullout resistance is over estimated. From a practical design perspective, it is advantageous to use equations where the bias is close to 1.0.

Each of the graphs in the following section are presented based on the configurations that were tested in the experimental test program. Because the data on the graph is based on the same measured test values, it provides a visual representation as to the accuracy of the equations used in Section 4.6.



4.7.1 Group-1 Set-1 - MW71  $S_T = 300$  mm

4.7.1.1 MW71 x MW71 50 x 300

Table 4-80 MW71 x MW71 50 x 300

|      | RE1  | RE2  | RE3  | Yu   |
|------|------|------|------|------|
| Mean | 1.00 | 1.01 | 0.94 | 1.08 |
| COV  | 0.09 | 0.08 | 0.08 | 0.11 |
| STD  | 0.09 | 0.08 | 0.07 | 0.12 |
| R    | 0.98 | 0.99 | 0.99 | 0.98 |

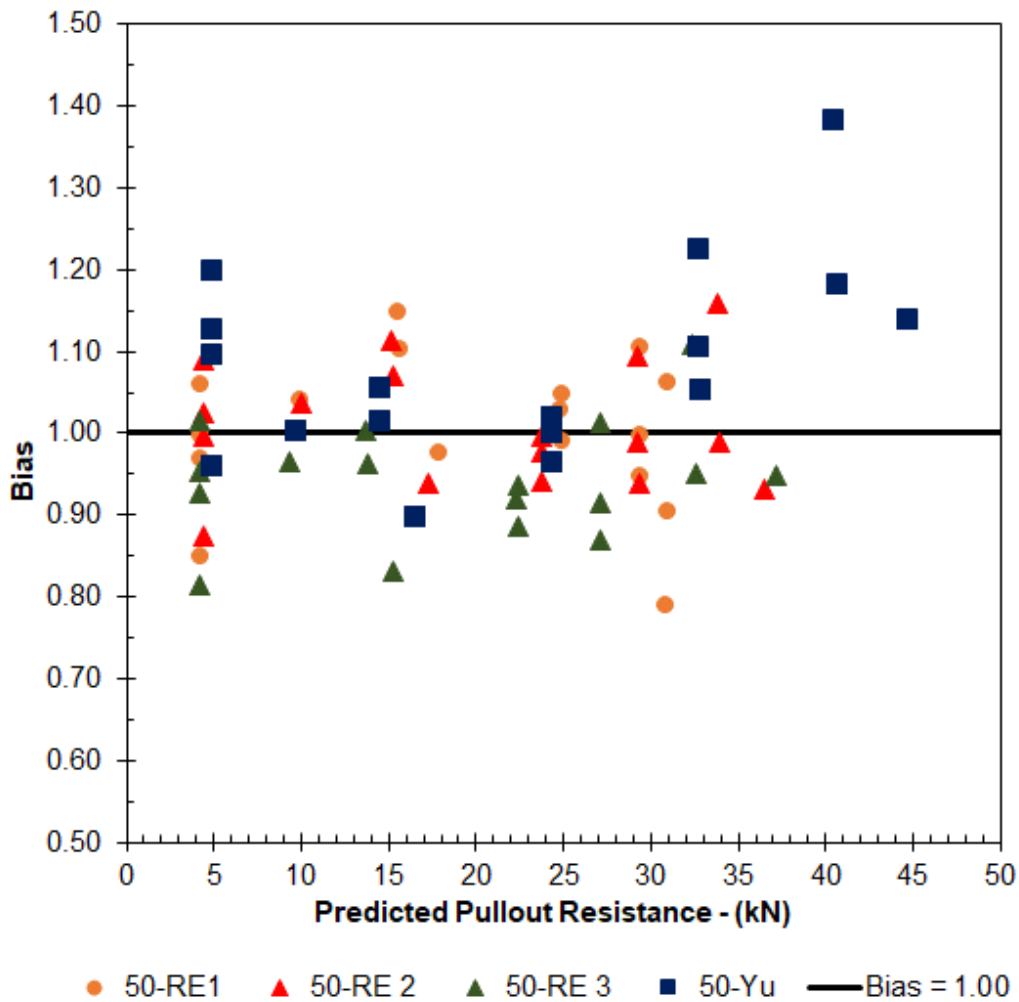


Figure 4-59 Bias (MW71 x MW71 - 50 x 300)

4.7.1.2 MW71 x MW71 100 x 300

Table 4-81 MW71 x MW71 100 x 300

|      | RE1  | RE2  | RE3  | Yu   |
|------|------|------|------|------|
| Mean | 0.98 | 1.00 | 1.02 | 1.08 |
| COV  | 0.14 | 0.04 | 0.05 | 0.05 |
| STD  | 0.14 | 0.04 | 0.05 | 0.05 |
| R    | 0.95 | 0.99 | 1.00 | 1.00 |

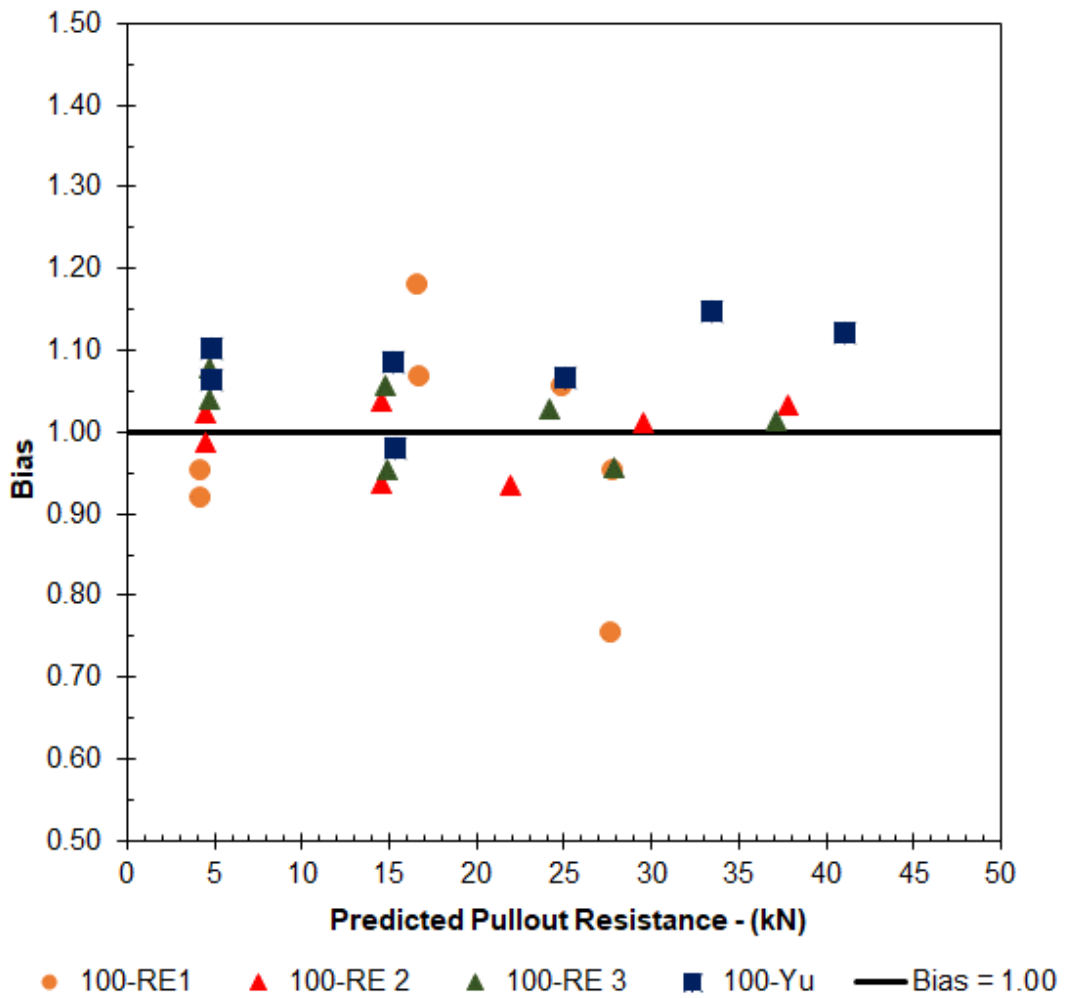


Figure 4-60 Bias (MW71 x MW71 - 100 x 300)

4.7.1.3 MW71 x MW71 200 x 300

Table 4-82 MW71 x MW71 200 x 300

|      | RE1  | RE2  | RE3  | Yu   |
|------|------|------|------|------|
| Mean | 0.99 | 1.01 | 0.97 | 1.10 |
| COV  | 0.18 | 0.11 | 0.10 | 0.07 |
| STD  | 0.17 | 0.11 | 0.10 | 0.08 |
| R    | 0.86 | 0.96 | 0.98 | 0.99 |

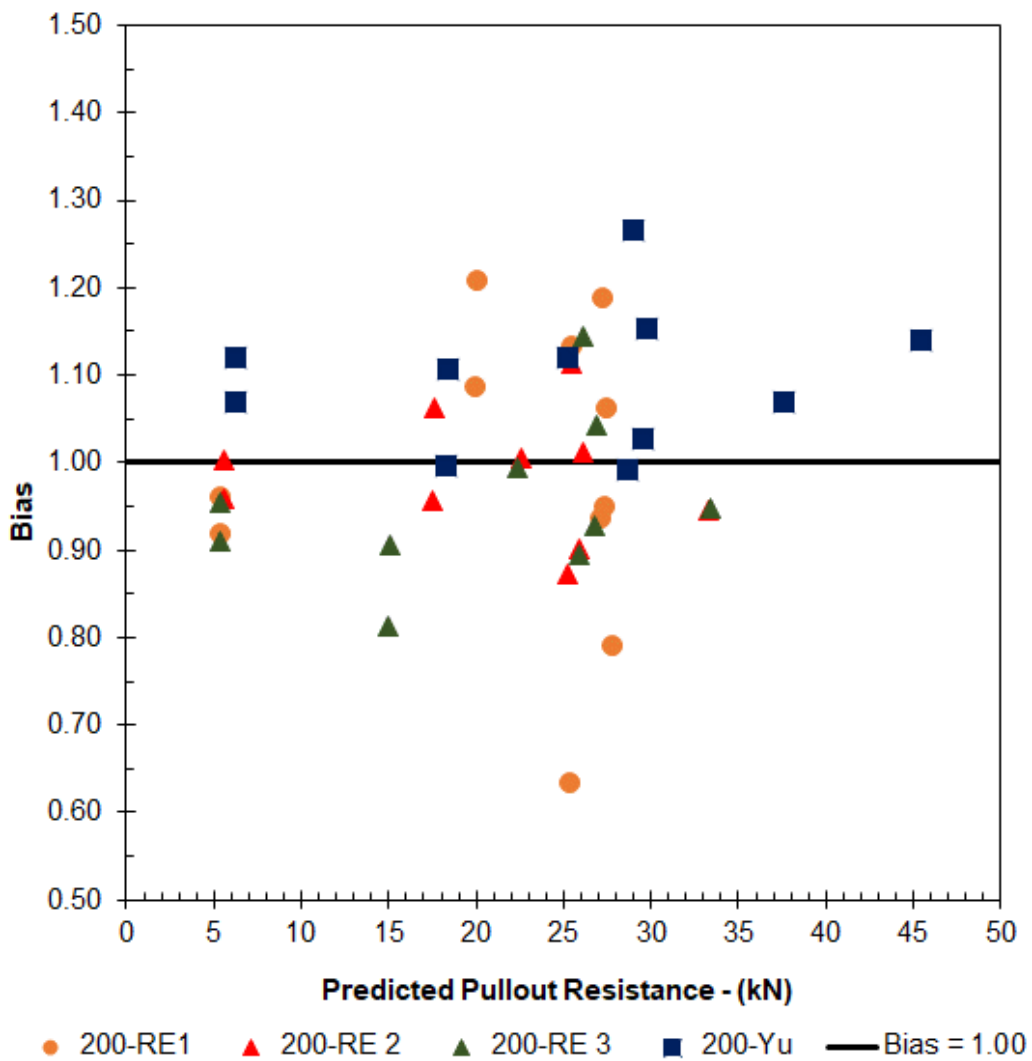


Figure 4-61 Bias ((MW71 x MW71 - 200 x 300))

4.7.2 Group-1 Set-2 – MW71  $S_T = 150$  mm

4.7.2.1 MW71 x MW71 50 x 150

Table 4-83 MW71 x MW71 50 x 150

|      | RE1  | RE2  | RE3  | Yu   |
|------|------|------|------|------|
| Mean | 1.00 | 1.00 | 1.01 | 0.89 |
| COV  | 0.17 | 0.06 | 0.10 | 0.07 |
| STD  | 0.17 | 0.06 | 0.10 | 0.06 |
| R    | 0.93 | 1.00 | 0.99 | 0.99 |

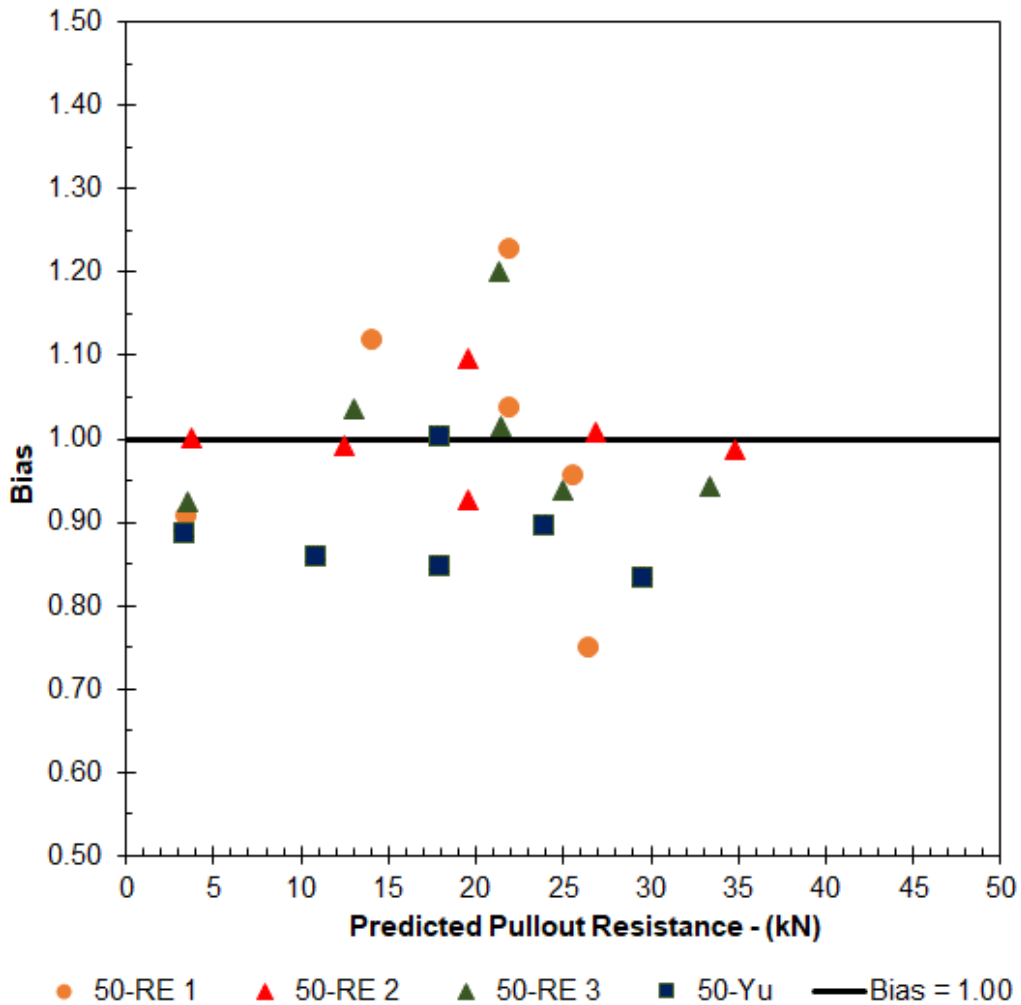


Figure 4-62 Bias (MW71 x MW71 - 50 x 150)

4.7.2.2 MW71 x MW71 100 x 150

Table 4-84 MW71 x MW71 100 x 150

|      | RE1  | RE2  | RE3  | Yu   |
|------|------|------|------|------|
| Mean | 1.00 | 1.00 | 0.98 | 0.92 |
| COV  | 0.09 | 0.05 | 0.05 | 0.05 |
| STD  | 0.09 | 0.05 | 0.05 | 0.05 |
| R    | 0.95 | 1.00 | 1.00 | 1.00 |

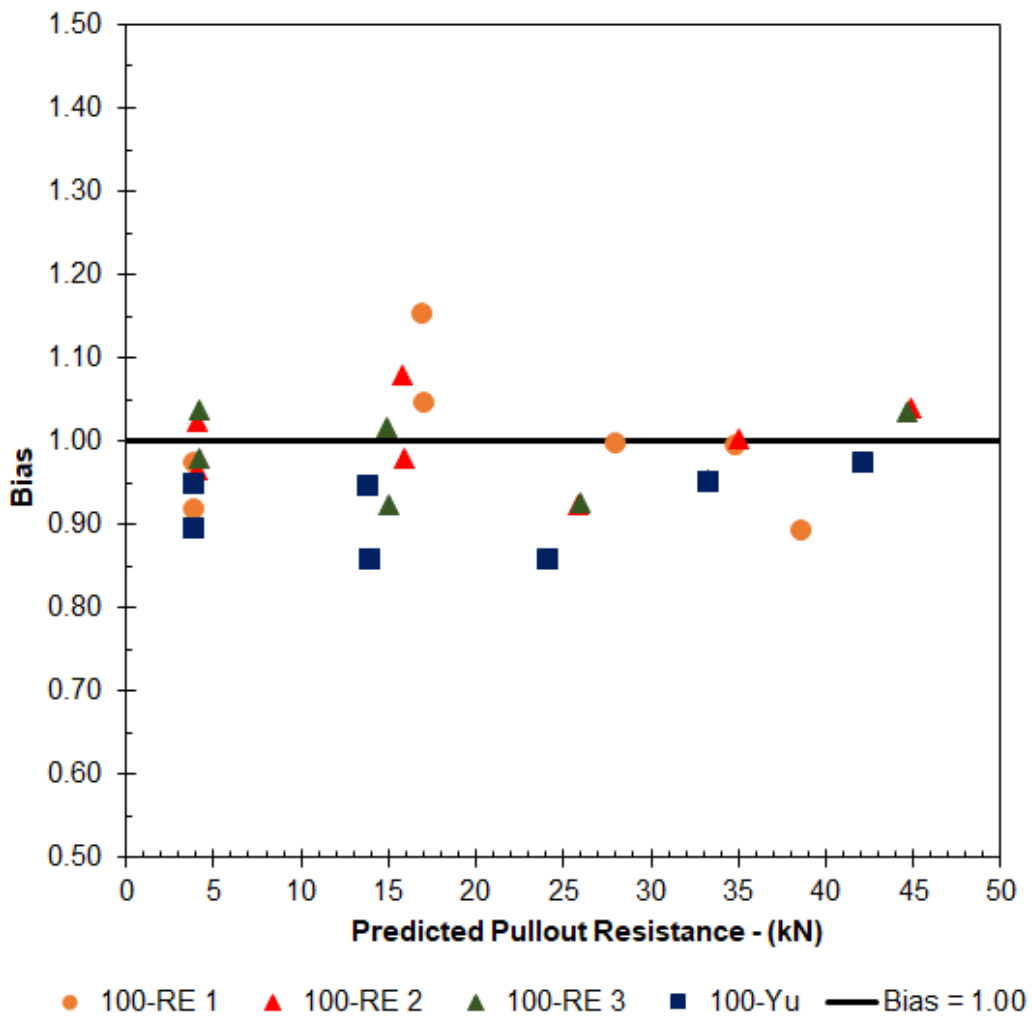


Figure 4-63 Bias (MW71 x MW71 - 100 x 150)

4.7.2.3 MW71 x MW71 - 200 x 150

Table 4-85 MW71 x MW71 - 200 x 150

|      | RE1  | RE2  | RE3  | Yu   |
|------|------|------|------|------|
| Mean | 0.99 | 1.01 | 0.83 | 0.85 |
| COV  | 0.22 | 0.12 | 0.14 | 0.08 |
| STD  | 0.21 | 0.12 | 0.12 | 0.07 |
| R    | 0.93 | 0.96 | 0.97 | 0.98 |

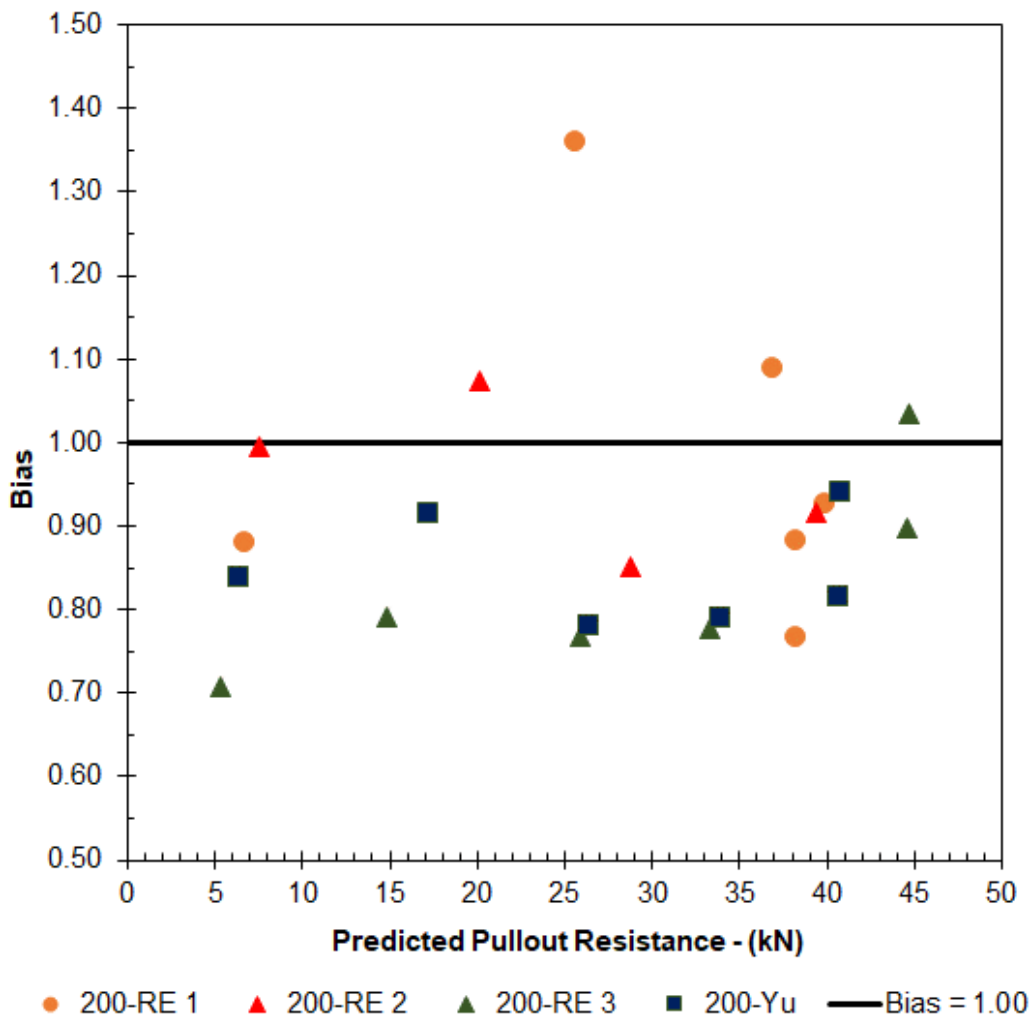


Figure 4-64 Bias (MW71 x MW71 - 200 x 150)

4.7.3 Group-1 Set-3 – MW71  $S_T = 1W$

4.7.3.1 MW71 x MW71 - 50 x 1W

Table 4-86 MW71 x MW71 - 50 x 1W

|      | RE1  | RE2  | RE3  | Yu   |
|------|------|------|------|------|
| Mean | 0.99 | 1.00 | 0.99 | 1.03 |
| COV  | 0.09 | 0.08 | 0.14 | 0.15 |
| STD  | 0.09 | 0.08 | 0.14 | 0.16 |
| R    | 0.99 | 0.98 | 0.95 | 0.96 |

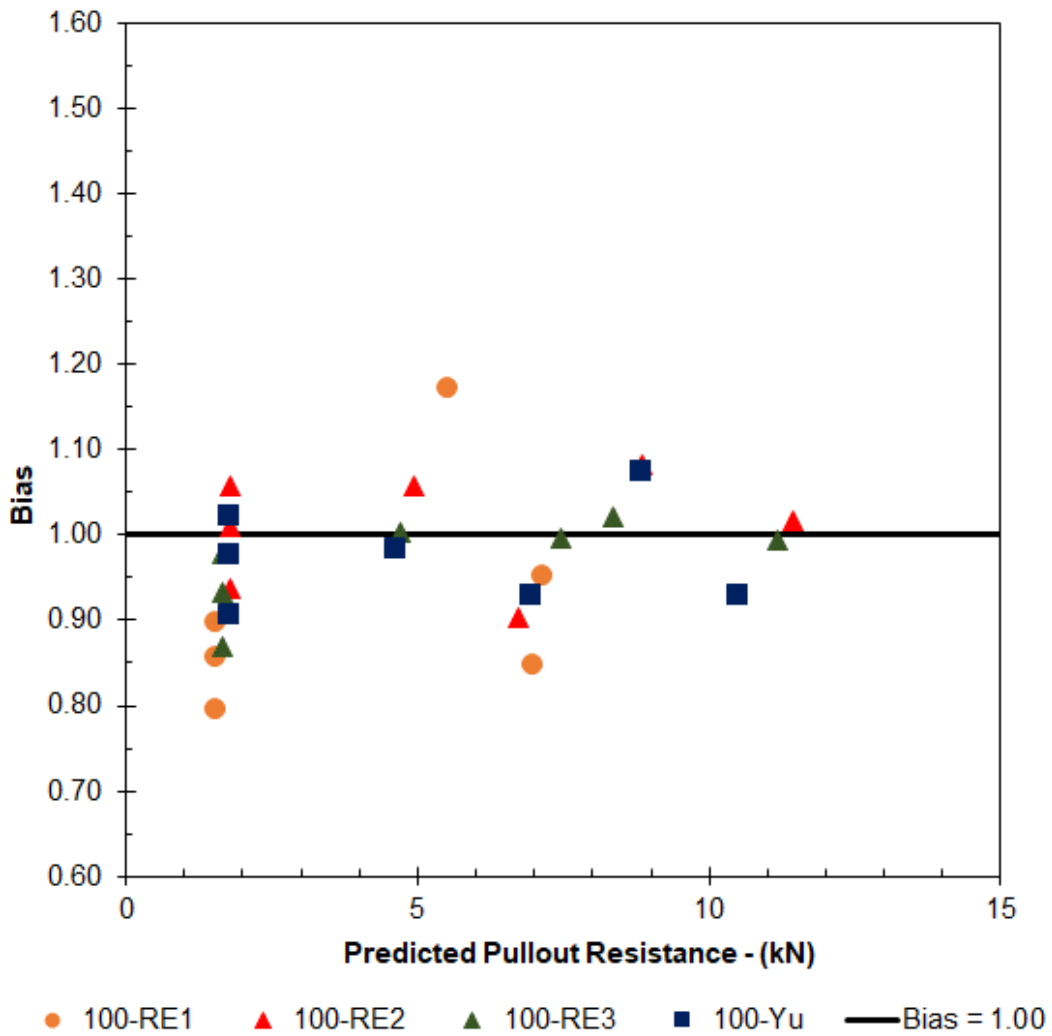


Figure 4-65 Bias (MW71 x MW71 - 50 x 1W)

4.7.3.2 MW71 x MW71 - 100 x 1W

Table 4-87 MW71 x MW71 - 100 x 1W

|      | RE1  | RE2  | RE3  | Yu   |
|------|------|------|------|------|
| Mean | 0.98 | 1.01 | 0.97 | 1.01 |
| COV  | 0.23 | 0.07 | 0.05 | 0.06 |
| STD  | 0.22 | 0.07 | 0.05 | 0.06 |
| R    | 0.86 | 0.99 | 1.00 | 0.99 |

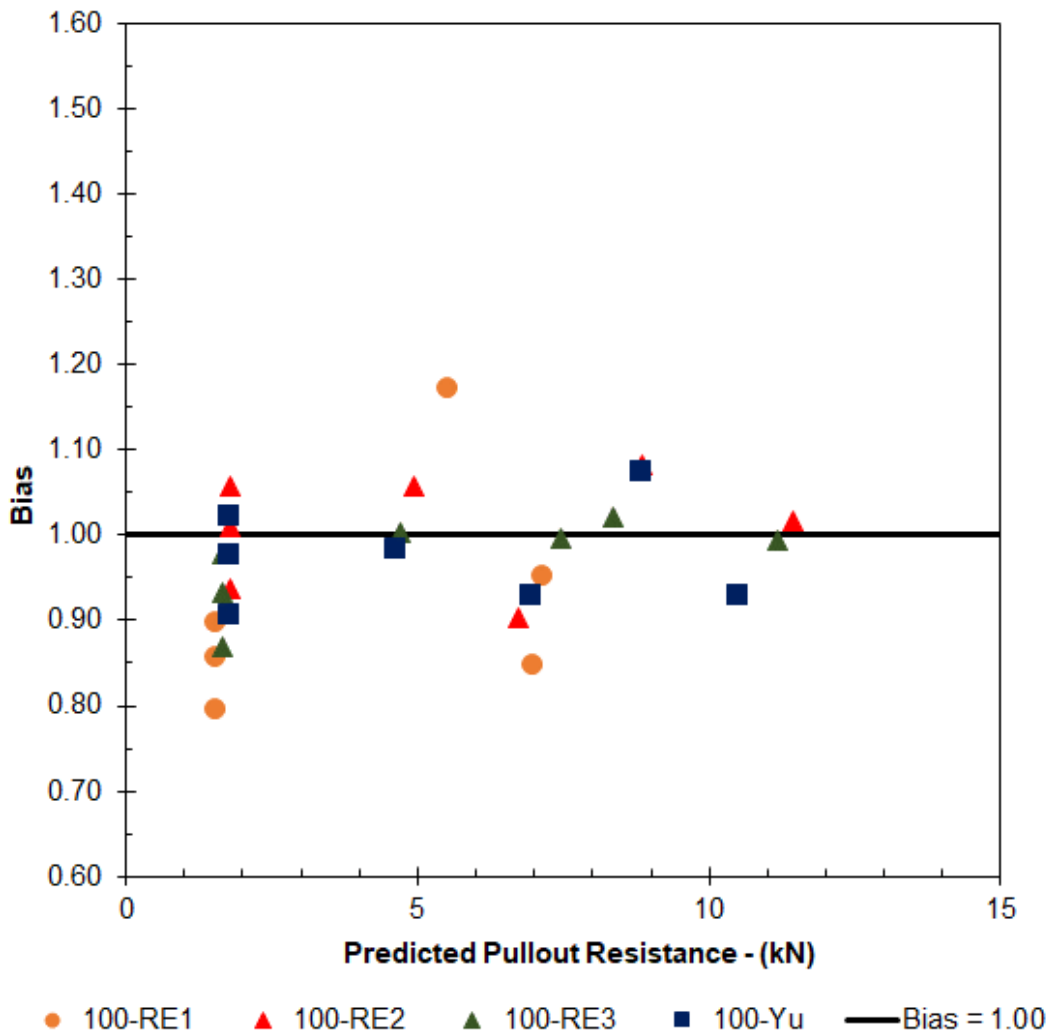


Figure 4-66 Bias (MW71 x MW71 - 100 x 1W)



4.7.3.3 MW71 x MW71 - 200 x 1W

Table 4-88 MW71 x MW71 - 200 x 1W

|      | RE1  | RE2  | RE3  | Yu   |
|------|------|------|------|------|
| Mean | 1.03 | 1.03 | 1.08 | 1.02 |
| COV  | 0.21 | 0.21 | 0.22 | 0.21 |
| STD  | 0.21 | 0.21 | 0.23 | 0.21 |
| R    | 0.99 | 1.00 | 1.00 | 0.99 |

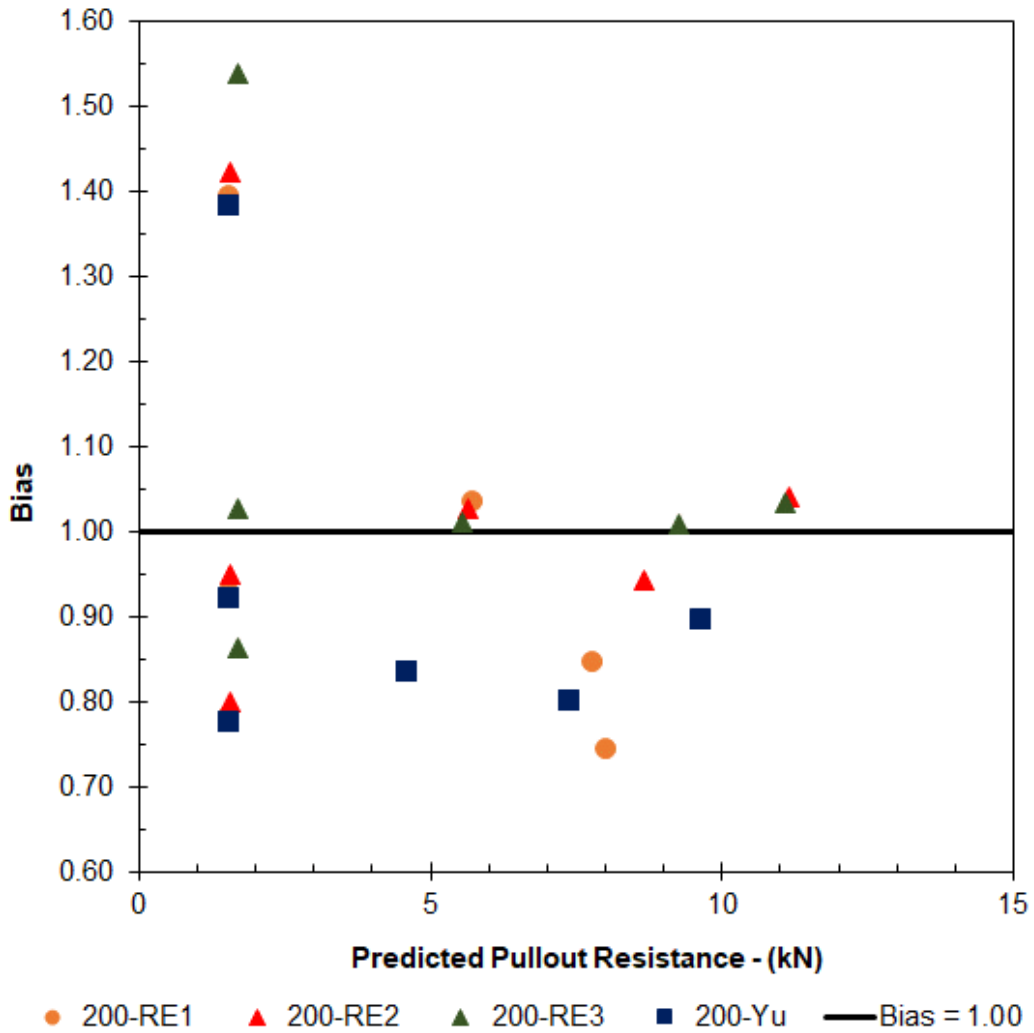


Figure 4-67 Bias (MW71 x MW71 - 200 x 1W)

4.7.4 Group-2 Set-1- MW45 ST = 300 mm

4.7.4.1 MW45 x MW45 - 50 x 300

Table 4-89 MW45 x MW45 - 50 x 300

|      | RE1  | RE2  | RE3  | Yu   |
|------|------|------|------|------|
| Mean | 0.94 | 1.01 | 0.91 | 1.02 |
| COV  | 0.28 | 0.08 | 0.12 | 0.07 |
| STD  | 0.27 | 0.08 | 0.11 | 0.07 |
| R    | 0.75 | 0.99 | 0.97 | 1.00 |

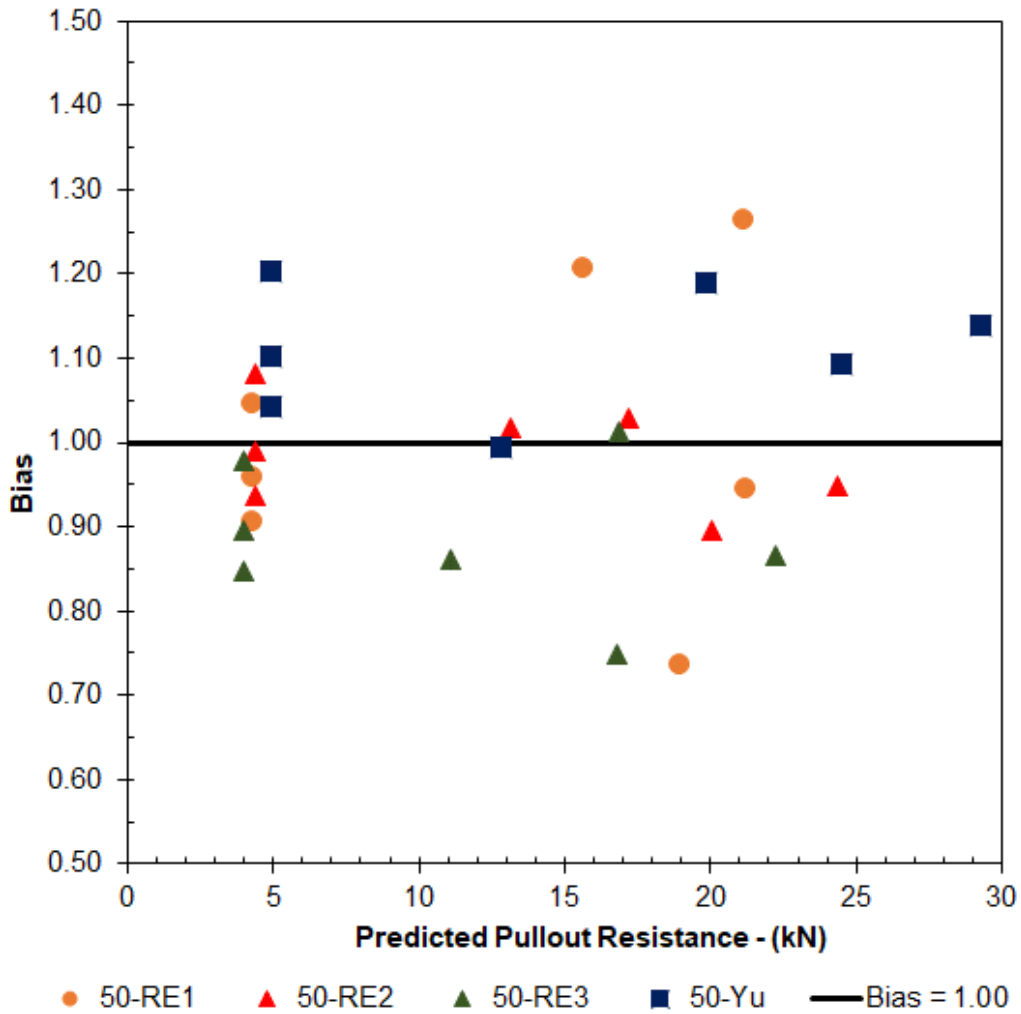


Figure 4-68 Bias (MW45 x MW45 - 50 x 300)

4.7.4.2 MW45 x MW45 - 100 x 300

Table 4-90 MW45 x MW45 - 100 x 300

|      | RE1  | RE2  | RE3  | Yu   |
|------|------|------|------|------|
| Mean | 1.00 | 1.00 | 0.93 | 1.01 |
| COV  | 0.14 | 0.07 | 0.08 | 0.07 |
| STD  | 0.14 | 0.07 | 0.08 | 0.07 |
| R    | 0.96 | 1.00 | 1.00 | 0.99 |

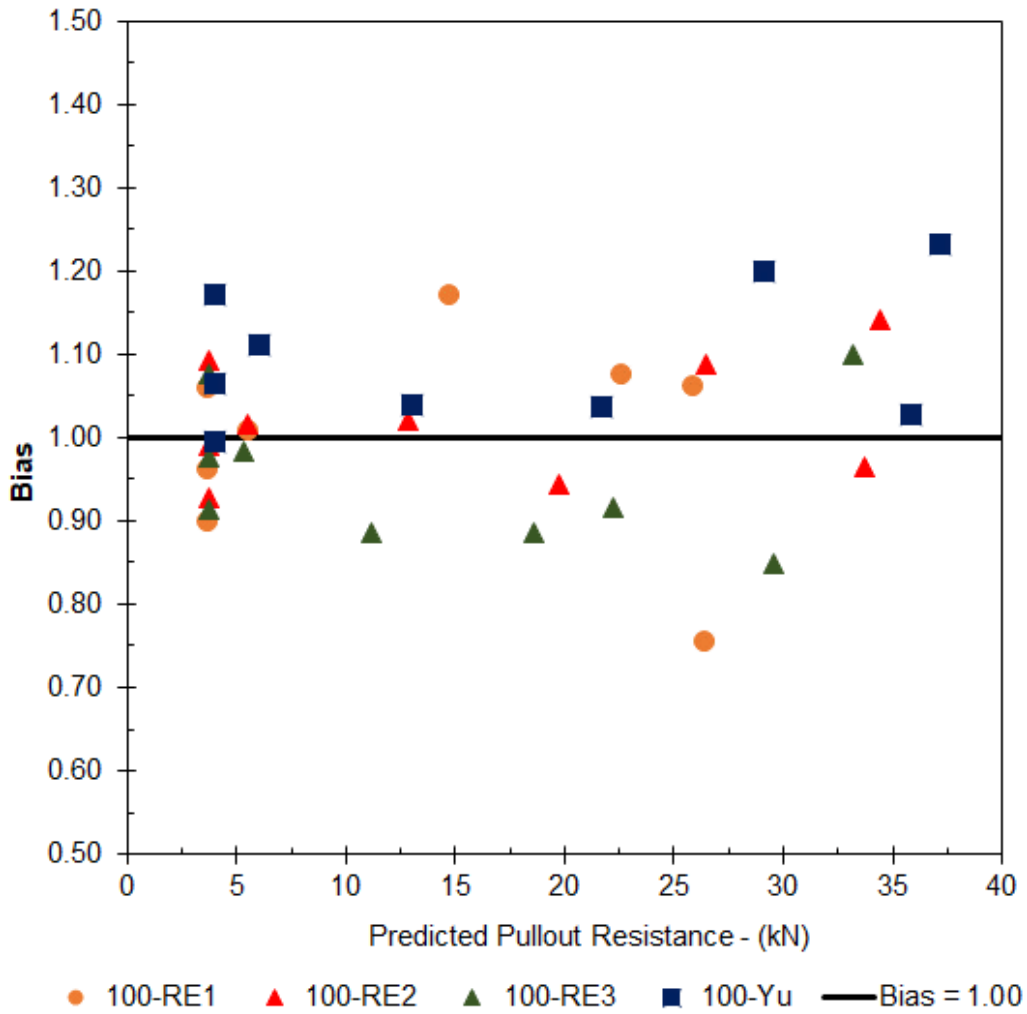


Figure 4-69 Bias (MW45 x MW45 - 100 x 300)

4.7.4.3 MW45 x MW45 - 200 x 300

Table 4-91 MW45 x MW45 - 200 x 300

|      | RE1  | RE2  | RE3  | Yu   |
|------|------|------|------|------|
| Mean | 0.91 | 0.92 | 0.88 | 0.92 |
| COV  | 0.29 | 0.29 | 0.29 | 0.29 |
| STD  | 0.27 | 0.26 | 0.25 | 0.27 |
| R    | 0.86 | 0.88 | 0.88 | 0.88 |

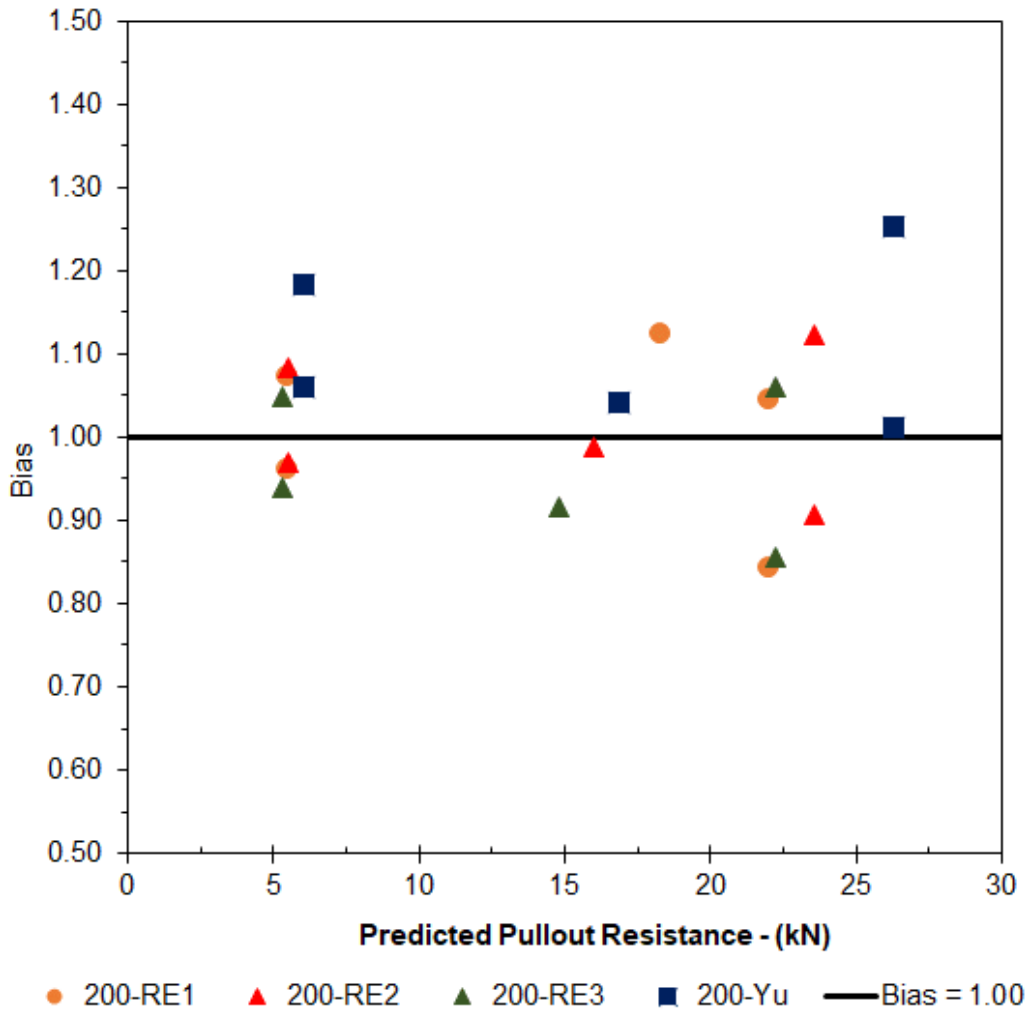


Figure 4-70 Bias (MW45 x MW45 - 200 x 300)

4.7.5 Group-2 Set-2 – MW45  $S_T = 150$  mm

4.7.5.1 MW45 x MW45 - 50 x 150

Table 4-92 MW45 x MW45 - 50 x 150

|      | RE1  | RE2  | RE3  | Yu   |
|------|------|------|------|------|
| Mean | 1.00 | 1.01 | 1.00 | 1.13 |
| COV  | 0.12 | 0.08 | 0.10 | 0.25 |
| STD  | 0.12 | 0.08 | 0.10 | 0.28 |
| R    | 0.98 | 1.00 | 1.00 | 1.00 |

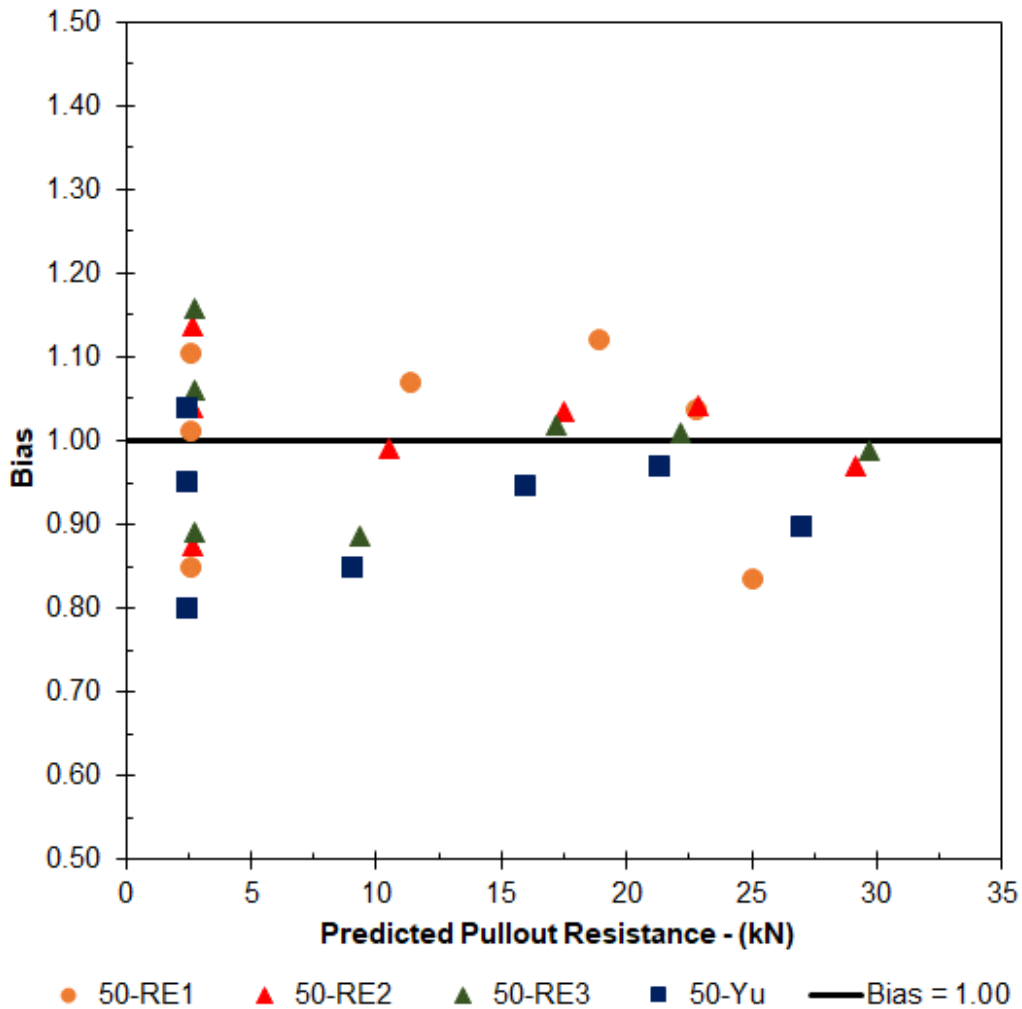


Figure 4-71 Bias (MW45 x MW45 - 50 x 150)

4.7.5.2 MW45 x MW45 - 100 x 150

Table 4-93 MW45 x MW45 - 100 x 150

|      | RE1  | RE2  | RE3  | Yu   |
|------|------|------|------|------|
| Mean | 0.99 | 0.99 | 0.88 | 0.98 |
| COV  | 0.15 | 0.15 | 0.15 | 0.13 |
| STD  | 0.15 | 0.14 | 0.13 | 0.13 |
| R    | 0.99 | 0.99 | 0.98 | 0.99 |

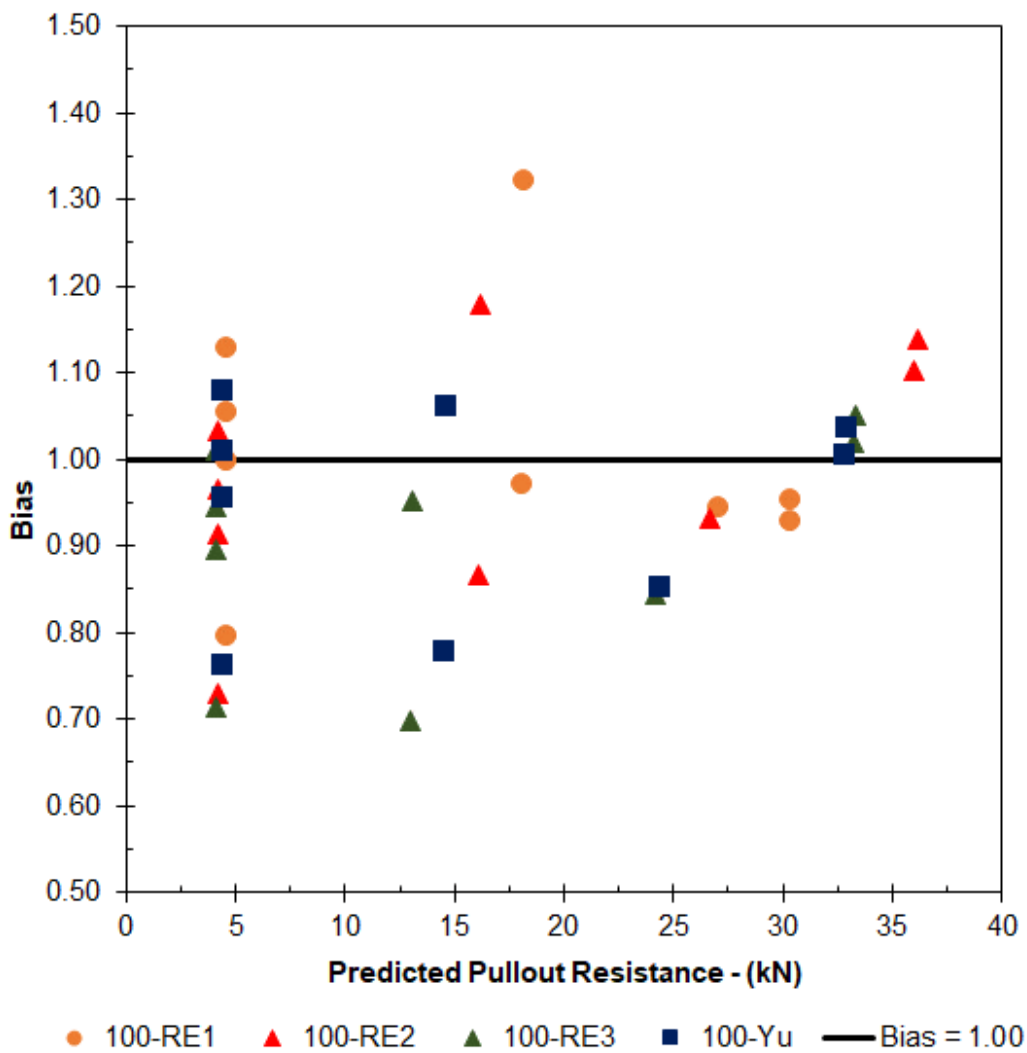


Figure 4-72 Bias (MW45 x MW45 - 100 x 150)

4.7.5.3 MW45 x MW45 - 200 x 150

Table 4-94 MW45 x MW45 - 200 x 150

|      | RE1  | RE2  | RE3  | Yu   |
|------|------|------|------|------|
| Mean | 1.00 | 1.00 | 0.87 | 1.01 |
| COV  | 0.80 | 0.04 | 0.09 | 0.07 |
| STD  | 0.80 | 0.04 | 0.08 | 0.07 |
| R    | 0.99 | 1.00 | 0.99 | 0.99 |

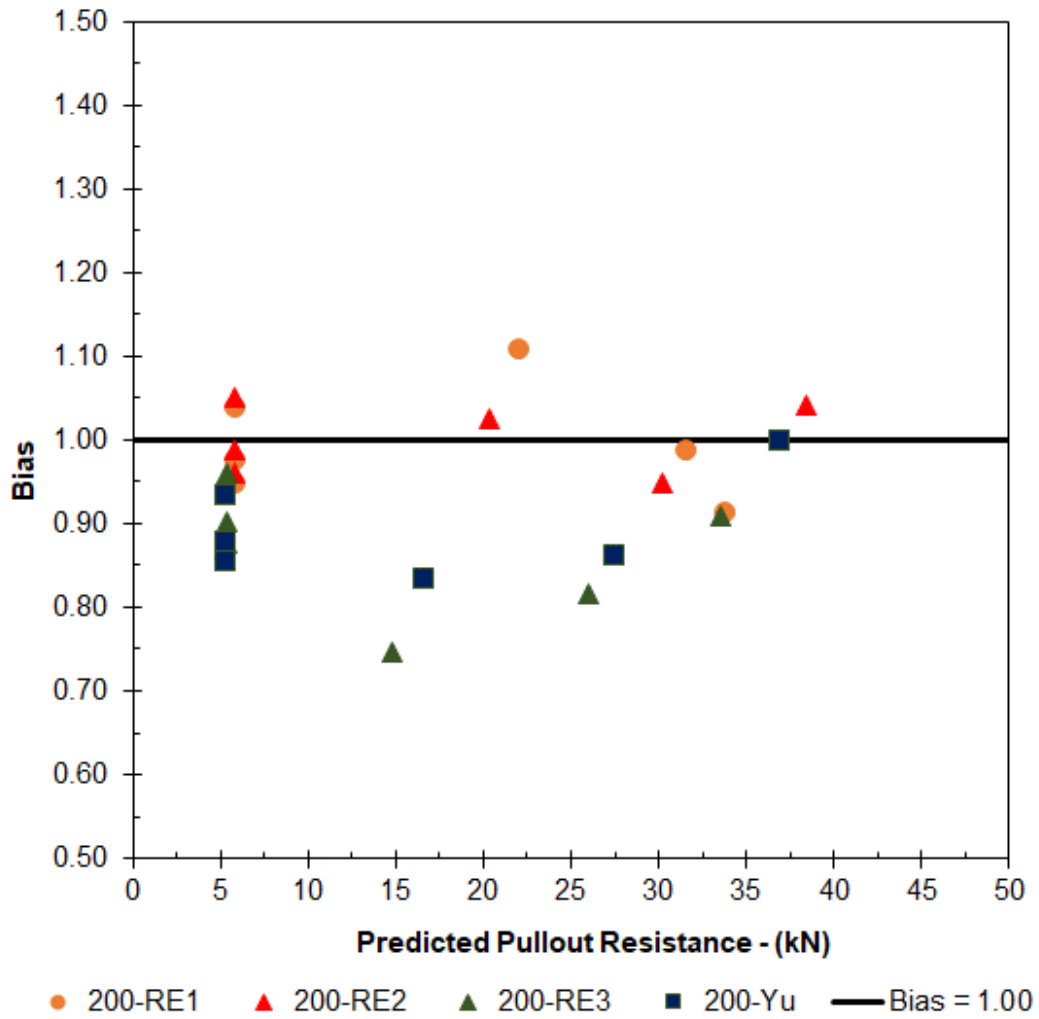


Figure 4-73 Bias (MW45 x MW45 - 200 x 150)

4.7.6 Group-2 Set-3 – MW45  $S_T = 1W$

4.7.6.1 MW45 x MW45 - 50 x 1W

Table 4-95 MW45 x MW45 - 50 x 1W

|      | RE1  | RE2                                   | RE3  | Yu   |
|------|------|---------------------------------------|------|------|
| Mean | 0.85 | 1.01                                  | 0.96 | 1.02 |
| COV  | 0.16 | 0.09                                  | 0.11 | 0.10 |
| STD  | 0.13 | 0.09 </td <td>0.11</td> <td>0.11</td> | 0.11 | 0.11 |
| R    | 0.95 | 0.98                                  | 0.97 | 0.98 |

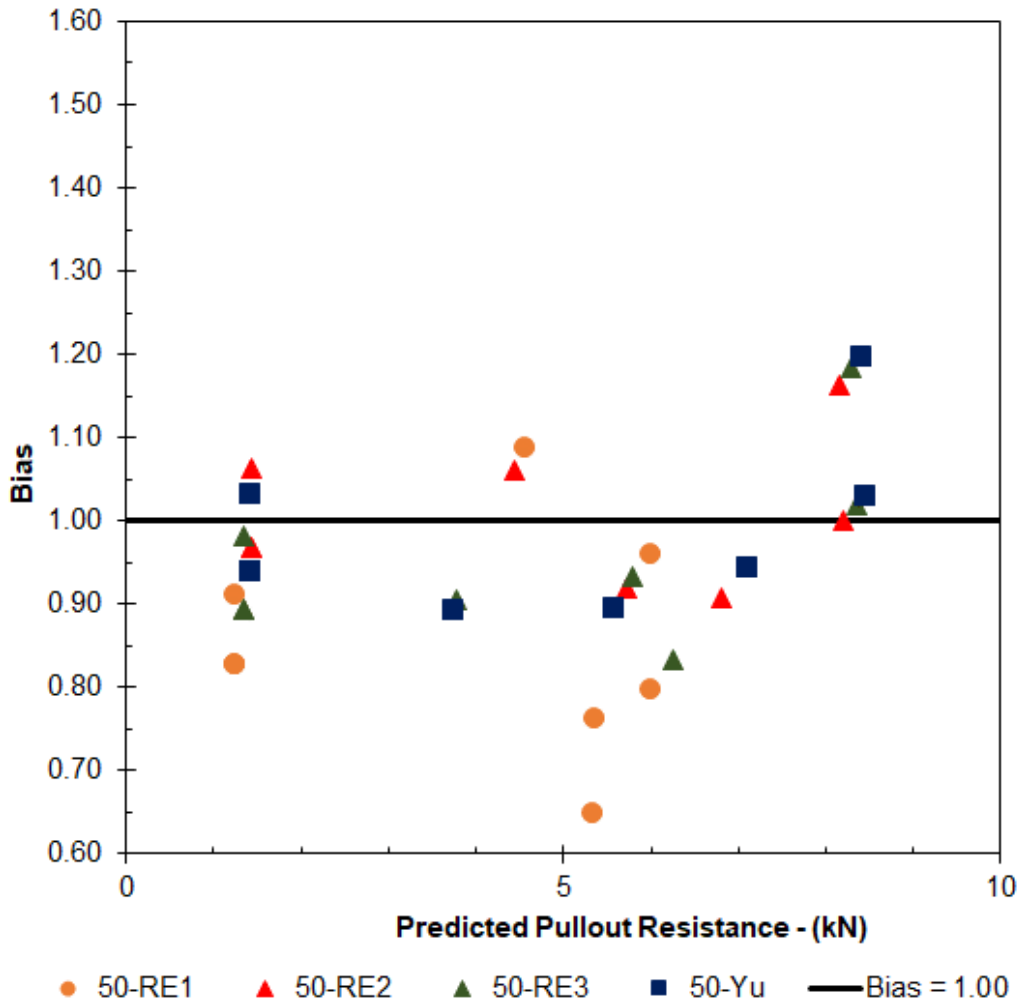


Figure 4-74 Bias (MW45 x MW45 - 50 x 1W)



4.7.6.2 MW45 x MW45 - 100 x 1W

Table 4-96 MW45 x MW45 - 100 x 1W

|      | RE1  | RE2  | RE3  | Yu   |
|------|------|------|------|------|
| Mean | 0.97 | 1.01 | 0.90 | 1.00 |
| COV  | 0.24 | 0.09 | 0.09 | 0.07 |
| STD  | 0.23 | 0.09 | 0.09 | 0.07 |
| R    | 0.87 | 0.99 | 0.99 | 1.00 |

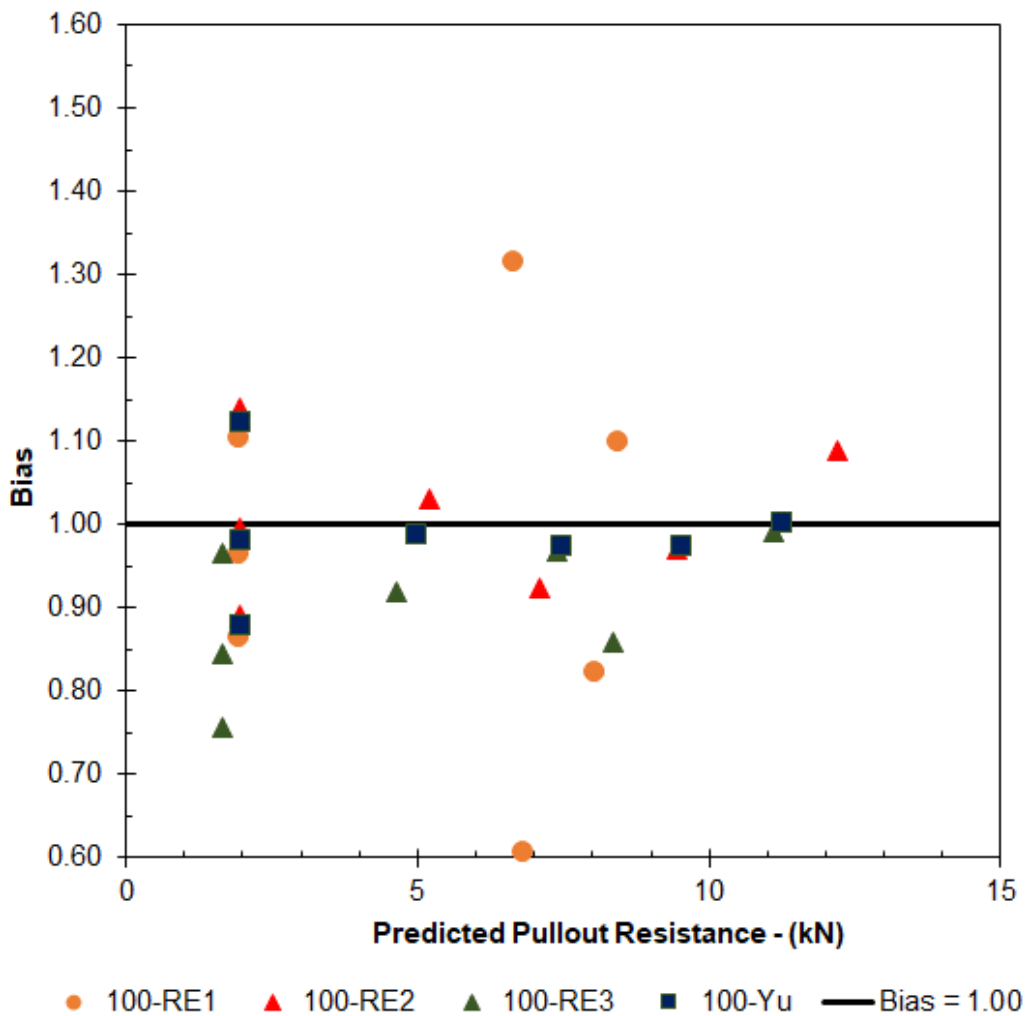


Figure 4-75 Bias (MW45 x MW45 - 100 x 1W)

4.7.6.3 MW45 x MW45 - 200 x 1W

Table 4-97 MW45 x MW45 - 200 x 1W

|      | RE1  | RE2  | RE3  | Yu   |
|------|------|------|------|------|
| Mean | 0.96 | 1.01 | 0.96 | 1.00 |
| COV  | 0.16 | 0.09 | 0.14 | 0.12 |
| STD  | 0.16 | 0.09 | 0.14 | 0.12 |
| R    | 0.93 | 1.00 | 0.99 | 0.99 |

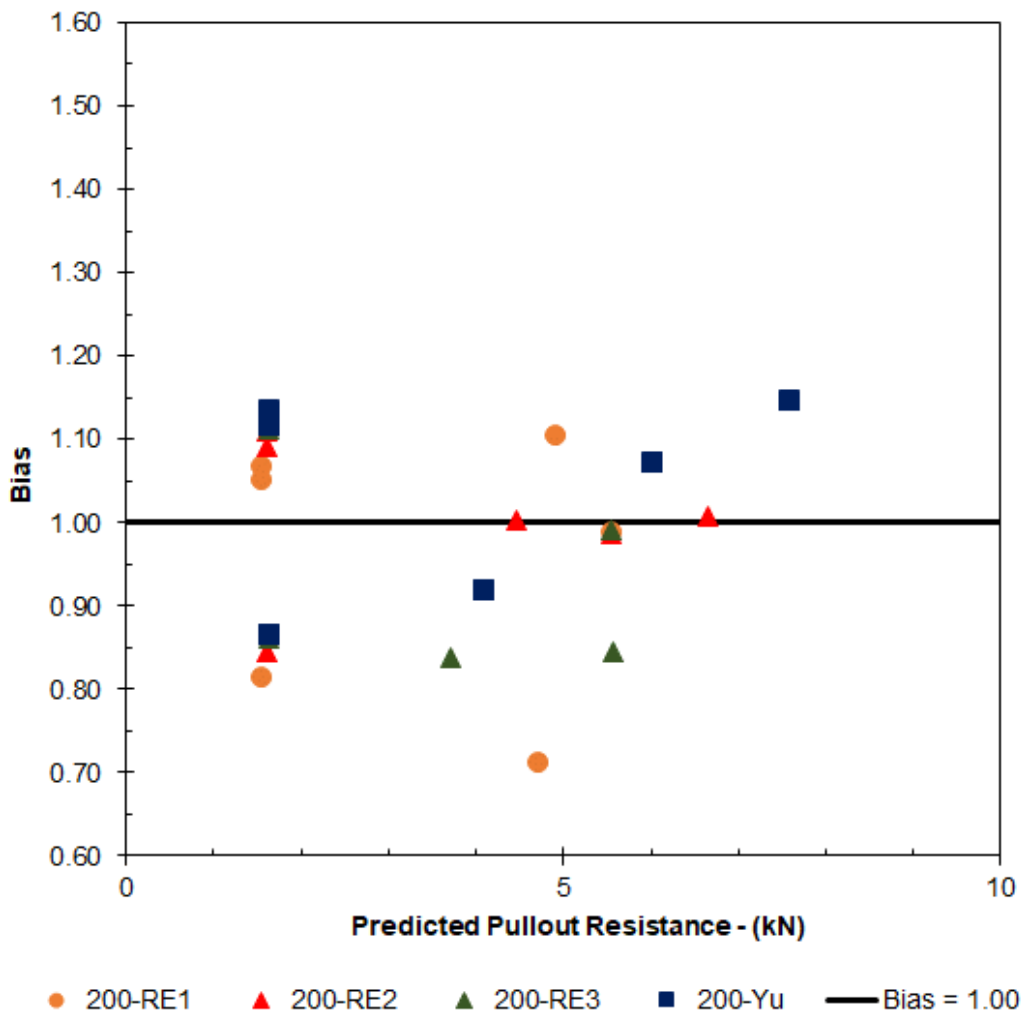


Figure 4-76 Bias (MW45 x MW45 - 200 x 1W)

#### 4.8 Equation Analysis for Predicting the Bearing Resistance Factor

Based on the statistical comparison between the four equations the RE2 equation is the best predictor of the pullout resistance of the 2-Wire element. This conclusion is based this pullout testing program and statistical correlations shown in Table 4-98 and Table 4-99.

Table 4-98 Statistical Values RE2 Equation (MW71)

|          | Mean | COV  | STD   | R    |
|----------|------|------|-------|------|
| Taylor 2 | 1.01 | 0.09 | 0.091 | 0.99 |

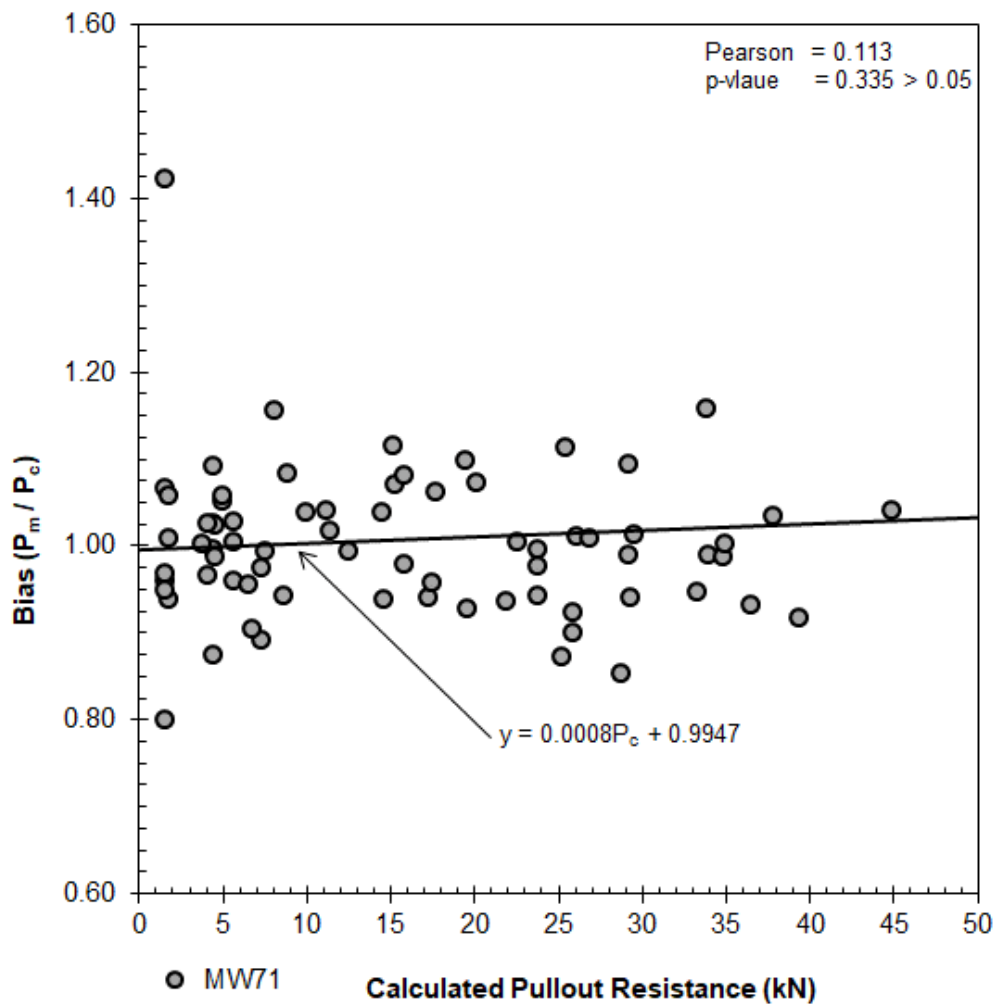


Figure 4-77 RE2 Equation MW71

Table 4-99 Statistical Values RE2 Equation (MW45)

|          | Mean | COV  | STD  | R    |
|----------|------|------|------|------|
| Taylor 2 | 0.99 | 0.12 | 0.12 | 0.99 |

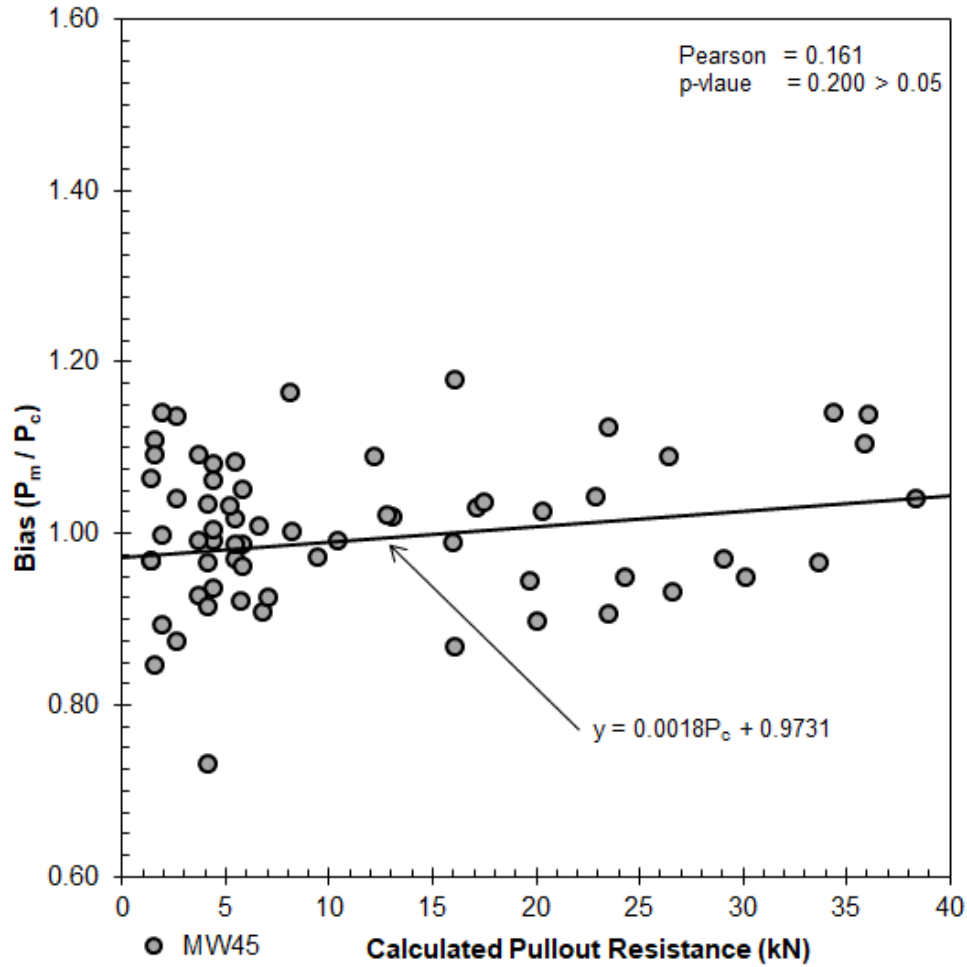


Figure 4-78 RE2 Equation MW45

#### 4.9 Spacing of Longitudinal and Transverse Elements

Based on the test results for a 2-Wire soil-reinforcing system, and the predict pullout resistance factor using equation RE2, the magnitude of the pullout resistance is influenced by, and is a function of, the spacing of the longitudinal and transverse

element. To demonstrate this, a normalized plot showing the pullout capacity for the 2-Wire system consisting of longitudinal and transverse elements sizes equal to MW71 and longitudinal spacings equal to 50 mm, 100 mm and 200 mm, and for transverse spacings equal to 300 and 150 mm, will be used. The data plot has been calculated using research equation RE2.

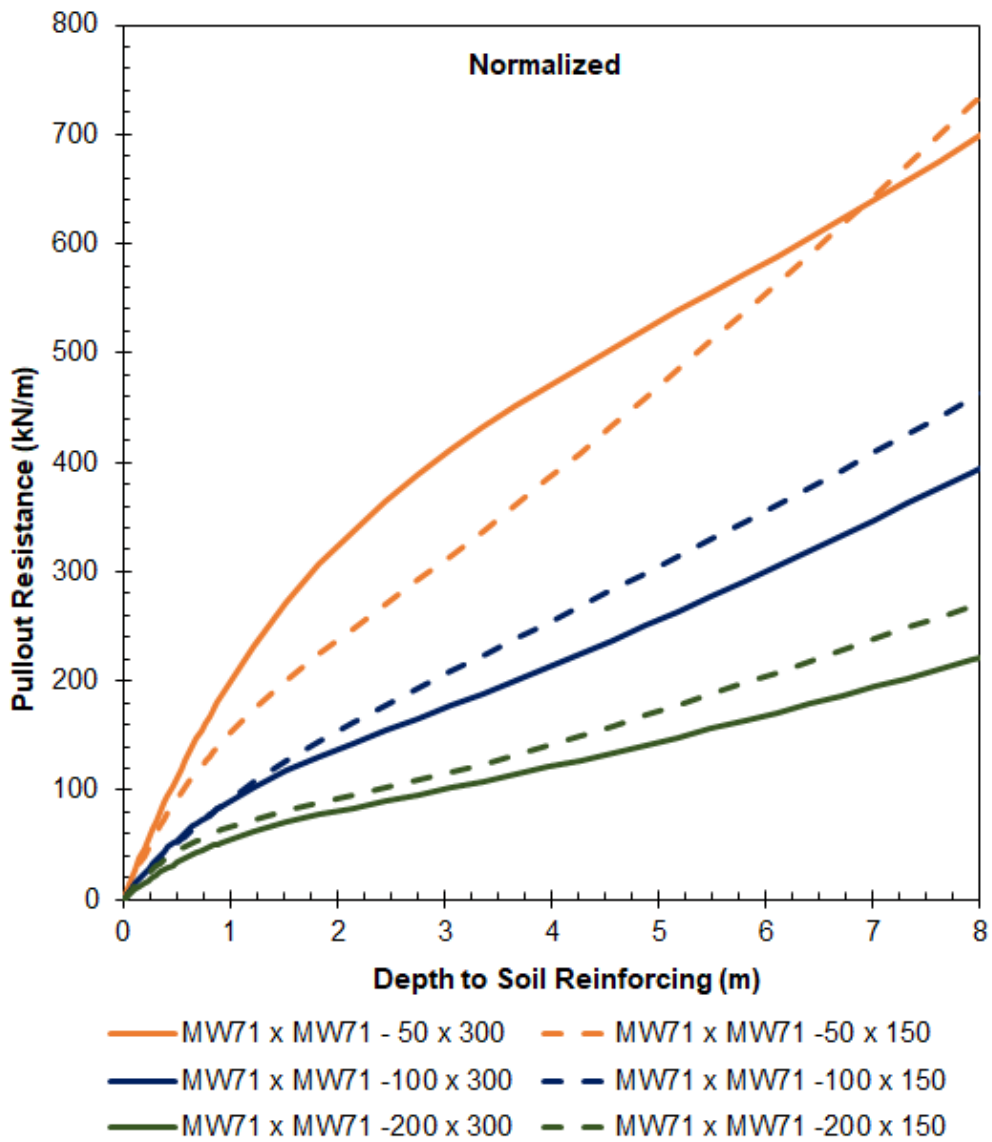


Figure 4-79 Pullout Resistance Based on Spacing of Transverse Element (RE2)

To use this graph, multiple the value from the graph by the width of the soil-reinforcing element. This will give a value in force per meter length of soil-reinforcing. Then multiple this value by the length of soil-reinforcing in the passive zone to get the pullout resistance of the element. As an example, the 2-Wire 50 mm x 300 mm will be used and compared to the results given in Table 4-29 from Section 4.6.1.2.

For a soil-reinforcing element located at a depth equal to 4.0 m, the pullout resistance is approximately equal to 475 kN/m. If this is multiplied by the spacing of the longitudinal wires equal to 0.050 meters, the pullout resistance is equal to 23.75 kN. The pullout tests were performed with a soil-reinforcing element equal to 1.222 m. At this length, the pullout resistance is equal to 23.75 kN multiplied by 1.222 m, or 29.02 kN. From Table 4-29, test numbers 11 and 12, in the  $P_{calc}$  column gives a calculated value equal to 29.22 kN which is nearly equal to the value calculated in this example. This shows that by normalizing the pullout resistance of the soil-reinforcing systems, that Figure 4-79 can be used to directly compare the systems.

As is shown in the normalized pullout resistance of Figure 4-79, each of the six systems have unique data sets and, therefore, unique pullout resistance. In some regions of the graph, the transverse element spacings equal to 300 mm have greater pullout resistance than the transverse element spacings equal to 150 mm. Furthermore, the pullout resistance for the system with the 50 mm longitudinal spacings has a normalized pullout resistance that is greater than the system with the 100 mm longitudinal spacings, and the pullout resistance for the system with the 100 mm longitudinal spacings has a normalized pullout resistance that is greater than the system with the 200 mm longitudinal spacings. It is still the case that the bearing area for the transverse element spacings equal to 150 mm has two times the bearing area as the

transverse element spacings equal to 300 mm. In addition, the 200 mm system has 2 times the bearing area for the same transverse element spacing when compared to the 100 mm spacing, and 4 times the bearing area for the same transverse element spacing when compared to the 50 mm spacing. It therefore can be concluded that the element spacing affects the resistance to pullout.

As discussed in Section 2.2.4, many of the equations that have been developed, and that are used to predict the pullout resistance of inextensible grid soil-reinforcing, are a function of the bearing area of the system. The bearing area of the system is a function of the number, length, and diameter of the transverse element. In the bearing area equations, the larger the bearing area, the greater the resistance to pullout is (Peterson et al., 1978, Bishop et al, 1979, Christopher, 1993, Bergado et al., 1993, NHI, 2009, AASHTO 2014). Figure 4-80 is the plot of the six systems shown in Figure 4-79 using the state-of-practice Simplified methodology that is presented in AASHTO (2017) and discussed in Section 2.1.3.4.4. As can be seen in Figure 4-80, for the same six systems, there are only two data lines that are noticeable. The other four data lines are there, they are just equal to the data line that is shown that has the same transverse spacing, i.e. bearing area. To expand on this, the data lines shown are defined by the transverse element spacing, i.e. one data set is for the transverse element spacings equal to 300 mm (continuous line) and one data set is for the transverse element spacings equal to 150 mm (dashed line). It is obvious that the data lines in Figure 4-80 have the same shape. It can also be surmised by looking at Figure 4-80 that the transverse element spacings equal to 150 mm have two times more resistance to pullout than the transverse element spacings that are equal to 300 mm.

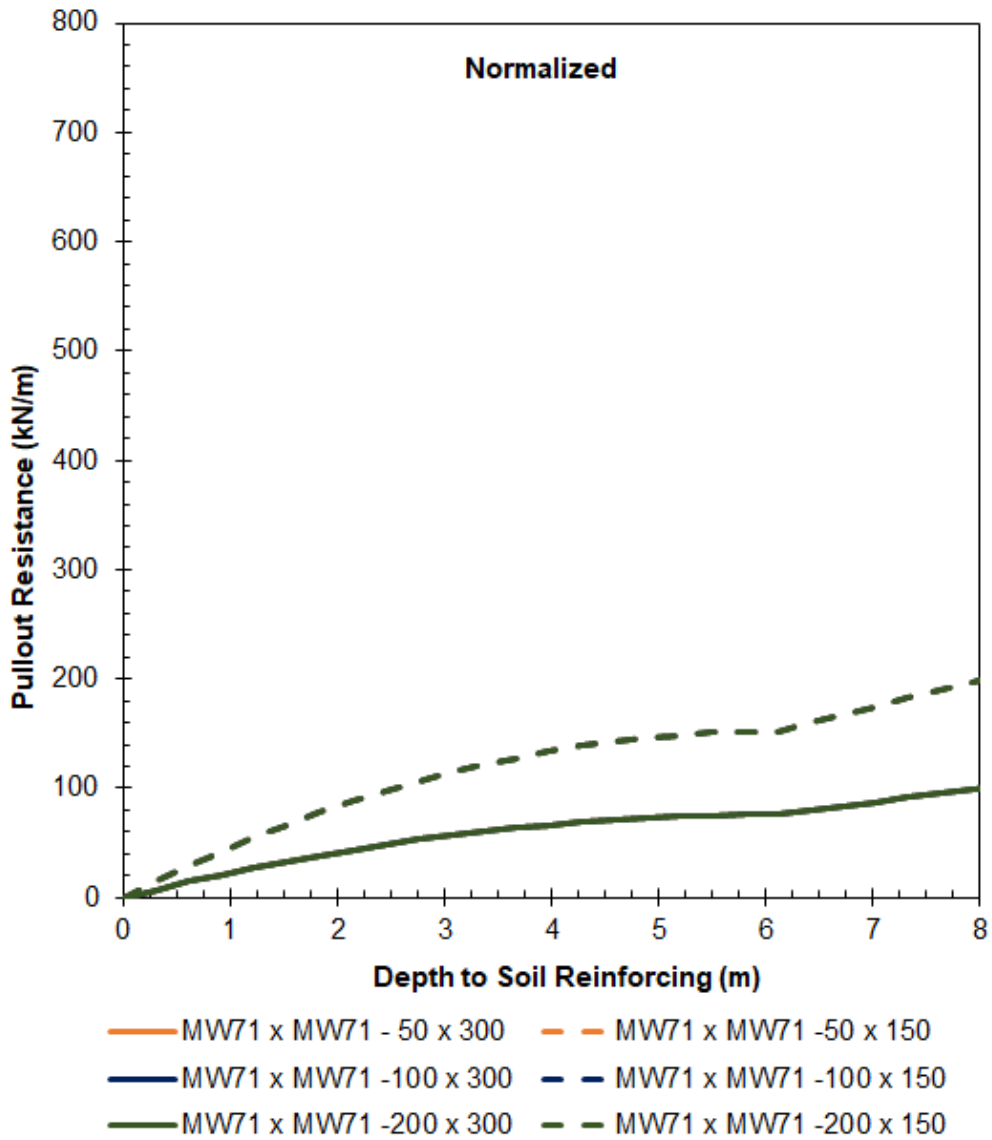


Figure 4-80 Pullout Resistance Based on Spacing of Transverse Element (AASHTO)

It is not apparent in Figure 4-79 that the shapes of the data lines are similar. The system with the 50 mm longitudinal spacing shows the two transverse spacings, i.e., 150 mm and 300 mm, having data lines intersecting at a depth nearly equal to 6.75 m. If Figure 4-79 is scaled up, the same phenomenon occurs with the 100 mm longitudinal spaced systems. That is, the two transverse spacings, i.e., 150 mm and 300 mm, have



data lines intersect as well. The shapes of the lines are the same, however, the scale of the lines is decreasing as the spacings increase.

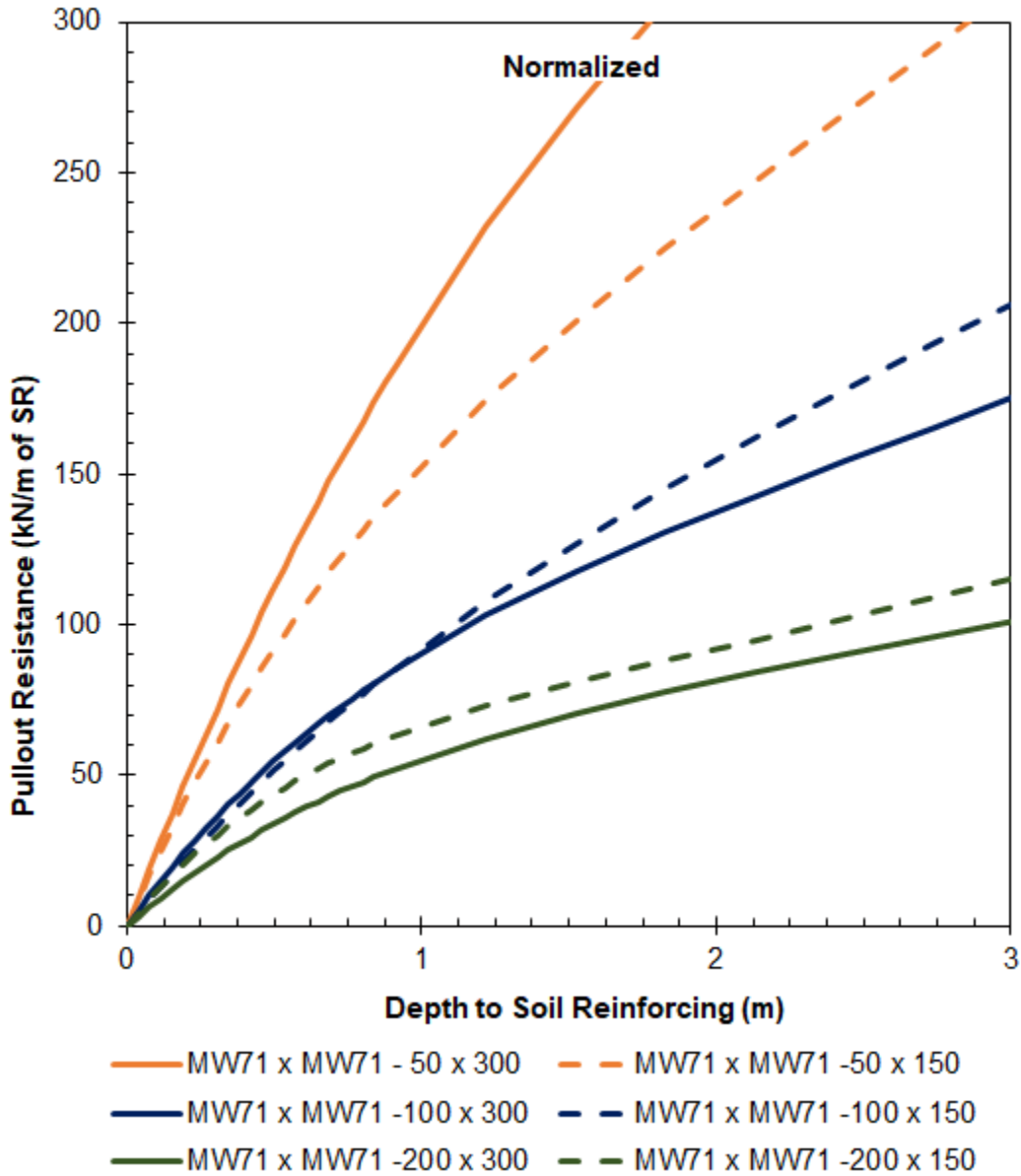


Figure 4-81 Pullout Resistance Based on Spacing of Transverse Element (RE2)

A regression analysis was performed on the normalized RE2 data to try and determine a mathematical a relationship that could justify the use of one equation that

would relate the systems by spacing. However, at this time, there was not a statistical relationship determined. This may be due to the number of data points. Although a mathematical relationship was not determined in this experimental program, there is clear indication that the pullout resistance is a function of the system configuration and is not based on the bearing area of the system.

#### 4.10 Bending of Transverse Element and Bearing Resistance

The bending of the transverse element also affects the bearing resistance of the 2-Wire soil-reinforcing element. Bending was measured with the three potentiometers that were attached to each of the weld junctions and at the mid-point of the transverse element. The magnitude of the bending was based on the difference of the average measured displacement of the two potentiometers located at each weld, and the measured displacement of the potentiometers at the mid-point.

The systems with a longitudinal spacing equal to 50 mm had transverse element bending that was less than 2.0 mm for all tested overburden pressures. During the tests, for both of the 50 mm spaced systems, i.e., MW71 and MW45, there was not any failure of the welds that join the transverse element to the longitudinal element. The 50 mm system is shown in Figure 4-82. The systems with longitudinal spacing equal to 100 mm had bending that was less than 1.0 mm for tested overburden pressures less than 30 kPa. The bending increased to 2.0 mm for tested overburden pressures less than 30 and 120 kPa. At the high overburden pressures greater than 90 kPa there was weld failure on some of the elements tested. This is shown in Figure 4-83. For the systems with longitudinal spacings equal to 200 mm, at a low overburden pressure equal to 6 kPa, the bending was less than 1 mm. At overburden pressures between 6 kPa and 30 kPa the

bending was less than 3 mm. At tested overburden pressures above 30 kPa there was noticeable bending of the transverse element. In addition, several of the test elements experienced failure at the junction of the welds. This is shown in Figure 4-84.

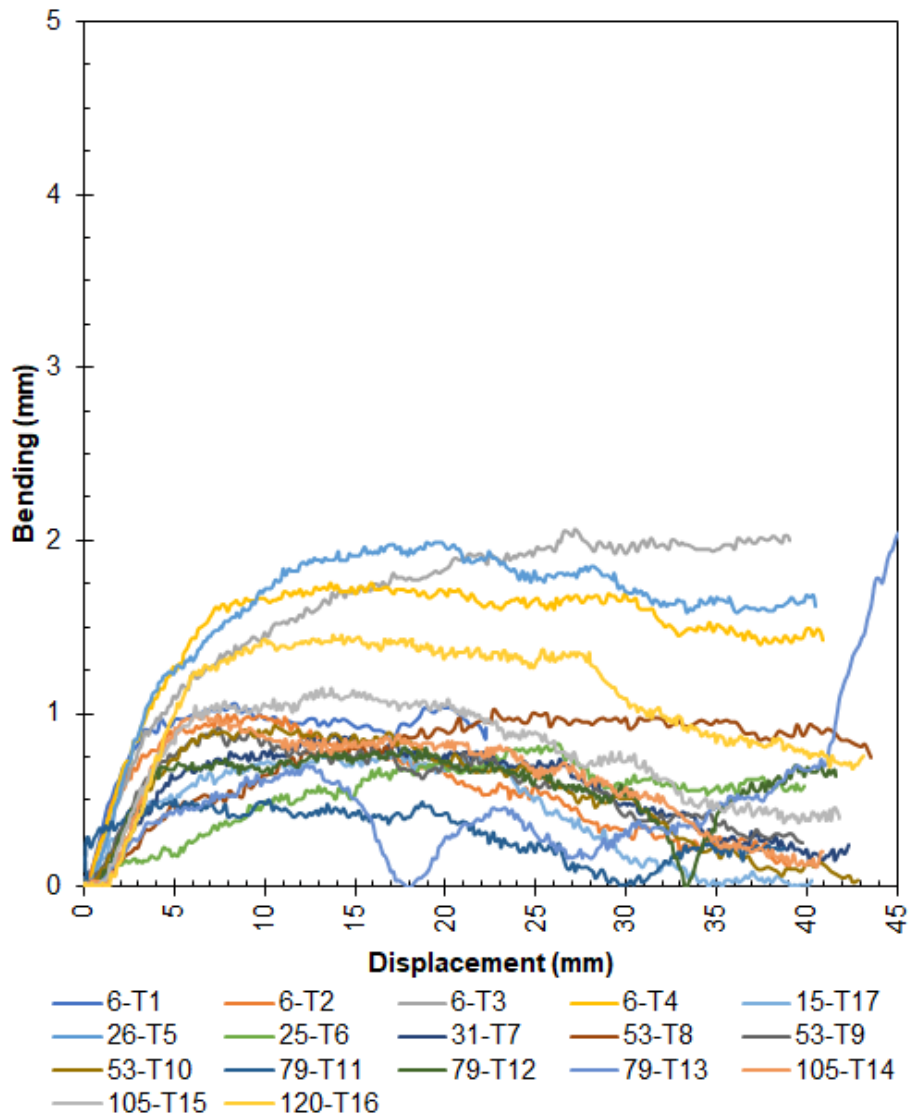


Figure 4-82 Transverse Bar Bending (MW71 x MW71 - 50 x 300)

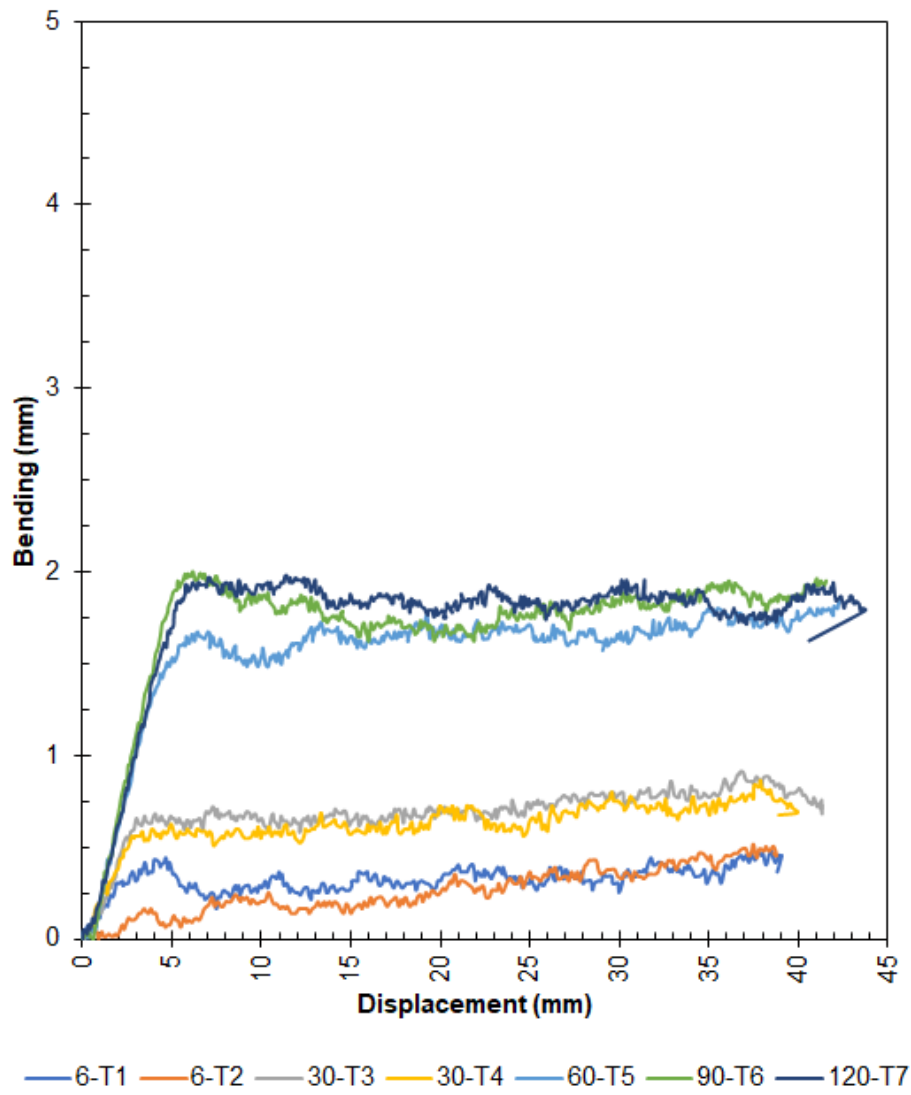


Figure 4-83 Transverse Bar Bending (MW71 x MW71 - 100 x 300)

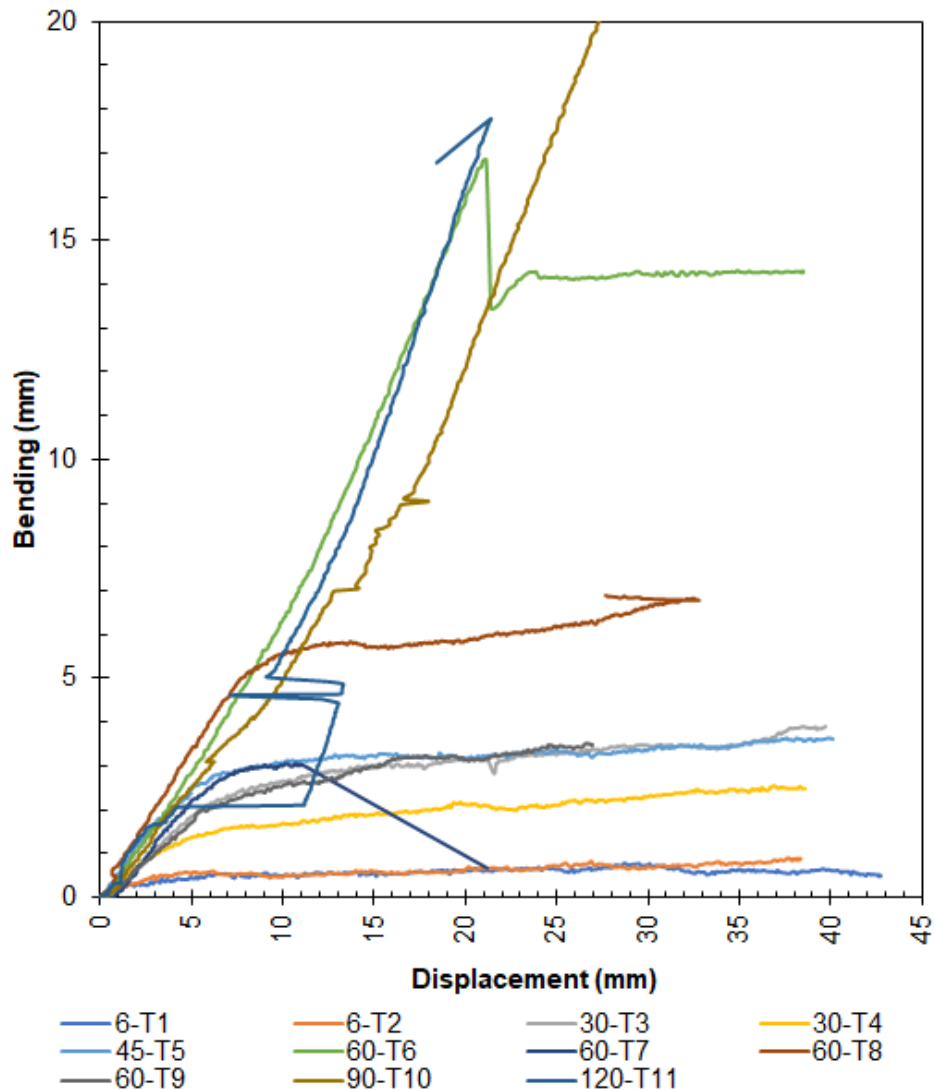


Figure 4-84 Transverse Bar Bending (MW71 x MW71 - 200 x 300)

\*The welds failed in test T6, T8, T10 and T11.

\*T6 was a failure of the connection point on the element and was not a weld failure.

In Figure 4-84 the test identified as T6, T8, T10 and T11 had weld failure. This can be seen on Figure 4-84. Typically, the bending is uniform as is shown on Figure 4-82, Figure 4-83 and portions of Figure 4-84. When weld failure occurs, there is a large spike in the data line, followed by a continuous increase in the data line.

Bending of the transverse element for grid soil-reinforcing systems has been documented in the literature as described in Section 2.2.4.5. Photograph 4-3 shows permanent deformation of the transverse element for the MW71 x MW71 - 200 x 300, 60-T8 test. As was described above, the system with longitudinal spacings equal to 100 mm (4 in.) and 200 mm (8 in.) experience bending at high overburden pressures and in some cases the system experienced weld failure as well, especially for the MW45 system. At high confinement, the systems longitudinal wires easily pull through the soil while the transverse element resists displacement.



Photograph 4-3 Transverse Bar Bending in MW71 x MW71 – 200 x 300



Photograph 4-4 Weld Failure MW71 x MW71 – 100 x 300

The failure of the welds occurs because of the moment that is being generated at the junction of the weld during bending. The 2-Wire element is fabricated in accordance with ASTM A1064. In the A1064 specification, it is a requirement that the weld shear capacity be greater than 240 MPa times the nominal area of the larger wire. In other words, if a shear force is applied to the wire on each side of the weld it must be able to withstand 50% of the tensile capacity of the wire. A weld shear testing apparatus and actual test is shown in Photograph 4-5.



Photograph 4-5 Weld Shear for Welded Wire Mesh

It can be seen in Photograph 4-5 that the method used to test the weld applies a shear force only, and there is no moment applied to the weld. As such, there is not a requirement for the moment capacity of the weld in the A1064 specification.

To investigate the bending mechanism in the transverse element a Plaxis-3D model was created. The model was developed for overburden pressure equal to 6 kPa, 30 kPa and 60 kPa, i.e., depth of soil equal to 0.305 m, 1.524 m, and 3.058 m. The MW71 x MW71 - 50 mm, 100 mm, and 200 mm, one -wire systems were modeled. A plan view of the model for the MW71 x MW71 – 200 mm x 1-Wire system is shown in Figure 4-85. The appendix has the material parameters used in the Plaxis 3D model.



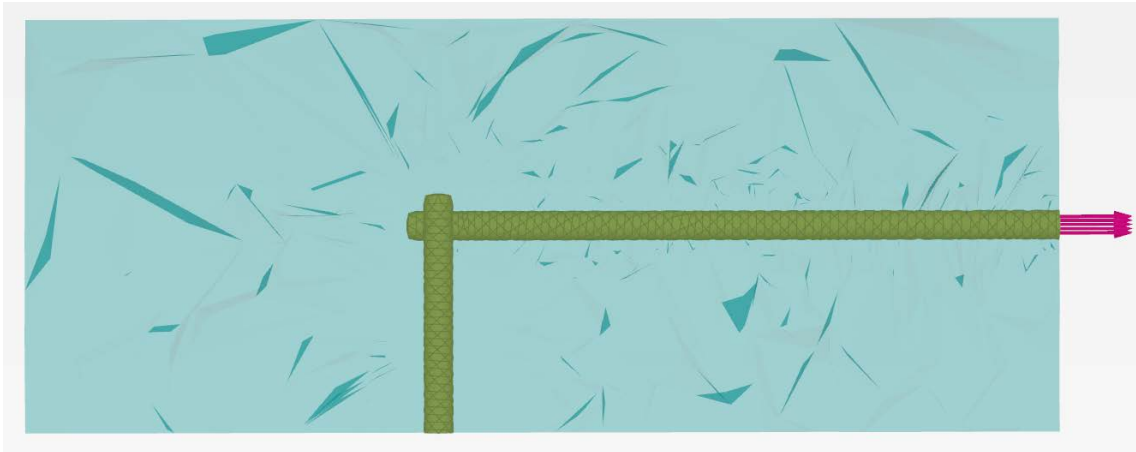


Figure 4-85 Plaxis 3D Model for MW71 x MW71 – 200 mm x 1-Wire

The moment diagram from the model, after 19 mm of longitudinal displacement is shown in Figure 4-86. The moment diagram shows that a moment does occur at the weld.

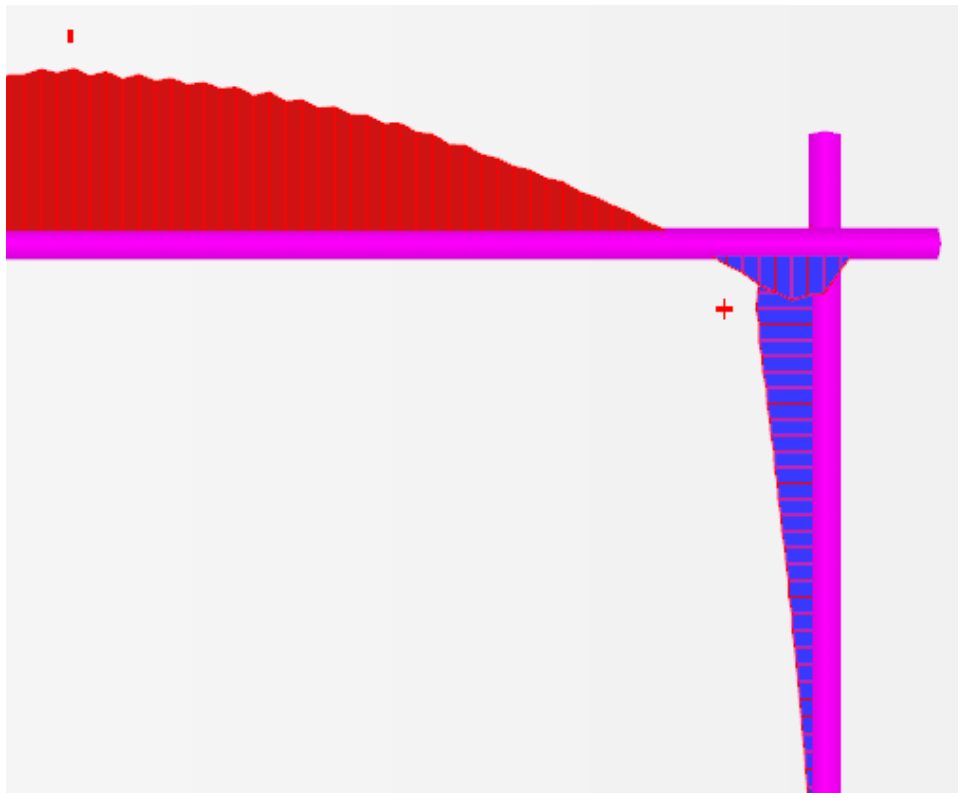


Figure 4-86 Moment Diagram for Transverse Bar Bending

Based on the results of the experimental test program and the data collected from the potentiometers the number of transverse elements does not influence the magnitude of the bending. For instance, the addition of more transverse element does not mean the system will experience less bending. It appears to be a function of the ability of the longitudinal element to freely displace in the soil. Figure 4-87 shows the difference of the mid-point transverse element displacement when compared to the average displacement of the transverse element located at the two weld junctions for the MW71 x MW71 – 50 mm x 150 mm system. This shows that bending is occurring in the transverse element. When the data in this graph is compared to the data in the Figure 4-82 graph, it shows a similar bending pattern. Figure 4-88 is the data bending graph for the MW71 x MW71 – 100 mm x 150 mm system. When the data in this graph is compared to the data in the Figure 4-83 graph, it shows a similar bending pattern. Figure 4-89 is the data bending graph for the MW71 x MW71 – 200 mm x 150 mm system. When the data in this graph is compared to the data in the Figure 4-84 graph, it shows a similar bending pattern.

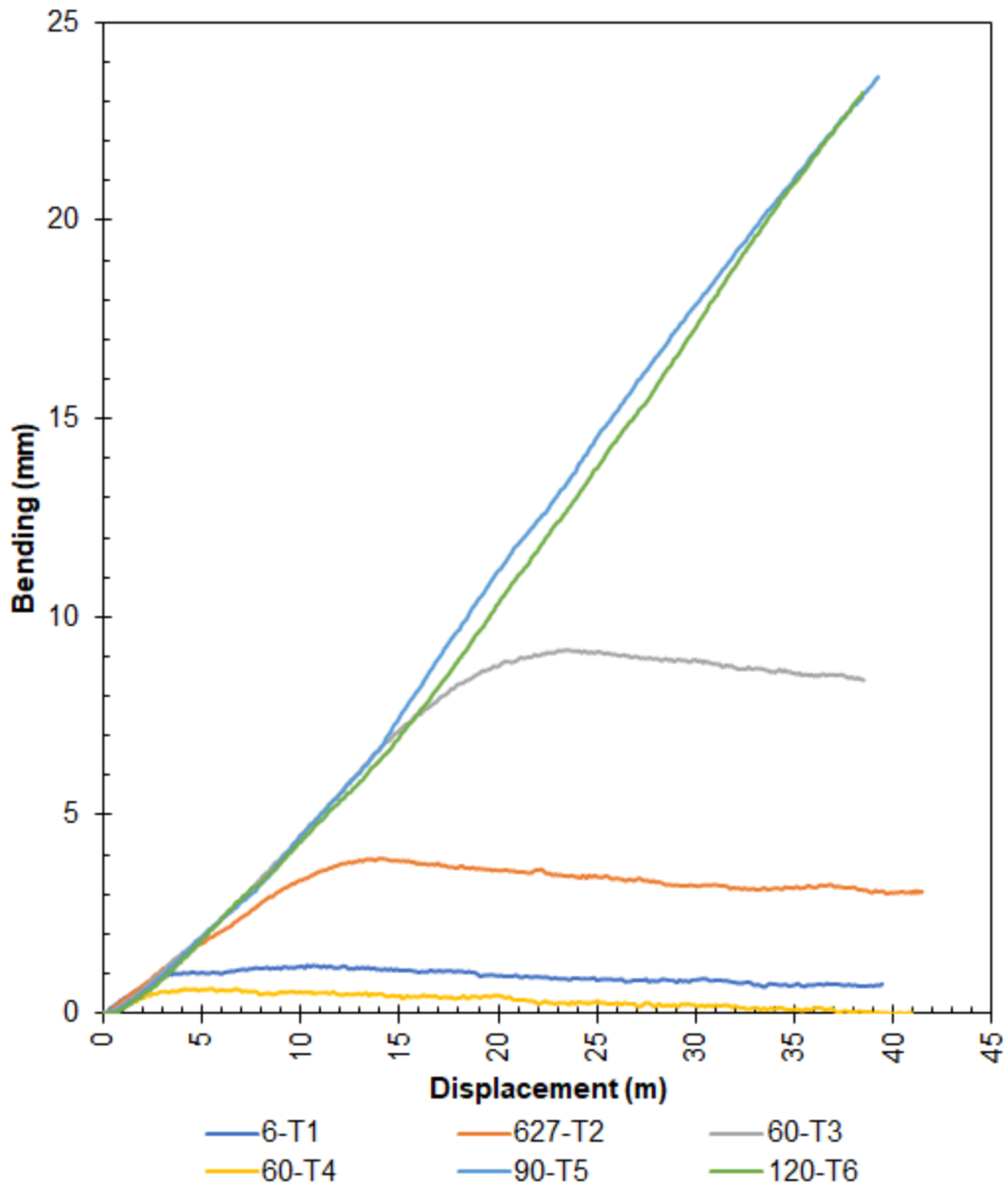


Figure 4-87 Transverse Bar Bending (MW71 x MW71 - 50 x 150)

Test T5 and T6 had a malfunction of the middle potentiometer

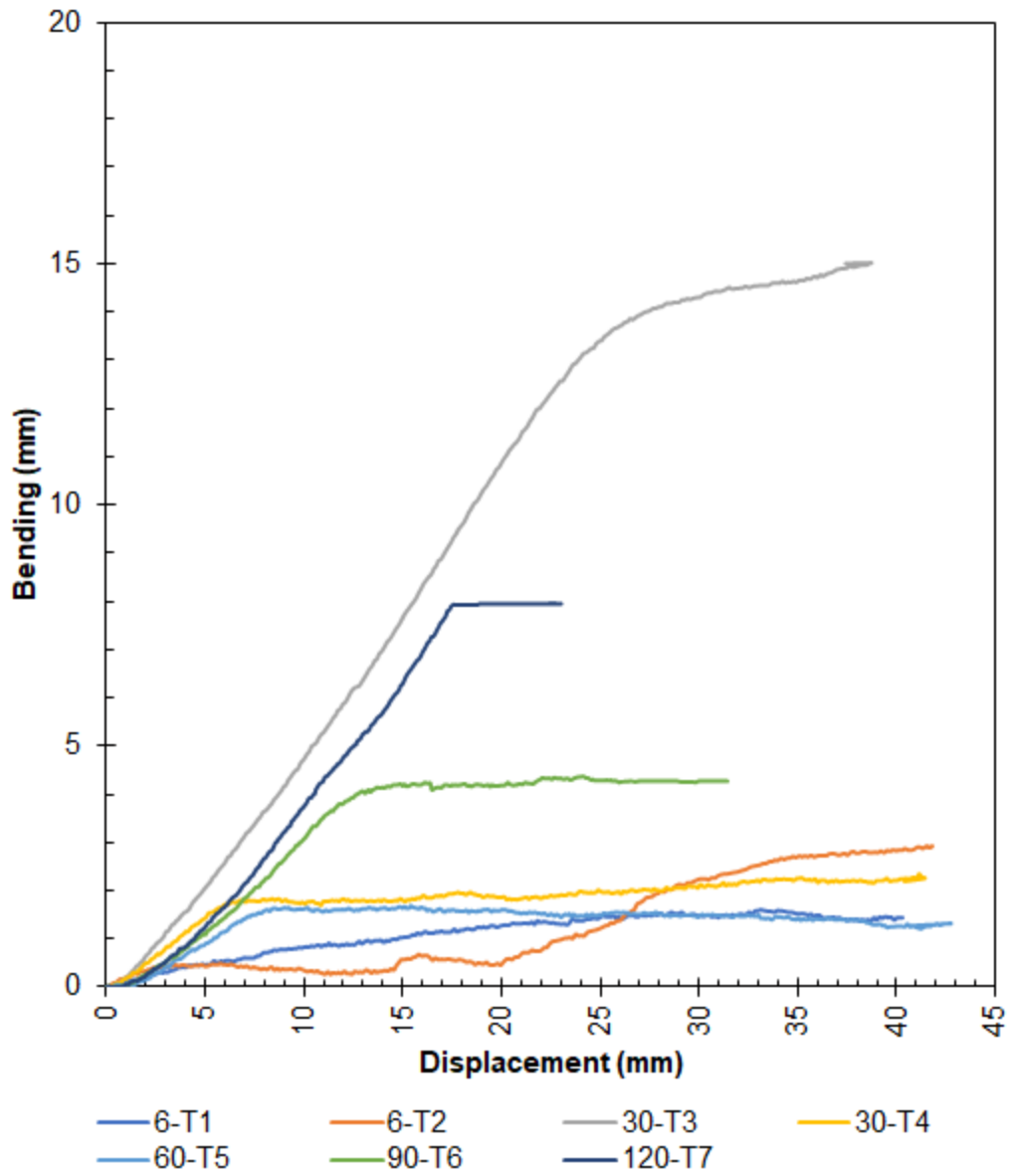


Figure 4-88 Transverse Bar Bending (MW71 x MW71 - 100 x 150)

The welds broke in test T6 and T7

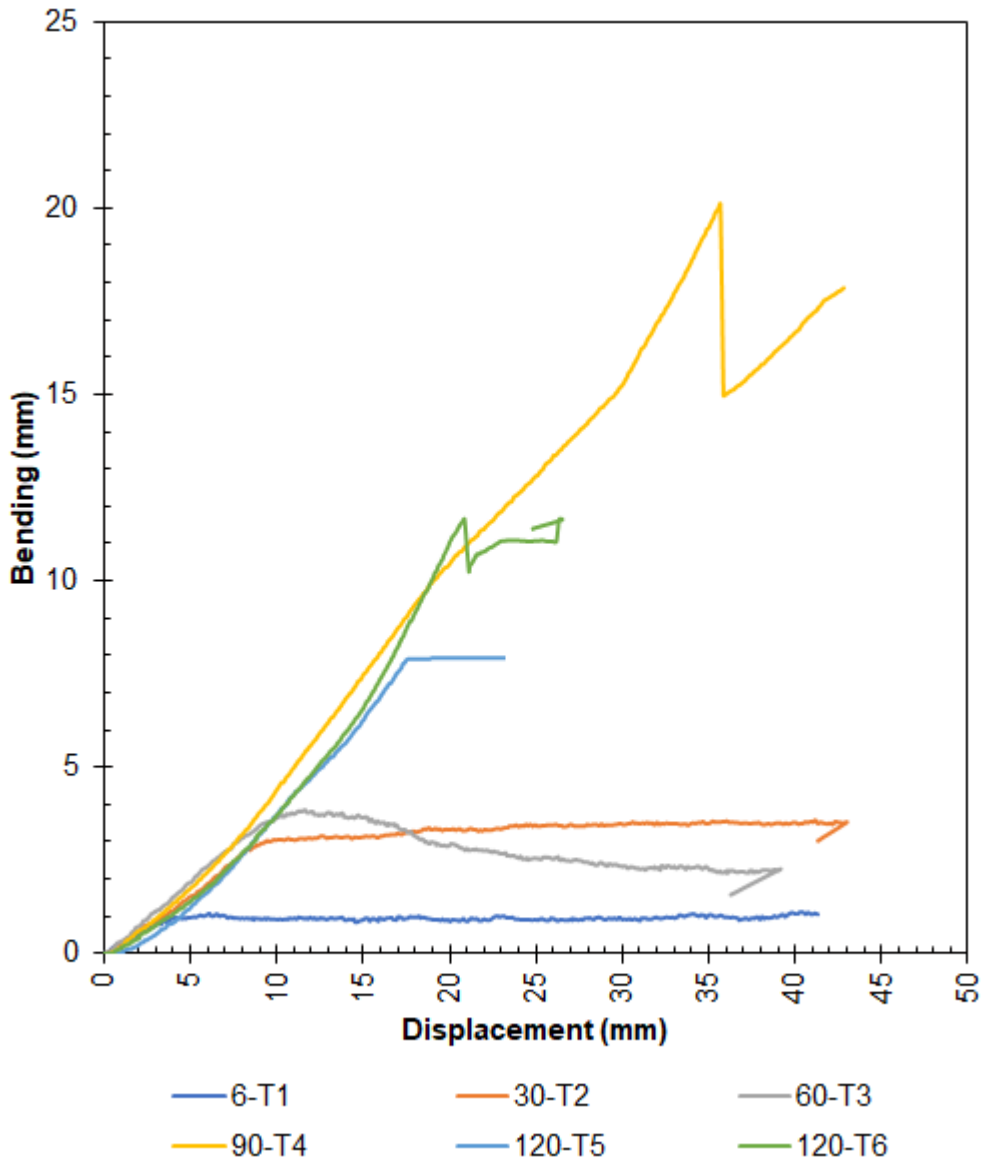


Figure 4-89 Transverse Bar Bending (MW71 x MW71 - 200 x 150)

The welds broke in test T4, T5 and T6

The Plaxis 3D model also showed that there is bending occurring in the transverse element that varies. It also shows that the degree of bending is different for different lengths of transverse elements, i.e., the spacing of the longitudinal element. As before, the degree of bending was determined by taking the difference between the

displacement of the weld and the displacement of the mid-point of the transverse element. The values shown in the following tables are based on the bending at the maximum system displacement equal to 19 mm. The degree of bending of each of the systems is shown in Table 4-100, Table 4-101, and in Table 4-102.

Table 4-100 Plaxis 3D Transverse Element Bending  
MW71 x MW71 – 50 x 1W

| Pressure | At Weld | Mid-Point | Difference |
|----------|---------|-----------|------------|
| 6        | 18.83   | 18.84     | 0.01       |
| 30       | 18.61   | 18.66     | 0.05       |
| 60       | 18.46   | 18.53     | 0.07       |

Table 4-101 Plaxis 3D Transverse Element Bending  
MW71 x MW71 – 100 x 1W

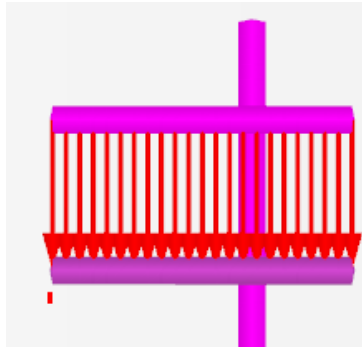
| Pressure | At Weld | Mid-Point | Difference |
|----------|---------|-----------|------------|
| 6        | 18.66   | 18.90     | 0.24       |
| 30       | 18.04   | 18.79     | 0.70       |
| 60       | 17.54   | 18.70     | 1.16       |

Table 4-102 Plaxis 3D Transverse Element Bending  
MW71 x MW71 – 200 x 1W

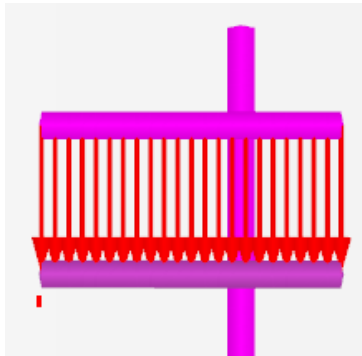
| Pressure | At Weld | Mid-Point | Difference |
|----------|---------|-----------|------------|
| 6        | 16.72   | 19.17     | 2.45       |
| 30       | 13.14   | 19.44     | 6.30       |
| 60       | 10.59   | 19.63     | 9.02       |

The bending of the transverse elements for each of the systems, as developed in the Plaxis-3D models, are shown in Figure 4-90 to Figure 4-92. The direction of displacement, or the application of the pullout force is toward the bottom of the figure.

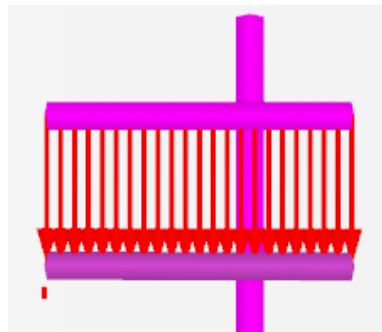
These diagrams will show how the bending increases with an increasing longitudinal spacing and overburden load.



6 kPa Overburden Pressure

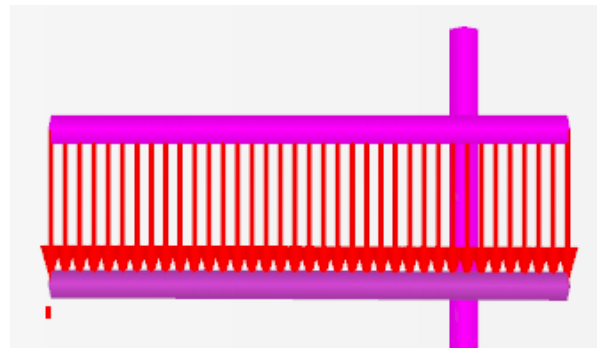


30 kPa Overburden Pressure

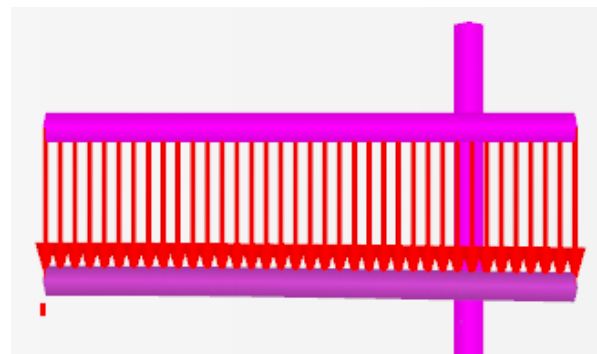


60 kPa Overburden Pressure

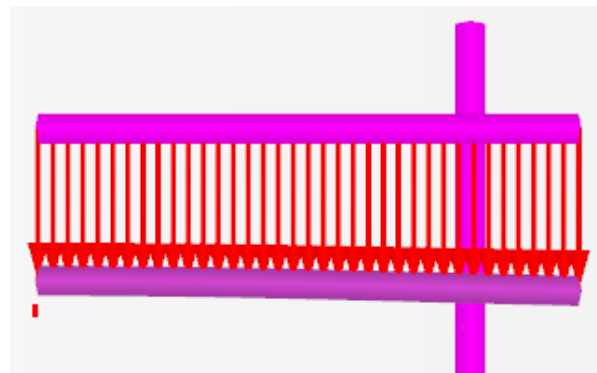
Figure 4-90 Element Bending (MW71 x MW71 - 50 x 1W Plaxis)



6 kPa Overburden Pressure



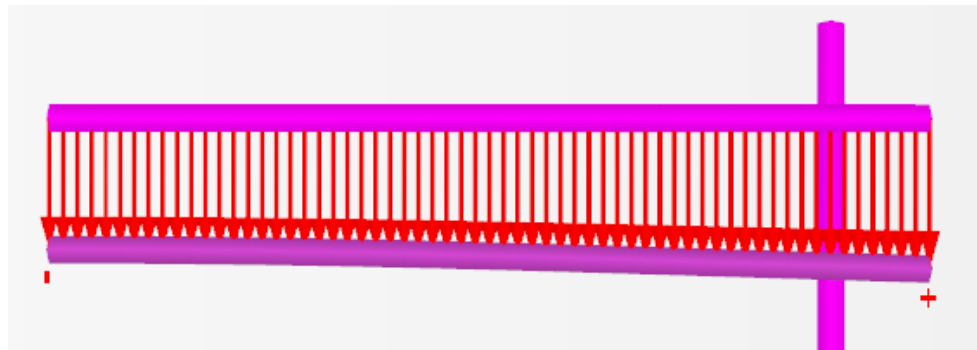
30 kPa Overburden Pressure



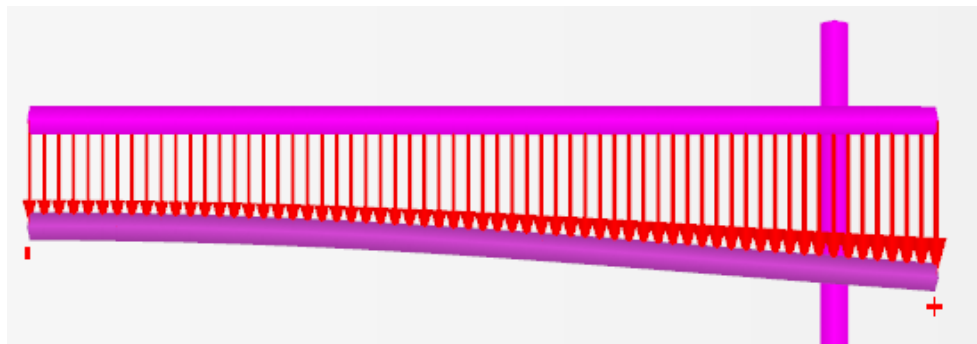
60 kPa Overburden Pressure

Figure 4-91 Element Bending (MW71 x MW71 - 100 x 1W Plaxis)

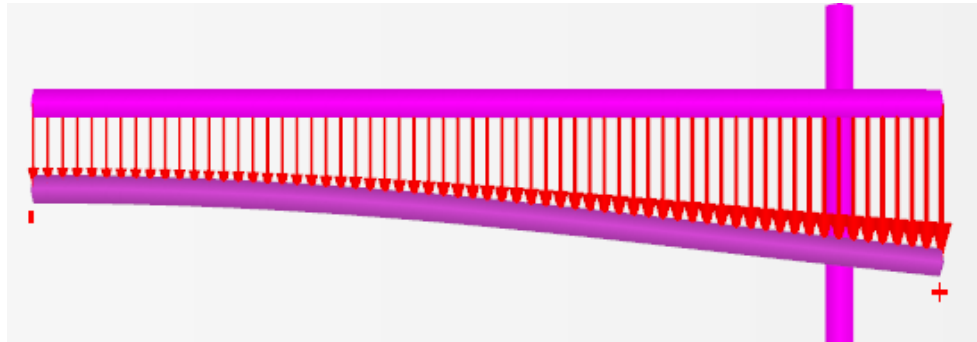




6 kPa Overburden Pressure



30 kPa Overburden Pressure

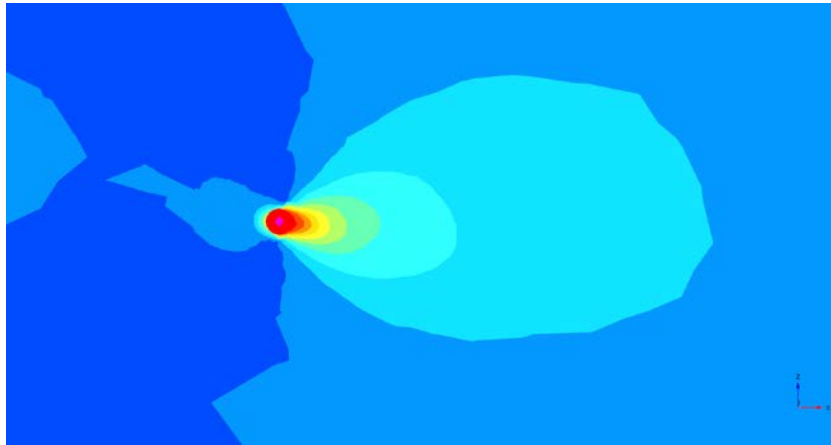


60 kPa Overburden Pressure

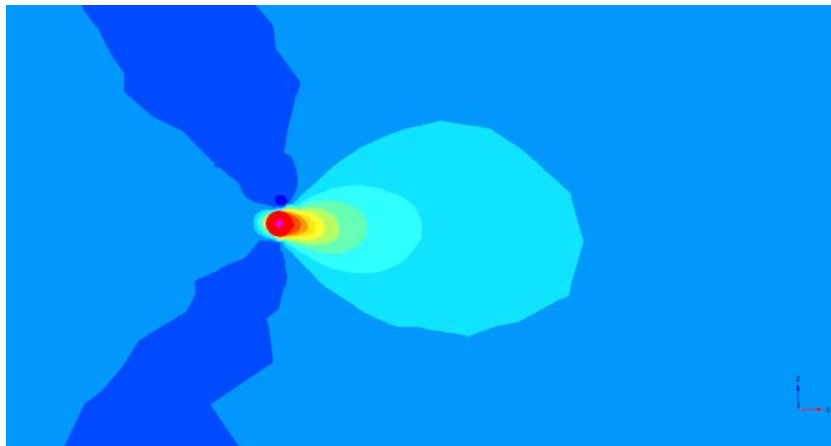
Figure 4-92 Element Bending (MW71 x MW71 - 200 x 1W Plaxis)

The displacement contours for each of the systems, developed from the Plaxis 3D models, are shown in Figure 4-93 to Figure 4-95. The displacement contours demonstrate that increasing confinement decreases the distance of the disturbance of the soil in front of the transverse member. The displacement contours also demonstrate that increasing longitudinal element spacings increases the distance of the disturbance

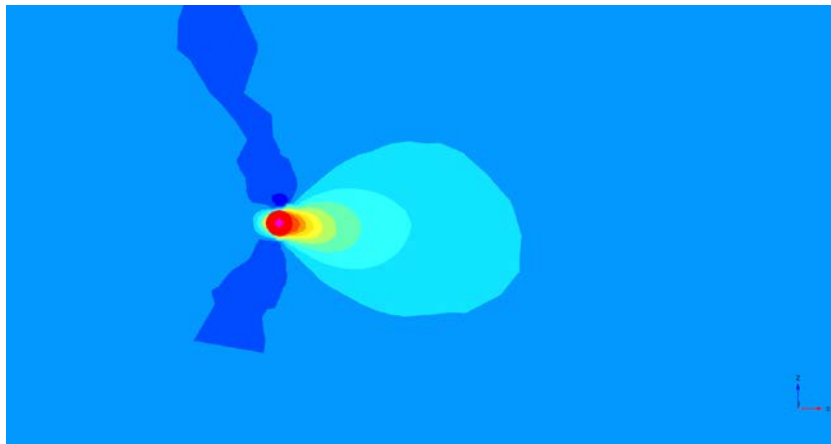
of the soil in the direction that is perpendicular to the transverse member. This demonstrates that the spacing of the longitudinal and transverse elements will influence the pullout resistance. In other words, the narrow soil-reinforcing element with large transverse spacings has smaller disturbance of the soil volume.



6 kPa Overburden Pressure

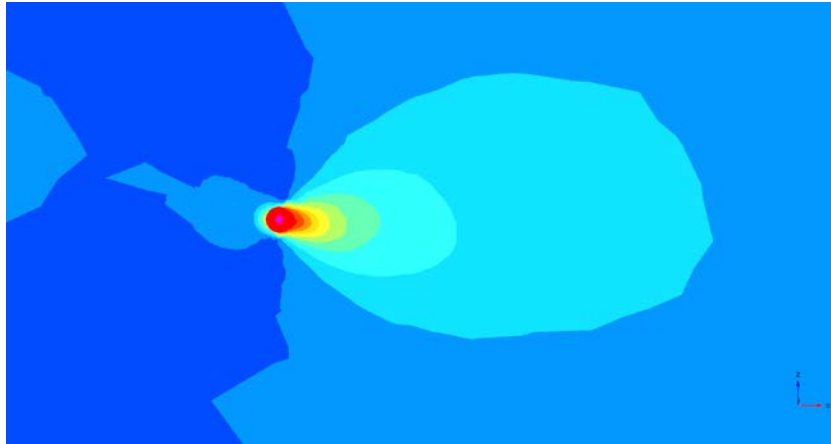


30 kPa Overburden Pressure

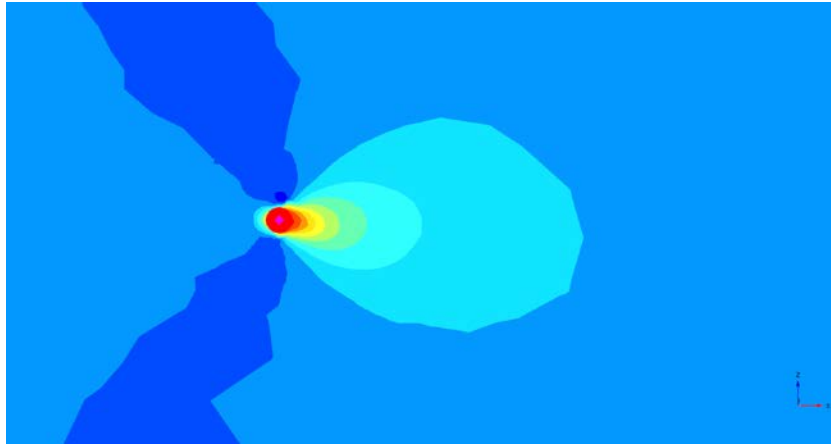


60 kPa Overburden Pressure

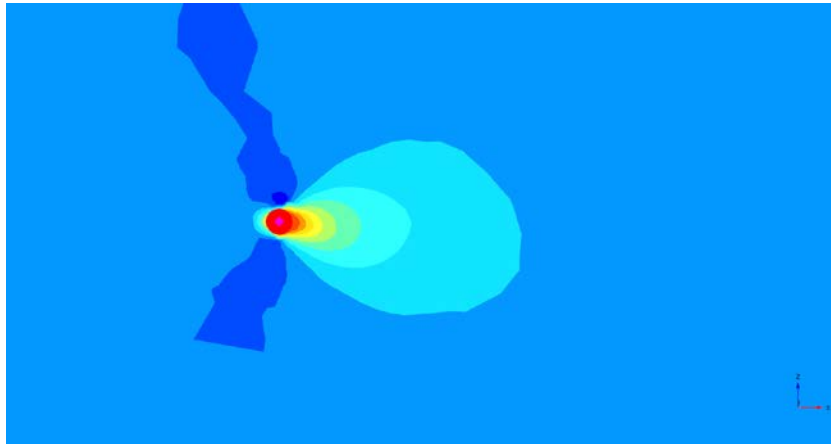
Figure 4-93 Total Displacement Contours for MW71 x MW71 – 50 x 1W



6 kPa Overburden Pressure

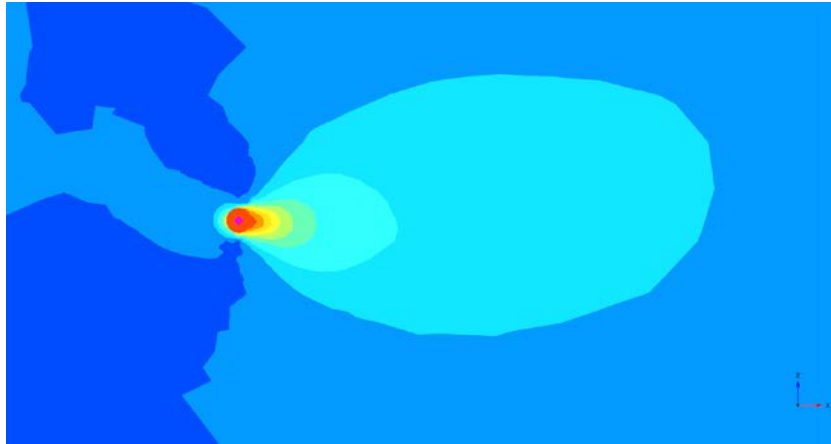


30 kPa Overburden Pressure

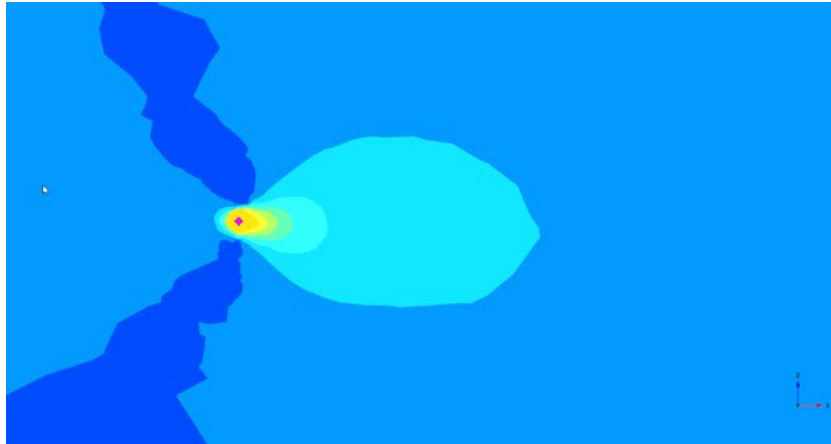


60 kPa Overburden Pressure

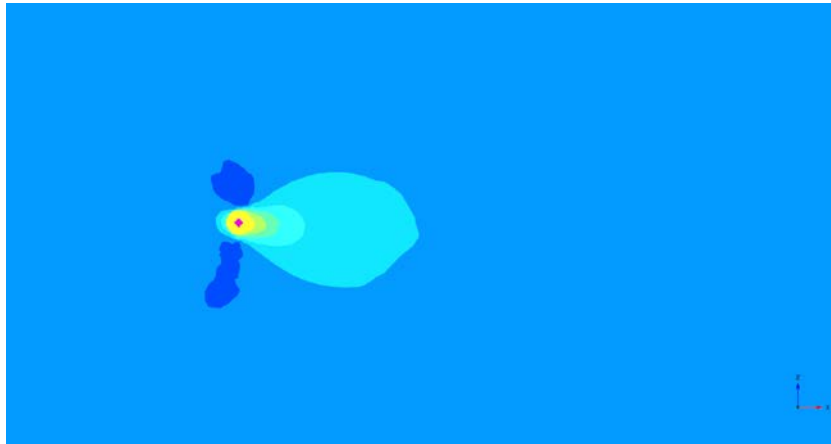
Figure 4-94 Total Displacement Contours for MW71 x MW71 – 100 x 1W



6 kPa Loading



30 kPa Loading



60 kPa Loading

Figure 4-95 Total Displacement Contours for MW71 x MW71 – 200 x 1W

#### 4.11 Using the Developed Equations for Design

Based on the methodology described for the internal stability analysis of the MSE structure in AASHTO (2014) Article 11.10.6.3.2 – *Reinforcement Pullout Design*, the required pullout resistance must be greater than, or equal to, the maximum tension force at each soil-reinforcing elevation as shown in Equation 4-12.

$$P_r \geq T_{\max} \quad \text{Equation 4-12}$$

Where:  $P_r$  = Pullout resistance (kN)

$T_{\max}$  = Maximum tension force to be resisted (kN)

As discussed in Section 4.8, equation RE2 can be used to determine the pullout resistance of a 2-Wire soil-reinforcing element. An example will be used to demonstrate how to calculate the pullout resistance and the corresponding capacity demand ratio (CDR) using the RE2 equation. The example will use RE2 to calculate the pullout resistance and will be a function of the depth of the soil-reinforcing as presented in Section 4.4.1. These results will be compared to the method used in the state-of-practice, as defined in AASHTO (2014) using Equation 1-1 and Equation 1-2.

For the comparison example, the following assumptions are used:

1. Backfill consists of Florida sand
  - a. Unit weight ( $\gamma_t$ ) of 19.6 kN/m<sup>3</sup>
  - b. Internal friction angle ( $\phi_t$ ) equal to 30 degrees.
  - c. Placed at 95% of standard proctor (ASTM D698).

2. Soil-reinforcing consists of a discrete linear strip using a 2-Wire soil-reinforcing system of the type defined by a MW71 x MW71 – 50 mm x 300 mm configuration.
3. The MSE cross-section wall height is equal to 9.144 m.
4. The soil-reinforcing length will be set equal to 70% of the wall height equal to 6.400 m.
5. The depth to soil-reinforcing under investigation, as measured from the MSE surface, is equal to 1.143 m.
6. A live load surcharge equal to 11.97 kPa is applied to the MSE surface.
7. The length of embedment ( $L_e$ ) will be based on the failure surface as defined in AASHTO (2014) figure 11.10.6.2.1-4. The length of embedment is calculated to be equal to 3.657 m.
8. The load factor to determine  $T_{max}$  is equal to the dead load factor EV equal to 1.35 as defined in AASHTO (2014) Section 3.
9. The resistance factor applied to the pullout resistance, as defined in AASHTO (2014) Section 11, Table 11.5.7-1 is equal to 0.90.
10. The MSE structure will be faced with a segmental concrete panel.
11. The tributary area for one 2-Wire soil-reinforcing element is equal to 0.774 m<sup>2</sup>.

The maximum horizontal force is calculated using AASHTO (2014), Section 11 and equation 11.10.6.2.1-1. The horizontal force is applied to the tributary area defined in item 11 specified above.

$$T_{\max} = K_r \cdot \gamma_{EV} \cdot (\gamma_f \cdot z + q) \cdot A_t \quad \text{Equation 4-13}$$

- Where:
- $T_{\max}$  = Maximum tension force to be resisted (kN)
  - $K_r$  = Horizontal earth pressure coefficient (dim)
  - $\gamma_{EV}$  = Load factor for vertical earth pressure (dim)
  - $\gamma_f$  = unit weight of backfill (kN/m<sup>3</sup>)
  - $z$  = Depth to soil-reinforcing (m)
  - $q$  = Live load surcharge (kPa)
  - $A_t$  = Tributary area for soil-reinforcing (m<sup>2</sup>)

$$K_r = \left( 1.7 - \frac{1.7 - 1.2}{6.1m} \cdot z \right) \cdot K_a \quad \text{Equation 2-22}$$

- Where:  $K_a$  = Active earth pressure coefficient (dim)

$$K_a = \tan^2 \left( 45^\circ - \frac{\phi_f}{2} \right) \quad \text{Equation 4-14}$$

- Where:  $\phi_f$  = Internal friction angle of soil (deg)

$$K_a = \tan^2 \left( 45^\circ - \frac{30^\circ}{2} \right) = 0.333$$

$$K_r = \left( 1.7 - \frac{1.7 - 1.2}{6.1m} \cdot 1.524m \right) \cdot 0.333 = 0.525$$

$$T_{req} = 0.556 \cdot 1.35 \cdot \left( 19.6 \frac{kN}{m^3} \cdot 1.143m + 11.97 \frac{kN}{m^2} \right) \cdot 0.774m^2 = 19.97 kN$$



The pullout resistance factor will be calculated using the RE2, Equation 4-7, and the appropriate values defined in Table 4-28, i.e.,  $F_0$  equal to 2.00,  $\alpha$  equal to 4.50, and  $\beta$  equal to 0.38.

$$F_q = F_0 + F_{\max} \cdot e^{-\beta \cdot z} \quad \text{Equation 4-7}$$

Where:

- $F_q$  = Bearing resistance factor (dim)
- $F_0$  = Minimum bearing resistance factor (dim)
- $\alpha$  = Maximum bearing resistance factor (dim)
- $z$  = depth to soil-reinforcing (m)

$$F_q = 2.00 + 4.50 \cdot e^{-0.38(1.144)} = 4.91$$

The pullout resistance for the 2-Wire soil-reinforcing is determined using Equation 4-4. The width of the soil-reinforcing,  $w$ , equal to 0.050 m, is used to replace the soil-reinforcing coverage ratio,  $R_c$ , for the tributary are defined above.

$$P_r = \phi_{po} \cdot F_q \cdot \alpha \cdot \sigma_v \cdot C \cdot w \cdot L_e$$

$$\sigma_v = \gamma_f \cdot Z \quad \text{Equation 4-4}$$

Where:

- $P_r$  = Pullout resistance (kN)
- $\phi_{po}$  = Pullout resistance factor (dim)
- $F_q$  = Bearing resistance factor (dim)
- $\alpha$  = Scale correction factor equal to 1.0 (dim)
- $C$  = Unit surface parameter equal to 2.0 (dim)
- $w$  = Width of soil-reinforcing element (mm)

$L_e$  = Length of embedment of soil-reinforcing (m)

$$P_r = 0.90 \cdot 4.91 \cdot 1.00 \cdot \left( 19.6 \frac{kN}{m^2} \cdot 1.144 m \right) \cdot 2.00 \cdot 0.050 m \cdot 3.657 m = 36.23 kN$$

The capacity demand ratio (CDR) for the LRFD is the measure of the structures capacity in relation to the required demand. A CDR greater than 1.0 means the structure capacity is greater than the required demand. A CDR less than 1.00 means that the required demand is greater than the supplied capacity.

$$CDR = \frac{Capacity}{Demand} \geq 1.00 \quad \text{Equation 4-15}$$

For RE2 the CDR is equal to the following:

$$CDR = \frac{P_r}{T_{max}} = \frac{36.23 kN}{19.26 kN} = 1.89$$

Following the same logic, the equation that was described in Section 4.4.1.1 that predicts the pullout resistance of the 2-Wire soil-reinforcing element based on the elevation that it is positioned within the MSE structure can be used to predict the pullout resistance as given in Equation 4-16.

$$P_r = (\alpha \cdot z^\beta) \cdot L_e \quad \text{Equation 4-16}$$

Where:  $P_r$  = Pullout resistance of soil-reinforcing (kN/m of SR)

$\alpha$  = Coefficient (dim)

$z$  = Depth to soil-reinforcing (m)

$\beta$  = Coefficient (dim)

$L_e$  = Length of embedment (m)

For the soil-reinforcing used in this example, MW71 x MW71 – 50 mm x 300 mm, the alpha ( $\alpha$ ) coefficient is equal to 8.0 and the beta ( $\beta$ ) coefficient is equal to 0.70 for the  $P_{50}$  equation as shown in Figure 4-4. Based on the soil-reinforcing positioned at a depth equal to 1.143 m and using the calculated length of embedment equal to 3.67 m, substituting these values into Equation 4-16, the pullout resistance can be predicted as shown below.

$$P_r = 8.0 \cdot (1.143 \text{ m})^{0.70} \cdot (3.67 \text{ m}) = 32.24 \text{ kN}$$

For depth  $P_{50}$  depth equation the CDR is equal to the following:

$$CDR = \frac{P_r}{T_{\max}} = \frac{32.24 \text{ kN}}{19.26 \text{ kN}} = 1.67$$

The AASHTO (2014) equation shown in Section 11, 11.10.6.3.2-1 (shown below as Equation 1-1) will be used to calculate the pullout resistance for the 2-Wire soil-reinforcing element defined using the assumptions stated above in item 2. The soil-reinforcing is defined as having a cross bar spaced ( $S_t$ ) at 300 mm on center, and a width ( $w$ ) equal to 0.050 m. As before, the reinforcing coverage ratio,  $R_c$ , will be replaced by substituting the width of the element,  $w$ . This substitution allows the pullout resistance to be calculated for one soil-reinforcing element.

$$P_r = N_p \cdot \frac{d_t}{S_t} \cdot \alpha \cdot \sigma_v \cdot L_e \cdot C \cdot w \quad \text{Equation 1-1}$$

where:  $P_r$  = Pullout resistance (kN)

$N_p$  = Pullout coefficient (dim)

$$= 20 - \frac{20 - 10}{10} \cdot z \leq 6 \text{ meters (AASHTO figure 11.10.6.3.2-2)}$$

- z = Depth to soil-reinforcing (m)
- d<sub>t</sub> = Diameter of transverse wire (m)
- S<sub>t</sub> = Spacing of transverse wire (m)
- α = Scale effect correction factor and is equal to 1 for inextensible systems (dim)
- σ<sub>v</sub> = Vertical pressure (kPa)
- L<sub>e</sub> = Length of reinforcement in resistive zone (m)
- C = Unit perimeter factor default value equal to 2 (dim)
- w = Width of soil-reinforcing element (m)

Substituting the required values into Equation 1-1, the pullout for the 2-Wire soil-reinforcing element is equal to 4.24 kN.

$$P_r = \left( 20 - \frac{20 - 10}{6.1 m} \cdot 1.144 m \right) \cdot \frac{0.0095 m}{0.300 m} \cdot 1.00 \cdot \left( 19.6 \frac{kN}{m^2} \cdot 1.144 m \right) \dots \dots \dots$$

$$\cdot 2.00 \cdot 0.050 m \cdot 3.657 m = 4.24 kN$$

For the AASHTO (2017) method, the CDR is equal to the following:

$$CDR = \frac{P_r}{T_{max}} = \frac{4.24 kN}{19.26 kN} = 0.22$$

As is evident by the method presented in AASHTO (2014) to determine the pullout resistance factor, described as lower bound values by FHWA (2010), the predicted pullout resistance of the MW71 x MW71 – 50 mm x 300 mm soil-reinforcing is 8.5 times lower than the pullout resistance predicted using the RE2 equation and the P<sub>50</sub> depth equation. It should also be noted that the RE2 equation and the P<sub>50</sub> equation, for

the specified MW71 x MW71 – 50 mm x 300 mm soil-reinforcing element give nearly equal pullout resistance magnitudes, 36.23 kN and 32.25 kN, respectively, and CDR values, 1.89 and 1.67, respectively. The full results for the 9.144 m wall height is shown in Table 4-103 and Table 4-104.

Table 4-103 Pullout Comparison Table of Forces

| Row | z (m) | $\sigma_v$ (kPa) | $K_r$ (dim) | $\sigma_H$ (kPa) | $T_{req}$ (kN) | $n_r$ (dim) | $L_e$ (m) |
|-----|-------|------------------|-------------|------------------|----------------|-------------|-----------|
| 1   | 0.381 | 7.48             | 0.556       | 14.61            | 33.9           | 3           | 3.66      |
| 2   | 1.143 | 22.44            | 0.535       | 24.87            | 57.8           | 3           | 3.66      |
| 3   | 1.905 | 37.40            | 0.515       | 34.30            | 79.7           | 3           | 3.66      |
| 4   | 2.667 | 52.35            | 0.494       | 42.88            | 99.6           | 3           | 3.66      |
| 5   | 3.429 | 67.31            | 0.473       | 50.62            | 117.6          | 4           | 3.66      |
| 6   | 4.191 | 82.27            | 0.452       | 57.53            | 133.6          | 4           | 3.66      |
| 7   | 4.953 | 97.23            | 0.431       | 63.59            | 147.7          | 5           | 3.89      |
| 8   | 5.715 | 112.19           | 0.411       | 68.81            | 159.8          | 5           | 4.34      |
| 9   | 6.477 | 127.14           | 0.400       | 75.12            | 174.5          | 6           | 4.80      |
| 10  | 7.239 | 142.10           | 0.400       | 83.20            | 193.2          | 6           | 5.26      |
| 11  | 8.001 | 157.06           | 0.400       | 91.28            | 212.0          | 7           | 5.72      |
| 12  | 8.763 | 172.02           | 0.400       | 99.35            | 230.8          | 7           | 6.17      |

Table 4-104 Pullout Comparison Table of Results

| Row | $F_q$ RE2 (kN) | $P_r$ RE2 (kN) | $CDR_{RE2}$ (dim) | $F_q$ AASHTO (kN) | $P_{50}$ (kN) | $CDR_{P50}$ (dim) | $P_r$ AASHTO (kN) | $CDR_{AASHTO}$ (dim) |
|-----|----------------|----------------|-------------------|-------------------|---------------|-------------------|-------------------|----------------------|
| 1   | 5.89           | 43.5           | 1.28              | 0.61              | 44.7          | 1.32              | 4.5               | 0.13                 |
| 2   | 4.91           | 108.9          | 1.89              | 0.57              | 96.4          | 1.67              | 12.7              | 0.22                 |
| 3   | 4.18           | 154.4          | 1.94              | 0.53              | 137.8         | 1.73              | 19.7              | 0.25                 |
| 4   | 3.63           | 187.8          | 1.89              | 0.49              | 174.4         | 1.75              | 25.6              | 0.26                 |
| 5   | 3.22           | 285.6          | 2.43              | 0.46              | 277.3         | 2.36              | 40.4              | 0.34                 |
| 6   | 2.92           | 315.8          | 2.36              | 0.42              | 319.1         | 2.39              | 45.0              | 0.34                 |
| 7   | 2.69           | 456.6          | 3.09              | 0.38              | 476.4         | 3.23              | 64.0              | 0.43                 |

Table 4-104 Pullout Comparison Table of Results

| Row | F <sub>q</sub><br>RE2<br>(kN) | P <sub>r</sub><br>RE2<br>(kN) | CDR <sub>RE2</sub><br>(dim) | F <sub>q</sub><br>AASHTO<br>(kN) | P <sub>50</sub><br>(kN) | CDR <sub>P50</sub><br>(dim) | P <sub>r</sub><br>AASHTO<br>(kN) | CDR <sub>AASHTO</sub><br>(dim) |
|-----|-------------------------------|-------------------------------|-----------------------------|----------------------------------|-------------------------|-----------------------------|----------------------------------|--------------------------------|
| 8   | 2.51                          | 551.0                         | 3.45                        | 0.34                             | 588.6                   | 3.68                        | 73.8                             | 0.46                           |
| 9   | 2.38                          | 785.8                         | 4.50                        | 0.32                             | 852.1                   | 4.88                        | 104.4                            | 0.60                           |
| 10  | 2.29                          | 922.9                         | 4.78                        | 0.32                             | 1008.8                  | 5.22                        | 127.8                            | 0.66                           |
| 11  | 2.22                          | 1252.7                        | 5.91                        | 0.32                             | 1372.2                  | 6.47                        | 179.1                            | 0.84                           |
| 12  | 2.16                          | 1445.5                        | 6.26                        | 0.32                             | 1579.4                  | 6.84                        | 211.8                            | 0.92                           |

## Chapter 5

### Summary, Conclusions, and Recommendations

#### 5.1 Summary

The present experimental test program investigated the pullout behavior of 2-Wire soil-reinforcing elements buried in sand. Testing was performed using a large-scale pullout apparatus fabricated in conformance with the recommendations of the ASTM D6706, *Standard Test Method for Measuring Geosynthetic Pullout Resistance in Soil*. The main components of the pullout apparatus include the soil-box, reaction frame, load frame, hydraulic system, instrumentation components, and the data acquisition system.

A series of 142 pullout tests was performed on 2-Wire soil-reinforcing elements. The 2-Wire soil-reinforcing elements consists of cold drawn steel wire that was fabricated in conformance with ASTM A1064. The soil-reinforcing elements were then hot-dip galvanized in conformance with ASTM A123. For the 2-Wire elements, three longitudinal element spacings were used and consisted of 50 mm, 100 mm, and 200 mm. For each of the longitudinal element spacings there were two different transverse element spacings consisting of 150 mm and 300 mm and systems with only 1-wire. Based on this, the tests included systems with 8, 4, and 1 transverse wires.

The soil used for the experimental test program consisted of a beach sand obtained in Jacksonville, Florida. The sand was classified as SP in conformance with the Unified Soil Classification. The sand material was selected to be used in the experimental test program because it is considered a lower-bound material that is used as backfill in MSE structures. Based on this, the results for this study can be conservatively used with other higher-bound materials. The target compaction of the

sand for the experimental test program was set equal to 95% of standard proctor in conformance with ASTM D698. The placed density of the sand, for each pullout test, was determined based on the use of a volume relationship.

Each of the sub-set of tests were performed at overburden depths equal to 300 mm (1 ft.), 1525 mm (5 ft.), 3050 mm (10 ft.), 4575 mm (15 ft.) and 6100 mm (20 ft.). This equates to 6 kPa (125 psf), 30 kPa (625 psf), 60 kPa (1250 psf), 90 kPa (1875 psf), and 120 kPa (2500 psf) pressures. The overburden pressure was applied using a pneumatic diaphragm and the top-mount reaction frame. The horizontal pullout force was applied using a hydraulic load system at rate of retraction equal to approximately 1 mm/min. The displacement of the 2-Wire element was recorded using two LVDT's positioned on each side of the connection clamp at the front of the soil-box, and three wire-rope potentiometers attached to the 2-Wire element to monitor the displacement and bending of the transverse element inside the soil-box. Two of the wire-rope potentiometers were placed at the location of the junction of the welds that join the longitudinal element to the transverse element. The third wire-rope potentiometer was placed at the midpoint of the transverse element. In conformance with ASTM D-6706, the front LVDT displacement points were used as the limiting criteria for the determination of the maximum pullout force. The maximum pullout force was recorded at 19 mm (3/4 in.) of displacement. If the maximum pullout force occurred before the 19 mm (3/4 in.) displacement, it was recorded as the maximum pullout force. Each test was performed to a maximum displacement of 38 mm (1 ½ in.). The maximum pullout force at 19 mm (3/4 in.) and 38 mm (1 ½ in.) was recorded for each of the tests.

The experimental test program results were presented in two forms. The first form was presented based on the measured pullout resistance as a function of depth. A



power function was used to represent a best-fit for the measured test data. The power function included two coefficients, alpha ( $\alpha$ ) and beta ( $\beta$ ). A regression analysis was performed on each of the test groups to determine the alpha and beta coefficients that provided a bias close to a value equal to 1.00 and P-Value less than 0.05. It was established through statistical analysis of the power function with the appropriate alpha and beta factors that it can be used to predict the pullout resistance for each soil-reinforcing system tested in this experimental program. It was also demonstrated that for the normalized measured pullout resistance that the pullout capacity is a function of the longitudinal and transverse wire spacing. An example was provided that demonstrated how the normalized pullout resistance from the power function could be correlated to actual measured test values.

The second form that was presented is based on the bearing resistance factor,  $F_q$ . The bearing resistance factor was back calculated using the state-of-practice pullout resistance equation provide in AASHTO (2014), Section 11, using the form given in Equation 4-5 that is shown again below.

$$F_q = \frac{P_r}{2 \cdot w \cdot L_e \cdot \sigma_v} \quad \text{Equation 4-5}$$

The experimental program pullout tests showed that there was a tendency for the bearing resistance factor, as a function of depth below the surface to the soil-reinforcing element, to have a shape of a decaying exponential function. At low overburden pressure the bearing resistance factor was higher than predicted by other equations for calculating the bearing resistance factor described in the literature review. It was also shown that the measured bearing resistance factor was substantially higher than the

relationship that is used in the state-of-practice defined in AASHTO (2014). The experimental program pullout tests also verified, as discussed in the literature review, that as the overburden pressure increased, the bearing resistance factor decreased.

A parametric study was used to determine the most efficient equation to calculate the bearing resistance factor. The parametric study investigated power functions, decaying exponential functions, and linear piece-wise functions. Regression analysis was used to estimate the coefficients required in each of the functions. The functions were then used to predict and compare the measure pullout resistance for the experimental test program. The predicted values were compared to the measured values by determining the bias. The bias was calculated using the ratio of the predicted pullout resistance to the measured pullout resistance. The statistical significance of each of the functions was determined using the Pearson Product Moment Correlation (PPMC) method. A bias that is less than one, correlates to a predicted pullout resistance that is less than the measured pullout resistance. Likewise, a bias greater than one correlated with a predicted pullout resistance greater than the measured pullout resistance. If the P-Value in the PPMC of the comparison of the measured pullout resistance to the predicted pullout resistance was less than 0.05 than a strong correlation existed. In addition, the P-Value was required to be greater than 0.05 for the comparison of the bias to the calculated pullout resistance. When these two conditions held true, the function was determined to be statistically significant and satisfactory to calculate the pullout resistance of the 2-Wire soil-reinforcing element. The four equations tested were the Research Equation 1 (RE1), Research Equation 2 (RE2), Research Equation 3 (RE3) and the equation provided in the literature by Yu et al., (2015).

Based on the statistical comparison between the four equations it was determined that the RE2 equation, shown in Equation 4-7 and again shown below, was the best predictor of the pullout resistance of the 2-Wire soil-reinforcing elements from this experimental test program.

RE2 
$$F_q = F_{\min} + F_{\max} \cdot e^{-\beta \cdot z}$$
 Equation 4-7

Where:

- $F_{\min}$  = Minimum bearing resistance factor (dim)
- $F_{\max}$  = Maximum bearing resistance factor (dim)
- $\beta$  = Coefficient (dim)
- $z$  = depth to soil-reinforcing (m)

It was demonstrated by the normalization of the measured pullout resistance for each of the systems tested and the predictions using RE2 equation, that the magnitude of the pullout resistance is influenced by the spacing of the longitudinal and transverse element of the 2-Wire soil-reinforcing system.

It was demonstrated though measured bending values of the transverse element that the bearing resistance factor of the 2-Wire soil-reinforcing element is influenced by the magnitude of bending. Bending of the transverse element was measured using potentiometers that were attached to the weld junctions and the mid-point of the transverse element. The systems with a longitudinal spacing equal to 50 mm had bending values that were all less than 2.0 mm for all tested overburden pressures. The systems with longitudinal spacing equal to 100 mm had bending values that varied from 1 mm to 4 mm and the magnitude was based on the magnitude of the overburden pressure. For the systems with longitudinal spacings equal to 200 mm, the magnitude of

the bending varied also as a function of the overburden pressure. At high overburden for longitudinal spacings equal to 100 mm and 200 mm, several specimens experienced weld failure. The weld failure was due to the bending moment that is created at the weld junction during bending of the transverse element. The bending moment was verified in the numerical model that was created in Plaxis-3D.

It was demonstrated that the number of transverse elements does not influence the degree of bending and is presumably due to the effect that that closely spaced transverse elements have on a decrease in the predicted pullout resistance. In the Plaxis-3D model the degree of bending was determined by taking the difference between the displacement of the transverse element at the junction of the weld and the mid-point, at a maximum system displacement equal to 19 mm. The displacement contours for each of the systems, developed from the Plaxis-3D models, demonstrated that increasing confinement decreases the distance of the disturbance of the soil in front of the transverse member, and that increasing longitudinal element spacings increases the distance of the disturbance of the soil in front and to the sides of the transverse element. The Plaxis-3D model demonstrates that the spacing of the longitudinal and transverse elements will influence the pullout resistance.

It was demonstrated using a worked example that compared to the research equation, RE2, to the state-of-practice pullout resistance equation in AASHTO (2014), that the state-of-practice equation underestimated the resistance to pullout by nearly 8.5 times for the MW71 x MW71 – 50 mm x 300 mm system.

## 5.2 Conclusions

The following conclusions for this experimental test program, based on the presentation of the results and the analysis as discussed in this dissertation, can be summarized as follows:

1. Pullout of 2-Wire soil-reinforcing elements are not a function of the total area of the bearing element contained in the soil.
2. The spacing of the longitudinal and transverse element affects the pullout resistance.
3. The pullout resistance of the 2-Wire soil-reinforcing element does not increase linearly with an increasing longitudinal spacing.
4. The pullout resistance of the 2-Wire soil-reinforcing element does not increase linearly with a number of transverse elements.
5. Test results showed that the pullout resistance of the 2-Wire soil-reinforcing element does not increase linearly with depth.
6. The bearing resistance factor of the 2-Wire soil-reinforcing element does not decrease linearly with depth.
7. The pullout resistance for 2-Wire soil-reinforcing elements is consistent with a power function that shows an increase in pullout resistance with the depth below the surface.
8. The bearing resistance factor is best-fit using a 3-parameter decaying exponential function.

9. The state-of-practice method of calculating the bearing resistance factor and corresponding pullout equation, that are presented in AASHTO and FHWA, underestimate the pullout resistance of the 2-Wire soil-reinforcing element in the upper portion of the structure by nearly 8 times.
10. The normalized pullout resistance for 2-Wire soil-reinforcing systems with narrower longitudinal element spacing have greater pullout resistance 2-Wire soil-reinforcing systems with a wider longitudinal element spacing.

### 5.3 Recommendations for Future Studies

The following recommendations are presented as suggestions for future studies:

1. Perform more test for each configuration used in this research program in conjunction with the same soil to improve the coefficients used in the equations to predict the pullout resistance and the bearing resistance factor of the 2-Wire soil-reinforcing system.
2. Expand the study to include differing frictional soil types.
3. Expand on the numerical models developed in Plaxis-3D.
4. Expand test matrix to include 3-Wire soil-reinforcing elements.
5. Explore boundary effects of the soil-box.

## References

- [1] AASHTO (2002). "Standard Specifications for Highway Bridges, 17th Edition", American Association of State Highway and Transportation Officials, Washington, DC
- [2] AASHTO (2009). "LRFD Bridge Design Specifications, 2009 Interims", American Association of State Highway and Transportation Officials, Washington, DC.
- [3] AASHTO (2010). "LRFD Bridge Design Specifications, 5th Edition", American Association of State Highway and Transportation Officials, Washington, DC.
- [4] AASHTO (2012). "LRFD Bridge Design Specifications, 6th Edition", American Association of State Highway and Transportation Officials, Washington, DC.
- [5] AASHTO (2014). "LRFD Bridge Design Specifications, 7th Edition", American Association of State Highway and Transportation Officials, Washington, DC.
- [6] Adib, M. E., (1988). "Internal Lateral Earth Pressure in Earth Walls", Ph.D. Dissertation, University of California, Berkley, Civil Engineering Department.
- [7] Allen, T.M., and Bathurst, R.J. (2001). "Application of the Ko-Stiffness Method to Reinforced Soil Limit States Design," Washington State Department of Transportation Report No. WA-RD 528.1, Olympia, WA.
- [8] Allen, T. M., Christopher, B. R., Elias, V., and DiMaggio, J. D. (2001). "Development of the simplified method for internal stability design of mechanically stabilized earth (MSE) walls." Research Rep. WA-RD 513.1, Washington State Dept. of Transportation, Olympia, WA, 96.
- [9] Allen T.M and Bathurst, R.J. (2003). " Prediction of Reinforcement Loads in Reinforced Soil Walls," Washington State Department of Transportation Report No. WA-RD 522.2, Olympia, WA
- [10] Allen, T. M., Nowak, A. S., and Bathurst, R. J. (2005). "Calibration to determine load and resistance factors for geotechnical and structural design." Circular E-C079, Transportation Research Board, National Research Council, Washington, DC.
- [11] Anderson, Loren R., et.al., (1985). "Performance of Rainier Avenue Welded Wire Wall", Seattle, Washington, Department of Civil and Environmental Engineering, Utah State University.

- [12] Anderson, P.L, (1991). "Subsurface Investigation and Improvements for MSE Structures Constructed on Poor Foundation Soils," 34th Annual Meeting, Association of Engineering Geologists," Environmental and Geological Challenges for the Decade, pp. 77-85
- [13] Anderson, P.L., Gladstone, R.A., and Withiam, J.L., (2010). "Coherent Gravity: The Correct Design Method for Steel-Reinforced MSE Walls," Proceedings of ER2010 Earth Retention Conference 3, ASCE, Bellevue, Washington
- [14] Anderson, P.L., Gladstone, R.A., and Sankey, J.E., (2012). "State of the Practice of MSE Wall Design for Highway Structures," Geotechnical Engineering State of the Art and Practice: Keynote Lectures from GeoCongress 2012, Oakland, California.
- [15] Bastick, M., Schlosser, F., Segrestin, P. Amar, S., and Canepa, Y. (1993). "Experimental Reinforced Earth Structure of Bourron Marlotte: Slender Wall and Abutment Test," Reinforcement Des Sols: Experimentations en Vraie Grandeur des Annees 80, Paris, pp. 201-228
- [16] Bathurst, R. J., Huang, B., and Allen, T. M. (2011). "Load and resistance factor design (LRFD) calibration for steel grid reinforced soil walls." *Georisk: Assess. Manage. Risk Eng. Syst. Geohards*, 5(3–4), 218–228.
- [17] Bathurst, R. J., Allen, T. M., Miyata, Y., and Huang, B. (2013). "LRFD calibration of metallic reinforced soil walls." *Geotechnical Special Publication 229*, ASCE, Reston, VA, 585–601.
- [18] Berg, R. B., Christopher, B. R., Samtani, N. C. (2009). "Design of Mechanically Stabilized Earth Walls and Reinforced Soil Slopes – Volume I", FHWA-NHI-10-024.
- [19] Bergado, D. T., Macatol, K. C., Amin, N. U., Chai, J. C., and Alfaro, M. C. (1993). "Interaction of lateritic soil and steel grid reinforcement." *Can. Geotech. J.*, 30(2), 376–384.
- [20] Bishop, J. a. and Anderson L. R. (1979). "Performance of a Welded Wire Wall", Report to the Hilfiker Company, Eureka California.
- [21] Bishop, Jerold A., (1980). "Evaluation of a Welded Wire Retaining Wall", M.S. Thesis, Utah State University, Civil and Environmental Engineering.



- [22] Bonczkiewicz, C.B., (1990). "Evaluation of Soil-Reinforcement Parameters and Interaction by Large Scale Pullout Test, Master of Science in Engineering Thesis submitted to Northwestern University, Evanston, Illinois.
- [23] Bounaparte R., and Schmertmann, G (1987). "Reinforcement Extensibility in Reinforced Soil Wall Design". Nat Advanced Research Workshop, Application of Polymeric Reinforcement in Soil Retaining Structures, Royal Military College of Canada, Kingston, Ontario.
- [24] Bowels, J.E. (1996). "Foundation Analysis and Design", 5th Edition. McGraw Hill Inc, Singapore.
- [25] Buisman, A. S. K. (1935). "De Weerstand Van Paalpunten in Zand." De Ingenieur, 50:25- 28, 31-35.
- [26] Caquot, A. (1934). "Equilibre des Massifs a Frottement Interne." Gauthier-Villars, Paris, France.
- [27] Chang, J. C., Hannon, J. B., and Forsyth, R. A. (1977). "Pull resistance and interaction of earthwork reinforcement and soil." Transportation Research Record 640, Transportation Research Board, Washington, DC, 1–6.
- [28] Christopher, B.R. and Bonczkiewicz, C.B., (1989). "Preliminary Results of Full Scale Field Test for Behavior of Reinforced Soil", Research Report to the U.S. Department of Transportation, Federal Highway Administration. FHWA Contract No. 61-84-C-00073.
- [29] Christopher, B.R., Gill, S.A., Juran, I., Mitchell, J.K., (1990). "Reinforced Soil Structures, Vol. 1, Design and Construction Guidelines", FHWA-RD-89-043.
- [30] Christopher, B.R., (1993). "Deformation Response and Wall Stiffness in relation to Reinforced Soil Wall Design", Ph.D. Dissertation, Purdue University
- [31] Clayton, C. R. I., Woods, R. I., Bond, A. J. and Militisky, J (2013). "Earth Pressure and Earth-Retaining Structures", 3rd Edition. CRC Press, New York.
- [32] Collin, J.G. (1988), "Earth Wall Design", Ph.D. Dissertation, University of California, Berkley, Civil Engineering Department.
- [33] Coulomb C.A., (1776). Essai Sur Une Application Des Regles des Maximis Et Minimis A Quelques Problemes De Statique Relatifs A L'architecture. Memoires de l'Academie Royale pres Divers Savants, Vol. 7

- [34] Crigler, J. R. (1999). "Mechanically Stabilized Retaining Wall System Having Adjustable Connection Means for Connecting Precast Concrete Facing Panels Thereto", U.S. Patent 5,971,669, October 22, 1999.
- [35] Das, B. M. and Shukla, S. K. (2013). "Earth Anchors", 2nd Edition. J. Ross Publishing Inc., Plantation, Florida.
- [36] De Beer, E. E., "Donnees Concernant la Resistance au Cisaillement Deduites des Essais de Penetration en Profondeur." *Geotechnique*, 1: 22-40 (1948).
- [37] De Beer, E. E., " Etude des Fondations sur Pilotis et Des Fondations Directes." *Annales des Travaux Publics de Belgique*,46: 1-78 (1945).
- [38] Duncan, J. M. and Chang, C. Y. (1970). "Nonlinear Analysis of Stress and Strain in Soils", *Journal of Soil Mechanics and Foundations Division, Proceedings of the American Society of Civil Engineers*, September 1970.
- [39] Duncan, J. M. and Seed, R. B. (1984). "SSCOMP: A Finite Element Analysis Program for Evaluation of Soil-Structure Interaction and Compaction Effects", Report No. UCB/GT/84-02, Department of Civil Engineering, University of California at Berkley.
- [40] Duncan, J. M., Byrne, P., Wong, K. S. and Marby, P (1980). "Strength, Stress-Strain and Bulk Modulus Parameters for Finite Element Analyses of Stresses and Movements in Soil". Report No. UCB/GT/80-01 College of Engineering, Office of Research Services, University of California, Berkeley, California.
- [41] Ehrlich, M.E. and Mitchell J.K., (1994). "Working Stress Design Method for Reinforced Soil Walls", *Journal of Geotechnical Engineering*, Vol 120, No. 4, pp. 625-645.
- [42] Fahmy, R. F. Wilson and Koerner, R. M. (1993). "Finite element modelling of soil-geogrid interaction with application to the behavior of geogrids in a pullout loading condition", *Geotextiles and Geomembranes*, Volume 12, Issue 5, Pages 479-501.
- [43] Florida Department of Transportation (2018), "Approved Product List", Retrieved from <https://fdotws1.dot.state.fl.us/ApprovedProductList/Products/Index/767>
- [44] Forsyth, R. A. (1978). "Alternate earth reinforcements." *Proc., ASCE Symp. on Reinforced Earth, Committee on Placement and Improvement of Soils of the Geotechnical Engineering Division of ASCE*, 358–370.

- [45] Han, Jei (2015). "Principles and Practices of Ground Improvement". John Wiley & Sons, Inc., Hoboken, New Jersey.
- [46] Handy, R. L. (1985). "The Arch in Soil Arching", *Journal of Geotechnical Engineering*, Volume III, No. 3, pages 302-317.
- [47] Handy, R. L. and Spangler, M. G. (2007). "Geotechnical Engineering: Soil and Foundation Principles and Practice, Fifth Edition". McGraw-Hill Companies, New York, New York, pg. 544-555
- [48] Hilfiker Retaining Walls (2018). Retrieved from <http://www.hilfiker.com/>
- [49] Huang, B., and Bathurst, R. J. (2009). "Evaluation of soil-geogrid pullout models using a statistical approach." *ASTM Geotech. Test. J.*, 32(6), 489–504.
- [50] Huang, B., Bathurst, R. J., and Allen, T. M. (2012). "Load and resistance factor design (LRFD) calibration for steel strip reinforced soil walls." *J. Geotech. Geoenviron. Eng.*, 10.1061/(ASCE)GT.1943-5606.0000665, 922–933.
- [51] Hunt, R. E., (1985). "Geotechnical Engineering Techniques and Practices". McGraw-Hill Inc.
- [52] Huntington, W. C. (1957). "Earth Pressures and Retaining Walls". John Wiley and Sons, Inc. London.
- [53] Jaber, M. (1989), "Behavior of Reinforced Soil Walls in Centrifuge Model Tests", Dissertation submitted in partial satisfaction of the requirements for the degree of Doctor of Philosophy, University of California, Berkeley, Department of Civil Engineering, March, 1989.
- [54] Janbu N., (ed.). "Static bearing capacity of friction piles". *Proceedings of the 6th European Conference on Soil Mechanics and Foundation Engineering*, 1976, Vol. 1.2, 479–488
- [55] Jaky, J. (1944). "The Coefficient of Earth Pressure at Rest", *Journal of the Society of Hungarian Architects and Engineers*, October, 1944, pp. 355-358.
- [56] Jaky, J., "On the Bearing Capacity of Piles", *Proceedings of the Second International Conference of Soil Mechanics and Foundation Engineering*, 1: 100-103, Rotterdam (1948).
- [57] Jayawickrama, P. W., Surles, J. G., Wood, T. A., and Lawson, W. D. (2013). "Pullout resistance of mechanically stabilized earth reinforcement in backfills

typically used in Texas: Volume 1.” Rep. No. 0-6493-1, Texas Dept. of Transportation, Austin, TX.

- [58] Jewell, R.A., (1984). “Reinforcement Bond Capacity”, *Geotechnique* 40, No. 3, 513-518.
- [59] Jewell, R. A., Milligan, G. W. E., Sarsby, R. W., and Dubois, D. (1984). “Interaction between soil and geogrids.” *Proc., Symp. on Polymer Grid Reinforcement in Civil Engineering*, Thomas Telford, London, 18–30.
- [60] Jones, C. J. F. P. (1985). “Earth Reinforcement and Soil Structures”, *Butterworths Advance Series in Geotechnical Engineering*.
- [61] Jumikis, A. R., (1962). “Soil Mechanics”, D. Van Nostrand Company, Inc., New York, New York.
- [62] Juran, I. (1985). "Behavior of Reinforced Soil Structures", Research Report No. 1 to the U.S. Department of Transportation, Federal Highway Administration, FHWA No. 61-84-C-00072, 31 p.
- [63] Juran, I., and Schlosser, F. (1978). “Theoretical Analysis of Failure in Reinforced Earth Structures”, *Proceedings, ASCE Symposium on Earth Reinforcement*, Pittsburgh, pp. 528-555.
- [64] Kerisel, J. (1961). Deep foundations in sands. Variation of ultimate bearing capacity with soil density, depth, diameter ,and speed. *Proc 5th ICSMFE Paris*
- [65] Keystone Retaining Wall Systems, (2018). Retrieved from <http://www.keystonewalls.com/>
- [66] Kondner, R.L. and Zelasko, J.S. (1963),” A Hyperbolic Stress-Strain Formulation of Sands”, *Proceedings of the 2nd Pan American Conference on Soil Mechanics and Foundation Engineering, Brazil, Vol 1*, pp 289-324
- [67] Lawson, W. D., Jayawickrama, P. W., Wood, T. A., and Surles, J. G. (2013). “Pullout resistance factors for inextensible mechanically stabilized earth reinforcements in sandy backfill.” *Transportation Research Record* 2363, Transportation Research Board, Washington, DC, 21–29.
- [68] Leshchinsky, D., Kang, B., Han, J., and Ling, H (2014). “Framework for Limit State Design of Geosynthetic-Reinforced Walls and Slopes”, *Journal of Transportation Infrastructure Geotechnology*.

- [69] Leshchinsky, D., Leshchinsky, O., Zelenko, B., and Horne, J. (2016). "Limit Equilibrium Design Framework for MSE Structures with Extensible Reinforcement", Report No. FHWA-HIF-17-004, Federal Highway Administration.
- [70] Macnab, A. (2002). "Earth Retention Systems Handbook". McGraw-Hill, New York.
- [71] Meyerhof, G. G. (1953). "The Bearing Capacity of Foundations Under Eccentric and Inclined Loads", Proceedings of the Third International Conference of Soil Mechanics and Foundation Engineering, Vol. 1, pp. 225-244.
- [72] Miyata, Y., and Bathurst, R. J. (2012). "Analysis and calibration of default steel strip pullout models used in Japan." Soils Found., 52(3), 481–497.
- [73] McKittrick, D.P. (1978). "Reinforced Earth: Application of Theory and Research to Practice", keynote paper, Symposium on Soil Reinforcing and Stabilizing Techniques, Sydney, Australia.
- [74] Mitchel, J.K. and Villet, W.B.C. (1987). "Reinforcement of Earth Slopes and Embankments", NCHRP Report No. 290, Transportation Research Board, Washington D.C.
- [75] Mitchel, R.J. (1983). "Earth Structures Engineering", Alan And Unwin, Inc., Pp. 39-61.
- [76] McGown, A., Andrawes, K. Z. and Al Hasani, M. M. (1978). "Effect of Inclusion Properties on the Behavior of Soils," Geotechnique 28, pp. 327-346.
- [77] NCHRP 290 (1987). "National Cooperative Highway Research Program Report 290, Reinforcement of Earth Slopes and Embankments," Transportation Research Board, Washington, D.C.
- [78] National Highway Institute (2009). "Design and Construction of Mechanically Stabilized Earth Walls and Reinforced Soil Slopes", FHWA-NHI-10-024 and 025, Volumes I and II, NHI Course Nos. 132042 and 132043, November 2009.
- [79] Neely, W. J. (1993). "Field Performance of a Retained Earth Wall", Reinforcement Des Sols: Experimentations en Vraie Grandeur des Annees 80, Paris, pp. 171-200.
- [80] Neely, W. J. (1995). "Pullout-out resistance of VSL bar mats for use with the FHWA structure stiffness design method." Demonstration Project No. 82, Federal Highway Administration, Washington, DC.

- [81] Nova, R. (2004). "Development of Elastoplastic Strain Hardening Models of Soil Behavior", *Degradations and Instabilities in Geomaterials*, International Centre for Mechanical Sciences Volume 461, 2004, pp 35-76.
- [82] Palmeira, E. M., and Milligan, G. W. E. (1989). "Scale and other actors affecting the results of pullout tests of grids buried in sand." *Geotechnique*, 39(3), 511–524.
- [83] Peterson, L. M., and Anderson, L. R. (1980). "Pullout resistance of welded wire mats embedded in soil." Dept. of Civil and Environmental Engineering, Utah State Univ., Logan, UT.
- [84] Plaxis 2D AE.02 (2014). "Reference Manual 2D" Plaxis B.V., Delft University of Technology, The Netherlands.
- [85] Plaxis 3D (2013). "Reference Manual 3D" Plaxis B.V., Delft University of Technology, The Netherlands.
- [86] Prandtl, L. (1920). "Uber die Harte plastischer Karper." *Nachrichten Kon. Gesell. der Wissenschaften, Math. Phys. Klasse*, 74-85, Gottingen.
- [87] Prandtl, L. (1921). "Uber die Eindringungsfestigkeit plastischer Baustoffe und die Festigkeit von Schneiden." *Zeitschrift fur Angewandte Mathematik und Mechanik*, 1: 1, 15-20.
- [88] Reissner, H. (1924), "Zurn Erddruckproblem." *Proc. First Intern. Conf. Applied Mech.*, 295-311, Delft.
- [89] Reese, L. C., (1964), "Load Versus Settlement of Axial Loaded Piles." *Proceedings of the Symposium on Bearing Capacity of Piles, Part 2*, Center Building Research Institute, Roorkee, India, Cement and Concrete, New Delhi, India, pp. 18-38.
- [90] Reinforced Earth Company (2018). Retrieved from <http://www.reinforcedearth.com/>.
- [91] Sampaoc, Casan L. (1994). "Behavior of Welded Wire Mesh Reinforced Soil Walls from Filed Evaluation and Finite Element Simulation", Ph.D. Thesis, Utah State University, Civil and Environmental Engineering
- [92] Schanz, T. and Vermeer, P.A. (1996). "Angles of Friction and Dilatancy of Sand", *Geotechnique* 46, No. 1, pg. 145-151

- [93] Schlosser, F. (1978). "History, Current Development, and Future Developments of Reinforced Earth", Symposium on Soil Reinforcing and Stabilizing Techniques, sponsored by New South Wales Institute of Technology and the University of Sydney, Austral.
- [94] Schlosser, F., and Elias, V. (1978). "Friction in reinforced earth". Proceedings of ASCE Symposium on earth Reinforcement, Pittsburg, PA, pp. 735-763.
- [95] Schlosser, F. (1990). "Mechanically Stabilized Earth Structures in Europe", Performance of Reinforced Earth Structures, Proceedings of the International Reinforced Soil conference, British Geotechnical Society, Glasgow.
- [96] Schmertmann, G., Chew, S.H., and Mitchell, J. (1989). "Finite Element Modelling of Reinforced Soil Wall Behavior," Geotechnical Engineering Report No. UCB/GT/89-01, University of California, Berkeley, September 1989.
- [97] Segrestin, P. and Bastick, M. (1996). "Comparative Study and Measurement of the Pullout Capacity of Extensible and Inextensible Reinforcements," International Symposium on Earth Reinforcement, Fukuoka, Kyushu,
- [98] Simac, M.R., Christopher, B.R., Bonczkiewicz, C. (1990). "Instrumented Field Performance of a 6-m Geogrid Soil Wall," Proceedings, 4th International Conference on Geotext.
- [99] Sine Wall (2018). Retrieved from <http://sinewall.com>.
- [100] Tanyu, B. F., Sabatini, P. J., and Berg, R. R. (2007). "Earth Retaining Structures", FHWA-NHI-07-071. National Highway Institute, Washington D.C.
- [101] Terzaghi, K (1936). "A Fundamental Fallacy in Earth Pressure Computations". Journal Boston Society of Civil Engineers reprinted in Contributions to Soil Mechanism 1924-1940 by the Society, Boston, Massachusetts.
- [102] Terzaghi, K (1943). "Theoretical Soil Mechanics". John Wiley and Sons, Inc., New York, New York.
- [103] Terzaghi, K, Peck, R. A. and Gholamreza, M (1996). "Soil Mechanics in Engineering Practice – 3rd Edition". John Wiley and Sons, Inc., New York, New York.
- [104] Vidal, H (1969) "The Principle of Reinforced Earth," Highway Research Record 282, pp. 1-16, 1969.

- [105] Vesic, A. B. (1963). "Bearing Capacity of Deep Foundations in Sand", Highway Research Record, No. 39, pp. 112-153.
- [106] Vesic, A. B. (1972). "Expansion of Cavities in Infinite Soil Mass", Journal of the Soil Mechanics and Foundations Division, Vol. 98, No. 3, pp. 661-688.
- [107] Weldu, M. T., Han, J., Rahmaninezhad, S. M., Parsons, R., L., and Kakrasul, J., I., (2015). " Pullout Resistance of Mechanically Stabilized Earth Wall Steel Strip Reinforcement in Uniform Aggregate". Report No. K-TRAN: KU-14-7, University of Kansas.
- [108] Wire Reinforcement Institute, Inc. (2016). "Manual of Standard of Practice – Structural Welded Wire Reinforcement (9th ed.)".
- [109] Winkerton, Hans F. and Fang, Hsai-Yang, (1975). "Foundation Engineering Handbook", Van Nostrand Reinhold Company, Chapters 3, 5, and 7.
- [110] Wong, Wing L. (1989). "Field Performance of Welded Wire Wall", M.S. Thesis, Utah State University, Civil and Environmental Engineering.
- [111] Vistawall, (2018). Retrieved from <https://www.bigrbridge.com/>
- [112] Xanthakos, P. P. (1991). "Ground Anchors and Anchored Structures". John Wiley and Sons, New York.
- [113] Zevgolts, I., and Bourdeau, P.L. (2007). "Mechanically Stabilized Earth and Wall Abutments for Bridge Support". FHWA/IN/JTRP-2006/38. Joint Transportation Research Program, Indiana Department of Transportation and Purdue University, West Lafayette Indiana.



## Biographical Information

Thomas (Tom) Patrick Taylor received a Bachelor of Science degree in Architectural Engineering from the University of Wyoming in 1990. He received a Master of Science in Civil Engineering from the University of Texas at Arlington in 2015. Tom worked as a design engineer until 1995. In February 1995 he founded T&B Structural Systems LLC. In February of 2007 T&B Structural Systems was acquired by the Atlantic Bridge Group. At that time T&B Structural Systems became Vistawall Systems. Tom is presently Vice President and Director of Research and Development for Vistawall Systems a division of Big-R Bridge. He is a registered professional engineer in 14 states and 2 Canadian provinces. Tom's research interests are in earth structures, ground improvements, and numerical modelling. He has 30 United States and Foreign patents and patents pending that are primarily concerned with Earth Structures. He has developed the proprietary software program MSE-Pro that is used in the design and analysis of Mechanically Stabilized Earth Structures.

**This Page Intentionally Left Blank**

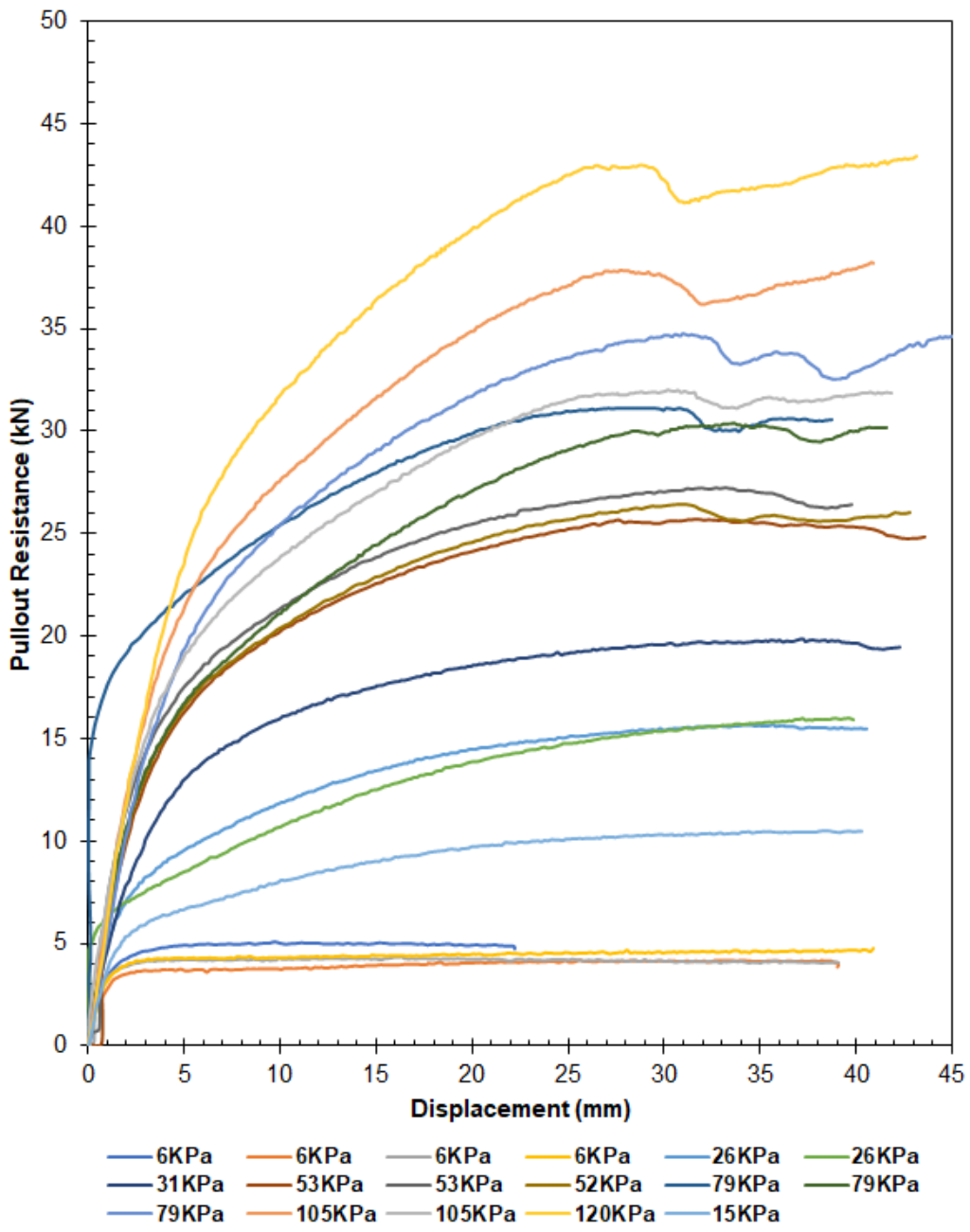
## **Appendix A**

### **Test Data**

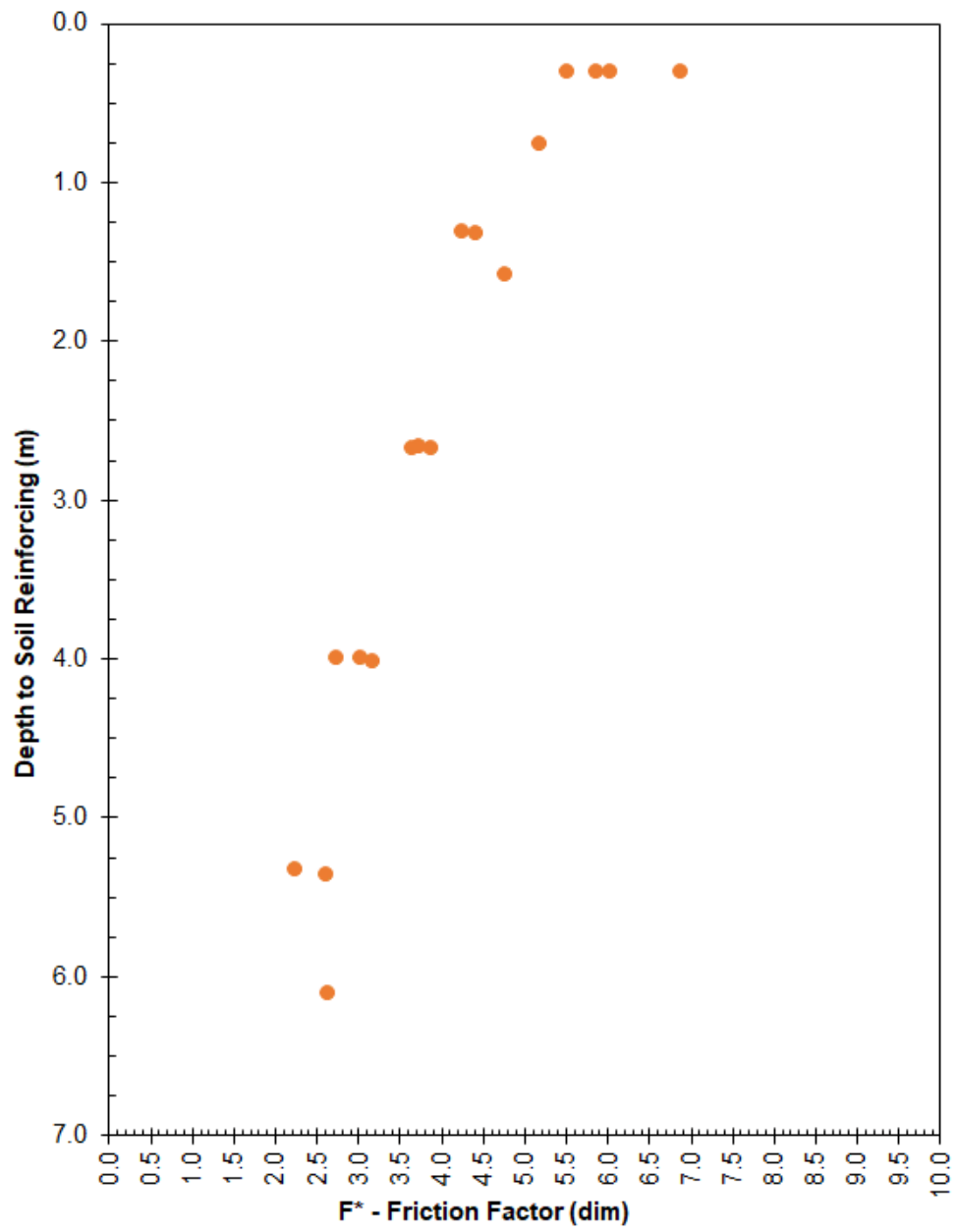
**This Page Intentionally Left Blank**

MW71 x MW71 – 50 mm x 300 mm

| <b>Test</b> | <b>Name</b> | <b>Surcharge<br/>(kPa)</b> | <b>P<sub>r,19 mm</sub><br/>(kN)</b> | <b>F*<sub>19 mm</sub><br/>(dim)</b> | <b>P<sub>r,peak</sub><br/>(kN)</b> | <b>F*<sub>peak</sub><br/>(dim)</b> |
|-------------|-------------|----------------------------|-------------------------------------|-------------------------------------|------------------------------------|------------------------------------|
| 1           | 6-T1        | 6                          | 5.10                                | 6.88                                | 5.10                               | 6.88                               |
| 2           | 6-T2        | 6                          | 4.09                                | 5.51                                | 4.19                               | 5.65                               |
| 3           | 6-T3        | 6                          | 4.35                                | 5.87                                | 4.35                               | 5.87                               |
| 4           | 6-T4        | 6                          | 4.48                                | 6.04                                | 4.75                               | 6.41                               |
| 5           | 26-T5       | 26                         | 14.30                               | 4.42                                | 15.68                              | 4.85                               |
| 6           | 25-T6       | 26                         | 13.64                               | 4.26                                | 16.01                              | 5.00                               |
| 7           | 31-T7       | 31                         | 18.36                               | 4.78                                | 19.83                              | 5.16                               |
| 8           | 53-T8       | 53                         | 23.86                               | 3.66                                | 25.69                              | 3.94                               |
| 9           | 53-T9       | 53                         | 25.25                               | 3.87                                | 27.27                              | 4.18                               |
| 10          | 53-T10      | 52                         | 24.29                               | 3.74                                | 26.43                              | 4.07                               |
| 11          | 79-T11      | 79                         | 29.54                               | 3.04                                | 31.13                              | 3.20                               |
| 12          | 79-T12      | 79                         | 26.71                               | 2.75                                | 30.40                              | 3.13                               |
| 13          | 79-T13      | 79                         | 31.18                               | 3.19                                | 34.76                              | 3.55                               |
| 14          | 105-T14     | 105                        | 34.31                               | 2.63                                | 38.23                              | 2.93                               |
| 15          | 105-T15     | 105                        | 29.21                               | 2.26                                | 32.00                              | 2.47                               |
| 16          | 120-T16     | 120                        | 39.19                               | 2.64                                | 43.41                              | 2.92                               |
| 17          | 15-T17      | 15                         | 9.62                                | 5.18                                | 10.51                              | 5.66                               |
| 18          |             |                            |                                     |                                     |                                    |                                    |
| 19          |             |                            |                                     |                                     |                                    |                                    |
| 20          |             |                            |                                     |                                     |                                    |                                    |



MW71 x MW71 – 50 mm x 300 mm

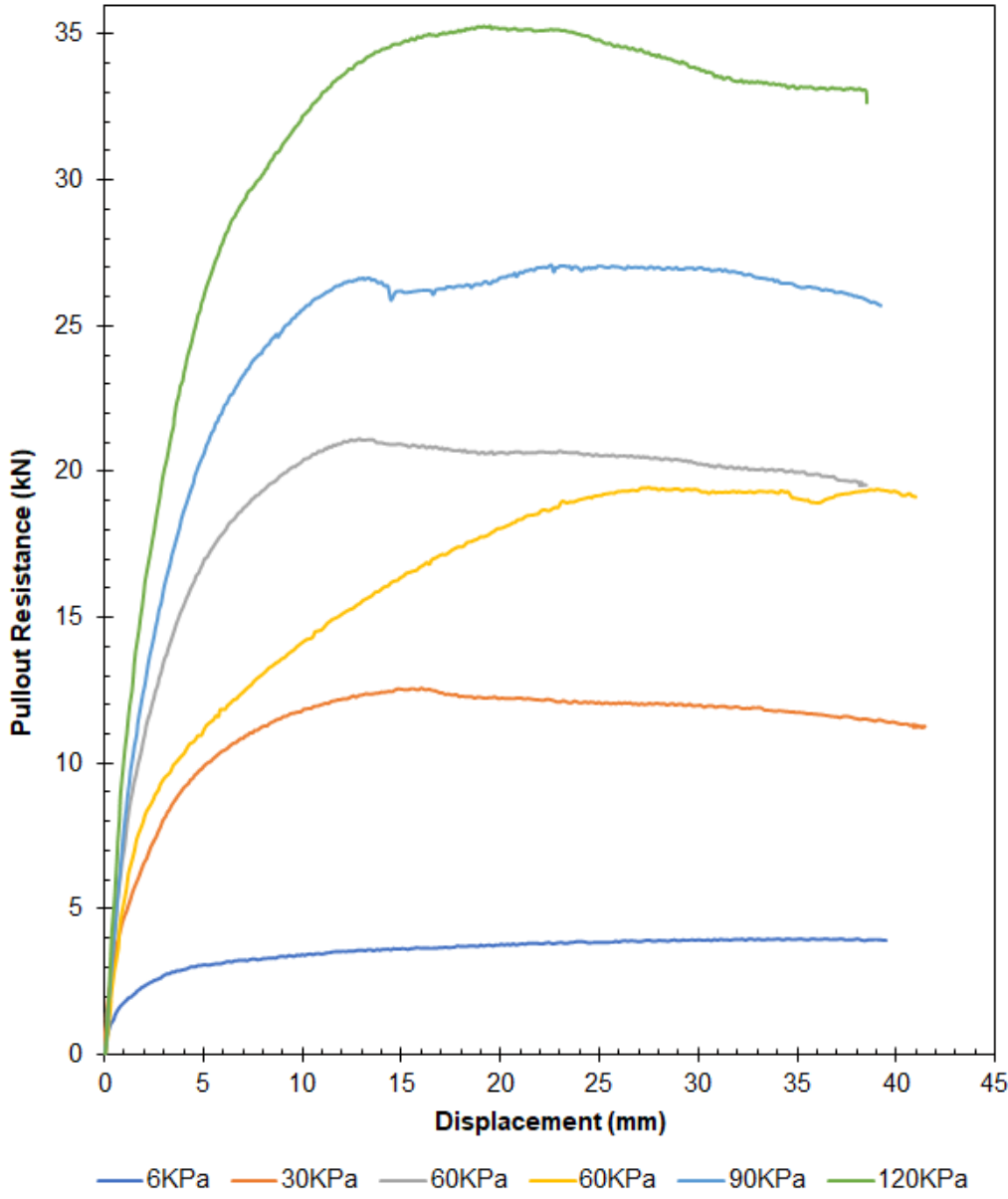


MW71 x MW71 – 50 mm x 300 mm

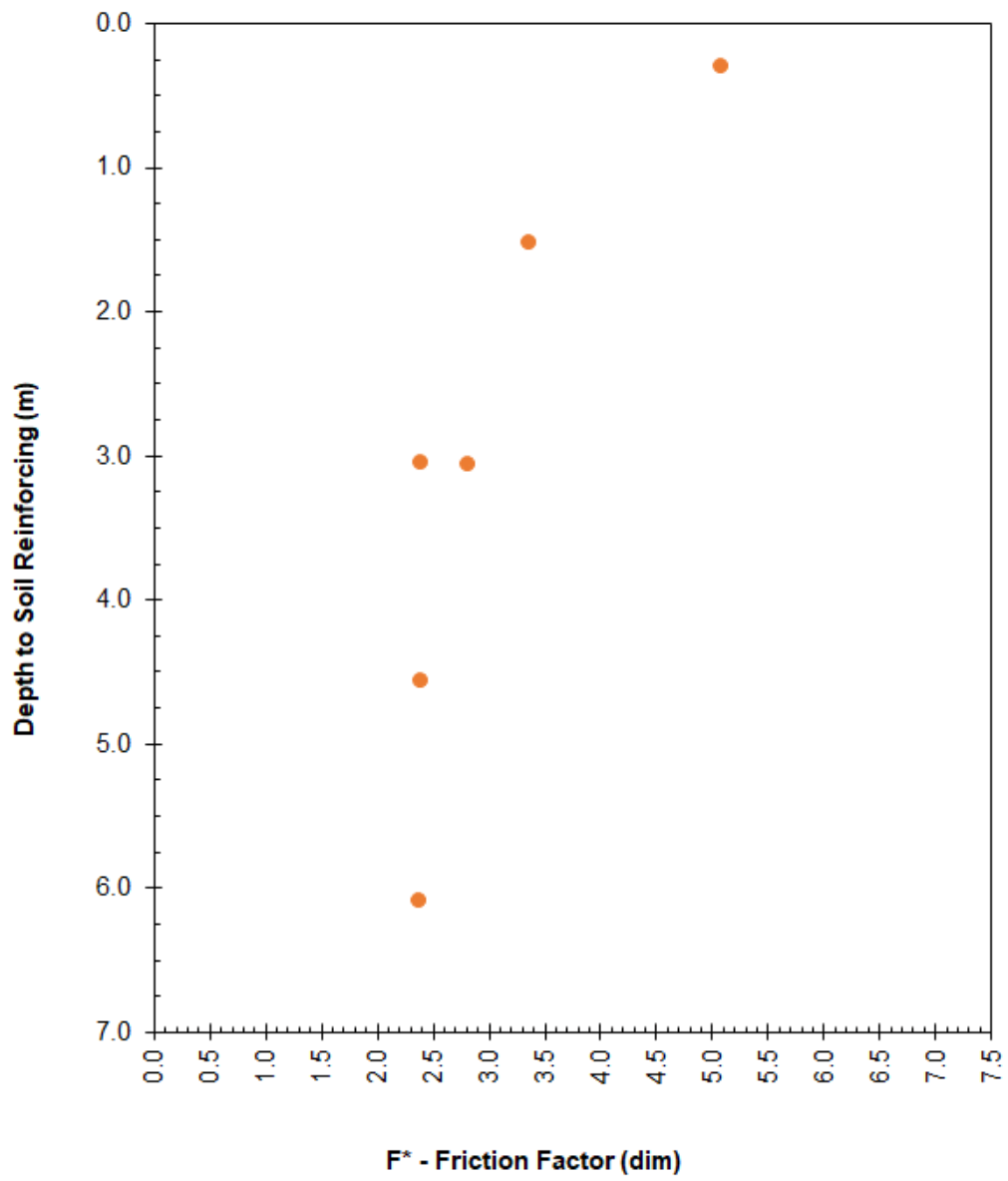
MW71 x MW71 – 50 mm x 150 mm

| <b>Test</b> | <b>Name</b> | <b>Surcharge<br/>(kPa)</b> | <b>P<sub>r_19 mm</sub><br/>(kN)</b> | <b>F*<sub>19 mm</sub><br/>(dim)</b> | <b>P<sub>r_peak</sub><br/>(kN)</b> | <b>F*<sub>peak</sub><br/>(dim)</b> |
|-------------|-------------|----------------------------|-------------------------------------|-------------------------------------|------------------------------------|------------------------------------|
| 1           | 6-T1        | 6                          | 3.77                                | 5.09                                | 3.98                               | 5.37                               |
| 2           | 30-T2       | 30                         | 12.55                               | 3.37                                | 12.55                              | 3.37                               |
| 3           | 60-T3       | 60                         | 21.10                               | 2.83                                | 21.10                              | 2.83                               |
| 4           | 60-T4       | 60                         | 17.79                               | 2.39                                | 19.48                              | 2.62                               |
| 5           | 90-T5       | 90                         | 26.63                               | 2.40                                | 27.06                              | 2.43                               |
| 6           | 120-T6      | 120                        | 35.30                               | 2.38                                | 35.32                              | 2.38                               |
| 7           |             |                            |                                     |                                     |                                    |                                    |
| 8           |             |                            |                                     |                                     |                                    |                                    |
| 9           |             |                            |                                     |                                     |                                    |                                    |
| 10          |             |                            |                                     |                                     |                                    |                                    |
| 11          |             |                            |                                     |                                     |                                    |                                    |
| 12          |             |                            |                                     |                                     |                                    |                                    |
| 13          |             |                            |                                     |                                     |                                    |                                    |
| 14          |             |                            |                                     |                                     |                                    |                                    |
| 15          |             |                            |                                     |                                     |                                    |                                    |
| 16          |             |                            |                                     |                                     |                                    |                                    |
| 17          |             |                            |                                     |                                     |                                    |                                    |
| 18          |             |                            |                                     |                                     |                                    |                                    |
| 19          |             |                            |                                     |                                     |                                    |                                    |
| 20          |             |                            |                                     |                                     |                                    |                                    |





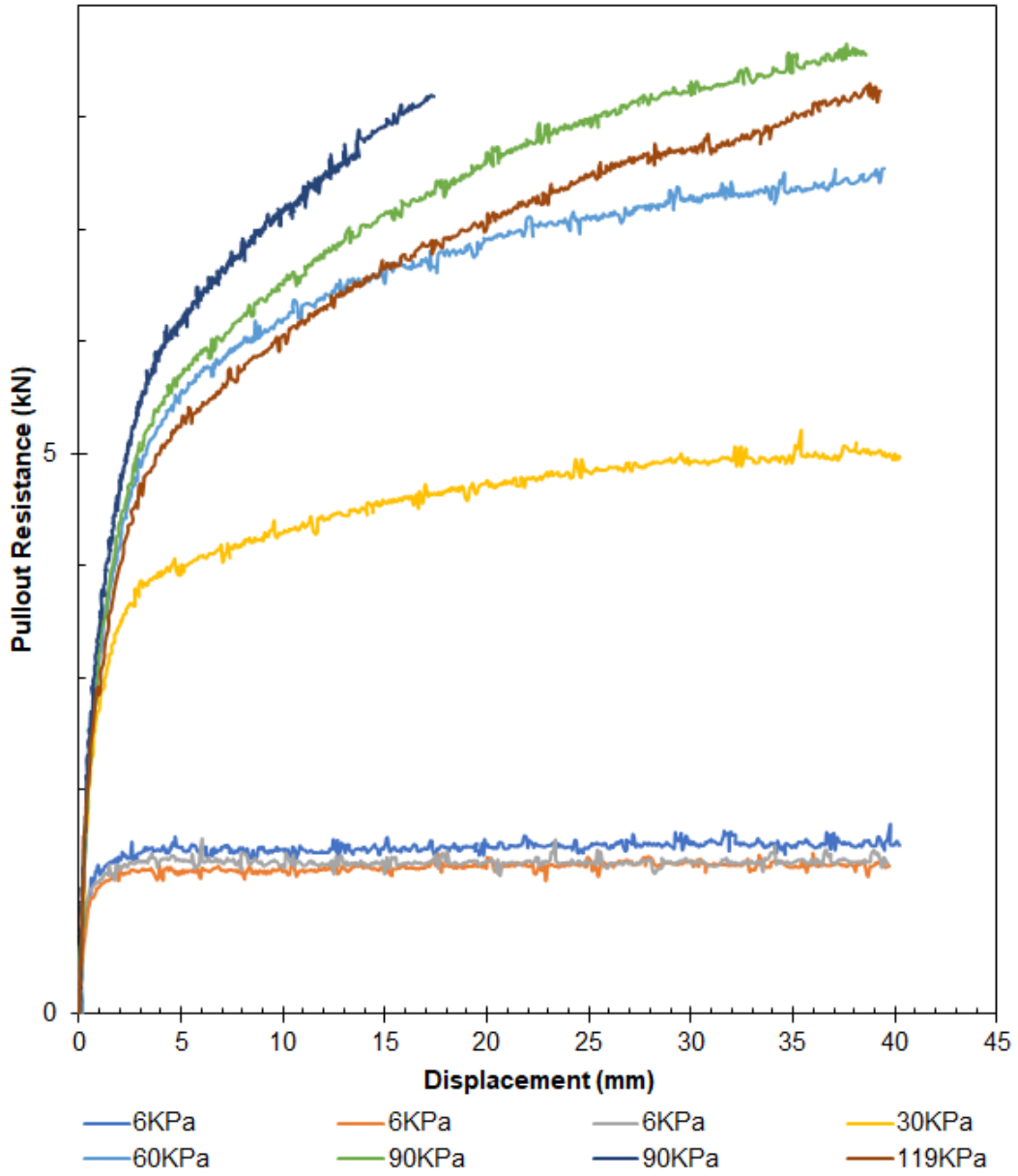
MW71 x MW71 – 50 mm x 150 mm



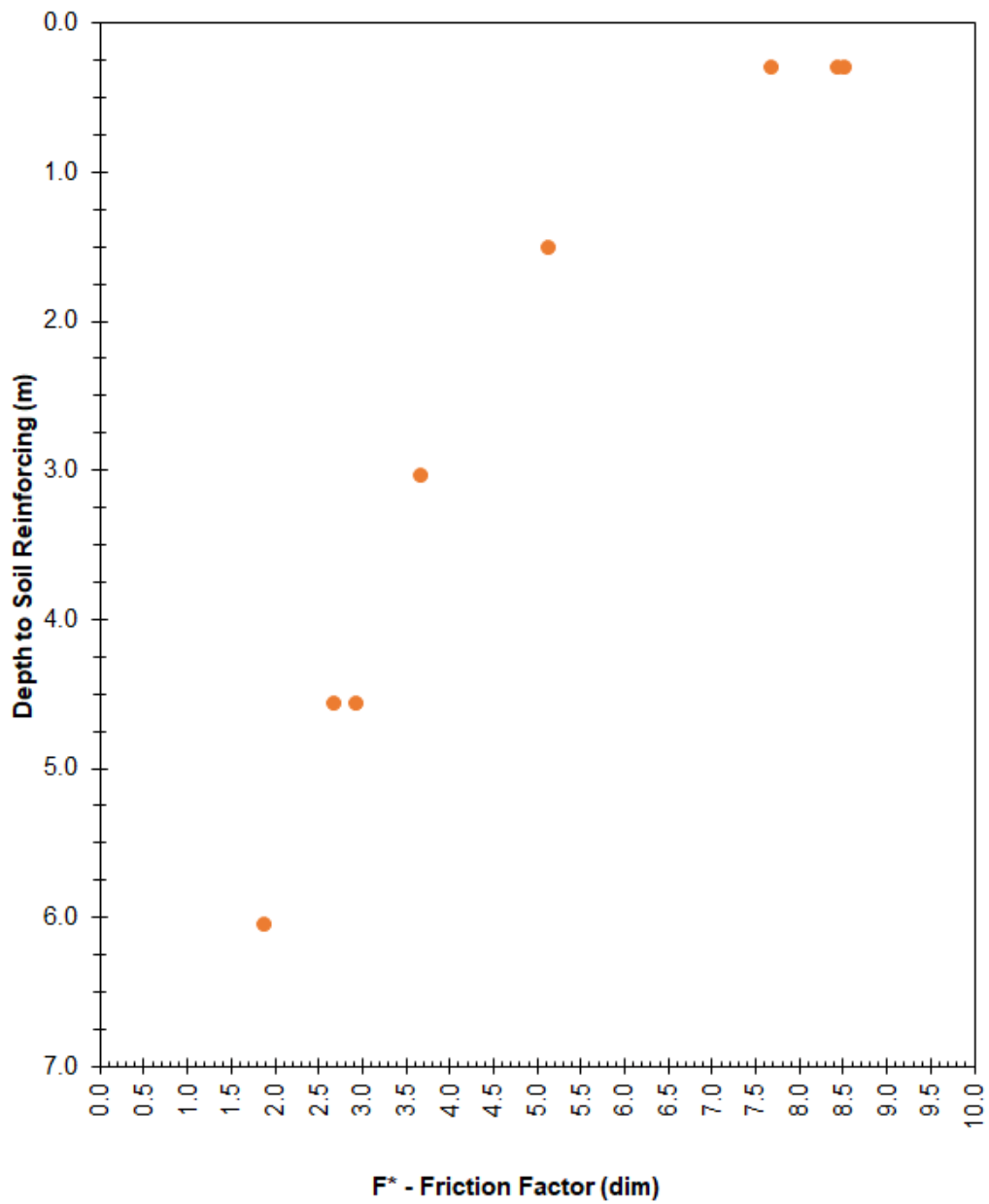
MW71 x MW71 – 50 mm x 150 mm

MW71 x MW71 – 50 mm x 1-Wire

| <b>Test</b> | <b>Name</b> | <b>Surcharge<br/>(kPa)</b> | <b>P<sub>r_19 mm</sub><br/>(kN)</b> | <b>F*<sub>19 mm</sub><br/>(dim)</b> | <b>P<sub>r_peak</sub><br/>(kN)</b> | <b>F*<sub>peak</sub><br/>(dim)</b> |
|-------------|-------------|----------------------------|-------------------------------------|-------------------------------------|------------------------------------|------------------------------------|
| 1           | 6-T1        | 6                          | 1.58                                | 8.54                                | 1.69                               | 9.14                               |
| 2           | 6-T2        | 6                          | 1.42                                | 7.69                                | 1.44                               | 7.77                               |
| 3           | 6-T3        | 6                          | 1.57                                | 8.45                                | 1.57                               | 8.45                               |
| 4           | 30-T4       | 30                         | 4.72                                | 5.14                                | 5.20                               | 5.67                               |
| 5           | 60-T5       | 60                         | 6.84                                | 3.69                                | 7.54                               | 4.07                               |
| 6           | 90-T6       | 90                         | 7.50                                | 2.70                                | 8.66                               | 3.11                               |
| 7           | 90-T7       | 90                         | 8.18                                | 2.94                                | 8.18                               | 2.94                               |
| 8           | 119-T8      | 119                        | 7.00                                | 1.90                                | 8.30                               | 2.25                               |
| 9           |             |                            |                                     |                                     |                                    |                                    |
| 10          |             |                            |                                     |                                     |                                    |                                    |
| 11          |             |                            |                                     |                                     |                                    |                                    |
| 12          |             |                            |                                     |                                     |                                    |                                    |
| 13          |             |                            |                                     |                                     |                                    |                                    |
| 14          |             |                            |                                     |                                     |                                    |                                    |
| 15          |             |                            |                                     |                                     |                                    |                                    |
| 16          |             |                            |                                     |                                     |                                    |                                    |
| 17          |             |                            |                                     |                                     |                                    |                                    |
| 18          |             |                            |                                     |                                     |                                    |                                    |
| 19          |             |                            |                                     |                                     |                                    |                                    |
| 20          |             |                            |                                     |                                     |                                    |                                    |



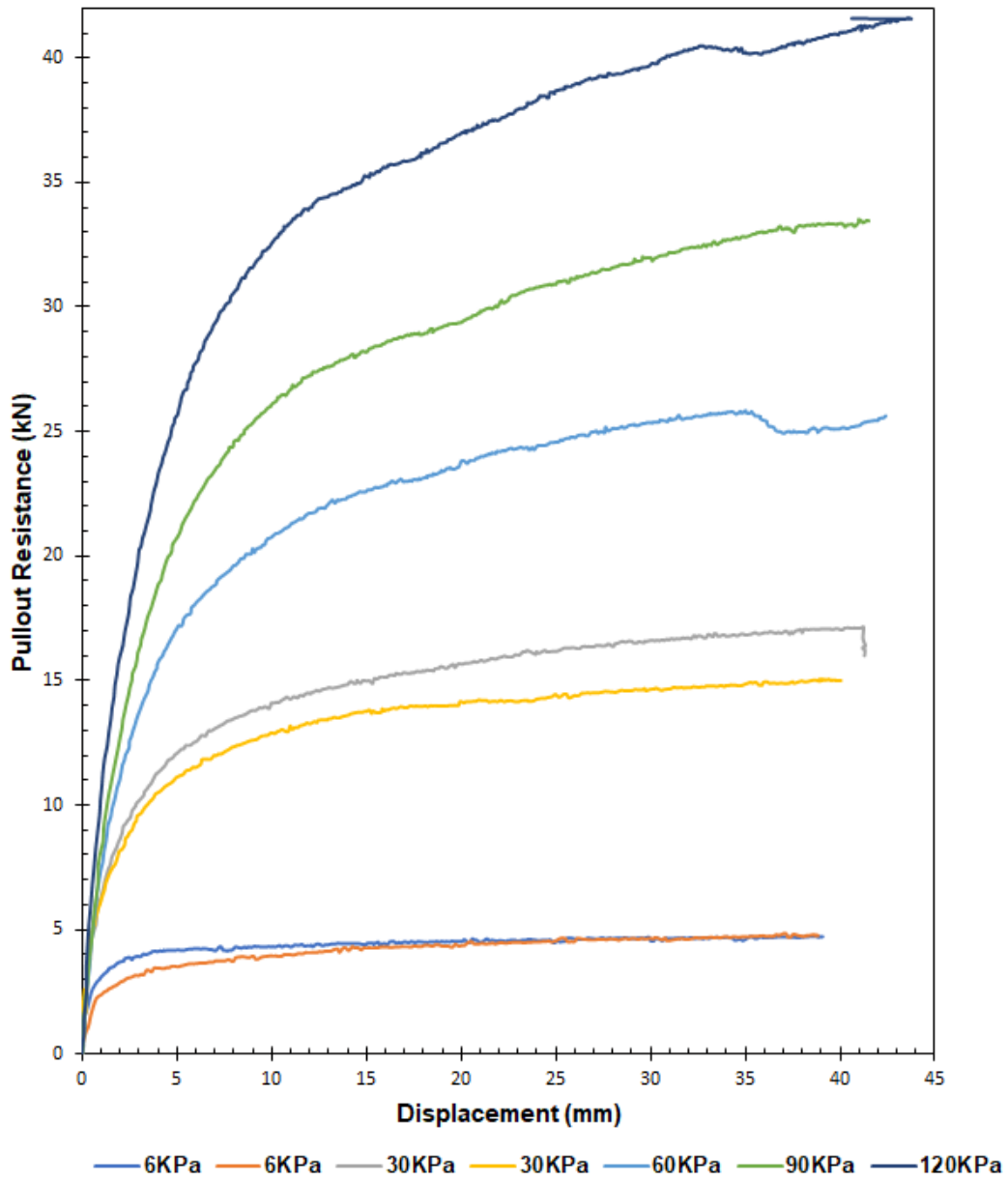
MW71 x MW71 – 50 mm x 1-Wire



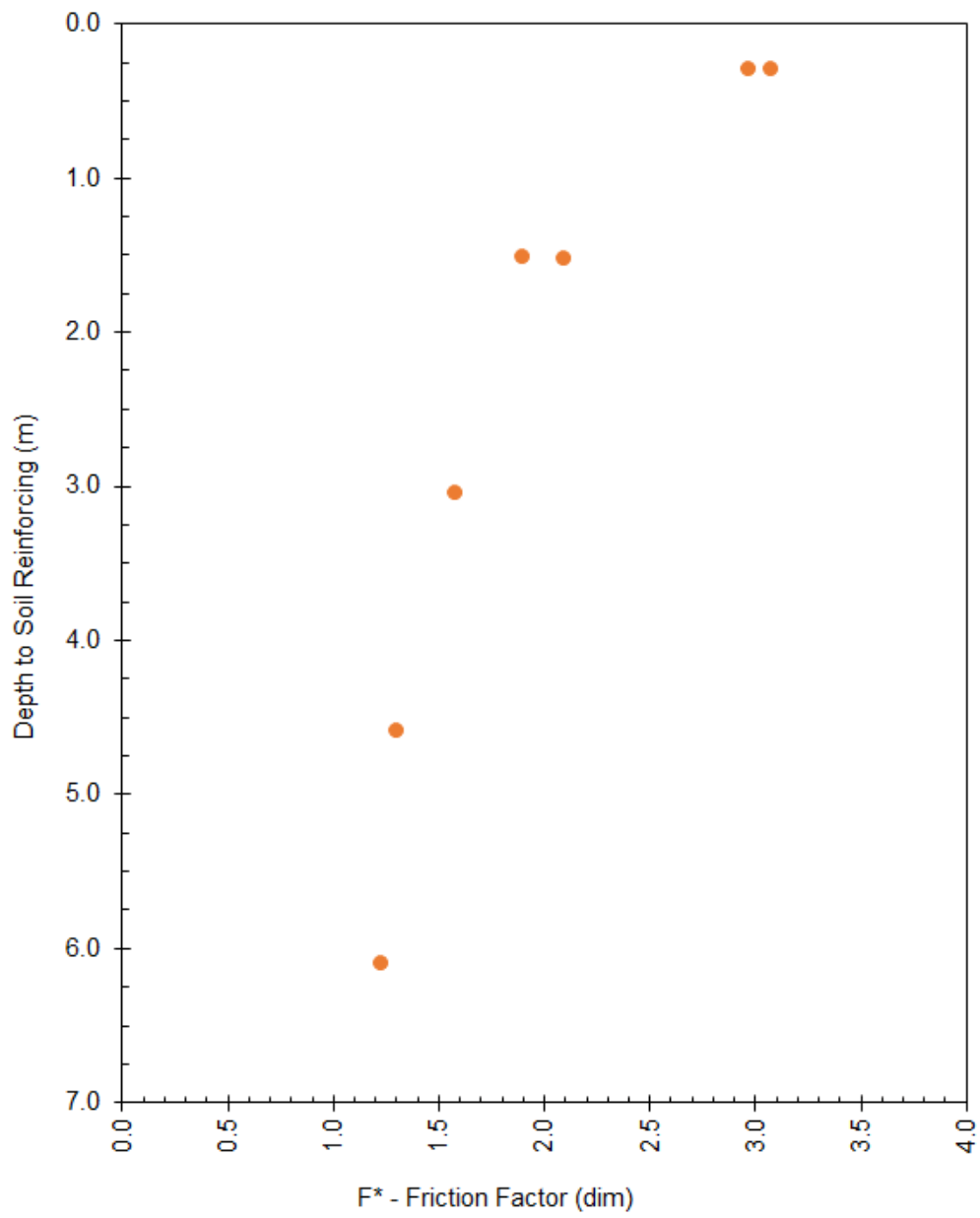
MW71 x MW71 – 50 mm x 1-Wire

MW71 x MW71 – 100 mm x 300 mm

| Test | Name   | Surcharge<br>(kPa) | P <sub>r_19 mm</sub><br>(kN) | F* <sub>19 mm</sub><br>(dim) | P <sub>r_peak</sub><br>(kN) | F* <sub>peak</sub><br>(dim) |
|------|--------|--------------------|------------------------------|------------------------------|-----------------------------|-----------------------------|
| 1    | 6-T1   | 6                  | 4.56                         | 3.08                         | 4.77                        | 3.21                        |
| 2    | 6-T2   | 6                  | 4.40                         | 2.97                         | 4.86                        | 3.28                        |
| 3    | 30-T3  | 30                 | 15.58                        | 2.10                         | 17.16                       | 2.31                        |
| 4    | 30-T4  | 30                 | 14.02                        | 1.90                         | 15.09                       | 2.04                        |
| 5    | 60-T5  | 60                 | 23.47                        | 1.58                         | 25.88                       | 1.74                        |
| 6    | 90-T6  | 90                 | 29.16                        | 1.31                         | 33.52                       | 1.50                        |
| 7    | 120-T7 | 120                | 36.57                        | 1.23                         | 41.61                       | 1.40                        |
| 8    |        |                    |                              |                              |                             |                             |
| 9    |        |                    |                              |                              |                             |                             |
| 10   |        |                    |                              |                              |                             |                             |
| 11   |        |                    |                              |                              |                             |                             |
| 12   |        |                    |                              |                              |                             |                             |
| 13   |        |                    |                              |                              |                             |                             |
| 14   |        |                    |                              |                              |                             |                             |
| 15   |        |                    |                              |                              |                             |                             |
| 16   |        |                    |                              |                              |                             |                             |
| 17   |        |                    |                              |                              |                             |                             |
| 18   |        |                    |                              |                              |                             |                             |
| 19   |        |                    |                              |                              |                             |                             |
| 20   |        |                    |                              |                              |                             |                             |



MW71 x MW71 – 100 mm x 300 mm



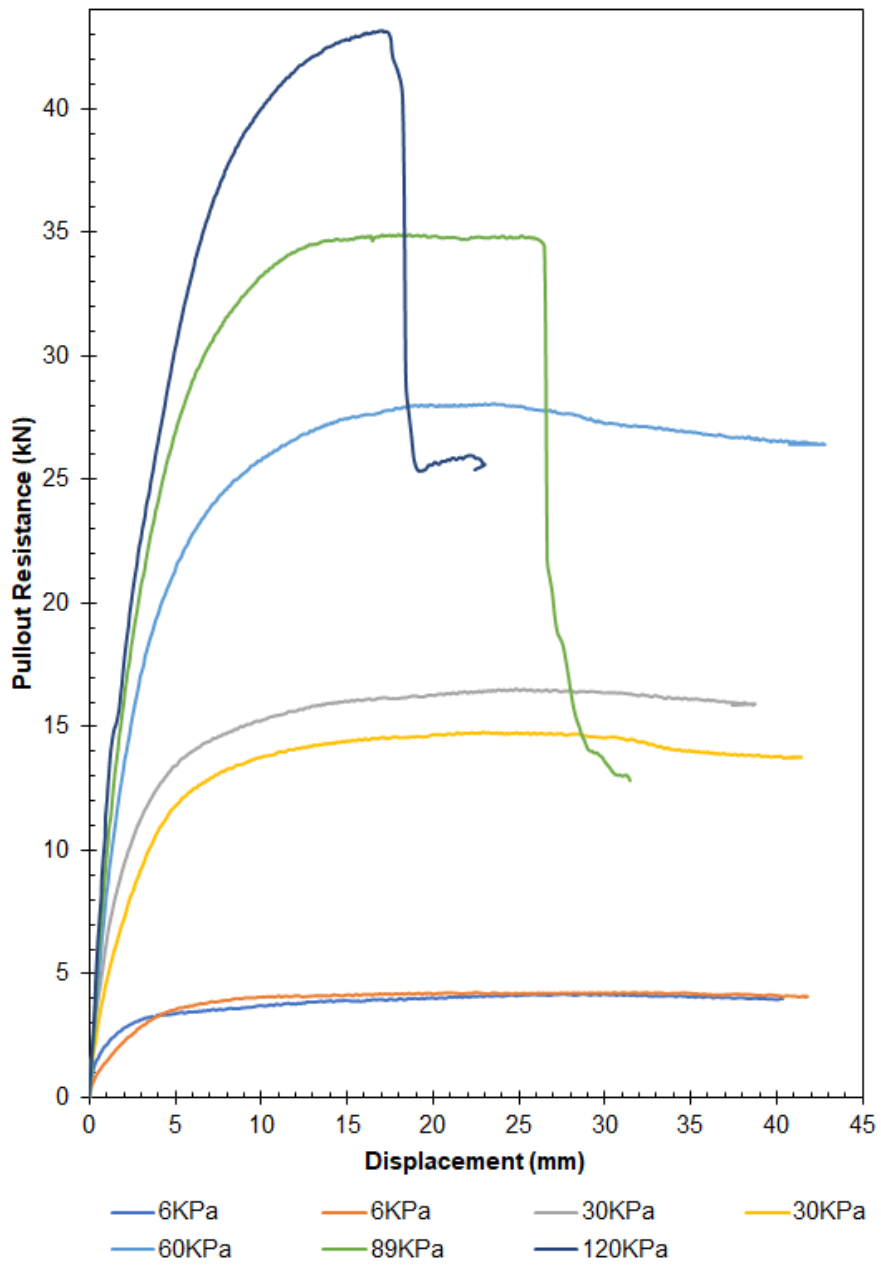
MW71 x MW71 – 100 mm x 300 mm



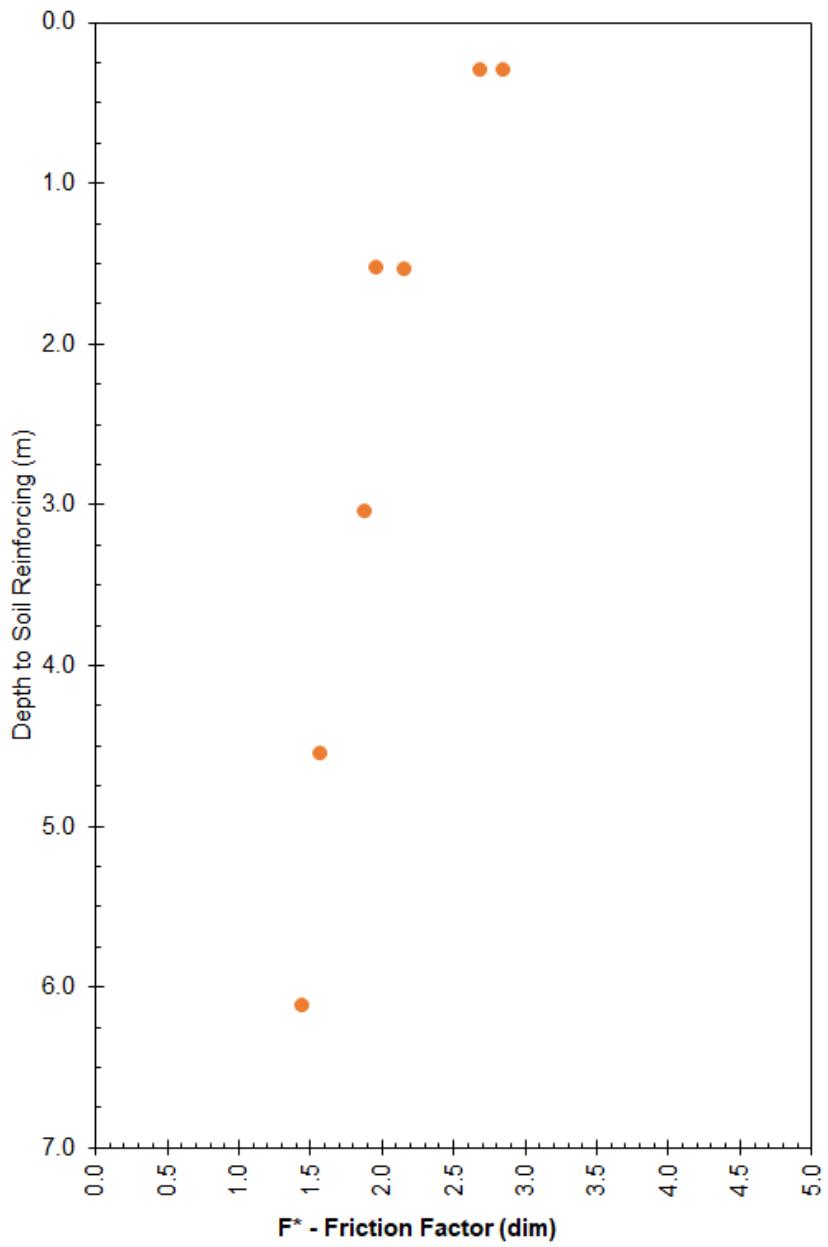
MW71 x MW71 – 100 mm x 150 mm

| Test | Name   | Surcharge<br>(kPa) | P <sub>r_19</sub><br>mm<br>(kN) | F* <sub>19 mm</sub><br>(dim) | P <sub>r_peak</sub><br>(kN) | F* <sub>peak</sub><br>(dim) |
|------|--------|--------------------|---------------------------------|------------------------------|-----------------------------|-----------------------------|
| 1    | 6-T1   | 6                  | 4.00                            | 2.70                         | 4.17                        | 2.81                        |
| 2    | 6-T2   | 6                  | 4.24                            | 2.86                         | 4.27                        | 2.88                        |
| 3    | 31-T3  | 31                 | 16.23                           | 2.16                         | 16.52                       | 2.20                        |
| 4    | 31-T4  | 31                 | 14.61                           | 1.96                         | 14.79                       | 1.99                        |
| 5    | 60-T5  | 60                 | 27.99                           | 1.89                         | 28.05                       | 1.89                        |
| 6    | 90-T6  | 90                 | 34.90                           | 1.58                         | 34.90                       | 1.58                        |
| 7    | 121-T7 | 121                | 43.17                           | 1.45                         | 43.17                       | 1.45                        |
| 8    |        |                    |                                 |                              |                             |                             |
| 9    |        |                    |                                 |                              |                             |                             |
| 10   |        |                    |                                 |                              |                             |                             |
| 11   |        |                    |                                 |                              |                             |                             |
| 12   |        |                    |                                 |                              |                             |                             |
| 13   |        |                    |                                 |                              |                             |                             |
| 14   |        |                    |                                 |                              |                             |                             |
| 15   |        |                    |                                 |                              |                             |                             |
| 16   |        |                    |                                 |                              |                             |                             |
| 17   |        |                    |                                 |                              |                             |                             |
| 18   |        |                    |                                 |                              |                             |                             |
| 19   |        |                    |                                 |                              |                             |                             |
| 20   |        |                    |                                 |                              |                             |                             |

Test 6 and Test 8 had weld failure



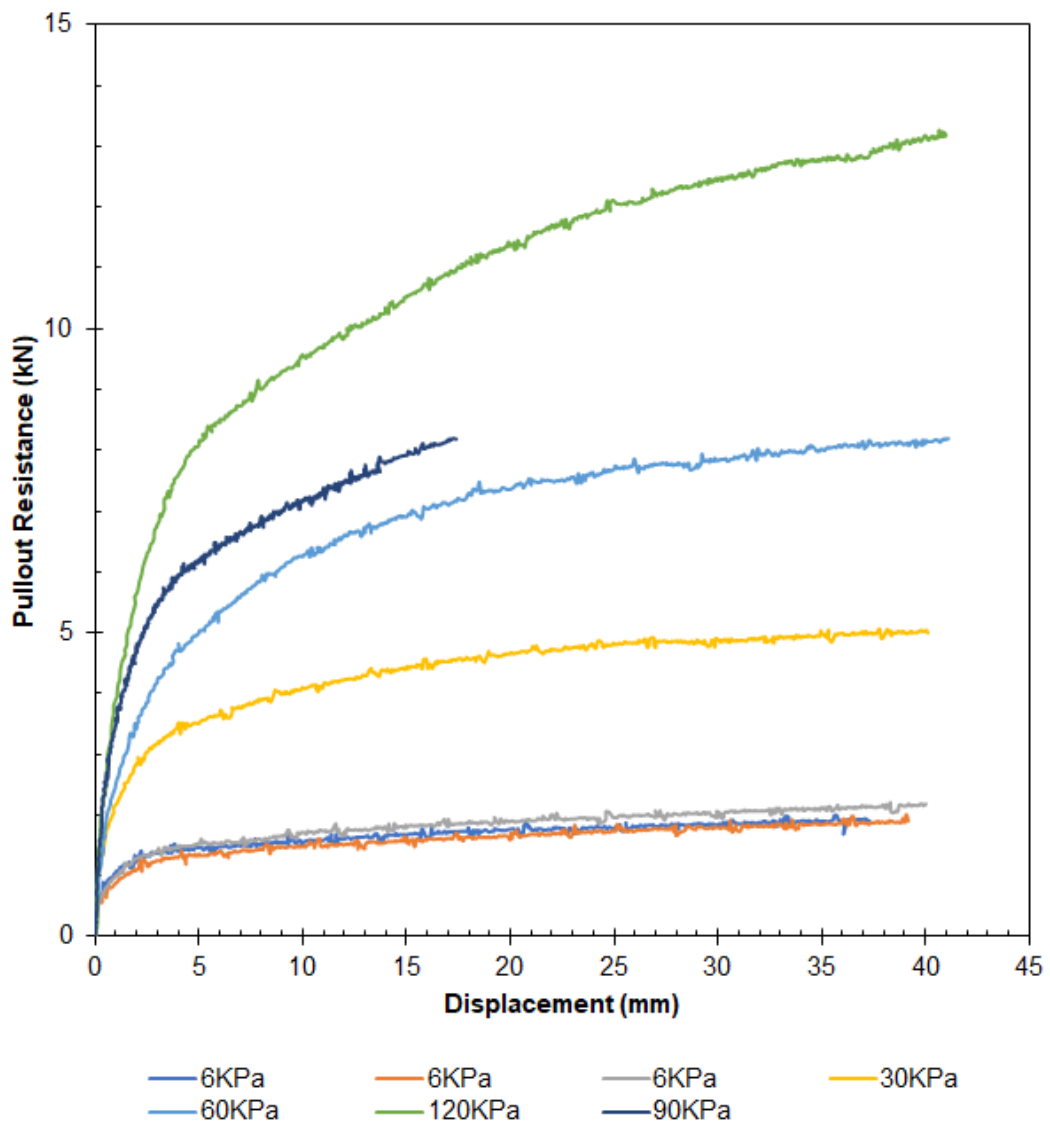
MW71 x MW71 – 100 mm x 150 mm



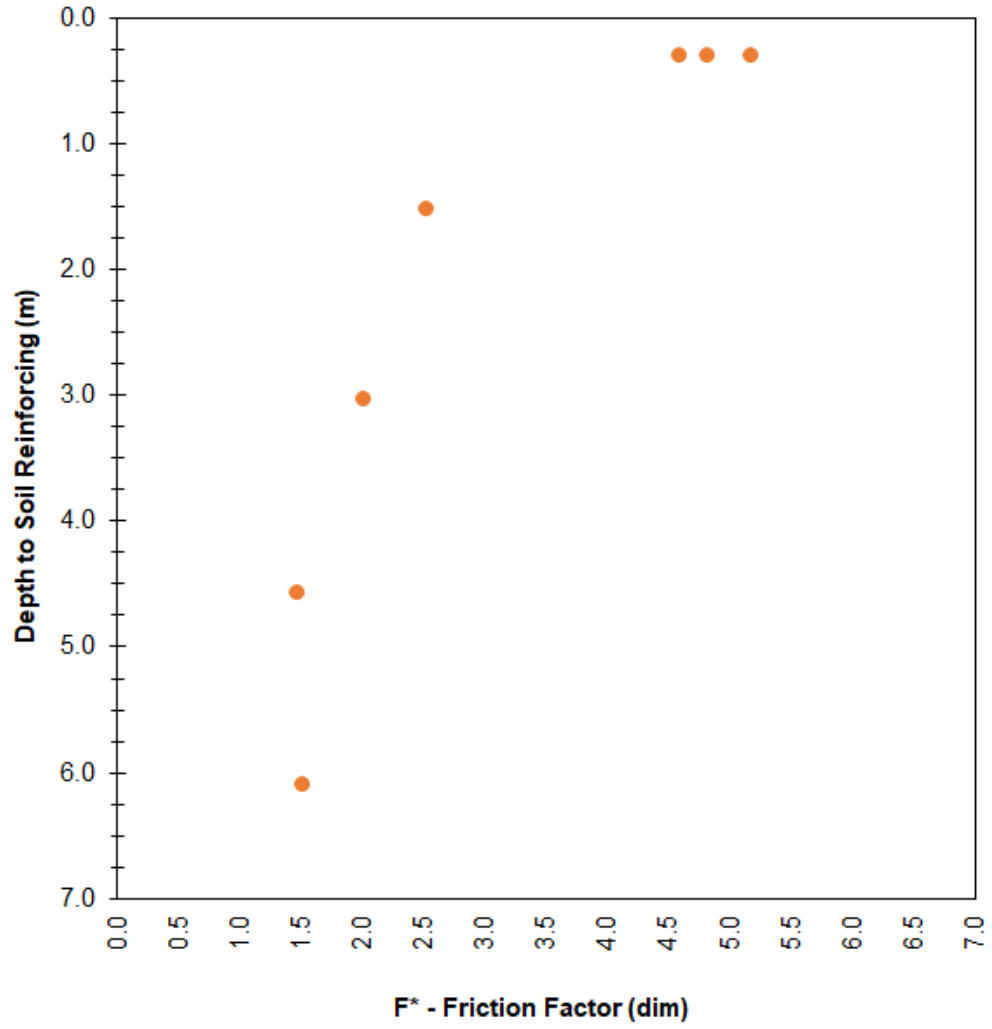
MW71 x MW71 – 100 mm x 150 mm

MW71 x MW71 – 100 mm x 1-Wire

| <b>Test</b> | <b>Name</b> | <b>Surcharge<br/>(kPa)</b> | <b>P<sub>r_19 mm</sub><br/>(kN)</b> | <b>F*<sub>19 mm</sub><br/>(dim)</b> | <b>P<sub>r_peak</sub><br/>(kN)</b> | <b>F*<sub>peak</sub><br/>(dim)</b> |
|-------------|-------------|----------------------------|-------------------------------------|-------------------------------------|------------------------------------|------------------------------------|
| 1           | 6-T1        | 6                          | 1.79                                | 4.82                                | 1.99                               | 5.36                               |
| 2           | 6-T2        | 6                          | 1.70                                | 4.60                                | 2.01                               | 5.43                               |
| 3           | 6-T3        | 6                          | 1.92                                | 5.18                                | 2.20                               | 5.93                               |
| 4           | 30-T4       | 30                         | 4.68                                | 2.53                                | 5.05                               | 2.73                               |
| 5           | 60-T5       | 60                         | 7.47                                | 2.02                                | 8.18                               | 2.21                               |
| 6           | 120-T6      | 120                        | 11.26                               | 1.52                                | 13.27                              | 1.79                               |
| 7           | 90-T7       | 90                         | 8.18                                | 1.47                                | 8.18                               | 1.47                               |
| 8           |             |                            |                                     |                                     |                                    |                                    |
| 9           |             |                            |                                     |                                     |                                    |                                    |
| 10          |             |                            |                                     |                                     |                                    |                                    |
| 11          |             |                            |                                     |                                     |                                    |                                    |
| 12          |             |                            |                                     |                                     |                                    |                                    |
| 13          |             |                            |                                     |                                     |                                    |                                    |
| 14          |             |                            |                                     |                                     |                                    |                                    |
| 15          |             |                            |                                     |                                     |                                    |                                    |
| 16          |             |                            |                                     |                                     |                                    |                                    |
| 17          |             |                            |                                     |                                     |                                    |                                    |
| 18          |             |                            |                                     |                                     |                                    |                                    |
| 19          |             |                            |                                     |                                     |                                    |                                    |
| 20          |             |                            |                                     |                                     |                                    |                                    |



MW71 x MW71 – 100 mm x 1-Wire



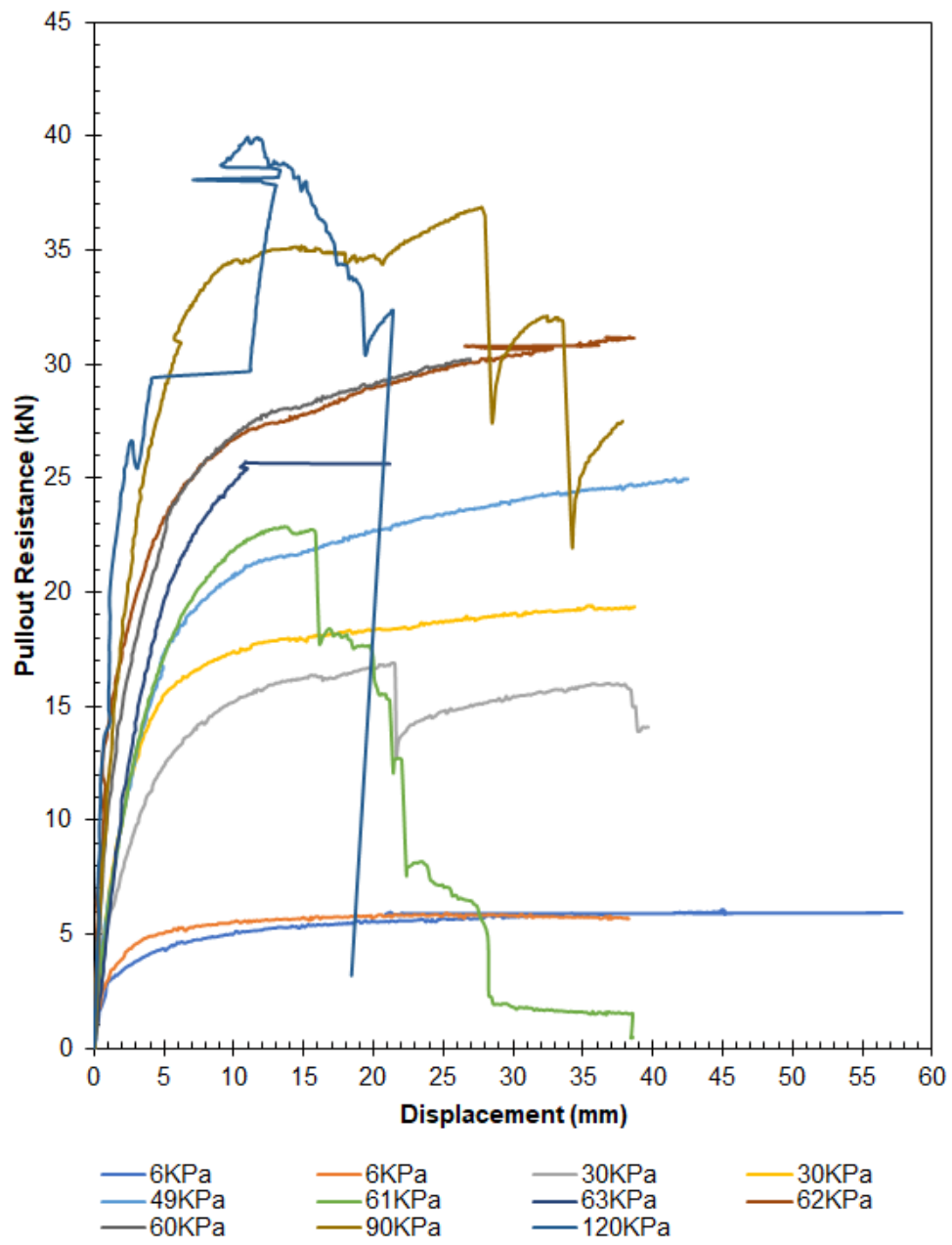
MW71 x MW71 – 100 mm x 1-Wire

MW71 x MW71 – 200 mm x 300 mm

| Test | Name    | Surcharge<br>(kPa) | $P_{r,19\text{ mm}}$<br>(kN) | $F^*_{19\text{ mm}}$<br>(dim) | $P_{r\_peak}$<br>(kN) | $F^*_{peak}$<br>(dim) |
|------|---------|--------------------|------------------------------|-------------------------------|-----------------------|-----------------------|
| 1    | 6-T1    | 6                  | 5.60                         | 1.89                          | 6.07                  | 2.05                  |
| 2    | 6-T2    | 6                  | 5.86                         | 1.98                          | 5.97                  | 2.01                  |
| 3    | 30-T3   | 30                 | 16.62                        | 1.10                          | 16.89                 | 1.12                  |
| 4    | 30-T4   | 30                 | 18.32                        | 1.23                          | 19.40                 | 1.30                  |
| 5    | 49-T5   | 49                 | 22.49                        | 0.93                          | 24.96                 | 1.03                  |
| 6    | 61-T6   | 61                 | 22.87                        | 0.76                          | 22.87                 | 0.76                  |
| 7    | 63-T7   | 63                 | 25.78                        | 0.83                          | 25.78                 | 0.83                  |
| 8    | 62-T8   | 62                 | 28.80                        | 0.93                          | 31.23                 | 1.01                  |
| 9    | 60-T9   | 60                 | 28.95                        | 0.98                          | 30.25                 | 1.02                  |
| 10   | 90-T10  | 90                 | 35.17                        | 0.79                          | 36.87                 | 0.83                  |
| 11   | 120-T11 | 120                | 39.94                        | 0.67                          | 39.94                 | 0.67                  |
| 12   |         |                    |                              |                               |                       |                       |
| 13   |         |                    |                              |                               |                       |                       |
| 14   |         |                    |                              |                               |                       |                       |
| 15   |         |                    |                              |                               |                       |                       |
| 16   |         |                    |                              |                               |                       |                       |
| 17   |         |                    |                              |                               |                       |                       |
| 18   |         |                    |                              |                               |                       |                       |
| 19   |         |                    |                              |                               |                       |                       |
| 20   |         |                    |                              |                               |                       |                       |

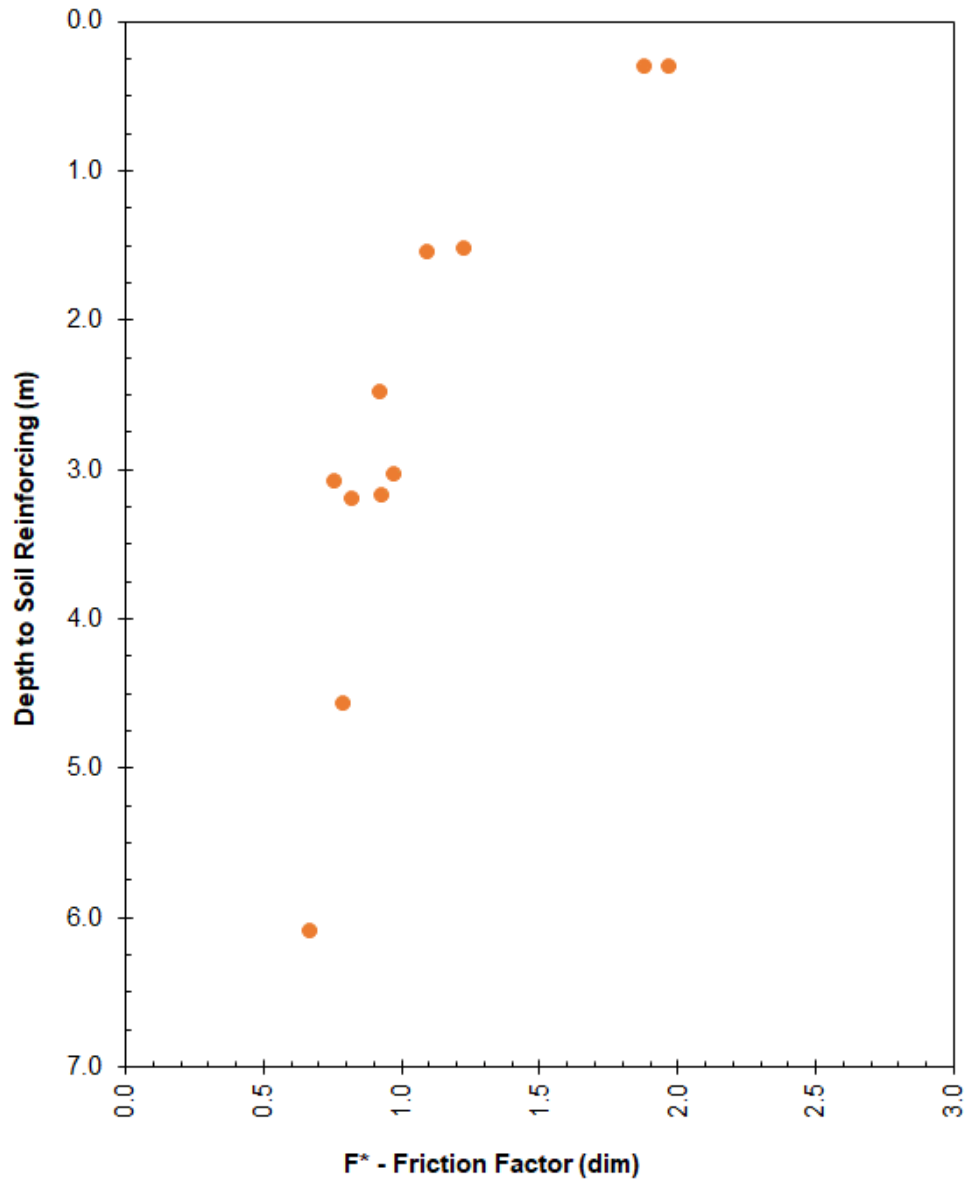
Test 6, 7, 10, and 11 had weld failure during test

Test 3 had lost load, then recovered (electrical)



MW71 x MW71 – 200 mm x 300 mm



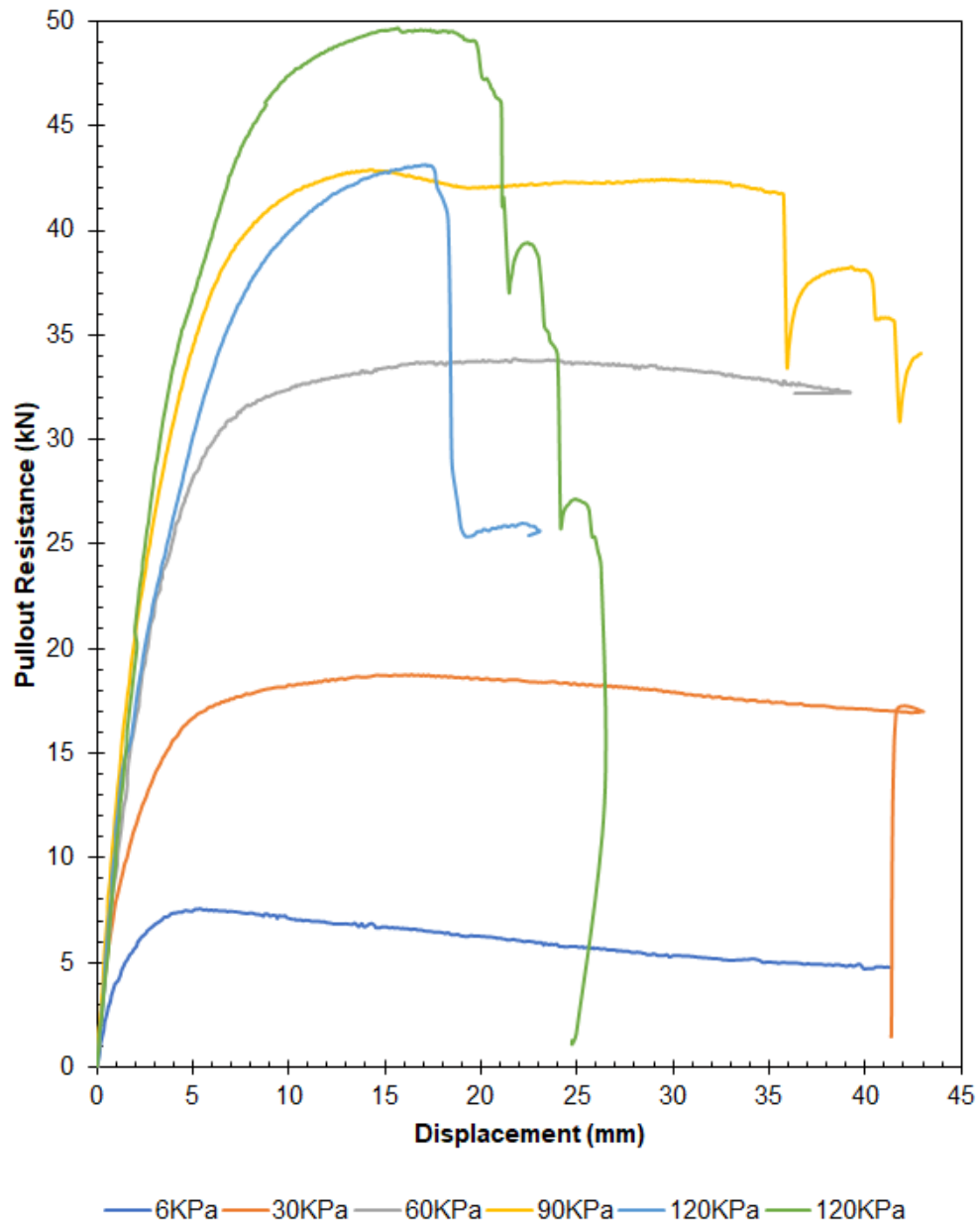


MW71 x MW71 – 200 mm x 300 mm

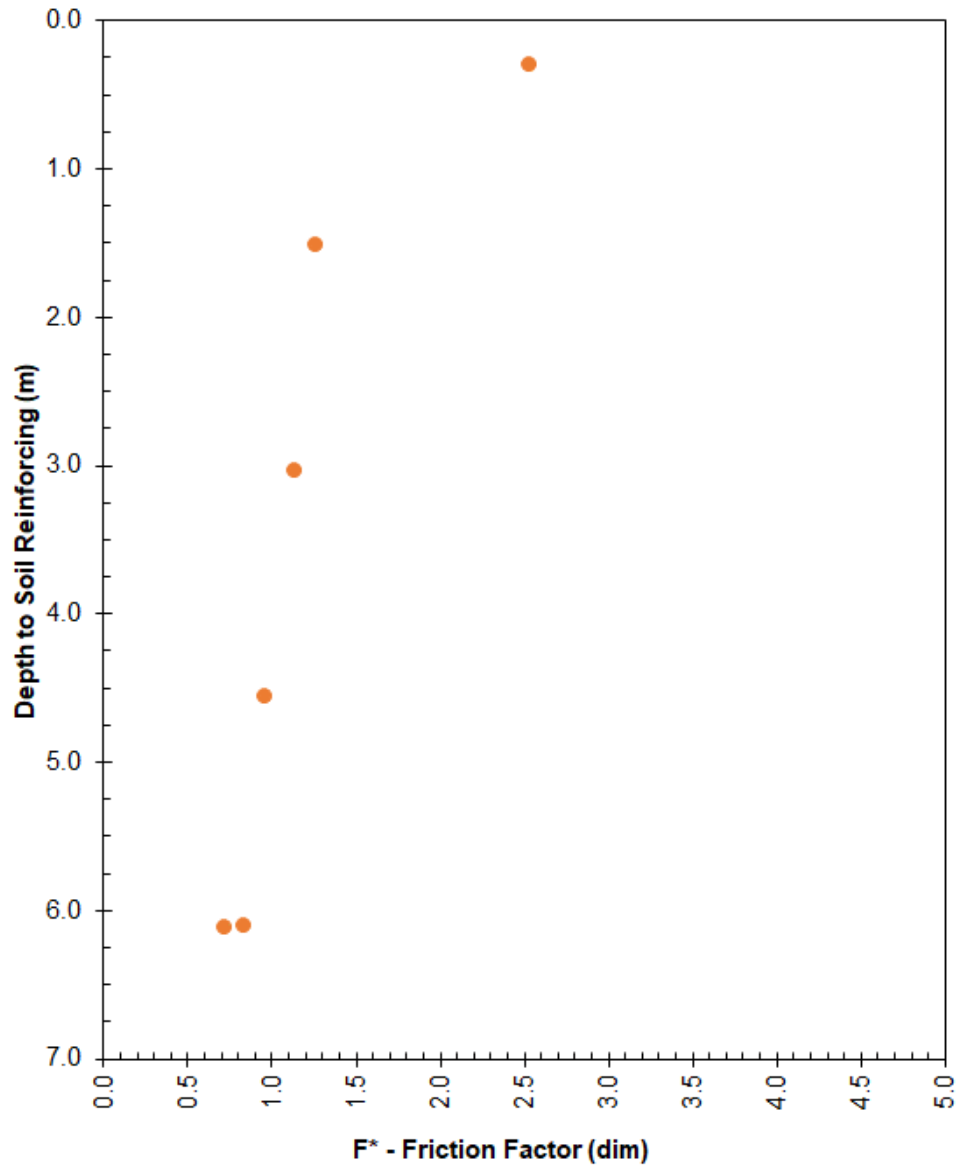
MW71 x MW71 – 200 mm x 150 mm

| Test | Name   | Surcharge<br>(kPa) | P <sub>r_19 mm</sub><br>(kN) | F* <sub>19 mm</sub><br>(dim) | P <sub>r_peak</sub><br>(kN) | F* <sub>peak</sub><br>(dim) |
|------|--------|--------------------|------------------------------|------------------------------|-----------------------------|-----------------------------|
| 1    | 6-T1   | 6                  | 7.53                         | 2.54                         | 7.53                        | 2.54                        |
| 2    | 29-T2  | 29                 | 18.75                        | 1.27                         | 18.75                       | 1.27                        |
| 3    | 59-T3  | 59                 | 33.78                        | 1.14                         | 33.90                       | 1.15                        |
| 4    | 89-T4  | 89                 | 42.91                        | 0.97                         | 42.91                       | 0.97                        |
| 5    | 120-T5 | 120                | 43.17                        | 0.72                         | 43.17                       | 0.72                        |
| 6    | 119-T6 | 119                | 49.72                        | 0.84                         | 49.72                       | 0.84                        |
| 7    |        |                    |                              |                              |                             |                             |
| 8    |        |                    |                              |                              |                             |                             |
| 9    |        |                    |                              |                              |                             |                             |
| 10   |        |                    |                              |                              |                             |                             |
| 11   |        |                    |                              |                              |                             |                             |
| 12   |        |                    |                              |                              |                             |                             |
| 13   |        |                    |                              |                              |                             |                             |
| 14   |        |                    |                              |                              |                             |                             |
| 15   |        |                    |                              |                              |                             |                             |
| 16   |        |                    |                              |                              |                             |                             |
| 17   |        |                    |                              |                              |                             |                             |
| 18   |        |                    |                              |                              |                             |                             |
| 19   |        |                    |                              |                              |                             |                             |
| 20   |        |                    |                              |                              |                             |                             |

Test 4, 5, and 6 had weld failure during test



MW71 x MW71 – 200 mm x 150 mm



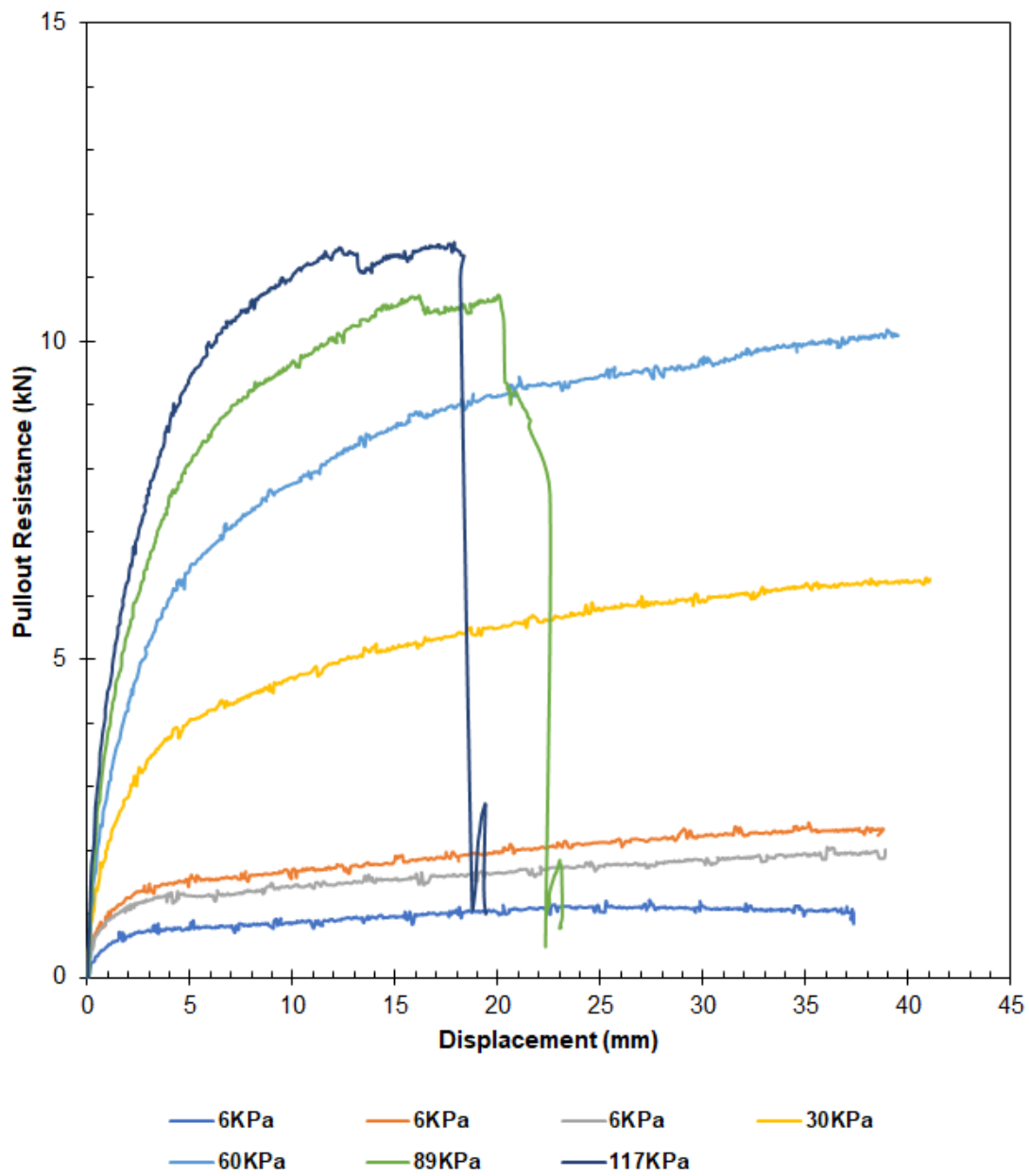
MW71 x MW71 – 200 mm x 150 mm

MW71 x MW71 – 200 mm x 1-Wire

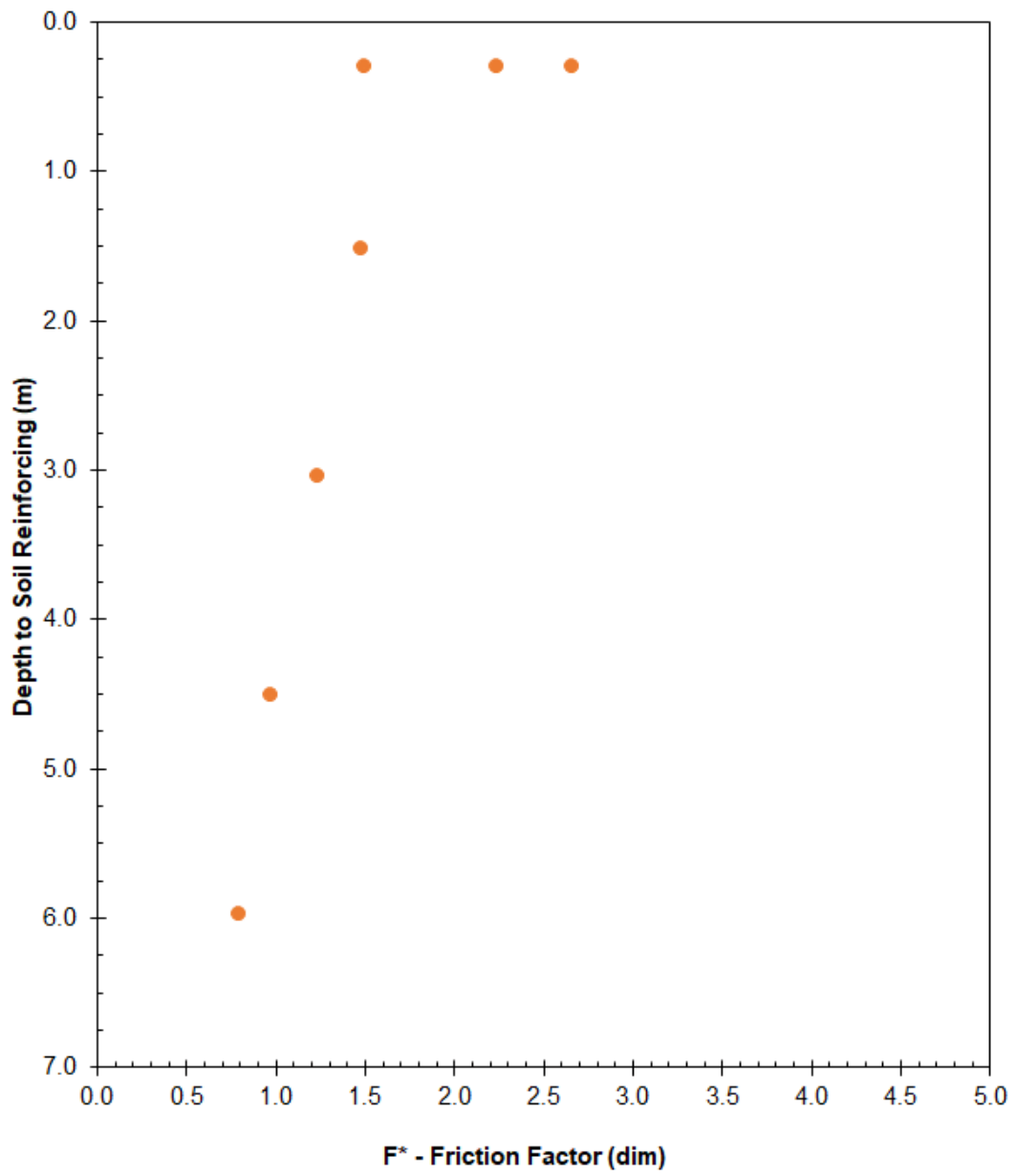
| Test | Name   | Surcharge<br>(kPa) | P <sub>r_19 mm</sub><br>(kN) | F* <sub>19 mm</sub><br>(dim) | P <sub>r_peak</sub><br>(kN) | F* <sub>peak</sub><br>(dim) |
|------|--------|--------------------|------------------------------|------------------------------|-----------------------------|-----------------------------|
| 1    | 6-T1   | 6                  | 110.81                       | 1.49                         | 122.04                      | 1.65                        |
| 2    | 6-T2   | 6                  | 197.42                       | 2.66                         | 243.84                      | 3.29                        |
| 3    | 6-T3   | 6                  | 166.21                       | 2.24                         | 205.14                      | 2.77                        |
| 4    | 30-T4  | 30                 | 550.24                       | 1.48                         | 628.04                      | 1.69                        |
| 5    | 60-T5  | 60                 | 917.67                       | 1.24                         | 1018.73                     | 1.38                        |
| 6    | 89-T6  | 89                 | 1071.89                      | 0.98                         | 1072.64                     | 0.98                        |
| 7    | 117-T7 | 117                | 1156.49                      | 0.80                         | 1156.49                     | 0.80                        |
| 8    |        |                    |                              |                              |                             |                             |
| 9    |        |                    |                              |                              |                             |                             |
| 10   |        |                    |                              |                              |                             |                             |
| 11   |        |                    |                              |                              |                             |                             |
| 12   |        |                    |                              |                              |                             |                             |
| 13   |        |                    |                              |                              |                             |                             |
| 14   |        |                    |                              |                              |                             |                             |
| 15   |        |                    |                              |                              |                             |                             |
| 16   |        |                    |                              |                              |                             |                             |
| 17   |        |                    |                              |                              |                             |                             |
| 18   |        |                    |                              |                              |                             |                             |
| 19   |        |                    |                              |                              |                             |                             |
| 20   |        |                    |                              |                              |                             |                             |

Test 6 and 7 had weld failure during test

The density of Test-1 was measured to be 88% of standard proctor



MW71 x MW71 – 200 mm x 1-Wire

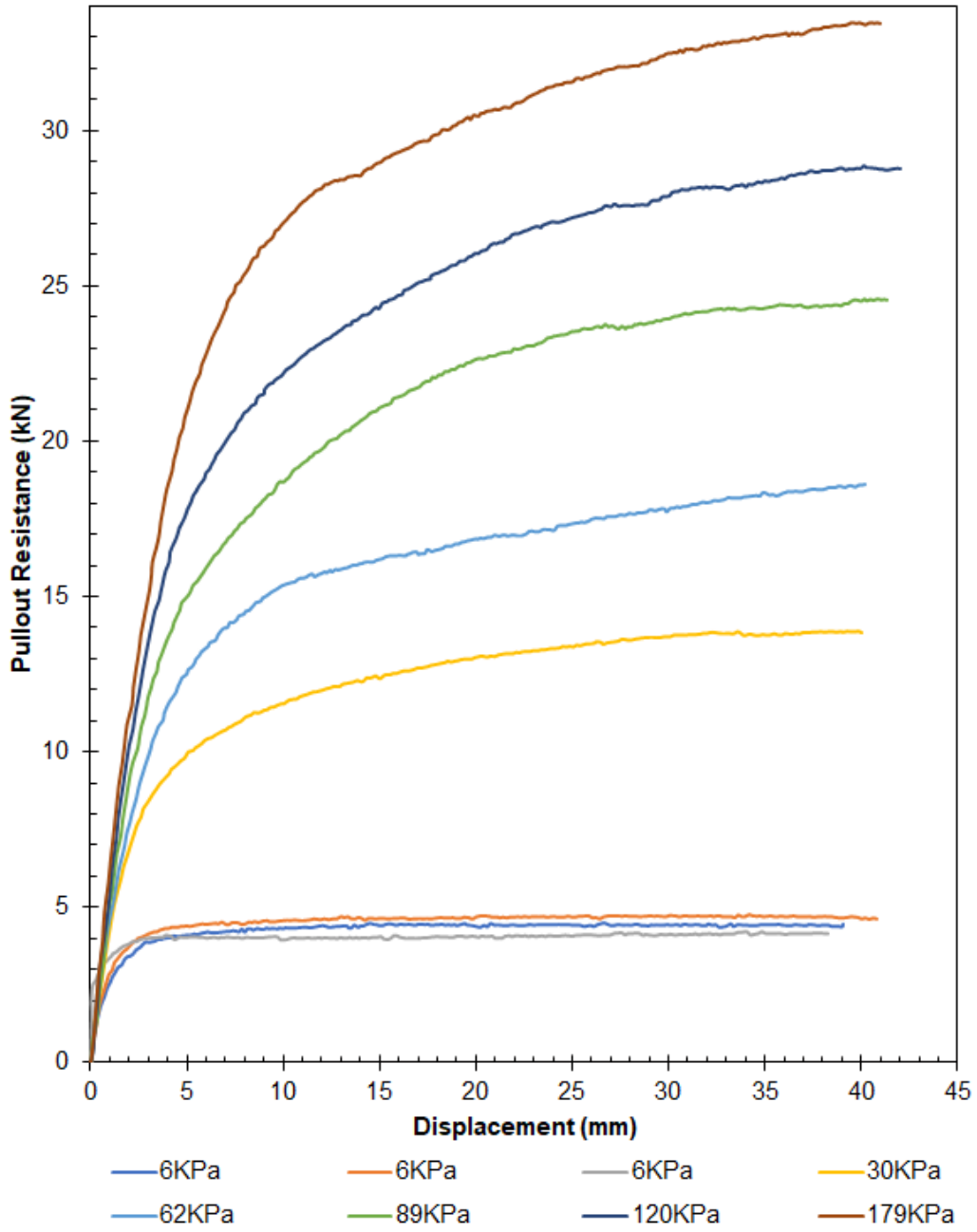


MW71 x MW71 -200 mm x 1-Wire

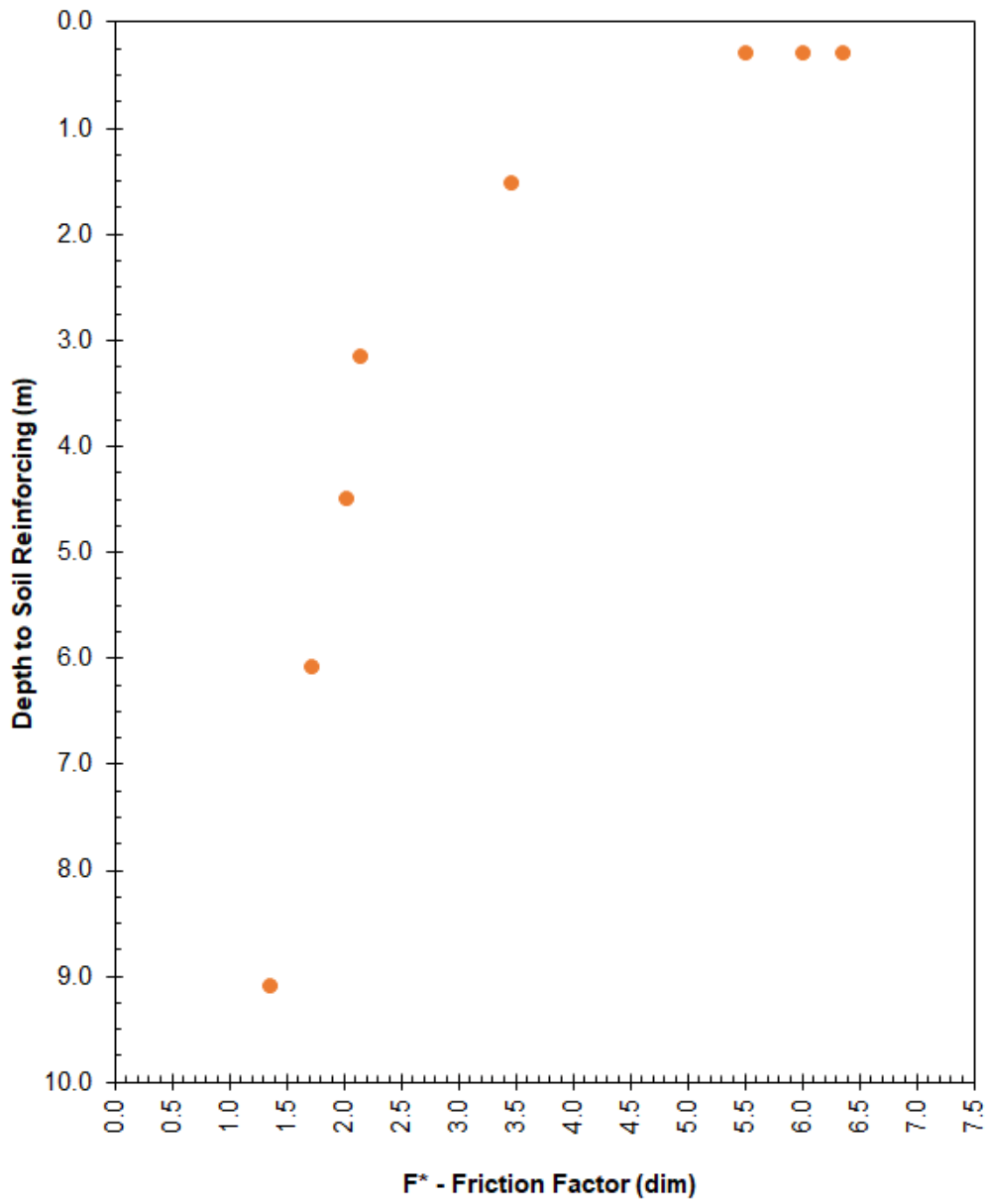
MW45 x MW45 –50 mm x 300 mm

| <b>Test</b> | <b>Name</b> | <b>Surcharge<br/>(kPa)</b> | <b>P<sub>r,19 mm</sub><br/>(kN)</b> | <b>F*<sub>19 mm</sub><br/>(dim)</b> | <b>P<sub>r,peak</sub><br/>(kN)</b> | <b>F*<sub>peak</sub><br/>(dim)</b> |
|-------------|-------------|----------------------------|-------------------------------------|-------------------------------------|------------------------------------|------------------------------------|
| 1           | 6-T1        | 6                          | 4.47                                | 6.02                                | 4.47                               | 6.03                               |
| 2           | 6-T2        | 6                          | 4.72                                | 6.37                                | 4.78                               | 6.45                               |
| 3           | 6-T3        | 6                          | 4.09                                | 5.52                                | 4.20                               | 5.67                               |
| 4           | 30-T4       | 30                         | 12.90                               | 3.48                                | 13.86                              | 3.74                               |
| 5           | 62-T5       | 62                         | 16.69                               | 2.16                                | 18.62                              | 2.41                               |
| 6           | 89-T6       | 89                         | 22.38                               | 2.04                                | 24.57                              | 2.24                               |
| 7           | 120-T7      | 120                        | 25.70                               | 1.73                                | 28.88                              | 1.95                               |
| 8           | 179-T8      | 179                        | 30.17                               | 1.36                                | 33.48                              | 1.51                               |
| 9           |             |                            |                                     |                                     |                                    |                                    |
| 10          |             |                            |                                     |                                     |                                    |                                    |
| 11          |             |                            |                                     |                                     |                                    |                                    |
| 12          |             |                            |                                     |                                     |                                    |                                    |
| 13          |             |                            |                                     |                                     |                                    |                                    |
| 14          |             |                            |                                     |                                     |                                    |                                    |
| 15          |             |                            |                                     |                                     |                                    |                                    |
| 16          |             |                            |                                     |                                     |                                    |                                    |
| 17          |             |                            |                                     |                                     |                                    |                                    |
| 18          |             |                            |                                     |                                     |                                    |                                    |
| 19          |             |                            |                                     |                                     |                                    |                                    |





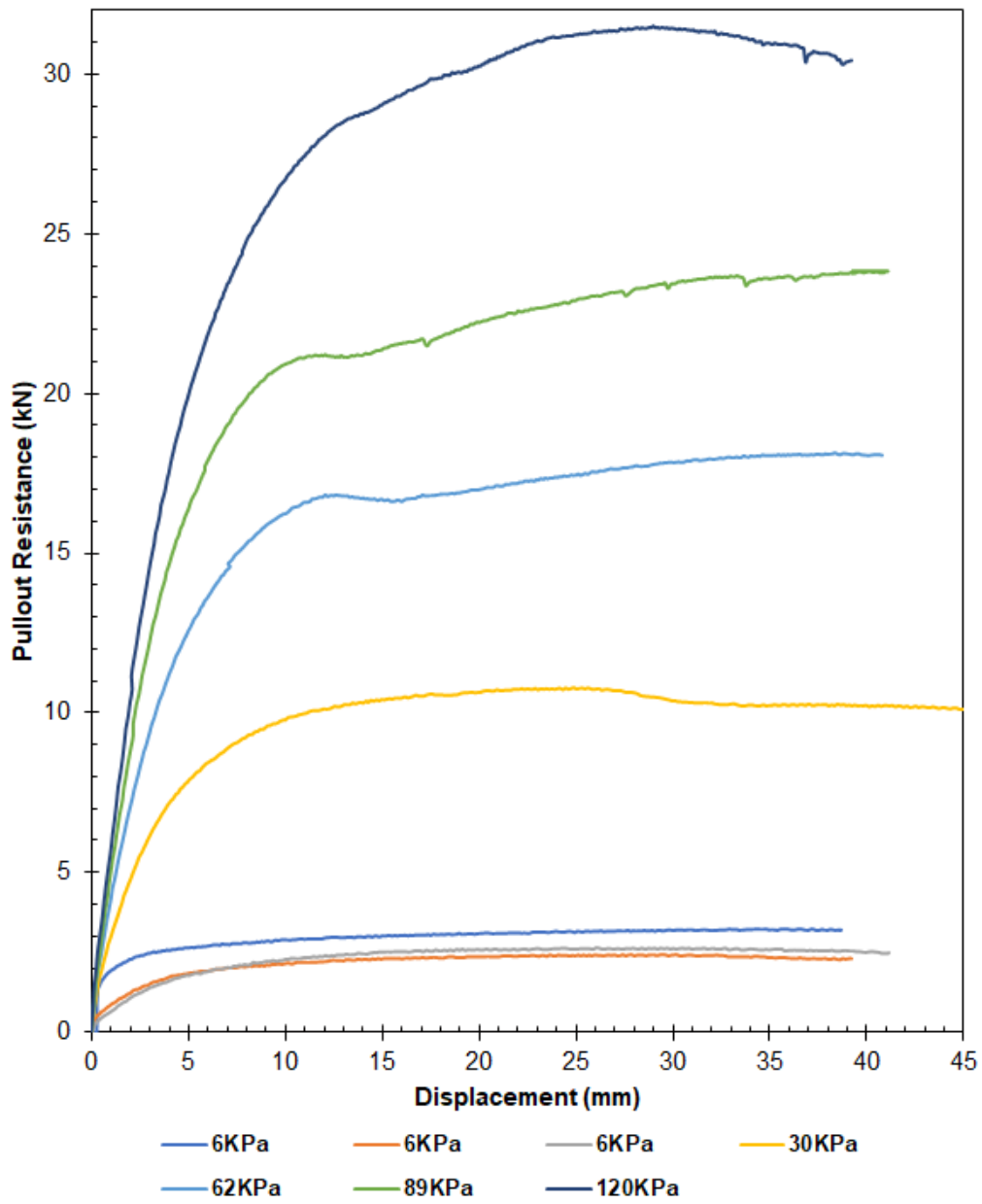
MW45 x MW45 -50 mm x 300 mm



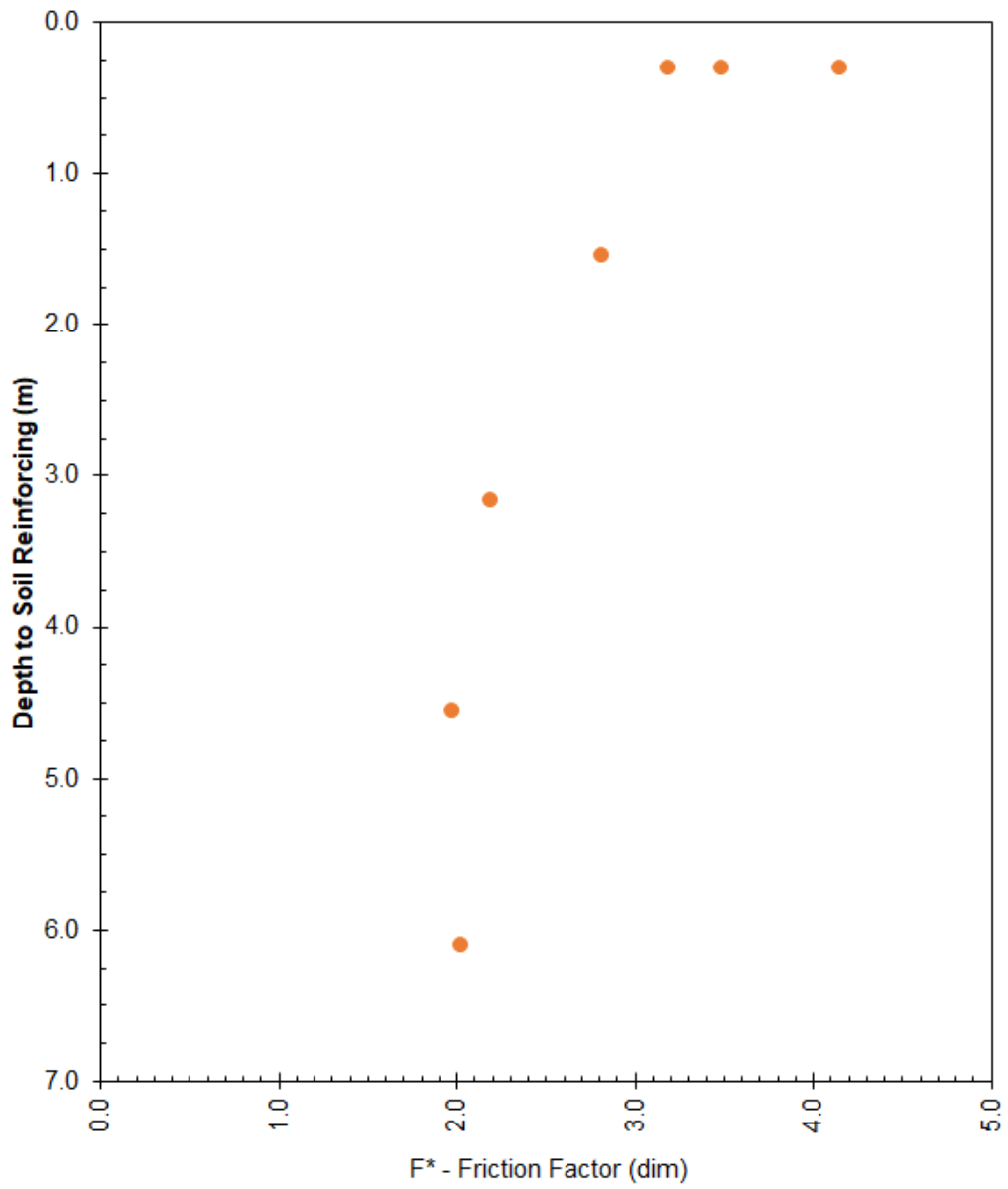
MW45 x MW45 -50 mm x 300 mm

MW45 x MW45 –50 mm x 150 mm

| <b>Test</b> | <b>Name</b> | <b>Surcharge<br/>(kPa)</b> | <b>P<sub>r_19 mm</sub><br/>(kN)</b> | <b>F*<sub>19 mm</sub><br/>(dim)</b> | <b>P<sub>r_peak</sub><br/>(kN)</b> | <b>F*<sub>peak</sub><br/>(dim)</b> |
|-------------|-------------|----------------------------|-------------------------------------|-------------------------------------|------------------------------------|------------------------------------|
| 1           | 6-T1        | 6                          | 2.37                                | 4.15                                | 2.44                               | 4.33                               |
| 2           | 6-T2        | 6                          | 2.59                                | 3.19                                | 2.63                               | 3.29                               |
| 3           | 6-T3        | 6                          | 10.58                               | 3.49                                | 10.77                              | 3.55                               |
| 4           | 31-T4       | 31                         | 16.89                               | 2.82                                | 18.14                              | 2.87                               |
| 5           | 63-T5       | 63                         | 21.99                               | 2.19                                | 23.83                              | 2.35                               |
| 6           | 91-T6       | 91                         | 30.05                               | 1.98                                | 31.49                              | 2.15                               |
| 7           | 122-T7      | 122                        | 0.00                                | 2.02                                | 0.00                               | 2.12                               |
| 8           |             |                            |                                     |                                     |                                    |                                    |
| 9           |             |                            |                                     |                                     |                                    |                                    |
| 10          |             |                            |                                     |                                     |                                    |                                    |
| 11          |             |                            |                                     |                                     |                                    |                                    |
| 12          |             |                            |                                     |                                     |                                    |                                    |
| 13          |             |                            |                                     |                                     |                                    |                                    |
| 14          |             |                            |                                     |                                     |                                    |                                    |
| 15          |             |                            |                                     |                                     |                                    |                                    |
| 16          |             |                            |                                     |                                     |                                    |                                    |
| 17          |             |                            |                                     |                                     |                                    |                                    |
| 18          |             |                            |                                     |                                     |                                    |                                    |
| 19          |             |                            |                                     |                                     |                                    |                                    |
| 20          |             |                            |                                     |                                     |                                    |                                    |



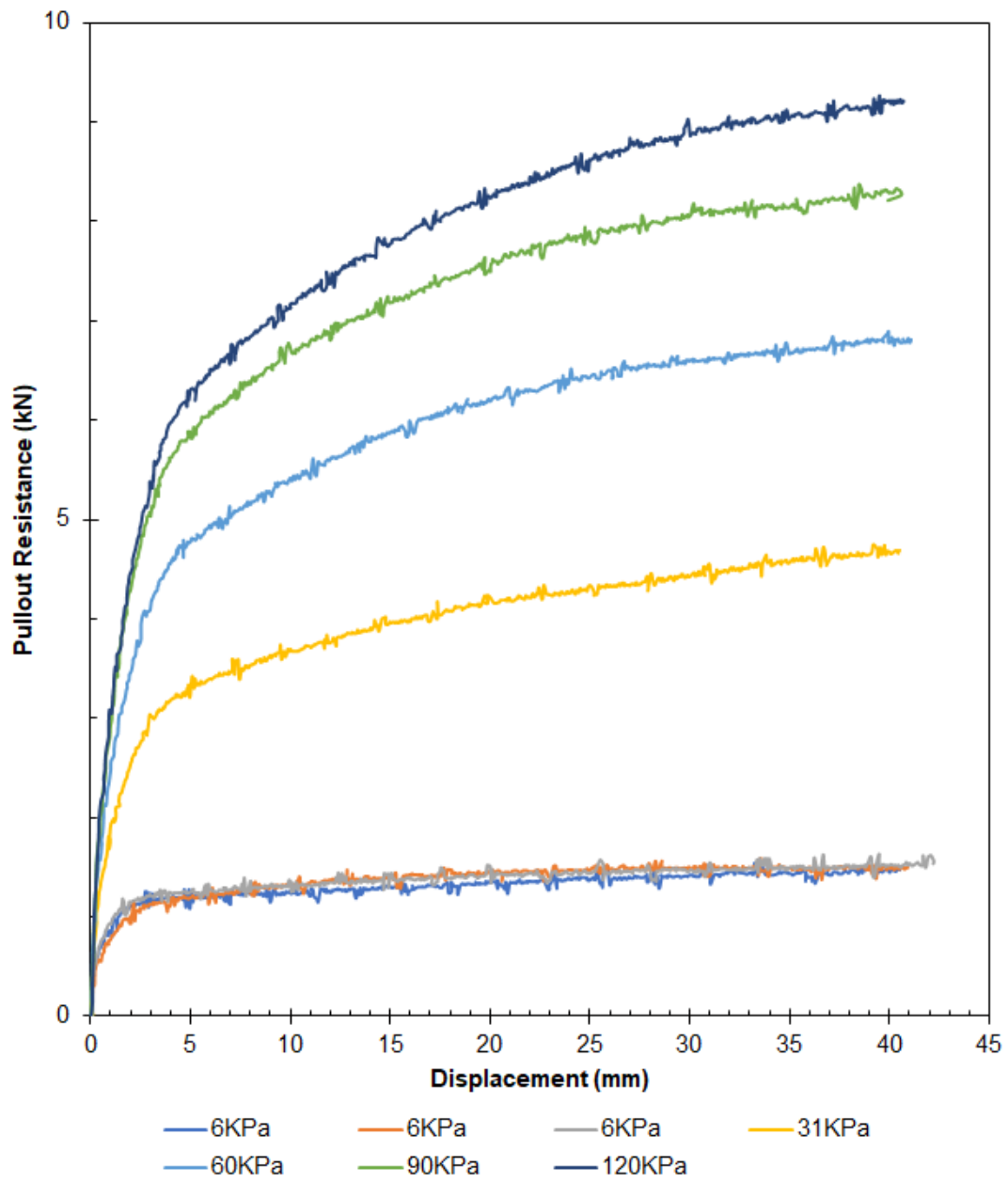
MW45 x MW45 –50 mm x 150 mm



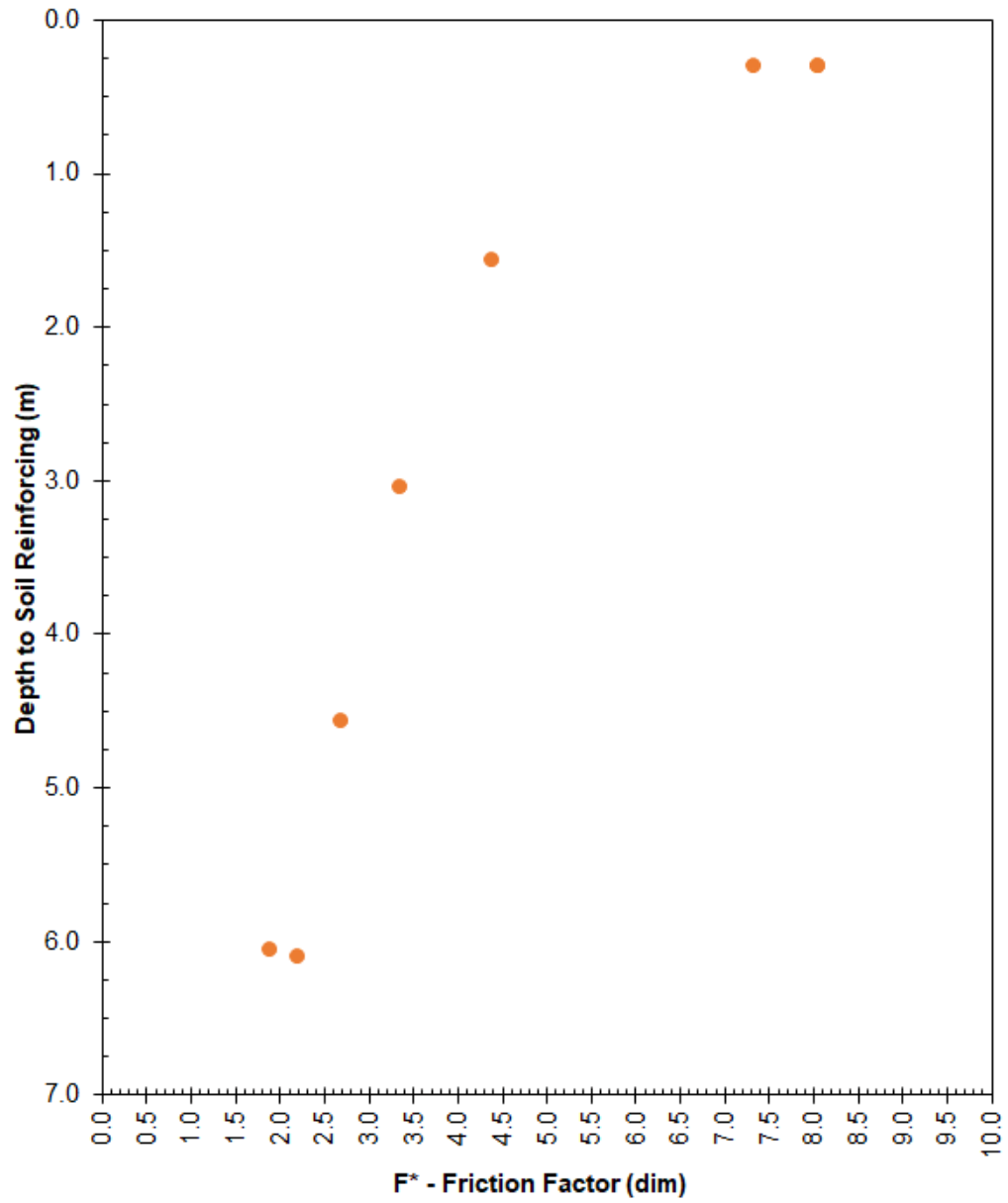
MW45 x MW45 –50 mm x 150 mm

MW45 x MW45 –50 mm x 1-Wire

| <b>Test</b> | <b>Name</b> | <b>Surcharge<br/>(kPa)</b> | <b>P<sub>r,19 mm</sub><br/>(kN)</b> | <b>F*<sub>19 mm</sub><br/>(dim)</b> | <b>P<sub>r,peak</sub><br/>(kN)</b> | <b>F*<sub>peak</sub><br/>(dim)</b> |
|-------------|-------------|----------------------------|-------------------------------------|-------------------------------------|------------------------------------|------------------------------------|
| 1           | 6-T1        | 6                          | 1.36                                | 7.33                                | 1.54                               | 8.30                               |
| 2           | 6-T2        | 6                          | 1.49                                | 8.06                                | 1.59                               | 8.58                               |
| 3           | 6-T3        | 6                          | 1.49                                | 8.06                                | 1.63                               | 8.78                               |
| 4           | 31-T4       | 31                         | 4.18                                | 4.39                                | 4.76                               | 5.00                               |
| 5           | 61-T5       | 61                         | 6.22                                | 3.35                                | 6.90                               | 3.72                               |
| 6           | 91-T6       | 91                         | 7.50                                | 2.70                                | 8.38                               | 3.01                               |
| 7           | 122-T7      | 122                        | 8.19                                | 2.21                                | 9.27                               | 2.50                               |
| 8           | 121-T8      | 121                        | 7.00                                | 1.90                                | 8.30                               | 2.25                               |
| 9           |             |                            |                                     |                                     |                                    |                                    |
| 10          |             |                            |                                     |                                     |                                    |                                    |
| 11          |             |                            |                                     |                                     |                                    |                                    |
| 12          |             |                            |                                     |                                     |                                    |                                    |
| 13          |             |                            |                                     |                                     |                                    |                                    |
| 14          |             |                            |                                     |                                     |                                    |                                    |
| 15          |             |                            |                                     |                                     |                                    |                                    |
| 16          |             |                            |                                     |                                     |                                    |                                    |
| 17          |             |                            |                                     |                                     |                                    |                                    |
| 18          |             |                            |                                     |                                     |                                    |                                    |
| 19          |             |                            |                                     |                                     |                                    |                                    |
| 20          |             |                            |                                     |                                     |                                    |                                    |



MW45 x MW45 –50 mm x 1-Wire

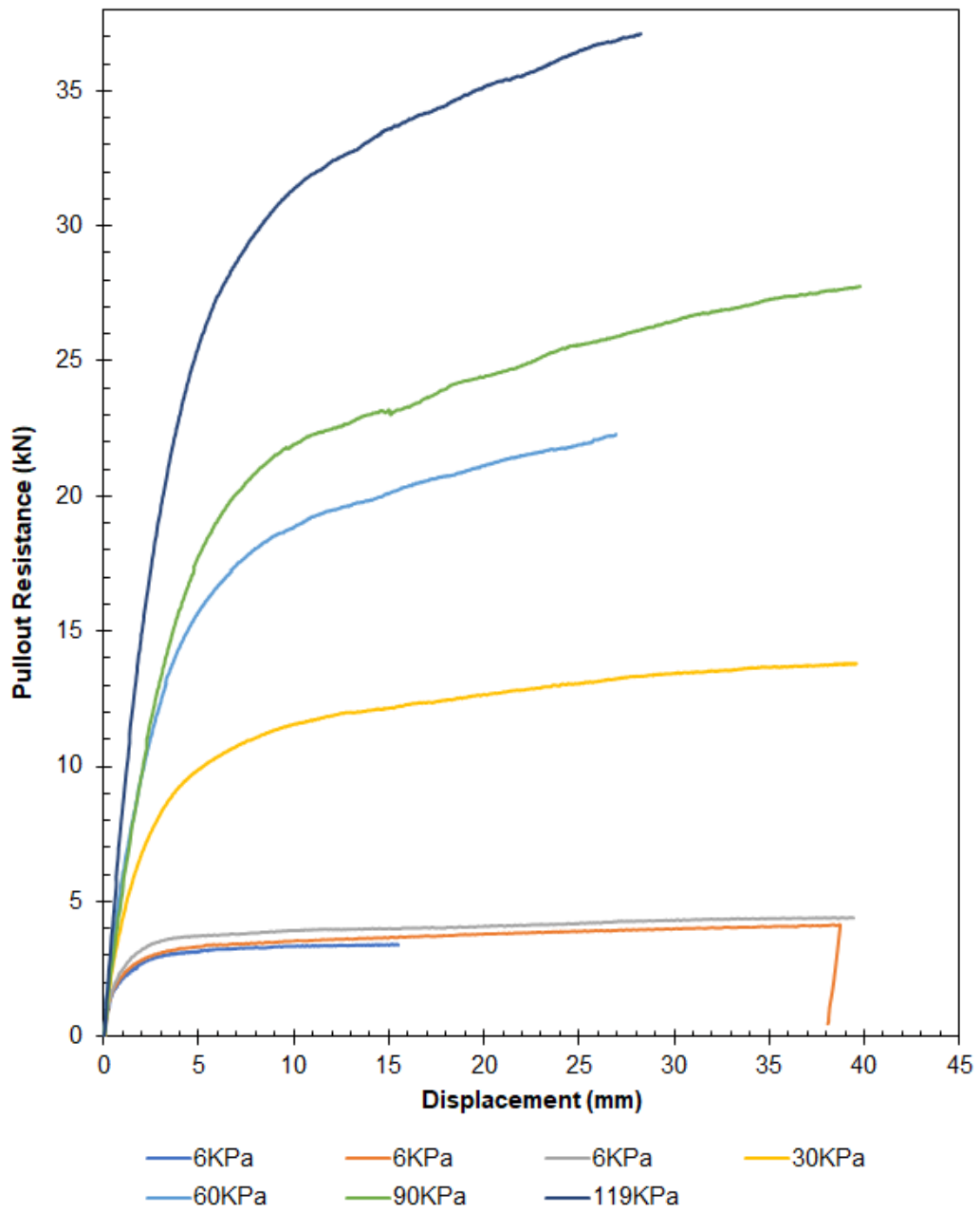


MW45 x MW45 -50 mm x 1-Wire

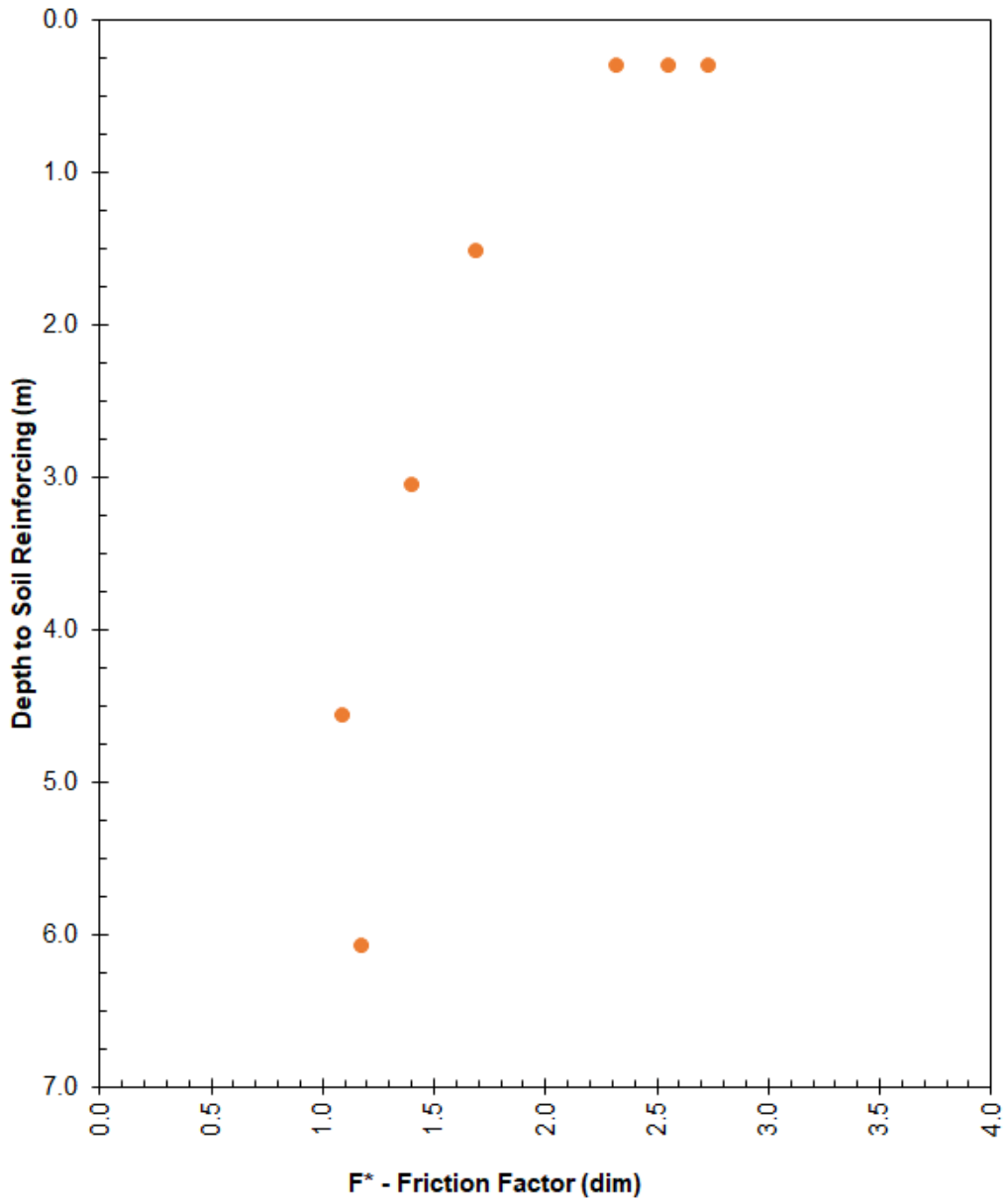


MW45 x MW45 –100 mm x 300 mm

| <b>Test</b> | <b>Name</b> | <b>Surcharge<br/>(kPa)</b> | <b>P<sub>r_19 mm</sub><br/>(kN)</b> | <b>F*<sub>19 mm</sub><br/>(dim)</b> | <b>P<sub>r_peak</sub><br/>(kN)</b> | <b>F*<sub>peak</sub><br/>(dim)</b> |
|-------------|-------------|----------------------------|-------------------------------------|-------------------------------------|------------------------------------|------------------------------------|
| 1           | 6-T1        | 6                          | 3.44                                | 2.32                                | 3.44                               | 2.32                               |
| 2           | 6-T2        | 6                          | 3.79                                | 2.56                                | 4.15                               | 2.80                               |
| 3           | 6-T3        | 6                          | 4.05                                | 2.73                                | 4.38                               | 2.96                               |
| 4           | 30-T4       | 30                         | 12.57                               | 1.70                                | 13.83                              | 1.87                               |
| 5           | 60-T5       | 60                         | 20.94                               | 1.41                                | 22.31                              | 1.50                               |
| 6           | 90-T6       | 90                         | 24.28                               | 1.09                                | 27.77                              | 1.25                               |
| 7           | 119-T7      | 119                        | 34.89                               | 1.18                                | 37.12                              | 1.25                               |
| 8           |             |                            |                                     |                                     |                                    |                                    |
| 9           |             |                            |                                     |                                     |                                    |                                    |
| 10          |             |                            |                                     |                                     |                                    |                                    |
| 11          |             |                            |                                     |                                     |                                    |                                    |
| 12          |             |                            |                                     |                                     |                                    |                                    |
| 13          |             |                            |                                     |                                     |                                    |                                    |
| 14          |             |                            |                                     |                                     |                                    |                                    |
| 15          |             |                            |                                     |                                     |                                    |                                    |
| 16          |             |                            |                                     |                                     |                                    |                                    |
| 17          |             |                            |                                     |                                     |                                    |                                    |
| 18          |             |                            |                                     |                                     |                                    |                                    |
| 19          |             |                            |                                     |                                     |                                    |                                    |
| 20          |             |                            |                                     |                                     |                                    |                                    |



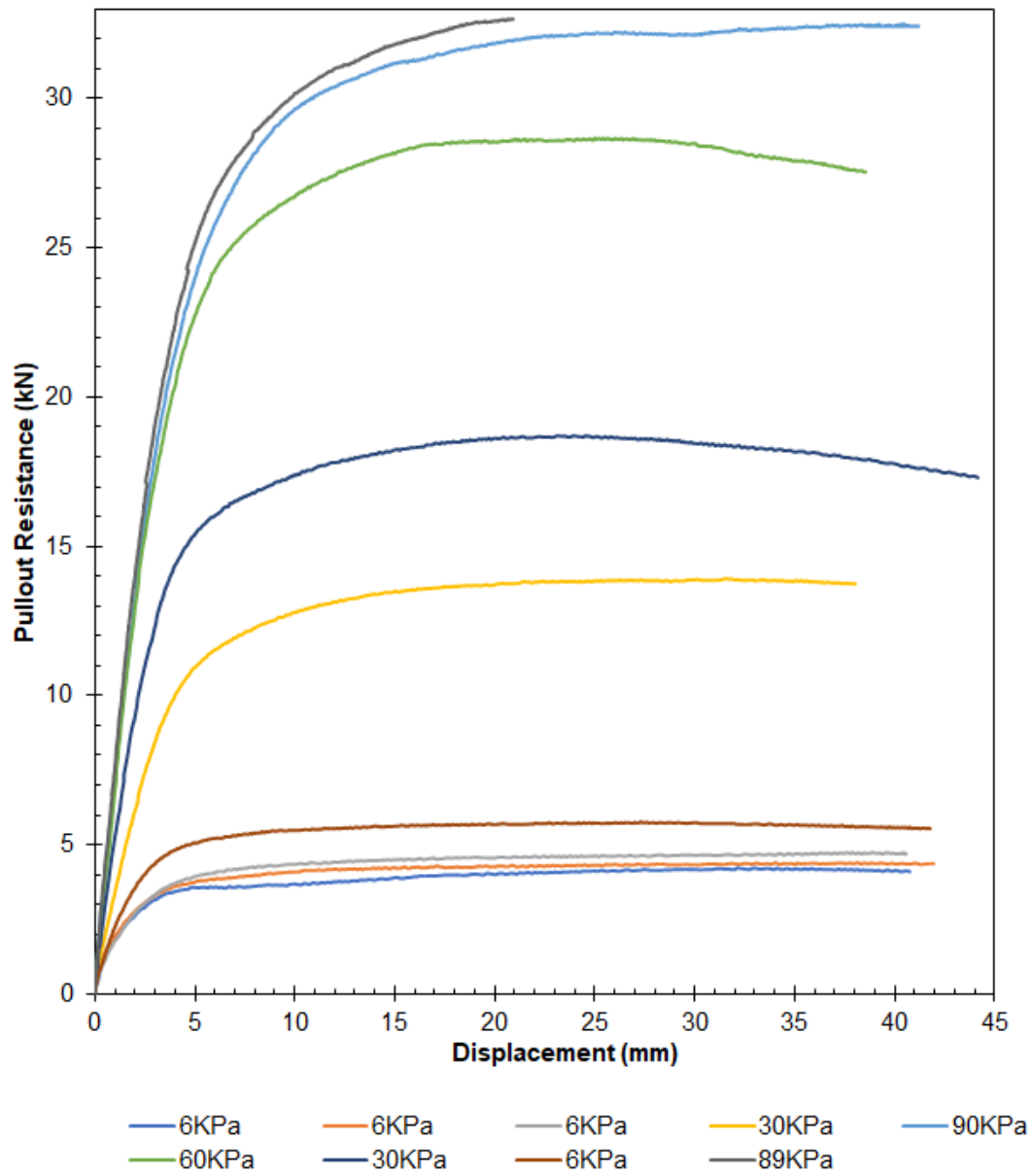
MW45 x MW45 –100 mm x 300 mm



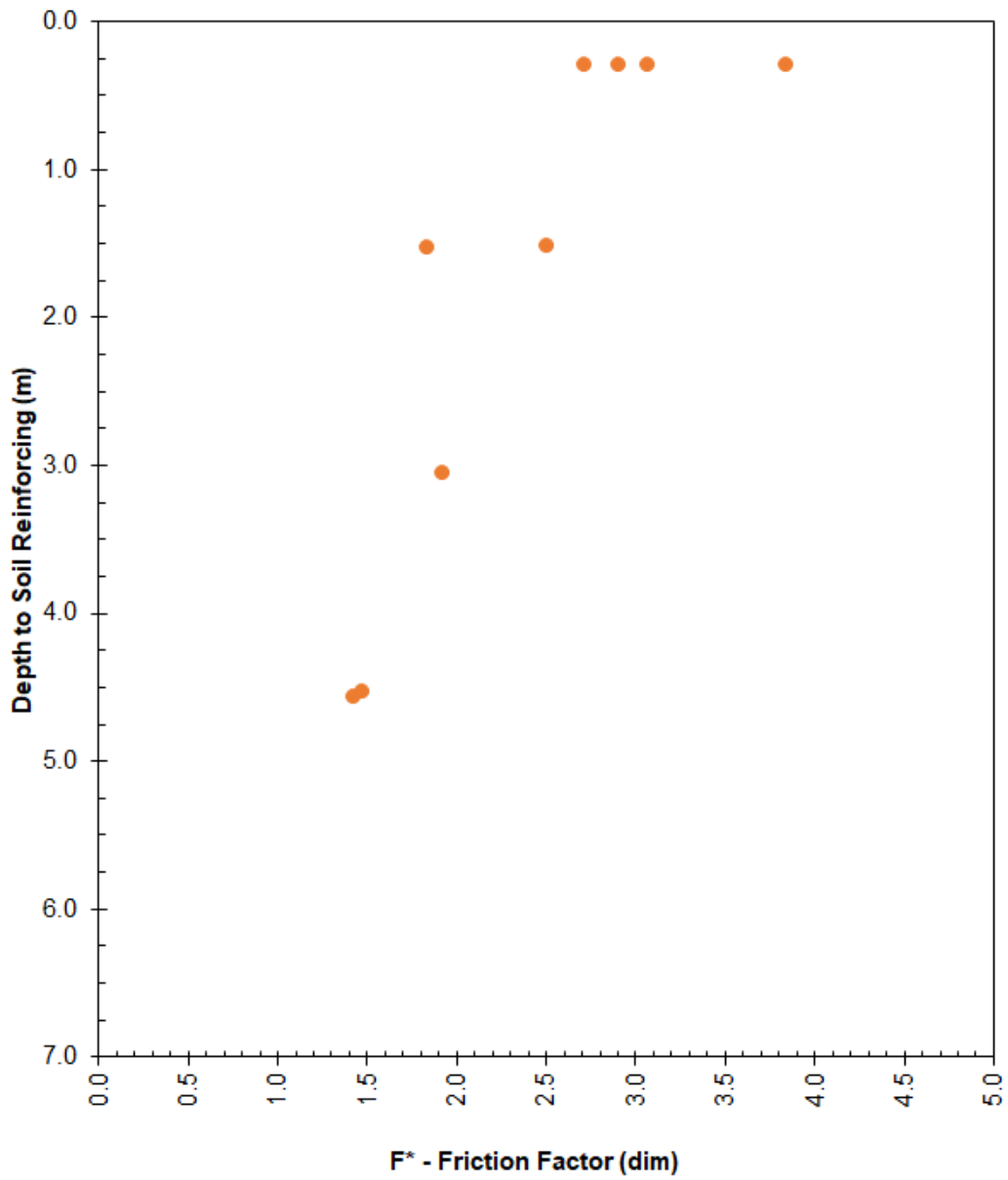
MW45 x MW45 –100 mm x 300 mm

MW45 x MW45 –100 mm x 150 mm

| <b>Test</b> | <b>Name</b> | <b>Surcharge<br/>(kPa)</b> | <b>P<sub>r_19 mm</sub><br/>(kN)</b> | <b>F*<sub>19 mm</sub><br/>(dim)</b> | <b>P<sub>r_peak</sub><br/>(kN)</b> | <b>F*<sub>peak</sub><br/>(dim)</b> |
|-------------|-------------|----------------------------|-------------------------------------|-------------------------------------|------------------------------------|------------------------------------|
| 1           | 6-T1        | 6                          | 4.03                                | 2.72                                | 4.24                               | 2.86                               |
| 2           | 6-T2        | 6                          | 4.32                                | 2.91                                | 4.43                               | 2.99                               |
| 3           | 6-T3        | 6                          | 4.56                                | 3.07                                | 4.72                               | 3.18                               |
| 4           | 30-T4       | 30                         | 13.70                               | 1.84                                | 13.92                              | 1.87                               |
| 5           | 90-T5       | 90                         | 31.75                               | 1.43                                | 32.50                              | 1.46                               |
| 6           | 60-T6       | 60                         | 28.60                               | 1.92                                | 28.70                              | 1.93                               |
| 7           | 30-T7       | 30                         | 18.60                               | 2.51                                | 18.73                              | 2.52                               |
| 8           | 6-T8        | 6                          | 5.71                                | 3.85                                | 5.79                               | 3.90                               |
| 9           | 89-T9       | 89                         | 32.58                               | 1.48                                | 32.69                              | 1.48                               |
| 10          |             |                            |                                     |                                     |                                    |                                    |
| 11          |             |                            |                                     |                                     |                                    |                                    |
| 12          |             |                            |                                     |                                     |                                    |                                    |
| 13          |             |                            |                                     |                                     |                                    |                                    |
| 14          |             |                            |                                     |                                     |                                    |                                    |
| 15          |             |                            |                                     |                                     |                                    |                                    |
| 16          |             |                            |                                     |                                     |                                    |                                    |
| 17          |             |                            |                                     |                                     |                                    |                                    |
| 18          |             |                            |                                     |                                     |                                    |                                    |
| 19          |             |                            |                                     |                                     |                                    |                                    |
| 20          |             |                            |                                     |                                     |                                    |                                    |



MW45 x MW45 –100 mm x 150 mm

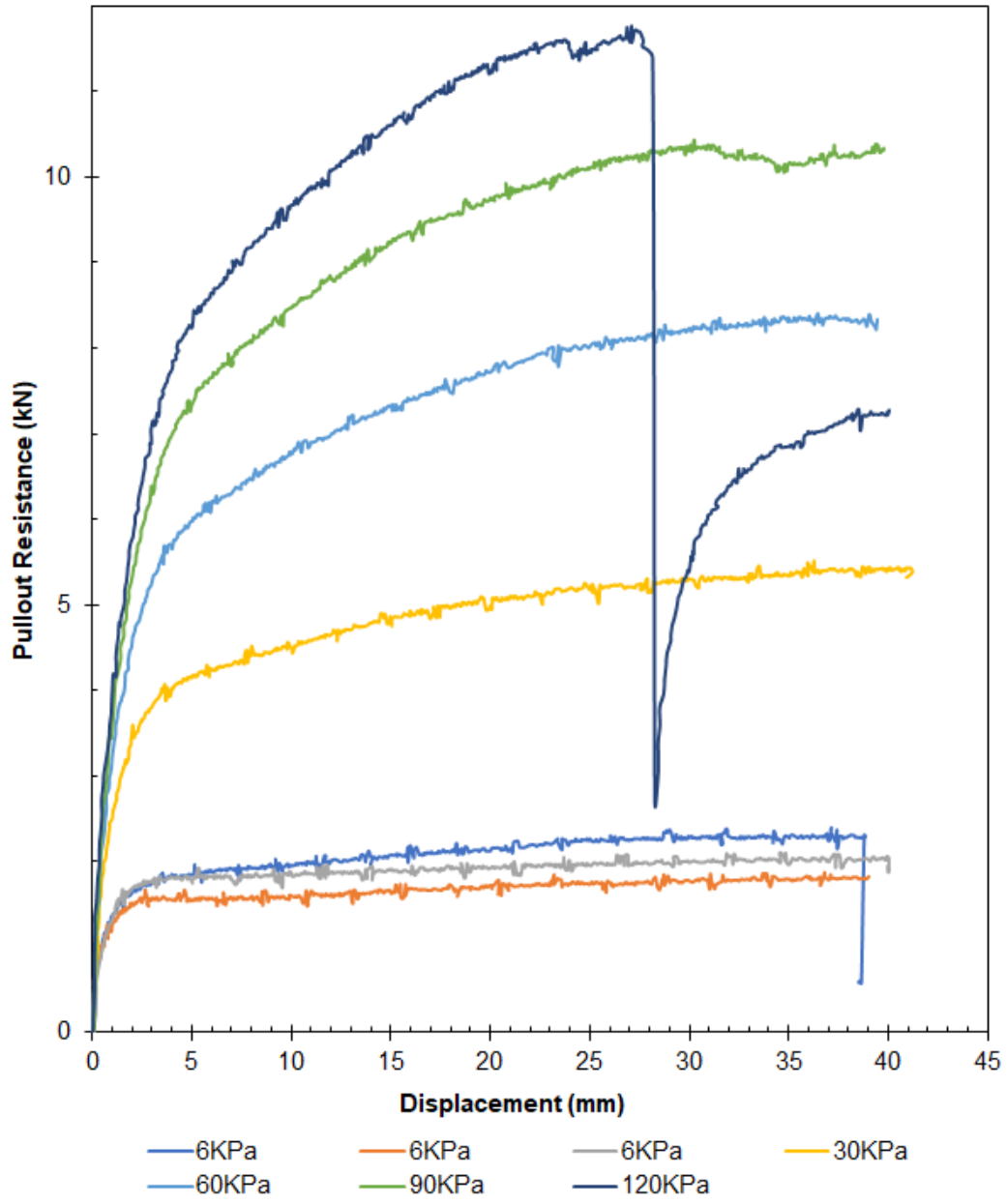


MW45 x MW45 –100 mm x 150 mm

MW45 x MW45 –100 mm x 1-Wire

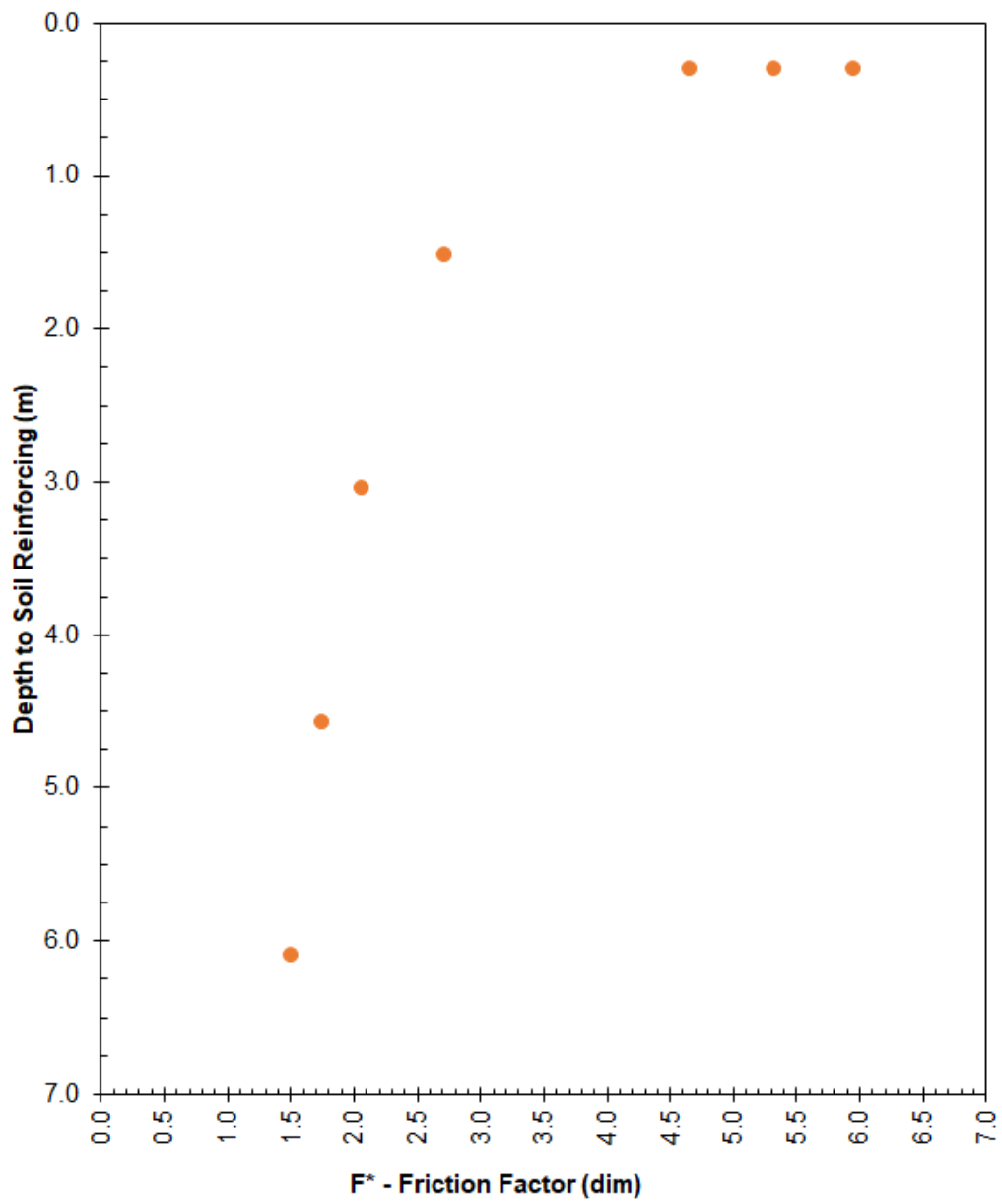
| Test | Name   | Surcharge<br>(kPa) | P <sub>r_19 mm</sub><br>(kN) | F* <sub>19 mm</sub><br>(dim) | P <sub>r_peak</sub><br>(kN) | F* <sub>peak</sub><br>(dim) |
|------|--------|--------------------|------------------------------|------------------------------|-----------------------------|-----------------------------|
| 1    | 6-T1   | 6                  | 2.21                         | 5.95                         | 2.39                        | 6.44                        |
| 2    | 6-T2   | 6                  | 1.73                         | 4.66                         | 1.86                        | 5.02                        |
| 3    | 6-T3   | 6                  | 1.97                         | 5.33                         | 2.09                        | 5.65                        |
| 4    | 30-T4  | 30                 | 5.04                         | 2.72                         | 5.52                        | 2.98                        |
| 5    | 60-T5  | 60                 | 7.66                         | 2.07                         | 8.41                        | 2.28                        |
| 6    | 90-T6  | 90                 | 9.74                         | 1.75                         | 10.44                       | 1.87                        |
| 7    | 120-T7 | 120                | 11.20                        | 1.51                         | 11.76                       | 1.59                        |
| 8    |        |                    |                              |                              |                             |                             |
| 9    |        |                    |                              |                              |                             |                             |
| 10   |        |                    |                              |                              |                             |                             |
| 11   |        |                    |                              |                              |                             |                             |
| 12   |        |                    |                              |                              |                             |                             |
| 13   |        |                    |                              |                              |                             |                             |
| 14   |        |                    |                              |                              |                             |                             |
| 15   |        |                    |                              |                              |                             |                             |
| 16   |        |                    |                              |                              |                             |                             |
| 17   |        |                    |                              |                              |                             |                             |
| 18   |        |                    |                              |                              |                             |                             |
| 19   |        |                    |                              |                              |                             |                             |
| 20   |        |                    |                              |                              |                             |                             |

Test 7 had weld failure during test.



MW45 x MW45 -100 mm x 1-Wire





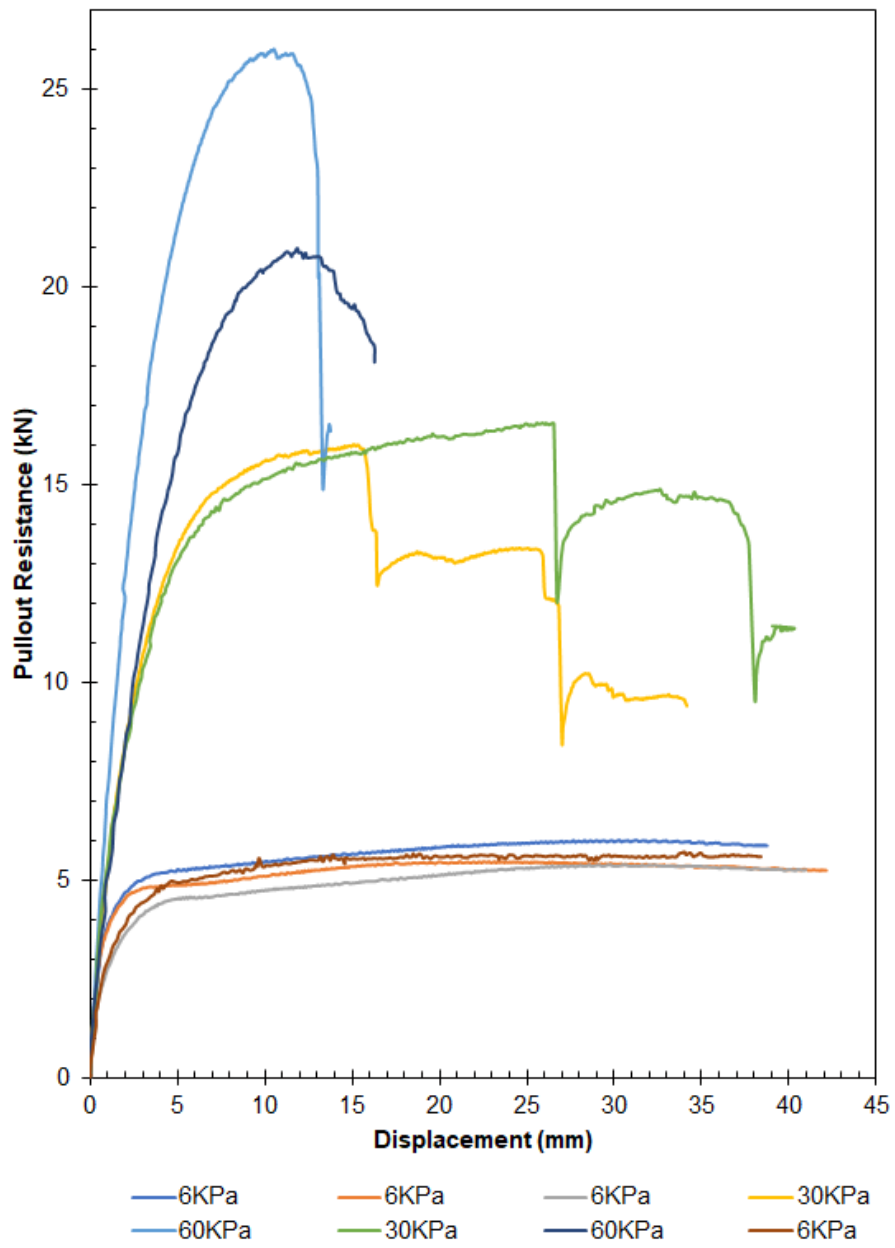
MW45 x MW45 –100 mm x 1-Wire

MW45 x MW45 –200 mm x 300 mm

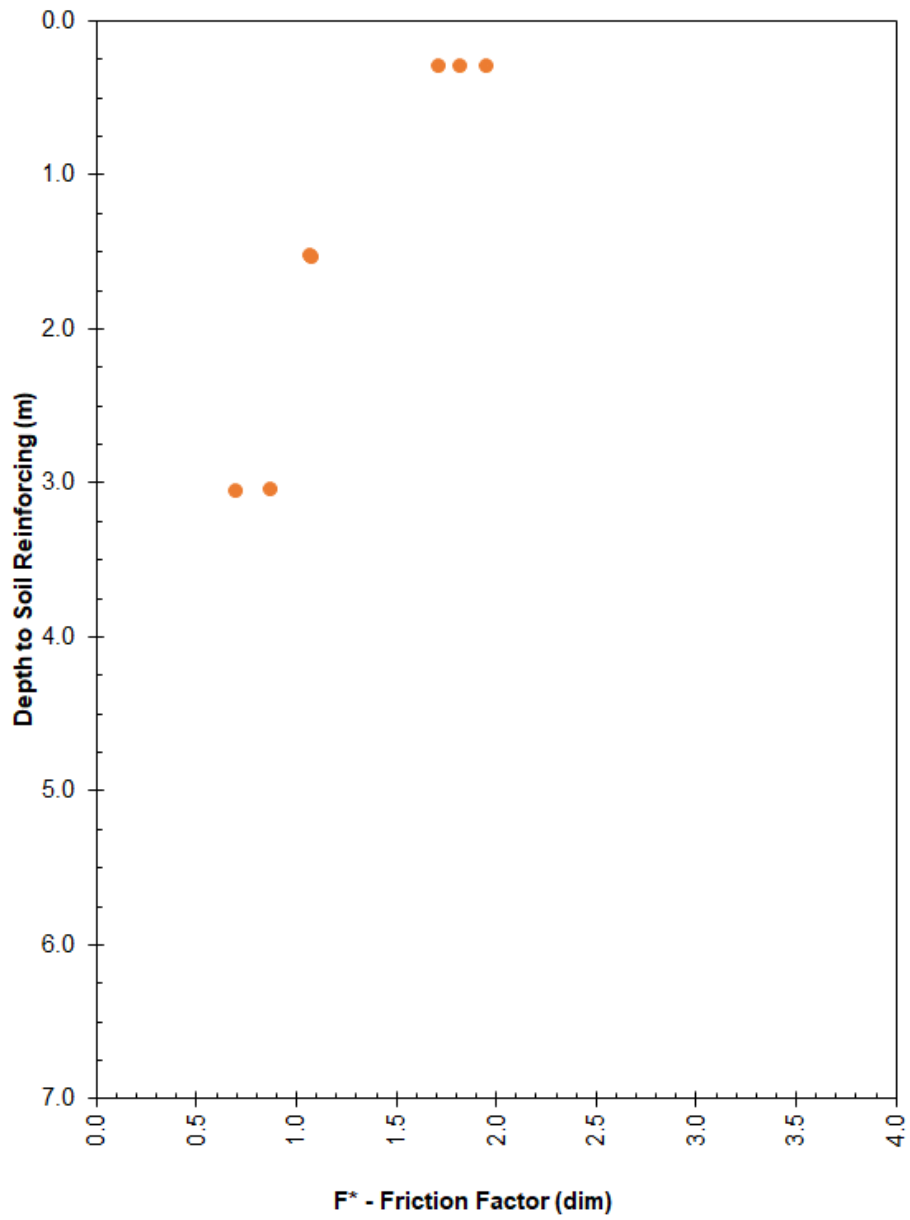
| Test | Name   | Surcharge (kPa) | P <sub>r_19 mm</sub> (kN) | F* <sub>19 mm</sub> (dim) | P <sub>r_peak</sub> (kN) | F* <sub>peak</sub> (dim) |
|------|--------|-----------------|---------------------------|---------------------------|--------------------------|--------------------------|
| 1    | 6-T1   | 6               | 5.80                      | 1.96                      | 6.00                     | 2.02                     |
| 2    | 6-T2   | 6               | 5.42                      | 1.83                      | 5.46                     | 1.84                     |
| 3    | 6-T3   | 6               | 5.09                      | 1.72                      | 5.39                     | 1.82                     |
| 4    | 30-T4  | 30              | 16.00                     | 1.08                      | 16.00                    | 1.08                     |
| 5    | 60-T5  | 60              | 26.03                     | 0.88                      | 26.03                    | 0.88                     |
| 6    | 30-T6  | 30              | 16.20                     | 1.08                      | 16.58                    | 1.11                     |
| 7    | 60-T7  | 60              | 20.99                     | 0.71                      | 20.99                    | 0.71                     |
| 8    | 125-T8 | 6               | 5.68                      | 1.92                      | 5.73                     | 1.93                     |
| 9    |        |                 |                           |                           |                          |                          |
| 10   |        |                 |                           |                           |                          |                          |
| 11   |        |                 |                           |                           |                          |                          |
| 12   |        |                 |                           |                           |                          |                          |
| 13   |        |                 |                           |                           |                          |                          |
| 14   |        |                 |                           |                           |                          |                          |
| 15   |        |                 |                           |                           |                          |                          |
| 16   |        |                 |                           |                           |                          |                          |
| 17   |        |                 |                           |                           |                          |                          |
| 18   |        |                 |                           |                           |                          |                          |
| 19   |        |                 |                           |                           |                          |                          |
| 20   |        |                 |                           |                           |                          |                          |

Test 4, 5, 6, and 7 had weld failure during test.

Because of weld failure testing was terminated at 3.048 m of fill



MW45 x MW45 –200 mm x 300 mm



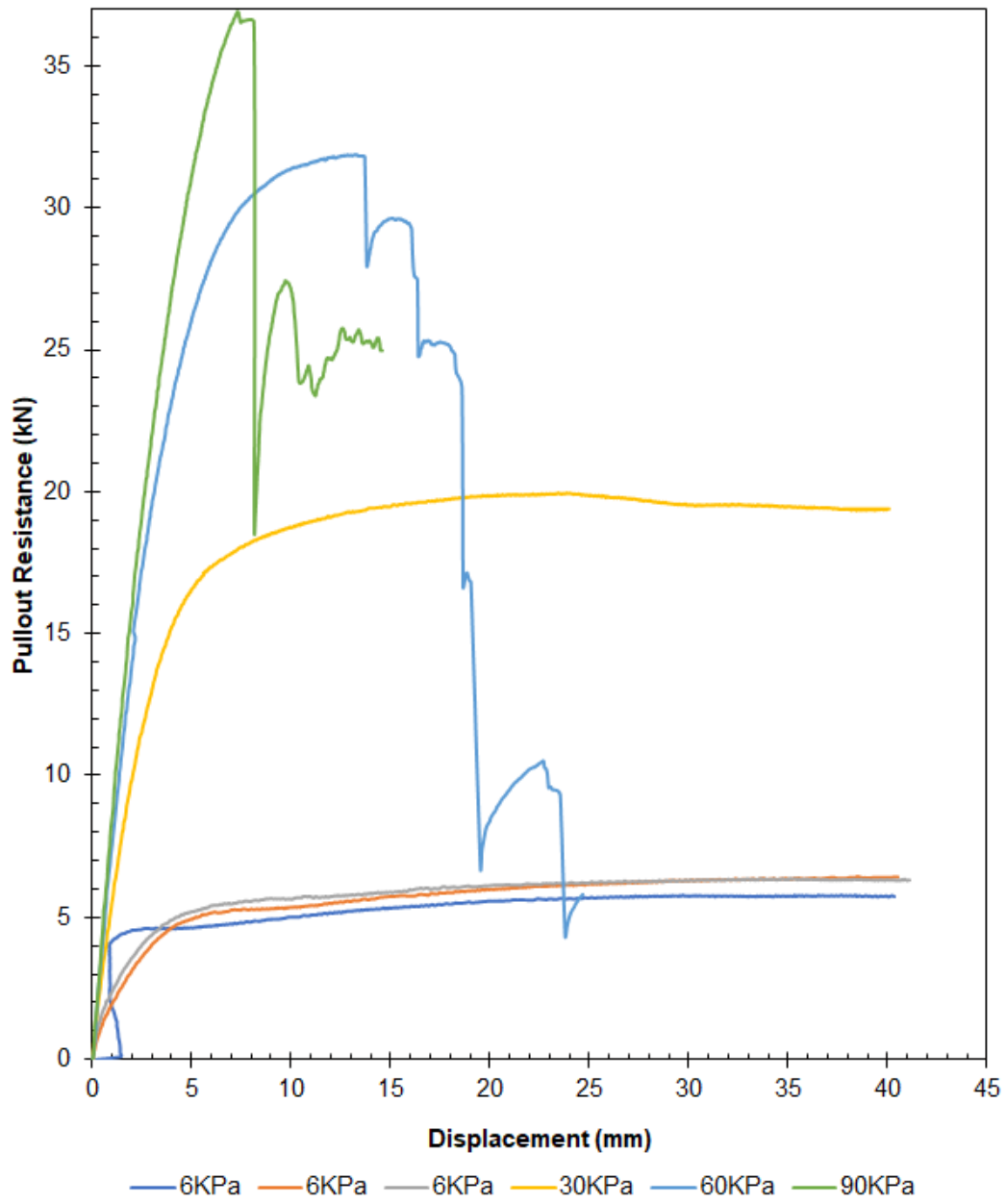
MW45 x MW45 –200 mm x 300 mm

MW45 x MW45 –200 mm x 150 mm

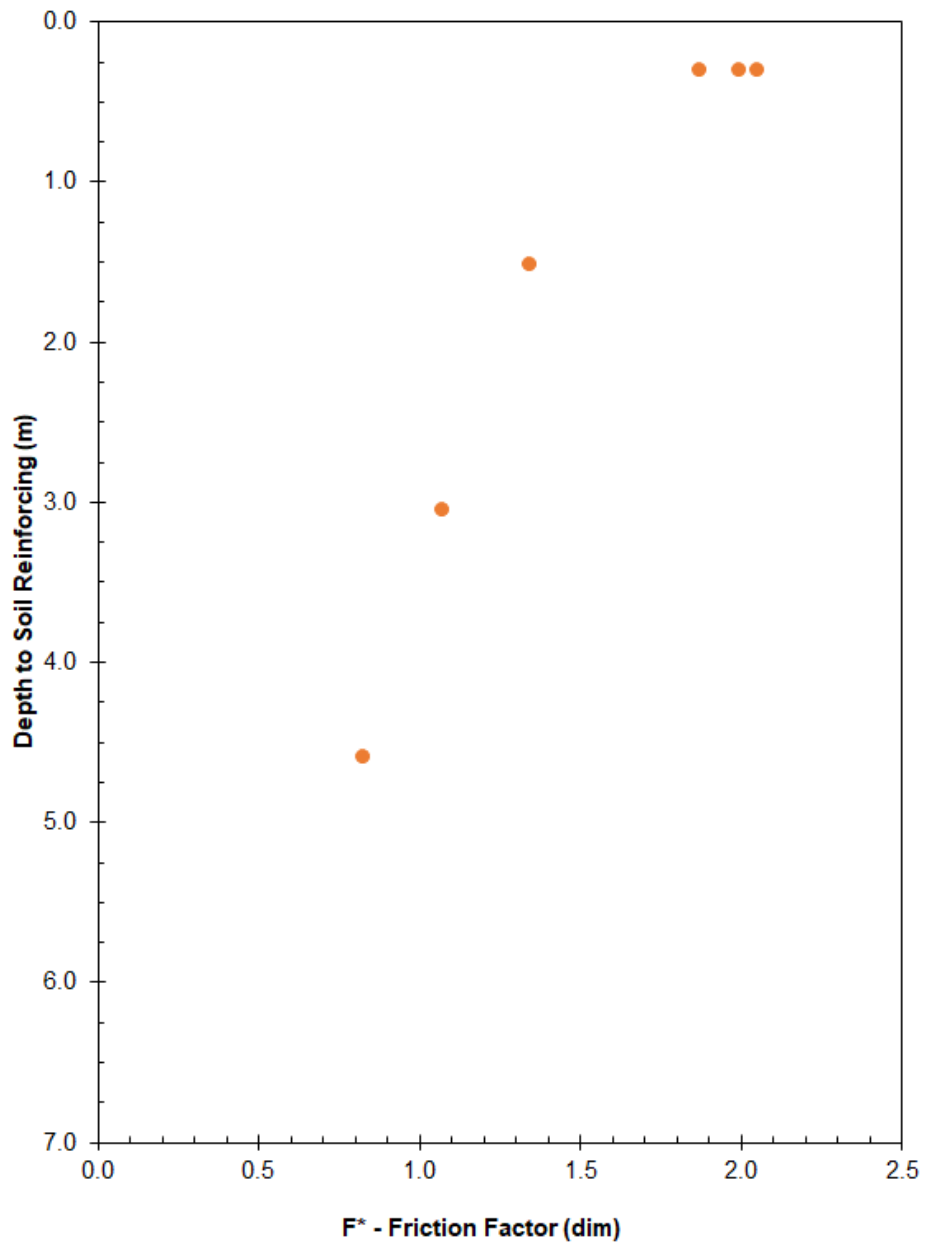
| Test | Name  | Surcharge<br>(kPa) | $P_{r_{19\text{ mm}}}$<br>(kN) | $F^*_{19\text{ mm}}$<br>(dim) | $P_{r_{\text{peak}}}$<br>(kN) | $F^*_{\text{peak}}$<br>(dim) |
|------|-------|--------------------|--------------------------------|-------------------------------|-------------------------------|------------------------------|
| 1    | 6-T1  | 6                  | 5.56                           | 1.87                          | 5.80                          | 1.96                         |
| 2    | 6-T2  | 6                  | 5.92                           | 2.00                          | 6.41                          | 2.16                         |
| 3    | 6-T3  | 6                  | 6.08                           | 2.05                          | 6.35                          | 2.14                         |
| 4    | 30-T4 | 30                 | 19.85                          | 1.34                          | 19.97                         | 1.35                         |
| 5    | 60-T5 | 60                 | 31.85                          | 1.07                          | 31.85                         | 1.07                         |
| 6    | 90-T6 | 90                 | 36.91                          | 0.83                          | 36.91                         | 0.83                         |
| 7    |       |                    |                                |                               |                               |                              |
| 8    |       |                    |                                |                               |                               |                              |
| 9    |       |                    |                                |                               |                               |                              |
| 10   |       |                    |                                |                               |                               |                              |
| 11   |       |                    |                                |                               |                               |                              |
| 12   |       |                    |                                |                               |                               |                              |
| 13   |       |                    |                                |                               |                               |                              |
| 14   |       |                    |                                |                               |                               |                              |
| 15   |       |                    |                                |                               |                               |                              |
| 16   |       |                    |                                |                               |                               |                              |
| 17   |       |                    |                                |                               |                               |                              |
| 18   |       |                    |                                |                               |                               |                              |
| 19   |       |                    |                                |                               |                               |                              |
| 20   |       |                    |                                |                               |                               |                              |

Test 5, and 6 had weld failure during test.

Test 1 potentiometer had a signal interruption



MW45 x MW45 -200 mm x 100 mm



MW45 x MW45 –200 mm x 150 mm

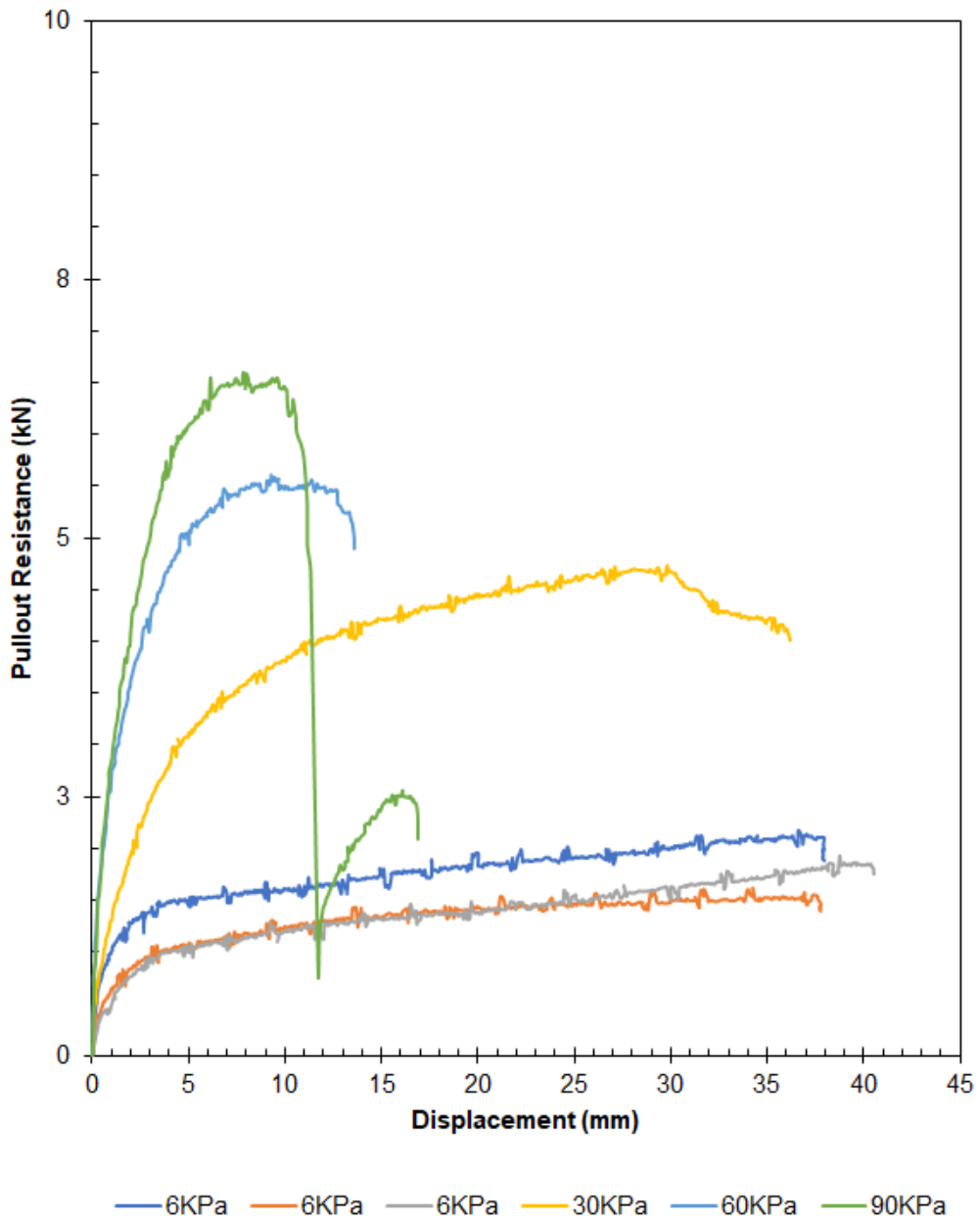
MW45 x MW45 –200 mm x 1-Wire

| Test | Name  | Surcharge (kPa) | P <sub>r_19 mm</sub> (kN) | F* <sub>19 mm</sub> (dim) | P <sub>r_peak</sub> (kN) | F* <sub>peak</sub> (dim) |
|------|-------|-----------------|---------------------------|---------------------------|--------------------------|--------------------------|
| 1    | 6-T1  | 6               | 1.89                      | 2.55                      | 2.18                     | 2.94                     |
| 2    | 6-T2  | 6               | 1.44                      | 1.95                      | 1.62                     | 2.19                     |
| 3    | 6-T3  | 6               | 1.47                      | 1.98                      | 1.93                     | 2.60                     |
| 4    | 30-T4 | 30              | 4.44                      | 1.19                      | 4.73                     | 1.27                     |
| 5    | 60-T5 | 60              | 5.61                      | 0.76                      | 5.61                     | 0.76                     |
| 6    | 90-T6 | 90              | 6.60                      | 0.59                      | 6.60                     | 0.59                     |
| 7    |       |                 |                           |                           |                          |                          |
| 8    |       |                 |                           |                           |                          |                          |
| 9    |       |                 |                           |                           |                          |                          |
| 10   |       |                 |                           |                           |                          |                          |
| 11   |       |                 |                           |                           |                          |                          |
| 12   |       |                 |                           |                           |                          |                          |
| 13   |       |                 |                           |                           |                          |                          |
| 14   |       |                 |                           |                           |                          |                          |
| 15   |       |                 |                           |                           |                          |                          |
| 16   |       |                 |                           |                           |                          |                          |
| 17   |       |                 |                           |                           |                          |                          |
| 18   |       |                 |                           |                           |                          |                          |
| 19   |       |                 |                           |                           |                          |                          |
| 20   |       |                 |                           |                           |                          |                          |

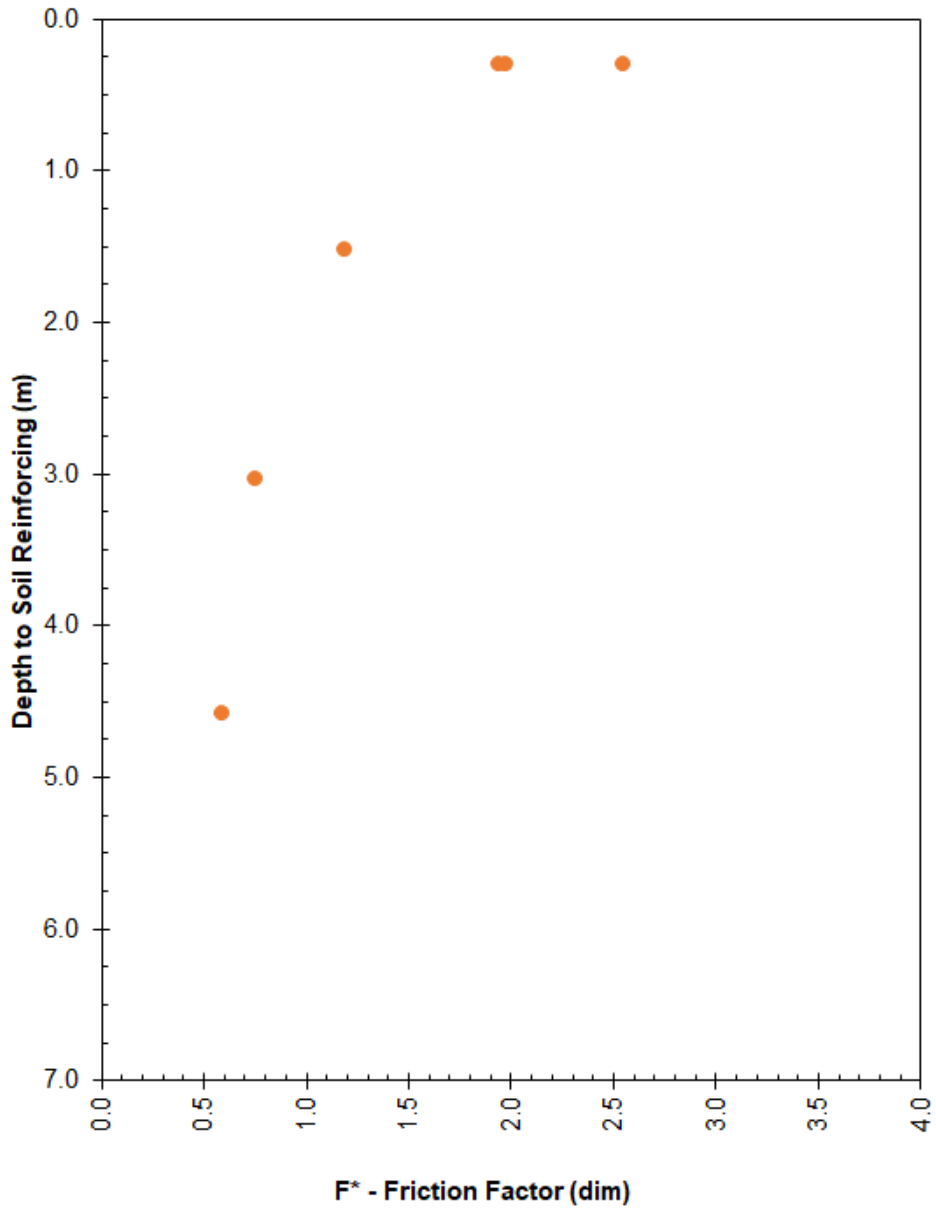
Test 4, 5, and 6 had weld failure during test.

Testing was stopped due to weld failure





MW45 x MW45 -200 mm x 1-Wire








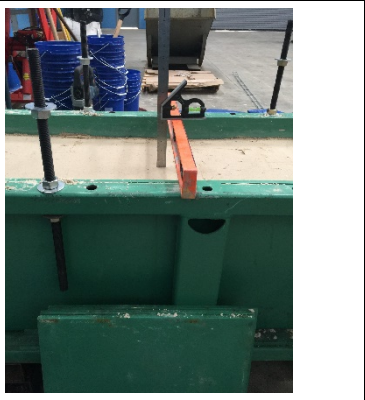
MW45 x MW45 –200 mm x 1-Wire

## **Appendix B**

### **Test Set-Up**

**This Page Intentionally Left Blank**

|     |  |   |
|-----|--|---|
| 1)  | Determine weight of soil at 2% below optimum moisture content.   |   |
| 2)  | Determine total weight of soil for test soil-box.  |   |
| 3)  | Determine weight of soil below elevation of soil-reinforcing element.  |   |
| 4)  | Determine weigh of soil above elevation of soil-reinforcing element.   |   |
| 5)  | Determine weight of reaction frame components.   |   |
| 6)  | Determine system pressure applied to soil-reinforcing.   |   |
| 7)  | Place front gate in pullout soil-box.  |   |
| 8)  | Place soil in the bottom of the soil-box using the required lift thickness and compact to required density. Repeat until soil is placed to the elevation required to place and connect the soil-reinforcing.                               |   |
| 9)  | Level the soil.  |   |
| 10) | <p>Place soil-reinforcing element.</p> <ul style="list-style-type: none"> <li>• Verify that the longitudinal wires are facing up</li> <li>• Verify the first transverse bar is at the edge of and completely inside the sleeve.</li> </ul> |  |

|  |   |
|--|---|
| <p>11) Hook the potentiometer wire-rope connectors on the soil-reinforcing in the required positions.</p>                      |    |
| <p>12) Place remaining front gate in pullout soil-box.</p>   |   |
| <p>13) Connect potentiometers at the back of pullout soil-box.</p>   |    |
| <p>14) Place soil in desired lift thickness and compact to required density. Verify volume relationship at each soil lift.</p> |   |
| <p>15) Level soil at top of the soil-box. This assures that the load is applied equally to the soil mass.</p>                  |  |

16) Place neoprene pad on top of soil.



17) Place air diaphragm on top of neoprene pad. Expand air diaphragm to properly position diaphragm in soil-box.



18) Place neoprene pad on top of air diaphragm.



19) Place reaction plate on top of air diaphragm.



20) Place reaction beams on top of reaction plate.



21) Place reaction cross beams on 19 mm all-thread columns.






22) Deflate air diaphragm. Check position of all reaction frame components in relationship to sides of soil-box.

23) Place load cell reaction beams and plates on reaction beams.





|  |   |
|--|---|
| <p>24) Place load cell and level reaction beam until the bottom of the reaction beam meets the load button on the load cell. Verify that the all-thread columns are secure by tightening the nut at the interface of the 50 mm x 50 mm beam.</p>   |   |
| <p>25) Move connection plate into proper position. Connect soil-reinforcing to connection load plate. Verify that connection plate is level. Secure bolts with air wrench and tighten with ratchet.</p>  |   |
| <p>26) Place LVDT at front of the pullout soil-box on each side of the horizontal actuator. Level and straighten the LVDT.</p>   |  |
| <p>27) Turn on the Campbell Scientific data acquisition system and perform the following:</p> <ul style="list-style-type: none"> <li>• Zero load cells.</li> <li>• Record the beginning positions of LVDTs</li> <li>• Calculate the position of the LVDT at 19 mm deformation and record the value</li> <li>•</li> </ul> |   |
| <p>28) Expand air bag until the load for the required overburden pressure is registering on the load cells. Verify that the loading on the plate is equal and the load cells are level. Check line pressure and air pressure.</p>  |   |

|     |   |
|-----|---|
| 29) | <ul style="list-style-type: none"> <li>• Verify the flow control position is set to testing position and is not in the set-up position.</li> <li>• Verify that the ball valve is in the neutral position.</li> <li>• Turn on the chiller.</li> <li>• Turn on the hydraulic pump.</li> </ul> |
| 30) | Clear the data in the data acquisition.   |
| 31) | Set up video cameras and start recording.   |
| 32) | Activate flow control to perform test.  |
| 33) | Stop test at 1 ½" displacement has been reached.  |
| 34) | Stop hydraulic pump.  |
| 35) | Save the test data from the data acquisition.   |
| 36) | Deflate the air bag.  |
| 37) | Remove the reaction frame.  |
| 38) | Remove the soil from the soil-box taking care to not disturb the soil-reinforcing. Pace the soil in the 5-gallon buckets to the required weight per bucket. Place on scale.   |
| 39) | At the elevation of the soil-reinforcing carefully exhume the soil.   |
| 40) | Examine the soil-reinforcing and photograph.  |
| 41) | Remove top plate of the connection clamp.   |
| 42) | Remove soil-reinforcing from soil-box.  |
| 43) | Level soil in base of soil-box and compact.   |
| 44) | Stop video recording and save video.  |
| 45) | Repeat test.  |

## **Appendix C**

### **Plaxis-3D Model Parameters**

**This Page Intentionally Left Blank**

## Plaxis Numerical Model

For the numerical model a 2-wire soil-reinforcing element with longitudinal spacings equal to 50, mm, 100 mm, and 200 mm and each containing only one transverse element were investigated. The model boundaries assumed symmetry and used a soil-reinforcing element that was dissected at the mid-point of the transverse bar. Based on this the extents of the model were set to 240 long (x) by 200 mm wide (y) by 500 mm tall (z). The soil-reinforcing element transverse bar was placed at the center of the x dimension. A plan view of the 200 mm model is shown below.



Prescribed displacements were initiated at the location of the longitudinal element at the interface where it exits the soil-box. The prescribed displacement was set equal to 19 mm. Three over burden pressures equal to 6 kPa, 30 kPa and 60 kPa were investigated for each soil-reinforcing configuration. The material properties for the steel and the soil are given in the following two tables.

### Steel Material Parameters

| Properties | Variable | Value                     |
|------------|----------|---------------------------|
| Material   |          | Linear Elastic            |
| Stiffness  | E        | 200.0E6 kN/m <sup>2</sup> |
|            | $\nu$    | 0.299                     |

### Soil Material Parameters

| Properties        | Variable    | Value                     |
|-------------------|-------------|---------------------------|
| Material          |             | Mohr-Coulomb              |
|                   |             | Drained                   |
| Unit Weight       | $\gamma$    | 20.00 kN/m <sup>3</sup>   |
| Dilatancy Cut-Off | $e_{init}$  | 0.500                     |
|                   | $e_{min}$   | 0.000                     |
|                   | $e_{max}$   | 999.0                     |
| Stiffness         | E           | 50.0E3 kN/m <sup>2</sup>  |
|                   | $\nu$       | 0.350                     |
| Alternatives      | G           | 18.52E3 kN/m <sup>2</sup> |
|                   | $E_{oed}$   | 80.25E3 kN/m <sup>2</sup> |
| Strength          | $c_{ref}$   | 0.1 kN/ m <sup>2</sup>    |
|                   | $\phi$      | 40 deg                    |
|                   | $\psi$      | 10 deg                    |
|                   | $R_{inter}$ | 0.75                      |